This document was produced by scanning the original publication.

Ce document est le produit d'une numérisation par balayage de la publication originale.

GEOLOGICAL SURVEY OF CANADA
BULLETIN 525

GEOLOGY AND NATURAL HAZARDS OF THE FRASER RIVER DELTA, BRITISH COLUMBIA

edited by
J.J. Clague, J.L. Luternauer, and D.C. Mosher

1998

Natural Resources Canada Ressources naturelles Canada

Canada

GEOLOGICAL SURVEY OF CANADA
BULLETIN 525

GEOLOGY AND NATURAL HAZARDS OF THE FRASER RIVER DELTA, BRITISH COLUMBIA

edited by
J.J. Clague, J.L. Luternauer, and D.C. Mosher

1998

©Her Majesty the Queen in Right of Canada, 1998

Catalogue No. M42-525E
ISBN 0-660-17651-3

Available in Canada from
Geological Survey of Canada offices:

601 Booth Street
Ottawa, Ontario K1A 0E8

3303-33rd Street N.W.
Calgary, Alberta T2L 2A7

101-605 Robson Street
Vancouver, B.C. V6B 5J3

A deposit copy of this publication is also available for reference
in selected public libraries across Canada

Price subject to change without notice

Cover illustration

Fraser River delta from space: satellite image, showing the Fraser delta and adjacent urbanized uplands of Greater Vancouver. Turbid waters of the Fraser River (blue grey) discharge into the Strait of Georgia. Image provided by G.F. Tomlins, copyright Pacific Geomatics Ltd., Surrey, British Columbia.

Critical reviewer
R.J.W. Turner

Authors' addresses

J.J. Clague
J.L. Luternauer
Geological Survey of Canada
605 Robson Street
Vancouver, British Columbia
V6B 5J3

D.C. Mosher
Geological Survey of Canada
Pacific Geoscience Centre
P.O. Box 6000
Sidney, British Columbia
V8L 4B2

CONTENTS

Introduction

J.J. Clague[1]

Clague, J.J., 1998: Introduction; in Geology and Natural Hazards of the Fraser River Delta, British Columbia, (ed.) J.J. Clague, J.L. Luternauer, and D.C. Mosher; Geological Survey of Canada, Bulletin 525, p. 1–6.

The Fraser River delta (Fig. 1), just south of Vancouver, British Columbia, is the largest, most populated, and most important delta in western Canada. Nearly 200 000 people live on the Fraser delta, and the population is expanding at an annual rate of about 2-3%, making this one of the fastest growing areas in the Lower Mainland. The Fraser delta is a major agricultural producer ($77 million revenue per year), an important waterfowl area, a vital link in the Fraser River salmon fishery, and a major commercial and industrial centre, sustaining over 90 000 jobs. It is also the location of critical facilities of regional and national importance, including the Vancouver International Airport, the Tsawwassen Ferry Terminal, and the Roberts Bank Deltaport. Electricity transmission cables supplying much of the power to southern Vancouver Island cross the delta slope.

The need to plan sensibly for future growth on the Fraser delta, while protecting vital natural resources, has become more acute in recent years as population has increased. Several environmental issues have been identified and studied. Human activity has contributed pollutants to the Fraser delta and degraded important coastal habitats. About 1 billion L of domestic and industrial waste are discharged into the Fraser River every day. Toxic chemicals seep from landfills, and accidental spills and illegal dumping contribute solvents, oils, and pesticides. Metals accumulate in sediments on the tidal flats and in deep water in the southern Strait of Georgia, and are released into the food chain. Causeways and other large structures, as well as river dredging, have altered sediment- and water-dispersal patterns and contributed to erosion of parts of the tidal flats. River training has concentrated sediment deposition in small areas at the mouths of the active distributary channels and thus promoted delta-slope failures (Fig. 1).

Le delta du fleuve Fraser (fig. 1), juste au sud de Vancouver, en Colombie-Britannique, est le plus vaste, le plus peuplé et le plus important de l'ouest du Canada. Une population de près de 200 000 habitants y vit et augmente à un rythme annuel de quelque 2 à 3 %, ce qui en fait une des régions des basses terres continentales où la croissance démographique est la plus élevée. Le delta du Fraser est une importante région agricole (77 millions de dollars en recettes par année), l'habitat de nombreux oiseaux aquatiques, un lien vital pour la pêche du saumon dans le fleuve Fraser et un centre d'activité commerciale et industrielle de premier plan; y sont concentrés plus de 90 000 emplois. C'est également là qu'ont été aménagées des installations cruciales pour l'économie régionale et nationale, notamment l'aéroport international de Vancouver, la gare maritime de Tsawwassen et le port de Roberts Bank. De plus, des câbles de transport d'électricité qui fournissent la presque totalité de l'énergie à la partie sud de l'île de Vancouver traversent le talus du delta.

Au cours des dernières années, l'augmentation de la population a mis en évidence la nécessité de planifier en toute connaissance de cause la croissance future dans la région du delta du Fraser. Plusieurs problèmes environnementaux ont été soulevés et ont fait l'objet d'études. Notamment, l'activité anthropique pollue le delta du Fraser et détériore d'importants habitats littoraux. Près d'un milliard de litres de déchets domestiques et industriels sont jetés dans le fleuve Fraser quotidiennement. Des produits chimiques toxiques s'infiltrent dans le sol à partir des décharges. Il arrive que des solvants, des carburants et des pesticides soient déversés accidentellement ou illégalement. Des métaux s'accumulent dans les sédiments des estrans et dans les eaux profondes de la partie sud du détroit de Georgia, s'immisçant ainsi dans la chaîne alimentaire. La construction de digues et d'autres gros ouvrages ainsi que le dragage du fleuve modifient la façon dont se dispersent les sédiments et les eaux et contribuent à l'érosion de certaines parties des estrans. Le redressement du cours du fleuve concentre le dépôt des sédiments dans de petites zones à l'embouchure des défluents actifs, ce qui a pour effet d'augmenter le nombre de ruptures du talus (fig. 1).

[1] Geological Survey of Canada, 605 Robson Street, Vancouver, British Columbia V6B 5J3

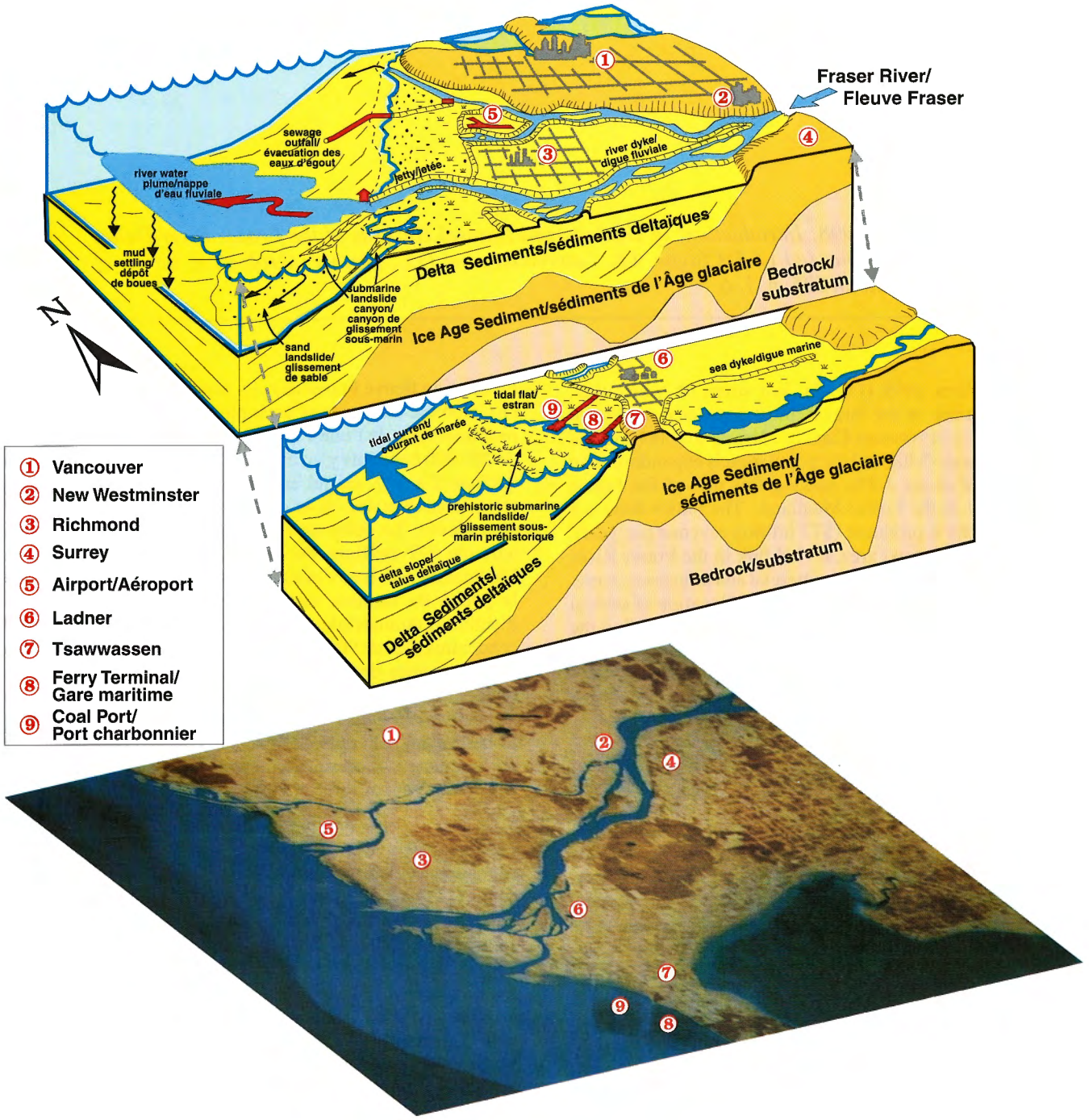

***Figure 1**. Cut-away block diagram of the Fraser delta, showing subsurface geology, important natural processes, cities and towns, and major delta-front facilities (from Turner et al., 1996). Locations of key sites are indicated on the block diagram and the satellite image below.*

***Figure 1**. Bloc diagramme du delta du Fraser, montrant la géologie souterraine, les processus naturels importants, les villes et les principales installations sur le front deltaïque (tiré de Turner et al., 1996). Les villes et les installations les plus importantes sont indiquées tant sur le bloc diagramme que sur l'image-satellite.*

People and property on the Fraser delta are at risk from earthquakes, landslides, floods, and sea-level rise. The Fraser delta lies within one of the most seismically active regions in Canada, and there is concern that shallow, subsurface, deltaic sediments might liquefy during a strong earthquake, increasing damage beyond that which would be caused by the ground shaking alone. Shaking might be stronger on some parts of the delta than on nearby firmer ground due to the peculiar geometry and physical properties of the deltaic deposits. The delta's protective dykes were built to withstand floods, not earthquakes, and could fail if seismic shaking was particularly strong or lengthy. Other natural hazards of concern are submarine landslides at the delta front, and burial and scour on the delta slope. Facilities vulnerable to these hazards include the ferry terminal, deltaport, and submarine cables and pipelines (Fig. 1). Finally, much of the delta plain lies only a metre or two above mean sea level, adjacent to the largest river in British Columbia; consequently, there is potential for damaging flooding, either directly from the river or from the sea during extreme storm events should sea level rise during the next century due to anticipated climatic warming.

Diverses catastrophes naturelles (tremblements de terre, inondations et hausse du niveau de la mer) menacent les personnes qui habitent sur le delta du Fraser et les propriétés qui y sont construites. Le delta du Fraser se trouve dans l'une des régions où la sismicité est la plus élevée du pays. Si un séisme de forte magnitude survenait, les sédiments deltaïques à faible profondeur pourraient se liquéfier, ajoutant ainsi aux dommages causés par les seuls ébranlements du sol. De plus, les secousses pourraient être plus fortes dans certaines parties du delta que dans les secteurs au sol plus dur du voisinage, à cause de la géométrie particulière et des propriétés physiques des sédiments deltaïques. Les digues de protection le long du delta ont été construites pour faire face aux crues, mais pas aux séismes; c'est pourquoi elles pourraient se rompre si des secousses sismiques étaient particulièrement intenses ou longues. Les autres risques naturels jugés menaçants pour le delta sont notamment les glissements de terrain sous-marins au niveau de son front ainsi que les phénomènes d'enfouissement et d'affouillement au niveau de son talus. Parmi les installations vulnérables à ces processus figurent la gare maritime, le port ainsi que les câbles et les conduites sur le fond marin (fig. 1). Enfin, la surface de la plaine deltaïque se trouve à tout juste un mètre ou deux au-dessus du niveau moyen de la mer et est à l'embouchure du plus grand fleuve de la Colombie-Britannique. Par conséquent, si le réchauffement climatique prévu faisait en sorte que le niveau de la mer augmentait au cours du prochain siècle, il se pourrait que des inondations causent des dommages à la suite du débordement du fleuve ou du déferlement de vagues océaniques pendant des tempêtes très violentes.

During the last three decades, the Geological Survey of Canada (GSC), in cooperation with other government agencies, universities, and the private sector, has conducted research to address many of these issues and concerns. Studies by the GSC have accomplished the following: 1) provided baseline geoscience data for other natural science surveys; 2) identified physical processes that affect the delta; 3) anticipated effects of natural processes and anthropogenic influences; 4) developed new technologies to more precisely describe the deposits beneath the delta; 5) designed methods to mitigate undesirable environmental changes; and 6) educated people about the environment in which they live.

Au cours des trois dernières décennies, la Commission géologique du Canada (CGC), en collaboration avec d'autres organismes gouvernementaux, des universités et le secteur privé, a mené des recherches pour étudier nombre de ces questions et préoccupations. Les scientifiques de la CGC ont ainsi réussi à obtenir les résultats suivants : 1) recueillir des données géoscientifiques de base pour d'autres levés en sciences naturelles; 2) déterminer les processus physiques qui modifient le delta; 3) prévoir les effets des processus naturels et des facteurs anthropiques sur le delta; 4) élaborer de nouvelles techniques pour en arriver à décrire avec plus de précision les dépôts du delta; 5) concevoir des méthodes pour atténuer les changements environnementaux non souhaitables et 6) fournir de l'information «grand public» sur l'environnement dans lequel vivent les habitants de cette région.

The 16 papers in this volume constitute a summary of recent research by GSC scientists and others on the geological architecture and environment of the Fraser delta, and the physical and chemical processes operating on it. The papers collectively cover all of the issues mentioned above, with the exception of contamination and flooding. They present the latest views on their subjects, and most contain extensive reference lists that provide additional information. The information in this Bulletin can be used to evaluate the possible impacts of natural processes and human activities on public safety, wildlife habitats, and development.

Les 16 articles que contient le présent bulletin résument les recherches menées récemment par les scientifiques de la CGC et d'autres individus sur le contexte géologique et l'environnement du delta du Fraser, ainsi que sur les processus physiques et chimiques qui le modifient. Les articles traitent de toutes les questions mentionnées ci-dessus, à l'exception de la contamination et des inondations. Ils présentent les données les plus récentes sur les sujets traités et la plupart contiennent une liste de référence exhaustive dans laquelle des informations supplémentaires sont fournies. Les données que contient ce bulletin pourront servir à évaluer les répercussions possibles des processus naturels et de l'activité de l'homme sur la sécurité publique, les habitats des espèces sauvages et l'expansion.

The first two papers are overviews of the geological and seismic setting of the Fraser delta; they provide background information for the more specific topical papers that follow. The character and origin of the landscape and earth materials in the Vancouver area are summarized in the first paper by Clague. The Fraser delta is a geologically young feature, formed since the end of the last glaciation about 10 000 years ago. The deltaic sediments overlie a thick succession of poorly consolidated glacial deposits, and these glacial deposits, in turn, rest on Tertiary sedimentary rocks which form part of the Georgia Basin (Fig. 1). The second paper, by Rogers, reviews the types, frequency, and causes of earthquakes in south-coastal British Columbia. About 10 moderate to large earthquakes have struck southwestern British Columbia and western Washington since the late 1800s, but none of these has damaged Vancouver. A local, shallow, crustal earthquake, or a much deeper quake within the subducting Juan de Fuca plate, poses the greatest threat to Vancouver, but much larger, rarer earthquakes (magnitude = 8+) at the boundary between the North America and Juan de Fuca plates could also damage the city.

Le deux premiers articles présentent les données de base utiles pour aborder les documents plus spécifiques qui suivent; l'un donne un aperçu du contexte géologique du delta du Fraser et l'autre en évalue les risques sismiques. L'article de Clague, le premier, décrit et explique comment se sont formés le paysage et les matériaux de la région de Vancouver. Du point de vue géologique, le delta du Fraser est un élément récent du paysage, sa formation s'étant amorcée à la fin de la dernière glaciation, voilà 10 000 ans. Les sédiments deltaïques reposent sur une épaisse succession de sédiments de l'Âge glaciaire faiblement consolidés qui, à leur tour, surmontent des roches sédimentaires du Tertiaire formant le substratum du bassin de Georgia (fig. 1). L'article de Rogers, le deuxième, fait état des séismes qui ont secoué la zone littorale de la Colombie-Britannique méridionale, en précisant les différents types, leur fréquence et leur cause. Environ 10 séismes de moyenne à forte magnitude ont ébranlé le sud-ouest de la Colombie-Britannique et l'ouest de l'État de Washington depuis la fin des années 1800, mais aucun n'a eu de répercussions sur Vancouver. Cette ville est surtout menacée par un séisme dont le foyer serait situé dans la croûte peu profonde des environs ou dans la plaque Juan de Fuca, beaucoup plus profonde et en cours de subduction; cependant, des séismes plus intenses et plus rares (magnitude ≥8) déclenchés à la limite entre les plaques nord-américaine et Juan de Fuca pourraient également y causer des dommages.

The next two papers are a summary of present-day sedimentary environments on the Fraser delta. The first of the two papers, by Luternauer et al., is a review of the full range of environments, from the floodplain to the delta slope, and sets the stage for later papers concerned with the stability of the delta front. Luternauer et al. point out that the delta's natural systems have been profoundly modified during the last century by dyking, river training, land clearing, and urbanization (Fig. 1). Consequences of these modifications are that sediment is no longer accumulating on the delta plain, Fraser River distributary channels are unable to migrate, and the river's load, reduced through dredging, is deposited in small areas off the mouths of the active distributaries. The second of the two papers, by Kostaschuk et al., is concerned with physical processes operating in the Main Channel of the Fraser River. During summer freshet, dunes migrate along the floor of the Main Channel, and large quantities of sand are delivered to the delta front at Sand Heads. The transport and deposition of silt and clay are influenced by a salt wedge that penetrates far up the Main Channel during rising tides and periods of low flow, and retreats to near the channel mouth during low tides and high flows. These processes complicate the dispersal of contaminants which are preferentially adsorbed onto clay minerals.

Les deux articles suivants présentent en résumé les milieux sédimentaires actuels du delta du Fraser. Dans le premier des deux, Luternauer et al. passent en revue l'éventail complet des milieux sédimentaires, allant de la plaine d'inondation au talus deltaïque, et jettent les prémisses d'autres articles traitant de la stabilité du front deltaïque. Il y est souligné que les systèmes naturels du delta ont été profondément modifiés au cours du dernier siècle par la construction de digues, le redressement du cours du fleuve, le déboisement et l'urbanisation (fig. 1). Les conséquences de ces modifications sont l'interruption de l'accumulation de sédiments sur la plaine deltaïque, l'incapacité des affluents du fleuve Fraser de migrer et la restriction du dépôt de la charge fluviatile (réduite par le dragage) à de petites zones à l'embouchure des défluents actifs. Kostaschuk et al. signent le deuxième article sur les processus physiques actifs dans le chenal principal du fleuve Fraser. Durant la période de crue estivale, les dunes migrent le long du lit du chenal principal et de grandes quantités de sable sont déposées au niveau des pointes de sable (Sand Heads) du front deltaïque. Le transport et le dépôt du silt et de l'argile sont modifiés par l'action d'une lame d'eau salée qui, d'une part, remonte loin dans le chenal principal durant les périodes de marée montante et de basses eaux (écoulement faible) et, d'autre part, recule presque jusqu'à l'embouchure du chenal durant les périodes de marée basse et de hautes eaux (écoulement fort). Les processus mentionnés ci-haut compliquent la dispersion des contaminants qui sont généralement adsorbés par les minéraux argileux.

A third group of papers deals with the geological architecture (lithostratigraphy) and biological structure (biofacies) of the Fraser delta. The first two papers in this group (Clague et al., Pullan et al.) provide detailed descriptions of the Holocene (postglacial) and Pleistocene ('Ice Age') deposits

Un troisième groupe d'articles traite de l'architecture géologique (lithostratigraphie) et de la structure biologique (biofaciès) du delta du Fraser. Les deux premiers (Clague et al. ainsi que Pullan et al.) décrivent en détail les dépôts de l'Holocène (postglaciaires) et du Pléistocène (l'Âge

beneath the dyked delta plain, determined from drilling, geotechnical testing, and geophysical surveys done by the GSC and others. The next contribution, by Hunter et al., is a review of the many geophysical techniques that have been employed to elucidate the subsurface structure of the terrestrial part of the Fraser delta. It is followed by a paper on the stratigraphy of the marine portion of the delta and the adjacent Strait of Georgia by Mosher and Hamilton. These papers make it clear that the sedimentary succession beneath the delta plain is far more complex than was thought, even five years ago. The Holocene deltaic deposits range from about 10 m to more than 300 m thick, and overlie Pleistocene sediments across an irregular surface with considerable local relief. The deltaic deposits show considerable lithologic variability over short vertical and horizontal distances, and do not display the simple layer-cake stratigraphy so often assumed. Seismic response models currently in use do not take into account this complexity and thus do not provide a good indication of surface ground motions that would result from a strong earthquake. The final paper in this group (Hutchinson et al.) provides the first published synthesis of Fraser delta biofacies. It is a summary of present-day and past plant, diatom, and foraminiferal communities on the delta, and discusses their use in paleoenvironmental reconstructions and stratigraphic correlation. This paper provides information on depositional environments of Pleistocene sediments beneath the Holocene delta and identifies a former channel of the Fraser River that discharged into Boundary Bay more than 6000 years ago.

A final group of papers is concerned with natural hazards and environmental issues. The first of these papers, by Clague et al., is a review of geological evidence for large prehistoric earthquakes in south-coastal British Columbia, and provides insights into the likely effects of a future comparable earthquake on the Fraser delta. Some of the earthquakes were larger than any that have occurred in the Vancouver area since the arrival of European settlers. A particularly large earthquake, about 1700 years ago, liquefied sand at shallow depths beneath the Fraser delta and caused the delta plain to subside. Were a similar earthquake to occur today, it would damage bridges, roads, utilities (gas, electricity, sewerage, water), and many buildings on the delta, and would probably trigger landslides at the delta front. Rogers et al. examine the ground-motion response on the Fraser delta from two moderate-sized historical earthquakes - the Pender Island earthquake in 1976 and the Duvall, Washington, earthquake in 1996. The records of these earthquakes provide important constraints on the spectral response of ground shaking during any future, larger earthquake. This work complements a study by Harris et al. of seismic-wave attenuation and amplification based on geological and geophysical data. Both studies show that the ground-motion response during an earthquake is likely to be complex, due in part to the heterogeneity of the Holocene deltaic deposits and to differences in the thickness of the deposits. Seismic waves most damaging to small structures (e.g. homes and low buildings) would be amplified in areas where deltaic sediments are thin and would

glaciaire) qui forment la plaine deltaïque endiguée, à partir de données de diagraphies, d'essais géotechniques et de levés géophysiques effectués par, entre autres, la CGC. L'article suivant de Hunter et al. fait état des nombreuses techniques géophysiques qui ont été utilisées pour établir la structure souterraine de la partie terrestre du delta du Fraser. Suit un article sur la stratigraphie de la portion marine du delta et du détroit de Georgia adjacent dont les auteurs sont Mosher et Hamilton. Il ressort clairement de ces contributions que la succession sédimentaire de la plaine deltaïque est beaucoup plus complexe qu'on ne le croyait, même il y a à peine cinq ans. L'épaisseur des sédiments holocènes du delta varie d'environ 10 mètres à plus de 300 mètres; ces matériaux reposent sur des sédiments pléistocènes dont la surface est irrégulière et très accidentée par endroits. Les dépôts deltaïques affichent une lithologie très variable sur de très courtes distances (tant verticales que horizontales) et leur stratigraphie ne correspond pas à l'image classique du «gâteau à étages». Les modèles sismiques actuellement utilisés ne tiennent pas compte de cette complexité et ne donnent donc pas une bonne indication des mouvements du sol en surface que produirait un séisme de forte magnitude. Le dernier article de ce groupe (Hutchinson et al.) constitue la première synthèse qu'on publie sur les biofaciès du delta du Fraser. Il donne un aperçu des communautés de plantes, de diatomées et de foraminifères qui existent ou qui ont existé dans l'environnement du delta et traite de leur utilisation dans les reconstitutions paléoenvironnementales et les corrélations stratigraphiques. Cet article renseigne sur les milieux de dépôts des sédiments pléistocènes (sous ceux de l'Holocène) ainsi que sur l'endroit où se trouvait un ancien défluent du fleuve Fraser qui se jetait dans la baie Boundary, il y a plus de 6 000 ans.

Un dernier groupe d'articles traite des risques naturels et des questions environnementales. Le premier de ceux-ci (Clague et al.) passe en revue les données géologiques sur les gros séismes préhistoriques qui ont frappé la zone littorale de la Colombie-Britannique méridionale et donne un aperçu des effets probables d'un séisme de cette magnitude dans la région du delta du Fraser. Certains séismes préhistoriques étaient plus forts que tous ceux qui ont ébranlé la région de Vancouver depuis l'arrivée des colons européens. Un tremblement de terre particulièrement violent, il y a quelque 1 700 ans, est à l'origine de phénomènes de liquéfaction du sable à de faibles profondeurs sous le delta du Fraser et de l'affaissement de la plaine deltaïque. Si un séisme d'une telle magnitude se produisait aujourd'hui, il endommagerait les ponts, les routes, les réseaux de services publics (gaz, électricité, égouts, aqueduc) et de nombreux bâtiments actuellement situés sur le delta, en plus de probablement déclencher des glissements de terrain au niveau du front deltaïque. Rogers et al. analysent les ébranlements du sol dans la région du delta du Fraser à la suite de deux séismes historiques d'intensité moyenne, soit celui de l'île Pender en 1976 et celui de Duvall (État de Washington) en 1996. Les traces laissées par ces séismes permettent de délimiter comment se comporteraient les matériaux du delta s'ils étaient soumis aux ondes d'un séisme de plus forte magnitude dans l'avenir. Ces travaux complètent une étude réalisée par Harris et al. sur l'atténuation et l'amplification des ondes sismiques basées sur des données géologiques et géophysiques. Les deux études

be reduced in intensity in areas of thick deltaic sediments. These sediments are thin at the margins of the delta and in a few other areas where Pleistocene deposits reach to shallow depths. In the next two contributions, Christian et al. and Christian, examine the stability of the Fraser delta front from a geotechnical perspective. The delta slope off southern Roberts Bank, where there are electricity transmission cables and major port facilities, is only marginally stable under present conditions and could liquefy or fail catastrophically during an earthquake. Christian et al. discuss the possibility that clays at the base of the Holocene deltaic sequence are being leached by seaward-flowing groundwater, and suggest that this may be a factor contributing to instability at the delta front. This hypothesis is consistent with results of groundwater flow modelling, presented in the next paper by Ricketts. Near-surface groundwater is derived mainly from local precipitation and the Fraser River, whereas deeper flow originates on the Pleistocene uplands that border the delta on the north and east. A hydraulic gradient drives this deeper flow towards the delta front. In the last paper in the volume, Dunn presents and interprets baseline geochemical data for seafloor sediments in the southern Strait of Georgia, including the Fraser delta slope. Although none of the analyzed samples has unusually high concentrations of heavy metals, some anthropogenic signal is discernible in the data. The baseline geochemical data will provide a yardstick for monitoring any future metal pollution at the delta front.

REFERENCE

Turner, R.J.W., Clague, J.J., and Groulx, B.J.
1996: Geoscape Vancouver - living with our geological landscape; Geological Survey of Canada, Open File 3309, 1 sheet.

montrent que les ébranlements du sol découlant d'un séisme devraient présenter une configuration complexe, à cause en partie de l'hétérogénéité des dépôts deltaïques de l'Holocène et des différences dans leur épaisseur. Les ondes sismiques qui détruisent le plus les petits ouvrages (par ex. les maisons et les bâtiments peu élevés) seraient amplifiées dans les zones où les sédiments deltaïques sont minces, alors qu'elles seraient atténuées dans celles où ils sont épais. Les dépôts de sédiments deltaïques sont minces en bordure du delta et dans quelques autres secteurs où les sédiments pléistocènes s'observent à faible profondeur. Dans les deux articles suivants, Christian et al. ainsi que Christian se penchent sur la stabilité du front deltaïque du Fraser selon une perspective géotechnique. Le talus deltaïque au large de la partie sud du banc Roberts, où traversent des câbles de transport d'électricité et où se trouvent d'importantes installations portuaires, est au seuil de la stabilité dans les conditions actuelles et pourrait se liquéfier ou subir une rupture catastrophique dans l'éventualité d'un séisme. Christian et al. abordent la possibilité que les argiles à la base de la séquence deltaïque de l'Holocène soient lessivées par des eaux souterraines s'écoulant vers la mer et émettent l'hypothèse que ce soit un facteur de l'instabilité du front deltaïque. Cette hypothèse corrobore les résultats de la modélisation de l'écoulement des eaux souterraines présentés dans l'article suivant (Ricketts). Les eaux souterraines qui circulent près de la surface proviennent surtout des précipitations locales et du fleuve Fraser, tandis que celles plus en profondeur sont issues des hautes terres pléistocènes longeant les parties nord et est du delta. Un gradient hydraulique oriente cet écoulement plus profond vers le front deltaïque. Dans le dernier article du volume, Dunn présente et interprète des données géochimiques de base sur les sédiments qui tapissent le plancher océanique dans le secteur sud du détroit de Georgia, secteur dont fait partie le talus du delta du Fraser. Même si aucun échantillon analysé n'a une teneur inhabituellement élevée en métaux lourds, les données révèlent l'existence d'une certaine pollution anthropique. Ces données géochimiques de base serviront de témoins pour suivre l'évolution de toute pollution future par les métaux dans le secteur du front deltaïque.

RÉFÉRENCE

Turner, R.J.W., Clague, J.J., et Groulx, B.J.
1996: Géopanorama de Vancouver : comprendre les processus géologiques, Commission géologique du Canada, dossier public 3309, 1 feuillet.

Geological setting of the Fraser River delta

J.J. Clague[1]

Clague, J.J., 1998: Geological setting of the Fraser River delta; in Geology and Natural Hazards of the Fraser River Delta, British Columbia, (ed.) J.J. Clague, J.L. Luternauer, and D.C. Mosher; Geological Survey of Canada, Bulletin 525, p. 7–16.

Abstract: The Fraser River delta is located in a structural depression near the west margin of the North America plate. The depression is underlain by three different basements which are exposed in the Coast Mountains to the north, the Cascade Range to the southeast, and Vancouver Island to the west. Basement rocks in the vicinity of the Fraser delta are overlain by thick, Late Cretaceous and Tertiary clastic sediments that have been shed from adjacent rising mountains, and by Quaternary sediments deposited mainly during Pleistocene glacial stages. The distribution of the mountains and low-lying areas of south-coastal British Columbia is a product of Cenozoic plate convergence, subduction, and dextral transpression. This physiography, however, has been considerably modified by Pleistocene glacial erosion and deposition over the last two million years. There has been comparatively less landscape change during the last 10 000 years (postglacial, or Holocene, time), although the Fraser delta has formed during this time. The tectonic processes that have shaped the landscape continue to operate today and are responsible for slow uplift and subsidence, earthquakes, and recent volcanic activity.

Résumé : Les sédiments du delta du fleuve Fraser se sont déposés dans une dépression structurale près de la marge ouest de la plaque nord-américaine. Le fond de la dépression consiste en trois types de substratum qui affleurent dans la chaîne Côtière, au nord, la chaîne des Cascades, au sud-est, et l'île de Vancouver, à l'ouest. Dans la région du delta du Fraser, les roches du substratum sont recouvertes d'une grande épaisseur de sédiments clastiques du Crétacé tardif et du Tertiaire qui ont été transportés depuis les montagnes adjacentes en cours d'édification, ainsi que de sédiments quaternaires déposés principalement durant les étages glaciaires du Pléistocène. La configuration des montagnes et des basses terres qui caractérise la zone littorale de la Colombie-Britannique méridionale est le produit d'une succession de régimes tectoniques au Cénozoïque (convergence de plaques, subduction et transpression dextre). Cette physiographie a cependant été considérablement modifiée par l'érosion et la sédimentation glaciaires au cours des deux derniers millions d'années du Pléistocène. Le paysage a été comparativement moins modifié depuis les derniers 10 000 ans (époque postglaciaire ou Holocène), même si le delta du Fraser s'est formé pendant cet intervalle de temps. Les processus tectoniques qui ont modelé le paysage se poursuivent encore aujourd'hui et sont la cause de divers phénomènes (lent processus de soulèvement et de subsidence, séismes et activité volcanique récente).

[1] Geological Survey of Canada, 605 Robson Street, Vancouver, British Columbia V6B 5J3

SCOPE OF PAPER

This paper provides background information on the tectonic setting and geology of the Vancouver area, and thus sets the stage for other papers in this Bulletin. It includes sections on the morphology of the Fraser delta, the tectonic environment, bedrock geology, and Quaternary geology.

MORPHOLOGY OF FRASER DELTA

The Fraser River delta is bordered to the north and east by uplands underlain by Pleistocene sediments. The delta plain, which is mainly below 2 m elevation (mean sea-level datum), extends 15-23 km west and south from a narrow gap in the uplands at New Westminster and contacts the sea along a perimeter of about 40 km (Fig. 1). Twenty-seven kilometres of this perimeter, adjacent to the distributary channels of Fraser River, face onto the Strait of Georgia; the remainder border Boundary Bay to the south. These two sections are separated by Point Roberts peninsula, an upland and a former island underlain by Pleistocene sediments. Very gently sloping tidal flats and the fringing subtidal part of the delta plain extend up to 9 km from the dyked edge of the delta to the subtidal delta slope. The western delta slope is inclined 1-23° (average 2-3°) towards the marine basin of the Strait of Georgia and terminates at about 300 m water depth, 5-10 km seaward of the edge of the tidal flats. The southern delta slope is ill-defined; it has a gentler gradient than the western delta slope and terminates in much shallower water (about 30 m).

BEDROCK GEOLOGY AND TECTONIC HISTORY

Regional geology

The Vancouver region is underlain by three different basements (Monger and Journeay, 1994). One of the basements, exposed in the Coast Mountains to the north, consists mainly of Jurassic and Cretaceous granitic rocks and remnants of their volcanic cover. A second basement, in the Cascade Range southeast of Vancouver, comprises Devonian through Cretaceous volcanic and sedimentary rocks. A third basement, on Vancouver Island to the west, consists of Devonian through Jurassic volcanic and sedimentary rocks and lesser granitic rocks. The elevated areas where these rocks are exposed are separated by the topographically low Georgia Depression and Fraser Lowland, which are underlain by thick Late Cretaceous and Tertiary clastic sedimentary rocks and Quaternary sediments.

Local bedrock geology

The Vancouver area is founded on a succession of Upper Cretaceous and Tertiary, clastic sedimentary rocks, which, in turn, unconformably overlie Lower Cretaceous granitic rocks in the Coast Mountains to the north (Roddick, 1965; Mustard, 1994; Mustard and Rouse, 1994). Upper Cretaceous sedimentary rocks occur widely in the subsurface in the Vancouver area, but are exposed only in North and West Vancouver and on the north side of Stanley Park, where they dip 10-15° south to southeast (Fig. 2). The rocks were deposited in alluvial-fan and fluvial environments from sources in the Coast Mountains to the north and northeast (Mustard and Rouse, 1994).

Tertiary sedimentary rocks underlie the Fraser delta. They disconformably overlie Upper Cretaceous strata in Stanley Park and elsewhere below the city of Vancouver (Fig. 3; Mustard, 1994; Mustard and Rouse, 1994). The Tertiary succession is dominated by Paleocene-Eocene sandstone, conglomerate, and minor coal deposited in high-energy fluvial systems (Mustard and Rouse, 1994). These rocks are up to 2.5 km thick below the Fraser Lowland and up to 6 km thick in the Bellingham area of northwest Washington state. Oligocene rocks are limited to scattered volcanic flows, and dykes, sills, and small stocks scattered throughout the Fraser Lowland (Hamilton and Dostal, 1994; Mustard and Rouse, 1994). A Miocene sequence of sandstone and mudstone, which does not crop out but is encountered locally in drillholes below the Fraser delta, is mainly fluvial in origin, but some facies contain marine microfossils suggesting deposition in an estuarine setting (Rouse et al., 1990; Mustard and Rouse, 1994).

Sedimentation in the Vancouver area may have been influenced by dextral strike-slip faulting in the early Tertiary (Johnson, 1984). Compression in the late Eocene deformed most rocks in the Georgia Depression into northwest-plunging folds (Mustard, 1994). North-northwest-trending folds in early Tertiary sedimentary rocks in northwest Washington may have also formed at this time (Johnson, 1984). Cretaceous strata in the western part of the basin were displaced along southwest-directed thrust faults (England and Calon, 1991), whereas those at the east margin of the basin seem only to have been tilted. The presence of northeast-striking, Neogene faults can be inferred from gravity and seismic profiles that cross the Fraser Lowland, and are also expressed in the modern physiography.

Tectonic evolution

Prior to the Late Cretaceous, the areas now occupied by the southern Coast Mountains and the northern Cascade Range were marine basins. In the early Late Cretaceous, rocks now found in the southwestern Coast Mountains and on Vancouver Island collided with earlier accreted crust to the east. This caused crustal thickening and rapid uplift, centred in the southeastern Coast Mountains, and initiated deposition of clastic sediments in the Georgia Depression (Monger and Journeay, 1994). The collision was probably associated with convergence between the North America plate and various Pacific plates. Following collision, the margin of North America stepped westward to a position near the west coast of Vancouver Island; however, intense intraplate contraction and dextral transpression, accompanied by metamorphism and intrusion, continued until about 40 Ma near the former plate boundary in the southeastern Coast Mountains and Cascade Range.

There was a change in tectonic activity in southwestern British Columbia about 40 Ma. A regime dominated by dextral transpression was replaced by one in which a continental magmatic arc developed above an easterly dipping subduction zone (Fig. 1; Monger and Journeay, 1994). This change may be linked to replacement of the northward-moving oceanic Kula plate by the more orthogonally convergent Juan de Fuca plate (Engebretson et al., 1985).

Today, the western margin of the North America plate is overriding the oceanic Juan de Fuca plate at a rate of about 45 mm/a (Riddihough and Hyndman, 1991). The Juan de Fuca plate descends to the east from near the bottom of the continental slope off Vancouver Island, reaching a depth of about 70 km below Vancouver (Rogers and Horner, 1991).

There is abundant evidence that the south-coastal region is presently tectonically active. 1) Faults and folds are present in Neogene and Quaternary sediments that have been scraped off the descending oceanic plate at the continental margin (Davis and Hyndman, 1989; Hyndman et al., 1990). 2) Earthquakes are common within both the North America plate and the upper part of the subducting Juan de Fuca plate (Rogers,

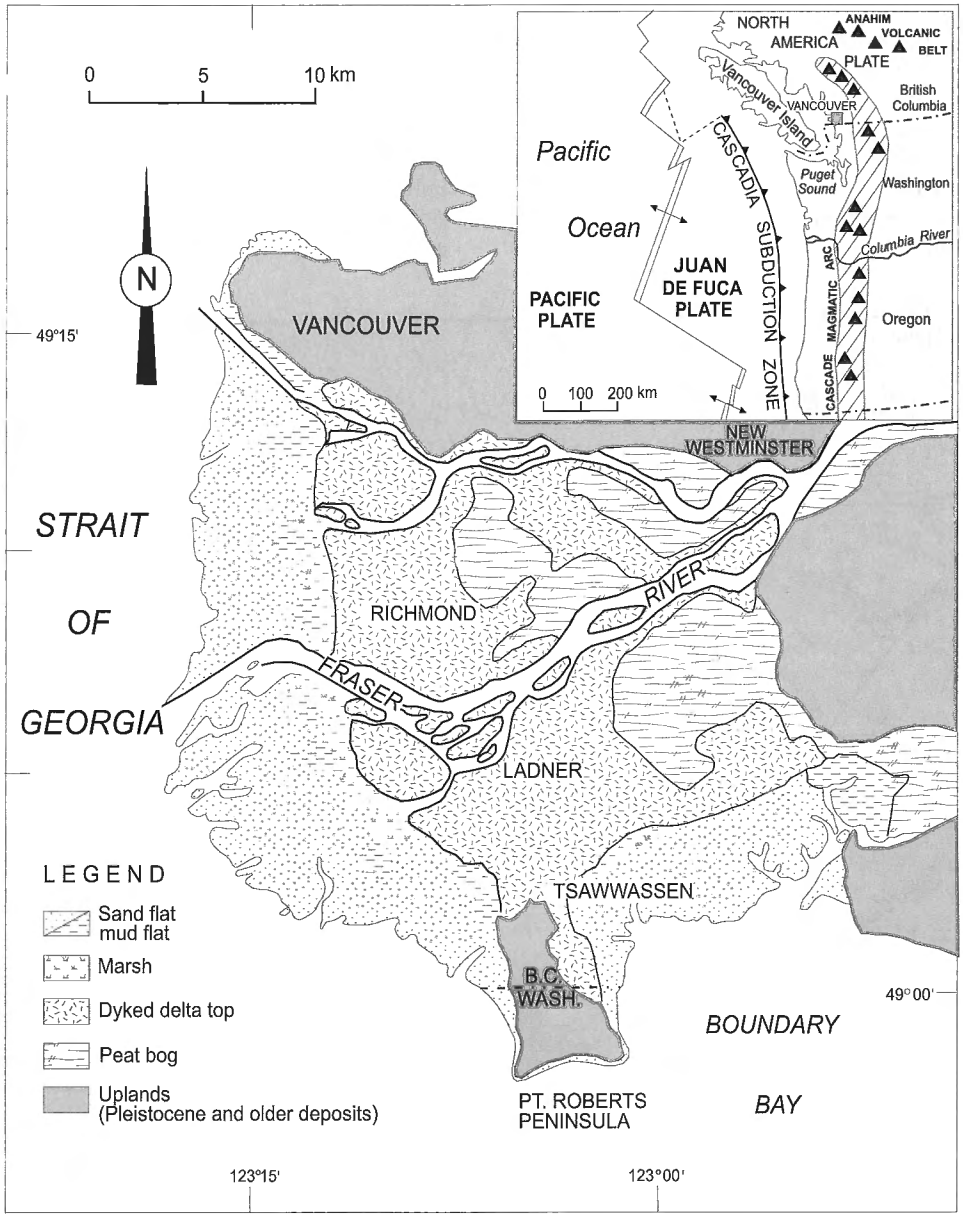

Figure 1. *Location and setting of the Fraser River delta. Inset: present-day major tectonic features of part of western North America, showing the Cascade magmatic arc (oblique ruled pattern) east of the subducting Juan de Fuca plate; triangles are Quaternary volcanoes.*

1994). 3) Vancouver Island, the Strait of Georgia, and the westernmost Coast Mountains are a forearc region of low crustal heat flow. This region is bordered on the east by an area of high heat flow, coincident with the Cascade magmatic arc (Lewis et al., 1992). 4) Geodetic data, long-term tidal data, and gravity measurements show that the margin of North America is deforming. The data show that the floor of the southern Strait of Georgia is subsiding at a rate of about 1 mm/a and parts of the Coast Mountains are rising at rates of 3-4 mm/a (Dragert, 1987; Holdahl et al., 1989). The strain probably is short-term and dominated by movements related to stress build-up across a locked subduction zone. Much of the stress may be released during episodic large earthquakes.

The present tectonic setting in this region is similar to that of the last 40 million years. This is shown by the longevity of the Cascade magmatic arc and by relative plate motions inferred from magnetic anomaly isochrons and seafloor topography (Engebretson et al., 1985; Atwater, 1989). However, the configuration of the plate margin probably has undergone some change during the last 20 million years. Brandon and Calderwood (1990) and Walcott (1993) documented such changes in the Olympic Mountains, where the Neogene accretionary complex is exposed on land. Walcott (1993) suggested that Neogene extension in Nevada, and consequent northwestward movement of northern California, caused shortening, crustal thickening, and uplift of rocks in the Olympic Peninsula as they were compressed against the salient of Vancouver Island. This may partly explain recent and continuing north-south compression in northwestern Washington state and southwestern British Columbia, indicated by earthquake first-motion studies and young crustal structures.

Ideas have been advanced to account for the present distribution of high and low areas in southwestern British Columbia. Phase changes in the descending oceanic slab (Rogers, 1983) have been invoked as a cause of forearc subsidence in the Georgia Depression. In addition, or alternatively, this subsidence may be related to lithospheric flexure, as Vancouver Island is tilted eastward by the subducting Juan de Fuca plate. Recently, Neogene subsidence of Queen Charlotte Basin, north of Vancouver Island, and synchronous uplift of the adjacent Coast Mountains have been attributed to simple shear on a lithosphere-scale, low-angle normal fault (Rohr and Currie, 1997). There is much evidence for late Cenozoic

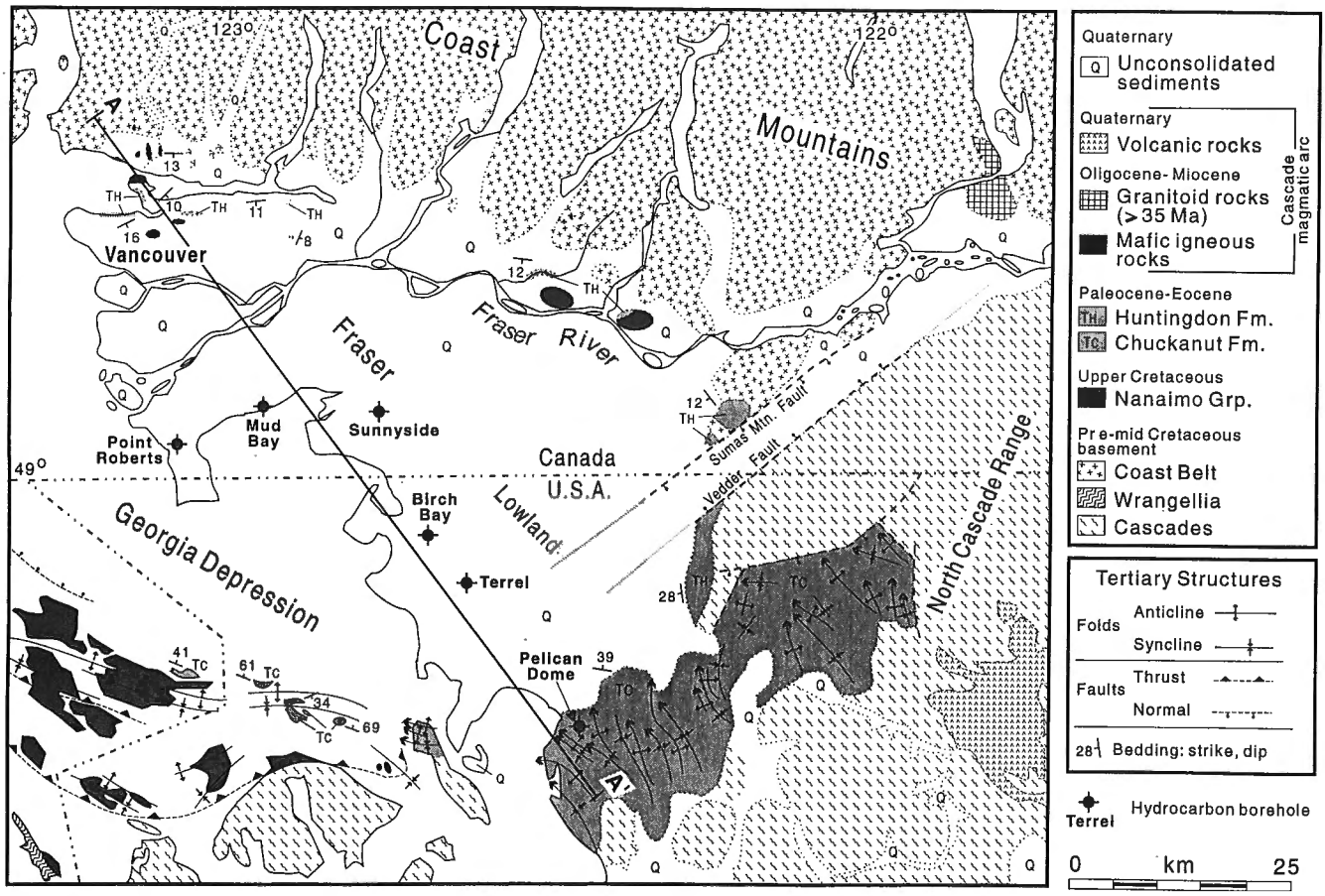

Figure 2. Simplified geological map of southwestern British Columbia and northwestern Washington state, showing the main physiographic elements and distribution of Late Cretaceous and younger rocks (Mustard et al., in press, Fig. 5). Also shown are the location of the cross-section of Figure 3 and oil and gas boreholes used to construct the cross-section.

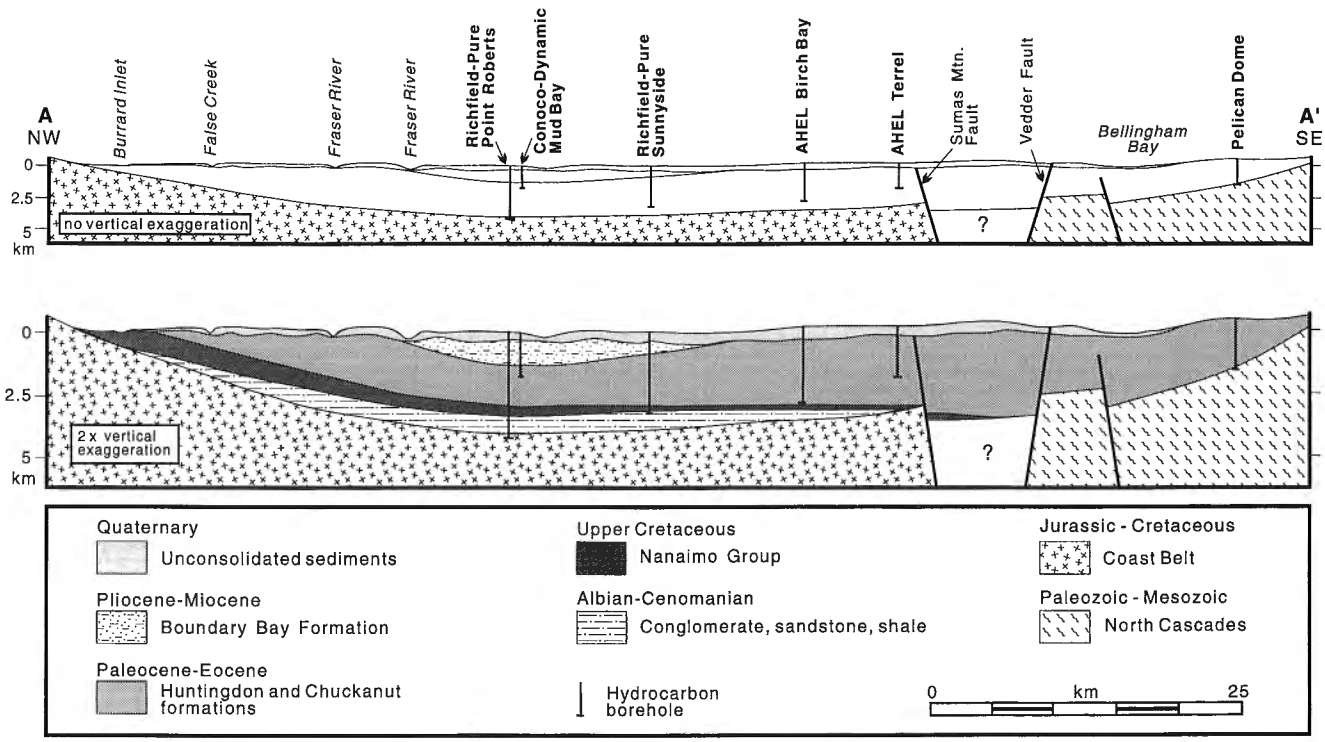

Figure 3. *Geological cross-section from Burrard Inlet in Vancouver to Bellingham, Washington (Mustard et al., in press, Fig. 6). The cross-section is based, in part, on data from oil and gas exploration wells located in Figure 2 and projected into the line of the section.*

uplift of the Coast Mountains north of about 52°N latitude. Originally flat-lying, late Miocene lavas rise to the west across the east flank of the Coast Mountains (Mathews, 1991). Parrish (1983), on the basis of a fission track study, paleogeographic arguments, and geomorphology, concluded that a large area of the southern Coast Mountains was uplifted more than 2 km over the last 10 million years, and he suggested that this might be due to thermal expansion related to high heat flow. The evidence for such large amounts of uplift south of 52°N latitude, however, is less compelling. Finally, basement features may influence physiography, as low areas coincide with the boundaries of the three basement complexes in this region.

QUATERNARY GEOLOGY

Pleistocene glaciation

South-coastal British Columbia is near the southwest margin of the former Cordilleran Ice Sheet, a system of confluent valley and piedmont glaciers, and mountain ice fields, that covered most of British Columbia and adjacent areas on several occasions during the Pleistocene Epoch (Clague, 1989). When the ice sheet was fully developed, its surface was above 2300 m elevation over much of southern British Columbia (Ryder et al., 1991). Glaciers from the southern Coast Mountains and the Vancouver Island Ranges coalesced over the Strait of Georgia to produce a great piedmont lobe that flowed south into the Puget Lowland of Washington state (Fig. 4; Armstrong et al., 1965; Waitt and Thorson, 1983). At the maximum of the last glaciation, about 15 ka BP, this piedmont lobe was about 2 km thick over the Vancouver area and terminated near Olympia, Washington, some 250 km to the south. (15 ka BP = 15 000 radiocarbon years before present. For simplicity, 'BP' is omitted from radiocarbon age designations in the remainder of the paper. It should be borne in mind, however, that radiocarbon and sidereal (calendric) ages are not the same because the amount of ^{14}C in the atmosphere has varied through time.)

The Cordilleran Ice Sheet did not fully develop during all Pleistocene glaciations. At the maxima of lesser glaciations, the major mountain systems supported networks of valley and piedmont glaciers, but large areas of the British Columbia interior remained ice free. Much of the Strait of Georgia and the Fraser Lowland may also have been ice-free at these times, although they were areas of proglacial sedimentation.

Glaciation has profoundly altered the landscape of the Vancouver area, just as it has the rest of British Columbia. Classic alpine landforms, including cirques, overdeepened valley heads, horns, and comb ridges abound in the higher parts of the southern Coast Mountains. Most mountain valleys have U-shaped cross-profiles, which also is a consequence of glacial erosion. Howe Sound and other fiords have been widened and deepened by glaciers, and the Strait of Georgia also bears evidence of glacial erosion.

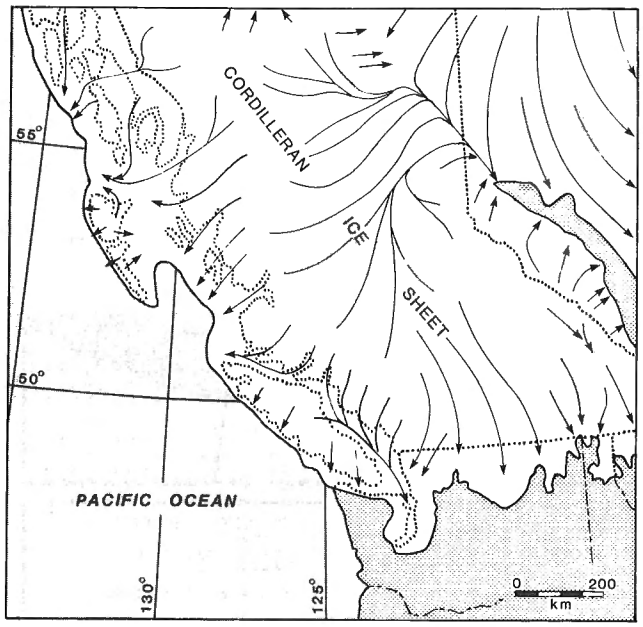

Figure 4. Cordilleran Ice Sheet at the maximum of the last glaciation (Clague, 1994, Fig. 2). Generalized flow pattern is shown by arrows.

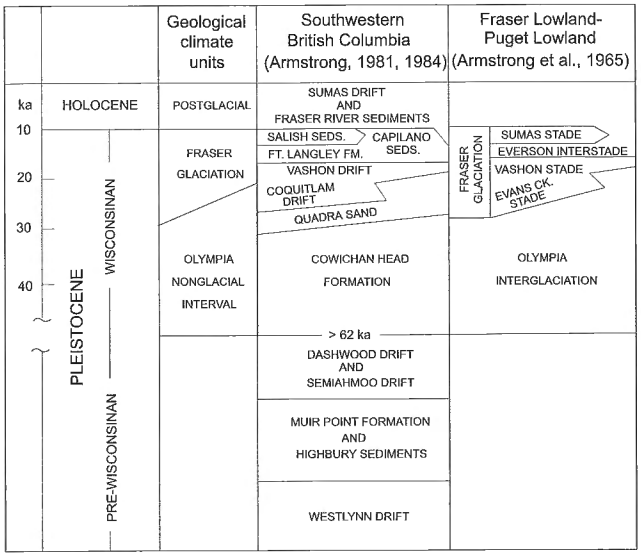

Figure 5. Subdivisions of Quaternary events and deposits in southwestern British Columbia (modified from Clague, 1994, Fig. 4).

Lowlands bordering the Fraser delta have been streamlined by south-flowing ice. Meltwater channels, raised deltas, kames, remnants of outwash plains, and relict shoreline and seafloor deposits also occur in these lowlands and collectively record the decay of the last glaciers at the end of the Pleistocene.

Quaternary stratigraphy and history

Quaternary sediments up to several hundred metres thick underlie parts of the Fraser Lowland, including the Fraser delta. In areas of thick sediments, there is little or no relation between the buried bedrock surface and the present land surface.

The Quaternary succession comprises sediments deposited during at least three glaciations and intervening interglaciations (Fig. 5; Armstrong et al., 1965; Armstrong and Clague, 1977; Armstrong, 1981, 1984; Hicock and Armstrong, 1981, 1983, 1985; Hicock and Rutter, 1986; Clague, 1994). Thick complex units of till and stratified drift were deposited beneath and at the margins of glaciers that advanced into the lowlands from adjacent mountains. These sediments were eroded both by the glaciers that flowed over them and by streams and the sea during subsequent interglaciations. As a consequence, the Quaternary succession is made up of packages of drift separated by unconformities. Significant bodies of interglacial sediment are of only local occurrence, and interglaciations are recorded throughout much of the Vancouver area by paleosols or unconformities.

Sediments older than the last glaciation are covered by younger deposits and have not been extensively studied. They crop out in sea cliffs, in natural exposures and gravel pits in mountain valleys, and on steep slopes within the Fraser Lowland. In addition, they have been encountered in many drillholes in the Vancouver area, including the Fraser delta. These older sediments have been grouped in the following units: 1) Middle or Early Pleistocene glacial deposits, assigned by Armstrong (1975) to the Westlynn Drift; 2) nonglacial fluvial, deltaic, and marine sediments of the Muir Point Formation and Highbury Sediments, deposited during the Sangamonian Stage about 125 ka (marine oxygen isotope stage 5e) (Hicock and Armstrong, 1983; Hicock, 1990); 3) drift of the penultimate glaciation (Early Wisconsinan; isotope stage 4?), termed Semiahmoo and Dashwood drifts (Fyles, 1963; Armstrong, 1975; Hicock and Armstrong, 1983); and 4) nonglacial fluvial, estuarine, and marine sediments of the Cowichan Head Formation, of Middle Wisconsinan age (isotope stage 3; ca. 25-65 ka) (Armstrong and Clague, 1977).

Fraser Glaciation

Most surface and near-surface sediments in the Vancouver area were deposited during the last (Late Wisconsinan or Fraser) glaciation which began about 25-30 ka and ended shortly after 11 ka (Clague, 1981). Early during the Fraser Glaciation, glaciers advanced down the Strait of Georgia and across the Fraser Lowland. The crust was depressed by the advancing glaciers, producing a broad, shallow moat or ramp on which glaciofluvial and glaciomarine sediments were deposited. These events are recorded in areas bordering the Strait of Georgia by a regionally extensive, diachronous body of sand and minor silt and gravel, termed Quadra Sand (Fig. 5; Clague, 1976, 1977, 1989). Quadra Sand was deposited in outwash plains, deltas, and subaqueous fans, and was progressively overridden and eroded by advancing glaciers (Fig. 6).

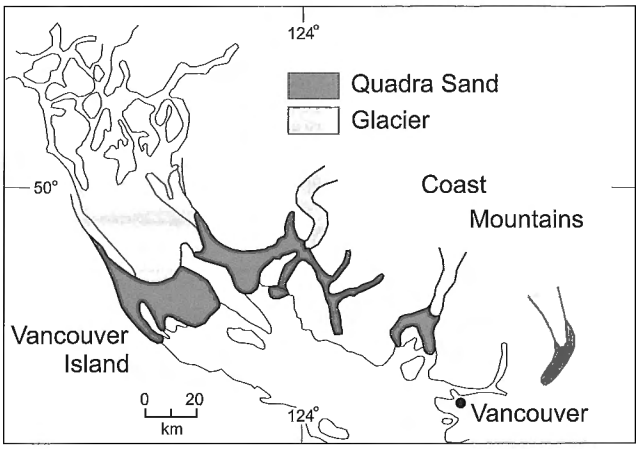

Figure 6. Origin of Quadra Sand (modified from Clague et al., 1987, Fig. 8). Aprons of sand formed in front of and along the margins of a glacier advancing down the Strait of Georgia during the Fraser Glaciation. The configuration shown in this figure dates to about 25 ka.

Evidence from several mountain valleys adjacent to the Fraser Lowland indicates that glaciers reached Vancouver after 25 ka. The deposits of this first incursion of ice into the Fraser Lowland during the Fraser Glaciation are termed Coquitlam Drift (Fig. 5), and include a wide variety of sediments of glaciolacustrine, glaciomarine, and glaciofluvial origin (Hicock and Armstrong, 1981). Glaciers subsequently retreated, and forests became re-established in the western Fraser Lowland and in the lower parts of some Coast Mountains valleys (Hicock et al., 1982; Hicock and Lian, 1995). The forests were overridden by readvancing ice about 17-18 ka during the climactic Vashon Stade of the Fraser Glaciation. Glaciolacustrine and glaciofluvial sediments and till of the Vashon Drift (Fig. 5) were deposited at this time, and a large piedmont glacier in the Strait of Georgia advanced to the south end of the Puget Lowland (Waitt and Thorson, 1983), achieving its maximum extent around 14.5 ka (Fig. 4; Mullineaux et al., 1965; Hicock and Armstrong, 1985).

Quadra Sand and Coquitlam Drift are generally capped by sandy Vashon till. In many places, however, till is absent and the erosion surface developed on Quadra Sand, Coquitlam Drift, and older Pleistocene units is directly overlain by late glacial and Holocene sediments.

About 13 ka, a calving embayment developed in northern Puget Sound and the Strait of Georgia, and glaciers rapidly retreated across isostatically depressed lowlands. Glaciomarine sediments of the Fort Langley Formation and Capilano Sediments (Fig. 5) were deposited during ice retreat (Amstrong, 1981). There are large raised deltas of sand and gravel (part of Capilano Sediments) at the mouths of mountain valleys just north of Vancouver; in some cases, gravel terraces extend up-valley considerable distances from the deltas (Armstrong, 1981). Thick deposits of stony silt and clay (Fort Langley Formation) in the central Fraser Lowland were deposited on the seafloor adjacent to a fluctuating ice margin. These sediments are complexly interbedded with diamicton, gravel, and sand, all deposited in close association with glacier ice.

A final, limited readvance of glaciers at the end of the Pleistocene left outwash and till (Sumas Drift, Fig. 5) on top of the Fort Langley Formation in the central Fraser Lowland. Sumas Drift has yielded radiocarbon ages ranging from about 11.5 to 11.1 ka (Clague, 1980, 1981; Saunders et al., 1987). Deglaciation of the Fraser Lowland was complete by shortly after 11 ka.

Holocene

The most significant change to the landscape of south-coastal British Columbia during the Holocene has been the growth of the Fraser River delta and floodplain (Fig. 7; Clague et al., 1983, 1991; Luternauer et al., 1994). The lowermost Fraser River occupies a valley that was covered by the sea and glacier ice at the end of the Pleistocene. The river rapidly prograded its floodplain to the west and began to construct a delta directly into the Strait of Georgia near New Westminster about 8-10 ka. The extensive delta plain west and southwest of New Westminster has been built since that time.

Waves and currents have eroded those parts of the coast backed by Quaternary sediments (Clague and Bornhold, 1980). Some shorelines may have retreated considerable distances during the middle and late Holocene as the sea rose relative to the land (see below).

Sea-level change and crustal deformation

The Cordilleran Ice Sheet depressed the crust of western Canada up to several hundred metres (Mathews et al., 1970; Clague, 1983). Gradual growth of glaciers during the early part of the Fraser Glaciation induced localized isostatic depression in the southern Coast Mountains. Lateral flow in the asthenosphere away from this area produced an outward-migrating forebulge which, together with eustatic effects, may have caused sea level to fall on the south coast. However, as glaciers expanded beyond the mountains, isostatically depressed areas grew in size, the coast began to subside, and the sea eventually rose above its present level relative to the land.

At the peak of the Fraser Glaciation, the entire region was isostatically depressed. The largest vertical displacements were in areas where ice was thickest, namely the Coast Mountains, Strait of Georgia, and Fraser Lowland (Clague, 1983). There were lesser displacements on western Vancouver Island and in northern Washington state.

Rapid deglaciation at the end of the Pleistocene was accompanied by isostatic uplift which, in this region, was greater than the coeval eustatic rise. Thus sea level fell as deglaciation progressed (Fig. 8; Mathews et al., 1970; Clague et al., 1982). Isostatic uplift occurred at different times during deglaciation due to diachronous retreat of the ice sheet (Clague, 1983). In general, areas that were deglaciated first rebounded earlier than those deglaciated later (Fig. 8). Uplift was accompanied by a fall in the level of the sea relative to the land. The pattern of sea-level change, however, was complicated

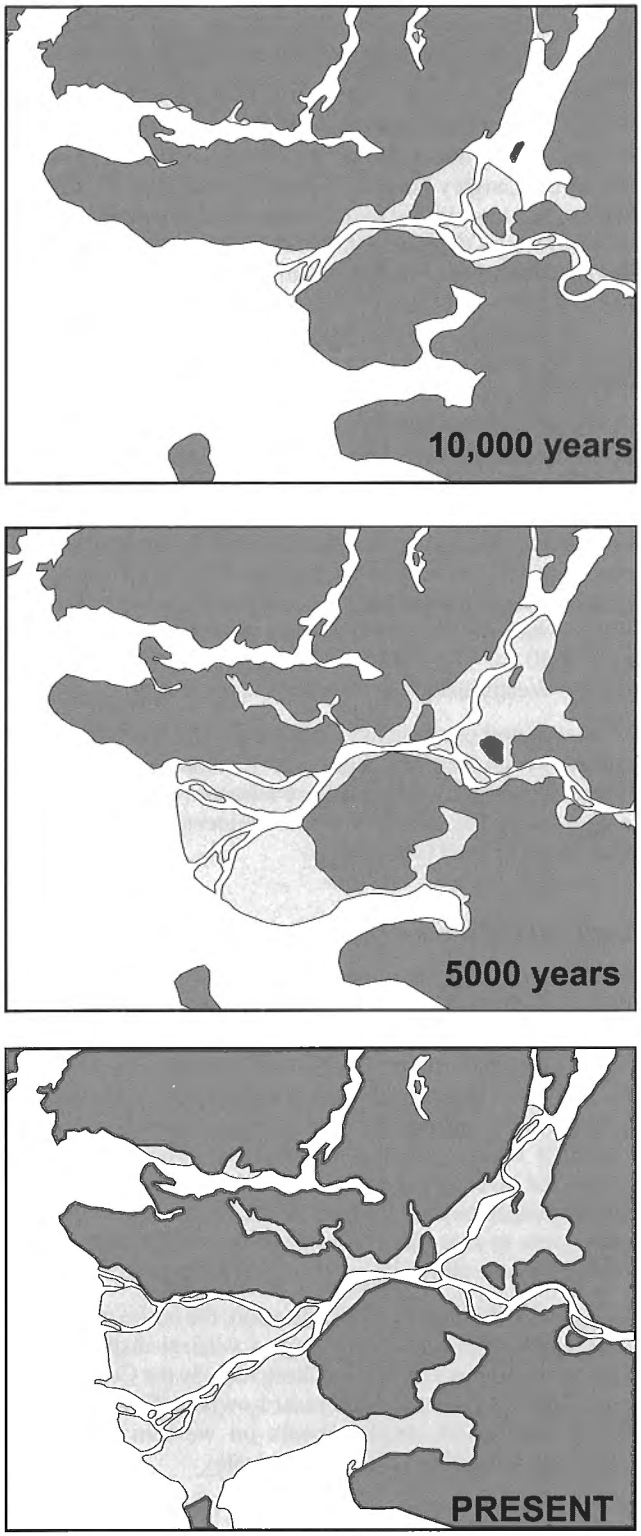

Figure 7. Holocene evolution of the Fraser River delta (modified from Clague et al., 1991, Fig. 9). Light shading – Holocene floodplains, fans, and peat bogs; dark shading – pre-Holocene landmass. Dates are approximate.

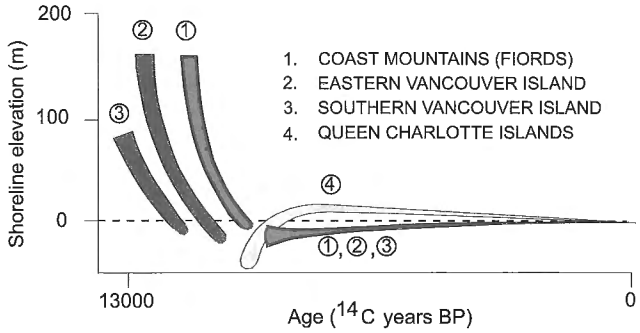

Figure 8. Generalized patterns of sea-level change on the British Columbia coast since the end of the last glaciation (modified from Clague, 1994, Fig. 11). Deglaciation and isostatic rebound occurred later in the southern Coast Mountains (Squamish) than on Vancouver Island (Victoria). Sea-level positions are approximate.

by variable rates and directions of eustatic changes, isostatic effects of local glacial stillstands and readvances, and possible displacements along faults.

The sea fell below its present level relative to the land between 12 and 10 ka (Mathews et al., 1970; Clague et al., 1982). Shortly thereafter, it reached its lowest Holocene level, which was at least 10 m below present sea level and perhaps much lower (Fig. 8). The subsequent rise in sea level during the middle and late Holocene may be largely eustatic, without compensatory isostatic uplift. During the last 2 ka, however, relative sea level has varied no more than 1 m, indicating that isostatic, tectonic, and residual isostatic effects have largely compensated for one another.

SUMMARY

The Fraser River delta is located near the western margin of the North America plate which is overriding the oceanic Juan de Fuca plate. The geology of this area is complex, the product of Cretaceous and Cenozoic convergence, subduction, and dextral transpression. Remnants of a thick fill of Upper Cretaceous, Tertiary, and Quaternary sediments are present in the Georgia Depression, the low-lying area bordered by the Coast, Cascade, and Insular Mountains. These sediments overlie three different basements which are exposed in the mountains surrounding the Georgia Depression.

Deposition of the Upper Cretaceous and Tertiary sediments occurred when oceanic rocks collided with ancestral North America in the vicinity of the present southeastern Coast Mountains. The collision elevated the Coast Mountains, and probably the Cascade and Insular Mountains. Continuing convergence and transpression during early Tertiary time deformed the molassic fill in the Georgia Depression, as well as the various basement rocks.

The tectonic regime of south-coastal British Columbia over the last 40 million years has been dominated by subduction of the Juan de Fuca plate and development of the Cascade

magmatic arc. Subduction and north-south compression, the latter perhaps related to impedance of northwest-moving crust by terranes in southwestern British Columbia, are the principal tectonic drivers in the region today. They are responsible for continuing uplift of the southern Coast Mountains, subsidence of the Georgia Depression, earthquakes, and recent volcanism.

Events of the Quaternary Period have left a strong imprint on south-coastal British Columbia. Of particular importance has been the repeated waxing and waning of the Cordilleran Ice Sheet. At its maximum, this ice sheet covered the entire south-coastal region and extended southward into Washington state.

Most of the Quaternary sediments in the lowlands around Vancouver were deposited near the margins of the glaciers that periodically advanced into, and retreated out of, the region. Heterogeneous sequences of Pleistocene proglacial, marine, fluvial, and deltaic sediments are bounded by unconformities and by nonglacial sediments similar to those accumulating in the area today.

The present landscape has been most strongly shaped by the last, or Fraser, glaciation (ca. 11-30 ka). During the climatic advance of the Fraser Glaciation, about 17-18 ka, lobes of the Cordilleran Ice Sheet advanced across the Fraser Lowland and down the Strait of Georgia. These glaciers eroded Pleistocene sediments and bedrock, and the Strait of Georgia and bordering lowlands attained something close to their present form at this time. During and following deglaciation, glaciomarine, marine, deltaic, and fluvial sediments were deposited on the glacially eroded landscape. The locus of much of the postglacial sedimentation has been the Strait of Georgia, fiords, and large lakes.

Most of the south coast experienced rapid isostatic uplift at the end of the last glaciation. Uplift decreased in a nonlinear fashion and, within a few thousand years, shorelines were lower than they are today. The subsequent, middle Holocene transgression may record a eustatic rise in sea level that was not fully compensated by residual isostatic uplift.

ACKNOWLEDGMENTS

P.S. Mustard prepared Figures 2 and 3, and granted me permission to reproduce them in this paper. T. Williams drafted some of the other illustrations. J.W.H. Monger and P.S. Mustard reviewed a draft of the paper and contributed to its improvement.

REFERENCES

Armstrong, J.E.
1975: Fraser Lowland - Canada; in The Last Glaciation, (ed). D.J. Easterbrook; IUGS-Unesco International Geological Correlation Program, Project 73-1-24, Guidebook for Field Conference, Western Washington University, Bellingham, p. 74-97.
1981: Post-Vashon Wisconsin glaciation, Fraser Lowland, British Columbia, Canada; Geological Survey of Canada, Bulletin 322, 34 p.

Armstrong, J.E. (cont.)
1984: Environmental and engineering applications of the surficial geology of the Fraser Lowland, British Columbia; Geological Survey of Canada, Paper 83-23, 54 p.

Armstrong, J.E. and Clague, J.J.
1977: Two major Wisconsin lithostratigraphic units in southwest British Columbia; Canadian Journal of Earth Sciences, v. 14, p. 1471-1480.

Armstrong, J.E., Crandell, D.R., Easterbrook, D.J., and Noble, J.B.
1965: Late Pleistocene stratigraphy and chronology in southwestern British Columbia and northwestern Washington; Geological Society of America Bulletin, v. 76, p. 321-330.

Atwater, T.
1989: Plate tectonic history of the northeast Pacific and western North America; in The Eastern Pacific Ocean and Hawaii, (ed.) E.L. Winterer, D.M. Hussong, and R.W. Decker; Geological Society of America, The Geology of North America, v. N, p. 21-72.

Brandon, M.T. and Calderwood, A.R.
1990: High-pressure metamorphism and uplift of the Olympic subduction complex; Geology, v. 18, p. 1252-1255.

Clague, J.J.
1976: Quadra Sand and its relation to the late Wisconsin glaciation of southwest British Columbia; Canadian Journal of Earth Sciences, v. 13, p. 803-815.
1977: Quadra Sand: a study of the late Pleistocene geology and geomorphic evolution of coastal southwest British Columbia; Geological Survey of Canada, Paper 77-17, 24 p.
1980: Late Quaternary geology and geochronology of British Columbia. Part 1: radiocarbon dates; Geological Survey of Canada, Paper 80-13, 28 p.
1981: Late Quaternary geology and geochronology of British Columbia. Part 2: summary and discussion of radiocarbon-dated Quaternary history; Geological Survey of Canada, Paper 80-35, 41 p.
1983: Glacio-isostatic effects of the Cordilleran Ice Sheet, British Columbia; in Shorelines and Isostasy, (ed.) D.E. Smith and A.G. Dawson; Academic Press, London, p. 321-343.
1989: Cordilleran Ice Sheet; in Chapter 1 of Quaternary Geology of Canada and Greenland, (ed.) R.J. Fulton; Geological Survey of Canada, Geology of Canada, no. 1 (also Geological Society of America, The Geology of North America, v. K-1), p. 40-42.
1994: Quaternary stratigraphy and history of south-coastal British Columbia; in Geology and Geological Hazards of the Vancouver Region, Southwestern British Columbia, (ed.) J.W.H. Monger; Geological Survey of Canada, Bulletin 481, p. 181-192.

Clague, J.J. and Bornhold, B.D.
1980: Morphology and littoral processes of the Pacific coast of Canada; in The Coastline of Canada, (ed.) S.B. McCann; Geological Survey of Canada, Paper 80-10, p. 339-380.

Clague, J.J., Evans, S.G., Fulton, R.J., Ryder, J.M., and Stryd, A.H.
1987: Quaternary geology of the southern Canadian Cordillera; International Union for Quaternary Research, XII International Congress, Ottawa, Excursion Guide Book A-18, 67 p.

Clague, J., Harper, J.R., Hebda, R.J., and Howes, D.E.
1982: Late Quaternary sea levels and crustal movements, coastal British Columbia; Canadian Journal of Earth Sciences, v. 19, p. 597-618.

Clague, J.J., Luternauer, J.L., and Hebda, R.J.
1983: Sedimentary environments and postglacial history of the Fraser Delta and lower Fraser Valley, British Columbia; Canadian Journal of Earth Sciences, v. 20, p. 1314-1326.

Clague, J.J., Luternauer, J.L., Pullan, S.E., and Hunter, J.A.
1991: Postglacial deltaic sediments, southern Fraser River delta, British Columbia; Canadian Journal of Earth Sciences, v. 28, p. 1386-1393.

Davis, E.E. and Hyndman, R.D.
1989: The structure and tectonic history of the northern Cascadia subduction zone: recent accretion and deformation; Geological Society of America Bulletin, v. 101, p. 1465-1480.

Dragert, H.
1987: The fall (and rise) of central Vancouver Island: 1930-1985; Canadian Journal of Earth Sciences, v. 24, p. 689-697.

Engebretson, D.C., Cox, A., and Gordon, R.G.
1985: Relative motions between oceanic and continental plates in the Pacific Basin; Geological Society of America, Special Paper 206, 59 p.

England, T.D.J. and Calon, T.J.
1991: The Cowichan fold and thrust system, Vancouver Island, southwestern British Columbia; Geological Society of America Bulletin, v. 103, p. 336-362.

Fyles, J.G.
1963: Surficial geology of Horne Lake and Parksville map areas, Vancouver Island, British Columbia; Geological Survey of Canada, Memoir 318, 142 p.

Hamilton, T.S. and Dostal, J.
1994: Middle Tertiary eruptive rocks in the Vancouver area; in Geology and Geological Hazards of the Vancouver Region, Southwestern British Columbia, (ed.) J.W.H. Monger; Geological Survey of Canada, Bulletin 481, p. 171-179.

Hicock, S.R.
1990: Late interglacial Muir Point Formation, Vancouver Island, British Columbia; Géographie physique et Quaternaire, v. 44, p. 337-340.

Hicock, S.R. and Armstrong, J.E.
1981: Coquitlam Drift: a pre-Vashon glacial formation in the Fraser Lowland, British Columbia; Canadian Journal of Earth Sciences, v. 18, p. 1443-1451.
1983: Four Pleistocene formations in southwest British Columbia: their implications for patterns of sedimentation of possible Sangamonian to early Wisconsinan age; Canadian Journal of Earth Sciences, v. 20, p. 1232-1247.
1985: Vashon Drift: definition of the formation in the Georgia Depression, southwest British Columbia; Canadian Journal of Earth Sciences, v. 22, p. 748-757.

Hicock, S.R. and Lian, O.B.
1995: The Sisters Creek Formation: Pleistocene sediments representing a nonglacial interval in southwestern British Columbia at about 18 ka; Canadian Journal of Earth Sciences, v. 32, p. 758-757.

Hicock, S.R. and Rutter, N.W.
1986: Pleistocene aminostratigraphy of the Georgia Depression, southwest British Columbia; Canadian Journal of Earth Sciences, v. 23, p. 383-392.

Hicock, S.R., Hebda, R.J., and Armstrong, J.E.
1982: Lag of Fraser glacial maximum in the Pacific Northwest: pollen and macrofossil evidence from western Fraser Lowland, British Columbia; Canadian Journal of Earth Sciences, v. 19, p. 2288-2296.

Holdahl, S.R., Faucher, F., and Dragert, H.
1989: Contemporary vertical crustal motion in the Pacific Northwest; in Slow Deformation and Transmission of Stress in the Earth, (ed.) H.C. Cohen and P. Vanicek; American Geophysical Union, IUGG Geophysical Monograph 49, v. 4, p. 17-29.

Hyndman, R.D., Yorath, C.J., Clowes, R.M., and Davis, E.E.
1990: The northern Cascadia subduction zone at Vancouver Island: seismic structure and tectonic history; Canadian Journal of Earth Sciences, v. 27, p. 313-329.

Johnson, S.Y.
1984: Stratigraphy, age, and paleogeography of the Eocene Chuckanut Formation, northwest Washington; Canadian Journal of Earth Sciences, v. 21, p. 92-106.

Lewis, T.J., Bentkowski, W.H., and Hyndman, R.D.
1992: Crustal temperatures near the Lithoprobe Southern Canadian Cordilleran Transect; Canadian Journal of Earth Sciences, v. 28, p. 195-208.

Luternauer, J.L., Barrie, J.V., Christian, H.A., Clague, J.J., Evoy, R.W., Hart, B.S., Hunter, J.A., Killeen, P.G., Kostaschuk, R.A., Mathewes, R.W., Monahan, P.A., Moslow, T.F., Mwenifumbo, C.J., Olynyk, H.W., Patterson, R.T., Pullan, S.E., Roberts, M.C., Robertson, P.K., Tarbotton, M.R., and Woeller, D.J.
1994: Fraser River delta: geology, geohazards and human impact; in Geology and Geological Hazards of the Vancouver Region, Southwestern British Columbia, (ed.) J.W.H. Monger; Geological Survey of Canada, Bulletin 481, p. 197-220.

Mathews, W.H.
1991: Physiographic evolution of the Canadian Cordillera; Chapter 11 in Geology of the Cordilleran Orogen in Canada, (ed.) H. Gabrielse and C.J. Yorath; Geological Survey of Canada, Geology of Canada, no. 4 (also Geological Society of America, The Geology of North America, v. G-2), p. 403-418.

Mathews, W.H., Fyles, J.G., and Nasmith, H.W.
1970: Postglacial crustal movements in southwestern British Columbia and adjacent Washington state; Canadian Journal of Earth Sciences, v. 7, p. 690-702.

Monger, J.W.H. and Journeay, J.M.
1994: Basement geology and tectonic evolution of the Vancouver region; in Geology and Geological Hazards of the Vancouver Region, Southwestern British Columbia, (ed.) J.W.H. Monger; Geological Survey of Canada, Bulletin 481, p. 3-25.

Mullineaux, D.R., Waldron, H.H., and Rubin, M.
1965: Stratigraphy and chronology of late interglacial and early Vashon glacial time in the Seattle area, Washington; United States Geological Survey, Bulletin 1194-O, 10 p.

Mustard, P.S.
1994: The Upper Cretaceous Nanaimo Group, Georgia Basin; in Geological and Geological Hazards of the Vancouver Region, Southwestern British Columbia, (ed.) J.W.H. Monger; Geological Survey of Canada, Bulletin 481, p. 27-95.

Mustard, P.S. and Rouse, G.E.
1994: Stratigraphy and evolution of Tertiary Georgia Basin and subjacent Upper Cretaceous sedimentary rocks, southwestern British Columbia and northwestern Washington State; in Geological and Geological Hazards of the Vancouver Region, Southwestern British Columbia, (ed.) J.W.H. Monger; Geological Survey of Canada, Bulletin 481, p. 97-169.

Mustard, P.S., Clague, J.J., Woodsworth, G.J., Hickson, C.J., Jackson, L.E., Jr., Luternauer, J.L., Monger, J.W.H., Ricketts, B.D., and Turner, R.J.W.
in press: Geology and geological hazards of the Greater Vancouver area in Urban Geology of Canadian Cities, (ed.) P.F. Karrow and O.L. White; Geological Association of Canada, Special Paper 42.

Parrish, R.R.
1983: Cenozoic thermal evolution and tectonics of the Coast Range of British Columbia: 1. fission track dating, apparent uplift rates, and patterns of uplift; Tectonics, v. 2, p. 601-631.

Riddihough, R.R. and Hyndman, R.D.
1991: Modern plate tectonic regime of the continental margin of western Canada; Chapter 13 in Geology of the Cordilleran Orogen in Canada, (ed.) H. Gabrielse and C.J. Yorath; Geological Survey of Canada, Geology of Canada, no. 4 (also Geological Society of America, The Geology of North America, v. G-2), p. 435-455.

Roddick, J.A.
1965: Vancouver North, Coquitlam, and Pitt Lake map areas, British Columbia, with special emphasis on the evolution of the plutonic rocks; Geological Survey of Canada, Memoir 335, 276 p.

Rogers, G.C.
1983: Seismotectonics of British Columbia; Ph.D. thesis, University of British Columbia, Vancouver, British Columbia, 247 p.
1994: Earthquakes in the Vancouver area; in Geological and Geological Hazards of the Vancouver Region, Southwestern British Columbia, (ed.) J.W.H. Monger; Geological Survey of Canada, Bulletin 481, p. 221-229.

Rogers, G.C. and Horner, R.B.
1991: An overview of western Canadian seismicity; in Neotectonics of North America, (ed.) D.B. Slemmons, E.R. Engdahl, M.D. Zoback, and D.D. Blackwell; Geological Society of America, Decade Map Volume 1, p. 69-76.

Rohr, K.M.M. and Currie, L.
1997: Queen Charlotte basin and Coast Mountains: paired belts of subsidence and uplift caused by a low-angle normal fault; Geology, v. 25, p. 819-822.

Rouse, G.E., Lesack, K.A., and White, J.M.
1990: Palynology of Cretaceous and Tertiary strata of Georgia Basin, southwestern British Columbia; in Current Research, Part F; Geological Survey of Canada, Paper 90-1F, p. 109-113.

Ryder, J.M., Fulton, R.J., and Clague, J.J.
1991: The Cordilleran Ice Sheet and the glacial geomorphology of southern and central British Columbia; Géographie physique et Quaternaire, v. 45, p. 365-377.

Saunders, I.R., Clague, J.J., and Roberts, M.C.
1987: Deglaciation of Chilliwack River valley, British Columbia; Canadian Journal of Earth Sciences, v. 24, p. 915-923.

Waitt, R.B., Jr. and Thorson, R.M.
1983: The Cordilleran ice sheet in Washington, Idaho, and Montana; in Late-Quaternary Environments of the United States, Volume 1, the Late Pleistocene, (ed.) S.C. Porter; University of Minnesota Press, Minneapolis, p. 53-70.

Walcott, R.
1993: Neogene tectonics and kinematics of western North America; Tectonics, v. 12, p. 326-333.

Earthquakes and earthquake hazard in the Vancouver area

G.C. Rogers[1]

Rogers, C.G., 1998: Earthquakes and earthquake hazard in the Vancouver area; in Geology and Natural Hazards of the Fraser River Delta, British Columbia, (ed.) J.J. Clague, J.L. Luternauer, and D.C. Mosher; Geological Survey of Canada, Bulletin 525, p. 17–25.

Abstract: Vancouver and the densely populated Lower Mainland region of southwest British Columbia are situated over an active subduction zone. The dynamic geological setting makes this region subject to frequent seismic activity and contributes to a higher risk of large damaging earthquakes than in other parts of Canada. Earthquakes that may present a hazard to the area occur in three distinct source regions: earthquakes within the continental crust, deeper earthquakes within the subducted oceanic plate, and earthquakes on the subduction boundary between the lithospheric plates. While Vancouver (incorporated in 1886) has not experienced a damaging earthquake in its short history, large earthquakes nearby have been strongly felt and there is paleoseismic evidence for very strong shaking in prehistoric time. Most of the region is placed in Seismic Zone 4 in the 1995 edition of the National Building Code of Canada. Ongoing microearthquake activity, and earthquakes strong enough to be felt occurring in most years, are reminders of the seismic hazard.

Résumé : Vancouver et le secteur densément peuplé des basses terres du Fraser (partie sud-ouest de la Colombie-Britannique) se trouvent sur le territoire d'une zone de subduction active. Ce contexte géologique, en raison de son dynamisme, fait en sorte que cette région est une cible fréquente de l'activité sismique et est, par rapport à l'ensemble du Canada, plus susceptible d'être secouée par de grands séismes dévastateurs. Les séismes qui représentent un danger pour la région sont de trois types : ceux ayant leur foyer dans la croûte continentale, ceux ayant leur foyer dans la plaque océanique en subduction et ceux engendrés à la limite de subduction entre les plaques lithosphériques. Vancouver, fondée en 1886, n'a pas connu de séismes destructeurs durant sa courte histoire; cependant, les séismes violents qui ont eu lieu dans les environs ont été fortement ressentis et il existe des indices paléosismiques de très fortes secousses à l'époque préhistorique. Presque toute la région se trouve dans la zone de risques sismiques 4 selon l'édition 1995 du Code national du bâtiment du Canada. Les microséismes, qui surviennent sur une base régulière, et les séismes suffisamment forts pour avoir été ressentis, dont la fréquence est presque annuelle, rappellent les risques qui guettent les habitants de cette région.

[1] Geological Survey of Canada, Pacific Geoscience Centre, P.O. Box 6000, Sidney, British Columbia V8L 4B2

INTRODUCTION

The southwest coast of British Columbia, including Vancouver and the densely populated Lower Mainland, is located in a dynamic geological setting (Fig. 1) that makes it one of the most seismically active regions of Canada. While Vancouver (incorporated in 1886) has not yet experienced a damaging earthquake, a number of large earthquakes have occurred close enough to have been strongly felt in the city and surrounding region (Table 1). Paleoseismic evidence on the Fraser delta, just to the south of Vancouver, confirms that large earthquakes have occurred in prehistoric time (Clague et al., 1992). Occurrences of earthquakes strong enough to be felt in most years (Fig. 2), and frequent microearthquake activity (Fig. 3), are reminders that the area is seismically active. This paper is adapted and updated from a previous version (Rogers, 1994).

Southwest British Columbia is situated over an active subduction zone, and thus is in an earthquake environment similar to the east coast of Japan, the south coast of Alaska, and most of the west coast of Central and South America. The oceanic Juan de Fuca and Explorer plates are being subducted in a northeast direction beneath the continental North American plate (Fig. 1). Earthquakes that may present a hazard to the area occur in three distinct source regions in this geological environment: continental crust earthquakes, deeper earthquakes within the subducted oceanic plate, and very large earthquakes on the subduction boundary between the lithospheric plates. The continental crust earthquakes, which are the most numerous, are driven by a compressive stress parallel to the continental margin, oriented north-northwest in southwest British Columbia, and include the damaging 1946 central Vancouver Island earthquake (magnitude (M) = 7.3) and the large prehistoric Seattle earthquake (M = 7+). The larger subcrustal earthquakes are caused by a tensional stress regime within the subducted plate in a depth range of 45 to 65 km and include damaging earthquakes in southern Puget Sound in 1949 (M = 7.0) and 1965 (M = 6.5). The subduction boundary, off the west coast of Vancouver Island, has not produced any earthquakes in historical time, but paleoseismic evidence shows that very large earthquakes have occurred at intervals of several centuries (Atwater, 1987; Adams, 1990;

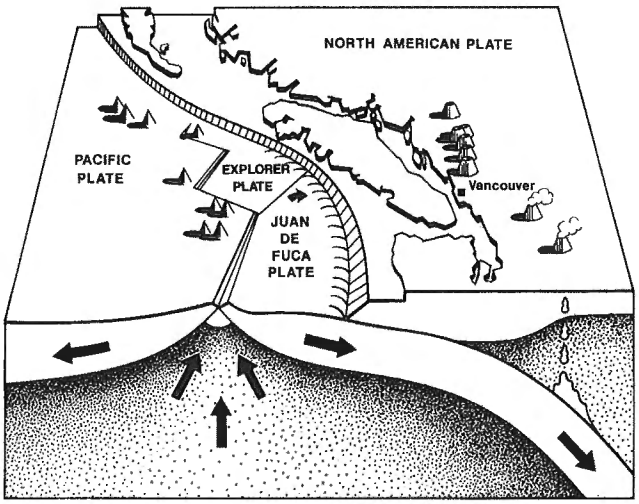

Figure 1. Cartoon of the tectonic setting of southwest British Columbia showing the oceanic Juan de Fuca and Explorer plates subducting beneath the continental North American plate.

Table 1. Some significant earthquakes felt in Vancouver.

Date	Location	Magnitude	Comment
~900	47.6°N 122.5°W	7+	Crustal earthquake; surface rupture and tsunami deposits in Puget Sound
1700/01/26	west of Vancouver Island	~9	Subduction earthquake; coastal native village destroyed and native houses on eastern Vancouver Island damaged
1864/10/29	48.75°N 123.25°W	~5.5	Probably deep, no reported aftershocks; felt strongly in the Lower Mainland
1872/12/15	48.5°N 121°W	~7.4	Crustal earthquake, many aftershocks; location uncertain, based on centre of isoseismals; felt strongly in the Lower Mainland
1909/01/11	48.7°N 122.8°W	~6.0	Probably deep, no reported aftershocks; felt strongly in the Lower Mainland
1918/12/06	49.4°N 126.2°W	~7.0	Crustal earthquake, many aftershocks; felt by most in the Lower Mainland; damage on the west coast of Vancouver Island
1920/01/24	48.6°N 123.0°W	~5.5	Probably deep, no reported aftershocks; felt strongly in the Lower Mainland
1946/06/23	49.8°N 125.3°W	7.3	Crustal earthquake, very few aftershocks; much damage on central Vancouver Island; felt strongly in the Lower Mainland
1949/04/13	47.1°N 123.0°W	~7.0	Depth 54 km; much damage at Seattle/Tacoma; felt by most in Lower Mainland
1965/04/29	47.4°N 122.3°W	6.5	Depth 63 km; much damage in Seattle; felt by most in the Lower Mainland
1975/11/30	49.2°N 123.6°W	4.9	Shallow, many aftershocks; felt by many in the Lower Mainland
1976/05/16	48.8°N 123.4°W	5.3	Depth 60 km, no aftershocks; felt by most in the Lower Mainland
1990/04/14	48.8°N 122.2°W	4.9	Shallow, many aftershocks; felt by many in the Lower Mainland
1996/05/03	47.8°N 121.9°W	5.0	Shallow, many aftershocks; felt by many in the Lower Mainland

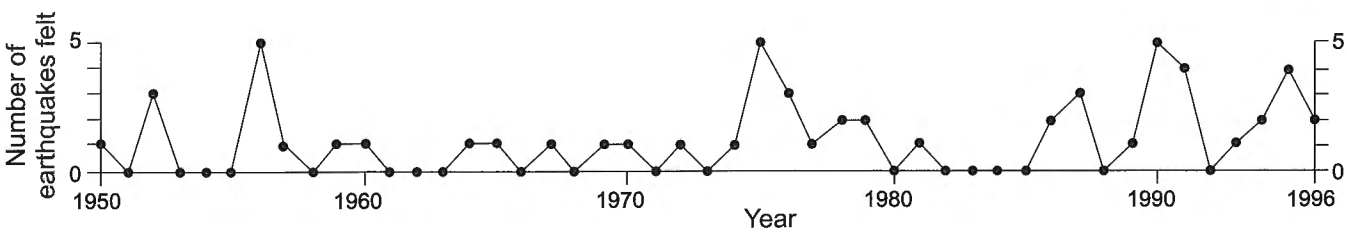

Figure 2. Number of earthquakes felt in Vancouver and the Lower Mainland from 1950 to 1996.

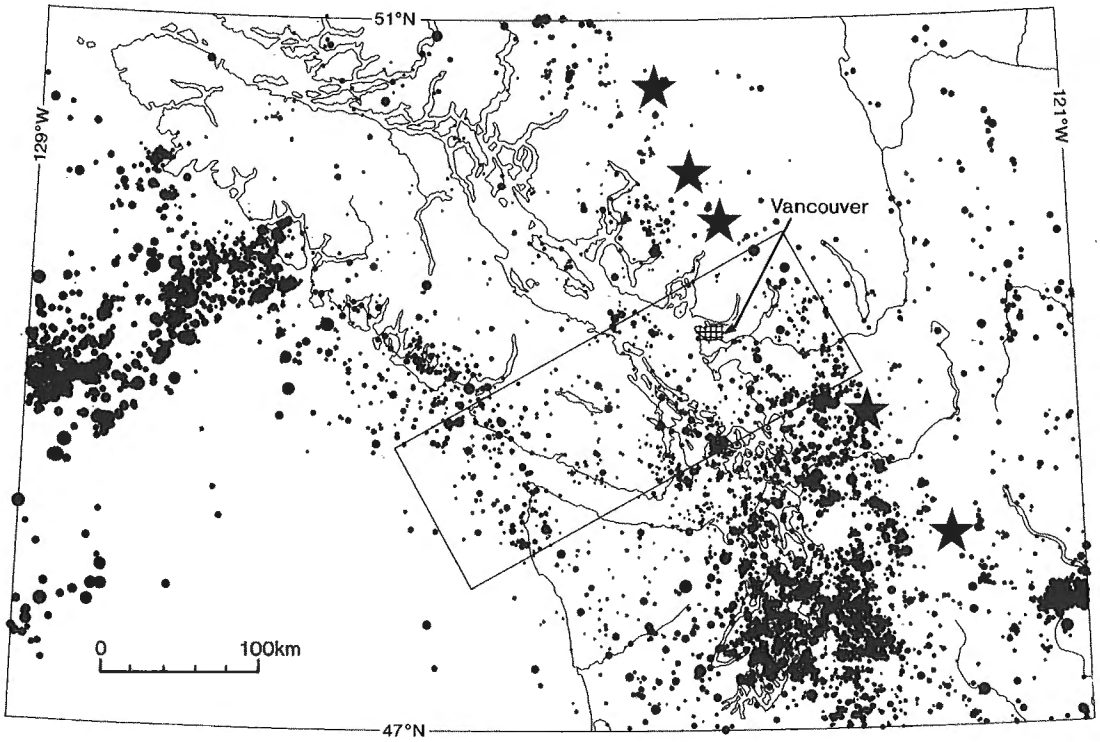

Figure 3. Seismicity in the Vancouver region from 1980 to 1991 inclusive. Dot size is proportional to magnitude. The smallest earthquakes plotted are magnitude 1, and the largest earthquake in this sample is an offshore event of magnitude 5.2. Earthquake data from the Geological Survey of Canada and the University of Washington have been combined to make this plot. The rectangle outlines the area used in the cross section in Figure 6. Stars are Quaternary volcanoes of the Cascade magmatic arc.

Atwater et al., 1995) with the most recent one on January 26, 1700 (Satake et al., 1996). Analysis of contemporary crustal deformation reveals that strain is accumulating for a future event (Dragert et al., 1994; Dragert and Hyndman, 1995). Subduction earthquakes are among the world's largest earthquakes. Those along the west coast of Vancouver Island are likely to exceed magnitude 8 (Rogers, 1988a; Hyndman et al., 1996), and to have effects comparable to the great Alaska earthquake (M = 9.2) in 1964 (Steinbrugge et al., 1967).

CRUSTAL EARTHQUAKES

About 90% of the small earthquakes in the Vancouver region occur in the continental crust of the North American plate. Forty years of earthquake monitoring in southwest British Columbia have revealed persistent crustal microearthquake activity (Milne et al., 1978; Rogers and Horner, 1991). Since the present seismograph network for monitoring the Lower Mainland and southern Vancouver Island regions was completed (early in 1983 for the Vancouver region), it has been possible to determine very accurately, to within a few kilometres horizontally and vertically, the locations of most small earthquakes (Fig. 3). Vancouver lies at the north end of an area of increased earthquake activity that extends to the south end of Puget Sound in Washington State. Concentrations of small events occur, but there are no distinct alignments of epicentres to convincingly mark the locations of active faults. However, the earthquakes die out to the east rather abruptly along a linear north-northwest trend, and this may be fault controlled. The vertical distribution of crustal earthquakes (Fig. 4) reveals that most occur at a considerable depth within the crust, on the order of 20 km, and it is perhaps not surprising that there appears to be little correlation with mapped surface faults. This depth range places most of the seismicity in this region deeper than earthquakes in California, where most earthquakes occur in the top 10 km of the crust and events deeper than 15 km are rare. The deeper source of most of the crustal events in southwest British Columbia means that there are fewer aftershocks than are typical for California earthquakes (e.g. Page, 1968).

The extra thickness of the brittle portion of the crust, where earthquakes can occur, is a direct result of the subduction environment. The subducting plate is colder than the asthenosphere into which it is descending and absorbs much of the heat flowing from the interior of the earth. The result is that there is very low heat flow through the upper crust and thus a thicker region of crust is in the temperature range that is cool enough to support brittle fracture in the form of earthquakes. Just to the west of the Quaternary volcanoes, which are part of the Cascade magmatic arc, the heat flow increases

markedly (Lewis, 1991), and a reduction in the seismicity rate appears to correlate with this change to a thinner section of brittle crust.

There have been three major crustal earthquakes affecting the region in historical time, in 1918 (M = 7) and 1946 (M = 7.3) on Vancouver Island (Rogers and Hasegawa, 1978; Cassidy et al., 1988), and in 1872 (M = 7.4) in northern Washington State (Malone and Bor, 1979) (Table 1, Fig. 5). The occurrence of these three large earthquakes is not obviously reflected in the pattern of earthquakes we see today. It should also be noted that all three of these larger earthquakes occurred away from the southern Strait of Georgia - Puget Sound lowland, which is the most intense region of seismicity reflected by the pattern of small earthquakes (Fig. 3).

There is a subset of the ongoing small earthquakes in the upper 10 km of the crust. Some of the larger of these very shallow events had long aftershock sequences, typical of California earthquakes, and may have occurred on faults that ruptured the surface. The November 30, 1975 earthquake (M = 4.9) in the central Strait of Georgia (Rogers, 1979); the April 13, 1990 Deming, Washington earthquake (M = 4.8), just south of Abbotsford (Qamar and Zollweg, 1990); and the May 3, 1996 Duvall, Washington earthquake (M = 5.0), just northeast of Seattle (Thomas et al., 1996) are three such events (Table 1, Fig. 5). There is also ample geological evidence that a large shallow prehistoric earthquake ruptured the surface in central Puget Sound, near Seattle, about 1100 years ago (Atwater and Moore, 1992; Bucknam et al., 1992). Such extremely shallow earthquakes are rare, but represent the greatest source of uncertainty in assigning seismic hazard in the region because their distribution and maximum magnitude are difficult to assess. Understanding the hazard they pose is important, however, because such near-surface sources can have very high accelerations in close proximity to them.

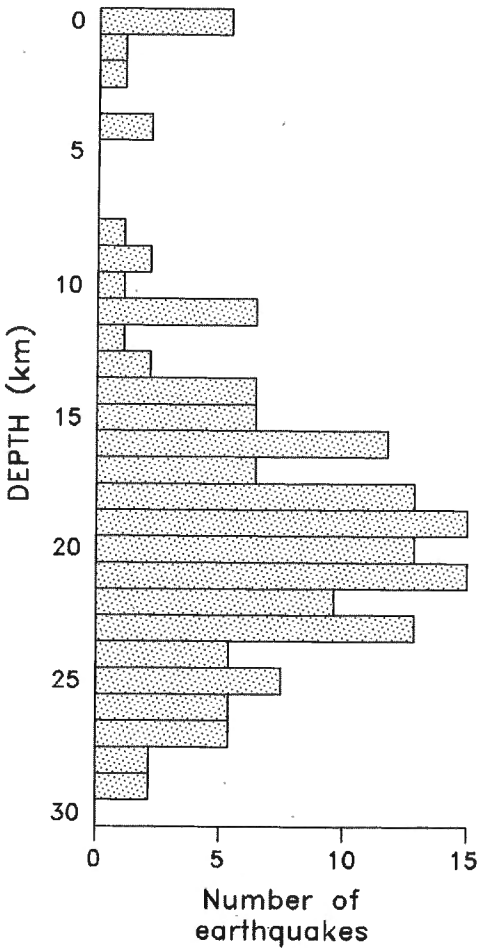

Figure 4. Depth distribution of a three-year sample of crustal earthquakes in the southern Strait of Georgia region, from 48°N to 49°N and from 122°W to 124°W.

Small crustal earthquakes in this region are a mixture of strike-slip and thrust events with a dominant north-northwest orientation of the principal stress axes (Mulder and Rogers, 1993) suggesting north-northwest compression. This is a different orientation from the apparent north-south compression observed just to the south in Washington State (Ma et al., 1996). It appears as if the compressive crustal stress is oriented parallel to the continental margin (Wang et al., 1995). This does not conflict with the observed crustal shortening (Savage et al., 1991; Dragert et al., 1994) perpendicular to the margin in the direction of the subducting plate, as the crustal deformation represents a change in stress, whereas the focal mechanisms of the earthquakes reflect the regional ambient stress. The origin of this stress regime has not yet been satisfactorily explained, but it may be a result of oblique subduction along most of the Cascadia margin (Rogers, 1979; Wang, 1996), compression from south of the subduction zone (Sbar, 1982), or rotation of a crustal block (Walcott, 1993).

SUBCRUSTAL EARTHQUAKES

Subcrustal earthquakes in this context refer to earthquakes within the subducting Juan de Fuca plate. This is the best quantified earthquake source region. Ongoing microearthquake activity delineates the subducted plate precisely (Fig. 6). The maximum earthquake size is constrained to about the magnitude 7 range because the brittle part of the young subducting plate is very thin, less than 10 km, and thus places an upper limit to rupture area for typical rupture lengths of less than 100 km. Because of their depth, these earthquakes rarely have aftershocks.

The earthquakes within the descending Juan de Fuca plate are concentrated in two regions. The first is in the vicinity of the west coast of Vancouver Island where the plate goes from horizontal below the ocean, to a shallow dip of 10 to 20° beneath Vancouver Island. The band of seismicity straddling the coast in Figure 3 represents this seismicity. The next concentration is below the Strait of Georgia and Puget Sound, where the plate bends further to a steeper dip of about 30° (Fig. 7). This is probably the region where the buoyancy of the subducting plate changes from positive to negative, because of phase changes in the rocks of the oceanic crust (Pennington, 1983; Rogers, 1983b). It is marked by a band of

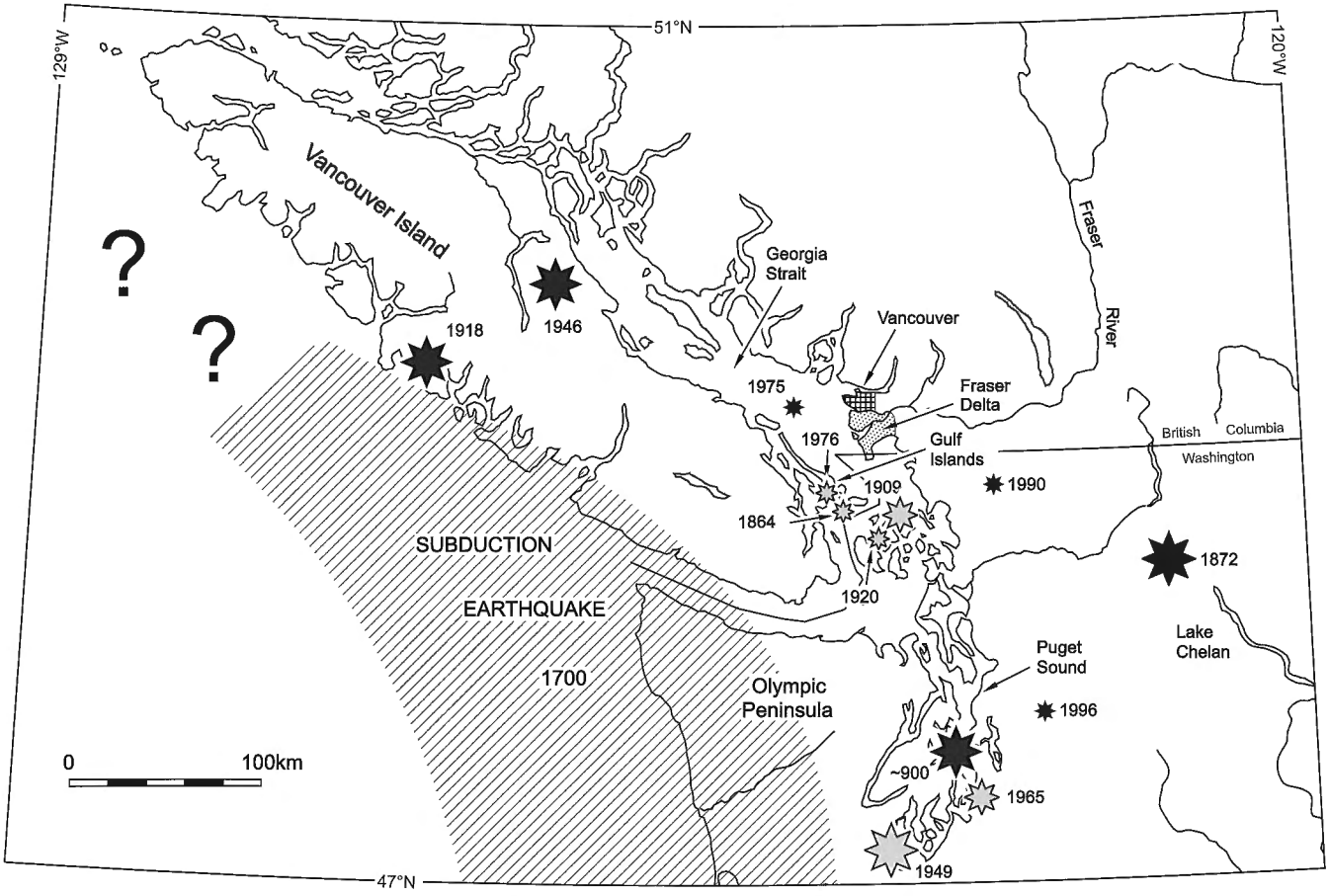

Figure 5. Significant earthquakes felt in Vancouver (see Table 1). Increasing size of symbols indicates magnitudes of 5 and greater, 6 and greater, and 7 and greater. Solid symbols are crustal earthquakes; shaded symbols are subcrustal events. Shaded area along the west coast of Vancouver Island is the maximum potential rupture surface for a subduction earthquake (adapted from Dragert et al., 1994); this surface may not extend as far east as shown.

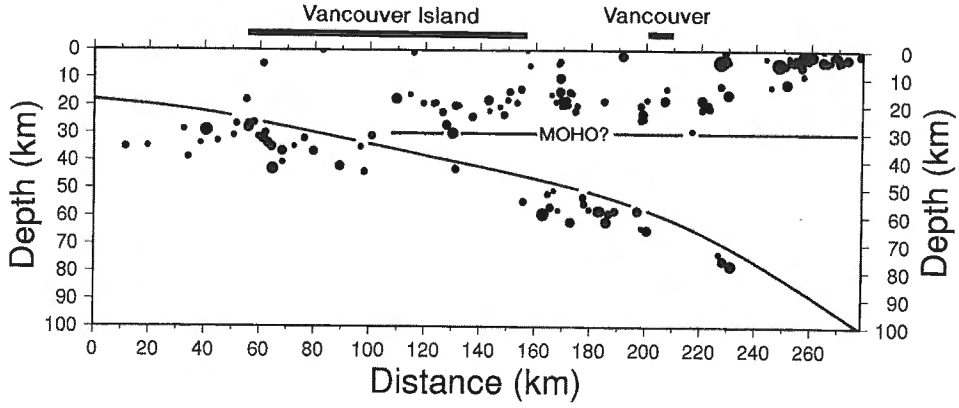

Figure 6. Earthquakes in the 100 km wide corridor shown in Figure 3, projected onto a cross-section through Vancouver. Only earthquakes with epicentral uncertainties of less than 3 km in depth are shown.

seismicity, mainly in the 45 to 65 km depth range, beneath the Strait of Georgia and Puget Sound (Fig. 6). This seismicity is also concentrated in a north-south sense between 47°N and 49.5°N, but continues at a much lower rate both to the north and to the south. The arching of the subducting plate in this region to accommodate the bend in the coast line (Rogers, 1983a; Crosson and Owens, 1987) is the likely cause of this north-south concentration.

The extent of the band of small subcrustal earthquakes defines a region where several significant earthquakes occurred before the installation of a modern seismograph network (Table 1, Fig. 5). Earthquakes in 1949 and 1965 at the south end of Puget Sound caused considerable damage. Earthquakes near the damage threshold (in the magnitude 5 to 6 range) occurred in the Gulf Islands/San Juan Islands region in 1864, 1909, 1920, and 1976. The larger subcrustal earthquakes are consistent with a down-dip tensional regime in the subducting plate (Rogers, 1983a), but smaller the earthquakes show a more complex stress regime (Ma et al., 1996).

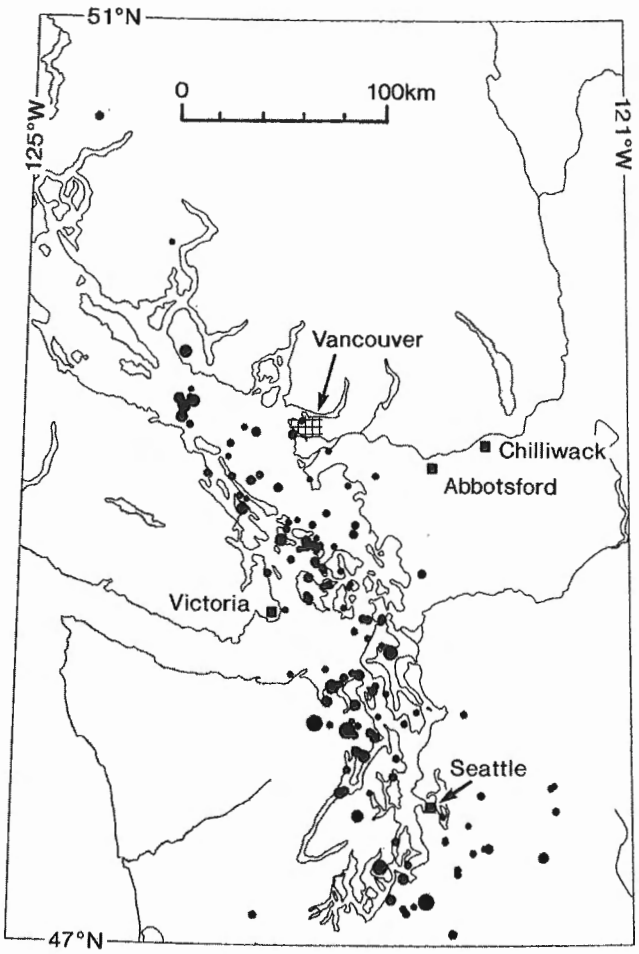

Figure 7. *Subcrustal earthquakes with depths of 50 km and greater (a subset of earthquakes shown in Fig. 3). The smallest earthquake plotted is magnitude 1 and the largest in the sample is magnitude 3.9.*

SUBDUCTION EARTHQUAKES

The potential for large earthquakes on the subduction interface at the Cascadia subduction zone has been discussed in the scientific literature for only about a decade (Heaton and Kanamori, 1984; Heaton and Hartzell, 1987; Rogers, 1988a), but the wide-ranging evidence for their occurrence has convinced most of the geoscience community that the hazard is real (Rogers, 1988b; Heaton, 1990). A number of different lines of evidence suggest that great subduction earthquakes have occurred in the past. In tidal marshes and estuaries on the west coast of Vancouver Island and along the outer coast of the United States, repeating sediment sequences of peat overlain by mud, often with a sand layer at the interface, are interpreted to result from abrupt subsidence events and tsunamis accompanying great earthquakes (Atwater, 1987; Clague and Bobrowsky, 1994; Atwater et al. 1995). Layers of coarse-grained sediments in deep-sea mud deposits are ascribed to turbidity currents originating from periodic strong shaking of the continental margin (Adams, 1990). Dating, using growth rings of trees killed suddenly by salt-water influx due to coastal subsidence, places the last great earthquake at about 1700 A.D. (Atwater and Yamaguchi, 1991), and back-calculating from the time of arrival of a tsunami in Japan gives the time of the great earthquake as 9 p.m., January 26, 1700 (Satake et al., 1996). This date is consistent with the oral traditions of the native peoples of the west coast of Vancouver Island who describe an earthquake and tsunami that came at night and destroyed the winter village of the Pachena Bay people (Arima et al., 1991). It is also consistent with a legend in the oral history of the Cowichan people of southern Vancouver Island which tells of a great earthquake that came at night and threw down houses and caused landslides in the days before the white man (Maud, 1978).

Elastic strain accumulating in the region has also been measured. Contemporary surface tilting and crustal shortening in a direction parallel to the movement of the subducting plate have been observed on Vancouver Island and the Olympic Peninsula. The rates are too great to be sustained over a long interval. A locked subduction zone that periodically releases the strain in huge earthquakes explains the observed pattern (Savage et al., 1991; Dragert et al., 1994).

Subduction earthquakes are rare but can be quantified. The magnitudes are large, magnitude 8 or greater, but constraints on potential ground motion can be made because the position of the plate interface is known from microearthquake activity (Rogers et al., 1990), and seismic reflection and refraction studies (Drew and Clowes, 1990; Hyndman et al., 1990). Information on rupture behaviour from other subduction zones can be used to obtain a realistic range of estimates of ground motion at the surface. The most important parameter for hazard estimates is the down-dip extent of the seismogenic zone. The maximum down-dip dimension of this potential rupture surface is determined by the length of the contact between the subducting plate and the brittle portion of the overlying continental crust, which is revealed by the depth of crustal earthquake activity (Fig. 4, 6). Temperature is probably the most important factor affecting the depth of brittle behaviour (Hyndman and Wang, 1993). Recent analysis

of crustal deformation on Vancouver Island (Dragert et al., 1994) places the currently locked portion of this zone mainly beneath the continental shelf, west of Vancouver Island (Fig. 5). The eastern limit of the down-dip end of the potential rupture coincides at the surface roughly with the west coast of Vancouver Island, at least 150 km west of Vancouver (Hyndman et al., 1996). The Explorer plate subduction regime (Fig. 1), about 250 km from Vancouver, is very poorly understood at present.

SEISMIC HAZARD

In the National Building Code of Canada (NBCC), seismic hazard is defined as the level of horizontal ground shaking (acceleration or velocity) which has a 10% probability of being exceeded over a 50 year period (a probability of 0.0021 per annum). Canada is divided into seven seismic hazard zones (0 and 1-6) based on the ground motion at this probability level (e.g. Heidebrecht et al., 1983). For each region there are two zoning values: Z_a, for small structures sensitive to damaging ground motions near 5 Hz; and Z_v, for large and high-rise structures sensitive to damaging ground motions near 1 Hz. For most of greater Vancouver and the Lower Mainland the 1995 NBCC zone values are $Z_a = 4$ and $Z_v = 4$, while points farther east than Chilliwack in the Fraser valley drop to zones $Z_a = 3$ and $Z_v = 3$. There is a small region immediately adjacent to the International Boundary that technically meets the criteria of $Z_a = 5$ (Weichert, 1994). The NBCC is a guide only; it is up to each community to adopt a seismic design value on the basis of municipal boundaries, relative economic considerations, and an understanding of the statistical nature of seismic hazard calculations.

The NBCC ground-motion levels are calculated for firm soil. Soils can amplify or attenuate earthquake shaking in selected frequency ranges that are defined by thicknesses and seismic velocities of the soil layers. Soil amplification is dealt with in the NBCC by using a multiplier to be applied to buildings constructed on soft soil deposits. The Fraser delta and alluvial deposits along the Fraser River are locales in the greater Vancouver area where soil amplification may be a concern for high-rise buildings (e.g. Sy et al., 1991). Amplifications at some sites may exceed the nominal multiplier in the NBCC. This is particularly likely near the edges of the delta where soil depths can be in the right range to allow resonances to occur in the frequency range of typical buildings. (Rogers et al., 1998). Amplification in the frequency range of very tall buildings or very large structures would be expected in the deepest part of the delta (Harris et al., 1995, 1998). At sites on the delta where strong ground motion has been recorded, there has been no amplification, or only modest attenuation, in higher frequency ranges that can damage typical one- or two-storey structures, the most common type of building on the Fraser delta (Rogers et al., 1998).

Besides shaking, soil failure by landslides or liquefaction also contributes to the seismic hazard. Many examples of soil failure occurred on Vancouver Island and around the Strait of Georgia during the 1946 M = 7.3 earthquake on central Vancouver Island (Mathews, 1979; Rogers, 1980), but Vancouver was just outside the affected region. Some steep slopes in the greater Vancouver region are prone to landslides (e.g. Eisbacher and Clague, 1981), and earthquake shaking may trigger landslides in these areas. Liquefaction deposits have been found on the Fraser delta (Clague et al., 1992), indicating the liquefaction susceptibility of some of the water-saturated sand deposits, and providing direct evidence that strong shaking from large earthquakes occurred in the past.

The 1995 NBCC does not consider a subduction earthquake. However, because the location of the subduction fault is known, ground motions can be estimated. The 150 km distance between Vancouver and the subduction fault means that seismic waves from subduction earthquakes will be significantly attenuated by the time they reach Vancouver. Research for the year 2000 NBCC demonstrates that ground motion from subduction earthquakes in the Vancouver region, while significant, will be less than ground-motion levels from probabilistic analysis of historical earthquakes which are used in the present code and proposed for the year 2000 NBCC (Adams et al., 1996). The main differences in hazard from great subduction earthquakes are the long duration of strong shaking associated with large rupture surfaces, and the large area of shaking which affects many communities. The long duration can adversely affect certain types of structures, and the liquefaction potential of saturated sands.

Good examples of the effects that a subduction earthquake produces are seen in the damage caused in the city of Anchorage by the great 1964 Alaska earthquake (M = 9.2) (Steinbrugge et al., 1967). Anchorage is about the same distance from the down-dip end of the Alaska seismogenic zone as Vancouver is from the Cascadia seismogenic zone. The estimated three minutes of strong shaking during the Alaska earthquake damaged numerous large structures. However, single-family wood-frame dwellings and other similar small wood-frame structures performed excellently as a class of construction, where not located in areas subject to soil failure.

SUMMARY

The dynamic geological setting of Vancouver and the Lower Mainland makes this region subject to frequent seismic activity and contributes to a higher risk of large damaging earthquakes than other parts of Canada. Earthquakes that may present a hazard to the area occur in three distinct source regions: earthquakes within the continental crust, deeper earthquakes within the subducted Juan de Fuca plate, and huge earthquakes on the subduction boundary between the two plates, about 150 km west of Vancouver. While Vancouver has not experienced a damaging earthquake in its short history, large earthquakes nearby have been strongly felt and there is paleoseismic evidence for very strong shaking in prehistoric time. Most of the region is placed in Seismic Zone 4 in the 1995 edition of the National Building Code of Canada. Ongoing microearthquake activity, and earthquakes strong enough to be felt occurring in most years, are reminders of the seismic hazard.

ACKNOWLEDGMENTS

Chris Spindler assisted with data files and computer plotting. Richard Franklin prepared the diagrams. Bob Horner has had the responsibility for earthquake location in this region since 1986. Precise locations near the International Boundary and plots of data south of the border are made possible by regular data exchange with the University of Washington. Reviews by Dieter Weichert and John Cassidy improved the paper.

REFERENCES

Adams, J.
1990: Cascadia subduction zone: evidence from turbidites off the Oregon-Washington margin; Tectonics, v. 9, p. 569-583.

Adams, J., Weichert, D.H., Halchuck, S., and Basham, P.W.
1996: Trial seismic hazard maps of Canada - 1995: final values for selected Canadian cities; Geological Survey of Canada, Open File 3283, 97 p.

Arima, E.Y., St. Clair, D., Clamhouse, L., Edgar, J., Jones, C., and Thomas, J.
1991: Between Ports Alberni and Renfrew: notes on west coast peoples; Canadian Museum of Civilization, Canadian Ethnology Service, Mercury Series Paper 121, 323 p.

Atwater, B.F.
1987: Evidence for great Holocene earthquakes along the outer coast of Washington State; Science, v. 236, p. 942-944.

Atwater, B.F. and Moore, A.L.
1992: A tsunami about 1000 years ago in Puget Sound, Washington; Science, v. 258, p. 1614-1617.

Atwater, B.F., and Yamaguchi, D.K.
1991: Sudden, probably coseismic submergence of Holocene trees and grass in coastal Washington State; Geology, v. 16, p. 706-709.

Atwater, B.F., Nelson, A.R., Clague, J.J., Carver, G.A., Yamaguchi, D.K., Bobrowsky, P.T., Bourgeois, J., Darienzo, M.E., Grant, W.C., Hemphill-Haley, E., Kelsey, H.M., Jacoby, G.C., Nishenko, S.P., Palmer, S.P., Peterson, C.D., and Reinhart, M.A.
1995: Summary of coastal geologic evidence for past great earthquakes on the Cascadia subduction zone; Earthquake Spectra, v. 11, p. 1-18.

Bucknam, R.C., Hemphill-Haley, E., and Leopold, E.B.
1992: Abrupt uplift within the past 1700 years at southern Puget Sound Washington; Science, v. 258, p. 1611-1614.

Cassidy, J.F., Ellis, R.M., and Rogers, G.C.
1988: The 1918 and 1957 Vancouver Island earthquakes; Bulletin of the Seismological Society of America, v. 78, p. 617-635.

Clague, J.J. and Bobrowsky, P.T.
1994: Evidence for a large earthquake and tsunami 100-400 years ago on western Vancouver Island British Columbia; Quaternary Research, v. 41, p. 176-184.

Clague, J.J., Naesgaard, E., and Sy, A.
1992: Liquefaction features on the Fraser delta: evidence for prehistoric earthquakes?; Canadian Journal of Earth Sciences, v. 29, p. 1734-1745.

Crosson, R.S. and Owens, T.J.
1987: Slab geometry of the Cascadia subduction zone beneath Washington from earthquake hypocentres and teleseismic converted waves; Geophysical Research Letters, v. 14, p. 824-827.

Dragert, H. and Hyndman, R.D.
1995: Continuous GPS monitoring of strain in the northern Cascadia subduction zone; Geophysical Research Letters, v. 22, p. 755-758.

Dragert, H., Hyndman, R.D., Rogers, G.C., and Wang, K.
1994: Current deformation and the width of the seismogenic zone of the northern Cascadia subduction thrust; Journal of Geophysical Research, v. 99, p. 653-668.

Drew, J.J. and Clowes, R.M.
1990: A re-interpretation of the seismic structure across the active subduction zone of western Canada; in Studies of Laterally Heterogeneous Structures Using Seismic Refraction and Reflection Data, (ed.) A.G. Green; Geological Survey of Canada, Paper 89-13, p. 115-132.

Eisbacher, G.H. and Clague, J.J.
1981: Urban landslides in the vicinity of Vancouver, British Columbia, with special reference to the December 1979 rainstorm; Canadian Geotechnical Journal, v. 18, p. 205-216.

Harris, J.B., Hunter, J.A., Luternauer, J.L., and Finn, W.D.L.
1995: Site response modelling of the Fraser River delta, British Columbia: preliminary results from two deep boreholes; in Current Research 1995-E, Geological Survey of Canada, p. 69-75.
1998: Site amplification modelling of the Fraser delta, British Columbia; in Geology and Natural Hazards of the Fraser River Delta, British Columbia, (ed.) J.J. Clague, J.L. Luternauer, and D.C. Mosher; Geological Survey of Canada, Bulletin 525, this volume.

Heaton, T.H.
1990: The calm before the quake?; Nature, v. 343, p. 511-512.

Heaton, T.H. and Hartzell, S.H.
1987: Earthquake hazards on the Cascadia subduction zone; Science, v. 236, p. 162-168.

Heaton, T.H. and Kanamori, H.
1984: Seismic potential associated with subduction in the northwestern United States; Bulletin of the Seismological Society of America, v. 74, p. 933-942.

Heidebrecht, A.C., Basham, P.W., Rainer, J.H., and Berry, M.J.
1983: Engineering applications of new probabilistic seismic ground-motion maps of Canada; Canadian Journal of Civil Engineering, v. 10, p. 670-680.

Hyndman R.D. and Wang, K.
1993: Thermal constraints on the zone of major thrust earthquake failure: the Cascadia subduction zone; Journal of Geophysical Research, v. 98, p. 2093-2060.

Hyndman, R.D., Rogers, G.C., Dragert, H., Wang, K., Clague, J.J., Adams, J., and Bobrowsky, P.T.
1996: Giant earthquakes beneath Canada's west coast; Geoscience Canada, v. 23, p. 63-72.

Hyndman, R.D., Yorath, C.J., Clowes, R.M., and Davis, E.E.
1990: The northern Cascadia subduction zone at Vancouver Island: seismic structure and tectonic history; Canadian Journal of Earth Sciences, v. 27, p. 313-329.

Lewis, T.
1991: Heat flux in the Canadian Cordillera; in Neotectonics of North America, (ed.) D.B. Slemmons, E.R. Engdahl, M.D. Zoback, and D.D. Blackwell; Geological Society of America, Decade Map Volume 1, p. 445-456.

Ma, L., Crosson, R.S., and Ludwin, R.
1996: Western Washington earthquake focal mechanisms and their relationship to regional tectonic stress; in Assessing Earthquake Hazard and Reducing Risk in the Pacific Northwest, (ed.) A.M. Rogers, T.J. Walsh, W.J. Kockelman, and G.R. Priest; United States Geological Survey, Professional Paper 1560, v. 1, p. 257-283.

Malone, S.D. and Bor, S.
1979: Attenuation patterns in the Pacific Northwest based on intensity data and the location of the 1872 North Cascades earthquake; Bulletin of the Seismological Society of America, v. 679, p. 531-576.

Mathews, W.H.
1979: Landslides of central Vancouver Island and the 1946 earthquake; Bulletin of the Seismological Society of America, v. 69, p. 445-450.

Maud, R.
1978: The Salish People (The Local Contribution of Charles Hill-Tout, Volume IV: the Sechelt and the South-eastern Tribes of Vancouver Island); Talon Books, Vancouver, British Columbia, 178 p.

Milne, W.G., Rogers, G.C., Riddihough, R.P., McMechan, G.A., and Hyndman, R.D.
1978: Seismicity of Western Canada; Canadian Journal of Earth Sciences, v. 15, p. 1170-1193.

Mulder, T.L. and Rogers, G.C.
1993: Crustal earthquakes in southwestern British Columbia ; Eos (Transactions, American Geophysical Union), v. 74, p. 201 (abstract).

Page, R.
1968: Focal depths of aftershocks; Journal of Geophysical Research, v. 73, p. 3897-3903.

Pennington, W.D.
1983: Role of shallow phase changes in the subduction of oceanic crust; Science, v. 220, p. 1045-1047.

Qamar, A. and Zollweg, J.
1990: The 1990 Deming, Washington earthquakes: a sequence of shallow thrust earthquakes in the Pacific northwest; Eos (Transactions, American Geophysical Union), v. 71, p. 1145 (abstract).

Rogers, G.C.
1979: Earthquake fault plane solutions near Vancouver Island; Canadian Journal of Earth Sciences, v. 16, p. 523-531.
1980: A documentation of soil failure during the British Columbia earthquake of 23 June, 1946; Canadian Geotechnical Journal, v. 17, p. 122-127.
1983a: Some comments on the seismicity of the northern Puget Sound - southern Vancouver Island region; in Proceedings of 1980 Conference on Earthquake Hazards of the Puget Sound Region, Washington State; United States Geological Survey, Open File Report 1983-19, p. 105-130.
1983b: Seismotectonics of British Columbia; Ph.D. thesis, University of British Columbia, Vancouver, British Columbia, 247 p.
1988a: An assessment of the megathrust earthquake potential of the Cascadia subduction zone; Canadian Journal of Earth Sciences, v. 24, p. 844-852.
1988b: Seismic potential of the Cascadia subduction zone; Nature, v. 332, p. 17.
1994: Earthquakes in the Vancouver area; in Geology and Geological Hazards of the Vancouver Region, Southwestern British Columbia, (ed.) J.W.H. Monger; Geological Survey of Canada, Bulletin 481, p. 221-229.

Rogers, G.C. and Hasegawa, H.S.
1978: A second look at the British Columbia earthquake of 23 June, 1946; Bulletin of the Seismological Society of America, v. 68, p. 653-676.

Rogers, G.C. and Horner, R.B.
1991: An overview of western Canadian seismicity; in Neotectonics of North America, (ed.) D.B. Slemmons, E.R. Engdahl, M.D. Zoback, and D.D. Blackwell; Geological Society of America, Decade Map Volume 1, p. 69-76.

Rogers, G.C., Cassidy, J.F., and Weichert, D.H.
1998: Variation in earthquake ground motion on the Fraser delta from strong motion seismograph records; in Geology and Natural Hazards of the Fraser River Delta, British Columbia, (ed.) J.J. Clague, J.L. Luternauer, and D.C. Mosher; Geological Survey of Canada, Bulletin 525, this volume.

Rogers, G.C., Spindler, C., and Hyndman, R.D.
1990: Seismicity along the Vancouver Island Lithoprobe corridor; in Proceedings of the Lithoprobe Southern Cordillera Symposium, University of Calgary, Calgary, Alberta, p. 166-169.

Satake, K., Shimazaki, K., Tsuji, Y., and Ueda, K.
1996: Time and size of a giant earthquake in Cascadia inferred from Japanese tsunami records of January 1700; Nature, v. 379, p. 246-249.

Savage, J.C., Lisowski, M., and Prescott, W.H.
1991: Strain accumulation in western Washington; Journal of Geophysical Research, v. 96, p. 14,493-14,507.

Sbar, M.L.
1982: Delineation and interpretation of seismotectonic domains in western North America; Journal of Geophysical Research, v. 87, p. 3919-3928.

Steinbrugge, K.V., Manning, J.H., and Degenklob, H.J.
1967: Building damage in Anchorage; in The Prince William Sound, Alaska, Earthquake of 1964 and Aftershocks, (ed.) F.J. Wood; United States Department of Commerce, Coast and Geodetic Survey, Publication 10-3, Vol. II, Part A, p. 7-217.

Sy, A., Lo, R.C., Henderson, P.W., Siu, D.Y., Finn, W.D.L., and Heidebrecht, A.C.
1991: Ground motion response for Fraser delta, British Columbia; Proceedings, 4th International Conference on Seismic Zonation, Stanford, California, v. 2, p. 232-350.

Thomas, G.C., Crosson, R.S., Cohee, B., and Qamar, T.
1996: The May 2, 1996 Duvall, Washington earthquake and aftershock sequence; Eos (Transactions, American Geophysical Union), v. 77, p. F523 (abstract).

Walcott, R.
1993: Neogene tectonics and kinematics of western North America; Tectonics, v. 12, p. 326-333.

Wang, K.
1996: Simplified analysis of horizontal stresses in a buttressed forearc sliver at an oblique subduction zone; Geophysical Research Letters, v. 223, p. 2021-2024.

Wang, K., Mulder, T., Rogers, G.C. and Hyndman, R.D.
1995: Case for very low coupling stress on the Cascadia subduction fault; Journal of Geophysical Research, v. 100, p. 12,907-12,918.

Weichert, D.H.
1994: Seismic acceleration zones in the Vancouver area; Canadian Journal of Civil Engineering, v. 21, p. 351-353.

Sedimentary environments of the Fraser delta

J.L. Luternauer[1], D.C. Mosher[2], J.J. Clague[1], and R.J. Atkins[3]

Luternauer, J.L., Mosher, D.C., Clague, J.J., and Atkins, R.J., 1998: Sedimentary environments of the Fraser delta; in Geology and Natural Hazards of the Fraser River Delta, British Columbia, (ed.) J.J. Clague, J.L. Luternauer, and D.C. Mosher; Geological Survey of Canada, Bulletin 525, p. 27–39.

Abstract: Sediments on the delta slope north of the Main Channel of the Fraser River are mainly sandy mud; sedimentation rates in this area are high due to northward transport of sediment from the river mouth. In contrast, little sediment is accumulating on the sandy slope south of the Main Channel. Failures near the crest of the slope trigger turbidity currents and debris flows in sea valleys off active distributary-channel mouths. Broad unvegetated tidal flats at the western and southern fronts of the delta are covered mainly by sand. The unvegetated tidal flats are bordered by a strip of intertidal marsh underlain by mud. The dyked, and now extensively urbanized delta plain is underlain by sand with a cap of several metres of silt. Domed peat bogs cover much of the eastern part of the delta plain. The two principal distributary channels of the Fraser River have highly mobile beds floored by sand. The channels and the foreshore are dyked, thus the delta plain is no longer subject to flooding.

Résumé : Au nord du chenal principal du fleuve Fraser, où les matériaux sur le talus deltaïque consistent en de la boue sableuse, les vitesses de sédimentation sont élevées et sont attribuables au transport vers le nord de particules provenant de l'embouchure du fleuve. Au sud du chenal principal, où les matériaux sur le talus deltaïque se composent de sable, les vitesses de sédimentation sont faibles. Les ruptures qui se produisent près de la crête du talus déclenchent des courants de turbidité et des coulées de débris dans les vallées sous-marines au large de l'embouchure des défluents actifs. Les vastes estrans sans végétation aux fronts ouest et sud du delta sont principalement recouverts de sable. Ils sont frangés par une bande de marécages intertidaux tapissés de boue. La plaine deltaïque endiguée et maintenant fortement urbanisée est constituée de sable que surmontent plusieurs mètres de silt. Des tourbières bombées couvrent presque toute la partie est de la plaine deltaïque. Les deux principaux défluents du fleuve Fraser ont un lit très mobile à fond sableux. Les défluents et la basse plage étant endigués, la plaine deltaïque est protégé contre les inondations.

[1] Geological Survey of Canada, 605 Robson Street, Vancouver, British Columbia V6B 5J3
[2] Geological Survey of Canada, Pacific Geoscience Centre, P.O. Box 6000, Sidney, British Columbia V8L 4B2
[3] Hay and Company Consultants Inc., 1 West 7th Avenue,Vancouver, British Columbia V5Y 1L5

INTRODUCTION

The Fraser River delta is a complex and dynamic sedimentary system that is evolving in response to natural processes and human disturbance. The main elements of this system — slope, tidal flats (including marsh), distributary channels, floodplain, and bogs — have been described in many previous reports (e.g. Ages and Woollard, 1976; Pharo and Barnes, 1976; Hebda, 1977; Swinbanks, 1979; Luternauer, 1980; Thomson, 1981; Clague and Luternauer, 1982; Clague et al., 1983; Luternauer and Finn, 1983; Church et al., 1992; Luternauer et al., 1994, 1995; Williams and Hamilton, 1994; and references therein). We draw upon these reports here to provide a summary of the present-day sedimentary regime of the Fraser delta. We also review some recent advances in understanding sedimentation in the estuary (Hay and Company Consultants, 1994, 1995, 1996; Kostaschuk et al., 1995; Liedtke et al., 1995; McLaren and Ren, 1995; Tarbotton and Harrison, 1996), that are helping address environmental concerns but are not covered elsewhere in this Bulletin.

SLOPE

Location and morphology

The western slope of the Fraser delta extends from the edge of the delta plain, about 10 m below lowest normal water level, to depths of 200-300 m in the Strait of Georgia (Fig. 1). It is a

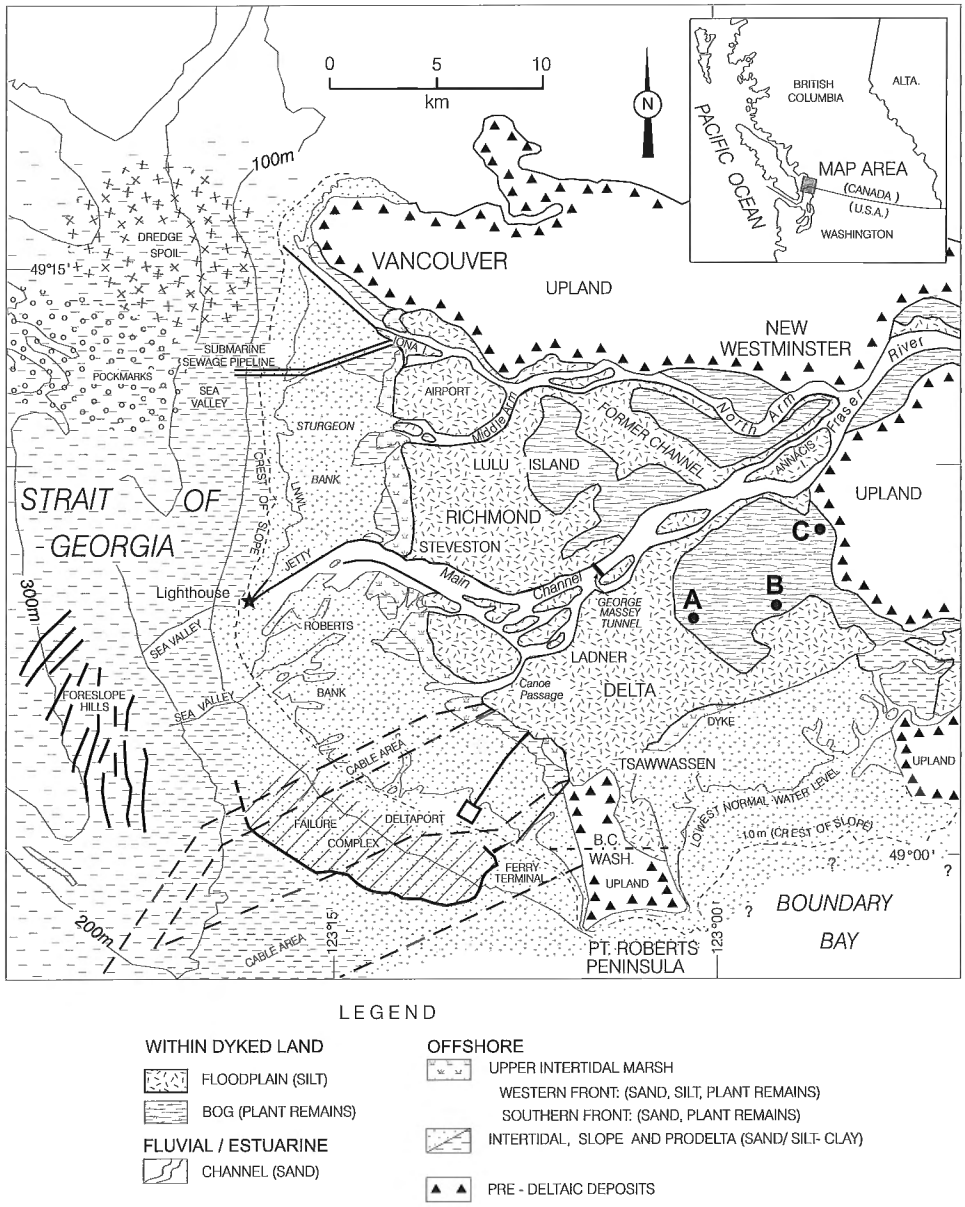

Figure 1. *Map of the Fraser River delta showing sedimentary environments. A, B, and C are locations of stratigraphic sections in Burns Bog, shown in Figure 9.*

fairly uniform apron, but is cut by two large submarine channels, or sea valleys, just off, and south of, the mouth of the Main Channel (Fig. 1). The slope dips 1-3° on average, but its crest is as steep as 14° and the walls of the sea valleys are inclined up to 23°. The southern slope of the delta, in Boundary Bay (Fig. 1), is ill-defined; it has a gentler gradient than the western delta slope and terminates in much shallower water.

Oceanography and sediment supply

Tidal currents over the delta slope generally follow bathymetric contours; flood currents are stronger and of longer duration than ebb currents, thus the dominant flow direction is to the northwest (Thomson, 1981). At times, the currents are strong enough to transport sand-sized sediment (Luternauer, 1980; Kostaschuk et al., 1995). Strong tidal currents also flow along the floor of the sea valley off the Main Channel (Shepard and Milliman, 1978).

A sediment-charged plume extends into the Strait of Georgia from the mouth of the Main Channel and, to a lesser extent, other distributaries during freshet (Thomson, 1981; Liedtke et al., 1995; Kostaschuk et al., 1998). The Coriolis effect acts in concert with tidal drag to deflect the plume towards the Sturgeon Bank slope on a flooding tide. Even on an ebbing tide, more fine-grained sediment is carried northward along the delta front because the southeasterly ebb tidal drag on the plume is balanced by the Coriolis effect and because surface water off Sturgeon Bank flows persistently to the north, regardless of tidal phase, during the summer (Giovando and Tabata, 1970; Tabata et al., 1971; Tabata, 1972). This northerly current on an ebbing tide, which is evident when the waters of the Strait of Georgia are well stratified, may result from the oblique breaking of internal gravity waves against the Sturgeon Bank slope (Thomson, 1975, 1981).

Sedimentology

Delta-slope sediments consist of mud and fine-grained sand deposited mainly from the Fraser River plume and sediment gravity flows, respectively (Luternauer et al., 1994). Cores collected within 250 m of the mouth of the Main Channel are dominated by thick beds of fine- to medium-grained sand; interbeds of mud and silt are more common in cores farther from the channel mouth.

Sediments on the Sturgeon Bank slope, north of the Main Channel, consist almost entirely of pervasively bioturbated, very fine-grained sandy mud (Luternauer, 1976; Pharo and Barnes, 1976; McLaren and Ren, 1995). Gas of biogenic origin is common in these muddy sediments and is responsible for pockmarks and other gas-related features on the seafloor on the northern part of the delta slope (Fig. 1; W.T. Collins, pers. comm., 1996; A.G. Judd, pers. comm., 1996).

Sediments on the Roberts Bank slope are mainly sand because the oceanographic regime limits the amount of finer-grained sediment that is carried into the area and deposited there. Most of the sand is relict and was probably deposited when the mouth of the main distributary channel of the Fraser River was south of where it is today. Minor amounts of sand, however, may wash off the Roberts Bank tidal flats and onto the slope. Sand is transported from the tidal flats onto the Sturgeon Bank slope by the same process, but, except near the crest of the slope off the North and Middle arms (Luternauer, 1980), it is mixed with more abundant silt and clay derived from the Fraser River plume.

Sedimentation rates range from <1 to 2 cm/a over much of the Sturgeon Bank slope and in the central Strait of Georgia, but are up to an order of magnitude higher just off the mouth of the Main Channel (Luternauer et al., 1994). In contrast, little or no sediment is being deposited today over most of the Roberts Bank slope.

Sandy sediments at depths of 20 to 120 m off southern Roberts Bank have been moulded into dunes (Kostaschuk et al., 1995; Fig. 1, 2c, 3, 4). The largest of these features exceeds 3 m in height and 100 m in wave length. Measurements of currents within 1 m of the seafloor in the dune field indicate net northwesterly sediment transport, presumably by the dominant flood tidal currents (Kostaschuk et al., 1995). An asymmetry of the dunes (Fig. 4) supports this interpretation. The presence of migrating dunes in an area that is not being replenished with sand suggests that the delta substrate may be eroding; this could affect the stability of nearby port facilities near the crest of the slope (Kostaschuk et al., 1995). Recently, however, Hay and Company Consultants (1996) concluded that, although sand is being carried away from this area, it is derived from material that was dumped there during the excavation of a ship-turning basin on the adjacent tidal flats (Fig. 3). Naturally deposited sediments are probably not being eroded because they are more compact and cohesive than the dredge spoil.

More than 3 x 10^6 m^3 of material have been dumped between 1968 and 1987 at a waste disposal site off North Arm (Fig. 1). Unauthorized disposal well outside the prescribed limits of the disposal site (Hart, 1992) has interfered with bottom fishing on the Sturgeon Bank slope. There are other, smaller, dump sites near the mouth of the Main Channel and off the Roberts Bank Deltaport.

Slope failures

Retrogressive failures and the resulting sediment gravity flows have eroded the active deep-sea valley off the mouth of the Main Channel (Kostaschuk et al., 1992b; Fig. 1, 2b, 5), smaller sea valleys off Canoe Passage and the North Arm, and relict valleys north and south of the Main Channel (Fig. 1). Most failures are linked to the rapid accumulation of sediment and may be triggered by tidal drawdown which can generate high interstitial pore pressures in these sediments (Christian et al., 1998). The high gas content of the sediments may play a significant roll in failure by raising pore pressures and decreasing grain-to-grain contact during tidal loading (McKenna et al., 1992; Chillarige et al., 1994, 1995; Christian et al., 1998).

Other, more problematic types of failures have been documented on the Fraser delta slope. Just south of the sea valley off the Main Channel is a zone of parallel ridges

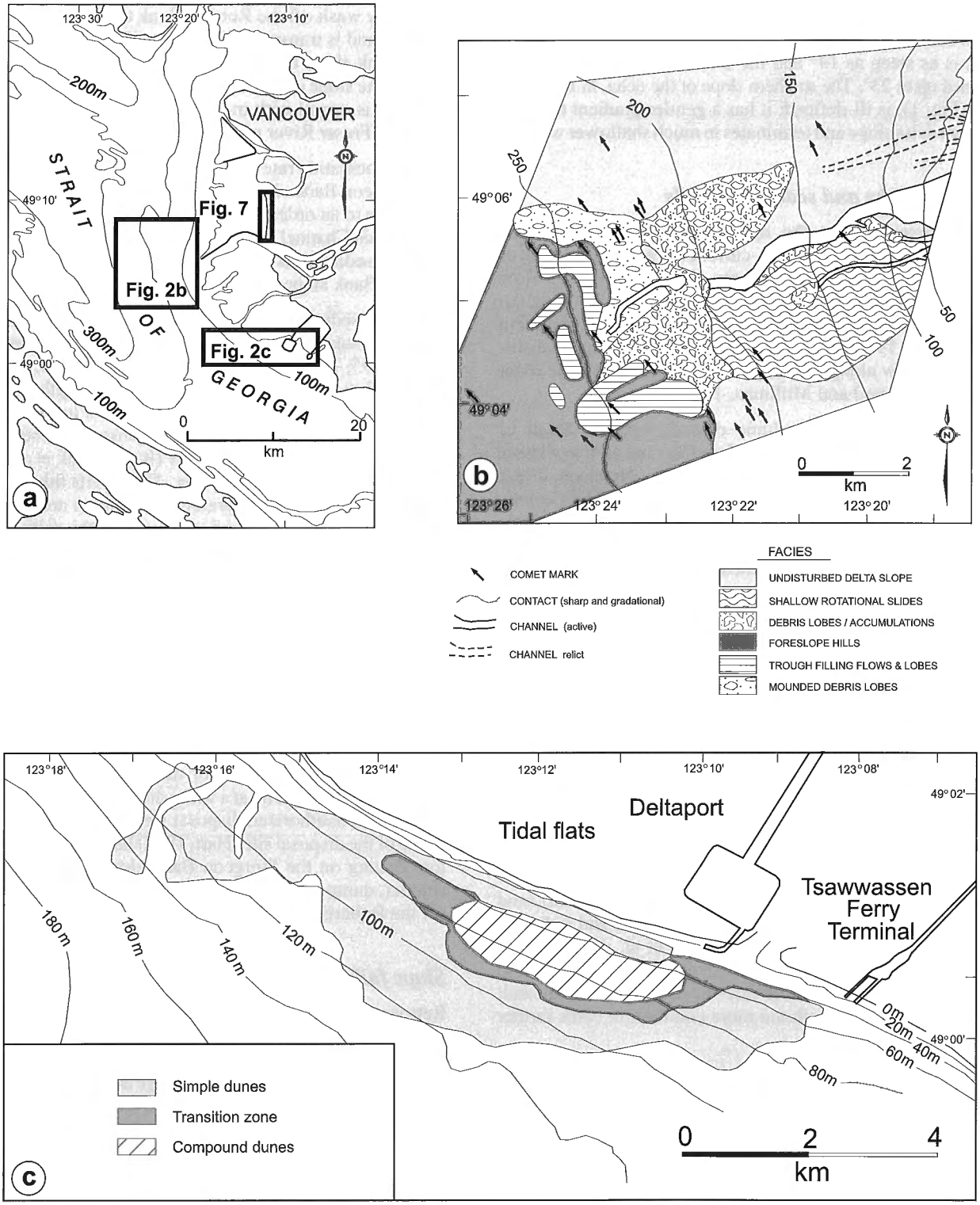

Figure 2. *Some features and deposits on the Fraser delta slope which are discussed in the paper.* ***a)*** *Location map for Figures 2b, 2c, and 7.* ***b)*** *Sedimentary deposits and features off the mouth of the Main Channel (modified from Hart et al., 1992a).* ***c)*** *Bedform distribution on the upper slope off southern Roberts Bank (modified from Kostaschuk et al., 1995).*

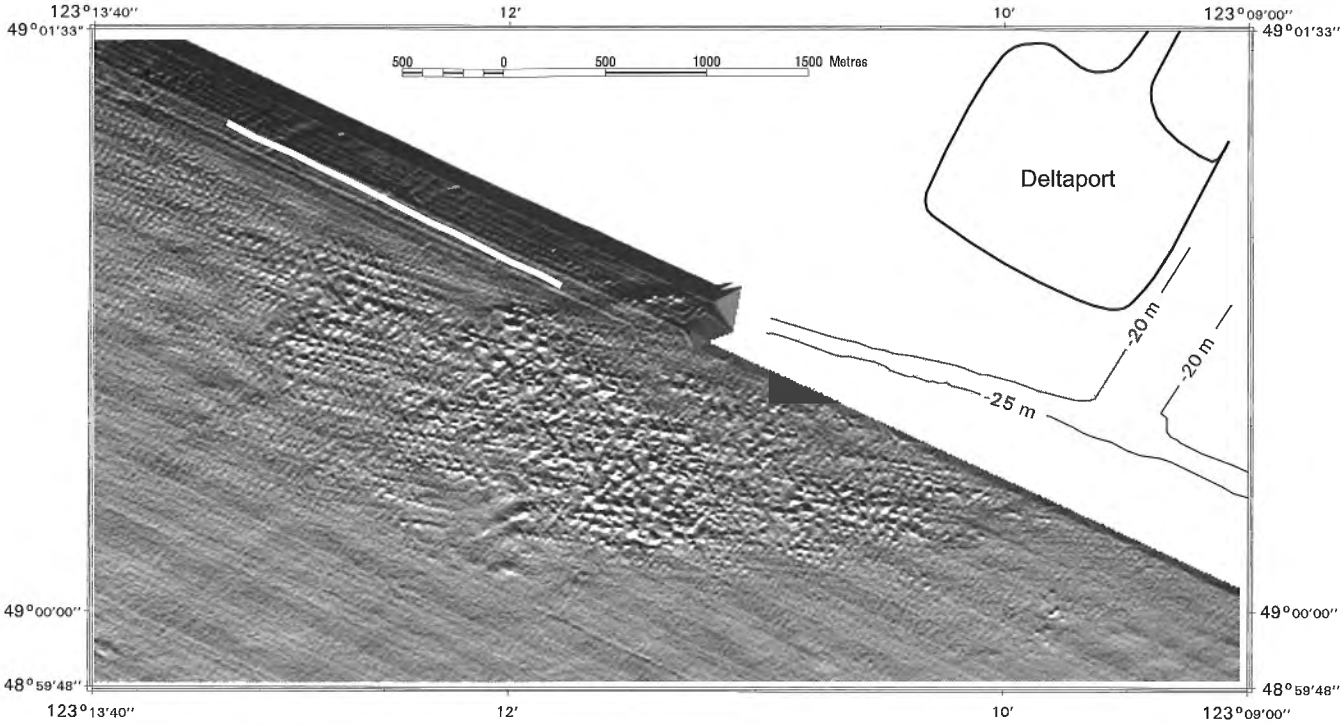

Figure 3. *Shaded relief image of bathymetry over a sand wave field off the Deltaport on southern Roberts Bank (modified from Currie and Mosher, 1996). The image was produced from swath bathymetric data and displays sand waves, dunes, and pockmarks developed on sediment dredged from a nearby ship-turning basin. The white line near the crest of the slope indicates the location of the trackline along which the images in Figure 4 were obtained. Sand waves and dunes are not readily apparent on the swath image in the vicinity of this trackline because the slope is relatively steep there.*

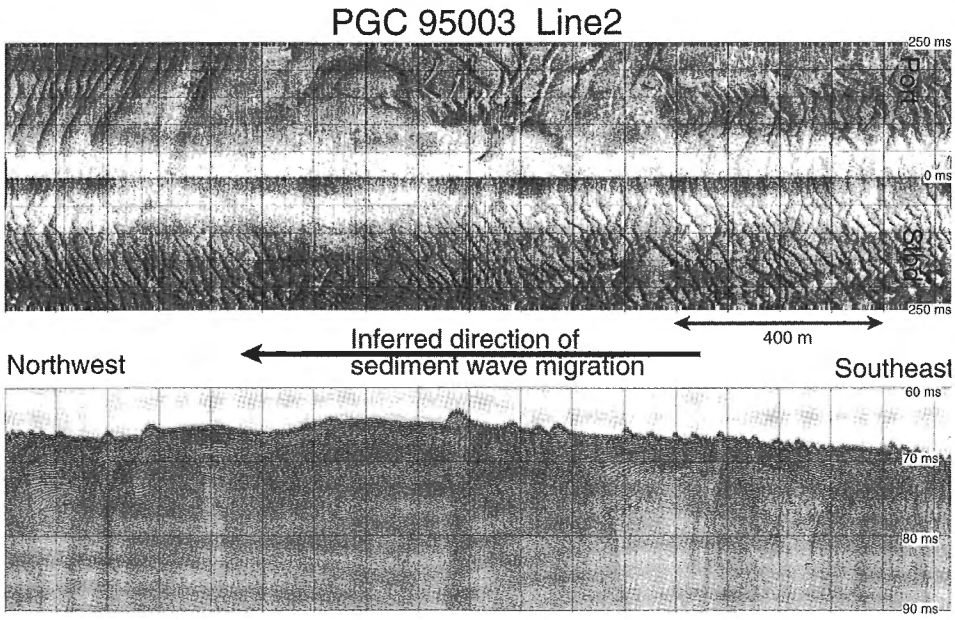

Figure 4. *Sidescan sonar image (top) and Seistec subbottom profile (bottom) over the sand-wave field on southern Roberts Bank (see Fig. 3 for location). The sidescan sonar record provides a plan view of the sand waves and dunes and illustrates the range of bedform sizes. The subbottom profile shows the amplitude of the bedforms and the direction of sediment transport inferred from their asymmetry. The scales are in ms (two-way traveltime).*

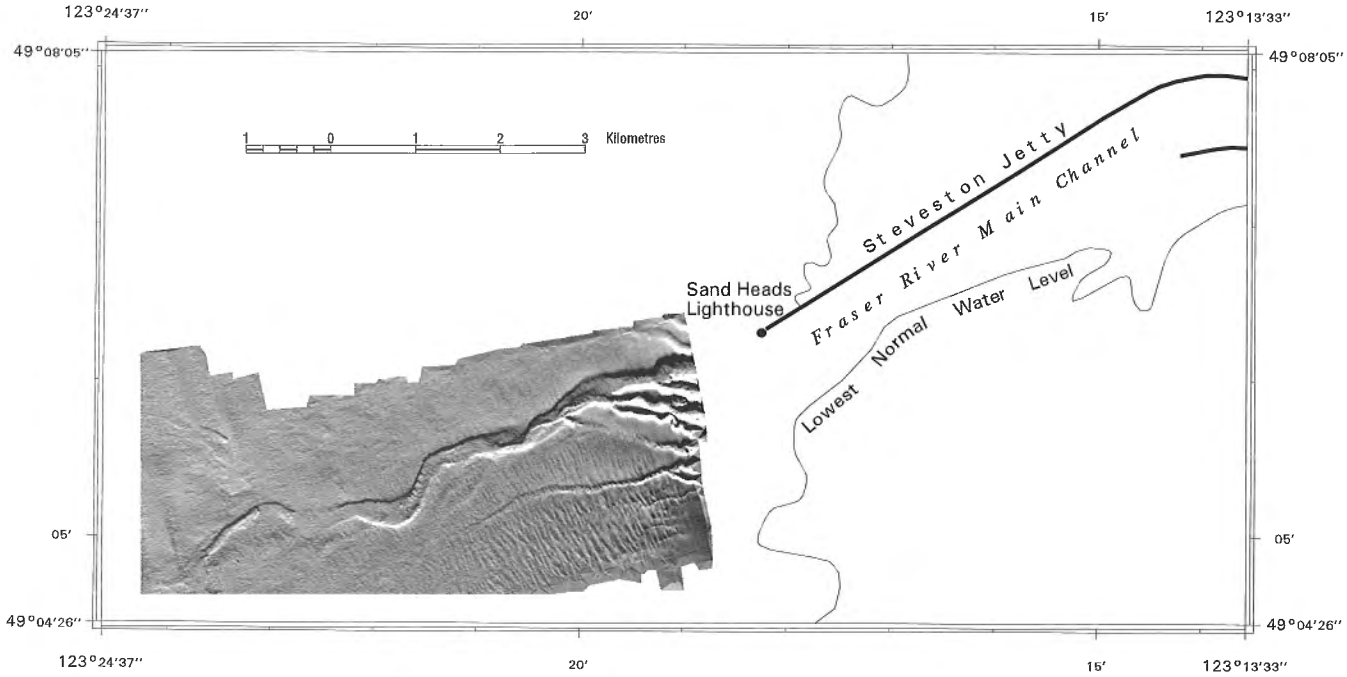

Figure 5. *Shaded relief image of bathymetry in the area of the Sand Heads sea valley system (modified from Currie and Mosher, 1996). The sea valley was formed by turbidity currents and debris flows triggered by failures at the crest of the slope off the mouth of the Main Channel. Parallel ridges on the slope south of the sea valley were probably generated by creep of cohesive delta slope sediments (Fig. 2b).*

(Fig. 1, 2b, 5), attributed to retrogressive sliding by Hart et al. (1992a) and Hart (1993a, b). In contrast, Christian et al. (1998) and Mosher and Hamilton (1998) conclude that these features have formed by creep of slope sediments. There is a much larger area of disturbed sediments on the southern Roberts Bank slope (Roberts Bank Failure Complex, Fig. 1), whose origin is still being debated but is interpreted by Mosher and Hamilton (1998) to be a former river-mouth failure complex. Finally, the Foreslope Hills, a 60 km^2 area of curvilinear troughs and ridges on the floor of the Strait of Georgia off the Main Channel (Fig. 1), may have formed by slumping of slope sediments above weak clayey sediments at the base of the Holocene deltaic sequence (Hart et al., 1992b; Hart, 1993a, b). In contrast, Christian et al. (1998) suggest that the Foreslope Hills may have developed in response to folding of subsurface layers ahead of a rapidly prograding delta, and Mosher and Hamilton (1998) believe that they are sedimentary bedforms.

TIDAL FLATS

Location and general morphology

An intertidal and shallow subtidal platform slopes 0.05° seaward from the dyked edge of the delta to the crest of the slope. The platform at the western delta front is as much as 9 km wide, and is largely intertidal (Fig. 1). It is narrower (about 7 km) at the southern delta front in Boundary Bay, and about half of it is subtidal there. The boundary between the platform and the slope also is less sharp on the south than on the west. A discontinuous fringe of marsh marks the landward edge of the tidal flats. Marshes are locally over 1 km wide along the western delta front, but are narrower at the southern front.

Oceanography and sediment supply

Tides at the delta front are mixed semi-diurnal and have a range of 4 to 5 m; the mean tidal height is 3 m (Thomson, 1981). Sturgeon and Roberts banks are exposed to waves from the northwest with a fetch of up to 120 km. Wave data collected during a twenty-four-month period from 1974-1976 indicate that maximum wave heights over both Sturgeon and Roberts banks are less than 4 m and exceed 1.2 m only 10% of the time (Thomson, 1981). Tidal conditions at Boundary Bay are similar to those at the western front, but wind-generated waves are not as large because the area is more sheltered.

Tidal flats at the western delta front are washed by river water emanating from the Main Channel, Middle Arm, and Canoe Passage. Silt and clay suspended in these waters are transported directly into the intertidal area where they accumulate in marshes and on adjacent unvegetated tidal flats. Fine-grained sediment is also carried into the upper intertidal area by rising tides which drive the sediment-charged river plume ashore. The Fraser River presently contributes little

sand to the tidal flats because the North Arm and Main Channel, which carry the bulk of the sediment load, are dredged and trained.

Tidal flats on the southern part of the delta are not exposed to river wash and have limited sediment supply (Swinbanks and Murray, 1981). Some fine-grained sediment carried by the Serpentine and Nicomekl rivers is deposited on the tidal flats at Mud Bay. Sea cliffs at Point Roberts, which consist of unconsolidated Pleistocene sediments, provide sand to western Boundary Bay.

Sedimentology and detailed morphology

Much of the western tidal platform is mantled by rippled and burrowed, fine-to medium-grained sand (Fig. 1). In places, including areas adjacent to jetties and marshes, the sand has been shaped by waves and longshore drift into swells with heights of 0.5 m and wave lengths of 50-100 m (Luternauer, 1980; Clague and Luternauer, 1982). Active, and abandoned, inactive distributary channels extend across the tidal flats.

Smaller channel systems have developed in response to dredging of the cargo-ship turning basin between the Deltaport and the Ferry Terminal on southern Roberts Bank (Luternauer et al., 1994; Tarbotton and Harrison, 1996). At this site, a network of creeks developed soon after dredging and eroded important eelgrass beds. Erosion was mitigated, in part, by constructing a rip-rap weir which caused the western creeks to fill in. In contrast, to the east, not only has erosion continued, albeit within fewer dominant channels, but part of the area also has been altered by sediment accretion. A lobe of sand, 600 m long, 100 m wide, and up to 0.5 m thick, began to accumulate at the head of a large creek between 1989 and 1991, smothering eelgrass beds (Luternauer et al., 1994). The sand was probably carried upstream along the channel by currents associated with flooding tides. This feature is continuing to grow, but at a slower rate in the last several years (Tarbotton and Harrison, 1996).

Marshes at the western delta front are brackish and are underlain by interbedded and interlaminated organic-rich mud and sand (Fig. 6). These marshes are dissected by creeks and contain shallow depressions. The landward limit of the marsh area is artificially fixed by a dyke.

Human activity may have altered the pattern and rates of sedimentation in the marshes at the western delta front. Williams and Hamilton (1994) concluded from a study of ^{137}Cs concentrations in marsh sediments on Sturgeon Bank that sedimentation rates were lower, by an average of 51%, in

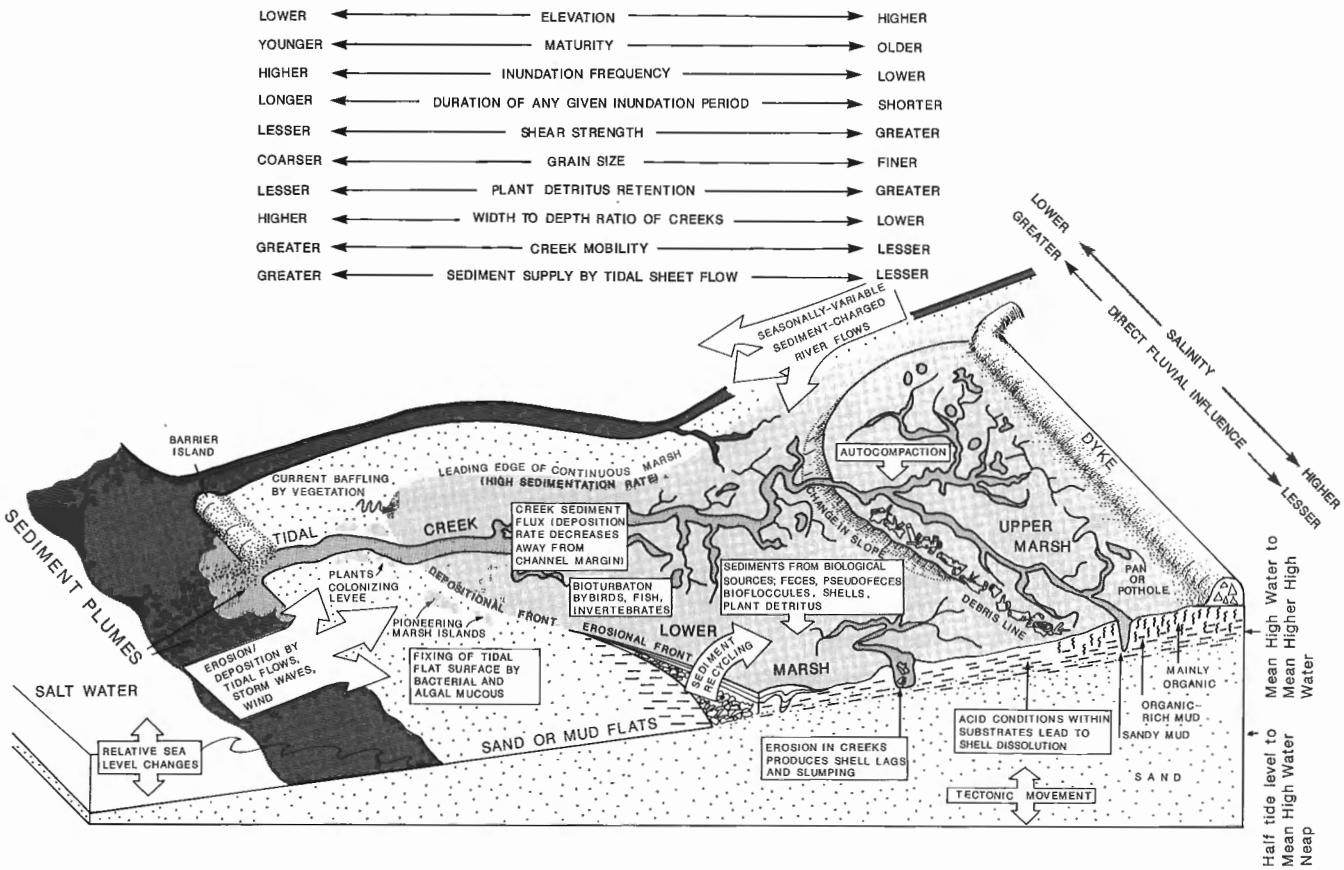

Figure 6. *Principal processes and characteristic features of a brackish marsh and adjacent tidal flat, like those at the western front of the Fraser delta (Luternauer et al., 1995; reprinted with permission of Elsevier Science-NL, Amsterdam, Netherlands).*

the period 1964-1981 compared to 1954-1964 (Fig. 2a, 7). They suggest "that the increased removal of sand by dredging in the Fraser River estuary has reduced sediment input and caused net erosive lowering throughout much of the sandy low marsh" (Williams and Hamilton, 1994, p. 1154). The study, however, is based on limited data; and because its conclusions have far-ranging implications for current and future developments that might affect sediment supply to the delta front, it is important that the results be confirmed.

Although dredging and channel entrainment have undoubtedly affected sediment supply to the delta front, quantifying their effects, as Williams and Hamilton (1994) have attempted to do, is difficult. The amount of sediment carried by the river varies significantly from year to year. Vegetation cover, biological activity such as bird foraging, and storms can significantly alter the balance between accretion and erosion. Also, the development and abandonment of even small tidal channels can drastically alter sedimentation at specific sites (Medley 1978; Luternauer et al., 1994).

The southern tidal flats at Boundary Bay consist almost entirely of well sorted, very fine- to fine-grained sand which gradually fines shoreward (Swinbanks and Murray, 1981). The sand occurs in waves that are similar to, although smaller than, those on the western tidal flats. Tidal channels cross the middle and outer parts of the flats. Tidal marshes just seaward of the dyke are narrower and less extensive than marshes at the western margin of the delta, and sediments, even there, are mainly sand. These marshes support vegetation adapted to more saline conditions than exist along much of the western delta front, and are true salt marshes (Luternauer et al., 1995). A broad algal mat zone on the tidal flat adjacent to the salt marshes is underlain by interlayered sand and algal matter (Swinbanks and Murray, 1981).

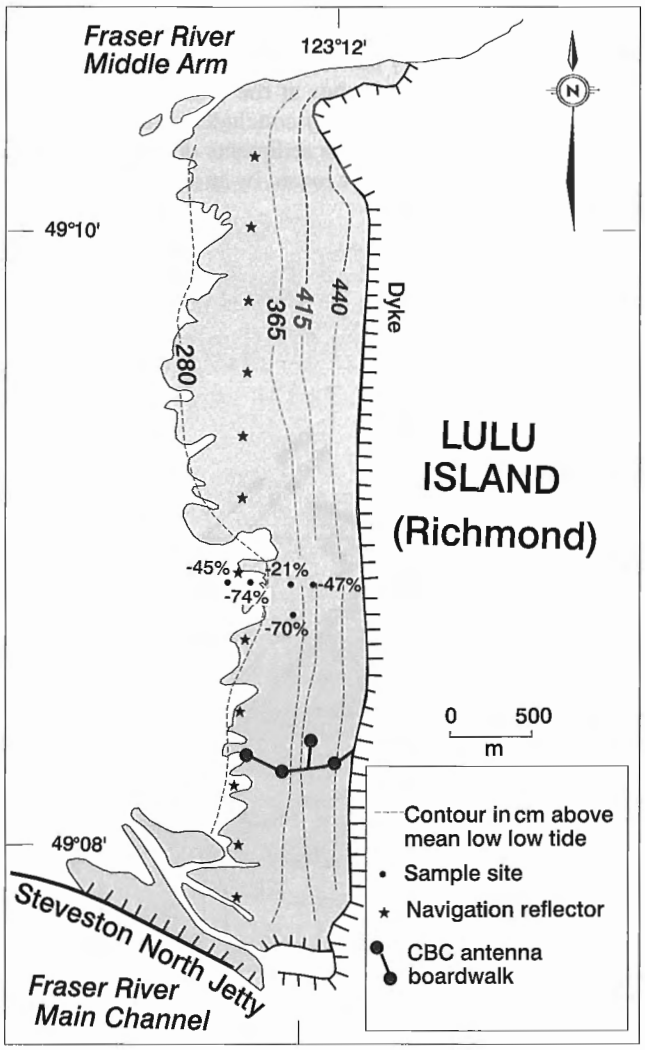

Figure 7. Calculated reduction in sedimentation rates between 1954-1964 and 1964-1981 in the marsh on central Sturgeon Bank based on ^{137}Cs data (modified from Williams and Hamilton, 1994). The marsh is shaded. See Figure 2a for location.

DISTRIBUTARY CHANNELS

Location and general morphology

The Fraser River splits into three channels at New Westminster (Fig. 1). Two of the channels recombine below Annacis Island to form the Main Channel which, in turn, divides farther downriver to form Canoe Passage. The third channel, North Arm, splits to form the Middle Arm in the northwestern corner of the delta. The Main Channel has a maximum width of up to 1250 m, but is more typically about 400 m wide and has a flow depth of about 10 m at low water (Church et al., 1992).

Estuarine circulation and sediment supply

The estuary extends from the mouths of the distributaries to the limit of tidal rise 75 km upstream of Sand Heads, well east of the Fraser delta (Fig. 1; Ages and Woollard, 1976; Church et al., 1992). Salinity stratification in the estuary varies with tidal conditions and river discharge (Kostaschuk et al., 1998). During periods of low discharge, a salt wedge intrudes more than 20 km upstream along the Main Channel, the deepest of the channels. During high discharge and a falling tide, the salt wedge can be driven out of the channel and into the Strait of Georgia.

The Fraser River supplies an average of 17.3 million t of sediment annually to the delta's distributaries, of which 35% is sand (Church et al., 1992). The Main Channel carries 80% or more of the total sediment load, including about 2.8 million t of fine- to very coarse-grained sand (0.18-2.0 mm). Sediment and water discharge exhibit strong seasonal variations and are largest during the late spring-early summer freshet.

Sedimentology and detailed morphology

The distributary channels are floored mainly with sand and muddy sand, except for the Middle Arm, in which sandy mud is common (McLaren and Ren, 1995). Both the North Arm

and the Main Channel are dredged to maintain navigable depths and to recover sand for construction purposes. The margins of the distributaries are dyked downstream to the tidal flats, and jetties further constrain the North Arm and the Main Channel as they cross the flats. Concern has been raised about sediment budget deficits at the river mouth because of increasing demands for dredged sand for construction and low supply in recent years due to low flows (Fraser River Estuary Management Program, unpublished meeting notes, 1996). These deficits could alter the sediment balance at the delta front which, in turn, could destabilize local fish and wildlife habitats.

Estuarine sediment transport and deposition have been studied in greatest detail along the lower reaches of the Main Channel. Sand bed-material in this part of the river has been moulded by river currents into dunes that are locally more than 5 m high and 100 m long (Kostaschuk and Macdonald, 1988; Kostaschuk et al., 1998). The dunes cause large turbulent vortices that are an important mechanism for entraining sand and suspending it higher than would ordinarily be the case, thus facilitating its transport down the river. A pre-freshet survey of the lower Main Channel (Fig. 8) suggests that the dunes may periodically migrate upstream (see also McLaren and Ren, 1995). This is likely related to intrusion of the salt wedge during periods of low river flow. The more vigorous downstream flows of spring-summer freshets reverse the direction of dune migration.

Suspended sediment in the Main Channel is transported seaward over the salt wedge. Sediment concentrations decrease seaward of the wedge tip because of interference in the exchange of sediment between the flow and the bed, reduced turbulence, flocculation of fine-grained sediment, and dilution of the sediment-water mixture (Kostaschuk et al., 1992a). Suspended sediment accumulates near the tip of the salt wedge, forming a turbidity maximum (Nichols and Biggs, 1985; Kostaschuk et al., 1992a). This is an ephemeral phenomenon that disappears when the salt wedge is flushed out of the channel at low tide, but it allows some pollutants to become concentrated in sediments (Luternauer et al., 1994).

Beyond the mouth of the Main Channel, suspended sediment spreads out in a plume in the Strait of Georgia (Luternauer et al., 1994; Liedtke et al., 1995; Kostaschuk et al., 1998). When the salt wedge is pushed out of the channel and river water comes into direct contact with the bed, sand bed material is resuspended and sediment concentrations increase in the plume. When the wedge lies within the channel and flow is stratified at the river mouth, concentrations of both fine- and coarse-grained sediment are reduced in the plume. Sediment concentrations in the plume decrease exponentially with distance seaward of the river mouth, but some fine-grained sediment is transported in suspension as far as the central Strait of Georgia and into lower Howe Sound before settling out onto the seafloor.

Most of the bed load of the Fraser River is carried in the Main Channel (Hay and Company Consultants Ltd., 1994, 1995). An average of 3.6 million m^3 /a of sand was supplied to the Main Channel between 1989 and 1994, but only 1.6 million m^3/a were deposited in the channel itself. The difference, about 2.0 million m^3/a, includes material carried through the channel to the mouth of the river, and material dredged for channel maintenance. An average of 2.7 million m^3/a of sand was dredged from the Main Channel between 1989 and 1994, resulting in a net loss of 1.1 million m^3/a of bed material.

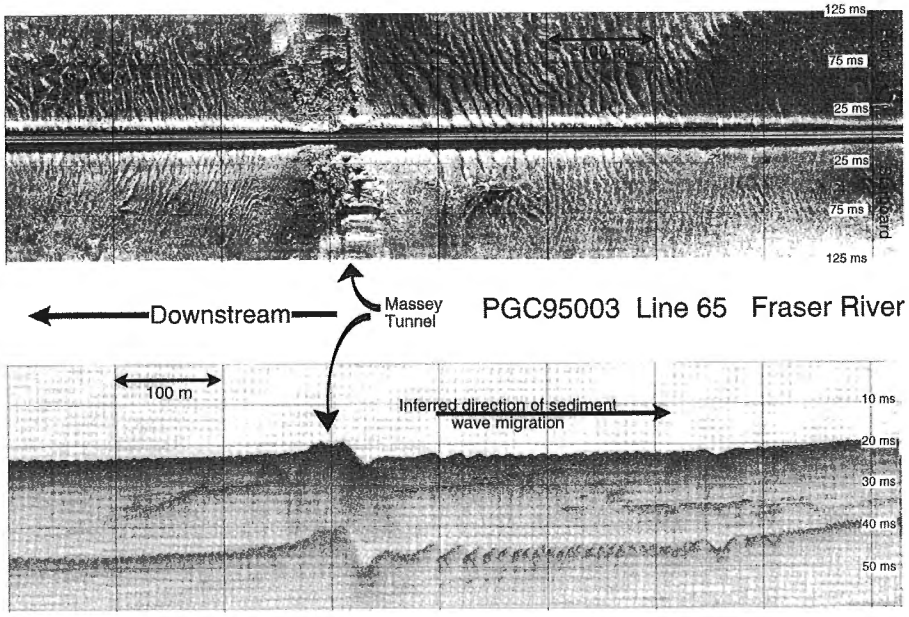

Figure 8. *Sidescan sonar image (top) and Seistec subbottom profile (bottom) of the Main Channel over the George Massey Tunnel (Fig. 1). Note the prominent sand dunes on the river bottom. The asymmetry of the dunes indicates upstream sediment transport (note: the subbottom profile was obtained in March 1994 before the freshet). The scales are in ms (two-way traveltime).*

The recent negative sand budget in the Main Channel is probably responsible for a lowering of the river bed (Hay and Company Consultants Ltd., 1995). Analysis of bed elevations at several river cross-sections has revealed a average net lowering of 0.11 m/a between 1980 and 1992. Much or all of this may be due to dredging, but considerable amounts of sand still reach the river mouth at Sand Heads.

Relatively little sand enters the North Arm. Dredging in recent years has resulted in an average net loss of sediment from this channel of about 1.2 million m^3/a. It is unlikely that dredging on this scale can continue for long without the channel being substantially deepened; yet the future demand for sand for construction purposes will probably exceed the combined 2.8 million m^3/a currently removed from the North Arm and the Main Channel.

FLOODPLAIN

The subaerial delta plain lies within a few metres of mean sea level and is underlain mainly by organic-rich mud and burrowed silt (Armstrong and Hicock, 1979, 1980). Over much of the delta plain, these fine-grained sediments are underlain at depths of a few metres by a thick sheet of distributary-channel sands (Monahan et al., 1993). The delta plain is crossed by active distributary channels of the Fraser River and, on eastern Lulu Island, by a former, now-infilled channel (Fig. 1).

Prior to dyking, part of the upper delta plain was flooded during very high tides and spring-summer freshets. Distributary channels and smaller creeks and sloughs were bordered by freshwater and brackish marshes and swamps (North and Teversham, 1984). These marshes and swamps disappeared when the land was cleared for agriculture. Construction of dykes and ditches has lowered the water table, but it is still within 2 m of the surface. Ditches on central and northeastern Lulu Island supply water from the Main Channel and the North Arm, respectively, for irrigation of agricultural lands, but are not a source of sediment (E. Gilfillan, pers. comm., 1996).

BOGS

Large domed peat bogs cover most of the eastern delta plain (Fig. 1; Johnston, 1921; Hebda, 1977; Clague and Luternauer, 1982; Styan and Bustin, 1983). The evolution of the largest of these bogs (Burns Bog) has been described by Hebda (1977) (Fig. 9). A sedge swamp became established at the present location of Burns Bog about 5500 years ago when the delta plain became built up above sea level. Abundant precipitation and poor drainage limited organic decomposition and promoted peat accumulation. Accumulation of sedge peat at the western edge of Burns Bog was briefly interrupted about 4500 to 5000 years ago by deposition of silt and sand during a brief incursion of the sea. This may have been caused by a northward shift of the main Fraser River distributary channel, the joining of the Fraser delta tidal flats to a former island (now Point Roberts Peninsula), or a rise in sea level. As its surface became more elevated, the swamp changed into a heath shrub land. Increased acidity resulting from the decomposition of plant remains favoured *Sphagnum* growth and gradually converted the shrub land into a moss bog. The *Sphagnum* phase began about 3000 years ago in the centre of Burns Bog, but not until considerably later along the eastern margin where a shrubby swamp persisted because of runoff from the nearby upland. Once the *Sphagnum* bog became established, its water-storage capacity increased markedly. This created conditions favourable for continued moss growth and accumulation, leading to the present domed-shaped bog that rises up to 5 m above the adjacent delta plain. The natural vegetation of Burns Bog and other bogs on the Fraser delta has been extensively modified by farming, peat mining, construction, waste disposal, and fire.

A recent editorial in the Vancouver Sun (Friday, July 19, 1996, p. A18), written in response to the fourth large fire in Burns Bog in this decade, noted that the bog has been mined for peat since the 1940s, has been ditched to improve drainage, and has had farms and a landfill established along its margins. This is in spite of it being a "unique and ecologically critical site... home to more than 150 species of birds as well as deer, bears, coyotes, beavers and muskrats." The editorial adds that, even though rainfall is the primary source of moisture for the bog, dyking of the delta plain and construction of a highway along the bog's eastern margin, have made it drier and more susceptible to fires.

STABILITY OF SEDIMENTARY ENVIRONMENTS

The sedimentary environments of the Fraser River delta continue to change in response to natural and human influences. The southern tidal flats and slope have been least affected by human activity and are probably the most stable parts of the delta. However, the paucity of sediment supply to Boundary Bay will likely diminish the capacity of its marshes to resist erosion in the event of a rise in sea level accompanying global warming.

The slope off Sturgeon Bank is prograding and displays little evidence of recent failures. In contrast, the Roberts Bank slope is sediment-starved and is experiencing localized erosion by currents. Large mass movements have occurred historically off the Main Channel, and earlier off the mouths of former distributary channels. Failures at former distributary mouths may have produced the large Roberts Bank Failure Complex. This complex may consist of overlapping sediment gravity-flow deposits emplaced as the river mouth shifted across the crest of the slope before flow was constrained by training walls and channel dredging (Christian et al., 1998; Mosher and Hamilton, 1998). Most future slope failures that are not triggered by earthquakes will probably occur off the Main Channel as this is the only place where significant volumes of sediment are presently accumulating on relatively steep slopes.

The western tidal flats are receiving adequate amounts of fine-grained sediment to maintain the local marshes, even if sea level were to rise. If, however, the Main Channel

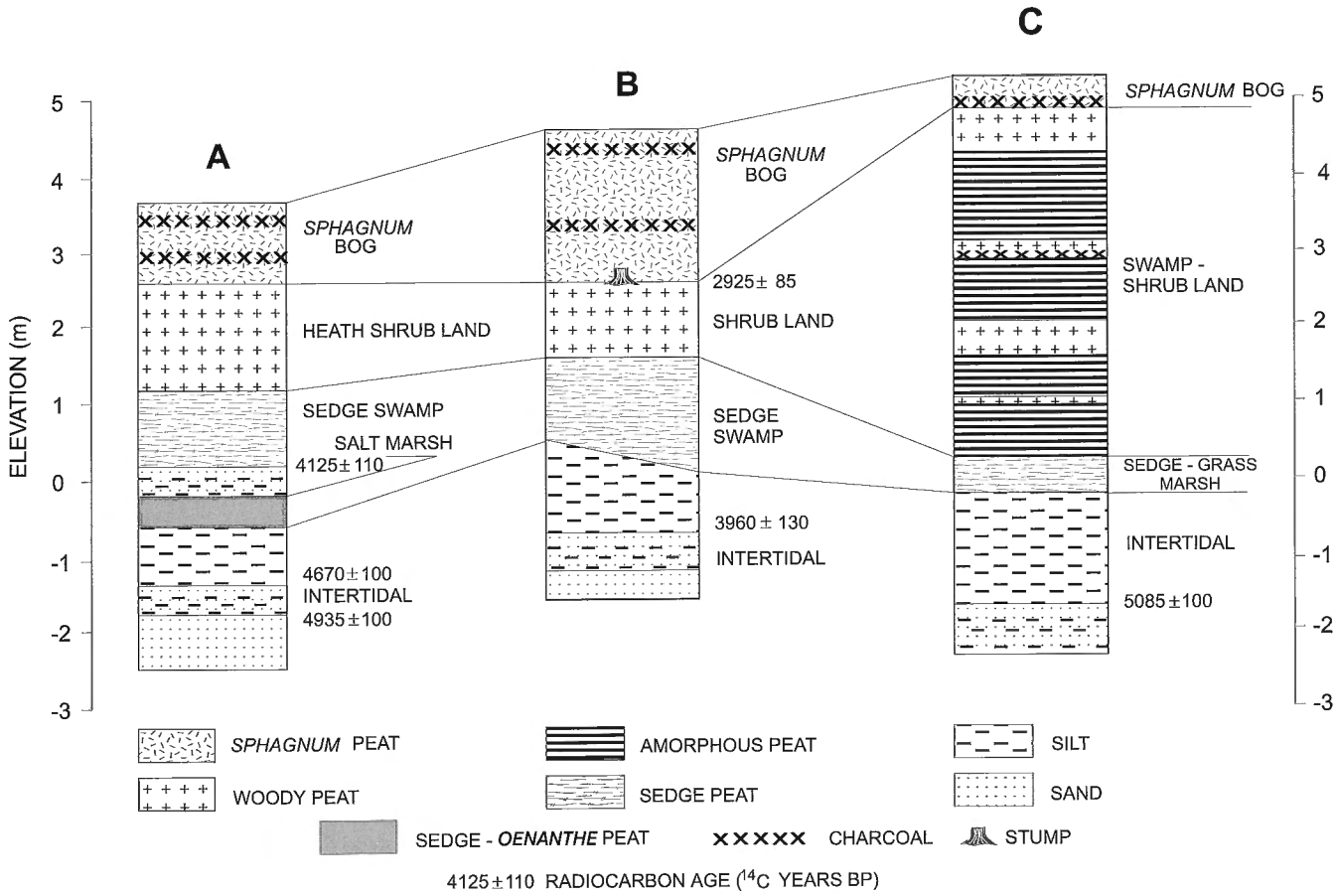

Figure 9. *Stratigraphic sections showing the evolution of Burns Bog during late Holocene time (modified from Clague and Luternauer, 1982). See Figure 1 for location.*

continues to be intensively dredged, and sand that is swept off the outer flats into deep water or carried inshore by prevailing currents and waves is not replenished, the marshes ultimately may be exposed to greater wave energy and begin to retreat. Deepening of the Main Channel due to dredging may not only further limit supply of sand to the tidal flats, but also destabilize channel margins.

Studies of sediment dynamics along the lower reach of the Main Channel have better defined mechanisms of sediment transport and have raised the possibility of contaminant concentration in channel sediments within the turbidity maximum near the tip of the salt wedge. The floodplain environment exists in name only because it is dyked and becoming increasingly urbanized. Large areas of bogs still exist, but in a form substantially altered by human activity.

ACKNOWLEDGMENTS

T. Williams drafted several figures, and B. Vanlier formatted and proofread the text. Critical reviews by V. Barrie and B. Tassone improved the paper.

REFERENCES

Ages, A. and Woollard, A.
1976: The tides in the Fraser River estuary; Canada Department of Environment, Marine Science Branch, Pacific Marine Science Report 76-5, 100 p.

Armstrong, J.E. and Hicock, S.R.
1979: Surficial geology, Vancouver, British Columbia; Geological Survey of Canada, Map 1486A, scale 1:250 000.
1980: Surficial geology, New Westminster, British Columbia; Geological Survey of Canada, Map 1484A, scale 1:250 000.

Chillarige, A.R.V., Morgenstern, N.R., Robertson, P.K., and Christian, H.
1995: Characterization of Fraser River delta sand; in Proceedings, 48th Canadian Geotechnical Conference, v. 2, p. 711-720.

Chillarige, A.R.V., Robertson, P.K., Morgenstern, N.R., Christian, H.A., and Woeller, D.J.
1994: Evaluation of wave effects on seabed instability in the Fraser River delta; in Proceedings, 47th Canadian Geotechnical Conference, p. 186a-186j.

Christian, H.A., Mosher, D.C., Barrie, J.V., Hunter, J.A., and Luternauer, J.L.
1998: Seabed instability on the Fraser River delta; in Geology and Natural Hazards of the Fraser River Delta, British Columbia, (ed.) J.J. Clague, J.L. Luternauer, and D.C. Mosher; Geological Survey of Canada, Bulletin 525, this volume.

Church, M., McLean, D.G., Kostaschuk, R.A., MacFarlane, S., Tassone, B., and Walton, D.
1992: Channel stability and management of lower Fraser River – field excursion guide; Environment Canada, Inland Waters Directorate, Water Resources Branch, Water Survey of Canada, Vancouver, British Columbia, 99 p.

Clague, J.J. and Luternauer, J.L.
1982: Excursion 30A: late Quaternary sedimentary environments, southwestern British Columbia; 11th International Congress on Sedimentology, Hamilton, Ontario, Guidebook, Field Excursion 30A, 167 p.

Clague, J.J., Luternauer, J.L., and Hebda, R.J.
1983: Sedimentary environments and postglacial history of the Fraser River delta and lower Fraser Valley, British Columbia; Canadian Journal of Earth Sciences, v. 20, p. 1314-1320.

Currie, R.C. and Mosher, D.C.
1996: Swath bathymetric surveys in the Strait of Georgia, British Columbia; in Current Research, 1996-E; Geological Survey of Canada, p. 33-40

Giovando, L.F. and Tabata, S.
1970: Measurements of surface flow in the Strait of Georgia by means of free-floating current-followers; Fisheries Research Board of Canada, Technical Report 163, 69 p.

Hart, B.S.
1992: Side-scan sonar observations of Point Grey dump site, Strait of Georgia, British Columbia; in Current Research, Part A; Geological Survey of Canada, Paper 92-1A, p. 55-61.
1993a: Stratigraphy of the delta slope and prodelta; delta slope sedimentation and erosion; submarine slope instability; in Applied Quaternary Research; Canadian Quaternary Association, Program with Abstracts and Field Guide, p. G 41 - G48.
1993b: Large scale *in situ* rotational failure on a low angle delta slope: the Foreslope Hills, Fraser Delta, British Columbia, Canada; Geo-Marine Letters, v. 13, p. 219 - 226.

Hart, B.S., Prior, D.B., Barrie, J.V., Currie, R.G., and Luternauer, J.L.
1992a: A river mouth submarine channel and failure complex, Fraser Delta, Canada; Sedimentary Geology, v. 81, p. 73-87.

Hart, B.S., Prior, D.B., Hamilton, T.S., Barrie, J.V., and Currie, R.G.
1992b: Patterns and styles of sedimentation, erosion and failure, Fraser delta slope, British Columbia; in Geotechnique and Natural Hazards; BiTech Publishers, Vancouver, British Columbia, p. 365-372.

Hay and Company Consultants Inc.
1994: Fraser River sand borrow study; Fraser River Harbour Commission, Vancouver, British Columbia, 39 p.
1995: Channel maintenance management study, lower Fraser River; Canadian Coast Guard, Public Works and Government Services Canada, Vancouver, British Columbia, 3 v., 140 p.
1996: Erosion at Roberts Bank, geophysical evaluation; Vancouver Port Corporation, Vancouver, British Columbia, 24 p.

Hebda, R.J.
1977: The paleoecology of a raised bog and associated deltaic sediments of the Fraser River delta; Ph.D. thesis, University of British Columbia, Vancouver, British Columbia, 202 p.

Johnston, W.A.
1921: Sedimentation of the Fraser River delta; Geological Survey of Canada, Memoir 125, 46 p.

Kostaschuk, R.A. and Macdonald, G.M.
1988: Multi-track surveying of large bedforms; Geo-Marine Letters, v. 8, p. 57-62.

Kostaschuk, R.A., Church, M.A., and Luternauer, J.L.
1992a: Sediment transport over salt wedge intrusions: Fraser River estuary, Canada; Sedimentology, v. 39, p. 305-317.

Kostaschuk, R.A., Luternauer, J.L., Barrie, J.V., LeBlond, P.H., and Werth von Deichmann, L.
1995: Sediment transport by tidal currents and implications for slope stability: Fraser River delta, British Columbia; Canadian Journal of Earth Sciences, v. 32, p. 852-859.

Kostaschuk, R.A., Luternauer, J.L., and Church, M.A.
1998: Sedimentary processes in the estuary; in Geology and Natural Hazards of the Fraser River Delta, British Columbia, (ed.) J.J. Clague, J.L. Luternauer, and D.C. Mosher; Geological Survey of Canada, Bulletin 525, this volume.

Kostaschuk, R.A., Luternauer, J.L., McKenna, G.T., and Moslow, T.F.
1992b: Sediment transport in a submarine channel system: Fraser River delta, Canada; Journal of Sedimentary Petrology, v. 62, p. 273-282.

Liedtke, J., Roberts, A., and Luternauer, J.
1995: Practical remote sensing of suspended sediment concentration; Photogrammetric Engineering & Remote Sensing, v. 61, p. 167-175.

Luternauer, J.L.
1976: Fraser River Delta sedimentation, Vancouver, B.C.; in Report of Activities, Part A; Geological Survey of Canada, Paper 76-1A, p. 213-219.
1980: Genesis of morphologic features on the western delta front of the Fraser River, British Columbia - status of knowledge; in The Coastline of Canada, Littoral Processes and Shore Morphology, (ed.) S.B. McCann; Geological Survey of Canada, Paper 80-10, p. 381-396.

Luternauer, J.L. and Finn, W.D.L.
1983: Stability of the Fraser River delta front; Canadian Geotechnical Journal, v. 20, p. 606-616.

Luternauer, J.L., Atkins, R.J., Moody, A.I., Williams, H.F.L., and Gibson, J.W.
1995: Salt marshes; Chapter 11 in Geomorphology and Sedimentology of Estuaries, (ed.) G.M.E. Perillo; Elsevier Science B.V., Developments in Sedimentology, 53, p. 307-332.

Luternauer, J.L., Barrie, J.V., Christian, H.A., Clague, J.J., Evoy, R.W., Hart, B.S., Hunter, J.A., Killeen, P.G., Kostaschuk, R.A., Mathewes, R.W., Monahan, P.A., Moslow, T.F., Mwenifumbo, C.J., Olynyk, H.W., Patterson, R.T., Pullan, S.E., Roberts, M.C., Robertson, P.K., Tarbotton, M.R., and Woeller, D.J.
1994: Fraser River delta: geology, geohazards and human impact; in Geology and Geological Hazards of the Vancouver Region, Southwestern British Columbia, (ed.) J.W.H. Monger; Geological Survey of Canada, Bulletin 481, p. 197-220.

McKenna, G.T. , Luternauer, J.L., and Kostaschuk, R.A.
1992: Large-scale mass wasting events on the Fraser River delta front near Sand Heads, British Columbia; Canadian Geotechnical Journal, v. 29, p. 141-156.

McLaren, P. and Ren, P.
1995: Sediment transport and its environmental implications in the lower Fraser River and Fraser delta; Environment Canada, Environmental Conservation, DOE FRAP 1995-03, 44 p.

Medley, E.
1978: Dendritic drainage channels and tidal flat erosion, west of Steveston, Fraser River delta, British Columbia; B.Sc. thesis, University of British Columbia, Vancouver, British Columbia, 70 p.

Monahan, P.A., Luternauer, J.L., and Barrie, J.V.
1993: A delta plain sheet sand in the Fraser River delta, British Columbia, Canada; Quaternary International, v. 20, p. 27-38.

Mosher, D.C. and Hamilton, T.S.
1998: Morphology, structure, and stratigraphy of the offshore Fraser delta and adjacent Strait of Georgia in Geology and Natural Hazards of the Fraser River Delta, British Columbia, (ed.) J.J. Clague, J.L. Luternauer, and D.C. Mosher; Geological Survey of Canada, Bulletin 525, this volume.

Nichols, M.M. and Biggs, R.B.
1985: Estuaries; in Coastal Sedimentary Environments, (ed.) R.A. Davis; Springer-Verlag, Toronto, Ontario, p. 77-186.

North, M.E.A. and Teversham, J.M.
1984: The vegetation of the floodplains of the lower Fraser, Serpentine and Nicomekl Rivers, 1859 to 1890; Syesis, v. 17, p. 47-66.

Pharo, C.H. and Barnes, W.C.
1976: Distribution of surficial sediments of the central and southern Strait of Georgia, British Columbia; Canadian Journal of Earth Sciences, v. 13, p. 684-696.

Shepard, F.P. and Milliman, J.D.
1978: Sea-floor currents on the foreset slope of the Fraser River delta, British Columbia (Canada); Marine Geology, v. 28, 245-251.

Styan, W. B. and Bustin, R.M.
1983: Sedimentology of Fraser River delta deposits: a modern analogue for some deltaic coals; International Journal of Coal Geology, v. 3, p. 101-143. Reprinted (1984) in Sedimentology of Coal and Coal-Bearing Sequences, (ed.) R.A. Rahmani and R.M. Flores; International Association of Sedimentologists, Special Publication 7, p. 241-271.

Swinbanks, D.D.
1979: Environmental factors controlling floral zonation and the distribution of burrowing and tube-dwelling organisms on Fraser Delta tidal flats, British Columbia; Ph.D. thesis, University of British Columbia, Vancouver, British Columbia, 273 p.

Swinbanks, D.D. and Murray, J.W.
1981: Biosedimentological zonation of Boundary Bay tidal flats, Fraser River delta, British Columbia; Sedimentology, v. 28, p. 201-237.

Tabata, S.
1972: The movement of Fraser River-influenced surface water in the Strait of Georgia as deduced from a series of aerial photographs; Canada Department of Environment, Marine Sciences Branch, Pacific Marine Science Report 72-6, 69 p.

Tabata, S., Giovando, L.F., and Devlin, D.
1971: Current velocities in the vicinity of the Greater Vancouver Sewerage and Drainage District's Iona Island outfall - 1968; Fisheries Research Board of Canada, Technical Report, 263, 110 p.

Tarbotton, M. and Harrison, P.G.
1996: A review of the recent physical and biological development of the southern Roberts Bank seagrass system, 1950 - 1994; report prepared for Roberts Bank Environmental Review Committee by Triton Consultants Ltd., Vancouver, British Columbia, 48 p.

Thomson, R.E.
1975: Longshore current generation by internal waves in the Strait of Georgia; Canadian Journal of Earth Sciences, v. 12, p. 472-488.
1981: Oceanography of the British Columbia coast; Canada Department of Fisheries and Oceans Canada, Canadian Special Publication of Fisheries and Aquatic Sciences, no. 56, 291 p.

Williams, H.F.L. and Hamilton, T.S.
1994: Sedimentary dynamics of an eroding tidal marsh derived from stratigraphic records of ^{137}Cs fallout, Fraser delta, British Columbia, Canada; Journal of Coastal Research, v. 11, p. 1145-1156.

Sedimentary processes in the estuary

R.A. Kostaschuk[1], J.L. Luternauer[2], and M.A. Church[3]

Kostaschuk, R.A., Luternauer, J.L., and Church, M.A., 1998: Sedimentary processes in the estuary; in Geology and Natural Hazards of the Fraser River Delta, British Columbia, (ed.) J.J. Clague, J.L. Luternauer, and D.C. Mosher; Geological Survey of Canada, Bulletin 525, p. 41–56.

Abstract: The lower Main Channel of the Fraser River estuary is now trained and fixed in position, but most of the flow could switch to the steeper Canoe Passage distributary. When river discharge is low and the tide is high, salt water intrudes into the channel to form a salt wedge. Currents are weak at this time and small amounts of sand are deposited at the salt-wedge tip. Some mud settles to form a turbidity maximum in the salt wedge, but most is transported seaward in a low-energy plume at the river mouth. High river discharge and low tide force the salt wedge out of the channel, producing strong currents and large amounts of sand in suspension. Mud is transported in a high-energy plume, but most sand is deposited on a bar. Mass flows at the river mouth transport sand down the delta slope in a submarine channel.

Résumé : Dans l'estuaire du fleuve Fraser, le cours inférieur du chenal principal a été redressé et ne bouge pas, mais il se peut quand même que la majeure partie de l'écoulement soit détourné vers le défluent à plus fort gradient du passage Canoe. Lorsque le débit du fleuve est faible et que la marée est haute, l'eau salée remonte dans le chenal pour former une lame. Les courants sont alors faibles et de petites quantités de sable sont déposées à l'extrémité de la lame d'eau salée. Une certaine quantité de boue se dépose et la turbidité est maximale dans la lame d'eau salée; cependant, la majeure partie de la boue est transportée vers la mer dans un panache à faible énergie à l'embouchure du fleuve. Lorsque le débit du fleuve est élevé et que la marée est basse, la lame d'eau salée est poussée vers l'extérieur du chenal produisant des courants forts et charriant de grandes quantités de sable en suspension. La boue est transportée dans un panache à forte énergie, mais presque tout le sable se dépose sur un banc. Le débit massique à l'embouchure du fleuve est tel qu'il transporte du sable vers le bas du talus deltaïque par l'intermédiaire d'un chenal sous-marin.

[1] Department of Geography, University of Guelph, Guelph, Ontario N1G 2W1
[2] Geological Survey of Canada, 605 Robson Street, Vancouver, British Columbia V6B 5J3
[3] Department of Geography, University of British Columbia, Vancouver, British Columbia V6T 1Z2

INTRODUCTION

An estuary is an inlet of the sea extending into a river valley as far as the upper limit of tidal influence (Fairbridge, 1980). Extending the notion of an 'inlet of the sea' to include river mouths, the estuary of Fraser River is the reach of the river between the Strait of Georgia and the upstream limit of the tide. During low river discharge, the tidal influence reaches 120 km upstream to Chilliwack, but during high river discharge it only reaches Mission, 75 km upstream from the Strait of Georgia (Thomson, 1981). The Fraser Estuary is usually operationally defined, however, as extending 55 km upstream to Kanaka Creek (Fig. 1A). The estuary is composed of the major distributary channels, Main Channel, North Arm, and Middle Arm, and a number of smaller distributary channels and tributary creeks (Fig. 1A). Main Channel has a sandy bed, North Arm has a muddy sand floor, and Middle Arm has a predominantly mud bed. Sand flats, mud flats, salt marshes, and tidal creeks are exposed at low tide along the margins of channels and on distributary islands. Salt water from Strait of Georgia intrudes into the lower reaches of estuary channels (Geyer and Farmer, 1989).

The Fraser Estuary is being profoundly affected by rapid industrial and urban growth, and many aspects of estuary management depend on our ability to describe and predict sedimentary processes. Large dunes in the lower reaches of Main Channel constitute a hazard to navigation (Kostaschuk et al., 1989a) and maintenance dredging is an ongoing activity. Deposition of sandy bed material at the mouth of Main Channel contributes to mass movements that may threaten coastal engineering structures (Kostaschuk and Atwood, 1990; McKenna et al., 1992; Christian et al., 1995). Contaminants

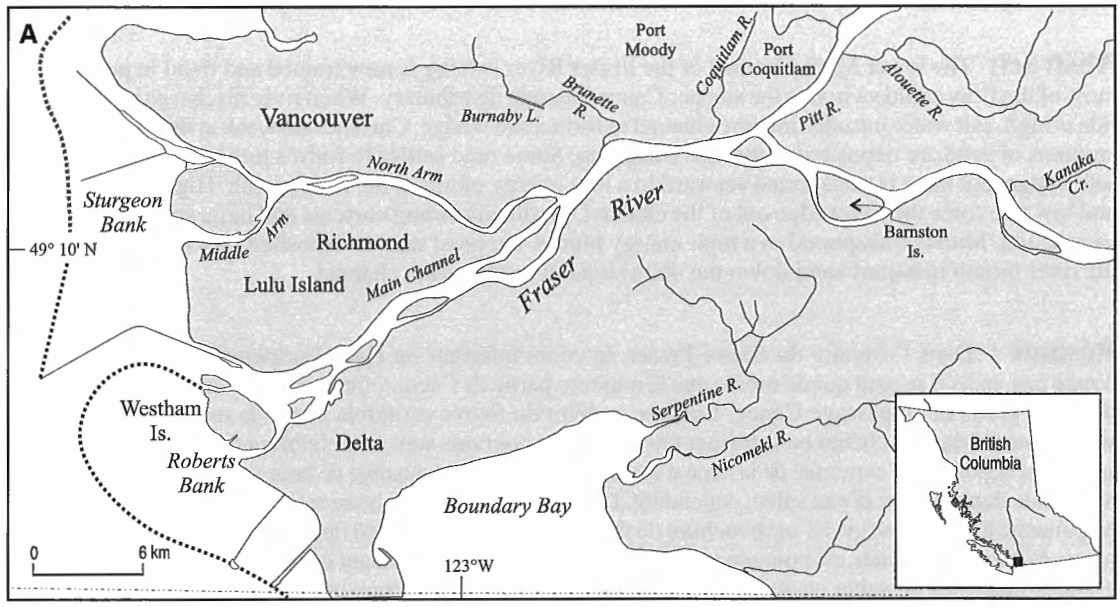

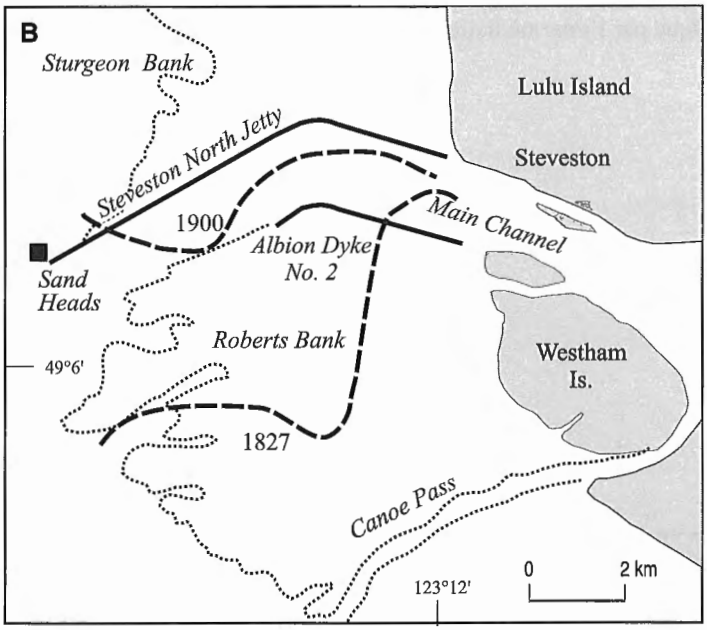

***Figure 1. A)** Fraser Estuary channels. **B)** Lower Main Channel. Channel positions in 1827 and 1900 are from Clague et al. (1983). The dotted line is the lowest normal water level (0 m).*

enter the estuary from several sources, including pulp mills and other industrial and municipal outfalls. Many contaminants are adsorbed on fine-grained sediment particles in suspension and are deposited in the estuary (Servizi, 1989; Venditti, 1995). Some toxins pass through the food chain and have been found in elevated levels in birds, mammals, and fish in the estuary (Servizi, 1989).

This paper is a summary of recent research on sedimentary processes in the lower Main Channel (Fig. 1B), the largest of the delta's distributaries. Our review includes the fluvial and marine conditions that affect the estuary, channel morphology and position, river and tidal effects on suspended sediment, the transport of sand and development of bedforms, salt-wedge sedimentation, sediment dynamics and mass movements at the river mouth, and a classification of the estuary. A conceptual model is used to summarize sedimentary processes in Main Channel.

FLUVIAL AND MARINE FRAMEWORK

The Fraser River is the largest river on the west coast of Canada. It is over 1200 km long and drains 250 000 km^2 of mountainous terrain in southern British Columbia. Mean annual discharge at Mission is 3400 m^3/s and daily discharge has a pronounced seasonal pattern (Fig. 2). In autumn, winter, and early spring, discharge is low, with minimum values around 1000 m^3/s. Rainstorm events can cause short-term increases in discharge during this period. Late spring and early summer are dominated by a snowmelt freshet of 6000-12 000 m^3/s. Discharges are moderate in late summer.

Sediment loads in the river can be divided into wash load and bed-material load. Wash load is clay, silt, and very fine-grained sand that is transported long distances in continuous suspension. It is not found in appreciable quantities on the bed. The coarser-grained bed-material load is transported episodically in suspension or along the bottom as bed load. McLean and Church (1986) suggest that the particle-size boundary between wash load and bed-material load at Mission is 0.125 mm. The concentration of suspended sediment at Mission, most of which is wash material, follows a similar annual pattern to discharge, but usually peaks before discharge during the freshet (Fig. 2). The post-peak decline in sediment concentration is more rapid compared to discharge, reaching pre-freshet values by July. The lag, or hysteresis, between discharge and concentration reflects the decline in the supply of wash load over the freshet season (Milliman, 1980). Wash load is derived directly from high banks along the river which are weathered by frost action during the winter. This material is quickly entrained in the spring, after which the supply of easily eroded sediment quickly declines, producing the lag effect. The Fraser River supplies an average of 17.3 million tonnes of sediment annually to the delta in the Strait of Georgia (McLean and Tassone, 1991). Thirty-five percent of this load is sand, a consequence of an energetic river emerging from a mountainous interior close to the sea. The Fraser delta is exceptional among large deltas for the high proportion of sand it delivers to the sea (Orton and Reading, 1993).

The Strait of Georgia is a semienclosed, high-energy marine basin. Waves in the Strait are fetch-limited with maximum significant heights of 2.1 m on Sturgeon Bank and 2.7 m on Roberts Bank (Thomson, 1981) (Fig. 1). Tides are primarily mixed, semidiurnal with a mean range of 3.1 m near the mouth of Main Channel. Distinct inequalities exist in the heights of the two high and low tides each day (Fig. 3). Differences in tidal range also occur fortnightly, with spring tides approaching 5 m and neap tides of the order of 2 m. Tidal range in Main Channel decreases both upstream of the river mouth and with increasing river discharge. Salt water intrudes from the Strait of Georgia into the lower estuary. The term 'salt wedge' is usually used to describe the salinity intrusion in Main Channel.

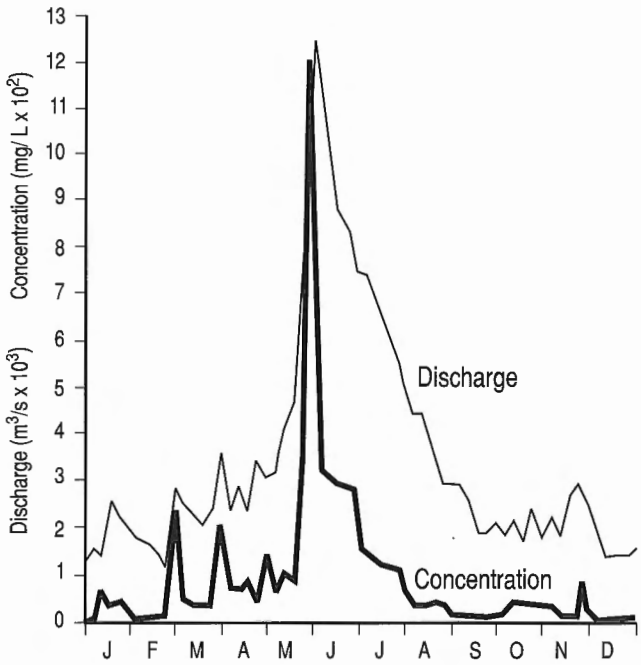

Figure 2. Daily mean discharge and suspended-sediment concentration for Fraser River at Mission, 1986. Data from the Water Survey of Canada.

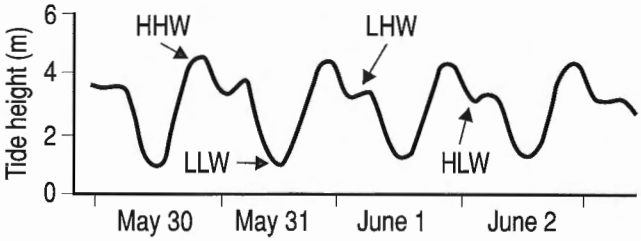

Figure 3. Tidal curve at Point Atkinson for selected days in 1987. HHW – higher high water, LHW – lower high water, HLW – higher low water, LLW – lower low water. Data from the Canadian Hydrographic Service.

CHANNEL MORPHOLOGY AND POSITION

The Main Channel upstream of Steveston has been remarkably stable in position during the late Holocene (Clague et al., 1983) and construction of dykes during the last century has prevented recent movement (Fig. 1A). In contrast, the channel downstream from Steveston shifted continuously over the tidal flats of Roberts Bank (Fig. 1B) prior to construction of the Steveston Jetty between 1911 and 1932. Early in the nineteenth century, the mouth of the channel was much further south and the orientation of a meander bend indicates that the channel was migrating to the south. By the end of the century, the channel had moved north close to its present position, with a meander bend in the same position as the bend in Steveston Jetty. There was also a second bend trending in the opposite direction just north of Sand Heads. Construction of the Steveston Jetty and Albion Dyke No. 2 has fixed the position of the channel. These structures maintained the upstream bend in the channel but removed the downstream bend, replacing it with a straight reach. This has important implications for the more recent behaviour of the channel.

Kostaschuk and Luternauer (1987) examined patterns of erosion and deposition in Main Channel and found intense scour on the outside of the bend at the base of the Steveston Jetty. They also found evidence of deposition across the channel on the inside of the bend where a large point bar had developed. These patterns are consistent with the behaviour of a meandering channel, although a natural channel would migrate toward the north. Kostaschuk and Luternauer (1987) also found deposition along the straight reach of the Steveston Jetty halfway between the bend and Sand Heads. They suggest that this may represent development of an incipient point bar similar in position to the one that existed in 1900 (Fig. 1B).

Deltaic distributary channels are highly unstable and channel switching is a common occurrence (e.g. Orton and Reading, 1993). McLaren and Ren (1995) believe that the flow presently following the Main Channel could be captured by Canoe Passage (Fig. 1B) because the distance to the Strait of Georgia is 2 km shorter. They point out that the emphasis in river control is to avoid the diversion of flow into Canoe Passage, but engineering control will become increasingly expensive as Main Channel extends further into the Strait. A major channel switch would have profound implications for navigation and for biotic and sedimentary environments on Roberts Bank.

RIVER AND TIDAL EFFECTS ON SUSPENDED SEDIMENT TRANSPORT

The Fraser River supplies large amounts of sand to the estuary, and the bed of Main Channel is composed almost entirely of sand. The sand has a mean particle size of 0.25-0.35 mm that varies little seasonally (Kostaschuk et al., 1989a; Kostaschuk and Ilersich, 1995; Villard, 1995). Villard (1995) examined particle-size distributions of suspended sediment in Main Channel and found that most samples were bimodal (Fig. 4). The coarse mode is interpreted as sandy bed material eroded episodically from the estuary floor, and the fine mode is wash load in continuous suspension. Erosion, transport, and deposition of suspended sediment in the estuary is controlled by a combination of river and tidal conditions.

Kostaschuk et al. (1989b) found that spatial and temporal variations in salinity and velocity in the estuary are controlled by river discharge, tidal height, and the position of the salt wedge (Fig. 5). The salt wedge is apparent at high tide in May and June near Sand Heads, and at Steveston in May (Fig. 1B). High river discharge in June prevents the salt wedge from migrating up river to Steveston. As the tide falls, the salt wedge is flushed downstream of Sand Heads and flow is unstratified at low tide. Currents are weak at high tide, and when the salt wedge is present, the fresh surface layer flows downstream. Slower currents in the lower layer are directed upstream at high tide. The full water column flows downstream during the falling tide and the velocity peaks just before low tide. In May, the rising tide produces a rapid deceleration of downstream currents, followed by weak upstream flow of the entire water column. Flow is downstream over the full tidal cycle in June at Steveston.

Suspended-sediment concentration is also related to river discharge, tides, and the salt wedge (Kostaschuk and Luternauer, 1989; Kostaschuk et al., 1989b). In the example shown in Figure 6, concentration at high tide is extremely low regardless of river discharge, except for June 8. The absence of the salt wedge at Steveston on June 8 resulted in unstratified flow and strong downstream velocities that kept sediment in suspension from the previous low tide. Flow becomes unstratified and accelerates as the tide falls, resulting in high concentrations of sandy bed material in suspension (e.g. Kostaschuk and Luternauer, 1989). Concentration remains relatively high as the tide begins to rise, then decreases rapidly to low values at high tide.

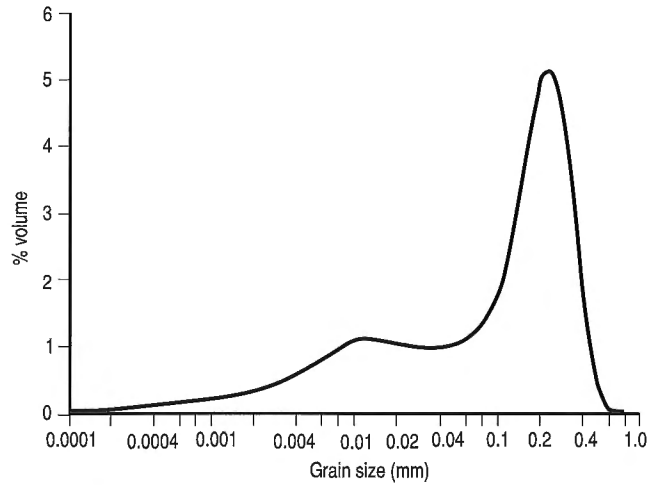

Figure 4. *Particle-size distribution for a pump sample taken 1 m above the bed in Main Channel near Steveston on June 21, 1994 (modified from Villard (1995)).*

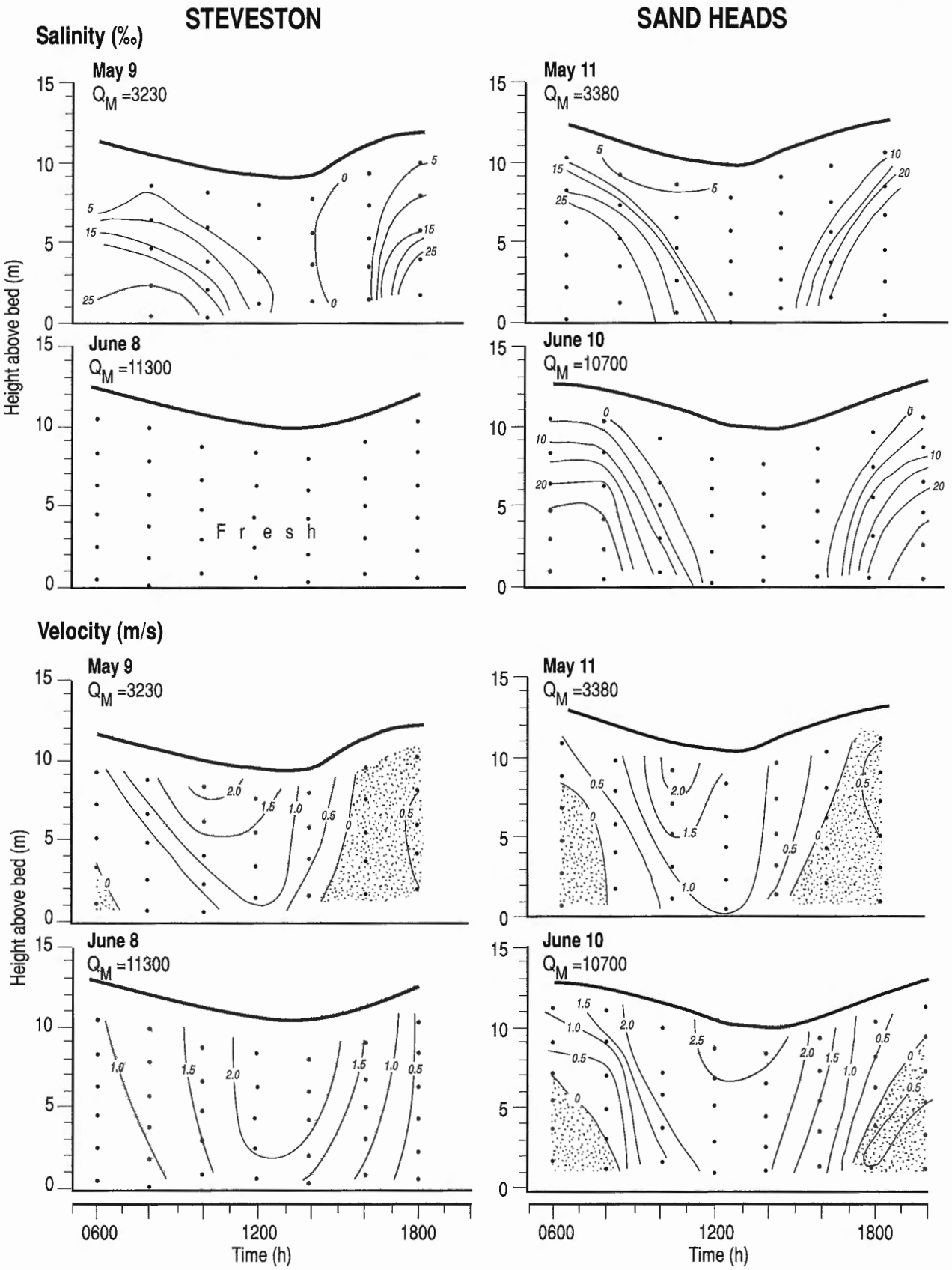

Figure 5. Salinity and velocity contours from anchor stations near Steveston and Sand Heads (Fig.1) in 1986. Q_M is mean daily discharge (m^3/s) at Mission. The stippled velocities represent upstream flow (modified from Kostaschuk et al. (1989b)).

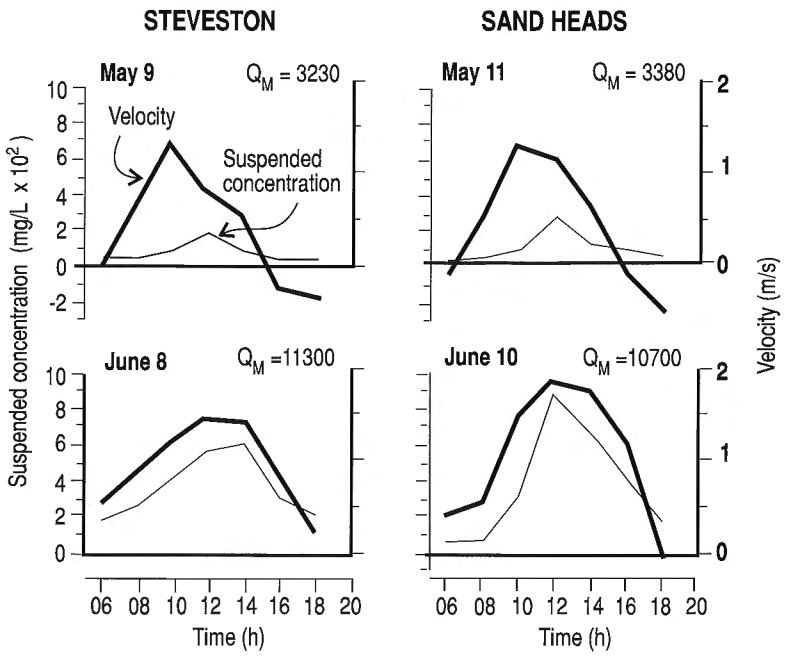

Figure 6.

Mean cross-sectional velocity and suspended sediment concentration near Steveston and Sand Heads (Fig. 1) in 1986. Q_M is mean daily discharge (m^3/s) at Mission. Tidal stage is illustrated in Figure 5 (modified from Kostaschuk et al. (1989b)).

Kostaschuk et al. (1989b) found that seasonal sediment concentration is lower than expected in July and September when river discharge is falling. In addition, peak concentration occurs after the peak in velocity over tidal cycles. The seasonal time-lag is referred to as fluvial hysteresis, and the tidal effect as tidal hysteresis. Fluvial hysteresis is clockwise, with the peak in sediment concentration preceding the peak in discharge (Fig. 2). Tidal hysteresis is counterclockwise (Fig. 7), with the peak in concentration following the peak in velocity (Fig. 6). This effect results from continued suspension of bed material after velocity begins to decrease, possibly because of high turbulence.

BEDFORMS AND BED-MATERIAL TRANSPORT

Sandy bed material in Main Channel is transported primarily during the period of unstratified flow surrounding low tide when river discharge is high. The current is strong and is directed downstream (Fig. 6). Bed material is moulded into large dunes that migrate downstream (Kostaschuk et al., 1989a). Recent surveys, however, suggest that upstream flows during low river discharge can generate small dunes that migrate upstream (Luternauer et al., 1998).

Dune morphology

Kostaschuk and MacDonald (1988) mapped the three-dimensional morphology of a group of large dunes near Sand Heads and described dunes with curved, concave-downstream planforms and depressions on crests and troughs. Some dunes appeared to be migrating over and burying smaller, possibly inactive, features. Dunes can exceed 5 m in height and 100 m in length in the estuary, but mean dune height is typically 1-2 m and mean length is 20-50 m (Pretious and Blench, 1951; Kostaschuk et al., 1989a; Kostaschuk and Ilersich, 1995) (Fig. 8). Dune size varies in a complex fashion with changes in flow velocity associated with river discharge and tidal conditions. Allen (1973) used surveys of Pretious and Blench (1951) to describe hysteresis in the relation between dunes and river flow. He found that dune height and length follow, but lag behind, seasonal changes in river discharge. Kostaschuk et al. (1989b) described the same pattern in later surveys (Fig. 9). Kostaschuk and Ilersich (1995) found a similar lag with weekly variations in tidal range. Bedform hysteresis is attributed to changes in bedform size and composition related to changing sediment transport rates (e.g. Allen, 1983). Time is required for sand within dunes to be remoulded into smaller or larger features that approach equilibrium with flow velocity. Larger dunes respond more slowly to changes in velocity because they contain more sediment.

Flow and sediment transport over dunes

Most dunes described in the literature (e.g. Allen, 1983) are dominated by bed-load transport and have lee-side flow separation and reversed flow. Velocity profiles over dunes in Main Channel (Fig. 10), however, provide no evidence for lee-side flow separation. Smith and McLean (1977) believe that similar dunes without flow separation in Columbia River, Washington, occur when sediment transport in suspension dominates over bed load. They suggest that suspended sand settles in the dune trough, reducing the lee-side angle and preventing the formation of a separation zone. Kostaschuk and Ilersich (1995) used data from dunes in Main Channel (Fig. 10) to test the hypothesis of suspension domination. They found that approximately 5% of the sediment trapped within migrating dunes is bed load and the remainder is deposited from suspension, confirming the hypothesis.

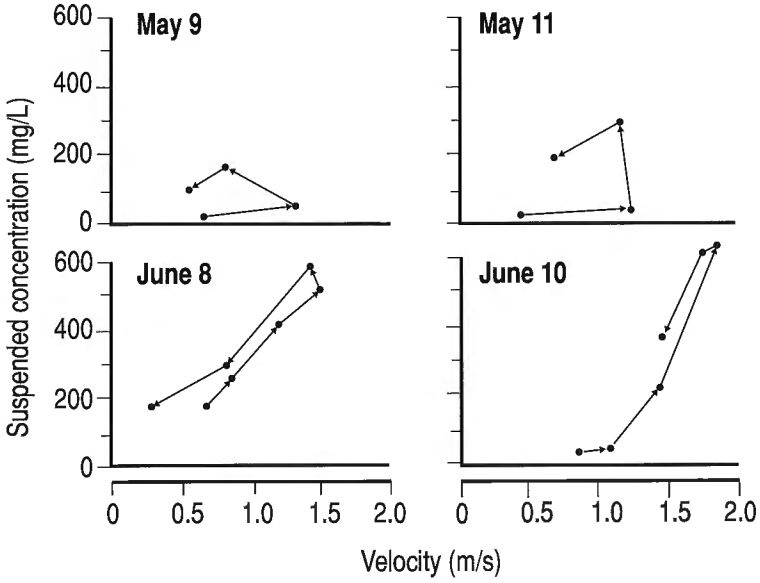

Figure 7.

Phase diagrams illustrating counterclockwise hysteresis in suspended-sediment concentration over tidal cycles in 1986 (modified from Kostaschuk et al. (1989b)).

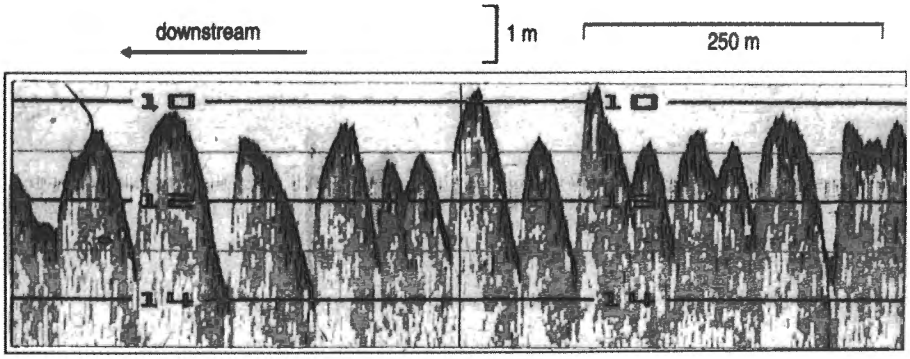

Figure 8. *Echo-sounding profile of dunes near Sand Heads on June 25, 1986.*

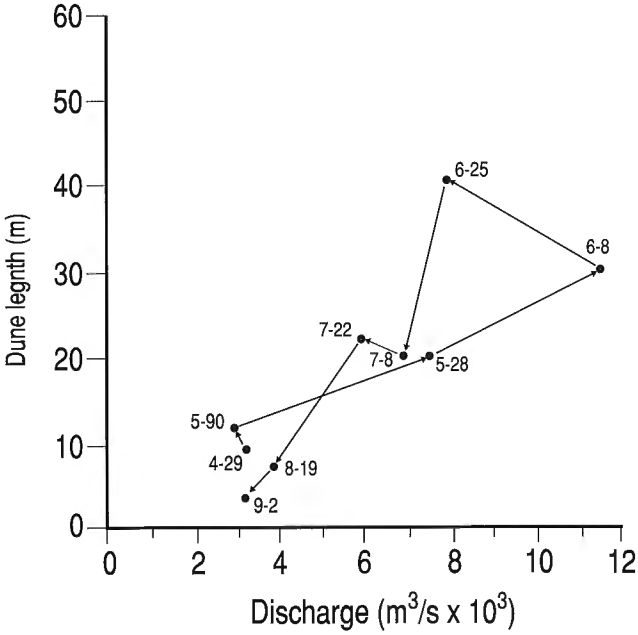

Figure 9.

Phase diagram of mean dune length near Steveston versus mean daily discharge at Port Mann Bridge in 1986. Numbers refer to the date (month-day) (modified from Kostaschuk et al. (1989a)).

Kostaschuk and Villard (1996a) classify dunes in Fraser estuary as symmetric (Fig. 10: June 21) and asymmetric (Fig. 10: June 27). Symmetric dunes have stoss and lee sides of similar length, stoss and lee slope angles less than 8°, and rounded crests. Asymmetric dunes have superimposed small dunes on stoss sides, sharp crests, stoss sides longer than lee sides, stoss side slopes less than 3°, and straight lee-side slopes up to 19°. Kostaschuk and Villard (1996a) suggest that dune symmetry and crest rounding of symmetric dunes are associated with high bed-material transport rates. High near-bed velocity and bed-load transport near dune crests result in crest rounding. Long, low-angle lee sides are produced by deposition of suspended sediment in dune troughs. Asymmetric dunes appear to be transitional features between large symmetric dunes and smaller dunes which have adjusted to lower flow-velocity and sediment-transport conditions. Small dunes on stoss sides reduce near-bed flow velocity and bed-load transport, causing a sharper dune crest. Bed load transported within the small dunes up the stoss side of asymmetric dunes likely accumulates at the crest of the main dune and avalanches down the lee side. Reduced deposition of suspended sediment in troughs results in a short, steeper lee slope.

Several criteria have been used to construct bedform diagrams defining stability fields for sandy bedforms such as ripples, dunes, plane bed, and antidunes (for a recent review, see Reid and Frostick, 1994). Bed configuration is generally characterized by sediment size and a measure of flow strength. These diagrams are based almost entirely on flume

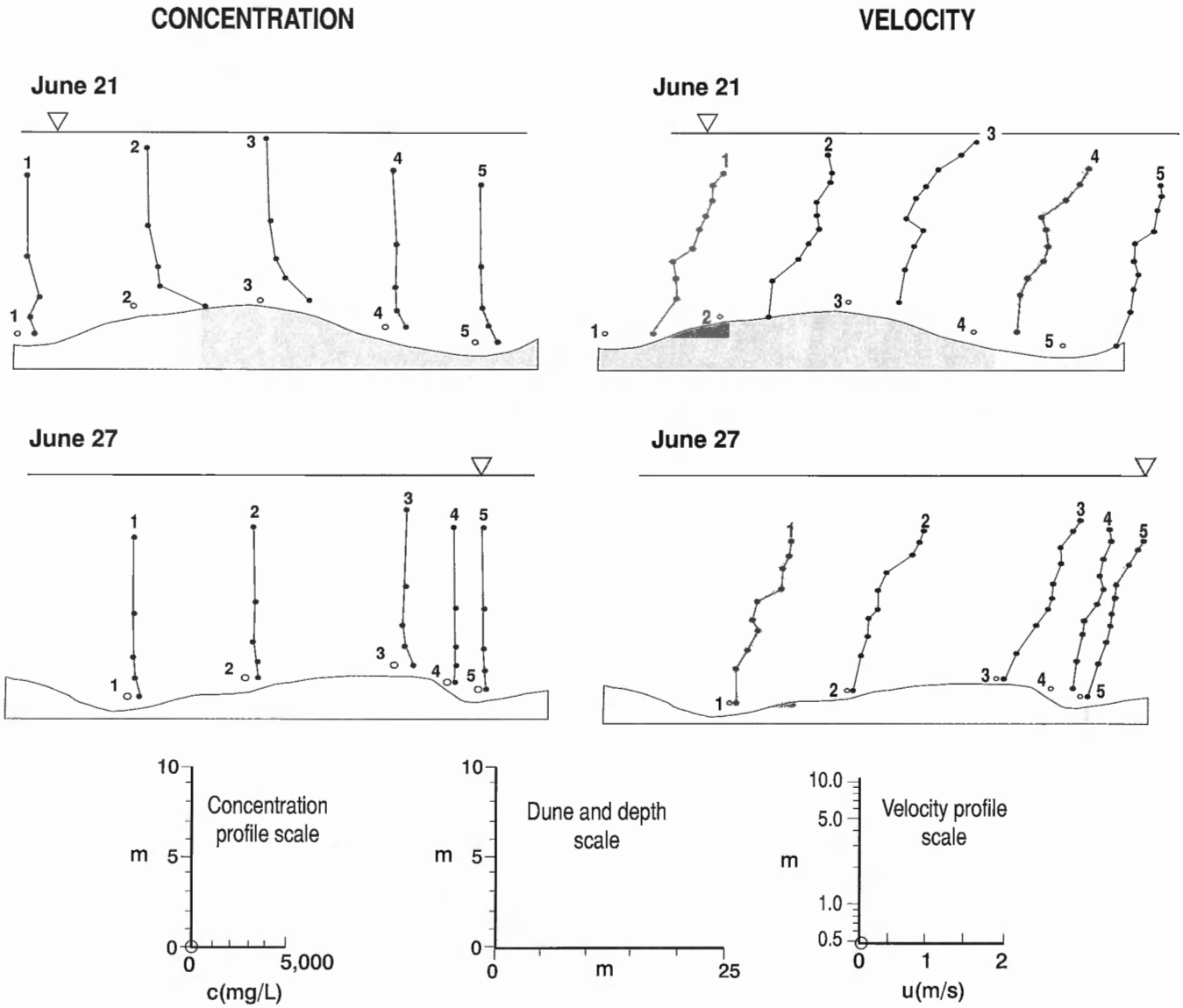

Figure 10. Velocity and suspended bed-material concentration profiles over dunes near Steveston in 1989. June 21 represents a symmetric dune, June 27 an asymmetric dune (modified from Kostaschuk and Villard (1996a)).

data, yet are commonly used to model flow-sediment-bedform relations in natural settings. Kostaschuk and Villard (1996a) plotted Fraser dunes on several diagrams and found that the bedforms fell into upper plane bed or antidune stability fields. There are at least two explanations for this. First, conventional stability diagrams based on flume studies may not apply to large dunes in deep natural flows. Perhaps it is not possible to scale down sedimentary processes in large rivers to small flumes. Second, dunes may not reach equilibrium with the flow during the relatively short period of bed-material transport around low tide. Additional research is required to resolve this issue.

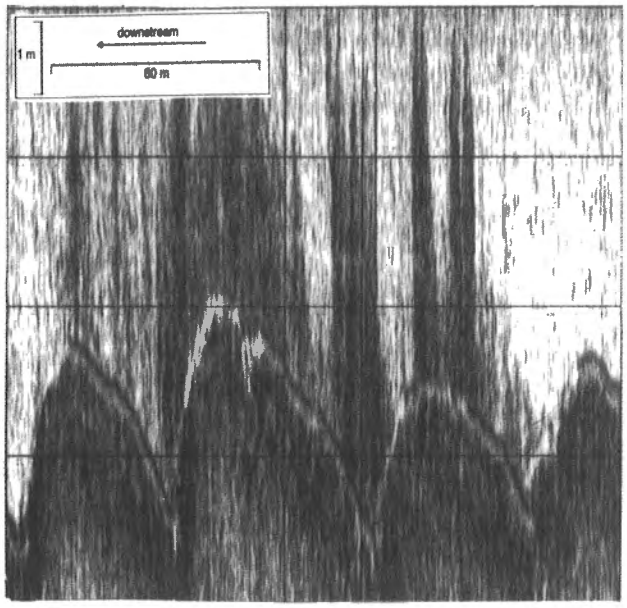

Figure 11. *Acoustic flow visualization of suspended-sediment events generated by dunes near Steveston on June 27, 1990.*

Turbulence and bed-material suspension

Turbulence is evident at the surface of most river and estuary flows as boils: circular patches of upwelling fluid (Best, 1993). Boils usually contain higher concentrations of suspended bed material than the surrounding flow (Rood and Hickin, 1989), showing that they are produced by turbulence originating at the bed. Matthes (1947) proposed that boils are the surface manifestation of vortices that he called 'kolks', an interpretation supported by Jackson (1976). Soundings in Main Channel using a high-resolution echo sounder have revealed acoustic 'clouds' in the flow (Fig. 11, 12). The clouds are interpreted as turbulent flow structures containing high concentrations of suspended bed material, possibly similar to Matthes' kolks (Kostaschuk and Church, 1993; Villard, 1995). Most of these suspension structures originate on the lower stoss sides of dunes, but some occur directly above dune crests (Fig. 11).

Soundings have also been used to examine time series of acoustic clouds passing an anchored research vessel (Fig. 12). These events are believed to be linked to the suspension structures generated over dunes (Fig. 11). Suspension structures appear to lift from the bed and rise to the surface as they migrate downstream, generating boils at the surface (Kostaschuk and Church, 1993). Kostaschuk and Villard (1996b) examined periods between events for several acoustic time series and found that they were randomly distributed over time in most cases. This implies that suspension structures are generated periodically and randomly at the bed.

SALT-WEDGE SEDIMENTARY PROCESSES

Salt-wedge position and channel deposition

The position of the salt wedge (Fig. 13) that migrates from the Strait of Georgia into Main Channel is primarily a function of river discharge and tidal height (Hughes and Ages, 1975; Hodgins et al., 1977; Ages, 1979). Ward (1976) determined

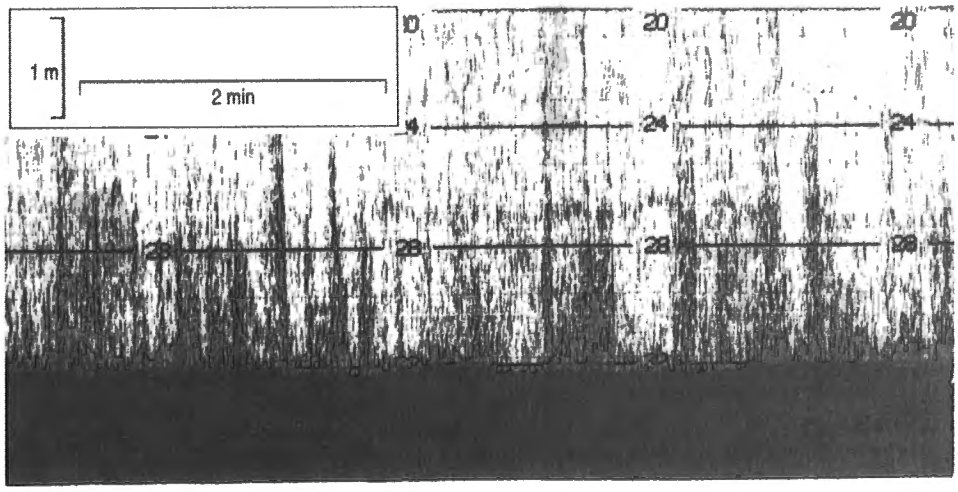

Figure 12. *Acoustic flow visualization time series taken at an anchor station near Steveston on June 17, 1992.*

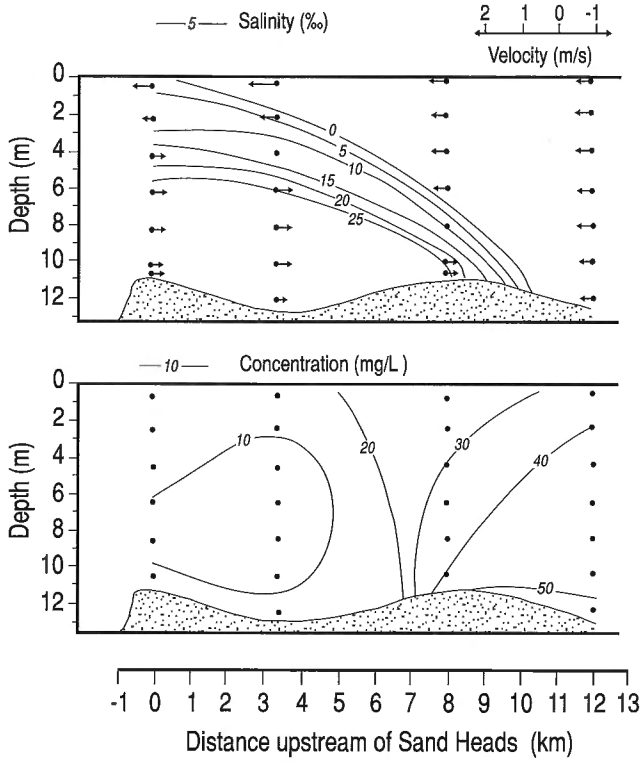

Figure 13. *Flow and suspended-sediment concentration at high tide on July 6, 1987. Downstream is to the left (modified from Kostaschuk et al. (1992a)).*

the effect of river discharge in Main Channel by examining the position of the wedge at the same high tide each lunar month, thus standardizing the tidal effect. He found a strong inverse relation between river discharge and the distance the salt wedge intrudes upstream. Kostaschuk and Atwood (1990) extended Ward's analysis to include both river discharge and tidal controls on salt-wedge position and developed an empirical, multiple-regression model for salt-wedge position. The model explains 85% of the variation in salt-wedge position, with discharge accounting for 44% and tidal height 41%.

Kostaschuk and Atwood (1990) used their model for salt-wedge position to predict patterns of bed-material deposition in Main Channel. They found that the salt wedge is consistently forced to the river mouth at Sand Heads during low tides below 1 m. The frequency of this occurrence increases with river discharge and thus is greatest in June. Bed-material transport is also greatest in June, so deposition in the channel should occur near the river mouth during this month. Surveys of bed erosion and deposition by Kostaschuk and Luternauer (1987) have confirmed this pattern. Persistent deposition occurred between April and September on the river-mouth bar at Sand Heads, with the greatest deposition in June. Deposition occurs on the bar because the flow is ramped up over salt water at the river mouth and bed material is rapidly deposited.

Suspended sediment transport above the salt wedge

Kostaschuk et al. (1992a) examined flow and suspended-sediment transport over the salt wedge in Main Channel at high tide (Fig. 13) and low tide (Fig. 14). At high tide, currents in the upper layer are weaker than those in the lower layer because the salt wedge moves upstream as the tide rises. In contrast, currents in the upper layer are stronger than those in the lower layer at low tide because flow accelerates and the salt wedge moves seaward as the tide falls. Both low- and high-tide observations show that the thickness of the upper layer decreases, and salinity and velocity increase, with distance downstream from the salt-wedge tip. The decrease in upper-layer thickness results from the downstream thickening of the salt wedge, and the increase in salinity is due to entrainment of saline water from the wedge. The slight downstream increase in velocity is related to the decrease in flow thickness, since the channel is confined by banks, jetties, and tidal flats (Fig. 1B) that restrict lateral expansion of the upper layer.

Kostaschuk et al. (1992a) found that suspended-sediment concentrations generally decrease seaward over the salt wedge. They suggest three reasons for this. First, the intrusion of the salt wedge interferes with sediment exchange between the flow and the bed (Kostaschuk and Luternauer, 1989). In unstratified flows, the transport of suspended bed material is intermittent, with continual exchanges of sediment between the bed and the water column. The salt wedge cuts off this exchange and sediment that is deposited is not replaced. Second, Kostaschuk and Church (1993) have shown that bed-material suspension in Main Channel is controlled by turbulence. When flow is stratified by the salt wedge, turbulence must work against buoyant forces. This causes a decrease in turbulent energy and, presumably, in suspended-sediment capacity. Third, salinity can cause fine-grained sediment to flocculate; the composite flocs have greater settling velocities than dispersed particles.

Kostaschuk et al. (1992a) developed a multiple-regression model to predict suspended-sediment concentration in the upper layer of the salt wedge. The model accounts for 66% of the variation in sediment concentration, with 30% of the variation explained by suspended-sediment concentration in the river, 11% by tidal height, and 25% by distance seaward along the salt wedge. The model shows that riverine processes and distance along the salt wedge are the primary controls of sediment concentration above the salt wedge.

RIVER-MOUTH PROCESSES

Plume

Outflow from Main Channel forms a plume in the Strait of Georgia (Stronach et al., 1988; Kostaschuk et al., 1993) (Fig. 15). Unstratified flow conditions occur at the river mouth when the salt wedge is pushed out of the channel and river water is in direct contact with the bed (Fig. 16A). Flow velocity during unstratified flow often exceeds 2 m/s at the mouth, and the velocity and thickness of the plume decrease seaward. Resuspension of sandy bed material occurs at the

mouth, and there are high concentrations of coarse-grained sediment in the plume (Fig. 17). When flow is stratified at the mouth (Fig. 16B), flow velocity is low and the plume is thin. Suspended sediment has already travelled over the salt wedge, resulting in low concentrations of fine-grained sediment (Fig. 17).

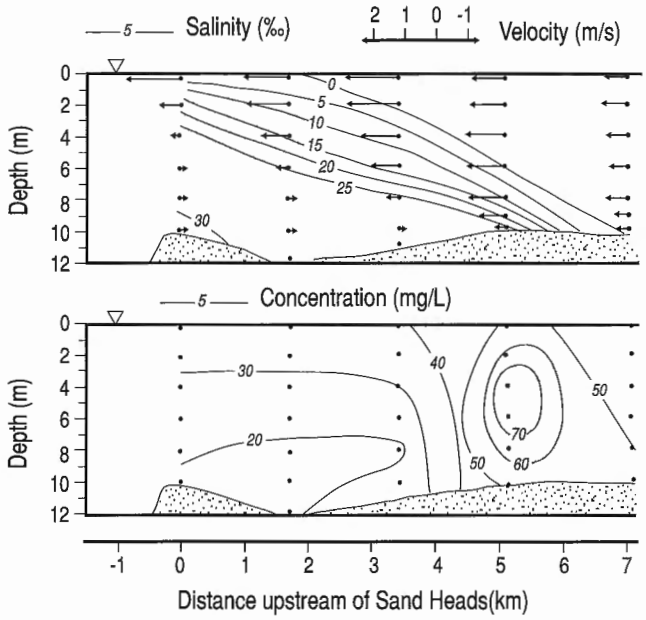

Figure 14. *Flow and suspended-sediment concentration at low tide on June 6, 1987. Downstream is to the left (modified from Kostaschuk et al. (1992a)).*

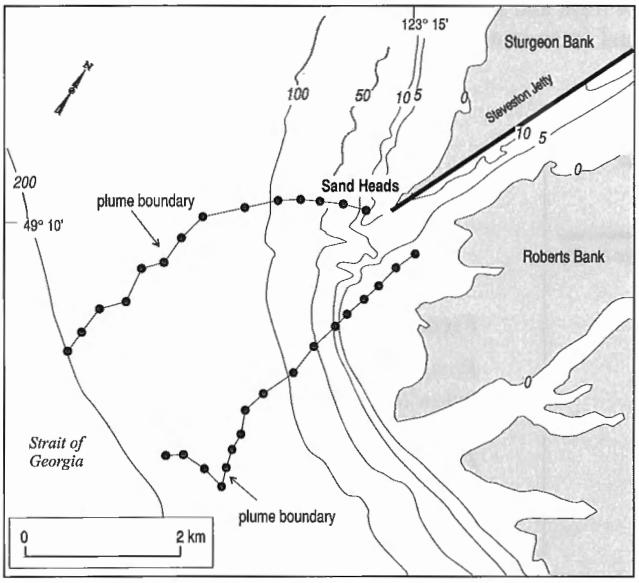

Figure 15. *Outline of the sediment plume at the river mouth on June 14, 1989. The plume edge was defined by taking microwave position fixes as the vessel ran along the plume boundary. Contours in metres below lowest normal low water (modified from Stephan (1990)).*

Concentrations of suspended sediment in the plume decline with distance seaward of the river mouth for three reasons (Kostaschuk et al., 1993). Water depth increases dramatically at the river mouth and the plume is not in contact with the bed, so sediment is not resuspended. Plume velocity and turbulence decrease seaward in the plume, reducing the ability of the flow to keep sediment in suspension. Flocculation of fine-grained sediment is enhanced in the saline water and the large flocs settle out of the plume.

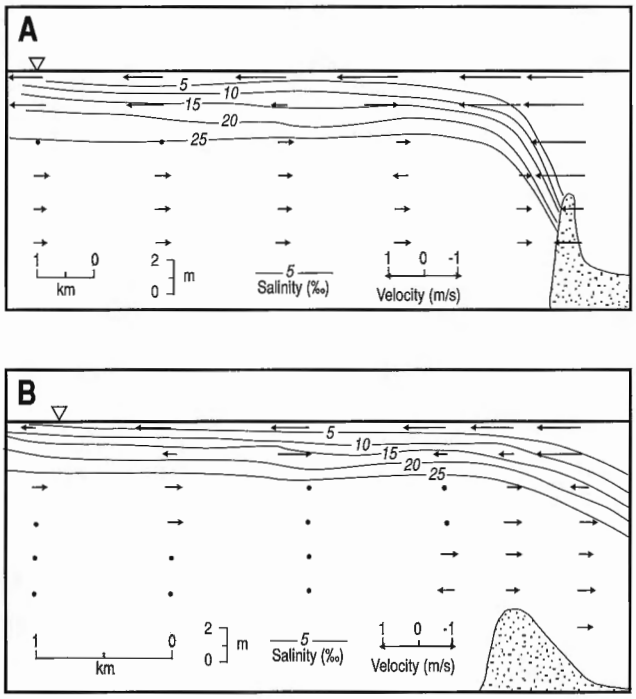

Figure 16. *Velocity and salinity in the centre of the plume during unstratified (**A**) and stratified (**B**) flow at the river mouth on May 20, 1989. Note the different horizontal scales (modified from Kostaschuk et al. (1993)).*

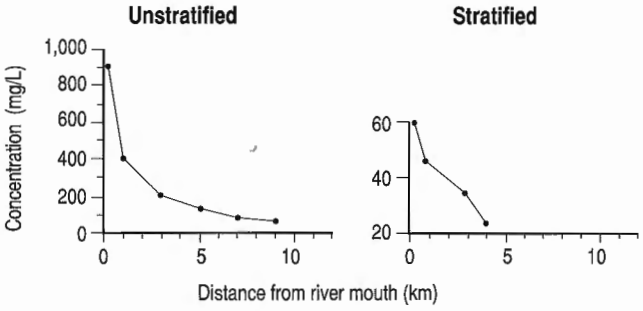

Figure 17. *Depth-integrated suspended-sediment concentration in the centre of the plume during unstratified and stratified flow at the river mouth on May 20, 1989 (modified from Kostaschuk et al. (1993)).*

Mass movements

The river mouth is a site of potential slope instability and the Sand Heads lighthouse (Fig. 1) is possibly at risk from these failures. McKenna et al. (1992) examined bathymetric charts from the river mouth (Fig. 18) and identified five large slope failures over a fifteen-year period. The largest failure occurred in 1985, involved over 1.4 x 10^6 m^3 of sand, and reached to within 100 m of the lighthouse (Atkins and Luternauer, 1991).

Failures usually occur after a long period of progradation of the river mouth, suggesting that their primary cause is rapid deposition (Christian et al., 1998; Mosher and Hamilton, 1998). Rapid deposition can load the underlying sediment and cause an increase in pore pressure that may lead to liquefaction. Construction of the Steveston North Jetty has confined the channel and enhanced deposition at the river mouth, probably increasing the potential for slope failure in that area (Christian et al., 1995). Christian et al. (1995) found that wave loading does not contribute to slope failure at Sand Heads. Earthquakes can shake sandy sediment until it liquefies, although historical slope failures at Sand Heads have not been triggered by earthquakes (Christian et al., 1995). Interstitial gas generated from decomposing organic matter in the sediment may increase pore pressures and reduce the strength of the sand (McKenna et al., 1992).

Failures at the river mouth generate mass flows that travel downslope in a submarine channel system that is over 5 km long and is situated on a depositional ridge (Hart et al., 1992; Kostaschuk et al., 1992b) (Fig. 19). Kostaschuk et al. (1992b) describe the channel system as consisting of several tributary channels that coalesce downslope into a single sinuous channel. The sinuous channel splits into small, shallow, distributary channels at the base of the delta slope. The tributary channels are relatively straight in plan and are deeply incised into the upper delta slope. The sinuous channel contains five distinct bends with levees along the banks and benches along the edge of the channel. The levees likely result from deposition as flows spills over the banks. Benches may represent deposition on the bed within the channel. Slumps and gullies are present on the outsides of bends, suggesting that the channel moves laterally. The distributary channels are situated on a subdued fan at the base of the depositional ridge, and slump scarps in this area indicate deformation along channel banks. Kostaschuk et al. (1992) conclude that the channel system has been produced by turbidity currents generated by periodic liquefaction of sandy sediment at the mouth of the river. Hart et al. (1992), however, believe that the channel complex is the result of submarine debris flows.

CLASSIFICATION OF MAIN CHANNEL OF THE FRASER ESTUARY

There are many ways to classify estuaries (Perillo, 1995). Fairbridge (1980) proposed a broad geomorphic scheme based on the origin of the estuary, sea-level history, tectonics, climate, and freshwater and sediment supply. This classification scheme includes fiords scoured by glacial processes, bar-built estuaries caused by longshore sediment transport across a river mouth, and delta-front estuaries consisting of distributary channels of marine deltas. The Fraser estuary is located on the surface of the Fraser delta, so is a delta-front estuary in Fairbridge's (1980) scheme.

Pritchard (1955) proposed three types of estuaries based on the relative importance of river velocity and tidal velocity in estuarine circulation. Salt-wedge estuaries are characterized by a dominance of river discharge over tides and limited mixing between fresh and marine water. These are highly stratified systems in which fresh river water flows above a landward-thinning wedge of denser salt water. Partially mixed estuaries have a stronger tidal effect and more mixing of fresh and salt water. Stratification is weaker, and both salt and fresh water are transferred vertically and horizontally.

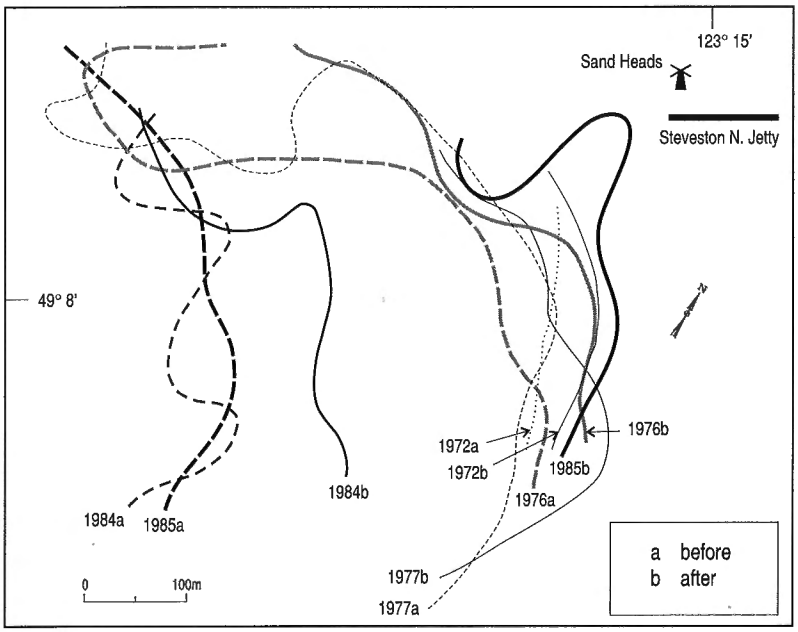

Figure 18.

Position of the 10 m bathymetric contour below lowest normal low water before (a) and after (b) mass movement events in 1972, 1976, 1977, 1984, and 1985. The 10 m contour is coincident with the crest of the delta front (modified from McKenna et al. (1992)).

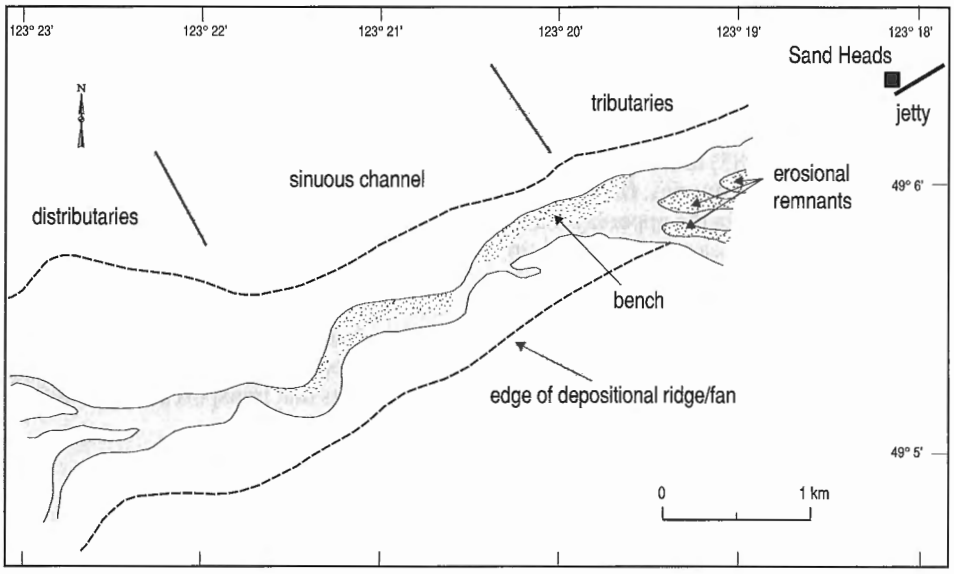

Figure 19. *Submarine mass-flow channel system. downslope is to the left (modified from Kostaschuk et al. (1992b)).*

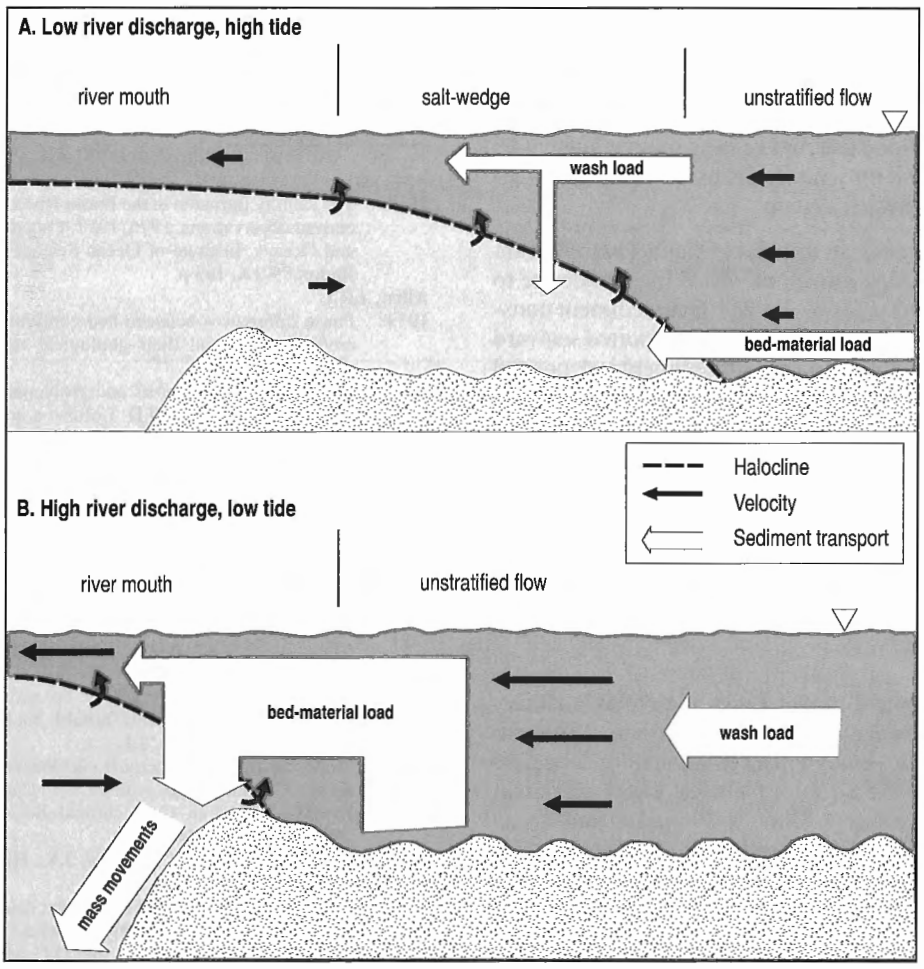

Figure 20. *Conceptual model of sedimentary processes in Main Channel of Fraser Estuary. See text for explanation.*

Fully mixed estuaries are dominated by tidal currents, and vertical salinity stratification is replaced by lateral variations in salinity.

Pritchard's (1955) classification of estuaries has been modified (e.g. Nicholls and Biggs, 1985) to include patterns of sediment movement. In salt-wedge estuaries, fine-grained suspended sediment is carried seaward in the upper layer and coarser-grained sediment is deposited near the landward tip of the intrusion. Riverine processes dominate suspended-sediment transport. The convergence of seaward transport of sediment by the river and landward transport by the tide in partially mixed estuaries produces a shoal on the bed and a turbidity maximum of suspended sediment in the water column. In fully mixed estuaries, fine-grained suspended sediment accumulates near the head of the estuary and coarse-grained sediment is transported both upstream and downstream in the channel.

Although Main Channel is usually classified as a salt-wedge estuary, it does not always behave as one. Kostaschuk et al. (1992a) examined the salinity intrusion at high tide and low tide during high river discharge and concluded that the estuary is a salt-wedge system. In contrast, Hodgins et al. (1977) measured salinity during low river discharge in winter and found that the increased tidal influence at that time of year results in stratification characteristic of a partially mixed estuary. Geyer and Farmer (1989) examined the salinity structure over the rise and fall of the tide during low river discharge. The salinity intrusion is a salt wedge as it migrates landward during the flood tide, but vertical mixing intensifies during the ebb tide and the salinity intrusion is more characteristic of a partially mixed system.

Sedimentary processes in the Main Channel are a variant of Pritchard's salt-wedge model, modified by a moderate to high tidal range. Riverine processes dominate sediment transport, fine-grained suspended sediment is transported seaward over the salt wedge, and coarse-grained sediment is deposited near the landward tip of the salt wedge (Kostaschuk et al., 1992a). These patterns are consistent with the salt-wedge model for microtidal coasts. However, a turbidity maximum of fine-grained sediment occurs near the salt-wedge tip (Kostaschuk et al., 1992a) (cf. Fig. 14), a feature characteristic of partially mixed estuaries on mesotidal coasts.

SUMMARY

Figure 20 is a conceptual model summarizing sedimentary processes in Main Channel. Sedimentary processes are controlled by the energetic, sandy Fraser River and the moderate to high tidal range in the Strait of Georgia. These processes function within unstratified flow, salt-wedge, and river-mouth zones. The salt wedge migrates into the channel when river discharge is low and all three zones are present (Fig. 20A). Low sediment concentrations supplied to the estuary by the river are primarily fine-grained wash load. Some wash load forms a turbidity maximum in the salt wedge, but most is transported into Strait of Georgia in a weak plume. Currents in the unstratified zone are weak and bed-material transport is limited to small amounts of bed-load movement close to the bed. Deposition of bed material occurs at the salt-wedge tip.

When river discharge is high and the tide is low, the salt wedge is forced out of the channel and unstratified flow and river-mouth zones are dominant (Fig. 20B). Wash-load concentrations supplied to the estuary by the river can be high. Current velocity is high in the unstratified zone and large amounts of bed material are suspended. Most wash load is transported seaward of the river mouth in the high-energy plume, but bed material is deposited on the bar at the river mouth. Deposition at the river mouth induces periodic mass movements that transport sand down the delta slope in a submarine channel.

ACKNOWLEDGMENTS

Funding was provided by the Natural Science and Engineering Research Council and the Geological Survey of Canada. Special thanks are extended to Ray Mackenzie and the Institute of Ocean Sciences for launch time and for supplying seasoned coxswains Randy Smith, Bob Taylor, and Ray Sanderson. Dave McLean and John Clague reviewed the manuscript and made many helpful comments.

REFERENCES

Ages, A.
1979: The salinity intrusion in the Fraser River: salinity, temperature and current observations, 1976, 1977; Canada Department of Fisheries and Oceans, Institute of Ocean Sciences, Pacific Marine Science Report 79-1A, 193 p.

Allen, J.R.L.
1973: Phase differences between bed configuration and flow in natural environments, and their geological relevance; Sedimentology, v. 20, p. 323-329.
1983: River bedforms: progress and problems; in Modern and Ancient Fluvial Systems, (ed.) J.D. Collinson and J. Lewin; International Association of Sedimentologists, Special Publication 6, p. 19-34.

Atkins, R.J. and Luternauer, J.L.
1991: Re-evaluation of slope failure volume estimates involving 3D computer graphics for the Fraser River delta front, British Columbia; in Current Research, Part E; Geological Survey of Canada, Paper 91-1E, p. 59-65.

Best, J.L.
1993: On the interactions between turbulent flow structure, sediment transport and bedform development: some considerations from recent experimental research; in Turbulence: Perspectives on Flow and Sediment Transport, (ed.) N.J. Clifford, J.R. French, and J. Hardisty; John Wiley & Sons, Sussex, England, p. 61-93.

Christian, H.A., Barrie, J.V., MacDonald, R., Monahan, P.A., Hunter, J.A., and Luternauer, J.L.
1995: Slope stability on Roberts Bank, Fraser River delta, Vancouver, British Columbia; Proceedings, 48th Canadian Geotechnical Conference, Canadian Geotechnical Society, Vancouver, British Columbia, p. 937-944.

Christian, H.A., Mosher, D.C., Barrie, J.V., Hunter, J.A., and Luternauer, J.L.
1998: Seabed instability on the Fraser River delta; in Geology and Natural Hazards of the Fraser River Delta, British Columbia, (ed.) J.J. Clague, J.L. Luternauer, and D.C. Mosher; Geological Survey of Canada, Bulletin 525, this volume.

Clague, J.J., Luternauer, J.L., and Hebda, R.J.
1983: Sedimentary environments and postglacial history of the Fraser River delta and lower Fraser Valley, British Columbia; Canadian Journal of Earth Sciences, v. 20, p. 1314-1320.

Fairbridge, R.W.
1980: The estuary: its definition and geodynamic cycle; in Chemistry and Biogeochemistry of Estuaries, (ed.) E. Olausson and I. Cato; John Wiley and Sons, Toronto, Ontario, p. 1-36.

Geyer, W.R. and Farmer, D.M.
1989: Tide-induced variation of the dynamics of a salt-wedge estuary; Journal of Physical Oceanography, v. 19, p. 1060-1072.

Hart, B.S., Prior, D.B., Barrie, J.V., Currie, R.G., and Luternauer, J.L.
1992: A river mouth submarine channel and failure complex, Fraser Delta, Canada; Sedimentary Geology, v. 81, p. 73-87.

Hodgins, D.O., Osborn, T.R., and Quick, M.C.
1977: Numerical model of stratified flow; American Society of Civil Engineers, Journal of the Waterways, Ports and Coastal Division, v. WW1, p. 25-42.

Hughes, C.C. and Ages, A.
1975: Salinity and temperature measurements in the lower Fraser River, 1966-1968, 1970-1973; Canada Department of Fisheries and Oceans, Institute of Ocean Sciences, Pacific Marine Science Report 75-2, 120 p.

Jackson, R.G.
1976: Sedimentological and fluid-dynamic implications of the turbulent bursting phenomena in geophysical flows; Journal of Fluid Mechanics, v. 77, p. 531-560.

Kostaschuk, R.A. and Atwood, L.A.
1990: River discharge and tidal controls on salt-wedge position and implications for channel shoaling; Canadian Journal of Civil Engineering, v. 17, p. 452-459.

Kostaschuk, R.A. and Church, M.A.
1993: Macroturbulence generated by dunes: Fraser River, Canada; Sedimentary Geology, v. 85, p. 25-37.

Kostaschuk, R.A. and Ilersich, S.A.
1995: Dune geometry and sediment transport: Fraser River, British Columbia; in River Geomorphology, (ed.) E.J. Hickin; John Wiley & Sons, Sussex, England, p. 19-36.

Kostaschuk, R.A. and Luternauer, J.L.
1987: Large-scale sedimentary processes in a trained, high-energy, sand-rich, salt-wedge estuary: Fraser River delta, British Columbia; in Current Research, Part A; Geological Survey of Canada, Paper 87-1A, p. 727-734.
1989: The role of the salt-wedge in sediment resuspension and deposition; Journal of Coastal Research, v. 5, p. 93-101.

Kostaschuk, R.A. and MacDonald, G.M.
1988: Multi-track surveying of large bedforms; Geo-Marine Letters, v. 8, p. 57-62.

Kostaschuk, R.A. and Villard, P.V.
1996a: Flow and sediment transport over large subaqueous dunes: Fraser River, Canada; Sedimentology, v. 43, p. 849-863.
1996b: Turbulent sand suspension events: Fraser River, Canada; in Coherent Flow Structures in Open Channels, (ed.) P.J. Ashworth, S.J. Bennett, J.L. Best, and S.J. McLelland; John Wiley & Sons, Sussex, England, p. 305-320.

Kostaschuk, R.A., Church, M.A., and Luternauer, J.L.
1989a: Bed material, bedforms and bed load in a salt-wedge estuary - Fraser River, British Columbia; Canadian Journal of Earth Sciences, v. 26, p. 1440-1452.
1992a: Sediment transport over salt-wedge intrusions: Fraser River estuary, Canada; Sedimentology, v. 39, p. 305-317.

Kostaschuk, R.A., Luternauer, J.L., and Church, M.A.
1989b: Suspended sediment hysteresis in a salt-wedge estuary - Fraser River, Canada; Marine Geology, v. 87, p. 273-285.

Kostaschuk, R.A., Luternauer, J.L., McKenna, G.T., and Moslow, T.F.
1992b: Sediment transport in a submarine channel system: Fraser River delta, Canada; Journal of Sedimentary Petrology, v. 62, p. 273-282.

Kostaschuk, R.A., Stephan, B.A., and Luternauer, J.L.
1993: Suspended sediment concentration in a buoyant plume: Fraser River, Canada; Geo-Marine Letters, v. 13, p. 165-171.

Luternauer, J.L., Mosher, D.C., Clague, J.J., and Atkins, R.J.
1998: Sedimentary environments of the Fraser delta; in Geology and Natural Hazards of the Fraser River Delta, British Columbia, (ed.) J.J. Clague, J.L. Luternauer, and D.C. Mosher; Geological Survey of Canada, Bulletin 525, this volume.

Matthes, G.H.
1947: Macroturbulence in natural stream flow; Transactions of the American Geophysical Union, v. 28, p. 255-262.

McKenna, G.T., Luternauer, J.L., and Kostaschuk, R.A.
1992: Large-scale mass-wasting events on the Fraser River delta front near Sand Heads, British Columbia; Canadian Geotechnical Journal, v. 29, p. 151-156.

McLaren, P. and Ren, P.
1995: Sediment transport and its environmental implications in the lower Fraser River and Fraser Delta; Canada Department of Environment, Environmental Conservation, DOE FRAP 1995-03, 37 p.

McLean, D.G. and Church, M.A.
1986: A re-examination of sediment transport observations in the lower Fraser River; Canada Department of Environment, Inland Waters Directorate, Water Survey of Canada, Sediment Survey Section, Report IWD-HQ-WRB-SS-86-6, 52 p.

McLean, D.G. and Tassone, B.
1991: A sediment budget of the lower Fraser River; Proceedings of the 5th Federal Interagency Sedimentation Conference, Las Vegas, Nevada, p. 2-33 - 2-40.

Milliman, J.D.
1980: Sedimentation in the Fraser River and its estuary, southwestern British Columbia (Canada); Estuarine and Coastal Marine Science, v. 10, p. 609-633.

Mosher, D.C. and Hamilton, T.S.
1998: Morphology, structure, and stratigraphy of the offshore Fraser delta and adjacent Strait of Georgia in Geology and Natural Hazards of the Fraser River Delta, British Columbia, (ed.) J.J. Clague, J.L. Luternauer, and D.C. Mosher; Geological Survey of Canada, Bulletin 525, this volume.

Nicholls, M.M. and Biggs, R.B.
1985: Estuaries; in Coastal Sedimentary Environments, (ed.) R.A. Davis; Springer-Verlag, New York, p. 77-186.

Orton, G.J. and Reading, H.G.
1993: Variability of deltaic processes in terms of sediment supply, with particular emphasis on grain size; Sedimentology, v. 40, p. 475-512.

Perillo, G.M.E.
1995: Definitions and geomorphologic classifications of estuaries; in Geomorphology and Sedimentology of Estuaries, (ed.) G.M.E. Perillo; Elsevier Science, Amsterdam, Netherlands, p. 17-47.

Pretious, E.S. and Blench, T.
1951: Final report on special observations of bed movement in lower Fraser River at Ladner reach during 1950 freshet; National Research Council of Canada, Fraser River Model Project, Technical Report no. 3, 17 p.

Pritchard, P.W.
1955: Estuarine circulation patterns; Proceedings of the American Society of Civil Engineers, v. 81, p. 717-1 - 717-11.

Reid, I. and Frostick, L.E.
1994: Fluvial sediment transport and deposition; in Sediment Transport and Depositional Processes, (ed.) K. Pye; Blackwell Scientific Publications, Edinburgh, United Kingdom, p. 89-156.

Rood, K.M. and Hickin, E.J.
1989: Suspended sediment concentration and calibre in relation to surface flow structure in Squamish River estuary, southwestern British Columbia; Canadian Journal of Earth Sciences, v. 26, p. 2172-2176.

Servizi, J.A.
1989: Protecting Fraser River salmon from wastewater: an assessment; in Proceedings of the National Workshop on Effects of Habitat Alteration on Salmonoid Stocks, (ed.) C.D. Levings, L.B. Holtby, and M.A. Henderson; Canadian Special Publication of Fisheries and Aquatic Sciences, no. 105, p. 136-153.

Smith, J.D. and McLean, S.R.
1977: Spatially averaged flow over a wavy bed; Journal of Geophysical Research, v. 82, p. 1735-1746.

Stephan, B. A.
1990: Sedimentary processes at the mouth of the Fraser River, British Columbia, Canada; M.Sc. thesis, University of Guelph, Guelph, Ontario, 134 p.

Stronach, J.A., Crean, P.B., and Murty, T.S.
1988: Mathematical modelling of the Fraser River plume; Water Pollution Research Journal of Canada, v. 23, p. 179-212.

Thomson, R.E.
1981: Oceanography of the British Columbia coast; Canadian Special Publication of Fisheries and Aquatic Sciences, no. 56, 291 p.

Venditti, J.
1995: Factors affecting the distribution of heavy metal contaminants in the bed sediments of Fraser Estuary; B.Sc. thesis, University of Guelph, Guelph, Ontario, 32 p.

Villard, P. V.
1995: Spatial and temporal behaviour of turbulent sand suspension over dunes: Fraser River, British Columbia; M.Sc. thesis, University of Guelph, Guelph, Ontario, 125 p.

Ward, P.R.B.
1976: Seasonal salinity changes in the Fraser River estuary; Canadian Journal of Civil Engineering, v. 3, p. 342-348.

Quaternary stratigraphy and evolution of the Fraser delta

J.J. Clague[1], J.L. Luternauer[1], P.A. Monahan[2], K.A. Edwardson[3], S.R. Dallimore[4], and J.A. Hunter[4]

Clague, J.J., Luternauer, J.L., Monahan, P.A., Edwardson, K.A., Dallimore, S.R., and Hunter, J.A., 1998: Quaternary stratigraphy and evolution of the Fraser delta; in Geology and Natural Hazards of the Fraser River Delta, British Columbia, (ed.) J.J. Clague, J.L. Luternauer, and D.C. Mosher; Geological Survey of Canada, Bulletin 525, p. 57–90.

Abstract: The Fraser River delta is underlain by thick Quaternary sediments and Tertiary sedimentary rocks separated by an unconformity with up to 800 m of relief. Pleistocene sediments consist mainly of sand and silt deposited in proglacial glaciomarine environments during several glaciations. These glacial sediments are separated by nonglacial marine deposits or, more commonly, by unconformities. The Pleistocene sequence is overlain by sediments of the Holocene Fraser River delta across a surface with up to 300 m of relief. The delta deposits comprise bottomset, foreset, and topset units. The bottomset unit consists mainly of clayey silt. Silty and sandy foreset deposits overlie the bottomset unit, and are unconformably overlain by 10 to 30 m of distributary-channel sands. The channel sands, which constitute the lower part of the topset unit, grade upward into several metres of intertidal and floodplain silts, and peat. The delta started to form about 10 000 years ago, when the Fraser River advanced its floodplain beyond the Pleistocene uplands at New Westminster. About 6000 years ago, the locus of deposition shifted from southward into Boundary Bay to westward into the Strait of Georgia proper.

Résumé : Le delta du Fraser consiste en d'épais sédiments quaternaires qui reposent sur des roches sédimentaires tertiaires; ces deux lithologies sont séparées par une discordance dont la surface présente une dénivellation pouvant atteindre 800 mètres. Les sédiments pléistocènes se composent principalement de sable et de silt déposés dans des milieux glaciomarins proglaciaires au cours de plusieurs glaciations. Les diverses accumulations de ces sédiments sont séparées par des sédiments marins non glaciaires ou, plus souvent, par des discordances. La séquence pléistocène est recouverte des sédiments holocènes du delta du fleuve Fraser; la surface de ce contact présente une dénivellation pouvant atteindre 300 mètres. Les dépôts deltaïques sont constitués d'une unité basale, d'une unité frontale et d'une unité sommitale. L'unité basale est principalement composée de silt argileux. Elle est surmontée du silt et du sable de l'unité frontale, qui à son tour est sous-jacente (contact discordant) à une épaisseur de 10 à 30 mètres de sable de défluent. Ce sable, qui forme la partie inférieure de l'unité sommitale, fait place vers le haut à plusieurs mètres de silt intertidal, de silt de plaine d'inondation, ainsi que de tourbe. Le delta a commencé à se former il y a environ 10 000 ans, lorsque la plaine d'inondation du fleuve Fraser s'est avancée au-delà des hautes terres du Pléistocène dans la région de New Westminster. Il y a quelque 6 000 ans, la sédimentation, qui se faisait vers le sud dans la baie Boundary, a changé de direction pour aller vers l'ouest dans le détroit de Georgia même.

[1] Geological Survey of Canada, 605 Robson Street, Vancouver, British Columbia V6B 5J3
[2] Monahan Petroleum Consulting, 1024 Benvenuto Avenue, Brentwood Bay, British Columbia V8M 1A1
[3] Geological Survey of Canada, P.O. Box 1006, Dartmouth, Nova Scotia B2Y 4A2
[4] Geological Survey of Canada, 601 Booth Street, Ottawa, Ontario K1A 0E8

INTRODUCTION

The Fraser River delta, just south of Vancouver, British Columbia, is the largest delta in western Canada. It is experiencing rapid urban and industrial growth, and is an important agricultural area and a vital link in the Fraser River salmon fishery. The Fraser delta also lies within one of the most seismically active regions in Canada, and the impact on the delta of a future strong earthquake is a growing concern.

The Fraser delta plain consists of upper and lower parts. The upper delta plain is east of the area of significant tidal influence and consists of the presently dyked portion of the delta. The lower delta plain, to the west, comprises tidal flats up to 9 km wide, extending from the dykes to the lowest level of tides. A shallow subaqueous platform extends another 2 km farther west from the low tide line to the top of the Fraser delta slope.

Stratigraphic information about the Fraser delta is important for several reasons: it improves our understanding of processes that have shaped the delta and that affect its stability (Luternauer et al., 1994); it allows possible aquifers and aquitards to be identified (Ricketts, 1998); and it is the basis for geotechnical assessments of earthquake hazards (Harris et al., 1995; Luternauer et al., 1995). This paper summarizes what is known about the stratigraphy, sedimentology, and structure of Quaternary deposits underlying the subaerial portion of the Fraser delta plain, discusses the geological history of the delta, and assesses the adequacy of available stratigraphic information for modelling the delta's response to earthquakes. The chapter includes 1) a compilation of previous work, 2) reference to field and laboratory methods used to interpret the stratigraphy of the delta, 3) a map and perspective views of the bedrock surface beneath the delta, 4) a list of important radiocarbon ages, 5) summary logs of representative cores collected by the Geological Survey of Canada and Simon Fraser University, 6) stratigraphic sections compiled from these cores and from industry data, and 7) photographs of selected sedimentary structures used for paleoenvironmental interpretation.

PREVIOUS STUDIES

The earliest substantive investigations of the Fraser delta, by Johnston (1921, 1923) and Mathews and Shepard (1962), concentrated on surficial deposits, but included some stratigraphic information from geotechnical boreholes and exploratory oil and gas wells (Mustard and Rouse, 1994). The first systematic subsurface investigation of the stratigraphy of the delta was conducted by Clague et al. (1983), who established the general architecture of the Fraser delta and outlined the evolution of the delta during the Holocene. They incorporated data from more than 1500 geotechnical boreholes in their interpretations and prepared representative stratigraphic sections for several parts of the delta. However, these interpretations were based on limited sampling and sediment descriptions, which precluded detailed stratigraphic correlation.

A scientific drilling and geophysical program to refine the stratigraphy of the Fraser delta commenced in the mid 1980s under the auspices of the Geological Survey of Canada and Simon Fraser University. Roberts et al. (1985) reported the results of a shallow coring program on the southern delta which discriminated subsurface fluvial and littoral sediments. Williams (1988) and Williams and Roberts (1989, 1990) investigated the uppermost topset deposits on Lulu Island using a series of shallow cores. They documented the interplay between sedimentation and sea-level rise during the middle to late Holocene. Luternauer et al. (1986, 1991), Jol (1988), Jol and Roberts (1988, 1992), Pullan et al. (1989), and Clague et al. (1991) presented results of seismic-reflection surveys and drilling on the southernmost part of the delta. They documented a thick, sandy, foreset sequence between thinner, finer-grained, bottomset and topset units, and commented on the age of delta progradation in the area. Patterson and Cameron (1991) and Patterson and Luternauer (1993) described late Quaternary foraminiferal faunas recovered from Geological Survey of Canada cores. Monahan et al. (1993a, b, 1995) documented the presence of distributary-channel sands beneath most of the delta plain from drillhole and geotechnical data. Williams and Luternauer (1991) and Hutchinson et al. (1995) identified a former distributary channel of the Fraser River that flowed into Boundary Bay during the early Holocene. Preliminary results of drilling and geotechnical testing in the Roberts Bank area have been presented by Christian et al. (1994a, b, 1995), and lithological, geotechnical, geophysical, and geochronological data for three 300 m holes drilled on Lulu Island in 1994 and 1996 have been summarized by Dallimore et al. (1995, 1996).

The requirement for high-quality subsurface geological and geophysical data for evaluating the stability of the delta slope, seismic ground motions, and the potential for liquefaction has been the catalyst for many recent studies on the Fraser delta (e.g. Campanella et al., 1983; Luternauer and Finn, 1983; Bazett and McCammon, 1986; Byrne and Anderson, 1987; Lo et al., 1991; Sy et al., 1991; Clague et al., 1992b, 1998; Naesgaard et al., 1992; Watts et al., 1992; Luternauer et al., 1994, 1995; Christian et al., 1995; Monahan et al., 1995; Luternauer and Hunter, 1996).

DATA COLLECTION

Logs of hydrocarbon exploratory wells, in particular four near the southern margin of the Fraser delta, provide information on the lithology of Tertiary sedimentary rocks beneath the delta (Mustard and Rouse, 1994) (Fig. 1). The form of the buried bedrock surface has been defined from 127 line-kilometres of multichannel seismic data provided by Dynamic Oil Ltd. (Britton et al., 1995). These seismic data were acquired between 1977 and 1989 with multivibrator energy sources.

The two principal sources of Quaternary stratigraphic information on the Fraser delta are drilling and seismic-reflection programs carried out by the Geological Survey of Canada and Simon Fraser University (Fig. 1). Geological Survey of Canada seismic-reflection surveys are described in more

detail by Hunter et al. and Pullan et al. in this volume; the reader is referred to these papers for information on methods and results. Details of the Simon Fraser University drilling programs are provided by Roberts et al. (1985), Luternauer et al. (1986), Williams (1988), Williams and Roberts (1989, 1990), Williams and Luternauer (1991), and Hutchinson et al. (1995). The Geological Survey of Canada has drilled 43 holes on the Fraser delta plain and at the delta front, ranging in depth from 16 to 367 m (Fig. 1, Appendix 1). The first six were drilled on the southern delta in 1986, with sampling limited to short, widely spaced, split-spoon cores. After this, most of the drilling involved continuous coring. Most onshore boreholes were cased and subsequently logged using a variety of geophysical methods (Hunter et al., 1994, 1995, 1998; Mwenifumbo et al., 1994). Some of the holes drilled recently have been geophysically logged, but not sampled. Relatively few of the boreholes penetrate the Pleistocene sequence (Luternauer et al., 1994; Dallimore et al., 1995, 1996; Luternauer and Hunter, 1996); consequently, much less is known about these deposits than the overlying Holocene sediments.

Preliminary description and subsampling of all cores were done in the field. The cores were photographed, visual estimates were made of grain size and composition, and sedimentary structures were identified. Samples were collected from the cores

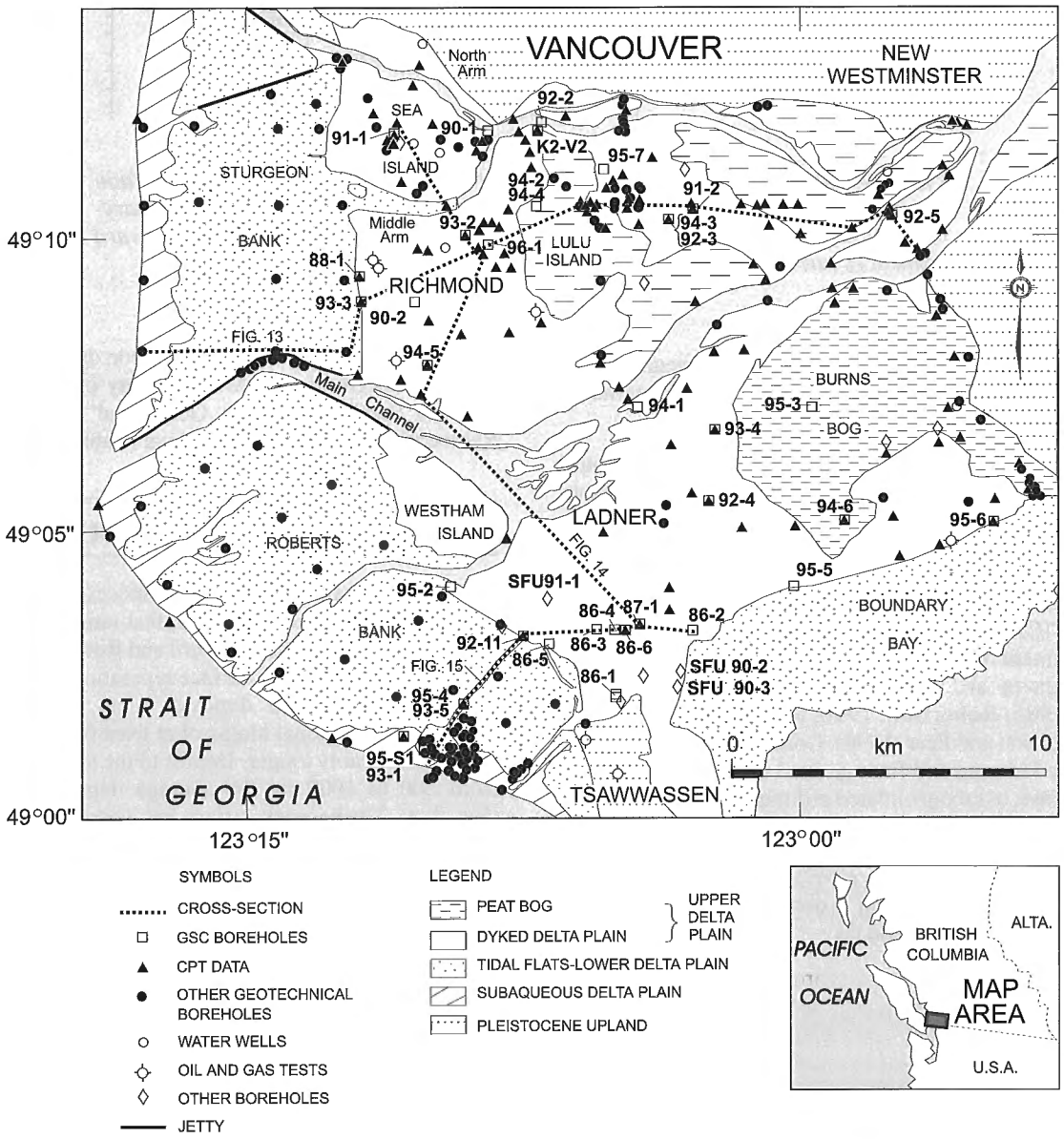

Figure 1. Map of the Fraser River delta showing locations of boreholes more than 20 m deep. Dotted lines indicate locations of cross-sections shown in Figures 13, 14, and 15. Numbered sites are boreholes illustrated in Figures 5 and 6 and Appendix 1 (Simon Fraser University holes are denoted by SFU; all other numbered sites are Geological Survey of Canada holes).

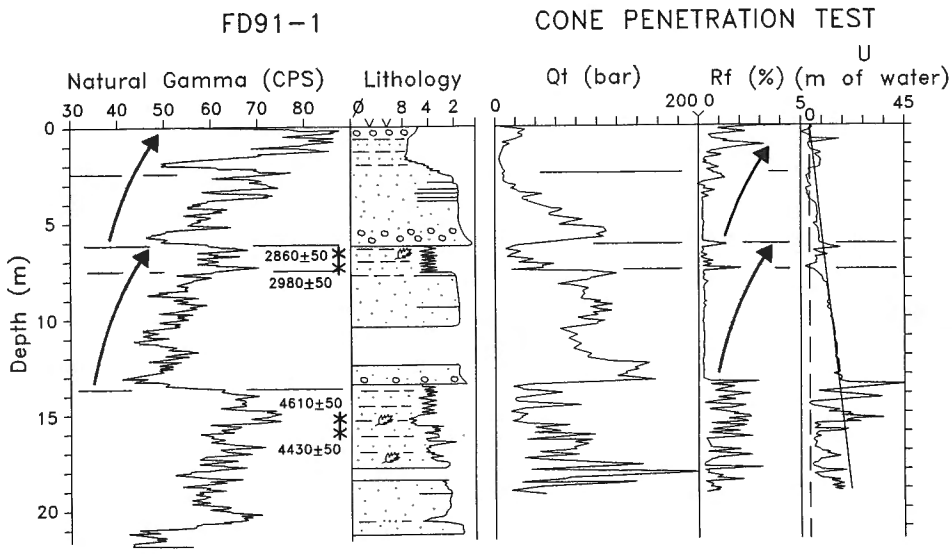

Figure 2. Gamma-ray and lithology logs from borehole FD91-1 and cone penetration test data from a nearby site. Sediments above 14 m depth are part of the distributary-channel sand sheet (see text). The sand sheet here consists of two fining-upward sequences (arrows). Refer to Appendix 1 for lithology legend.

for grain-size analysis, Atterberg limits, water content, salinity, radiocarbon dating, and microfossil analysis (Luternauer et al., 1994; Dallimore et al., 1995, 1996).

A vast amount of geotechnical data gathered during publicly funded construction projects, and derived mainly from standard penetration and cone penetration tests, supplements subsurface data collected by the Geological Survey of Canada and Simon Fraser University (Fig. 1; Monahan et al., 1993b; Monahan and Luternauer, 1994). In particular, the cone penetration test (CPT) provides continuous measurements from which sediment types and properties can be interpreted (Campanella et al., 1983; Robertson and Campanella, 1983a, b, 1985; Robertson, 1990; Monahan et al., 1993b, 1995; Robertson and Fear, 1996). Cone penetration tests can be performed in sand and finer grained sediments, but not in gravel or dense, overconsolidated sediments such as till. They have been used extensively, together with borehole data, to interpret the stratigraphy of the upper part of the Holocene deltaic sequence (Fig. 2). Most CPTs on the delta have depths of 20 to 40 m (e.g. Woeller et al., 1993a, b, 1994); the deepest is 100 m (Christian et al., 1994a).

DATA ANALYSIS

Geological Survey of Canada cores were re-examined in the laboratory. Grain-size, Atterberg limits, and other geotechnical analyses of samples collected from deep boreholes were performed at the Geological Survey of Canada sedimentology laboratories in Ottawa and Sidney (see Dallimore et al., 1995, for description of methods). Most grain-size descriptions of cores from shallow boreholes (<100 m) are based on visual inspection. Samples of fossil wood and marine shells, extracted from cores, were radiocarbon dated at the accelerator mass spectrometry (AMS) facility of the University of Toronto (IsoTrace) or the Geological Survey of Canada Radiocarbon Laboratory in Ottawa (Table 1).

BEDROCK AND ITS BURIED SURFACE

The Fraser delta is underlain by a succession of clastic sedimentary rocks, up to 4 km thick, that range in age from Late Cretaceous to Miocene (Mustard and Rouse, 1994; Britton et al., 1995). The erosional surface separating this bedrock from overlying Pleistocene deposits is an unconformity that records a depositional hiatus of at least 6 million years, perhaps considerably longer. Depths to the top of bedrock range from 200 to 1000 m; the average depth is about 500 m (Fig. 3, 4). The bedrock surface has a crude linear form, with northwest-trending ridges and intervening troughs and basins. There are no data for the urban area of Richmond, but surveys just to the south suggest that a broad bedrock basin underlies the city (Britton et al., 1995).

PLEISTOCENE DEPOSITS

The drilling and surface and downhole geophysical surveys that have provided information on the distribution, stratigraphy, and characteristics of Pleistocene sediments beneath the Fraser delta are summarized in Figures 5-12, Tables 2 and 3, and Appendix 1 (see also Bazett and McCammon, 1986; Clague et al., 1991; Luternauer et al., 1991, 1994; Dallimore et al., 1995, 1996; Luternauer and Hunter, 1996). The Pleistocene sequence has been penetrated in 12 Geological Survey of

Table 1. Radiocarbon ages on samples from Fraser River delta boreholes.

Borehole	Depth (m)	Radiocarbon age[1] (^{14}C years BP)	Laboratory no.[2]	Material	Reference
FD86-1	7	3540 ± 50*	TO-870	shell	Clague et al., 1991
FD86-2	31	6710 ± 90	TO-576	wood	Clague et al., 1991
FD86-2	46	6370 ± 90	TO-577	wood	Clague et al., 1991
FD86-5	31	5280 ± 70	TO-583	wood	Clague et al., 1991
FD86-5	31	5400 ± 80*	TO-583a	shell	Clague et al., 1991
FD86-6	18	6380 ± 70	TO-588	wood	Clague et al., 1991
FD87-1	40	5820 ± 60	TO-777	wood	Clague et al., 1991
FD87-1	66	6380 ± 60*	TO-778	shell	Clague et al., 1991
FD87-1	99	6250 ± 80	TO-779	wood	Clague et al., 1991
FD87-1	143	7470 ± 60	TO-780	wood	Clague et al., 1991
FD87-1	158	8310 ± 70*	TO-781	shell	Clague et al., 1991
FD87-1	168	9150 ± 70*	TO-782	shell	Clague et al., 1991
FD87-1	171	9410 ± 70*	TO-783	shell	Clague et al., 1991
FD87-1	179	9950 ± 80*	TO-784	shell	Clague et al., 1991
FD87-1	184	11 920 ± 90*	TO-1094	shell	Clague et al., 1991
FD87-1	201	37 460 ± 660	TO-785	wood	Luternauer et al., 1991
FD87-1	219	46 430 ± 880*	TO-1095	shell	Luternauer et al., 1991
FD87-1	223	26 880 ± 200	TO-786*	shell	Luternauer et al., 1991
FD87-1	247	33 490 ± 270	TO-787	wood	Luternauer et al., 1991
FD87-1	267	24 460 ± 160	TO-788	wood	Luternauer et al., 1991
FD90-A	35	9590 ± 70	TO-2749	shell	Patterson and Luternauer, 1993
FD90-B	19	6630 ± 60	TO-2748	shell	Patterson and Luternauer, 1993
FD90-B	35	6400 ± 80	TO-2747	wood	Patterson and Luternauer, 1993
FD91-1	7	2860 ± 50	TO-2756	wood	Patterson and Luternauer, 1993
FD91-1	8	2980 ± 50	TO-2757	wood	Patterson and Luternauer, 1993
FD91-1	14	4610 ± 50	TO-2758	wood	Patterson and Luternauer, 1993
FD91-1	15	4430 ± 50	TO-2759	wood	Patterson and Luternauer, 1993
FD91-1	22	8940 ± 100	TO-2754	shell	Patterson and Luternauer, 1993
FD91-1	23	7870 ± 90	TO-2755	shell	Patterson and Luternauer, 1993
FD91-1	25	6380 ± 60	TO-2750	bryophyte	Patterson and Luternauer, 1993
FD91-1	27	7510 ± 60	TO-2751	shell	Patterson and Luternauer, 1993
FD91-1	29	8620 ± 700	TO-2752	shell	Patterson and Luternauer, 1993
FD91-2	4	2740 ± 50	TO-2760	wood	Patterson and Luternauer, 1993
FD91-2	5	2850 ± 50	TO-2761	wood	Patterson and Luternauer, 1993
FD91-2	10	3940 ± 50	TO-2762	wood	Patterson and Luternauer, 1993
FD91-2	26	4700 ± 50	TO-2763	wood	Patterson and Luternauer, 1993
FD91-2	41	10 530 ± 90	TO-3307	shell	Patterson and Luternauer, 1993
FD92-2A	21	9690 ± 80	TO-40 94	shell	
FD92-4	12	6990 ± 70	TO-4098	shell	
FD92-4	38	8570 ± 70	TO-4095	shell	
FD92-11	85	6540 ± 170	TO-4097	shell	
FD92-11	100	10 010 ± 70	TO-4894	shell	
FD93-1	20	1060 ± 80	TO-3977	leaf	
FD93-1	21	1120 ± 50	TO-3978	wood	
FD93-1	53	1690 ± 60	TO-4096	wood	
FD93-2	8	3760 ± 90	GSC-5790	wood	
FD93-2	17	5120 ± 100	GSC-5792	wood	
FD93-2	41	8220 ± 110	GSC-5802	wood	
FD93-2	29	7600 ± 70	TO-4142	wood	
FD93-2	46	6710 ± 80	TO-4143	wood	
FD93-3	5	2740 ± 50	TO-4148	shell	
FD93-3	9	3200 ± 90	GSC-5785	wood	
FD93-3	20	3670 ± 50	TO-4149	wood	
FD93-3	44	5940 ± 60	TO-4150	shell	
FD93-4	16	1890 ± 70	GSC-5804	wood	
FD93-4	21	8140 ± 70	TO-4215	shell	
FD93-4	47	9050 ± 100	TO-4216	shell	
FD93-5	8	600 ± 60	TO-4281	wood	
FD93-5	15	3420 ± 60	TO-4217	shell	
FD93-5	38	2460 ± 50	TO-4281	wood	
FD93S-1	10	230 ± 50	TO-4371	wood	
FD93S-1	24	1670 ± 50	TO-4370	shell	
FD93S-2	16	170 ± 70	TO-4372	wood	
FD94-1	9	10 ± 60	TO-4374	wood	Monahan et al., 1995
FD94-1	26	9060 ± 80	TO-4595	shell	Monahan et al., 1995
FD94-3	15	4620 ± 70	TO-4461	wood	Dallimore et al., 1995
FD94-3	85	40 290 ± 780	TO-4462	wood	Dallimore et al., 1995
FD94-3	120	46 530 ± 1100	TO-4463	wood	Dallimore et al., 1995
FD94-3	151	41 970 ± 680	TO-4464	wood	Dallimore et al., 1995
FD94-4	32	9130 ± 80	TO-4464	shell	Dallimore et al., 1995
FD94-4	119	8920 ± 80	TO-4466	shell	Dallimore et al., 1995
FD94-4	142	9710 ± 100	TO-4467	shell	Dallimore et al., 1995
FD94-4	158	9520 ± 90	TO-4468	shell	Dallimore et al., 1995
FD94-4	170	9540 ± 90	TO-4469	shell	Dallimore et al., 1995
FD94-4	235	10 870 ± 100	TO-4470	shell	Dallimore et al., 1995
FD94-6	8	5120 ± 60	TO-4895	wood	
FD94-6	22	8790 ± 70	TO-4896	shell	
FD95-6	19	8600 ± 70	TO-5418	shell	
FD95-6	24	8760 ± 70	TO-5419	shell	
FD96-1	13	3770 ± 60	Beta-93808	wood	Dallimore et al., 1996
FD96-1	77	8500 ± 60	Beta-93809	shell	Dallimore et al., 1996
FD96-1	110	10 020 ± 50	Beta-93891	shell	Dallimore et al., 1996
FD96-1	151	8770 ± 60	Beta-93810	shell	Dallimore et al., 1996
FD96-1	269	10 180 ± 50	Beta-93811	shell	Dallimore et al., 1996
FD96-1	305	10 980 ± 60	Beta-93812	shell	Dallimore et al., 1996
K2V2	20	4430 ± 50	TO-4897	wood	Monahan et al., 1995

[1] Ages as reported by the laboratory – those with an asterisk (old TO shell ages) are normalized to $\delta^{13}C$ = 0‰ PDB, equivalent to a reservoir correction of 410 years; all others are normalized to $\delta^{13}C$ = -25.0‰ PDB and have no reservoir correction. Laboratory-reported error terms are 2σ for GSC ages and 1σ for TO ages.

[2] Laboratories: Beta, Beta Analytic; GSC, Geological Survey of Canada; TO, IsoTrace (University of Toronto).

Canada boreholes (Fig. 5, 6, 11, 12, 13) and in several other holes drilled by geotechnical firms and hydrocarbon exploration companies (Table 2; Luternauer and Hunter, 1996).

Sedimentology

The Pleistocene succession beneath the Fraser delta is several hundred metres thick and displays complex changes in sediment type both vertically, at individual sites, and laterally between sites (Fig. 5, 6; Appendix 1). The dominant sediments are sand and silt, occurring as massive and stratified facies. Diamicton is less common, but is present at or near the top of the Pleistocene succession in some boreholes. Diamicton also occurs at greater depths, near the bottoms of some of the deepest holes. Gravel is rare in the cored Pleistocene sequence. In a general sense, fine-grained sediments dominate the deeper part of the Pleistocene succession, whereas coarser grained sediments are more common toward the top; this is best seen where deltaic deposits are thin, as at borehole FD94-3 (Fig. 5B) and in the logs of hydrocarbon exploration wells. Pleistocene sediments penetrated in five of the Geological Survey of Canada boreholes, which were drilled specifically to characterize deep Holocene and underlying deposits, are described below (see also Clague et al., 1991; Luternauer et al., 1991; Dallimore et al., 1995, 1996).

Borehole FD87-1

A 2 m thick layer of silty clay with scattered pebbles marks the top of the Pleistocene sequence in borehole FD87-1 on the southern Fraser delta (Fig. 5A; Luternauer et al., 1991). A shell from this layer yielded an AMS radiocarbon age of 11 920 ± 90 BP (12 330 ± 90 BP if normalized to $\delta^{13}C$ = -25.0‰, which is the present standard; TO-1094, Table 1). Below the silty clay, at a depth of 185 m, is about 1 m of diamicton. Seven metres of sheared clayey silt with scattered shell fragments directly underlie the diamicton. The sheared clayey silt is itself underlain by 120 m of interbedded massive to laminated clayey silt with sand and pebble layers, and silt-sand couplets. Radiocarbon ages on wood and shell from this part of the sequence range from 24 460 ± 160 to 46 430 ± 880 BP (TO-788, TO-1095). Load casts and convolutions are

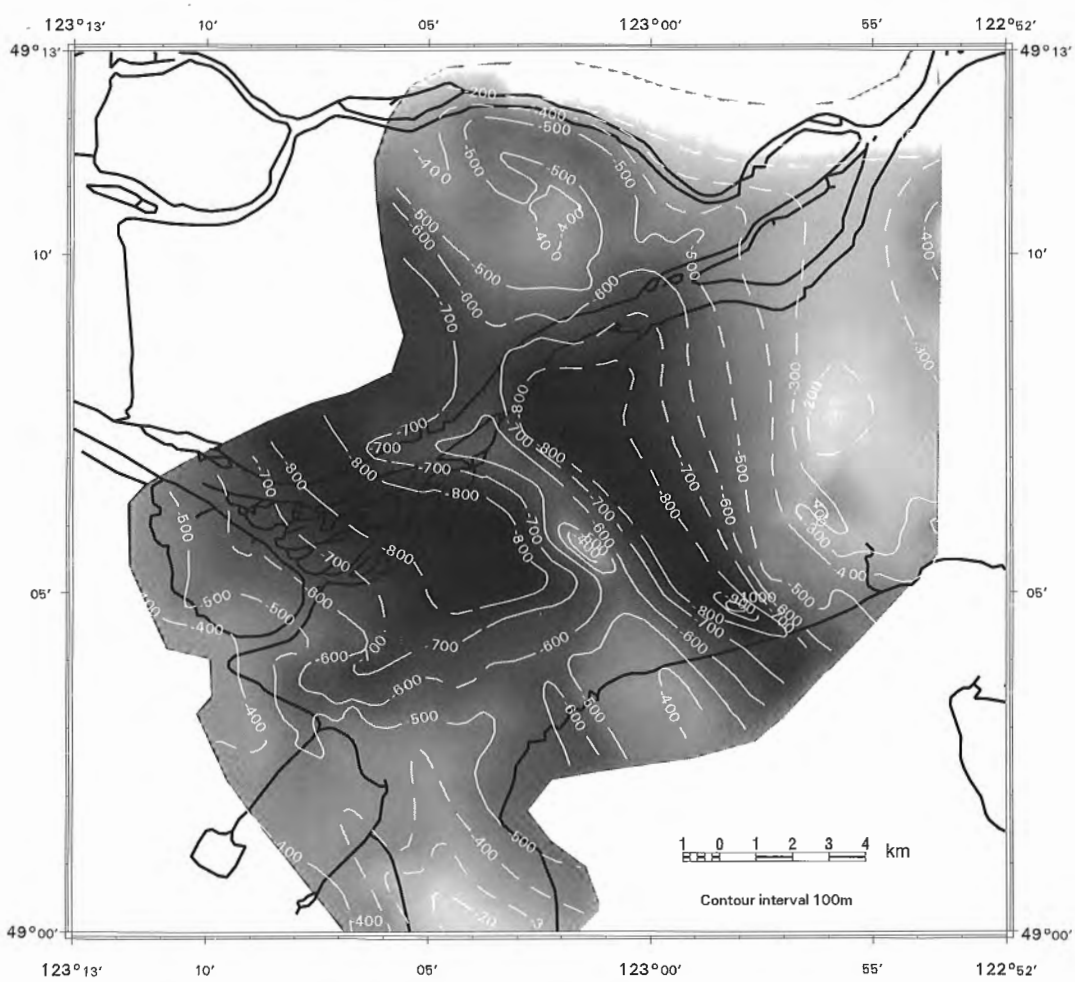

Figure 3. *Shaded contour map of the depth (m) of the Tertiary bedrock surface beneath the Fraser delta plain (adapted from Britton et al., 1995).*

common between 192 and 242 m depth. This thick stratified sequence lies on 1 m of diamicton at 312 m depth. The diamicton, in turn, successively overlies 27 m of massive to weakly stratified, pebbly sand, 5 m of clast-rich diamicton, and 10 m of clast-poor diamicton. The lowest 12 m of sediment penetrated in the borehole, to a depth of 367 m, consist of massive, deformed, silty clay with scattered granules and pebbles.

Borehole FD94-3

Two hundred and eighty-five metres of Pleistocene sediments were penetrated in borehole FD94-3, located near the centre of the Fraser delta (Fig. 5B, 6, 7; Dallimore et al., 1995). The Pleistocene-Holocene boundary is marked by a thin gravelly horizon at 19 m depth. The magnetic susceptibility response of the sediments increases markedly at this level (Hunter et al., 1995), as has been found at the

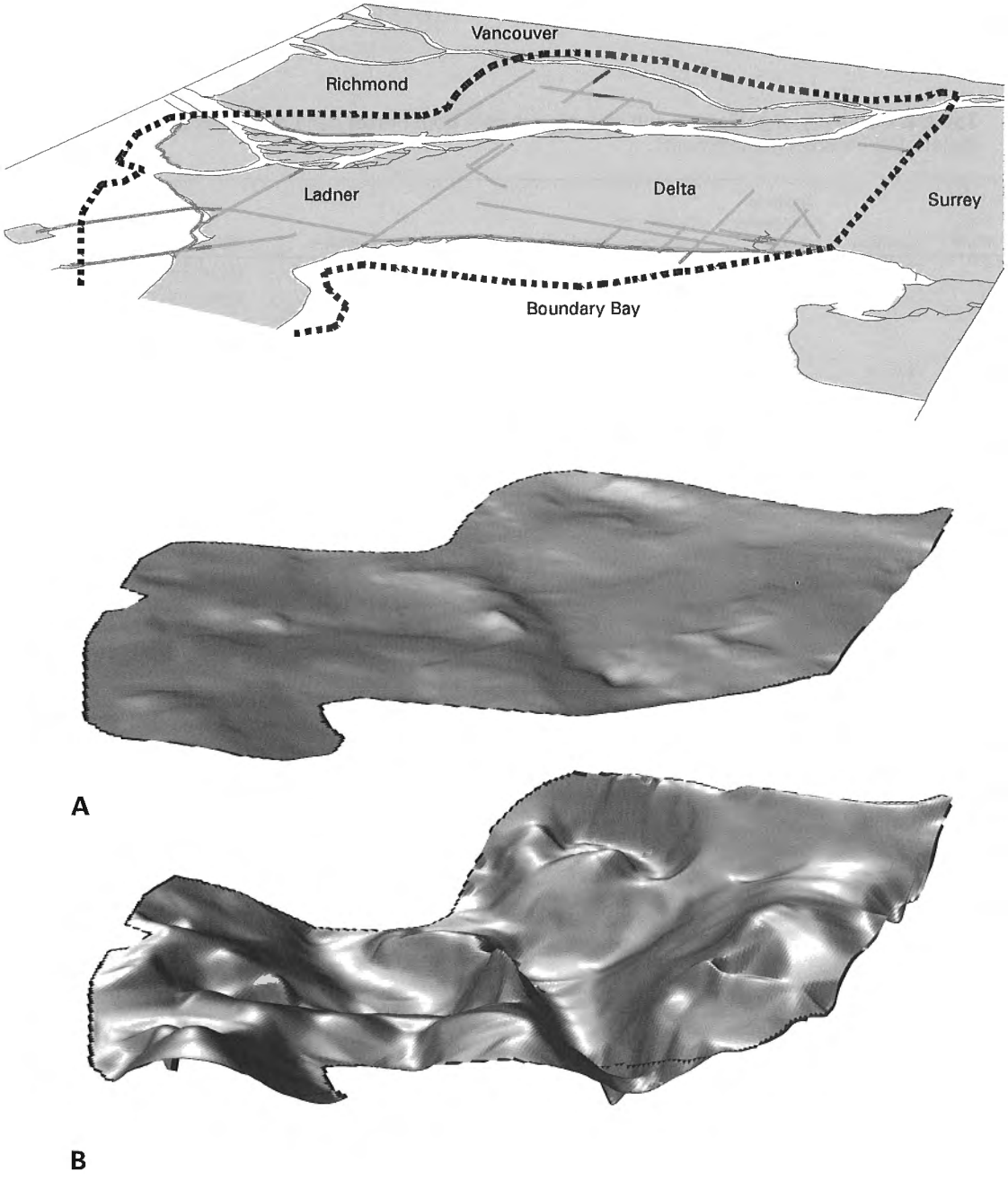

Figure 4. Oblique views of the buried Tertiary bedrock surface beneath the Fraser delta, created from data in Figure 3; views to the northwest and illumination from the southwest. ***A)*** *No exaggeration;* ***B)*** *5x vertical exaggeration.*

Pleistocene-Holocene boundary in several other boreholes on the delta (Luternauer and Hunter, 1996). An AMS radiocarbon age of 40 290 ± 780 BP (TO-4462) at 85 m depth suggests that sediments below the discontinuity are Pleistocene, although it is possible that the dated wood has been reworked and thus is older than the enclosing sediments.

The Pleistocene sequence in FD94-3 comprises 75 m of massive to stratified, fine-grained sand overlying 210 m of interbedded, mainly massive, very fine- to fine-grained sand and bioturbated, laminated to thin-bedded, clayey silt. No diamicton was encountered in the thick Pleistocene sequence in this borehole.

Two types of deformation were noted in the Pleistocene sediments. Convolute bedding (Fig. 7A) and high-angle stratification (Fig. 7B) are common in stratified clayey silt and fine-grained sand. These structures are confined to zones several centimetres to 3 m thick from 123 m depth to the bottom of the borehole at 305 m. The deformed zones are separated by undisturbed beds. The second type of deformation is manifested by sheared surfaces in dense clayey silt (Fig. 7C).

Table 2. Summary of geological and geophysical data from Fraser delta boreholes that penetrated Pleistocene sediments.

Site, Fig. 9	Borehole	Depth to Pleistocene (m)	Lithology of Pleistocene deposits	Geophysical method	Reference
A	FD86-1	8	8-85 DIAMICTON	SEE site Z in Table 3	Clague et al.,1991
B	FD86-5	51[1]	51-88 GRAVEL, CLAY, DIAMICTON	SHEAR VELOCITY MAGNETIC SUSCEPTIBILITY CONDUCTIVITY; SEE also site Y in Table 3	Clague et al., 1991
C	FD87-1A	185	185-367 CLAY, SILT, SAND, minor DIAMICTON		Clague et al., 1991; Luternauer et al., 1991, 1994
D	FD90-1	35	35-43 DIAMICTON	SHEAR VELOCITY MAGNETIC SUSCEPTIBILITY CONDUCTIVITY	Hunter et al., 1994
E	SFU90-3	53	stiff drilling below 53 m[2]	SEE site R in Table 3	M.C. Roberts, pers. comm., 1996
F	GA-111	66	66-81 DIAMICTON 81-115 SILT and SAND with silty CLAY at base 115-122 DIAMICTON 122-145 CLAY		Bazett and McCammon, 1986
G	FD92-2	32	32-35 DIAMICTON	SHEAR VELOCITY MAGNETIC SUSCEPTIBILITY CONDUCTIVITY	Hunter et al., 1994
H	FD92-11	100	100-101 CLAY, SILT, very fine SAND	MAGNETIC SUSCEPTIBILITY CONDUCTIVITY	Christian et al., 1994a
I	FD94-3	19	19-305 CLAY, SILT, SAND	SHEAR VELOCITY MAGNETIC SUSCEPTIBILITY; SEE also site DD in Table 3	Dallimore et al., 1995
J	FD94-4	236	236-301 DIAMICTON with SILT and CLAY intervals at 280-289	SHEAR VELOCITY MAGNETIC SUSCEPTIBILITY CONDUCTIVITY	Dallimore et al., 1995
K	FD95-S1	109	109-122 DIAMICTON 122-124 sandy SILT 124-144 clayey and sandy SILT	SHEAR VELOCITY MAGNETIC SUSCEPTIBILITY CONDUCTIVITY	Christian et al., 1995
L	FD95-2	52	stiff drilling below 52 m[2]	SHEAR VELOCITY MAGNETIC SUSCEPTIBILITY CONDUCTIVITY; SEE also site EE in Table 3	
M	FD95-4	91	stiff drilling below 91m[2]	MAGNETIC SUSCEPTIBILITY CONDUCTIVITY	
N	FD95-8	50	stiff drilling below 50 m	SEE site AA in Table 3	
O	MUD BAY d-95-D	186	186-266 SAND 266-447 CLAY, SILTSTONE	conventional industry electrical and sonic logs indicating a decreasing conductivity gradient and a P-wave discontinuity	J. Britton, pers. comm., 1996
P	FD96-1	305	305-328 DIAMICTON	SHEAR VELOCITY MAGNETIC SUSCEPTIBILITY CONDUCTIVITY	Dallimore et al., 1996
Q	DH-10	78	78-80 DIAMICTON		Swan Wooster Engineering, pers. comm., 1996

[1] Depth based on geophysical anomaly is 33 m.
[2] No samples were collected.

Table 3. Summary of shear-wave refraction data for sites where Pleistocene sediments are suspected or have been identified.

Site, Fig. 9	Depth to top Pleistocene[1] (m)	Holocene shear-wave velocity range (m/s)	Pleistocene shear-wave velocity range (m/s)	Survey description
R	86 (70-110)	120-340	450-550	reversed refraction array length 480 m
S	78 (77-79)	80-300	450-730	reversed refraction array length 480 m
T	>190	180-350		single-ended refraction array length 490 m
U	>235	100-420		reversed refraction array length 600 m
V	>246	135-400		single-ended refraction array length 650 m
W	>274	140-390		single-ended refraction array length 790 m
X	>161	90-350		single-ended refraction array length 540 m
Y	69 (50-87)	110-270	550	reversed refraction array length 300 m
Z	11 (4-18)	130-200	400-650	reversed refraction array length 270 m
AA	77 (70-84)	80-300	450-550	reversed refraction array length 270 m
BB	90 (50-130)	50-250	750	reversed refraction array length 330 m
CC	24 (16-32)	100-270	600-740	reversed refraction array length 100 m
DD	26 (19-33)	120-210	320-460	reversed refraction array length 270 m
EE	72 (69-75)	85-260	395-545	reversed refraction array length 270 m
FF	52 (50-54)	75-322	375-660	reversed refraction array length 330 m

[1] Mean (range).
Note: sites Y, Z, AA, BB, CC, DD are, respectively, sites 5, 9, 30, 36, 38, and 70 of Hunter et al. (1992).

Borehole FD94-4

About 1 m of sandy silt with scattered granules and pebbles caps the 64 m thick Pleistocene sequence in borehole FD94-4, located on central Lulu Island 4 km west of FD94-3 (Fig. 5C, 6; Dallimore et al., 1995). The silt is underlain across a gradational contact at 238 m depth by massive to weakly stratified diamicton, consisting of clayey sandy silt with 15-25% subangular to angular, striated pebbles (Fig. 8A). Below 255 m, the diamicton contains layers of pebbly clayey silty sand with rare shell fragments, and laminated to thin-bedded sandy silt. The diamicton sequence is sharply underlain, at 281 m depth, by weakly laminated, compact, sheared and slickensided, clayey silt with scattered shell fragments. At a depth of 287 m, the silt grades down into weakly stratified, silty to sandy diamicton; drilling ended in this unit at 301 m.

Borehole 95S-1

Pleistocene deposits were encountered between 109 and 152 m in this borehole (Appendix 1; Christian et al., 1995). The uppermost 4 m of the Pleistocene sequence consist of clayey sandy silt with up to 5% scattered pebbles. This unit overlies 10 m of dense sandy diamicton. The lower part of the penetrated sequence comprises massive to laminated, sandy and clayey silt with some pebbles (K.W. Conway, pers. comm., 1996).

Borehole FD96-1

Pleistocene sediments were penetrated at depths from 305 to 328 m in this borehole (Fig. 5D), located in downtown Richmond 2 km southwest of FD94-4 (Fig. 5C, 6). Massive to weakly laminated clayey silt with scattered pebbles and granules occurs between 305 and 307 m. This unit is underlain by 18 m of dominantly rhythmically bedded clayey silt, comprising 2-3 cm thick couplets (Fig. 8B) and containing scattered shells and shell fragments. The lowest unit, at 325-328 m, is massive clast-poor diamicton.

Depositional environments and age

The Pleistocene succession beneath the Fraser delta includes diamicton units of glacial and glaciomarine origin, but is dominated by glaciomarine and marine sand and silt. The succession, on the whole, is more heterogeneous than the Holocene deltaic sequence. Most of the nondiamictic sediments are probably subaqueous outwash deposited at various distances from glacier margins during the waxing and waning stages of glaciations. The gross mineralogy of the sediments supports this inference: Pleistocene sands contain abundant quartz and feldspar, probably derived from the Coast Mountains to the north, whereas Holocene deltaic sands are dominated by darker lithic detritus derived from the Cascade Mountains to the east.

With the exception of the finest grained bioturbated facies, the Pleistocene sediments were deposited relatively rapidly. High sedimentation rates and the antiquity (Early-Middle Pleistocene age; see below) of the lowest sediments in borehole FD94-3 imply that there are significant breaks in the sequence. If one assumes that sedimentation rates are even grossly comparable to those of the Holocene, the Pleistocene succession can only record, at most, a few tens of thousands of years of deposition. The hundreds of thousands of years which are not represented must, therefore, be associated with one or more unconformities.

Fraser Glaciation

Thin, pebbly, silt layers at the top of the Pleistocene sequence in boreholes FD87-1, FD94-4, FD95S-1, and FD96-1 (Fig. 5) are glaciomarine deposits dating to the end of the Fraser Glaciation, which was the last Pleistocene glaciation of British Columbia (Capilano Sediments of Armstrong, 1981, 1984). The radiocarbon age of 11 920 ± 90 BP from the pebbly silt layer in FD87-1 is consistent with this age assignment. These sediments probably accumulated on the seafloor near the terminus of a glacier. The coarse-grained fraction of the sediment is interpreted to be ice-rafted debris derived

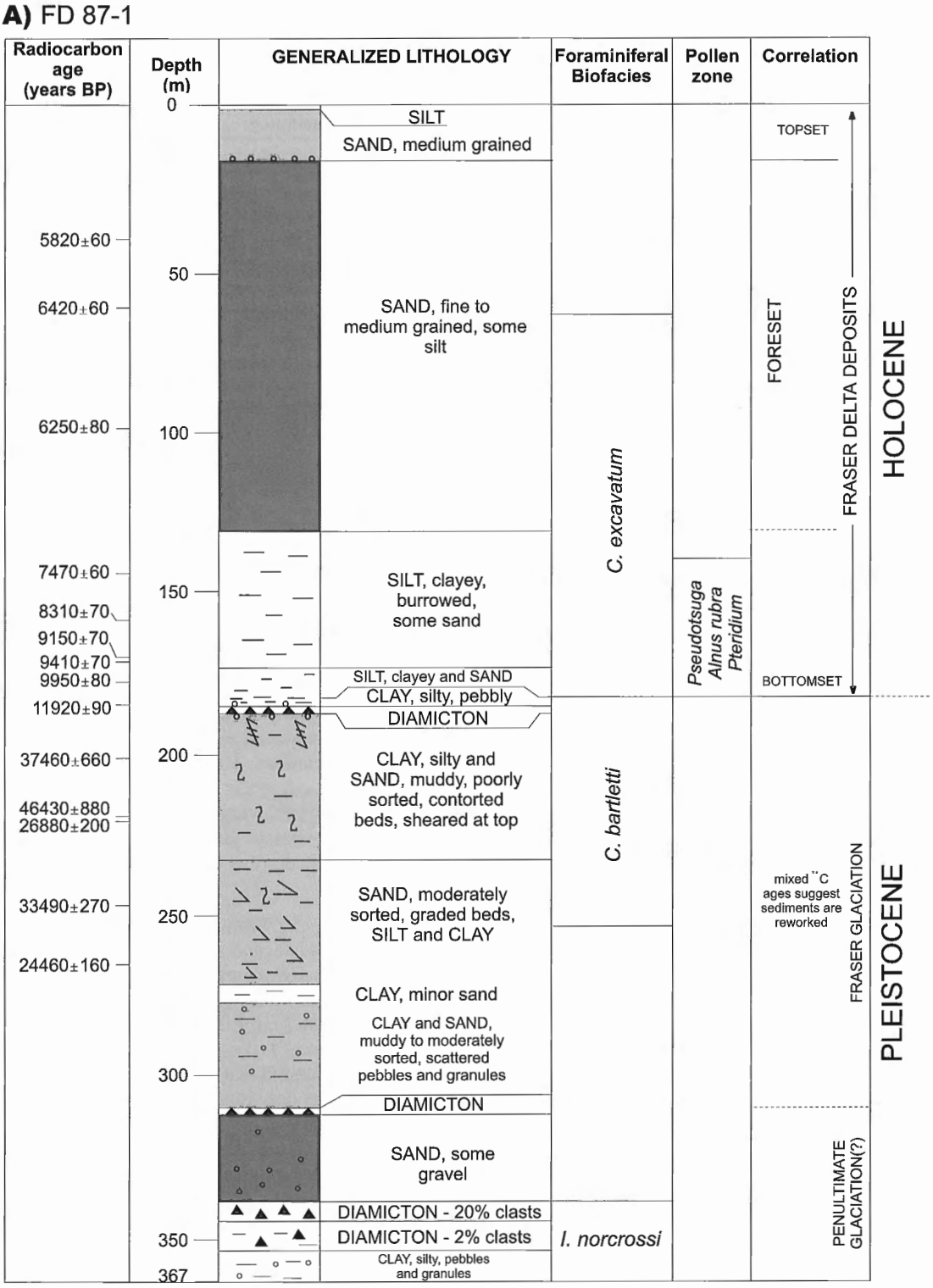

Figure 5. *Stratigraphy, sedimentology, and chronology of Geological Survey of Canada deep boreholes.* ***A)*** *FD87-1, southwestern Fraser delta;* ***B)*** *FD94-3, central Lulu Island;* ***C)*** *FD94-4, west-central Lulu Island;* ***D)*** *FD96-1, western Lulu Island (see Fig. 1 for locations and Clague et al., 1991; Luternauer et al., 1991; and Dallimore et al., 1995, 1996, for additional details. Radiocarbon ages are reported in Table 1 (a reservoir correction of 410 years, equivalent to a fractionation correction to a base of* $\delta^{13}C = 0‰$*, has been applied to all shell ages).*

B) FD 94-3

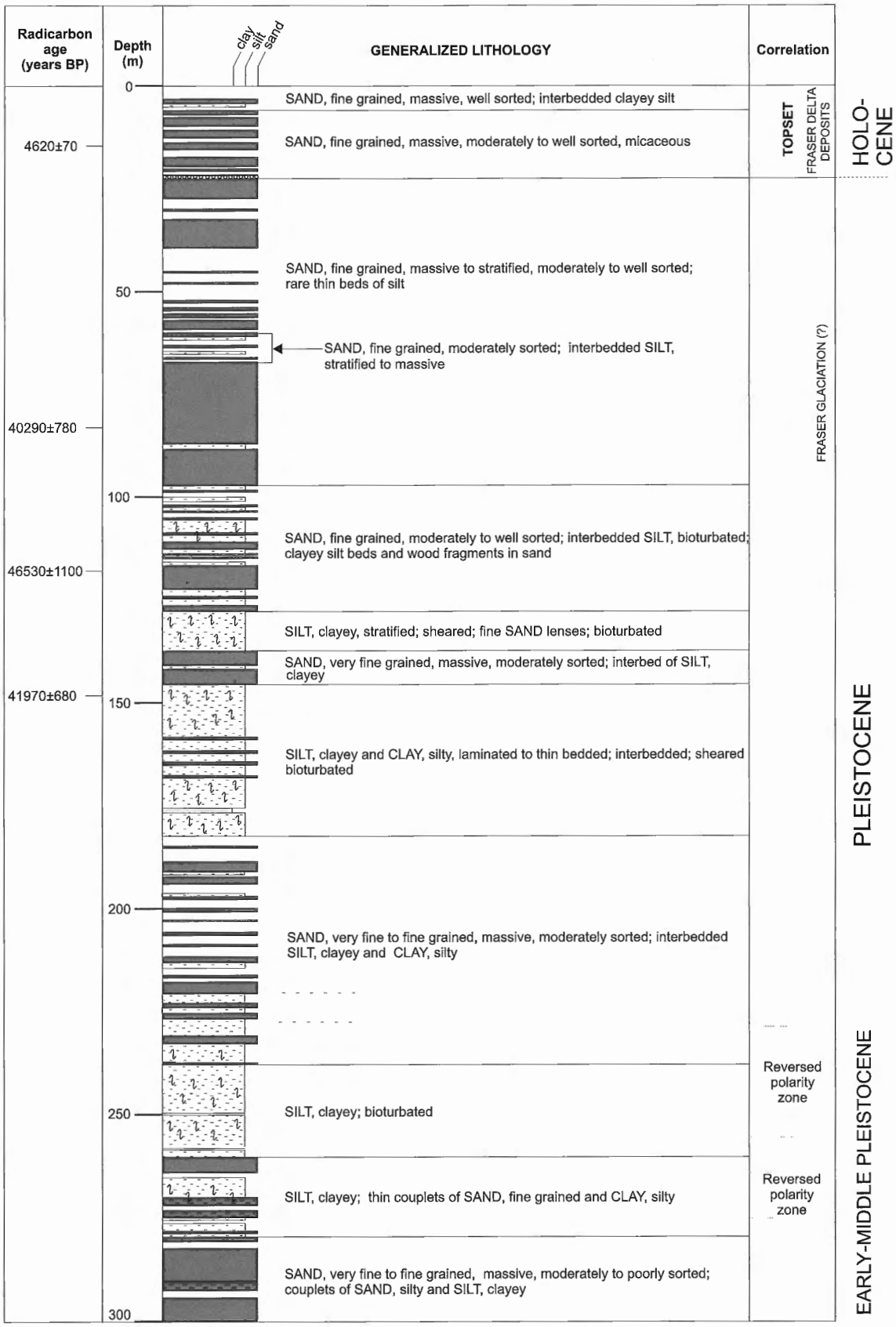

Figure 5. (cont.)

C) FD 94-4

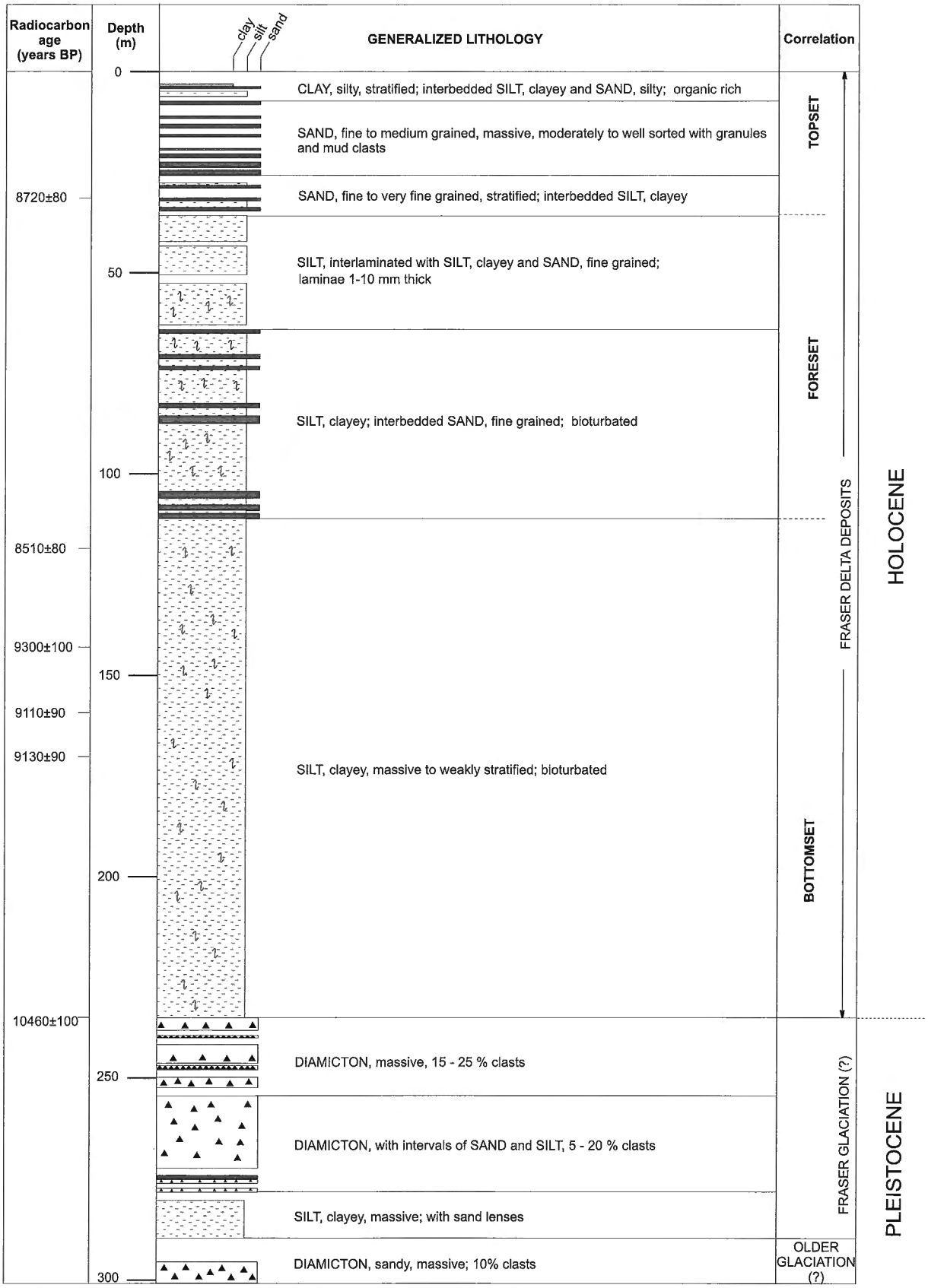

Figure 5. (cont.)

D) FD 96-1

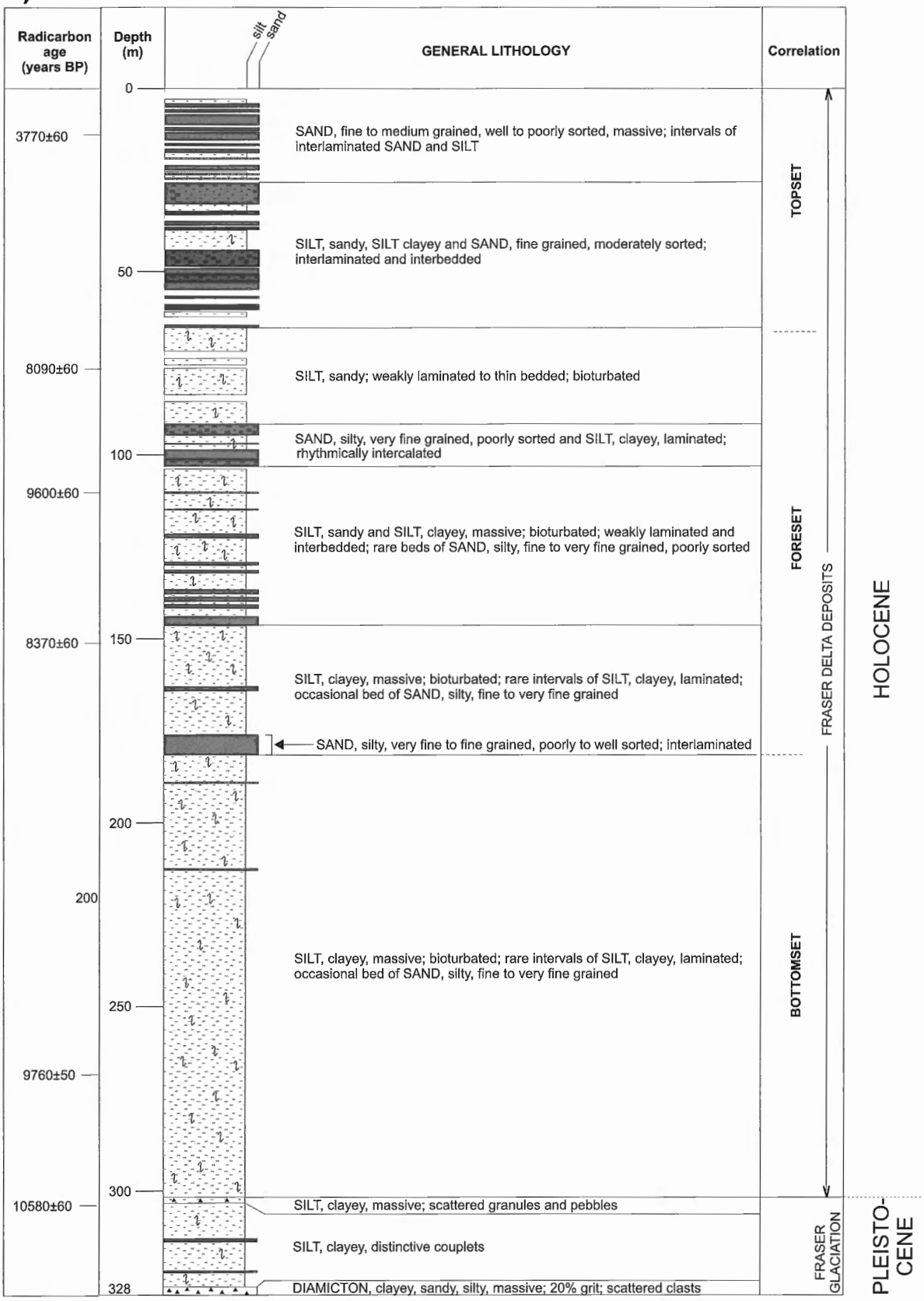

Figure 5. *(cont.)*

from a glacier margin or from icebergs calved off the glacier. In borehole FD96-1, the number and size of stones decrease upward, signifying either retreat of the glacier terminus or a decrease in the supply of coarse-grained clastic material. Couplets of clayey silt below the pebbly silt in FD96-1 (Fig. 8B) record relatively rapid sedimentation in a glaciomarine environment, perhaps close to the glacier terminus. Cowan and Powell (1990) describe rapidly deposited couplets at the tidewater terminus of McBride Glacier in Alaska. They suggest that tidal fluctuations play a role in the deposition of these couplets, but that similar rhythmic sediments may result from diurnal or seasonal variations in sediment supply.

Sandy diamicton below the thin, pebbly, silt unit in boreholes FD87-1, FD94-4, FD95S-1, and FD96-1 is interpreted to be till deposited directly from a glacier flowing southward down the Strait of Georgia during the Fraser Glaciation. The glacier eroded underlying Pleistocene deposits and produced the irregular surface on which the Holocene Fraser delta accumulated. It also sheared some clayey silt intervals within the Pleistocene sequence (e.g. at 192-196 m in FD87-1 and 280-285 m in FD94-4).

Silty and sandy sediments beneath the capping diamicton in FD87-1, to a depth of about 256 m, contain a foraminiferal fauna indicative of deposition in cold marine waters more than 150 m deep (Patterson and Cameron, 1991). These sediments contain pebble bands deposited by energetic meltwater

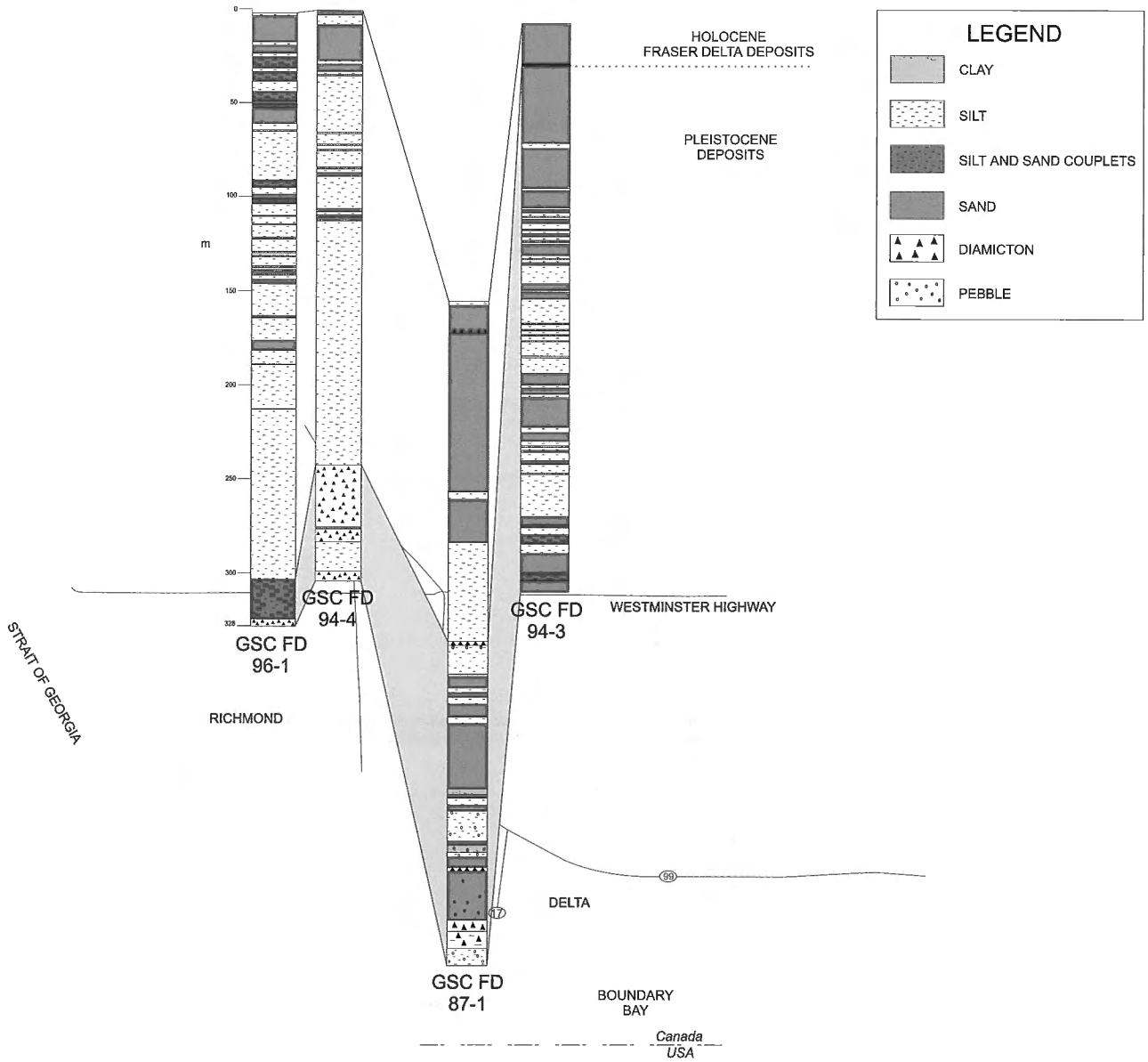

Figure 6. *Fence diagram showing generalized stratigraphy and correlation of deep Geological Survey of Canada boreholes (see Fig. 1 for borehole locations). The stratigraphic logs are positioned at their respective locations on the delta.*

flows or turbid underflows. The sediments probably record the advance of glaciers into the area during the early part of the Fraser Glaciation between about 25 000 and 16 000 ^{14}C years ago (Clague et al., 1980). They are likely the marine equivalent of sandy glaciofluvial deposits (Quadra Sand) which underlie some uplands at the margins of the Fraser delta (Clague, 1977, 1998). Radiocarbon ages from the glaciomarine sediments do not, as one might expect, become older downward (Fig. 5A), which indicates that the dated material has been reworked and that the ages should be considered minima for the time of sediment deposition.

The upper part of the Pleistocene sequence in FD94-3, above 148 m, is dominated by well sorted, fine-grained sand. The thickness of this mainly sandy sequence, the probable wedge shape of the deposit, and the presence of syndepositional deformation structures indicative of episodic mass movement are consistent with rapid deposition on a subaqueous fan or a delta near a glacier margin. These sediments may correlate with the above-mentioned, early Fraser Glaciation deposits in FD87-1.

Pre-Fraser glaciation(s)

Deposits of one or more pre-Fraser, Pleistocene glaciations are present in FD87-1, FD-94-3, and FD94-4, as well as in some other boreholes. Sandy diamicton at the base of FD87-1 and FD94-4 is interpreted to be till deposited during the penultimate glaciation (Semiahmoo Glaciation of Armstrong, 1984),

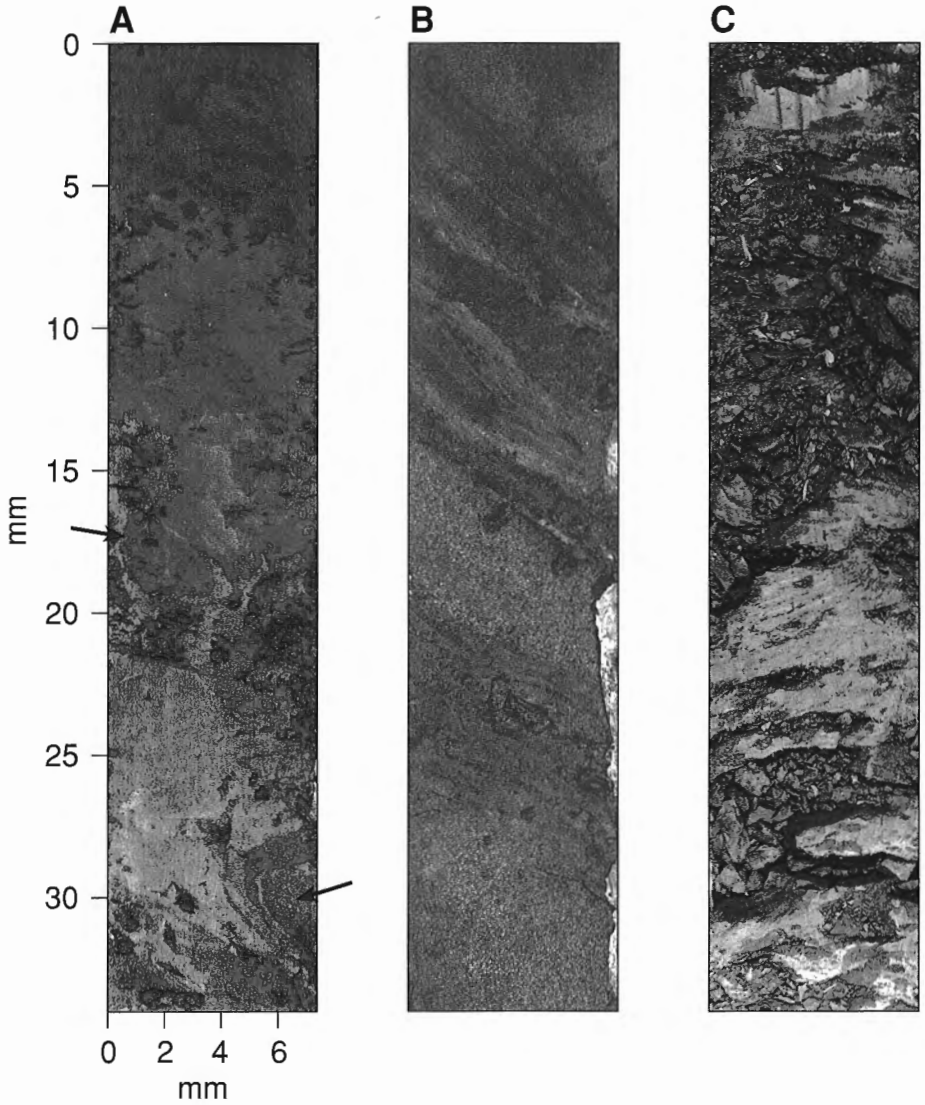

Figure 7. *Deformation features in cores of Pleistocene sediments from borehole FD94-3.* ***A)*** *Convolute bedding (arrows), 124 m depth.* ***B)*** *High-angle stratification, 216 m depth.* ***C)*** *Sheared surfaces within dense clayey silt, 155 m depth. The deformation in A and B is syndepositional to early postdepositional; that in C is postdepositional.*

which occurred more than 65 000 but less than 100 000 years ago (Clague et al., 1992a; Clague, 1998), or possibly during an older Pleistocene glaciation. In FD87-1, this sandy diamicton is underlain by clast-poor, foraminifera-bearing diamicton and pebbly silty clay of glaciomarine origin. Foraminiferal assemblages are dominated by two species, *Cassidulina reniforme* and *Islandiella norcrossi*, which are characteristic of ice-proximal glaciomarine environments (Scott et al., 1989; Patterson and Cameron, 1991). The stratigraphic position and foraminiferal assemblages of these sediments suggest that they date to the end of the penultimate glaciation, although they could possibly be older.

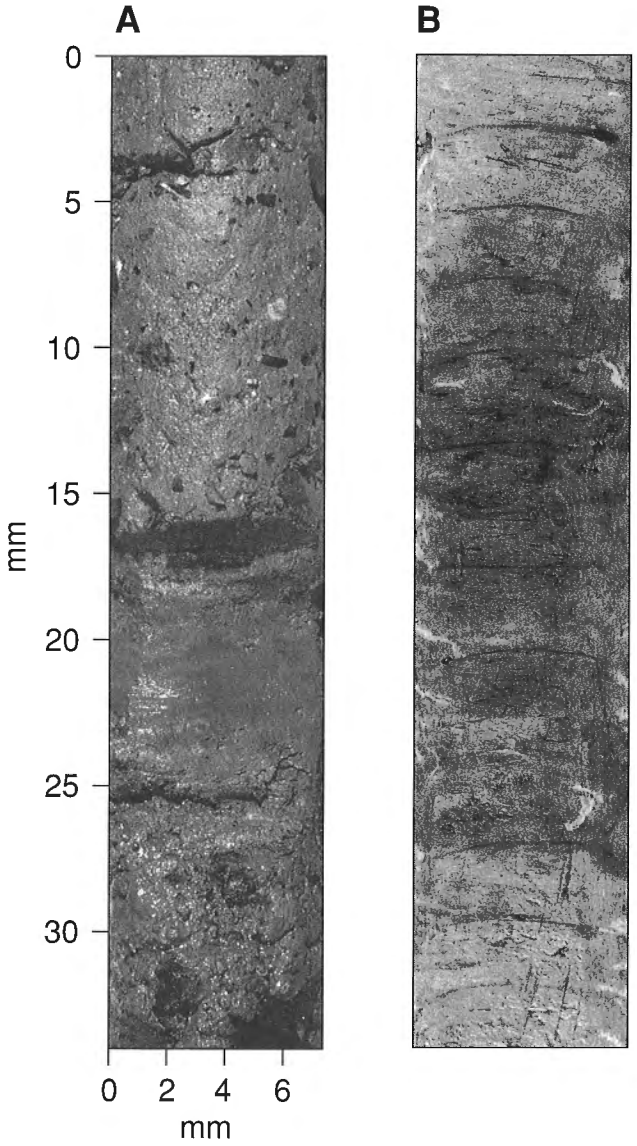

Figure 8. *Examples of Pleistocene sediments encountered in deep boreholes on the Fraser delta.* ***A)*** *Diamicton and thin beds of poorly sorted sandy silt, FD94-4, 240 m depth.* ***B)*** *Rhythmic couplets of clayey silt, FD96-1, 302 m depth.*

Sediments in the lower part of the Pleistocene sequence in borehole FD94-3 are mainly interbedded, bioturbated, clayey silt and very fine-grained sand. These fine-grained sediments are interpreted to be distal glaciomarine or nonglacial marine deposits of Middle or Early Pleistocene age.

Their age is constrained by geomagnetic inclination data (Fig. 5B; Dallimore et al., 1995). There are two magnetically reversed intervals in the core, one from 230 to 259 m and another from 270 to 280 m; the remainder of the sequence has normal magnetic polarity. The reversely magnetized sediments are older than 790 000 years, which is the approximate age of the boundary between the Brunhes Normal Polarity Chron and the Matuyama Reversed Polarity Chron (Johnson, 1982). The older, reversely magnetized zone may predate the Matuyama Chron or it may be a subzone within that chron. In either case, sediments below 230 m are no younger than Middle Pleistocene and thus are older than the penultimate (Semiahmoo) glaciation in southwestern British Columbia (Clague et al., 1992a; Clague, 1998). If, as suggested earlier, the dominantly sandy part of the sequence above 148 m dates to the early part of the Fraser Glaciation, there must be one or more unconformities between it and the highest magnetically reversed sediments at 230 m.

THE PLEISTOCENE SURFACE

The surface separating Pleistocene deposits from overlying Holocene deltaic sediments has been penetrated in numerous boreholes near the margins of the Fraser delta, but in relatively few boreholes nearer the centre (Fig. 9). Figures 10 and 11 show the depths of this surface where it is known from drilling and geophysical surveys, and Figure 12 shows the surface in several profiles across the delta.

The Pleistocene surface is more than 150 m deep beneath most of the delta, but it is highly irregular. A northwest-trending Pleistocene ridge extends beneath the tidal flats near Point Roberts (Christian et al., 1994a), and Pleistocene sediments as shallow as 19 m are present beneath central Lulu Island (Dallimore et al., 1995). In contrast, in Richmond on western Lulu Island, the Pleistocene surface is more than 300 m deep (Dallimore et al., 1996). We attribute this considerable relief to erosion of the Pleistocene succession by glaciers during the Fraser Glaciation.

HOLOCENE DEPOSITS

The Holocene deltaic succession has a maximum known thickness of 305 m and can be divided into topset, foreset, and bottomset units. The uppermost, topset, unit comprises generally flat-lying sediments deposited in floodplain, tidal-flat, river-channel, and bog environments. The foreset unit sharply underlies the topset and consists of gently dipping delta-slope sediments. The bottomset unit interfingers with, and grades up into, the foreset unit; it consists of flat to very gently dipping beds deposited beyond the base of the slope.

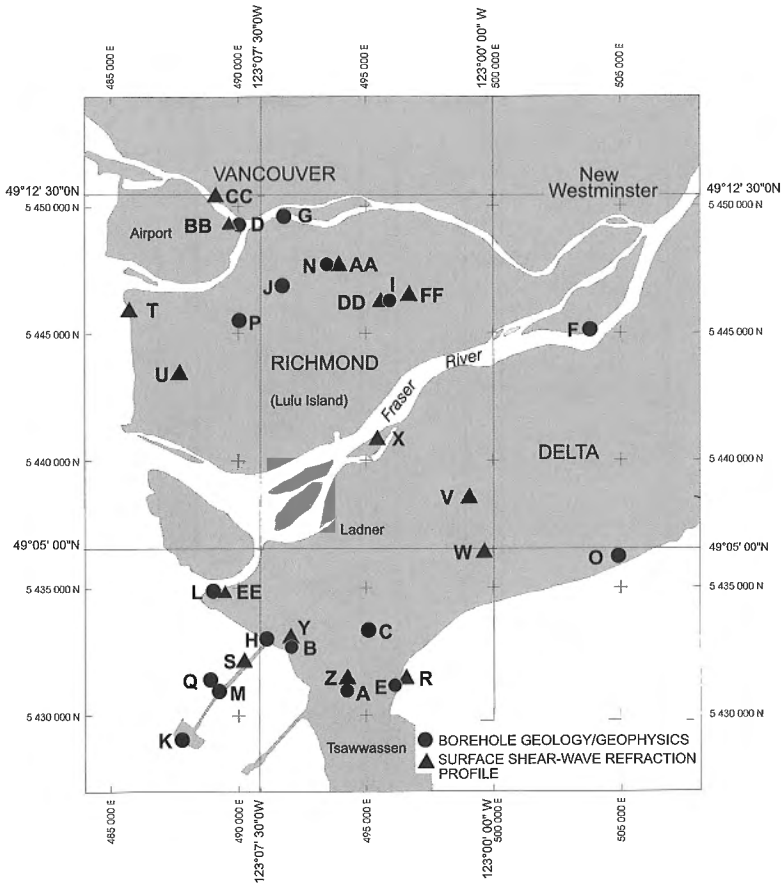

Figure 9.

Locations where the depth (or minimum depth) to the top of the Pleistocene sequence has been determined by drilling or geophysical surveying. See Tables 2 and 3 for borehole and survey details, and Figure 10 for depths (from Luternauer and Hunter, 1996).

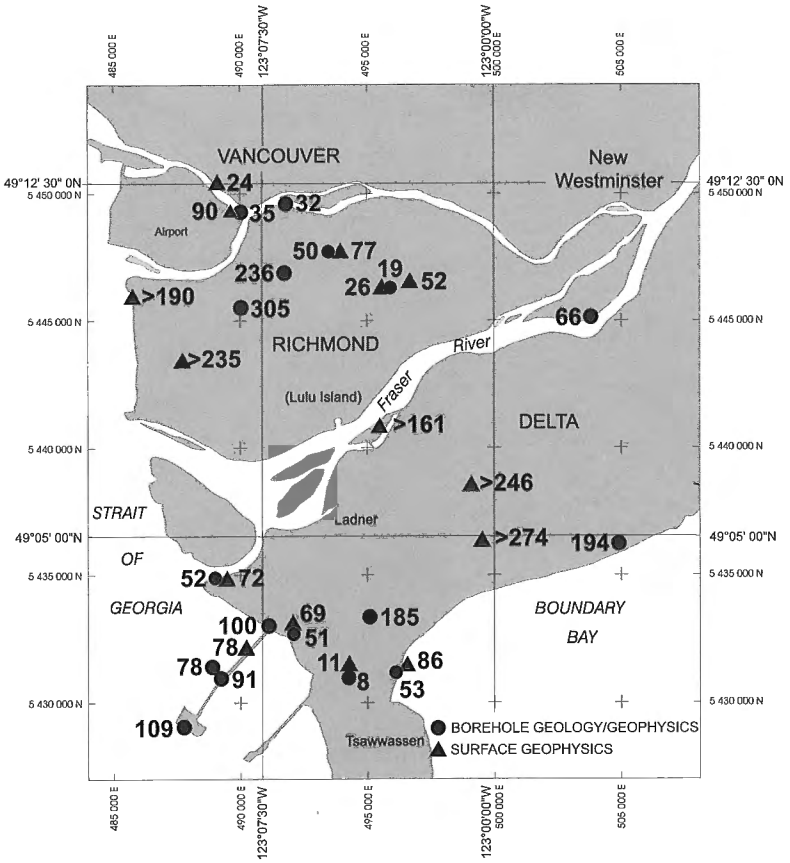

Figure 10.

Depth to the top of the Pleistocene sequence based on borehole geological and geophysical data, and shear-wave refraction surveys (from Luternauer and Hunter, 1996).

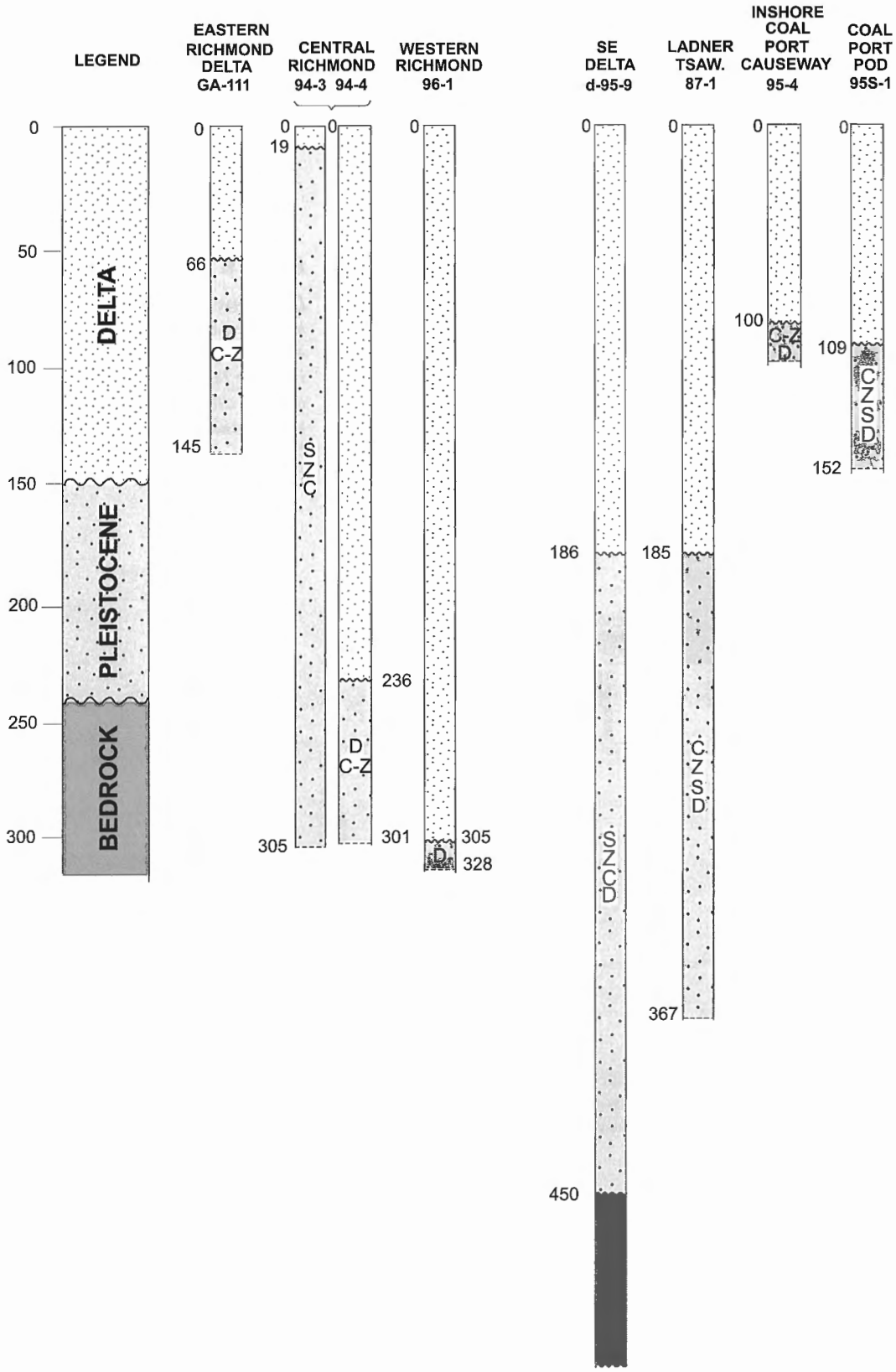

Figure 11. Generalized stratigraphy of boreholes which penetrated Pleistocene deposits or bedrock beneath the Fraser delta, and an earlier geological section used in geotechnical assessments of potential ground motion amplification. Sediment types are listed in order of decreasing abundance; C - clay, Z - silt, S - sand, D - diamicton.

Topset

The topset unit thins from about 40 m at the apex of the Fraser delta to 20 m or less at the western margin of the dyked upper delta plain (Fig. 13, 14, 15; Clague et al., 1983; Monahan et al., 1993a, b). The westward thinning of the topset is due to the delta being constructed at a time when relative sea level was rising (Clague et al., 1983; Williams and Roberts, 1989, 1990); i.e., the oldest part of the topset, nearer the apex, was deposited at a time of lower sea level, whereas the youngest part of the topset, at the western margin of the delta, was deposited when sea level was near its present position.

The western, southern, and central parts of the upper delta plain are underlain by organic-rich, laminated, clayey silt, interpreted to be a floodplain deposit (Williams, 1988; Williams and Roberts, 1989; Hutchinson et al., 1995). This deposit thickens eastward, from less than 1 m at the western margin of the dyked delta plain to more than 10 m at the apex of the delta (Fig. 13; Clague et al., 1983; Williams, 1988; Williams and Roberts, 1989). Mazama tephra (ca. 6800 ^{14}C years BP) has been identified in floodplain silt underlying the eastern part of the upper delta plain (Williams, 1988; Williams and Roberts, 1989). Domed peat bogs have developed on the floodplain in this area (Hebda, 1977; Clague and Luternauer, 1982; Clague et al., 1983).

The floodplain deposit is underlain in some areas by up to 5 m of burrowed silt and sand containing an intertidal fossil fauna (Williams, 1988; Williams and Roberts, 1989; Monahan et al., 1993a, b; Hutchinson et al., 1995).

The lowest, and thickest, part of the topset unit is an 8-30 m thick deposit of sand (Fig. 13), which has an erosional base (Fig. 16) with several metres of local relief, and is organized into one or more decametre-scale fining-upward sequences. The sand is fine to medium grained (Fig. 17) and commonly contains silt and clay rip-up clasts (Fig. 18). Very fine-grained gravel is present within the sand, generally at the base of fining-upward sequences. The sand forms a sheet-like deposit that underlies almost all of the dyked upper delta plain and extends westward beneath the lower delta plain,

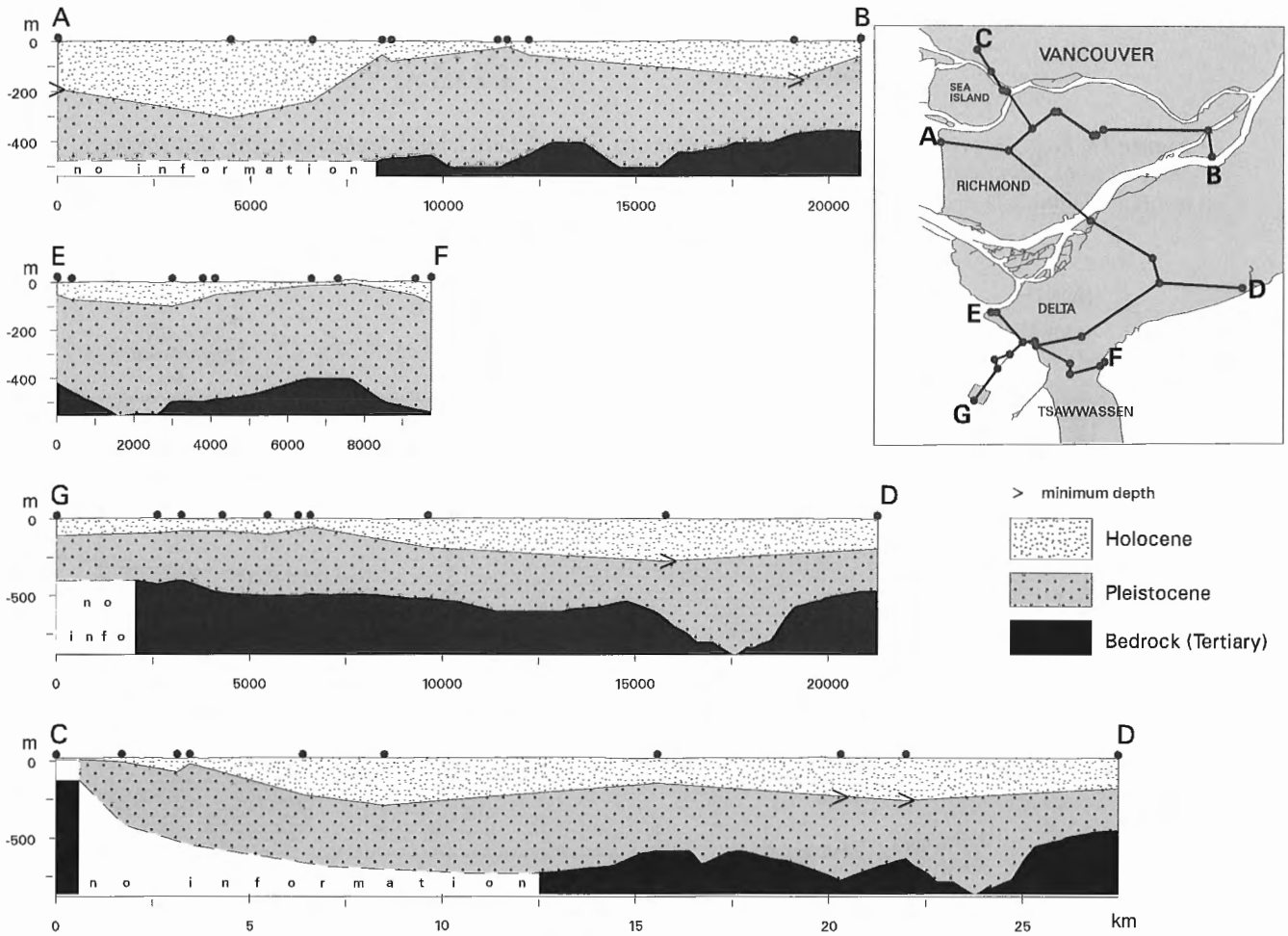

Figure 12. *Cross-sections showing variations in the thickness of Holocene and Pleistocene deposits beneath the Fraser delta, based on drilling and geophysical surveys. The position of the bedrock surface is based on data from Figure 3. The depth of the Pleistocene surface is known only at sites designated by black dots; the position of the surface between data points is uncertain. Note differences in the vertical scales.*

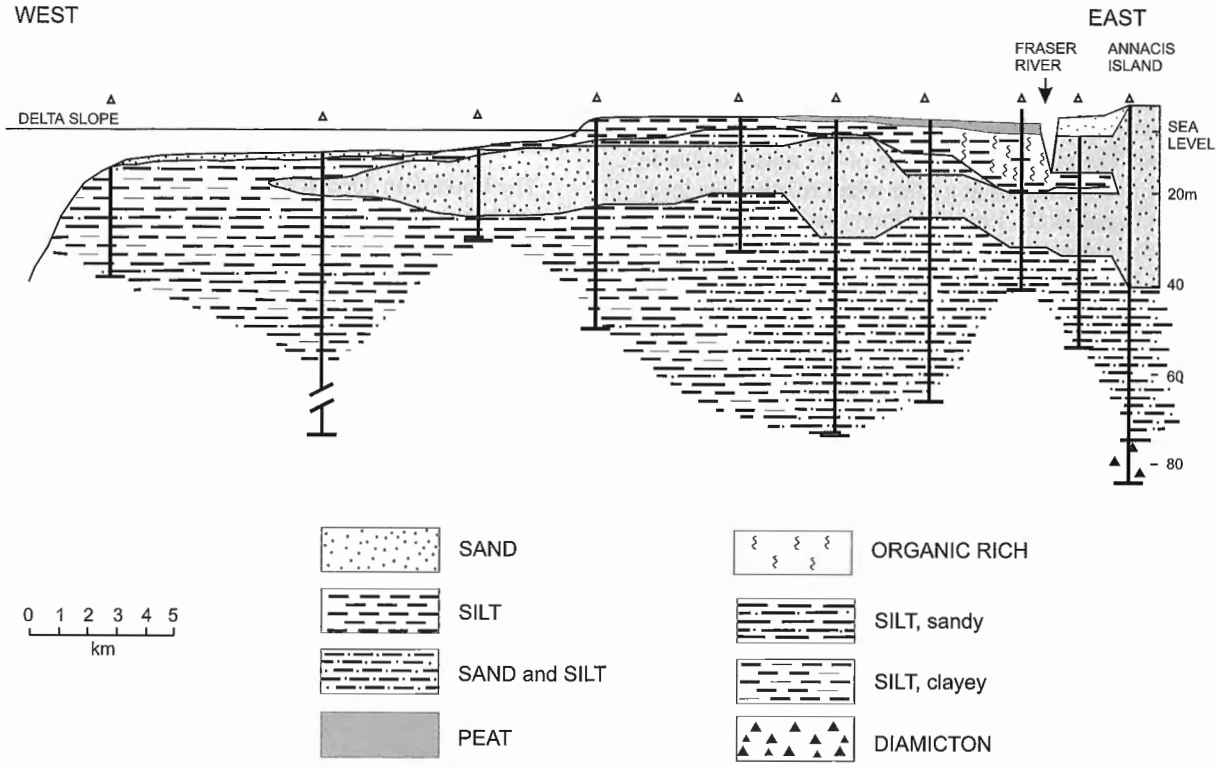

Figure 13. *East-west cross-section of Holocene deposits beneath Lulu Island, highlighting the distributary-channel sand sheet (stippled shaded unit); see Figure 1 for location. The section is based on cone penetration test (CPT) data.*

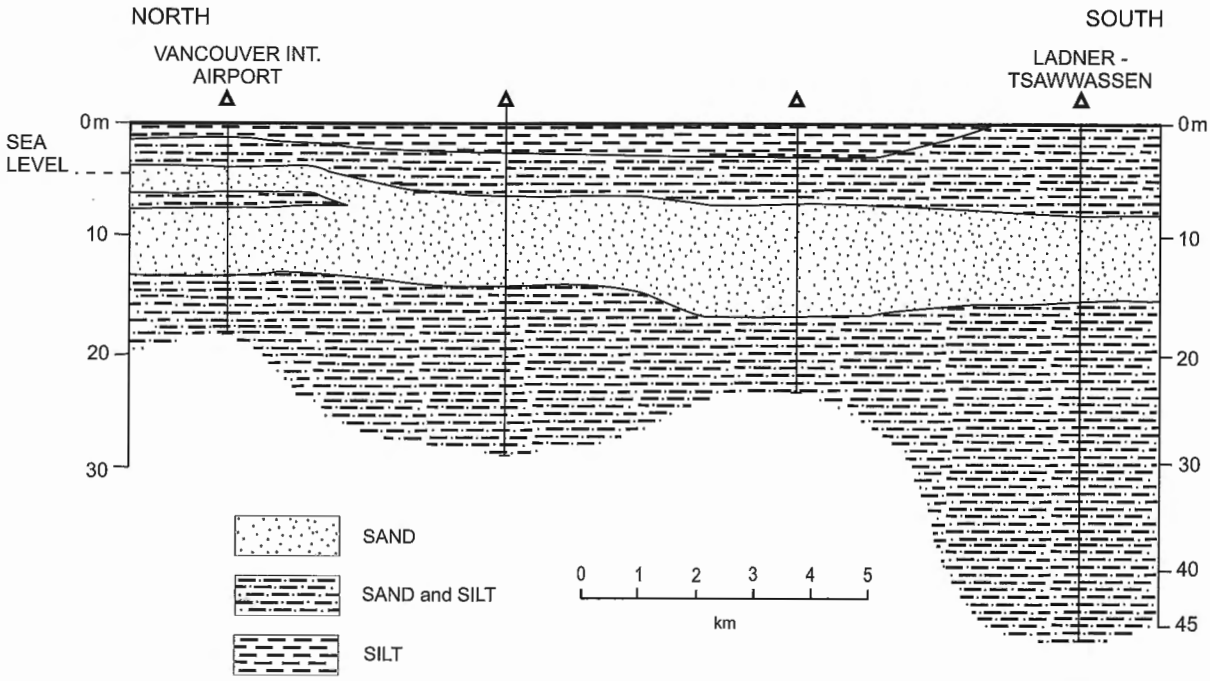

Figure 14. *North-south cross-section of Holocene deltaic deposits showing the distributary channel sand sheet overlying thick delta-slope silt and sand; see Figure 1 for location. The section is based on cone penetration test (CPT) data.*

approximately halfway across Sturgeon Bank and almost to the seaward edge of the tidal flats off southern Roberts Bank (Fig. 13, 14, 15; Williams and Luternauer, 1991; Monahan et al., 1993a, b; 1995; Hutchinson et al., 1995).

The sharp erosional base of the sand sheet and the multiple fining-upward sequences within it are indicative of deposition in a distributary-channel environment. Three distinct subfacies are recognized (Monahan et al., 1993a, b, 1995). An intertidal subfacies consists of sand deposited in distributary channels in a tidal-flat environment. Sand of this subfacies contains shell debris, particularly at its base (Fig. 18), and grades upward into the overlying, above-mentioned, burrowed silt and fine-grained sand, interpreted to be an intertidal deposit. This subfacies is widespread beneath both the modern tidal flats and the upper delta plain. The second subfacies is sand deposited in channels on the upper delta plain. The sand is devoid of shell debris, contains a freshwater diatom assemblage, and is capped by well bedded and laminated sand and silt. High-angle planar crossbedding is common in the upper part of this subfacies (Fig. 17; Williams and Luternauer, 1991; Monahan et al., 1993a, b, 1995; Hutchinson et al., 1995). This subfacies occurs as broad bands which cross the upper delta plain (for examples, see Williams and Luternauer, 1991; Hutchinson et al., 1995; Monahan et al., 1995). The third subfacies comprises thin (2-5 m) accumulations of sand at the seaward limit of the distributary-channel sand sheet (Monahan et al., 1995). This subfacies has also been recognized locally at the base of the sand sheet near the centre of the delta, where it has been preserved because of the subsequent rapid rise in sea level during the middle Holocene (Williams and Roberts, 1989; Monahan et al., 1995). Elsewhere, the subfacies was eroded by migrating channels.

Locally, ribbon-like bodies of interbedded sand and silt up to 20 m thick occur in place of the upper part of the sand sheet. These bodies record relatively low-energy sedimentation in channels during their abandonment (Monahan, 1993; Hutchinson et al., 1995; Monahan et al., 1995).

Historical records show that distributaries migrated extensively where they crossed the modern tidal flats (Johnston, 1923; Clague and Luternauer, 1982; Clague et al., 1983; Luternauer and Finn, 1983). Although distributary channels on the modern upper delta plain have been more stable, some channel migration has occurred in historical times (Johnston, 1923; North et al., 1979; Monahan et al., 1993a, b, 1995). A large, long-abandoned channel, which crosses eastern Lulu Island from the present Main Channel to North Arm (Johnston, 1923; Clague et al., 1983), demonstrates that major avulsive events have occurred on the upper delta plain. Repeated avulsion on the upper delta plain and channel migration on the lower delta plain explain the widespread extent of the distributary-channel sand sheet (Monahan et al., 1993b; Hutchinson et al., 1995).

Foreset

The distributary-channel sand sheet sharply overlies up to 165 m of seaward-dipping sand and silt, interpreted to be delta slope deposits (Fig. 5A, C, D, 15; Pullan et al., 1989,

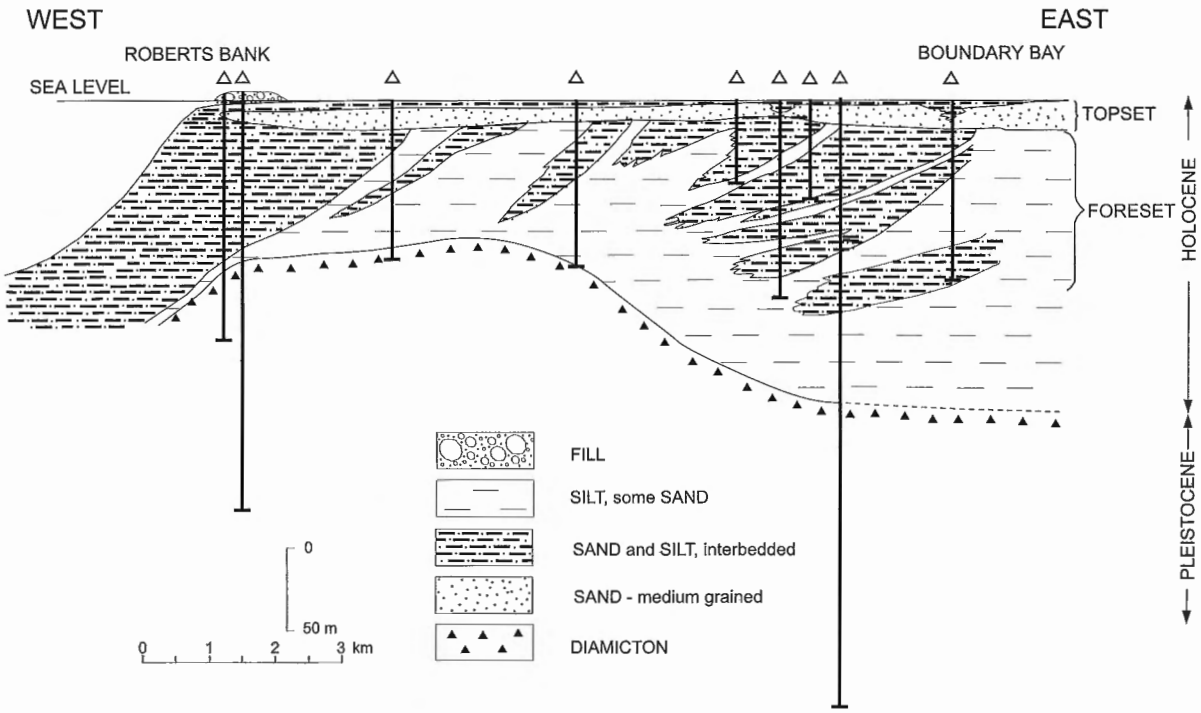

Figure 15. *East-west cross-section of Holocene deposits beneath the southernmost Fraser delta, showing the distributary-channel sand sheet and underlying foreset deposits; see Figure 1 for location. The section is based on cone penetration test (CPT) data.*

1998; Clague et al., 1991; Monahan et al., 1993b, 1995). Locally, some interbedded sand and silt directly below the distributary-channel sand sheet may be tidal-flat or subaqueous-platform deposits.

The foreset deposits are interlaminated and interbedded on a variety of scales (Fig. 16, 19, 20). Coarser grained facies include laminated, very fine- to fine-grained sand deposited from suspension, and metre-thick fining-upward beds of very fine- to medium-grained sand with shells and rip-up clasts (Fig. 20, 21), interpreted to be sediment gravity-flow deposits. Fine-grained sediments deposited on the upper delta slope (<50 m water depth) range in texture from sandy to clayey silt, are laminated, and contain thin, very fine-grained sand interbeds (Fig. 19). These sediments are commonly arranged into metre-scale coarsening-upward sequences of sand and silt, interpreted as annual deposits (Monahan et al., 1994, 1995; B.S. Hart, pers. comm., 1993). During spring freshet, the peak in suspended load precedes the peak in river discharge (Milliman, 1980; Kostaschuk et al., 1986, 1989). Consequently, silty sediments are transported out of the river mouth and onto the slope before sands, which are most efficiently transported during peak flow. Fine-grained sediments deposited on the lower slope (>50 m water depth) are commonly bioturbated and become progressively finer with depth (Christian et al., 1994a, b; Dallimore et al., 1995).

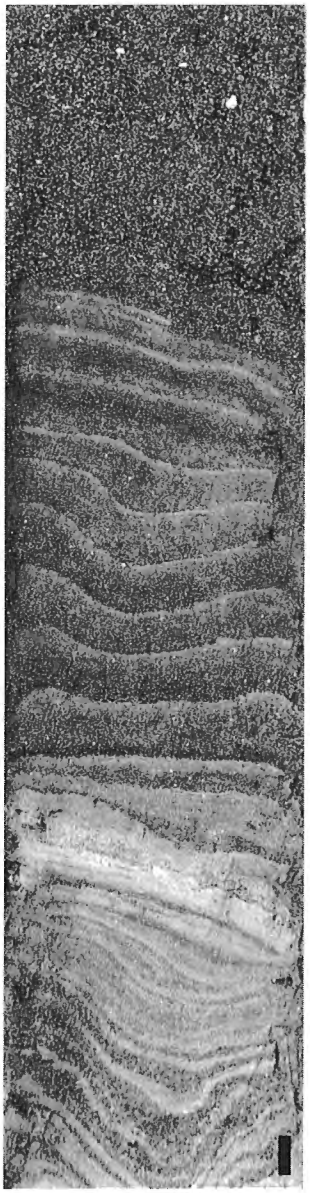

Figure 16. *Erosional base of the distributary-channel sand sheet, showing truncation of underlying, laminated foreset silt and sand; FD93-5, 20.68-20.98 m depth (see Fig. 1 for location). Vertical bar at lower right is 1 cm.*

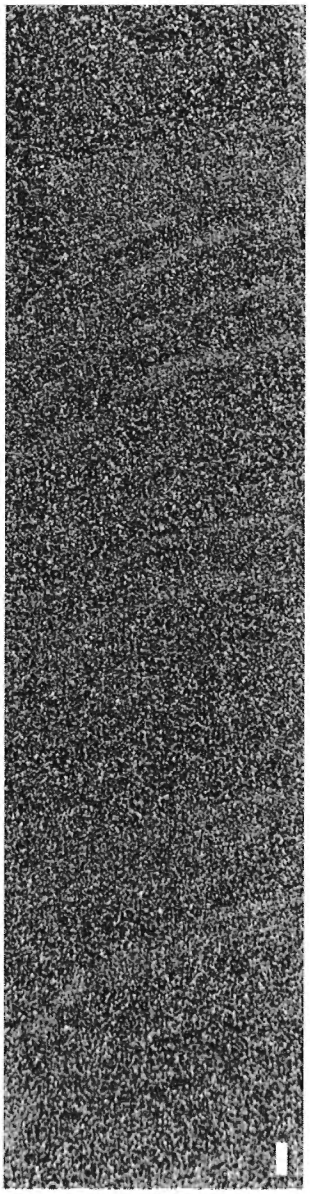

Figure 17. *Cross-bedded sand of the distributary-channel sand sheet; K2V2, 7.50-7.80 m depth (see Fig. 1 for location). Vertical bar at lower right is 1 cm. (From Monahan et al., 1997.)*

Sand is most common in the upper portion of the foreset unit. In the southern part of the delta, sand-dominated zones up to 30 m thick are interbedded with much thinner silty zones and extend to depths of 130 m (Fig. 17; Clague et al., 1991; Luternauer et al., 1991). Farther north, the foreset unit is much siltier, although localized sandy zones up to 30 m thick can be found directly below the distributary-channel sand sheet (Monahan et al., 1993a, b; Luternauer et al., 1994). These sands were probably deposited close to active river distributary-channel mouths. Sandy sediment gravity deposits are locally interbedded with silty foreset beds (Monahan, 1993; Luternauer et al., 1994; Christian et al., 1995).

Bottomset

Foreset deposits overlie up to 120 m of nearly flat-lying bioturbated clayey silt (Clague et al., 1983, 1991; Luternauer et al., 1994). These fine-grained sediments are interpreted to be the bottomset of the delta and are analogous to sediments presently accumulating in deep water in the Strait of Georgia. The bottomset deposits conformably overlie Late Pleistocene glaciomarine sediments (Hamilton, 1991; Hart and Hamilton, 1993; Hart et al., 1995).

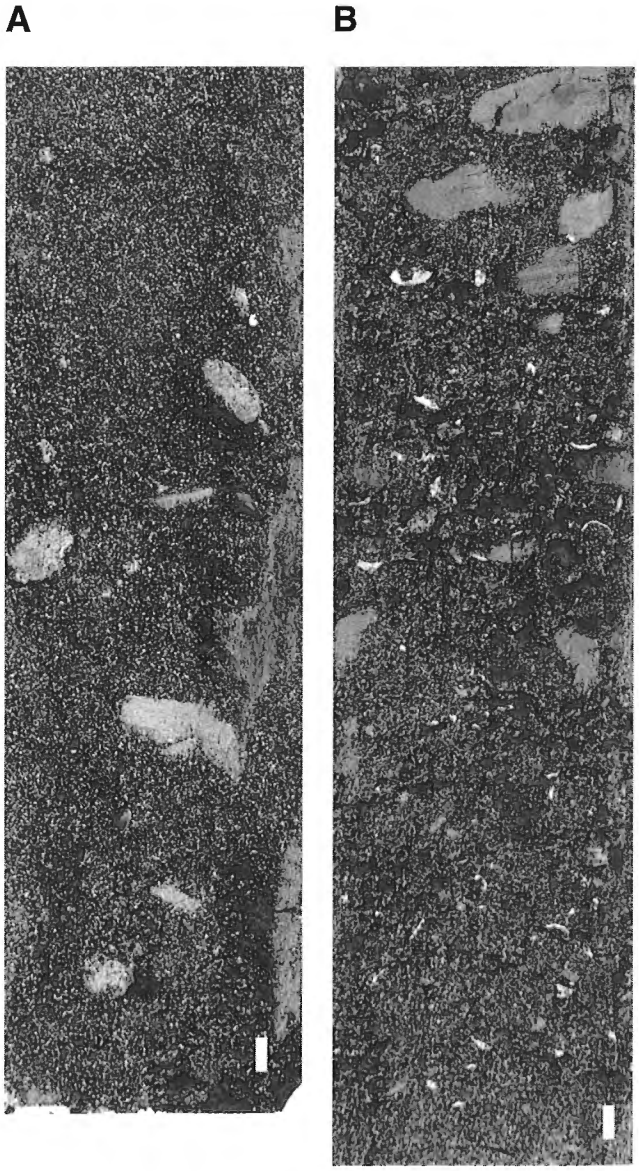

Figure 18. *Sand with silt clasts and shell fragments from the base of the distributary-channel sand sheet.* ***A)*** *FD93-3, 18.58-18.88 m;* ***B)*** *FD93-5, 20.08-2038 m depth (see Fig. 1 for locations). The sand was deposited in channels that migrated across a tidal flat. Vertical bar at lower right is 1 cm. (A from Monahan et al., 1997.)*

Figure 19. *Laminated silt and very fine-grained sand of the foreset unit; FD92-11, 25.32-25.62 m depth (see Fig. 1 for location). Vertical bar at lower right is 1 cm. (From Monahan et al., 1997.)*

HOLOCENE EVOLUTION OF THE DELTA

The chronology of Fraser delta growth is based largely on radiocarbon ages on shell and detrital wood (Table 1). Delicate unabraded samples were selected for radiocarbon analysis to minimize the danger of dating reworked organic material, which would give anomalously old ages. Nevertheless, in boreholes where several samples were dated, some younger samples underlie older ones, indicating that this problem was not entirely overcome (Clague et al., 1991; Luternauer et al., 1991; Dallimore et al., 1995). Such age inversions commonly involve restricted intervals of time, thus a general chronology of delta growth can be determined.

Radiocarbon ages show that foreset deposits were being deposited near the apex of the Fraser delta shortly after 10 000 ^{14}C years BP (Fig. 22; Williams and Roberts, 1989). The delta front had advanced to central Lulu Island by 9000 ^{14}C years BP and to the western edges of the modern peat bogs by 8000 ^{14}C years BP (Table 1). By or shortly after 8000 ^{14}C years BP, floodplain deposits were accumulating at the apex of the delta (Williams and Roberts, 1989).

The sea rose, relative to the land, from about -12 m to a few metres below its present level between 8000 and 5000 ^{14}C years BP (Mathews et al., 1970; Clague et al., 1982; Williams

Figure 20. *Lower part of a sandy gravity-flow deposit, erosionally overlying laminated foreset silt and sand; FD94-4, 31.75-32.07 m depth (see Fig. 1 for location). The sediment gravity-flow deposit consists of fine-grained sand with silt clasts and shell debris. Vertical bar at lower right is 1 cm.*

Figure 21. *Clast- and shell-bearing sand interpreted to be a sediment gravity-flow deposit; FD95-S1, 64.60- 64.90 m depth (see Fig. 1 for location). This deposit is within the foreset unit. Vertical bar at lower right is 1 cm.*

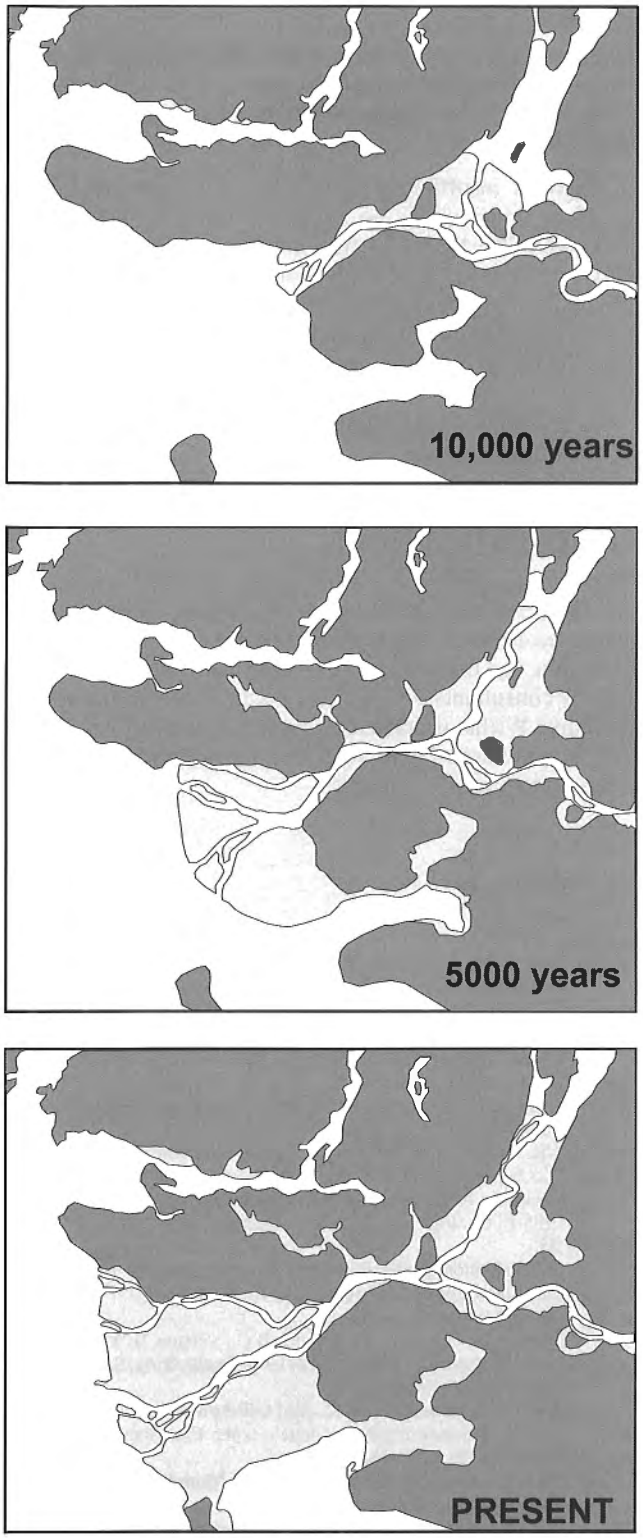

Figure 22. Holocene evolution of the Fraser delta. Light shading – Holocene floodplains, fans, and peat bogs; dark shading – pre-Holocene landmass. Dates are approximate. (Adapted from Clague et al., 1991.)

and Roberts, 1989). Delta progradation slowed during this period, not only because sea level rose, but also because the delta advanced into deeper water along a wider front (Williams and Roberts, 1989).

The delta front extended as far west as the modern delta shoreline by approximately 5000 ^{14}C years BP. The island that now is Point Roberts peninsula became connected to the mainland by tidal flats at about that time. The delta prograded beyond the modern Boundary Bay shoreline about 6000 ^{14}C years BP, and the distributary channel that flowed into the bay was abandoned shortly thereafter (Hutchinson et al., 1995).

About 5000 ^{14}C years BP, the rate of relative sea-level rise decreased to the point that peat bogs began to develop on the eastern part of the delta. Since then, the bogs have expanded and deepened, and the delta has advanced along its western front.

Radiocarbon ages from deep boreholes show that the foreset sequence accumulated rapidly: 100 m in about 1600 ^{14}C years at FD87-1 near Tsawwassen (Clague et al., 1991) and 140 m in about 800 ^{14}C years at FD94-4 on central Lulu Island (Dallimore et al., 1995). These high rates, however, apply to specific sites and restricted intervals of time, i.e., when the delta slope was advancing past a site. Deposition was not occurring at these high rates over the entire delta front throughout the Holocene.

Sedimentation on the delta has been profoundly affected by human intervention: dyking of the river channels and the shoreline; training of the lower reaches of the two main distributaries; intensive dredging to maintain navigable depths and recover sand for construction; and construction of jetties across the tidal flats to alter coastal water circulation or to access major port facilities (Luternauer et al., 1994, 1998). As a result, the Fraser River no longer deposits sediment on the floodplain, sand deposition is restricted to that part of the western delta front adjacent to distributary-channel mouths, and less sand reaches the delta front (Luternauer et al., 1998). The tidal flats and foreslope south of the Main Channel are generally starved of both fine- and coarse-grained sediment.

ADEQUACY AND IMPLICATIONS OF STRATIGRAPHIC INFORMATION FOR SEISMIC HAZARD ASSESSMENT

Thick accumulations of deltaic sediments can amplify ground motions during an earthquake. Past studies of the response of the Fraser delta to earthquake shaking employed a simple stratigraphic model, in which a thick till layer with a relatively flat base lay below Holocene deltaic deposits (e.g. Byrne and Anderson, 1987; Sy et al., 1991). Information obtained in recent years, which is summarized in Figures 9-12, shows that this model is incorrect. Diamicton constitutes less than 20% of the total Pleistocene section, there are profound unconformities within the sequence, and both the Tertiary and Pleistocene surfaces have relief of hundreds of metres. The existing database, however, is not adequate to define either the Tertiary or Pleistocene surface, as required for two- or three-dimensional, seismic ground-motion amplification studies (Luternauer and Hunter, 1996). Both surfaces are

highly irregular, and materials directly above and below them vary spatially. The irregular buried topography will reflect and refract seismic energy in a complex fashion; consequently, the pattern of surface ground motions during a strong earthquake is much more difficult to predict than previously thought (Luternauer et al., 1995; Hunter et al., 1998).

The sands of the Fraser delta topset are susceptible to earthquake-induced liquefaction (Byrne, 1978; Clague et al., 1992b; Watts et al., 1992). The physical properties and shear-wave velocity characteristics of the topset unit have been defined (Hunter et al., 1998; Pullan et al., 1998), and work is underway to define the distribution of deposits within the topset that are most susceptible to liquefaction (Monahan et al., 1994, 1996). The latter include the ribbon-like bodies of silt and fine-grained sand deposited in abandoned channels and sloughs, and young parts of the distributary-channel sand sheet which commonly occur in and adjacent to the Main Channel. Areas of lower liquefaction hazard include some of the older parts of the delta, where channel sands are overlain by up to 15 m of floodplain silt (Monahan et al., 1994, 1996).

SUMMARY

Tertiary sedimentary rocks underlie thick Quaternary sediments beneath the Fraser River delta. The unconformable surface that marks the top of the Tertiary sequence has considerable relief, ranging in depth from 200 to 1000 m. The Pleistocene succession consists mainly of sand and silt deposited in glaciomarine and marine environments; gravel and diamicton constitute less than 20% of the Pleistocene deposits drilled to date. An irregular surface with up to 300 m of relief separates the Pleistocene sequence from Holocene deltaic deposits. The deep architecture of the delta determined from recent deep drilling and geophysical work contrasts sharply with the simple stratigraphic model used in the past to assess seismic ground-motion amplification.

The Holocene Fraser delta comprises topset, foreset, and bottomset units. The topset unit consists of a sheet of distributary-channel sand overlain by intertidal and floodplain silt and sand, and, on the eastern part of the delta, peat. The distributary-channel sand sheet overlies a thick foreset unit of silt and sand deposited in a delta-slope environment. Foreset sediments interfinger both vertically and laterally with bottomset silt and clay which are identical to sediments presently accumulating in deep waters of the Strait of Georgia.

The Fraser delta began to form shortly after 10 000 ^{14}C years BP. Initial progradation was rapid — the delta plain reached about halfway to the present crest of the slope about 8000 ^{14}C years BP. Progradation slowed between 8000 and 5000 ^{14}C years BP as sea level rose relative to the land and as the delta advanced into deep water along a longer front. After 5000 ^{14}C years BP, the rate of sea-level rise slowed enough for peat to begin to accumulate on the eastern delta plain, leading to the establishment of peat bogs.

Natural deltaic processes have been extensively altered by human activities, including dyking, training and dredging of the main distributary channels, and construction of jetties on the tidal flats. The Fraser River no longer floods the subaerial delta plain, most sand is now deposited off the mouths of the two active distributary channels, and little new fine-grained sediment reaches either the tidal flats or the slope south of the Main Channel.

There is insufficient deep stratigraphic information to model ground motions on the Fraser delta during a strong earthquake. The buried Tertiary and Pleistocene surfaces will likely produce an extremely complex pattern of seismic ground motions. The stratigraphic database for the upper part of the Holocene deltaic sequence is adequate for assessing the potential for near-surface liquefaction during an earthquake. Sediments most susceptible to liquefaction are young channel sands and abandoned channel silts and fine-grained sands in the delta topset unit.

ACKNOWLEDGMENTS

This paper is a summary of our own work, that of students and colleagues at Simon Fraser University, the University of British Columbia, and the Geological Survey of Canada, and studies done by consultants in the private sector. Andrew Makepeace and Tonia Williams drafted the figures. Greg Brooks, Robert Gerath, and Susan Pullan reviewed the manuscript and contributed to its improvement.

REFERENCES

Armstrong, J.E.
1981: Post-Vashon Wisconsin glaciation, Fraser Lowland, British Columbia; Geological Survey of Canada, Bulletin 322, 34 p.
1984: Environmental and engineering applications of the surficial geology of the Fraser Lowlands, British Columbia; Geological Survey of Canada, Paper 83-23, 54 p.

Bazett, D.J. and McCammon, N.R.
1986: Foundations of the Annacis cable-stayed bridge; Canadian Geotechnical Journal, v. 23, p. 458-471.

Britton, J.R., Harris, J.B., Hunter, J.A., and Luternauer, J.L.
1995: The bedrock surface beneath the Fraser River delta in British Columbia based on seismic measurements; in Current Research 1995-E; Geological Survey of Canada, p. 83-89.

Byrne, P.H.
1978: An evaluation of the liquefaction potential of the Fraser Delta; Canadian Geotechnical Journal, v. 15, p. 32-46.

Byrne, P.H. and Anderson, D.L.
1987: Earthquake design in Richmond, B.C., version II; University of British Columbia, Department of Civil Engineering, Soils Mechanics Series, no. 109, 90 p.

Campanella, R.G., Robertson, P.K., and Gillespie, D.
1983: Cone penetration testing in deltaic soils; Canadian Geotechnical Journal, v. 20, p. 23-35.

Christian, H.A., Barrie, J.V., MacDonald, R., Monahan, P.A., Hunter, J.A., and Luternauer, J.L.
1995: Slope instability on Roberts Bank, Fraser River delta, Vancouver, British Columbia; in Proceedings, 48th Canadian Geotechnical Conference, Vancouver, British Columbia, Preprint Volume 2, p. 937-946.

Christian, H.A., Monahan, P.A., and Barrie, J.V.
1994a: Deep hole geotechnical investigation adjacent to the B.C. Hydro Canoe Pass submarine cable terminal, Fraser River delta, British Columbia; Geological Survey of Canada, Open File 2861, 72 p.

Christian, H.A., Mulder, T., Courtney, R.C., Mosher, D.C., Barrie, J.V., Currie, R.G., Olynyk, H.W., and Monahan, P.A.
1994b: Slope instability on the Fraser River delta foreslope, Vancouver, British Columbia; in Proceedings, 47th Canadian Geotechnical Conference, Halifax, Nova Scotia, p. 155-165.

Clague, J.J.
1977: Quadra Sand: a study of the late Pleistocene geology and geomorphic history of coastal southwest British Columbia; Geological Survey of Canada, Paper 77-17, 24 p.
1998: Geological setting of the Fraser River delta; in Geology and Natural Hazards of the Fraser River Delta, British Columbia, (ed.) J.J. Clague, J.L. Luternauer, and D.C. Mosher; Geological Survey of Canada, Bulletin 525, this volume.

Clague, J.J. and Luternauer, J.L.
1982: Excursion 30A: late Quaternary sedimentary environments, southwestern British Columbia; 11th International Congress on Sedimentology, Hamilton, Ontario, Guidebook, Field Excursion 30A, 167 p.

Clague, J.J., Armstrong, J.E., and Mathews, W.H.
1980: Advance of the late Wisconsin Cordilleran Ice Sheet in southern British Columbia since 22 000 yr B.P.; Quaternary Research, v. 13, p. 322-326.

Clague, J.J., Easterbrook, D.J., Hughes, O.L., and Matthews, J.V., Jr.
1992a: The Sangamonian and early Wisconsinan stages in western Canada and northwestern United States; in The Last Interglacial-Glacial Transition in North America, (ed.) P.C. Clark and P.C. Lea; Geological Society of America, Special Paper 270, p. 253-268.

Clague, J.J., Harper, J.R., Hebda, R.J., and Howes, D.E.
1982: Late Quaternary sea levels and crustal movements, coastal British Columbia; Canadian Journal of Earth Sciences, v. 19, p. 597-618.

Clague, J.J., Luternauer, J.L., and Hebda, R.J.
1983: Sedimentary environments and postglacial history of the Fraser River delta and lower Fraser Valley, British Columbia; Canadian Journal of Earth Sciences, v. 20, p. 1314-1320.

Clague, J.J., Luternauer, J.L., Pullan, S.A., and Hunter, J.A.
1991: Postglacial deltaic sediments, southern Fraser River delta, British Columbia; Canadian Journal of Earth Sciences, v. 28, p. 1386-1393.

Clague, J.J., Naesgaard, E., and Mathewes, R.W.
1998: Geological evidence for prehistoric earthquakes; in Geology and Natural Hazards of the Fraser River Delta, British Columbia, (ed.) J.J. Clague, J.L. Luternauer, and D.C. Mosher; Geological Survey of Canada, Bulletin 525, this volume.

Clague, J.J., Naesgaard, E., and Sy, A.
1992b: Liquefaction features on the Fraser River delta: evidence for prehistoric earthquakes?; Canadian Journal of Earth Sciences, v. 29, p. 1734-1745.

Cowan, E.G. and Powell, R.R.
1990: Suspended sediment transport and deposition of cyclically interlaminated sediment in a temperate glacial fjord, Alaska, U.S.A.; in Glacimarine Environments: Processes and Sediments, (ed.) J.A. Dowdeswell and J.D. Scourse; Geological Society of London, Special Publication 53, p. 75-89.

Dallimore, S.R., Edwardson, K.A., Hunter, J.A., Clague, J.J., and Luternauer, J.L.
1995: Composite geotechnical logs for two deep boreholes in the Fraser River delta, British Columbia; Geological Survey of Canada, Open File 3018, 1 sheet.

Dallimore, S.R., Edwardson, K.A., Hunter J.A., Meldrum, J.L., Luternauer, J.L., and Clague, J.J.
1996: Lithologic, geotechnical and geophysical logs for a deep borehole at Richmond City Hall, British Columbia; Geological Survey of Canada, Open File 3356, 2 sheets and 2 diskettes.

Hamilton, T.S.
1991: Seismic stratigraphy of unconsolidated sediments in the central Strait of Georgia: Hornby Island to Roberts Bank; Geological Survey of Canada, Open File 2350, 9 maps, scale 1:125 000.

Harris, J.B., Hunter, J.A., Luternauer, J.L., and Finn, W.D.L.
1995: Site response modelling of the Fraser River delta, British Columbia: preliminary results from two deep boreholes; in Current Research 1995-E; Geological Survey of Canada, p. 69-75.

Hart, B.S. and Hamilton, T.S.
1993: High resolution acoustic mapping of shallow gas in unconsolidated sediments beneath the Strait of Georgia, British Columbia; Geo-Marine Letters, v. 13, p. 49-55.

Hart, B.S., Hamilton, T.S., Barrie, J.V., and Prior, D.B.
1995: Seismic stratigraphy and sedimentary framework of a deep-water Holocene delta: The Fraser delta, Canada; in Geology of Deltas, (ed.) M.N. Oti and G. Postma; A.A. Balkema, Rotterdam, Netherlands, p. 167-178.

Hebda, R.J.
1977: The paleoecology of a raised bog and associated deltaic sediments of the Fraser River delta; Ph.D. thesis, University of British Columbia, Vancouver, British Columbia, 202 p.

Hunter, J.A., Burns, R.A., Good, R.L., Wang, Y., and Evans, M.E.
1995: Borehole magnetic susceptibility measurements in unconsolidated overburden of the Fraser River delta, British Columbia; in Current Research 1995-E; Geological Survey of Canada, p. 77-82.

Hunter, J.A., Douma, M., Burns, R.A, Good, R.L., Pullan, S.E., Harris, J.B., Luternauer, J.L, and Best, M.E.
1998: Testing and application of near-surface geophysical techniques for earthquake hazards studies, Fraser River delta, British Columbia; in Geology and Natural Hazards of the Fraser River Delta, British Columbia, (ed.) J.J. Clague, J.L. Luternauer, and D.C. Mosher; Geological Survey of Canada, Bulletin 525, this volume.

Hunter, J.A., Luternauer, J.L., Neave, K.G., Pullan, S.E., Good, R.I., Burns, R.A., and Douma, M.
1992: Shallow shear-wave velocity-depth data in the Fraser delta, from surface refraction measurements, 1989, 1990, 1991; Geological Survey of Canada, Open File 2504, 270 p.

Hunter, J.A., Luternauer, J.L., Roberts, M.C., Monahan, P.A., and Douma, M.
1994: Borehole geophysical logs, Fraser River delta (92G), British Columbia; Geological Survey of Canada, Open File 2841, 30 p.

Hutchinson, I., Roberts, M.C., and Williams, H.F.L.
1995: Stratigraphy, diatom biofacies, and palaeogeomorphology of a mid Holocene distributary channel system, Fraser River delta, British Columbia, Canada; Canadian Journal of Earth Sciences, v. 32, p. 749-757.

Johnson, R.G.
1982: Brunhes-Matuyama magnetic reversal dated at 790,000 yr B.P. by marine-astronomical correlations; Quaternary Research, v. 17, p. 135-147.

Johnston, W.A.
1921: Sedimentation of the Fraser River delta; Geological Survey of Canada, Memoir 125, 46 p.
1923: Geology of the Fraser River delta map area; Geological Survey of Canada, Memoir 135, 87 p.

Jol, H.M.
1988: Seismic stratigraphic analysis of the southwestern Fraser River delta, British Columbia; M.Sc. thesis, Simon Fraser University, Burnaby, British Columbia, 176 p.

Jol, H.M. and Roberts, M.C.
1988: The seismic facies of a delta onlapping an offshore island: Fraser River Delta, British Columbia; in Sequences, Stratigraphy, Sedimentology: Surface and Subsurface, (ed.) D.P. James and D.A. Leckie; Canadian Society of Petroleum Geologists, Memoir 15, p. 137-142.
1992: The seismic facies of a tidally influenced Holocene delta: Boundary Bay, Fraser River delta, B.C.; Sedimentary Geology, v. 77, p. 173-183.

Kostaschuk, R.A., Luternauer, J.L., and Church, M.A.
1989: Suspended sediment hysteresis in a salt-wedge estuary: Fraser River, Canada; Marine Geology, v. 87, p. 273-285.

Kostaschuk, R.A., Luternauer, J.L., and Millard, T.H.
1986: Sediment transport in the outer Main Channel of the Fraser River Estuary during the 1985 freshet; in Current Research, Part A; Geological Survey of Canada, Paper 86-1A, p. 565-570.

Lo, R.C., Sy, A., Henderson, P.W., Siu, D.Y., Finn, W.D.L., and Heidebrecht, A.C.
1991: Seismic site amplification study for Fraser Delta, British Columbia; in Proceedings, 6th Canadian Conference on Earthquake Engineering, Toronto, Ontario, p. 509-516.

Luternauer, J.L. and Finn, W.D.L.
1983: Stability of the Fraser River delta front; Canadian Geotechnical Journal, v. 20, p. 606-616.

Luternauer, J.L. and Hunter, J.A.
1996: Mapping Pleistocene deposits beneath the Fraser River delta: preliminary geological and geophysical results; in Current Research 1996-E; Geological Survey of Canada, p. 41-48.

Luternauer, J.L., Barrie, J.V., Christian, H.A., Clague, J.J., Evoy, R.W., Hart, B.S., Hunter, J.A., Killeen, P.G., Kostaschuk, R.A., Mathewes, R.W., Monahan, P.A., Moslow, T.F., Mwenifumbo, C.J., Olynyk, H.W., Patterson, R.T., Pullan, S.E., Roberts, M.C., Robertson, P.K., Tarbotton, M.R., and Woeller, D.J.
1994: Fraser River delta: geology, geohazards and human impact; in Geology and Geological Hazards of the Vancouver Region, Southwestern British Columbia, (ed.) J.W.H. Monger; Geological Survey of Canada, Bulletin 481, p. 197-220.

Luternauer, J.L., Clague, J.J., and Feeney, T.D.
1991: A 367 m core from southwestern Fraser River delta, British Columbia; in Current Research, Part E; Geological Survey of Canada, Paper 91-1E, p. 127-134.

Luternauer, J.L., Clague, J.J., Hamilton, T.S., Hunter, J.A., Pullan, S.E., and Roberts, M.C.
1986: Structure and stratigraphy of the southwestern Fraser River delta: a trial shallow seismic profiling and coring survey; in Current Research, Part B; Geological Survey of Canada, Paper 86-1B, p. 707-714.

Luternauer, J.L., Harris, J.B., Hunter, J.A., and Finn, W.D.L.
1995: Fraser River delta geology: modeling for seismic hazard assessment; The B.C. Professional Engineer, v. 46, p. 10-14.

Luternauer, J.L., Mosher, D.C., Clague, J.J., and Atkins, R.J.
1998: Sedimentary environments of the Fraser delta; in Geology and Natural Hazards of the Fraser River Delta, British Columbia, (ed.) J.J. Clague, J.L. Luternauer, and D.C. Mosher; Geological Survey of Canada, Bulletin 525, this volume.

Mathews, W.H. and Shepard, F.P.
1962: Sedimentation of the Fraser River delta, British Columbia; American Association of Petroleum Geologists Bulletin, v. 46, p. 1416-1438.

Mathews, W.H., Fyles, J.G., and Nasmith, H.W.
1970: Postglacial crustal movements in southwestern British Columbia and adjacent Washington state; Canadian Journal of Earth Sciences, v. 7, p. 690-702.

Milliman, J.D.
1980: Sedimentation in the Fraser River and its estuary, southwestern British Columbia (Canada); Estuarine and Coastal Marine Science, v. 10, p. 609-633.

Monahan, P.A.
1993: Stratigraphy of the delta plain; in Applied Quaternary Research, Program with Abstracts and Field Guide; Canadian Quaternary Association, Victoria, British Columbia, p. G35-G40.

Monahan, P.A. and Luternauer, J.L.
1994: Greater Vancouver Geotechnical Database (British Columbia): Richmond Pilot Project; in Current Research 1994-E; Geological Survey of Canada, p. 85-91.

Monahan, P.A., Luternauer, J.L., and Barrie, J.V.
1993a: A delta topset "sheet" sand and modern sedimentary processes in the Fraser River delta, British Columbia; in Current Research, Part A; Geological Survey of Canada, Paper 93-1A, p. 263-272.
1993b: A delta plain sheet sand in the Fraser River delta, British Columbia, Canada; Quaternary International, v. 20, p. 27-38.
1994: Application of cone penetration test data to facies analysis on the Fraser River delta; Geological Society of America, Abstracts with Programs, v. 26, p. A-253.
1995: The geology of the CANLEX Phase II sites in Delta and Richmond, British Columbia; in Proceedings, 48th Annual Canadian Geotechnical Conference, British Columbia, Preprint Volume 1, p. 59-68.
1996: Facies analysis for earthquake hazard mapping in the Fraser River delta; in Abstracts, Pan Pacific Hazards '96, Vancouver, British Columbia, p. 177.
1997: The topset and upper foreset of the modern Fraser River delta, British Columbia, Canada; in Core conference , June 5-6, 1997, (comp.) J. Wood and W. Martindale; Canadian Society of Petroleum Geologists, Calgary, Alberta, p. 491-517.

Mustard, P.S. and Rouse, G.E.
1994: Stratigraphy and evolution of Tertiary Georgia Basin and subjacent Upper Cretaceous sedimentary rocks, southwestern British Columbia and northwestern Washington State; in Geological and Geological Hazards of the Vancouver Region, Southwestern British Columbia, (ed.) J.W.H. Monger; Geological Survey of Canada, Bulletin 481, p. 97-169.

Mwenifumbo, C.J., Killeen, P.G., and Elliott, B.
1994: Downhole logging measurements in the Fraser Delta, British Columbia; in Current Research 1994-E; Geological Survey of Canada, p. 77-84.

Naesgaard, E., Sy, A., and Clague, J.J.
1992: Liquefaction sand dykes at Kwantlen College, Richmond, B.C.; in Geotechnique and Natural Hazards; BiTech Publishers, Vancouver, British Columbia, p. 159-166.

North, M.E.A., Dunn, M.W., and Teversham, J.M.
1979: Vegetation of the southwestern Fraser Lowland, 1858-1880; Canada Department of Environment, Lands Directorate, Vancouver, British Columbia, scale 1:50 000.

Patterson, R.T. and Cameron, B.E.
1991: Paleoenvironmental significance of the foraminiferal biofacies succession in the late Quaternary sediments of the Fraser River delta, British Columbia; Journal of Foraminiferal Research, v. 21, p. 228-243.

Patterson, R.T. and Luternauer, J.L.
1993: Holocene foraminiferal faunas from cores collected on the Fraser River delta, British Columbia: a paleoecological interpretation; in Current Research, Part A; Geological Survey of Canada, Paper 93-1A, p. 245-254.

Pullan, S.E., Hunter, J.A., Jol, H.M., Roberts, M.C., Burns, R.A., and Harris, J.A.
1998: Seismostratigraphic investigations of the southern Fraser River delta; in Geology and Natural Hazards of the Fraser River Delta, British Columbia, (ed.) J.J. Clague, J.L. Luternauer, and D.C. Mosher; Geological Survey of Canada, Bulletin 525, this volume.

Pullan, S.E., Jol, H.M., Gagne, R.M., and Hunter, J.A.
1989: Compilation of high resolution 'optimum offset' shallow seismic reflection profiles from the southern Fraser River delta, British Columbia; Geological Survey of Canada, Open File 1992, 8 p.

Ricketts, B.D.
1998: Groundwater flow beneath the Fraser River delta, British Columbia; a preliminary model; in Geology and Natural Hazards of the Fraser River Delta, British Columbia, (ed.) J.J. Clague, J.L. Luternauer, and D.C. Mosher; Geological Survey of Canada, Bulletin 525, this volume.

Roberts, M.C., Williams, H.F.L., Luternauer, J.L., and Cameron, B.E.B.
1985: Sedimentary framework of the Fraser River delta, British Columbia: preliminary field and laboratory results; in Current Research, Part A; Geological Survey of Canada, Paper 85-1A, p. 717-722.

Robertson, P.K.
1990: Soil classification using the cone penetration test; Canadian Geotechnical Journal, v. 27, p. 151-158.

Robertson, P.K. and Campanella, R.G.
1983a: Evaluation of liquefaction potential using the cone penetration test; University of British Columbia, Department of Civil Engineering, Soil Mechanics Series, no. 64, 54 p.
1983b: Interpretation of cone penetration tests. Part I, sand; Canadian Geotechnical Journal, v. 20, p.718-733.
1985: Liquefaction potential of sands using the cone penetration test; American Society of Civil Engineers, Journal of Geotechnical Division, v. 22, p. 298-307.

Robertson, P.K. and Fear, C.E.
1996: Soil liquefaction and its evaluation based on SPT and CPT; in Recent Developments in Seismic Liquefaction Assessment; Cone-Tec Investigations Ltd., Vancouver, British Columbia, 52 p.

Scott, D.B., Baki, V., and Younger, C.D.
1989: Late Pleistocene-Holocene paleoceanographic changes on the eastern Canadian margin: stable isotopic evidence; Palaeogeography, Palaeoclimatology, Palaeoecology, v. 74, p. 279-295.

Sy, A., Henderson, P.W., Lo, R.C., Siu, D.Y., Finn, W.D.L., and Heidebrecht, A.C.
1991: Ground motion response for Fraser delta, British Columbia; in Proceedings, 4th International Conference on Seismic Zonation, Stanford, California, v. 2, p. 343-350.

Watts, B.D., Seyers, W.C., and Stewart, R.A.
1992: Liquefaction susceptibility of Greater Vancouver area soils; in Geotechnique and Natural Hazards; BiTech Publishers, Vancouver, British Columbia, p. 145-157.

Williams, H.F.L.
1988: Sea-level change and delta growth; Fraser Delta, British Columbia; Ph.D. thesis, Simon Fraser University, Burnaby, British Columbia, 256 p.

Williams, H.F.L. and Luternauer, J.L.
1991: Shallow structure and growth of the southern Fraser River delta: preliminary field results; in Current Research, Part A; Geological Survey of Canada, Paper 91-1A, p. 85-90.

Williams, H.F.L. and Roberts, M.C.
1989: Holocene sea-level change and delta growth: Fraser River Delta, British Columbia; Canadian Journal of Earth Sciences, v. 26, p. 1657-1666.
1990: Two middle Holocene marker beds in vertically accreted floodplain deposits, lower Fraser River, British Columbia; Géographie physique et Quaternaire, v. 44, p. 27-32.

Woeller, D.J., Hunter, J.A., and Luternauer, J.L.
1993a: Results of SCPT and SASW testing of the Fraser River delta sediments, British Columbia (92G/2,3); Geological Survey of Canada, Open File 2714, 224 p.

Woeller, D.J., Luternauer, J.L., and Hunter, J.A.
1993b: Presentation and interpretation of seismic cone penetration test data, Fraser River delta, British Columbia (92G/2,3); Geological Survey of Canada, Open File 2715, 86 p.

Woeller, D.J., Hunter, J.A., and Luternauer, J.L.
1994: Results of seismic cone penetration testing in the Fraser River delta, February-March, 1994; Geological Survey of Canada, Open File 2956, 158 p.

Appendix 1

Legend (**A**) and lithological logs (**B-E**) for representative holes which were drilled primarily to obtain information on the Holocene deltaic sequence. Locations are shown in Figure 1. Logs are grouped according to regions: B and C - southwestern region; D - southeastern and central regions; E - northern region.

A

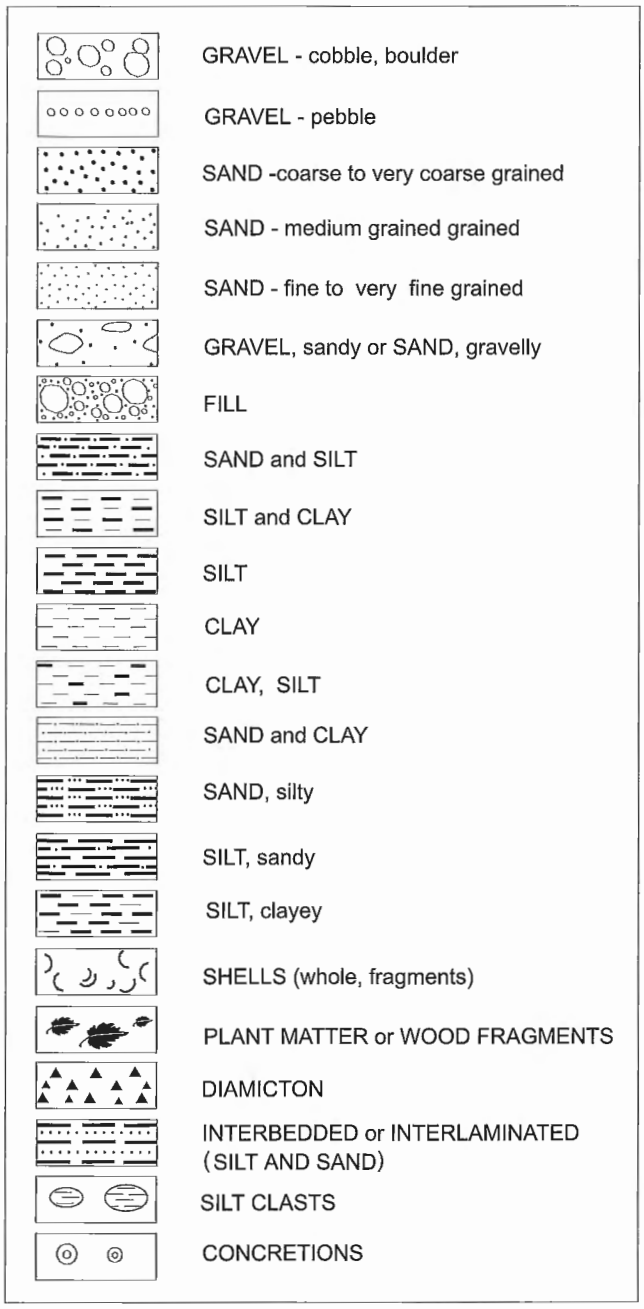

B

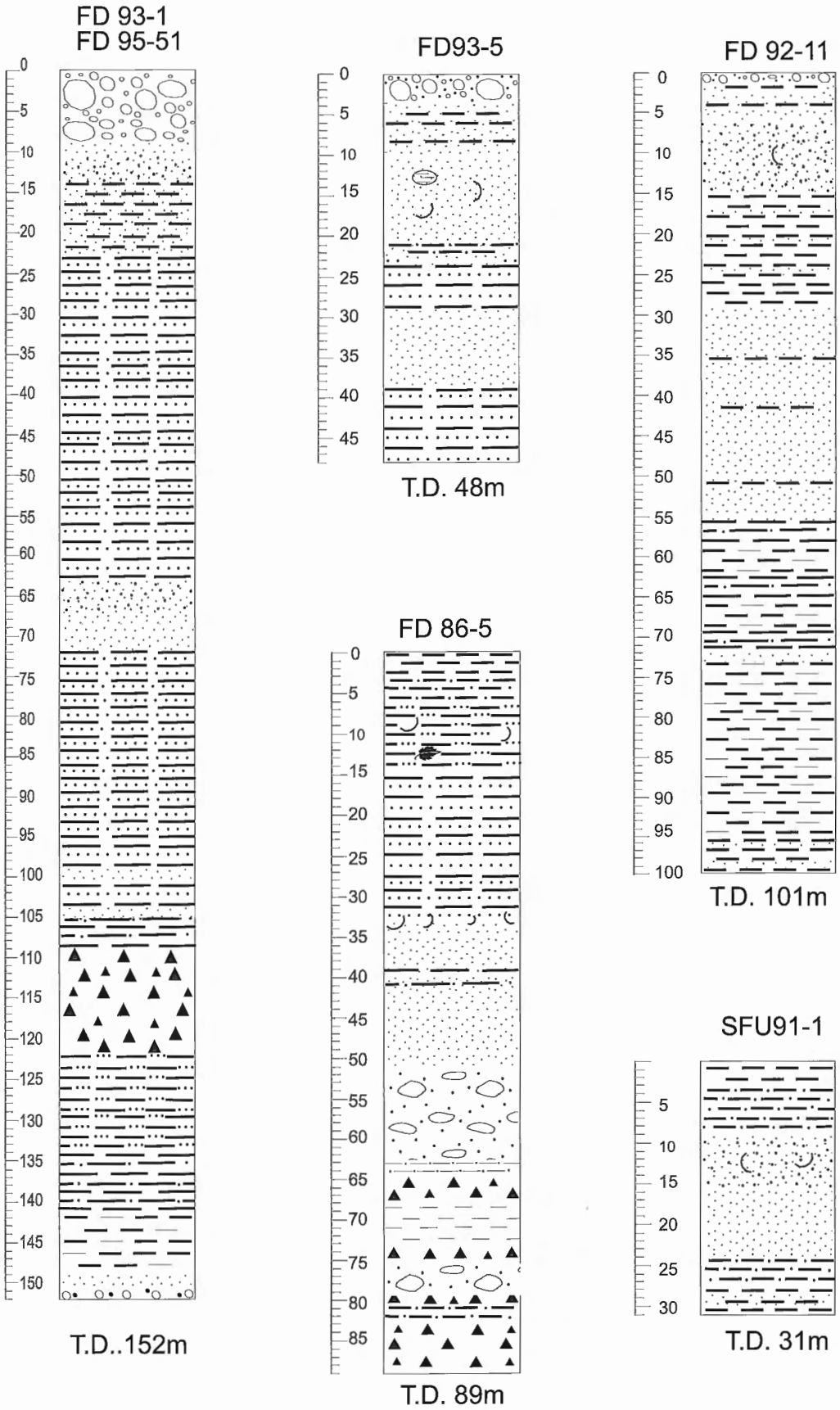
FD 93-1
FD 95-51
T.D..152m
FD93-5
T.D. 48m
FD 92-11
T.D. 101m
FD 86-5
T.D. 89m
SFU91-1
T.D. 31m

C

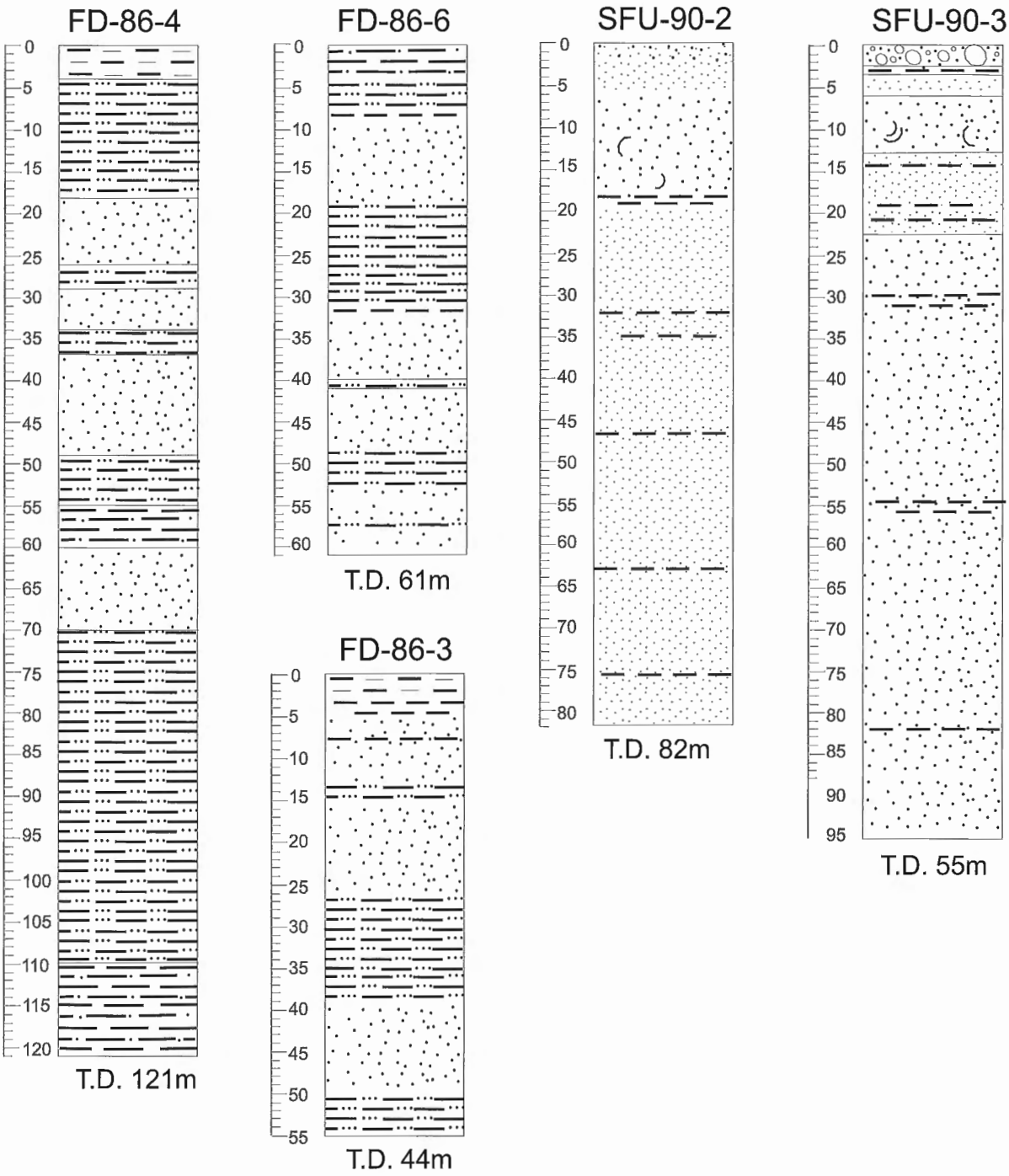
FD-86-4
0
5
10
15
20
25
30
35
40
45
50
55
60
65
70
75
80
85
90
95
100
105
110
115
120
T.D. 121m
FD-86-6
0
5
10
15
20
25
30
35
40
45
50
55
60
T.D. 61m
FD-86-3
0
5
10
15
20
25
30
35
40
45
50
55
T.D. 44m
SFU-90-2
0
5
10
15
20
25
30
35
40
45
50
55
60
65
70
75
80
T.D. 82m
SFU-90-3
0
5
10
15
20
25
30
35
40
45
50
55
60
65
70
75
80
85
90
95
T.D. 55m

D

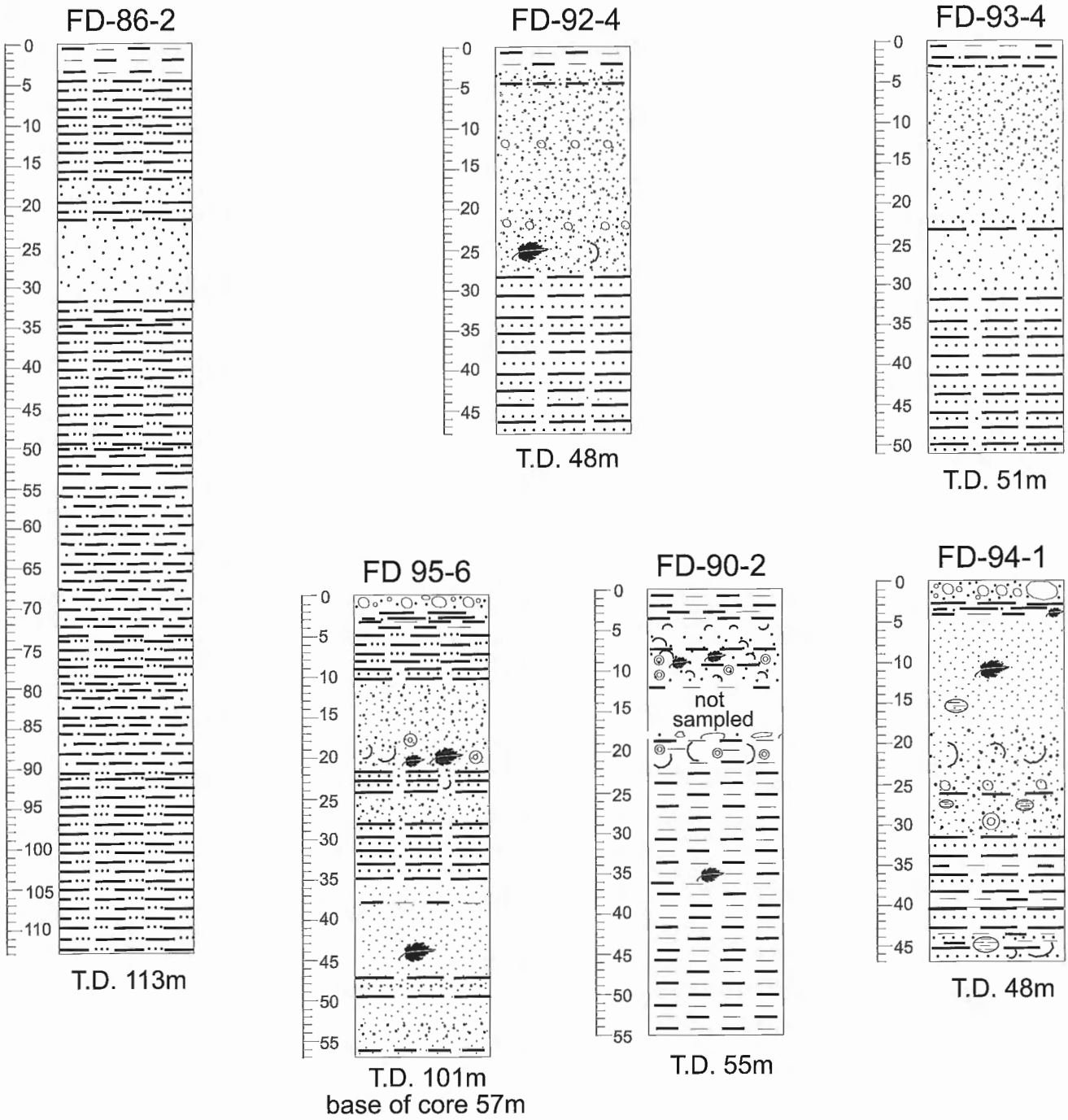
FD-86-2
T.D. 113m
FD-92-4
T.D. 48m
FD-93-4
T.D. 51m
FD 95-6
T.D. 101m
base of core 57m
FD-90-2
not sampled
T.D. 55m
FD-94-1
T.D. 48m

E

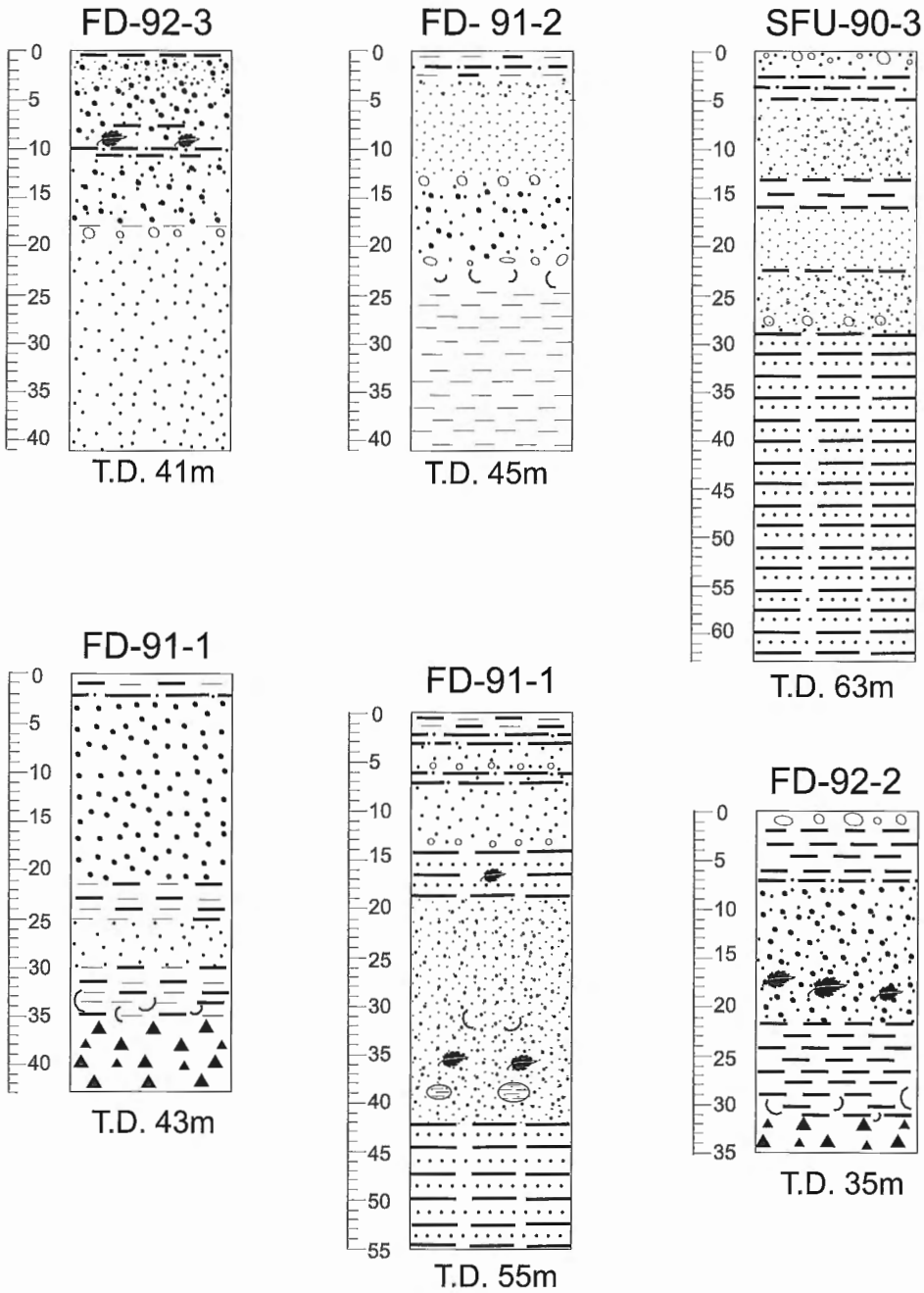
FD-92-3
0
5
10
15
20
25
30
35
40
T.D. 41m
FD- 91-2
0
5
10
15
20
25
30
35
40
T.D. 45m
SFU-90-3
0
5
10
15
20
25
30
35
40
45
50
55
60
T.D. 63m
FD-91-1
0
5
10
15
20
25
30
35
40
T.D. 43m
FD-91-1
0
5
10
15
20
25
30
35
40
45
50
55
T.D. 55m
FD-92-2
0
5
10
15
20
25
30
35
T.D. 35m

Seismostratigraphic investigations of the southern Fraser River delta

S.E. Pullan[1], J.A. Hunter[1], H.M. Jol[2], M.C. Roberts[3], R.A. Burns[1], and J.B. Harris[4]

Pullan, S.E., Hunter, J.A., Jol, H.M., Roberts, M.C., Burns, R.A., and Harris, J.B., 1998: Seismostratigraphic investigations of the southern Fraser River delta; in Geology and Natural Hazards of the Fraser River Delta, British Columbia, (ed.) J.J. Clague, J.L. Luternauer, and D.C. Mosher; Geological Survey of Canada, Bulletin 525, p. 91–122.

Abstract: Between 1985 and 1995, the Geological Survey of Canada acquired approximately 60 line-kilometres of shallow seismic reflection data on the Fraser River delta. Most of these data were obtained on the southern delta in the mid 1980s using the 'optimum offset' technique. The fine-grained, water-saturated surface sediments provide an excellent medium for application of high-resolution, compressional-wave, seismic reflection methods, and data with dominant frequencies of 200-300 Hz were consistently obtained. These data have provided an opportunity for detailed examination of the subsurface structure of the delta to depths of up to 170 m. Unfortunately, in many areas the depth of investigation was severely limited by the presence of gas in the shallow sediments. More recently, common-midpoint (CMP) data, using both compressional and shear waves, have been acquired in an attempt to find alternative methods for exploring the deeper structure of the delta.

Résumé : Entre 1985 et 1995, la Commission géologique du Canada a fait des levés de sismique réflexion peu profonde sur environ 60 kilomètres de lignes réparties sur le territoire du delta du Fraser. La plupart des données recueillies portent sur la partie sud du delta et ont été acquises au milieu des années quatre-vingts par la technique de l'«écart optimal». Les sédiments superficiels à grain fin saturés en eau sont un excellent matériau pour appliquer les méthodes de sismique réflexion à haute résolution utilisant les ondes de compression. Les fréquences de 200 à 300 Hz sont celles auxquelles les données obtenues ont été les plus consistantes. Ces données ont permis d'analyser en détail la structure souterraine du delta jusqu'à des profondeurs de 170 mètres. Malheureusement, dans de nombreuses zones, la profondeur d'analyse a été limitée par la présence de gaz dans les sédiments peu profonds. Plus récemment, des données de points milieux communs, utilisant les ondes de compression et de cisaillement, ont été acquises en vue de trouver des méthodes de remplacement pour explorer la structure plus profonde du delta.

[1] Geological Survey of Canada, 601 Booth Street, Ottawa, Ontario K1A 0E8
[2] Department of Geography, University of Wisconsin - Eau Claire, Eau Claire, Wisconsin 54702-4004
[3] Departments of Earth Sciences and Geography, Simon Fraser University, Burnaby, British Columbia V5A 1S6
[4] Department of Geology, Millsaps College, 1701 N. State Street, Jackson, Mississippi 39210

INTRODUCTION

The Fraser River delta lies just south of the city of Vancouver (Fig. 1), and is rapidly being urbanized and industrialized. In the past, much of this development has taken place without detailed knowledge of the subsurface structure of the delta, or an appreciation of the seismic hazard that may be associated with the thick alluvial and deltaic deposits in one of the most seismically active areas in Canada.

In recent years, the Geological Survey of Canada has directed considerable effort towards understanding the evolution and structure of the delta, and this Bulletin summarizes much of that work. The delta is an extremely complex sedimentary system, and it is difficult to delineate its three-dimensional structure. Boreholes are costly and can provide only limited sampling of the subsurface. The development of shallow seismic reflection techniques in the 1980s (e.g. Doornenbal and Helbig, 1983; Hunter et al., 1984, 1989; Knapp and Steeples, 1986a, b) provided a tool capable of yielding less expensive and more laterally continuous information on the stratigraphy and structure of the Quaternary deposits beneath the present-day delta.

Seismic reflection surveys are based on the principle that seismic energy is partially reflected at every subsurface boundary across which there is a contrast in acoustic impedance. Because such contrasts are generally associated with lithological boundaries, seismic techniques can be used to obtain subsurface structural information. Surveys involve laying out a series of receivers (geophones) on the ground surface, and recording ground motions as a function of time in response to the detonation of a small explosive/shotgun source or the impact of a weight drop or sledgehammer. Energy travels along the ground surface, is refracted along interfaces, such as the water table, where large increases in seismic velocity occur, and is reflected from subsurface horizons such as lithological boundaries or erosional surfaces.

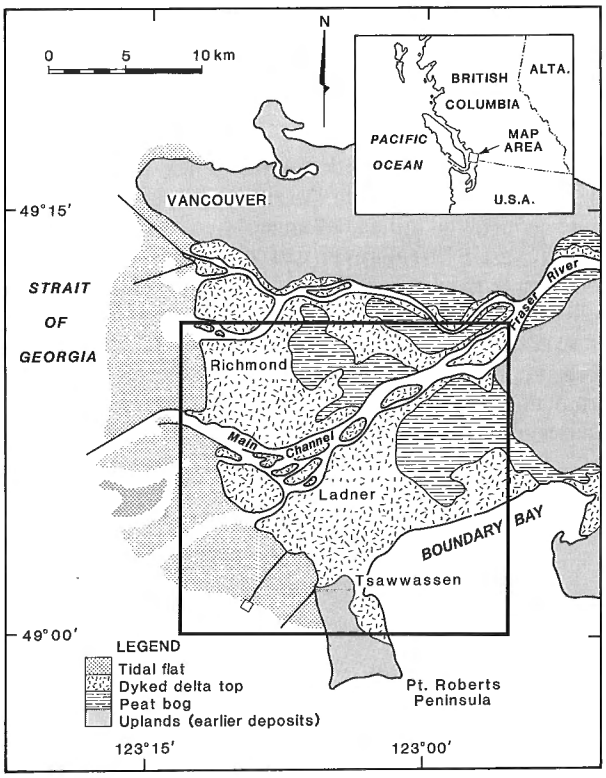

Figure 1. Location map of the Fraser River delta. The central box outlines the survey area shown in Figure 2.

This paper presents the results of a variety of shallow seismic reflection surveys that have been carried out on the Fraser River delta by the Geological Survey of Canada since 1985 (Fig. 2). An 'optimum offset', compressional-wave, shallow, seismic reflection survey conducted in August 1985 proved that excellent data could be obtained from the southern part of the Fraser delta and, under favourable conditions, could define the subsurface structure to depths of approximately 170 m (Luternauer et al., 1986). Further work using this profiling technique was carried out on the southern delta in 1986 and 1987 (Pullan et al., 1989), in conjunction with drilling, borehole logging, sample analyses, and cone penetrometer tests (Luternauer, 1988). In 1988, the survey area was extended north into the Richmond area, and tests of the technique in imaging subsurface structure to depths of approximately 400 m were carried out northeast of Tsawwassen. In total, 53 line-kilometres of 'optimum offset' shallow seismic reflection data have been acquired on the delta (Fig. 2).

Common-midpoint (CMP) seismic reflection surveys were conducted along selected profiles in 1989 and 1990, to test the potential for delineating deeper structure (Luternauer, 1990, 1991). In 1991, two boreholes were drilled with a Minipac Gas Detector attached to the mud line to substantiate the interpretation that large-amplitude reflections on the seismic profiles indicated the presence of gas within the shallow sediments. A compressional-wave CMP survey was shot in 1995 in the vicinity of borehole FD94-3 (Fig. 2) to extend the borehole information laterally. In 1992, the first shear-wave CMP data were acquired, and two more short shear-wave CMP lines were shot in 1995. Shear waves were used to 'see through' the shallow gas that effectively masked the deeper structure on many compressional-wave sections. Approximately 9 line-kilometres of CMP profiles were acquired on the Fraser delta by the Geological Survey of Canada between 1989 and 1995 (Fig. 2).

This paper starts with a brief discussion of seismic reflection theory, and then outlines the survey methods and recording parameters used in the Fraser delta surveys. The results of the surveys are presented in terms of geological units or depositional sequences, starting with the youngest sediments. Most of the information obtained from the seismic sections pertains to the Holocene deltaic deposits; the discussion includes sections on topset and foreset sequences, evidence for gas within the shallow sediments, and the interpretation of slumps and faults. Some information on the Holocene-Pleistocene boundary has been obtained from seismic reflection records northeast of Tsawwassen where the depth of penetration was not limited by the presence of gas, and from

shear-wave sections. These surveys have also provided limited information on Pleistocene sediments and the Tertiary bedrock surface.

SEISMIC REFLECTION PROFILING

Seismic reflection methods involve measurement of the time taken for seismic energy to travel from the source at or near the surface, down to an acoustical discontinuity in the ground, and back up to a receiver or series of receivers on the ground surface. These methods require digitization of the seismic wave train and at least some degree of computer processing of the data. Data are usually acquired continuously along a survey line, and processed to produce a seismic section which is a two-way traveltime cross-section of the subsurface. Velocity-depth functions calculated from the data (ideally supplemented with seismic or acoustic logs in nearby boreholes) are used to translate the two-way traveltime into depth.

Seismic energy is reflected from any interface across which there is a change in acoustic impedance (product of velocity and density). A large contrast in acoustic impedance will cause most of the impinging seismic energy to be reflected back towards the surface rather than transmitted to deeper horizons. However, coherent reflections can result from small changes in acoustic impedance; for example, in unconsolidated sediments, it has been shown that subtle changes in density or water content are sufficient to produce observable reflections on shallow seismic reflection sections (Slaine et al., 1990).

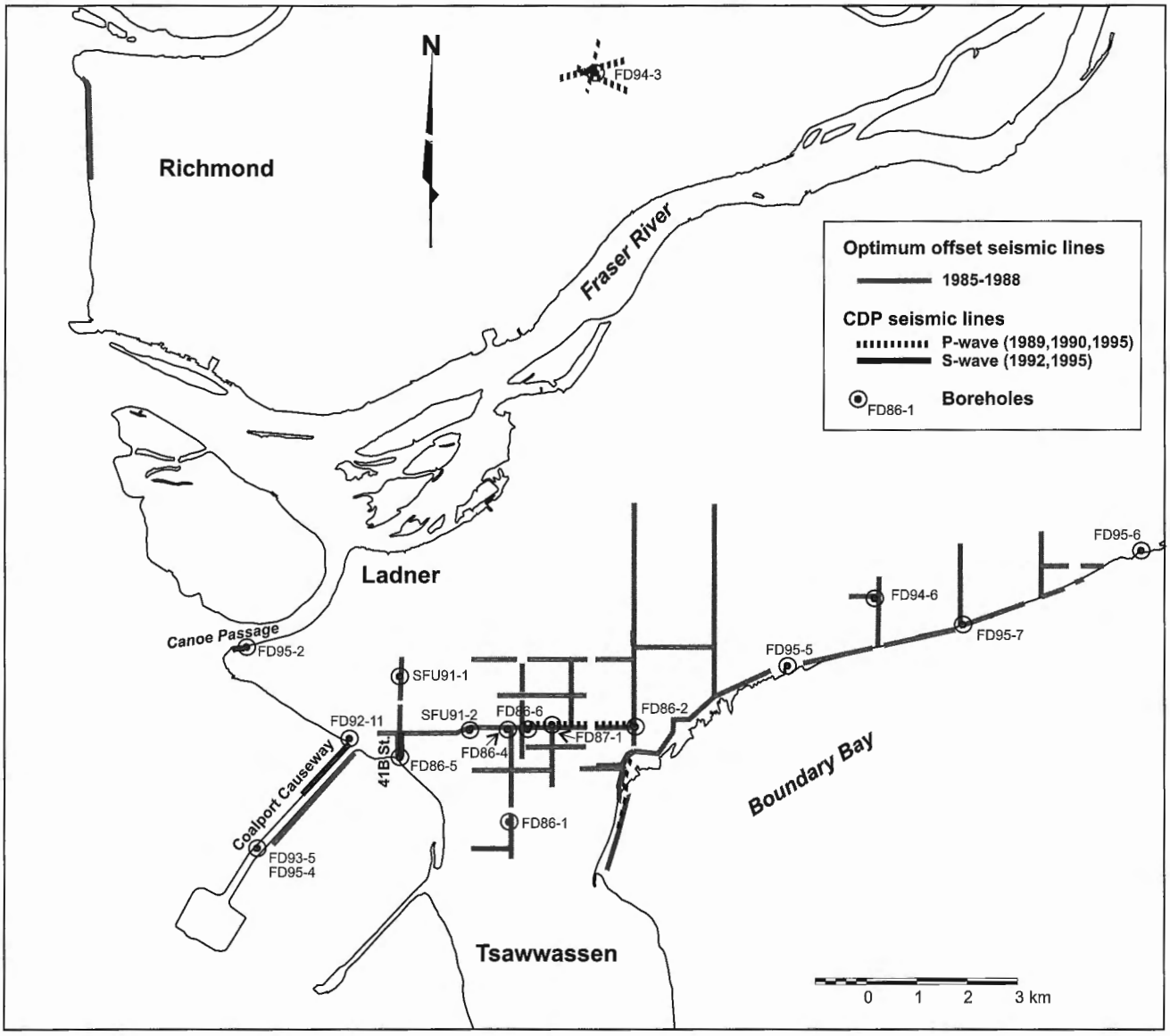

Figure 2. Map of the Fraser River delta showing locations of seismic reflection profiles and associated boreholes drilled by the Geological Survey of Canada and Simon Fraser University.

'Optimum offset' and common-midpoint (CMP) profiling

Details on the application and methods used in shallow seismic reflection surveys can be found in Hunter et al. (1989), Pullan and Hunter (1990), and Steeples and Miller (1990). These papers summarize the development of two different shallow seismic reflection methods – the 'optimum offset' technique, which in its simplest form is a single-channel, constant-offset, profiling technique requiring a minimum of data processing, and the common-midpoint (CMP) method which is an adaptation of the methods employed extensively in the petroleum industry.

The 'optimum offset' method evolved in the early 1980s, in part to avoid the dependence of CMP methods on mainframe computer processing, and in part to avoid the costs and time involved in storing and processing large amounts of data (Hunter et al., 1984). It is the simplest possible form of shallow reflection profiling, in which each trace of the final section is obtained by recording the output of a single geophone separated from the source by a given offset. The offset is chosen after examining test records from around the survey area; it must be large enough that the target reflection can be observed without interference from ground roll or a ground-coupled airwave. The section is then produced trace-by-trace by moving the position of the source and the recording geophone progressively down the line in constant increments (Fig. 3). The processing required is largely cosmetic and consists of the application of static corrections (usually the alignment of first arrivals), digital filtering, and gain controls (Pullan and Hunter, 1990). A velocity-depth function determined from analyses of multichannel records that are recorded along with the optimum offset data is used to calculate a depth scale corresponding to the two-way travel-time of the seismic section. Under favourable conditions, where the signal-to-noise ratio is high enough for reflections from the target horizon(s) to be clearly visible on the field records, the optimum offset method has proved to be a very useful tool for mapping bedrock topography and Quaternary stratigraphy (Whiteley et al., 1986; Pullan et al., 1987, 1992; Hunter et al., 1989; Pullan and Hunter, 1990; Slaine et al., 1990; Roberts et al., 1992; Sharpe et al., 1992).

In CMP surveys, multichannel (12, 24, or more) data are recorded for each shotpoint (Steeples and Miller, 1990). This is accomplished by laying out a large number of geophones and using a 'roll-along' switching box (either internal or external to the recording seismograph) that allows a multichannel record with the chosen offset and receiver geometry to be recorded for every shot. During processing, these data are sorted according to their common midpoints or common depth points (Fig. 4); each trace of these CMP gathers is corrected for offset according to a velocity-depth function determined from the data, and then the traces are stacked (summed) together. This stacking procedure is the essence of

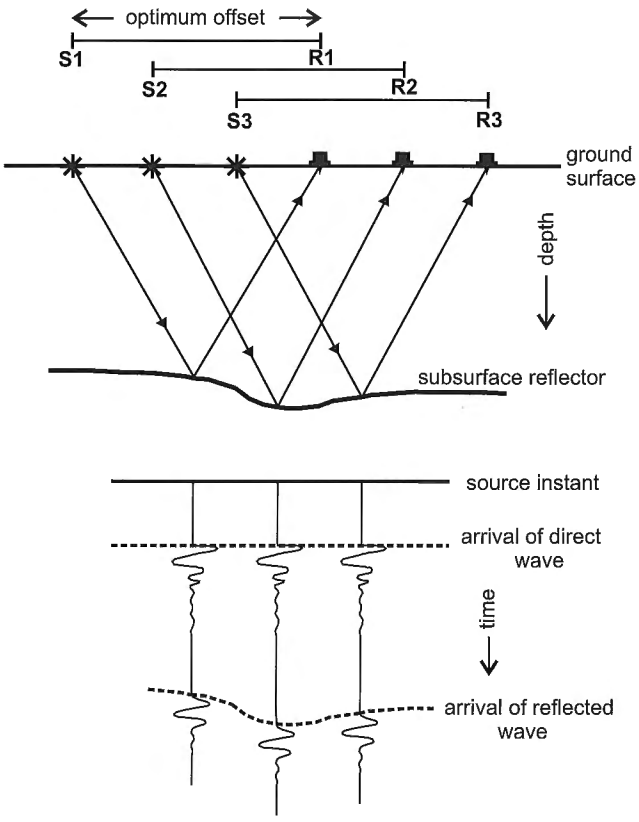

Figure 3. Field setup (top) and resulting schematic optimum offset section (bottom). The optimum offset traces were produced by shooting first from S1 (source position 1) and recording the output from R1 (receiver 1), then from S2 to R2, and finally from S3 to R3.

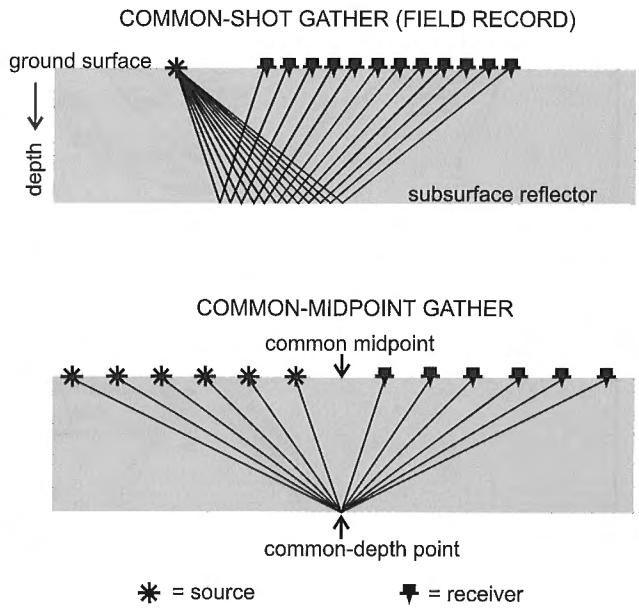

Figure 4. Schematic diagram showing the subsurface travel paths of reflections from field records (upper panel) that have been sorted into a common midpoint (CMP) gather (lower panel). All of the traces in a CMP survey that are characterized by a common midpoint between the source and receiver are processed and stacked together to form a single trace on the final section.

the CMP technique and allows a potential improvement in the signal-to-noise ratio of the data according to the square root of the fold (number of traces summed to create one trace on the final processed section). The CMP technique requires the storage, handling, and processing of a large amount of data, and this makes it significantly more time consuming and costly than the optimum offset method. However, in many study areas the signal enhancement capabilities of the CMP method are critical to successfully acquiring the desired subsurface information (Pullan et al., 1991b).

During the last decade, technological improvements in engineering seismographs, personal computers, and data storage capabilities, and the availability of new PC-based software have overcome many of the limiting factors that led to the development of the optimum offset technique. Common-midpoint data are now routinely collected in the field, allowing common-offset panels to be pulled from the data set and examined before a final decision on the requirement for CMP processing is made (Pullan et al., 1991b). This procedure gives the interpreter the flexibility to exploit the advantages of either technique, depending on the particular problem and site conditions involved.

Compressional (P-) and shear (S-) waves

The type of elastic wave used in most seismic reflection surveying is the compressional wave or P-wave, an elastic body wave in which particle motion is in the direction of propagation of the wave. In unconsolidated sedimentary deposits, the velocity of P-waves is strongly influenced by the presence of water in pore spaces. Typical velocities in water-saturated clays, silts, and sands range from 1500 to 1700 m/s (velocity in water is ~1470 m/s); coarse-grained gravels or compact tills may have significantly higher velocities (in some cases up to 3000 m/s). However, the P-wave velocity in dry, unconsolidated materials is likely to be only a few hundred metres per second. This makes the water table a very significant interface in shallow P-wave reflection surveys.

Shear waves, or S-waves, are body waves in which the particle motion is perpendicular to the direction of wave propagation. S-waves are generated by all sources and also by the partitioning of energy across an acoustic impedance interface in the subsurface (Telford et al., 1976, p. 251; Helbig, 1987; Norminton, 1990). They are not usually observed on P-wave sections because a typical compressional-wave survey discriminates against the recording of shear-wave energy by using vertical geophones, filters, and a record length that minimize the effect of all 'interfering' (i.e. non P-wave reflection) events. Shear-wave data are acquired using horizontal geophones, oriented either in line with the source-receiver spread in the case of vertically polarized shear-wave (SV) surveys, or perpendicular to the survey line for horizontally polarized shear-wave (SH) surveys. True SH waves do not undergo mode conversion (P-SV or SV-P) at subsurface interfaces (Norminton, 1990), so shear-wave reflection surveys are often conducted in this mode to minimize converted-wave interference. Shear-wave surveys generally use some form of polarized source; for example, a railway tie oriented perpendicular to the seismic line (in SH mode) and struck at each end with a sledgehammer. In this way, S-waves of opposite polarities are recorded, and the records can be subtracted to enhance the signal strength of the shear waves and reduce P-wave contamination.

The use of shear waves for shallow seismic reflection profiling offers two potential advantages over compressional waves. First, in well consolidated materials the velocity of shear waves is typically half the P-wave velocity (V_P), and it can be much less than that (0.1-0.2 times V_P) in poorly consolidated sediments. Although high-frequency S-waves are difficult to produce, the lower velocity means that even 50 Hz shear waves have significantly shorter wavelengths than 100-200 Hz P-waves, and hence can result in higher subsurface resolution. Second, shear waves do not exist in fluids and are largely unaffected by the presence of water or gas in the pore spaces of a sediment. This suggests that in areas where high-frequency compressional-wave data are difficult to obtain (e.g. where a low water table results in severe attenuation of high-frequency P-wave energy at the source, or P-waves are attenuated by gas), a shear-wave survey may be more successful in imaging the subsurface target. At present, the use of shear-wave reflection surveys for shallow applications is by no means routine, but considerable effort has been devoted to the testing and development of this method during the last decade (e.g. Hasbrouck, 1987; Zhang, 1990; Pullan et al., 1991a; Johnson and Clark, 1992; Dobecki, 1993; Clark et al., 1994; Bates, 1996).

Potential and limitations of shallow seismic reflection methods

The potential of shallow seismic reflection surveys for providing detailed subsurface structural information has been well demonstrated during the last decade (Hunter et al., 1989; Pullan and Hunter, 1990; Steeples and Miller, 1990; Miller et al., 1992; Roberts et al., 1992; Sharpe et al., 1992; Clark et al., 1994, Bates, 1996). The successful application of any shallow reflection survey depends on the detection of high-frequency energy reflected from velocity discontinuities of interest within the subsurface. The dominant wavelength of the recorded data (wavelength = velocity/frequency) must be small enough to image the target reflector. The required frequency will depend on the objective of the particular survey, with the highest frequencies required for imaging very shallow (i.e. 10-20 m depth) or small (on the order of a few metres in either lateral or horizontal extent) targets. Unfortunately, earth materials, and especially unconsolidated sediments, are strong attenuators of high-frequency energy. Thus, seismic waves in the 10-100 Hz range, commonly used in hydrocarbon exploration, may be reflected from depths of thousands of metres, but energy with frequencies above 150 Hz normally only travel tens or hundreds of metres. The ability of a particular site to transmit high-frequency energy is a major factor in determining the quality and the ultimate resolution of a shallow reflection survey.

Much of the attenuation of high-frequency energy occurs in near-surface materials where the seismic energy is produced. The optimum conditions for shallow reflection surveys exist where the surface materials are fine grained and

water saturated; reflections with dominant frequencies of 300-500 Hz can be obtained in such situations. These frequencies correspond to seismic wavelengths in unconsolidated, water-saturated sediments of 3-5 m, with a potential subsurface structural resolution of approximately 1-2 m (one-third the dominant wavelength; Miller et al., 1995). When surface materials are coarse grained and dry, however, dominant frequencies of the recorded data can be less than 100 Hz. In such areas, seismic wavelengths below the water table may exceed 15 m, and the resolution of the data may not be sufficient to obtain the desired subsurface information. Corrections can be made for variations in topography along a survey line during data processing; however, surface conditions and the depth to the water table are likely to vary with the topography, and these changes may affect the frequency characteristics and resolution of the data. High-resolution seismic reflection surveys are generally not successful in areas where the surface sediments are gas charged (e.g. areas of fill, swamps, bogs), as the attenuation of high-frequency energy in such areas is extreme.

Reflections from very shallow interfaces arrive at times that are close to the arrival times for energy that has travelled directly along the surface of the ground or has been refracted from shallow interfaces such as the water table. For this reason it is often not possible to separate shallow reflection signals from other interfering events. The depth to the first separable reflection horizon depends on the frequency of the signals and source-receiver offsets, but in general, horizons within 10-15 m of the surface cannot be easily delineated using shallow seismic reflection methods.

SURVEY METHODS AND RECORDING PARAMETERS

Initial tests of the shallow seismic reflection technique on the Fraser delta in 1985 indicated that data of excellent quality could be obtained there (Luternauer et al., 1986). The surface sediments are fine grained and water saturated, and provide a near-ideal medium for high-resolution reflection surveys (see also Doornenbal and Helbig, 1983; Jongerius and Helbig, 1988). The dominant frequency of the reflection data is between 300 and 500 Hz, corresponding to wavelengths of 3 to 5 m, and the potential subsurface resolution is on the metre scale.

Two logistical problems were encountered in locating survey lines on the delta. First, many areas of the delta are urbanized (e.g. City of Richmond), and therefore not easily accessible for seismic surveying. Second, much of the eastern part of the delta is covered by peat bogs (Fig. 1), which precludes the use of shallow reflection methods. Severe attenuation of high-frequency energy was observed in seismic tests even beyond the limits of the peat bogs, presumably due to the presence of thin subsurface peat layers or to gas trapped in near-surface sediments. Because of these limitations, the optimum offset surveys were carried out predominantly in the southern rural parts of the delta, near Ladner and Tsawwassen (Fig. 2).

Optimum offset surveys

Most of the shallow seismic reflection sections presented in this paper were produced using the optimum offset technique described above (Hunter et al., 1984, 1989; Pullan and Hunter, 1990). The recording parameters for the surveys are listed in Table 1. The low-frequency components of the data were suppressed before digital recording by high-frequency geophones (50 or 100 Hz) and high-pass analog filters on the seismograph. A 12-gauge 'Buffalo gun' (a simple mechanical device used to detonate a 12-gauge shell just below the ground surface; Pullan and MacAulay, 1987) was the seismic source. For optimum seismic coupling, the geophones and the source were planted in the bottom of water-filled drainage ditches.

The data were collected using 12-channel engineering seismographs with fixed-gain amplifiers, hence the requirement for reducing the low-frequency components of the signal prior to analogue/digital conversion. The seismographs were state-of-the-art instruments at the time, but have been significantly surpassed by present-day technology. Data with 8-bit digital resolution were acquired with Nimbus 1210F and Bison 8012A seismographs. In 1987, two lines were acquired with a prototype 12-channel Scintrex S-2 Echo seismograph which featured 12-bit digital resolution.

All data were transferred to an Apple II+ or IIe microcomputer, stored on floppy disk, and processed using software developed by the Geological Survey of Canada (Norminton and Pullan, 1986). Static corrections, a digital filter, an automatic gain control, and gain tapers were applied to the data. The seismic profiles are sections in two-way traveltime rather than depth. The depth scales shown on the optimum offset sections in this paper were calculated from a velocity-depth function determined from uphole seismic surveys in several boreholes in the area (Appendix A). Under good conditions, these parameters allowed observation of subsurface structures from 10-170 m depth (Pullan et al., 1989).

Common-midpoint surveys

By 1989, advancements in engineering-seismograph and microcomputer technology were starting to overcome the problems of recording, storing, and processing large amounts of data that had led to the development of the optimum offset technique. It was also apparent from the previous surveys that there were large areas of the Fraser delta where the presence of gas within the deltaic sequence severely limited the effective penetration of compressional wave energy (see "Gas in the sediments"). No optimum offset data were collected after 1988; instead CMP seismic reflection data were acquired in an effort to provide deeper, subsurface, structural information, and to assess whether such surveys could provide additional information in areas where optimum offset surveys had been limited by gas. These data have been acquired, stored, and processed in IBM format using commercially available software packages.

Compressional-wave CMP surveys

The first compressional-wave CMP survey was conducted in 1989 using a Scintrex S-2 Echo seismograph (still a fixed-gain instrument, but specially fitted with 14-bit A/D converters). Soon thereafter, in 1990, CMP data were recorded on the first state-of-the-art, instantaneous floating-point seismograph, a Geometrics ES-2401 instrument. Both of these surveys repeated sections of optimum offset lines (Fig. 2). The 1989 survey recorded 400 ms of 6-fold CMP data along a line where penetration of seismic energy on the optimum offset section was limited to 180 ms. The aim of this survey was to evaluate whether higher fold data would allow delineation of deeper structure. The 1990 data were collected along the edge of the tidal flats at the west side of Boundary Bay. The geometry and recording parameters for this line were designed to investigate structure at depths of several hundred metres below the surface in an area where there is no gas in the shallow sediments. The recording parameters for both surveys are listed in Table 1. A standard CMP sequence of processing steps, including trace editing, static corrections, bandpass filtering, gain scaling, velocity analysis, and stacking, were applied to the data using Eavesdropper™ software.

An additional 3.2 km of P-wave CMP data were collected under contract in 1995 along three intersecting lines centred on a 300 m deep borehole (FD94-3, see Dallimore et al., 1995) in the north-central part of the study area (Fig. 2, Table 1). These data were subject to strong interference from airport beacons and are currently being processed and analyzed.

Shear-wave CMP surveys

Three short, shear-wave CMP surveys have been conducted in the western part of the study area (Fig. 2) to test the potential of this method for mapping the Holocene-Pleistocene boundary (Harris et al., 1996). The locations of these profiles were chosen, in part, because of their proximity to boreholes where Pleistocene sediments were encountered. The shear-wave energy source for the Coalport (Deltaport) Causeway line (shot in 1992) was a 7.3 kg sledgehammer striking a large angled steel plate. The signals from four blows (two blows in each direction) were stacked in the seismograph with opposite polarities for the two impact directions. The source for both the 41B Street and Canoe Passage lines (acquired in 1995) was similar, except that a small steel I-beam was used as the mass instead of the angled plate. The Coalport Causeway and 41B Street profiles were shot in SH mode, with source and receivers (8 Hz horizontal geophones) aligned perpendicular to the line. The Canoe Passage profile was shot in SV mode, with source and receivers oriented in line. The recording parameters for these surveys are summarized in Table 1. A simple, standard CMP sequence of processing

Table 1. Recording parameters of seismic reflection surveys conducted on the Fraser River delta between 1985 and 1995.

Year	Survey type	Seismograph	No. of channels	Source	Geophones	Geophone spacing (m)	Source offset (m)	Record length (ms)	Total line-km
1985*	P-wave optimum offset	Nimbus 1210F	12	12-gauge shotgun	50 or 100 Hz	5, 2.5	20, 25	100, 200	5.5
1986*	P-wave optimum offset	Nimbus 1210F, Bison 8012A	12	12-gauge shotgun	50 or 100 Hz	3	24	200	10
1987*	P-wave optimum offset	Nimbus 1210F, Bison 8012A, S-2 Echo	12	12-gauge shotgun	50 or 100 Hz	3	24	200	33.8
1988**	P-wave optimum offset	Nimbus 1210F	12	12-gauge shotgun	50 Hz	3	12	200	2.2
1988**	P-wave optimum offset	Nimbus 1210F	12	12-gauge shotgun	50 Hz	3	42, 66, 72	500	1.5
1989**	P-wave CMP (6-fold)	S-2 Echo	12	12-gauge shotgun	50 Hz	5	20	400	2
1990**	P-wave CMP (6-fold)	ES-2401	12	8-gauge shotgun	50 Hz (x3)	5	120	1000	1.5
1995**	P-wave CMP (12-fold)	Strataview S-24	24	10-gauge shotgun	50 Hz	5	30	1000	3.2
1992**	S-wave CMP (6-fold)	Strataview R-24	24	hammer on angled plate	8 Hz horizontal (SH mode)	3	1.5	2000	1.4
1995**	S-wave CMP (12-fold)	Strataview R-24	24	hammer on angled I-beam	8 Hz horizontal (SH/SV mode)	3	1.5	1000	0.6

* Data in Pullan et al. (1989).
** Unpublished data.

steps, including trace editing, bandpass filtering, gain scaling, velocity analysis, and stacking, were applied to the data using Eavesdropper™ software.

RESULTS

The seismic reflection profiles presented in this paper (Fig. 5), in conjunction with borehole data, indicate that the sedimentary sequence beneath the southern Fraser River delta comprises four main units: Holocene topset (unit 1) and foreset (unit 2) deposits, underlying Pleistocene sediments (unit 3), and Tertiary bedrock (unit 4) (see also Pullan and Hunter, 1987; Clague et al., 1991; Jol and Roberts, 1988, 1992). These units are discussed in detail in the sections that follow.

Holocene sediments (units 1 and 2)

Units 1 and 2 constitute the Holocene sequence of the Fraser River delta. All seismic sections provide some information on these sediments. The discussion below is subdivided into topset sequence (unit 1), foreset sequence (unit 2), gas within the shallow sediments, and Holocene slumps and faults. No bottomset sediments have been identified on these seismic sections. In most cases, the seismic energy has been attenuated at shallower depths by the presence of gas.

Topset sequence (unit 1)

The shallowest unit observed on optimum offset seismic reflection profiles is a sequence of flat-lying, low- to moderate-amplitude reflections which have been interpreted to be deltaic topset deposits (Clague et al., 1991). Drilling has shown that this unit ranges from a few metres to more than 20 m thick, and consists of interbedded mud, sandy silt, and silty fine-grained sand, in places capped by peat. The unit increases in thickness in an easterly direction towards the apex of the delta, probably as a result of relative changes in sea level during Holocene time (Clague et al., 1982, 1983). The topset deposits aggraded in response to a rise in sea level between about 8000 BP and the present day (Williams and Roberts, 1989, 1990).

The sedimentary character of these deposits is largely dependent on their relationship to laterally stable or laterally migrating distributary channels. Where a distributary channel crosses the Fraser's subaerial delta plain, its ability to migrate laterally is inhibited be vegetated banks of cohesive bank material. These stable channels shift by avulsion rather than more gradual lateral migration (Hutchinson et al., 1995). During times of flood, overbank deposits accrete vertically in areas adjacent to the distributary channels. Where the distributary channels cross the unvegetated tidal flats, lateral migration is not restricted by cohesive banks and lateral accretion deposits are dominant (Monahan et al., 1993).

This uppermost sedimentary unit is not always evident on the optimum offset seismic reflection profiles for two reasons. First, the non-zero offset (source-receiver separation) that is necessary to avoid interference between surface waves (ground roll) and reflections from deep horizons compromises the resolution of very shallow structure (see "Potential and limitations of shallow seismic surveys"). The offset used for most of the profiles (24 m) was chosen to observe structure at depths of 10-170 m. Second, the lithological contrast between the topset sediments and the underlying foreset deposits, and hence the acoustic contrast at the interface between the two units, is a subtle one. As a result, the reflection associated with this boundary is generally relatively small in

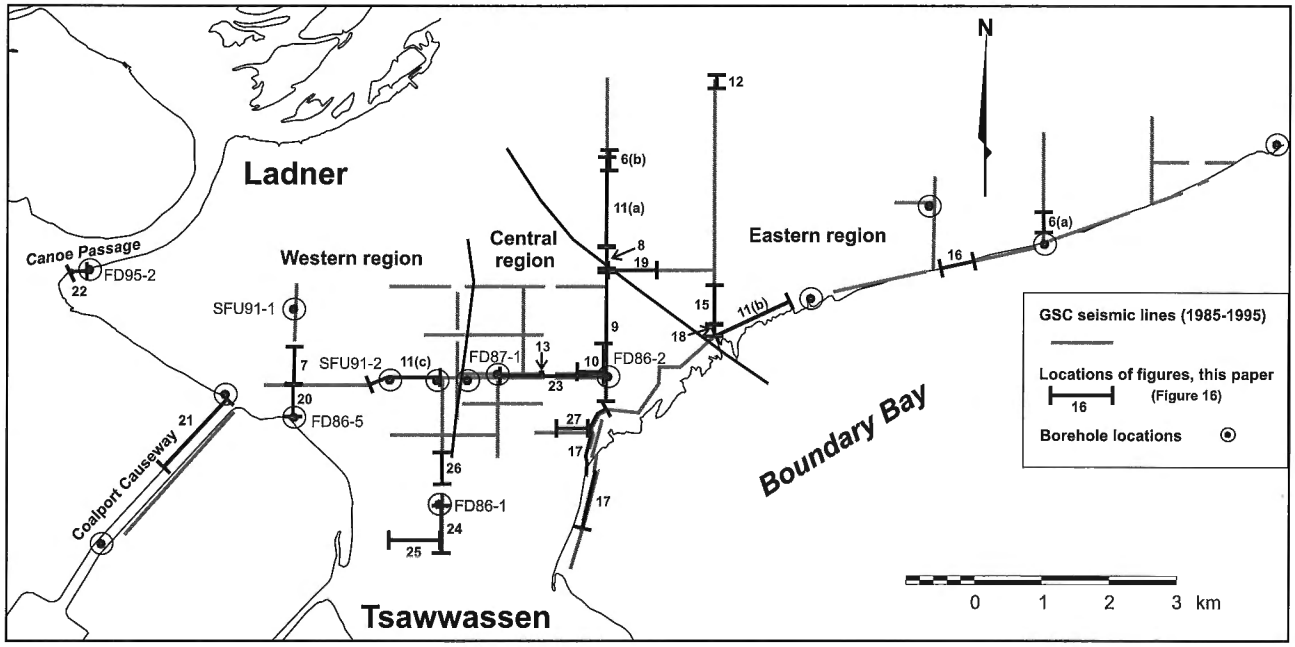

Figure 5. Locations of seismic sections shown as figures in this paper.

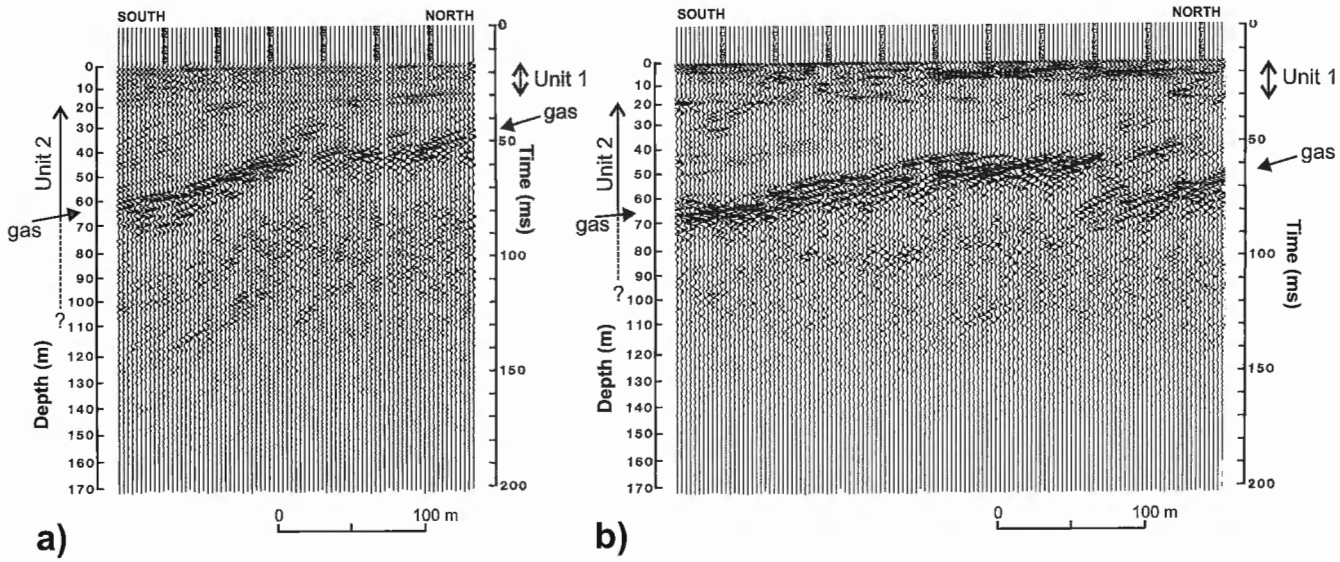

*Figure 6. North-south optimum offset section from the **a)** southeastern and **b)** central parts of the study area, showing thick topset deposits (unit 1) and limited penetration of seismic energy in the foreset sequence below (unit 2). The large-amplitude reflection that masks all underlying structure is caused by gas in the deltaic sediments.*

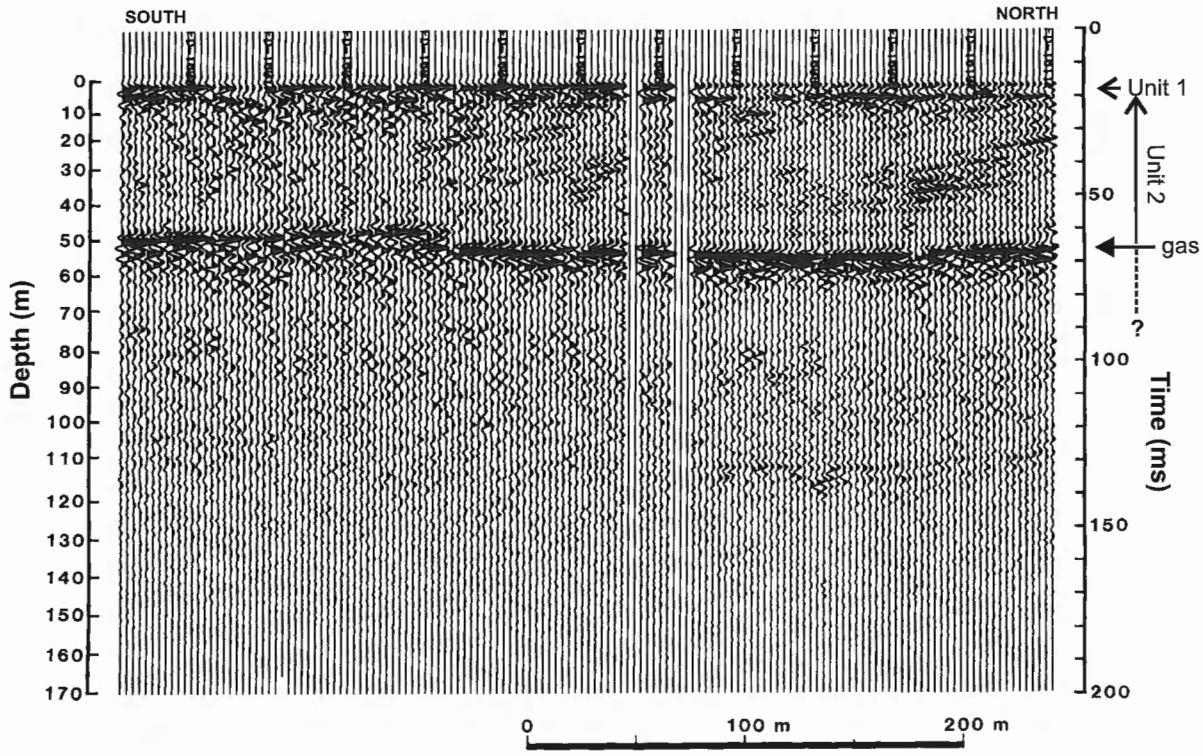

Figure 7. North-south optimum offset section from the western part of the study area showing a flat-lying reflection at a depth of 5-10 m that is interpreted to be the base of unit 1 (topset deposits). The relatively flat-lying, large-amplitude reflection at approximately 50 m depth masks all deeper structure and is interpreted to be the top of sediments containing gas.

amplitude. On the southern Fraser delta, the topset unit tends to be most clearly defined on north-south profiles along the depositional dip, where it unconformably overlies the dipping sequence of foreset beds. Where the foreset unit is also characterized by relatively flat-lying reflections, such as along a depositional strike section, it is difficult to accurately identify the base of the topset sequence.

Figures 6 and 7 show examples of optimum offset sections where the topset sequence can be observed. These are north-south sections along which the topset deposits are clearly nonconformable with the underlying dipping foreset beds. Figure 6 shows examples from the southeastern and central regions of the study area where the topset deposits are approximately 20 m thick. Figure 7 is an example from the western edge of the dyked delta plain, where the topsets are much thinner. In this example the base of the topset deposits is interpreted to be a very shallow reflection, best observed at the north end of the profile, at a depth of 5-10 m.

Seismic reflection surveys can be designed for better resolution of the shallow subsurface structure. Figure 8 is an example of a north-south optimum offset section recorded with an offset of 12 m, a geophone spacing of 1.5 m, and a record length of 100 ms. The topset unit is clearly depicted in this section. The unit is approximately 20 m thick and is separated from the underlying foreset sequence by a sharp, nearly planar surface. Just to the right of the centre of this figure is a shallow channel-like feature cut into the foreset deposits. The channel is approximately 100 m wide and 5 m deep, and may represent an old distributary channel of the Fraser River.

Foreset sequence (unit 2)

Optimum offset reflection surveys have revealed that the topset sequence, over a large portion of the survey area, is underlain by a thick unit of dipping reflections (Fig. 8). A 2 km long north-south section (Fig. 9) shows a typical sequence of these reflections dipping to the south. Dip angles can reach 7-8°, although the average is 1.5-3°. Deeper reflections, in general, dip at lower angles than those higher in the sequence. A perpendicular line intersecting this section shows that the reflections do have a small component of dip to the west (Fig. 10). Thus, the true dip direction of the foreset beds in this area is south-southwest. At the south end of the section shown in Figure 9, the unit of dipping reflections is more than 130 m thick. This unit is interpreted to be a progradational sequence of foreset beds deposited on the foreslope of the ancestral Fraser delta (Jol and Roberts, 1988; Clague et al., 1991), based on the seismostratigraphy observed on the sections, the uniformity of dip, and the measured angles of dip.

Several Geological Survey of Canada drillholes have penetrated this unit in the survey area (Clague et al., 1991; Fig. 9), and have shown that the foreset sequence there is dominantly sand and silty sand. There is a good correlation between many of the seismic reflections and subtle changes in lithology. For example, the boundary between sandy silt and silty sand at approximately 74 m depth in borehole FD86-2 correlates well with a reflection package at approximately 90 ms at the same site (Fig. 9). Detailed geophysical logging and grain-size data from borehole FD87-1 (Fig. 2) also support the contention that small changes in lithology can be correlated with reflections on the optimum offset seismic

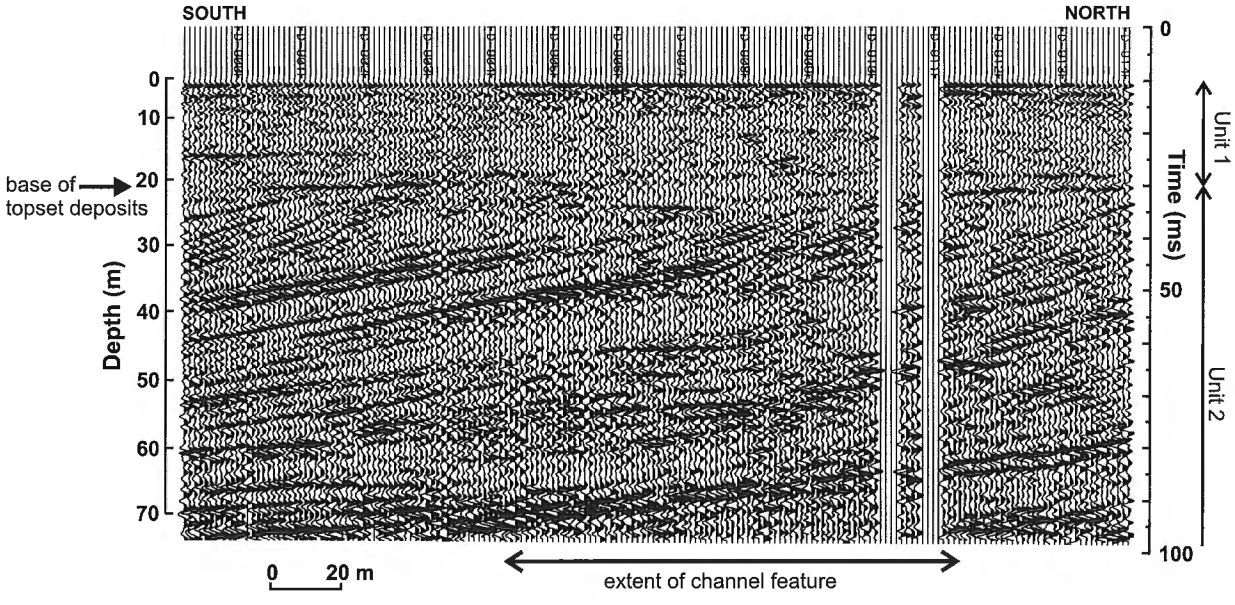

Figure 8. North-south optimum offset section from the central part of the study area, recorded with an offset of 12 m and a geophone spacing of 1.5 m. These parameters allow for higher resolution in the uppermost few tens of metres of the sediment sequence. This section shows the interface between the uppermost flat-lying Holocene topset sediments (unit 1) and the underlying foreset sequence (unit 2) at a depth of 20-25 m.

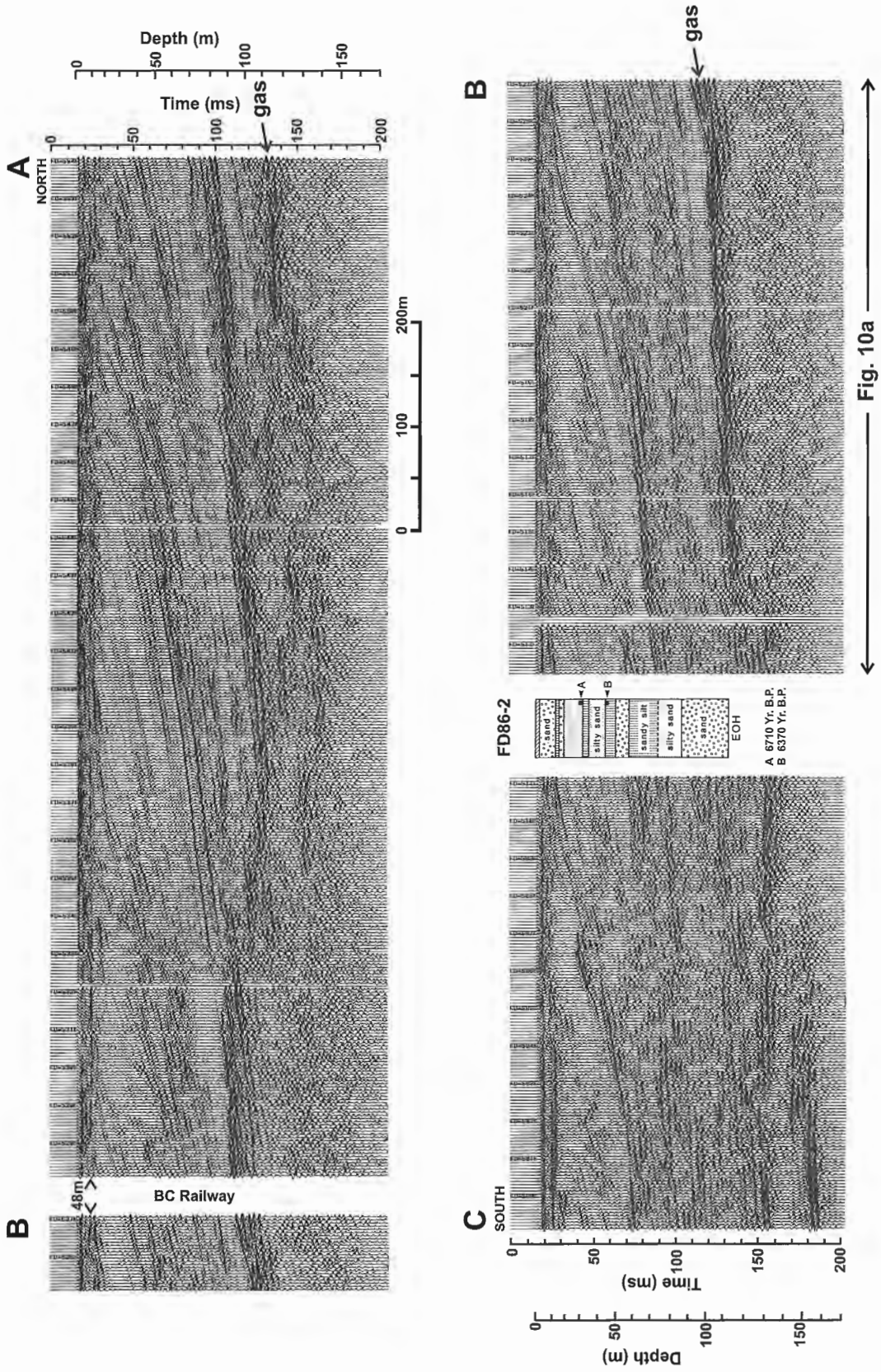

Figure 9. *A 2 km long, north-south optimum offset section showing a sequence of reflections dipping to the south, interpreted to be Holocene foreset deposits; at the south end of the section (C), the foreset sequence is at least 130 m thick.*

sections. Thus, it is believed that the reflections seen on these seismic sections are produced by small density and/or velocity changes across bed boundaries within the sandy sequence.

The thick foreset sequence seen in Figures 9 and 10 is not as apparent on seismic reflection profiles acquired elsewhere in the study area. Only in a limited area north of Tsawwassen do the seismic profiles delineate the full sequence of Holocene deltaic deposits and image lower stratigraphy. Elsewhere a large-amplitude reflection(s) within the foreset sequence effectively masks deeper structure. Examples of the decrease in the effective penetration of compressional wave energy to the north, east, and west of borehole FD86-2 are shown in Figure 11. The large-amplitude reflections observed on all these profiles are interpreted to be the result of gas trapped within the deltaic sequence. Observations that have led to this conclusion are discussed below.

Gas in the sediments

The presence of gas in sediments can have a profound effect on the quality of seismic reflection data ('gas' in this context means any substance in the gaseous state, from air to hydrocarbons). Acoustic attenuation, velocity, and reflection coefficients for liquid-saturated sediments differ significantly from those of partially saturated, gas-bearing sediments. For example, gas saturations of only 1% (i.e. gas occupies 1% of the pore space) in a quartz sand can cause the velocity to decrease to as little as one-fifth that of the fully

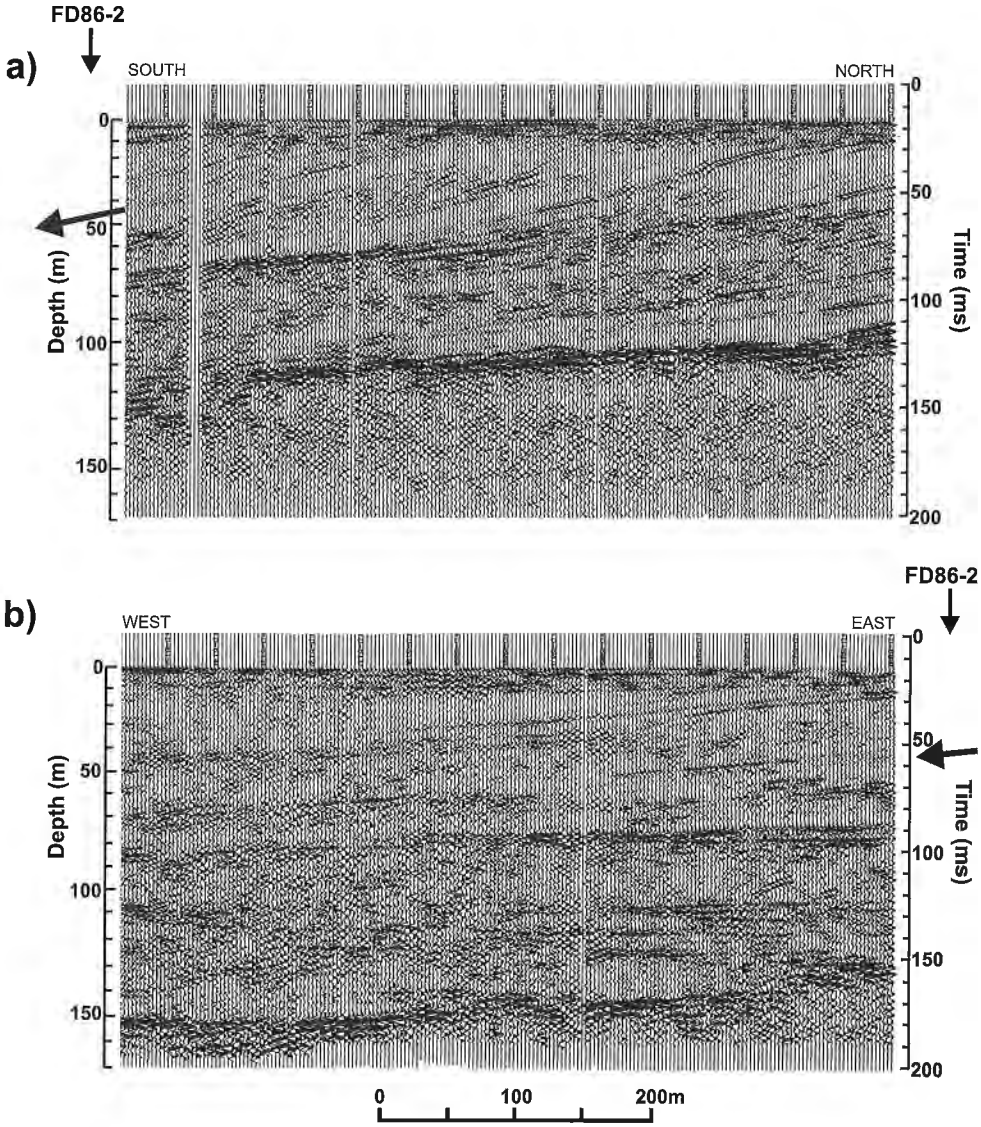

Figure 10. North-south (a) and east-west (b) optimum offset sections at borehole FD86-2. The two sections show that the dip of the foreset beds (arrows) is south-southwest.

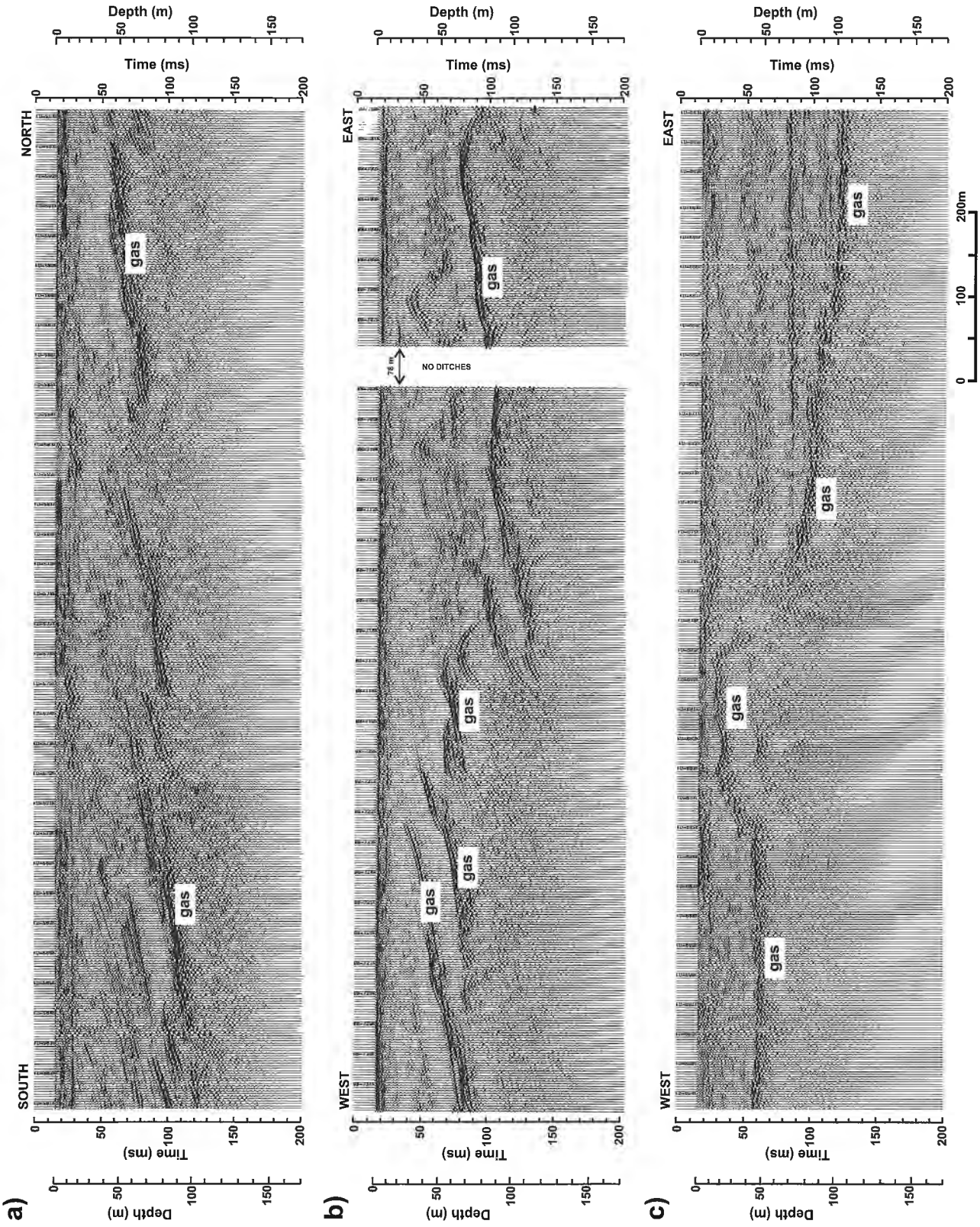

Figure 11. *Examples of the change in seismic character and decrease in effective penetration of seismic energy* ***a)*** *north,* ***b)*** *east, and* ***c)*** *west of borehole FD86-2.*

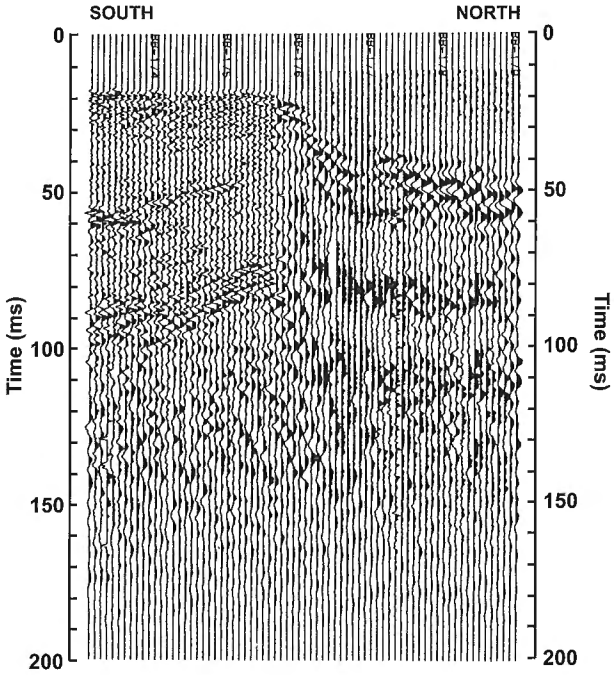

Figure 12. Example of the abrupt deterioration of high-frequency energy due to the presence of a small amount of gas in the pore space of near-surface sediments.

water-saturated sediment (Brandt, 1960). The reduction in velocity is depth dependent; the effect becomes less pronounced as the depth of burial increases. However, even at considerable depths, the velocity changes caused by the presence of gas are significant in comparison to those associated with typical lithological boundaries within unconsolidated sediments.

As well as producing a substantial decrease in velocity, gas in sediments greatly increases the attenuation of seismic signals. When gas is present in near-surface materials, the resulting attenuation of high-frequency energy can be severe enough to preclude the use of shallow seismic reflection techniques altogether. The presence of near-surface gas in some areas of the Fraser delta is clearly indicated by 'wipeout' or no-record zones in the seismic sections. An example of severe attenuation of high-frequency energy and abrupt deterioration in record quality in one of these zones is shown in Figure 12. The increased time delay to the first arrivals on the right side of the figure indicates a sudden decrease in the velocity of the surface materials which is accompanied by a loss of high-frequency signal (>100 Hz). Such deterioration in data quality is common in the eastern part of the survey area.

As has already been noted, penetration of high-frequency, compressional-wave seismic energy is severely limited in many areas of the Fraser delta, in some cases to only a few tens of metres (Fig. 6, 7, 11). Typically, a blind zone with no coherent reflections occurs beneath a large-amplitude reflection on the seismic section. The large-amplitude reflection indicates an interface across which there is a significant contrast (either increase or decrease) in acoustic impedance. Drilling has provided no evidence of major lithological changes which might produce such reflections. The presence of gas in the sediments below the interface could be the cause of both the large-amplitude reflection and the masking of deeper structure.

Two additional seismic indicators that are diagnostic of the presence of gas have been observed in reflection profiles from the southern Fraser delta:

1. There are abrupt lateral variations in the amplitude of reflections in many seismic sections, which cannot be explained by changes in stratigraphy or structure (Fig. 11; see also discussion below).
2. The large-amplitude reflections are a distinct boundary between high-frequency signals and low-amplitude, low-frequency signals at greater traveltimes (Fig. 13). The increased attenuation below this boundary is consistent with the presence of gas.

Gas within the deltaic sequence may have been formed locally by diagenesis of organic matter, or could be migrating into the sediments from deeper stratigraphic levels. Within the foreset sequence, gas would be trapped beneath finer grained layers, while permeating upward with ease through coarse-grained material. Gas trapped beneath a bed in one area but having permeated higher in the sequence to another bed in an adjacent area could explain the observed lateral discontinuities.

The seismic data strongly suggest that gas is present within the Holocene deltaic sequence beneath much of the Fraser River delta, but they do not directly measure it. In 1991, a Minipac Gas Detector was used during the drilling of

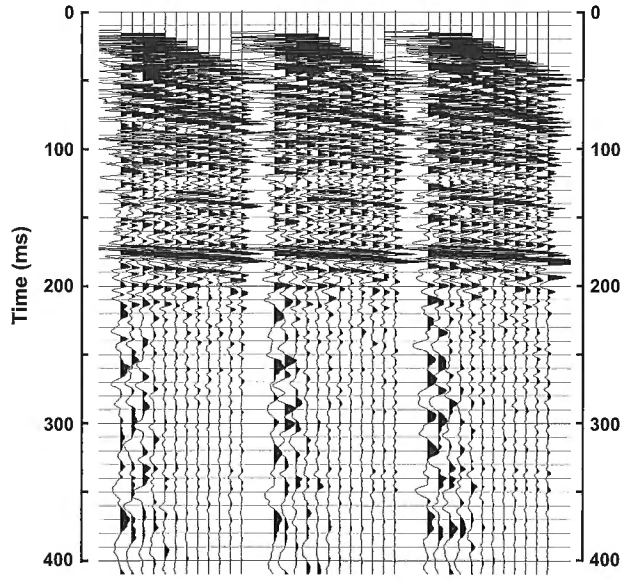

Figure 13. Three field records from a 1989 compressional-wave CMP survey showing that the large-amplitude reflection at approximately 180 ms is a marked boundary between high-frequency signals and low-amplitude, low-frequency signals at greater traveltimes. No gain control or filtering was applied to these records; true relative amplitudes are displayed.

two boreholes by Simon Fraser University (SFU91-1 and SFU91-2; Fig. 5) to definitively document the existence of gas. The instrument, which is commonly used in the petroleum industry, measures and records the presence of combustible gases in the gas/air mixture retrieved from the drilling fluid. Because gas is easily lost before it reaches the gas trap in the mud tank at the surface, the readouts are very sensitive to drilling operations (e.g. speed of drilling and mud weight). The objective of this experiment, however, was not to measure gas concentrations, but simply to document the presence of combustible gases at sites where large-amplitude reflections were observed at relatively shallow depths.

The results from SFU91-2 are shown in Figure 14, along with a natural gamma log and interval P-wave velocities calculated from a downhole seismic survey (see Appendix A). There is clearly a correspondence between the gas activity recorded by the Minipac Gas Detector and low seismic velocities below 12 m depth. P-wave velocities in saturated sediments which are less than those in water (1470 m/s) strongly suggest the presence of gas. A few samples from SFU91-1 and SFU91-2 were also analyzed for gas. A single sample from borehole SFU91-2 (22.5 m depth) did not yield any measurable methane, but one sample from SFU91-1 gave a value of 800 ppmv (R. Cranston, personal communication, 1991). Even that measurement suffered from a loss of perhaps 99% of the available gas (R. Cranston, personal communication, 1991).

The results of this experiment substantiate the interpretation that the large-amplitude reflections and strong attenuation observed on the seismic profiles are due to the presence of gas within the deltaic sequence. It is clear that many of the seismic profiles are dominated by these characteristics, but the eastern and western parts of the study area (Fig. 5) differ substantially in how the characteristics are manifested. This is attributed to differences in depositional environments and is discussed in the two following sections.

Eastern region

Records from the eastern part of the survey area, north of Boundary Bay (Fig. 5), show foreset deposits characterized by high-amplitude, steeply dipping (up to 7-8°), and laterally discontinuous reflections (Fig. 6, 11a,b). In general, the depth of penetration of seismic energy decreases to the north and east where older sediments are found nearer the surface (the delta having prograded to the south-southwest). The deepest reflection observed in the eastern part of the study area is generally a large-amplitude event showing abrupt lateral discontinuities over distances of a few hundred metres (Fig. 15). The eastern region is also characterized by a number of 'no--record' zones (Fig. 12). The limited penetration of seismic energy is attributed to the presence of gas trapped in sediments at shallow depth, and the no-record zones to areas where gas has permeated up to the surface.

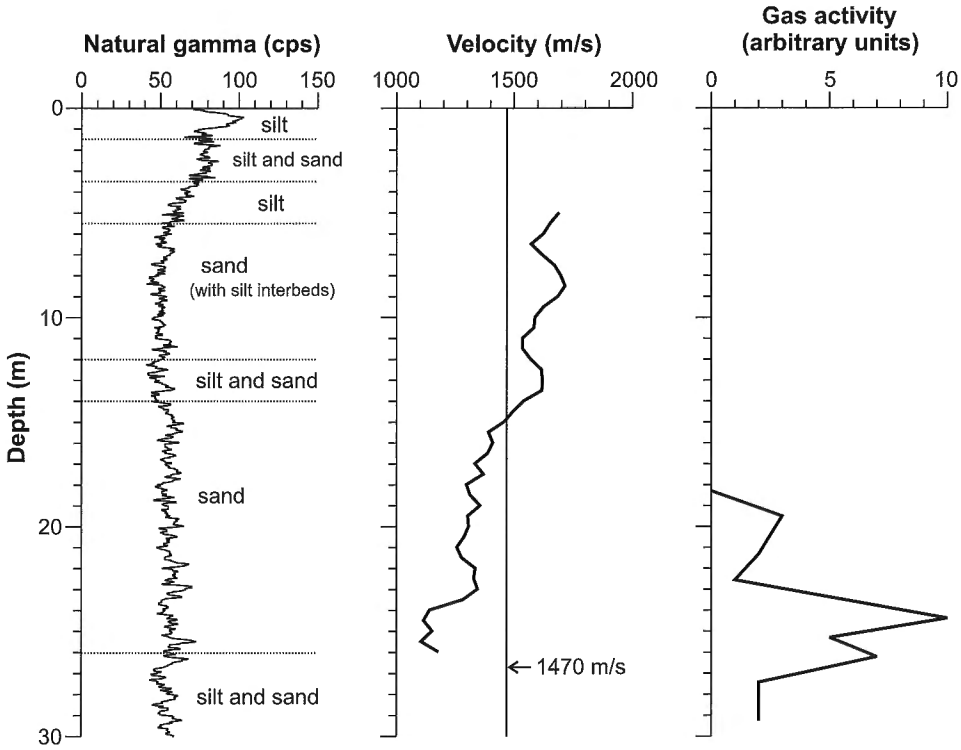

Figure 14. Natural gamma, P-wave seismic velocities, and gas readouts obtained with the Minipac Gas Detector in borehole SFU91-2 on the Fraser delta north of Tsawwassen. P-wave velocities in the sediments containing gas are lower than the velocity in water (vertical line).

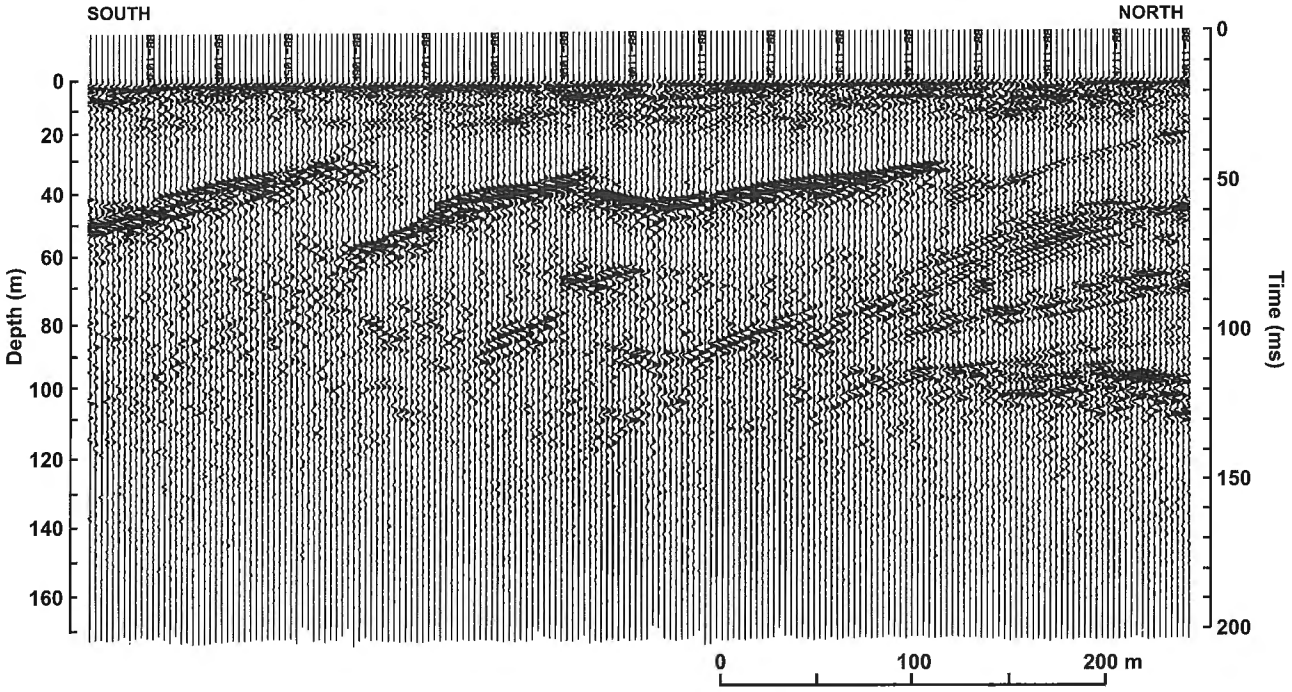

Figure 15. *North-south optimum offset section showing the limited penetration of seismic energy and abrupt lateral shifts of large-amplitude reflections typically observed on seismic profiles from the eastern part of the study area.*

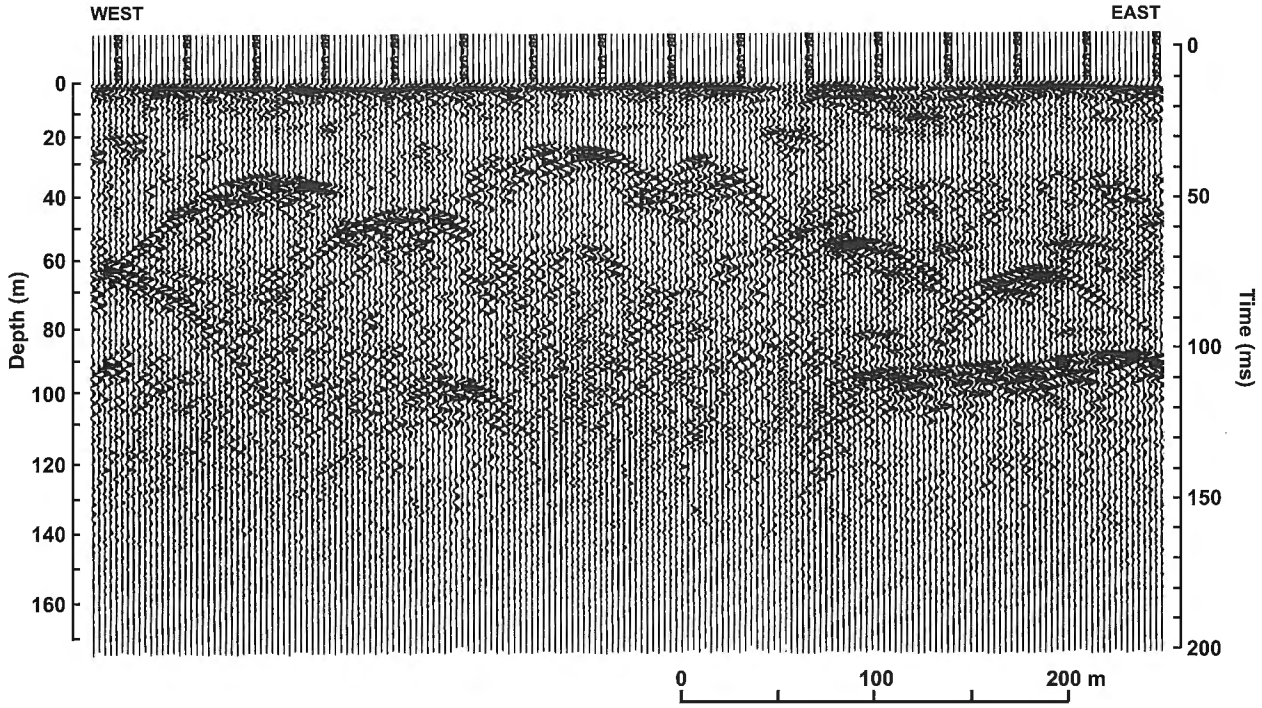

Figure 16. *East-west optimum offset section along the Boundary Bay dyke showing several examples of the hyperbolic diffractions discussed in the text.*

Distinctive, high-amplitude, hyperbolic diffractions are a common feature on several east-west sections along the Boundary Bay dyke (Fig. 16). The distinctive hyperbolic shape is caused by the scattering of seismic energy from a small subsurface feature. By comparing the diffractions with calculated diffraction curves, it is estimated that the subsurface structures range from 12 to 42 m in width along the strike of the foreset sequence (Jol, 1988). However, these may be linear features in the dip direction, as there are no indications of diffractions on north-south sections north of Boundary Bay.

The large amplitudes of these hyperbolic features, the abrupt lateral changes in reflection characteristics, and the masking of deeper horizons are characteristics associated with gas. However, the linear nature of the features appears to be unique to this part of the delta. Possible alternative explanations for the features, suggested by Jol (1988), are 1) some natural process that has incised the slope (e.g. gullying of the sea floor by mass wasting and/or turbidity currents), and 2) localized slope failure or slumping.

Western region

Many seismic profiles from the western part of the survey area, north and west of Point Roberts (Fig. 5), are dominated by a single, continuous, high-amplitude reflection at shallow depth (Fig. 7, 11c). This horizon is relatively flat, but shallows slightly in the northern part of the region. There is no indication of deeper structure on the seismic sections. Above the reflection, there are weak indications of foreset beds, with apparent dips to the southwest. Maximum observed dip angles are 6° (e.g. north end of Fig. 7), but the thick sequences of delta foreset deposits seen in the eastern region are not in evidence here. The relatively thin (<60 m) sequence of foreset beds above the large-amplitude reflection appears to have been deposited on a fairly flat surface, because the lowest beds of the sequence are flat-lying. There is no evidence that the large-amplitude reflection truncates either underlying or overlying strata.

Gas trapped beneath a fine-grained layer at the depth of the large-amplitude reflection explains both the amplitude of the reflection and the lack of seismic energy returning from deeper stratigraphic horizons. The continuity of the reflection suggests that the sediments are uniform over a large area. In a few places, shallow anomalous 'bumps' disrupt the lateral continuity of the reflection (Fig. 11c). Two such anomalies have been drilled, but in neither case has a significant lithologic change been identified at the depth of the reflection. These features are interpreted to be areas where gas has invaded shallow sediments.

It appears that the deltaic sediments in the western part of the survey area were deposited under a different regime than those north of Boundary Bay. The gentle dips of the foreset beds in the western region, and the assumption that the large-amplitude reflection must be stratigraphically controlled even if the amplitude is related primarily to the presence of gas, suggest that this portion of the delta was not built out into as deep a basin as north of Boundary Bay, but rather were deposited in a quiet shallow-water environment. These deposits may have accumulated on an old Pleistocene platform, perhaps the subsurface extension of the Pleistocene deposits of Point Roberts (see 'Pleistocene sediments (unit 3)').

Holocene slumps and faults

There is evidence on the optimum offset sections for both slumps and faults within the Holocene deltaic sequence on the southern Fraser delta. An excellent example of a slump can be seen in the upper panel of Figure 17 (this section is the southern extension of the line shown in Figure 9 and is discussed in detail by Jol and Roberts, 1988). A lump of material at a depth of about 100 m at the base of the deltaic sequence has been interpreted to be a subaqueous landslide deposit that was emplaced when sediments slid down the north-dipping unconformity visible on this section, and came to rest on the surface of the deltaic sediments then being built southwards (Jol and Roberts, 1988). Alternatively, it could be part of the foreset sequence which slid down the south-dipping delta foreslope and came to rest in the small basin formed where the foreset beds lap onto the southward-rising unconformity (Jol and Roberts, 1992). The displaced mass is large – approximately 30 m high in the centre and over 300 m long. Its width is not known, as no seismic lines cross the feature perpendicular to the line shown in Figure 17. The presence of reflections within the block suggests that the material moved as a coherent mass with relatively little internal disturbance.

Other features, which are interpreted to be smaller slumps, are fairly common on shallow seismic profiles that are parallel to the dip of the foreset deposits. An example, shown in Figure 18, has a maximum thickness of approximately 10 m and a length of about 100 m.

Slope failures are common at the present-day delta front (e.g. McKenna et al., 1992), and similar failures have occurred throughout the Holocene as the Fraser delta has built out into the Strait of Georgia. Factors that may trigger these failures include seismic activity (Milne et al., 1978), cyclic wave loading, rapid sediment loading during freshet, and tidal drawdowns (McKenna et al., 1992; Christian et al., 1998).

There is abundant evidence for Tertiary folding and faulting in the Georgia Basin (Mustard and Rouse, 1994), but the existence of young faults beneath the southern Fraser delta is more problematic. However, Figure 19 shows an example of possible fault disruption of the foreset sequence. This section does not show the regular coherent reflections that characterize other east-west sections in the area (e.g. the east side of Fig. 11c). Rather, the foreset beds are disrupted at several sites. It is possible that such disturbed strata indicate faulting associated with tectonic processes, or syndepositional movements related to slope failure or sediment loading. Such disturbance is uncommon in the seismic records; there are just one or two sections of line that show such features in the 60 line-kilometres collected to date. Without independent evidence, the identification of Holocene faults in this area remains speculative.

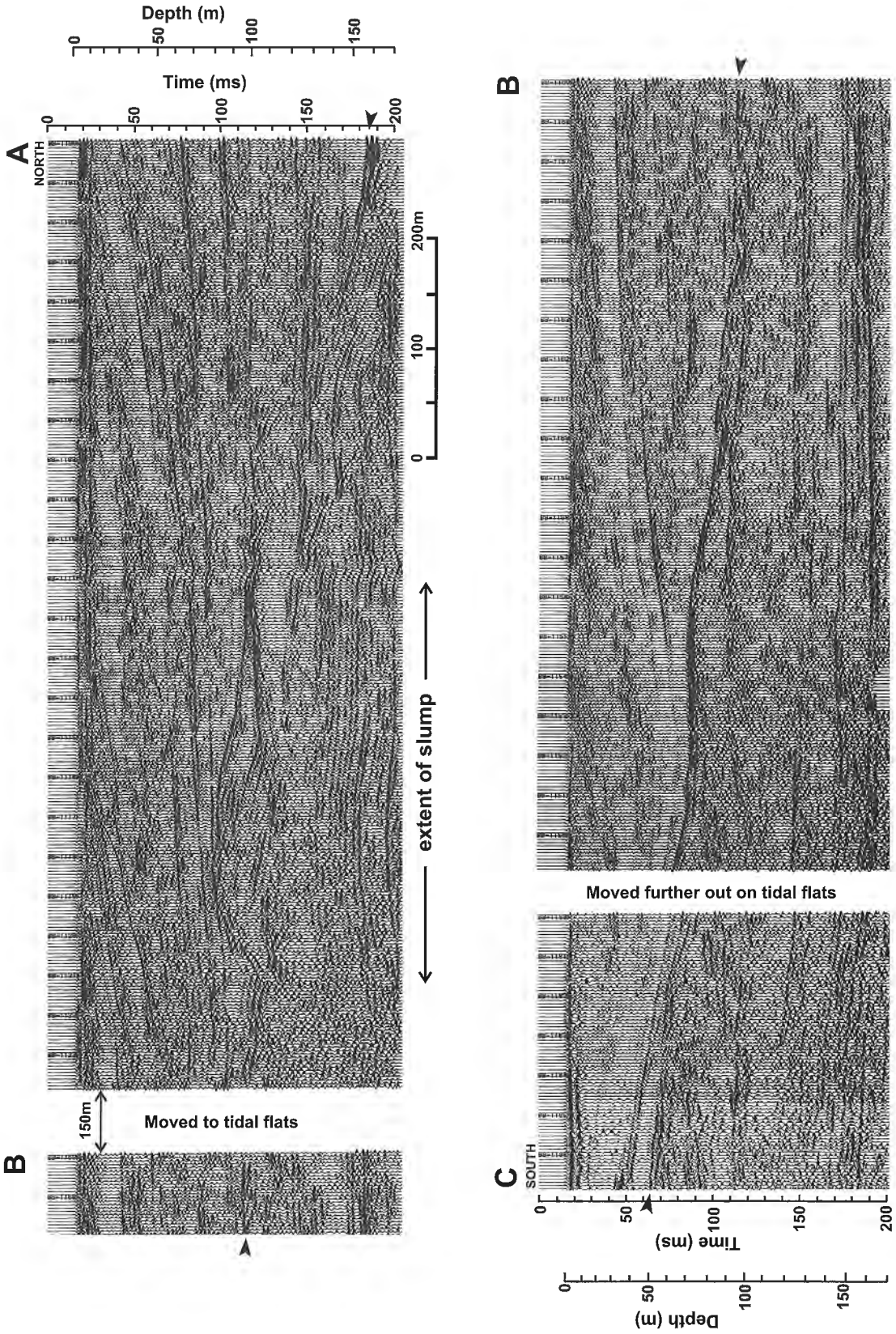

Figure 17. Approximately north-south optimum offset section extending south from location C in Figure 9. This profile shows an unconformity (arrowed) shallowing towards Point Roberts and overlain by foreset beds. The unconformity has a maximum depth of 155 m at the north end of the profile (A) and rises to within 50 m of the surface at the south end (C). The irregular mass of material north of B at 95 m depth is interpreted to be a large slump (see text).

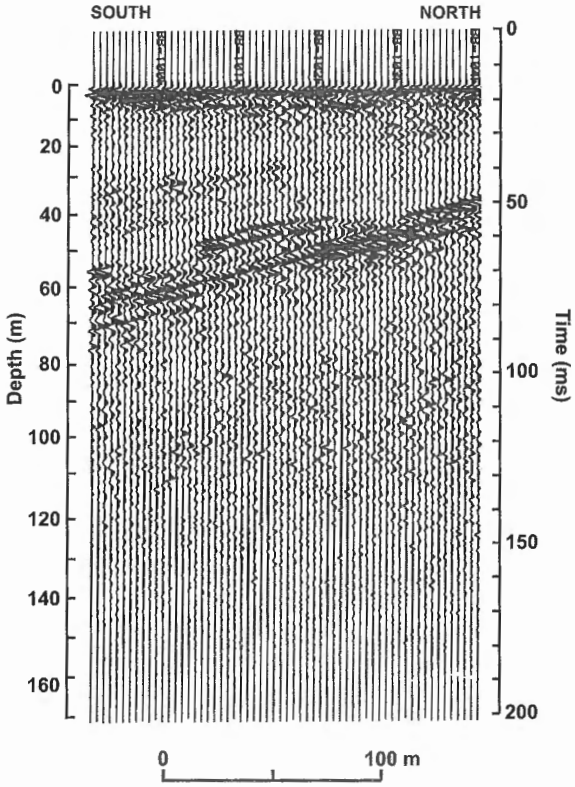

Figure 18. North-south optimum offset section showing a possible small slump within the foreset sequence. This type of feature is common on seismic sections from the southern Fraser delta.

Holocene-Pleistocene boundary

The depth and configuration of the Holocene-Pleistocene surface are important to understanding the growth and evolution of the delta, and to modelling the response of the ground to seismic shaking (Harris et al., 1995; Luternauer and Hunter, 1996). Unfortunately, limited penetration of energy, due to the presence of gas within the deltaic sediments, has meant that the seismic reflection profiles only provide information on this boundary in some areas. Recent drilling has shown that the Pleistocene surface ranges in depth from a few metres to more than 300 m (Clague et al., 1991; Dallimore et al., 1995), hence seismic surveys aimed at delineating this surface have to be designed to target this wide range of depths. Experimentation with both P- and S-wave CMP seismic reflection techniques over the last few years has largely been done with this objective in mind.

The southernmost part of the survey area, immediately north of Point Roberts, is one region where gas does not pose a problem, and information on the deeper stratigraphy has been obtained from the compressional-wave seismic reflection surveys. Point Roberts is an upland underlain by stratified Pleistocene sediments and capped by till. At one time, these older deposits formed an island in the Strait of Georgia. During the Holocene, the delta of the Fraser River prograded onto this upland. Seismic profiles show some of the structures that formed as the Point Roberts upland became connected to the Fraser delta.

The Holocene-Pleistocene boundary is evident on the optimum offset profile shown Figure 17. A 150 m thick sequence of dipping reflections, interpreted as foreset

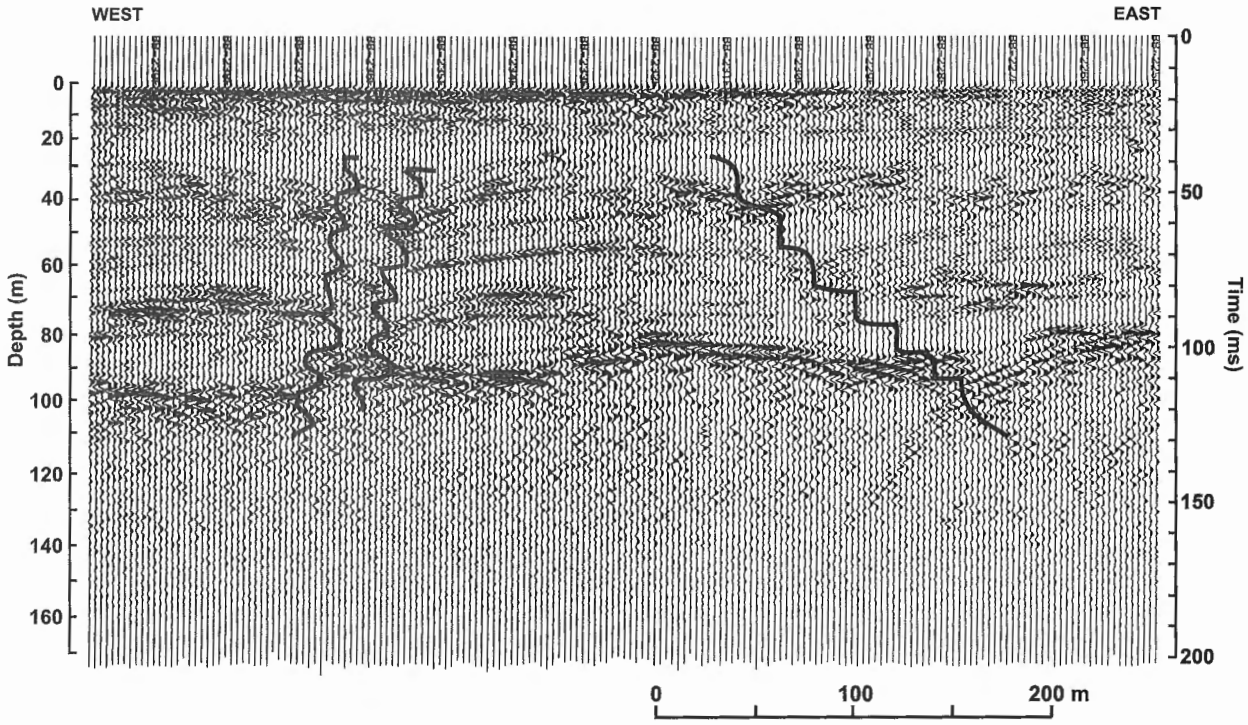

Figure 19. East-west optimum offset section showing several areas where foreset beds have been disrupted, possibly by faulting.

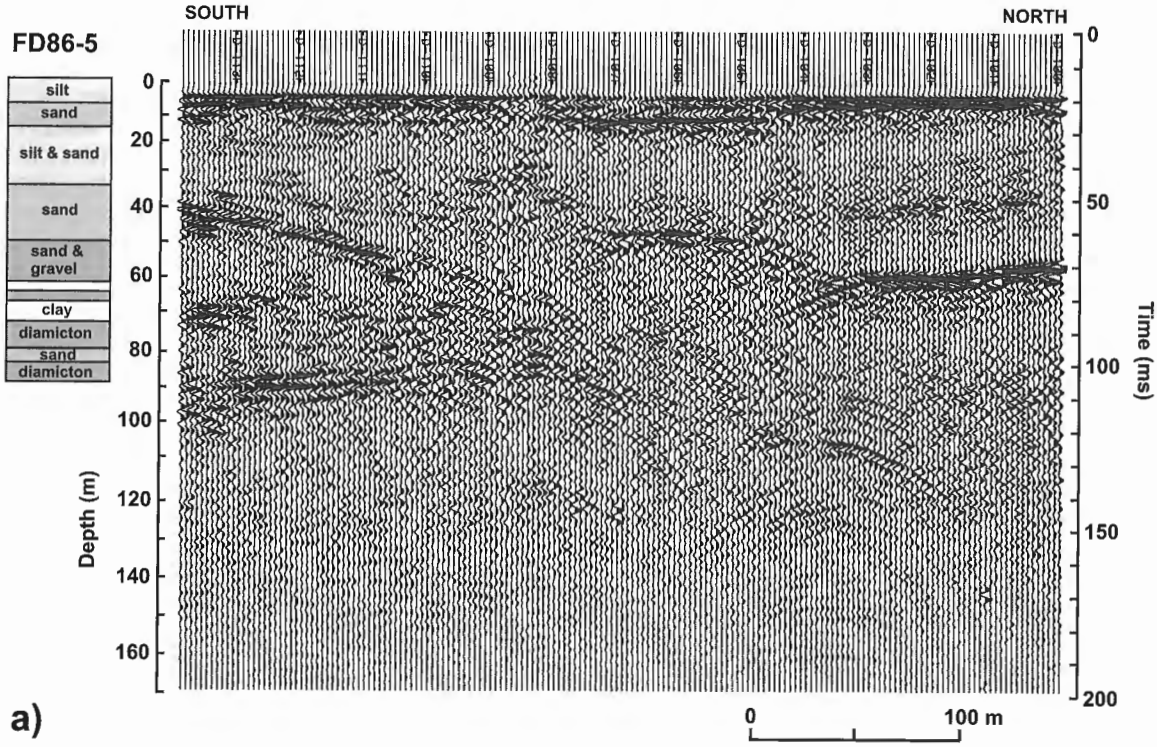

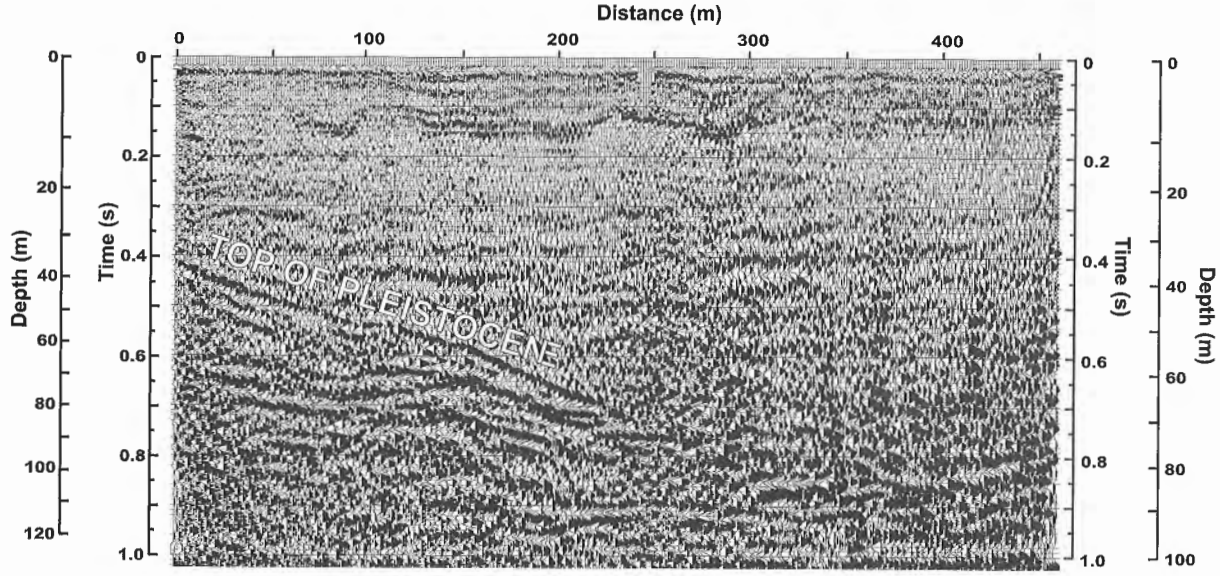

Figure 20. a) Optimum offset section northwest of Point Roberts. The reflector dipping to the north from the south end of the profile is interpreted to be the top of the Pleistocene sequence. The large-amplitude reflection at 60 m depth at the north end of the profile is attributed to gas. b) Shear-wave CMP section shot along the same line as a) and plotted at approximately the same aspect ratio for comparison. The dipping Pleistocene surface is a strong reflector at the south end of the profile and can be traced across the section in spite of the increase in noise towards the north.

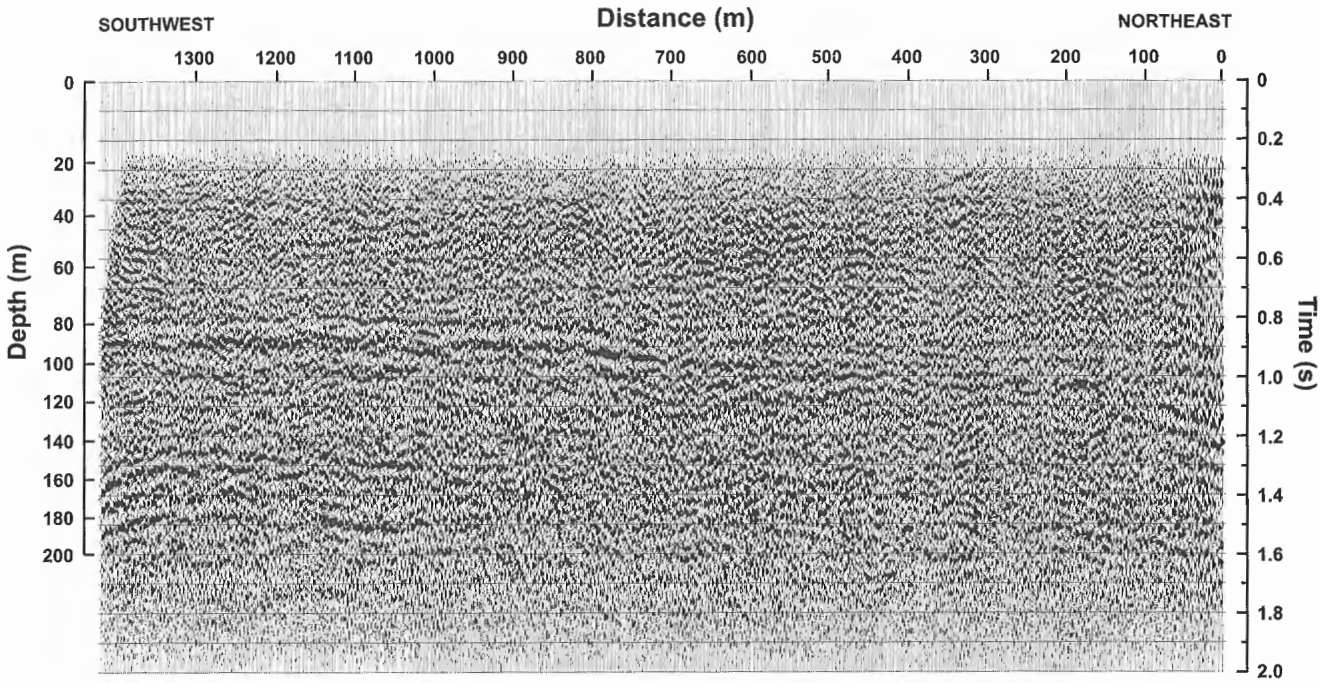

Figure 21. *Northeast-southwest shear-wave CMP section along the Coalport (Deltaport) Causeway at the western front of the Fraser delta. The reflection at 80 m depth is interpreted to be the top of the Pleistocene sequence. It dips gently to the northeast along this profile.*

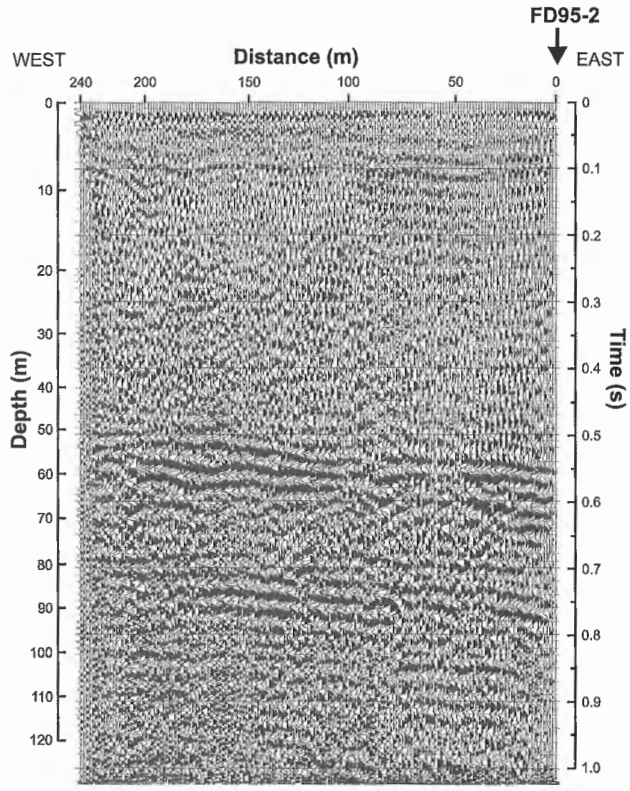

Figure 22.

East-west shear-wave CMP section along the dyke at the mouth of Canoe Passage, southwest of Ladner. The reflection at 50-60 m depth is interpreted to be the top of the Pleistocene sequence, in agreement with data from borehole FD95-2.

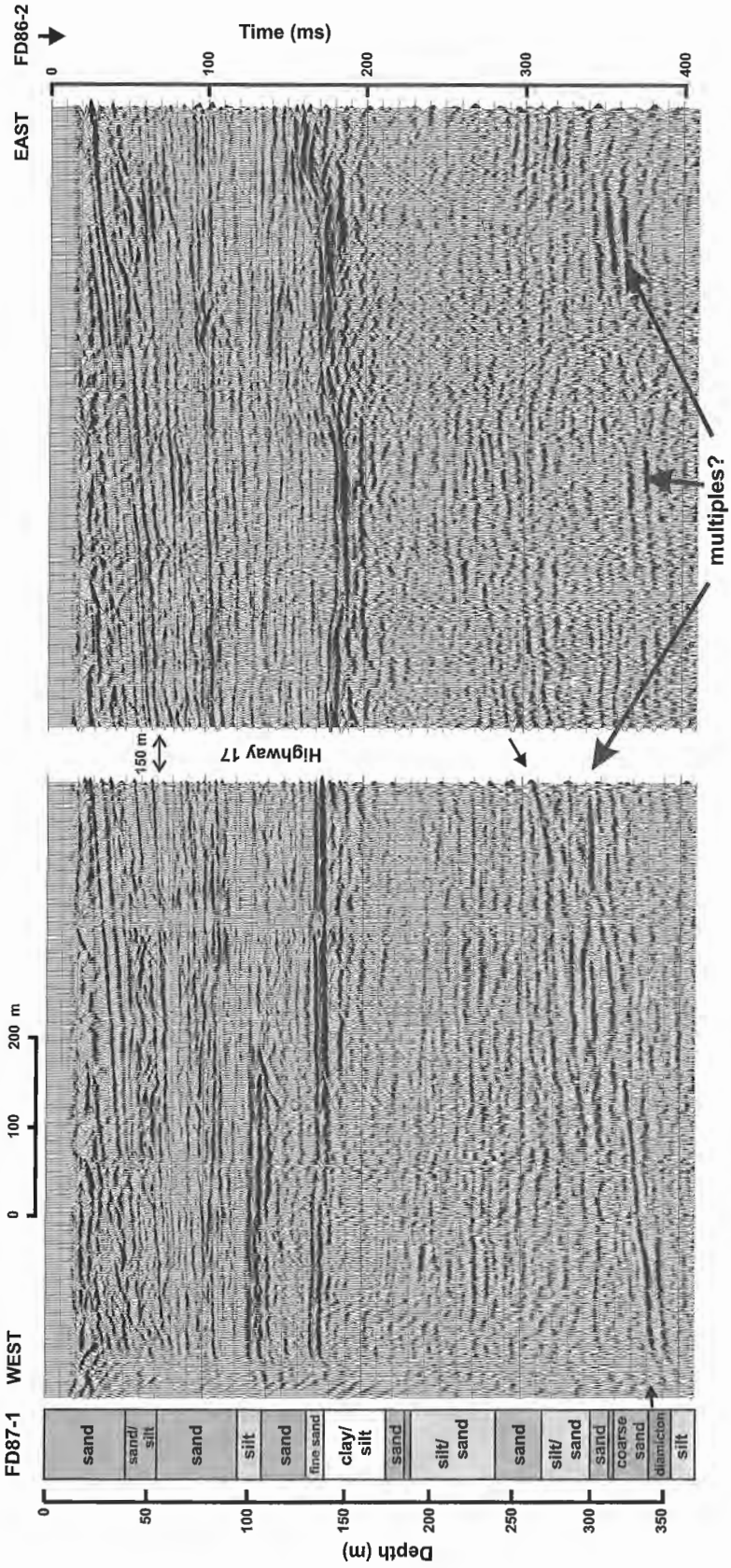

Figure 23. *Six-fold P-wave CMP section between boreholes FD86-2 and FD87-1, north of Tsawwassen. The large-amplitude reflection at approximately 140 m depth is attributed to gas (Fig. 13). The Holocene-Pleistocene boundary which is 185 m deep in FD87-1 is not apparent on the section. Some structure can be seen in the Pleistocene sequence; notably, a west-dipping reflection (arrowed) that can be correlated with the lowest diamicton in FD87-1. However, true structure at this depth is at least partially obscured by the presence of multiples (seismic energy that has been reflected more than once from an interface higher in the section).*

deposits, overlies an unconformity that rises to the south, reaching a depth of about 50 m at the south end of the profile. The deposits beneath the unconformity predate the Fraser delta and are Pleistocene in age. The shallowing of the unconformity towards Point Roberts suggests that these deposits are related to the sediments that underlie Point Roberts peninsula. The unconformity rises approximately 100 m along the 2.3 km length of the line, implying an average northerly dip of 2.5°.

The Pleistocene surface can also be clearly seen as a strong reflection dipping steeply to the north on an optimum offset seismic section northwest of Point Roberts (Fig. 20a). Unfortunately, the reflection can only be followed for about 200 m before the seismic energy is lost beneath high-amplitude reflections higher up in the section, which are attributed to gas. A CMP shear-wave reflection survey was conducted along the same line in 1995, and the results are shown in Figure 20b for comparison. The same northerly dipping surface can be traced across the entire profile, reaching a depth of 80 m at its north end. However, the signal-to-noise ratio of the data deteriorates as the surface deepens and the line approaches a busy road at the north end of the section. The seismic sections are interpreted to show that the Pleistocene surface drops approximately 45 m over a distance of 250 m, implying a dip of about 10°.

A simplified geological log for borehole FD86-5 is plotted in Figure 20a. The borehole is approximately 10 m from the road and ditch where the seismic data were collected. The seismic sections suggest that the Pleistocene surface lies at a depth of approximately 35 m at the nearest approach to the borehole. This corresponds with the top of a sandy horizon that overlies coarse-grained sediments at 50 m depth. Other geophysical logs (Hunter et al., 1998) from this borehole support the interpretation of the top of the sand as the Pleistocene surface.

Other shear-wave CMP surveys have successfully mapped the Pleistocene surface. For example, Figures 21 and 22 clearly show a reflection at depths that correspond to the Pleistocene surface in nearby boreholes, though the signal-to-noise ratio is poor. Little structural information on the Holocene sequence can be seen on these or other shear-wave sections acquired to date. The technique clearly shows promise for delineating the Pleistocene surface in areas where gas limits penetration of compressional-wave energy, but more work needs to be done in testing sources and surveying parameters in order to improve the quality of the shear-wave results.

Figure 23 shows a compressional-wave CMP section that was shot between two boreholes north of Tsawwassen. The Holocene-Pleistocene boundary was determined to be at a depth of 185 m in borehole FD87-1 at the west end of the section (Clague et al., 1991; Luternauer et al., 1991), but it has no obvious seismic signature. The boundary is marked by a thin (<2 m) diamicton, but otherwise there is no major lithological change; above it lie muds interpreted to be deposited in the ancestral Strait of Georgia, while below it is a thick (>100 m) sequence of interbedded mud and sand of glaciomarine origin (Luternauer et al., 1991). It appears that, with the loss of energy at the large-amplitude reflection at 170-180 ms (Fig. 13), there is an insufficient contrast in acoustic impedance at the Pleistocene surface to produce a visible coherent reflection.

Pleistocene sediments (unit 3)

Although the top of the Pleistocene sequence does not produce an identifiable reflection on the CMP section shown in Figure 23, there are weak reflections from within this sequence. These are most notable between 230 and 300 m depth, an interval in borehole FD87-1 marked by numerous sharp contacts and changes in grain size, and at approximately 350 m depth, where a west-dipping reflection can be correlated with the only major diamicton encountered in the borehole (Luternauer et al., 1991). This west-dipping reflection is interpreted to be an erosional unconformity within the Pleistocene sequence.

Another such unconformity can be seen in Figure 24; this figure shows a very shallow, high-amplitude reflection plunging sharply towards Point Roberts, directly north of the Tsawwassen upland. Drilling (FD86-1) has established that this reflector is the top of a compact Pleistocene diamicton, more than 75 m thick (Clague et al., 1991). The diamicton is older than the surface till that mantles Point Roberts peninsula (Vashon till, Armstrong, 1984) since, according to the seismic section, it is approximately 110 m below the surface at the north edge of the upland. An east-west line (Fig. 25), perpendicular to that of Figure 24, shows that the unconformity also dips to the west. The stratified sediments above the unconformity are relatively flat-lying on both these lines, and like the diamicton, they appear to extend beneath the exposed Pleistocene sediments of Point Roberts peninsula (Fig. 24). Thus, the seismic sections in this area define a remnant of Pleistocene stratified sediments which underlie Point Roberts and overlie glacial deposits that predate the last glaciation. All of these sediments may have been faulted, as indicated by the sagging and misalignment of reflections at the west side of Figure 25.

The Pleistocene sediments encountered in borehole FD86-1 cannot be confidently traced northward from the borehole because of a break in the seismic section necessitated by a major highway crossing and the presence of gas in near-surface sediments farther north. Figure 26 is the northward extension of Figure 24; the two figures are separated by a gap of 250 m. The south end of Figure 26 shows a reflection dipping north from 50 ms to about 70 ms. The reflection is interpreted to be the Pleistocene surface, here overlain by Holocene deltaic sediments (this interpretation is based on correlation of seismic profiles with a borehole 1.5 km to the north). The northward-dipping reflection may correlate with the southward-dipping unconformity on Figure 24, in which case it records sediments that are older than the last glaciation. Alternatively, it may delineate the Holocene-Pleistocene surface. This reflection disappears completely beneath a shallower large-amplitude reflection only 250 m farther north along the section. The shallower reflection is attributed to the presence of gas, though it is again presumed to be stratigraphically controlled (i.e. gas trapped beneath a fine-grained layer).

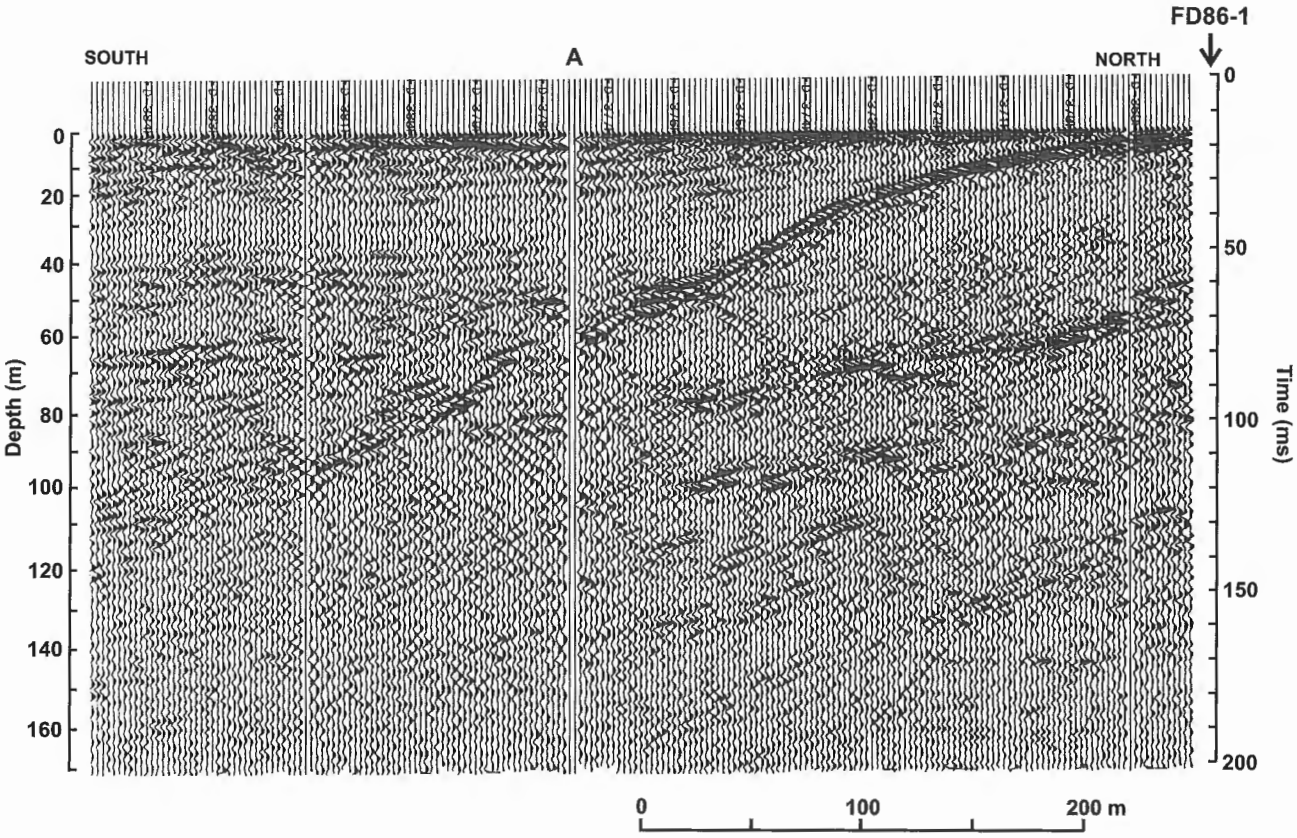

Figure 24. North-south optimum offset section abutting against the Point Roberts upland to the south. Till at a depth of less than 10 m in borehole FD86-1 appears to dive under the upland, and is therefore presumably older than the Pleistocene deposits exposed there. A marks the intersection of this line and the east-west profile shown in Figure 25.

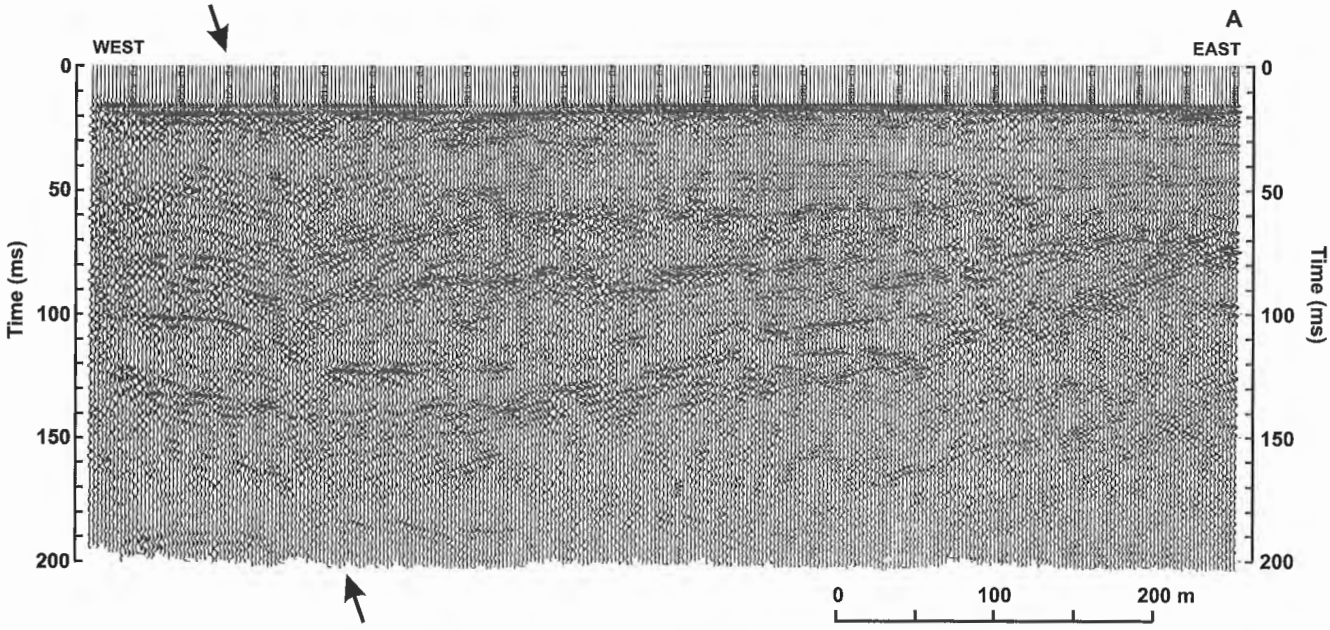

Figure 25. East-west optimum offset section perpendicular to the profile in Figure 24, showing the east-west extension of a 100 m deep basin filled with sediments interpreted to be Pleistocene in age. A possible near-vertical fault (arrowed) is indicated by the disruption of reflections in the middle of the sequence.

There is evidence of deeper structure at the south end of the section shown in Figure 26. Weak reflections between 150 and 200 ms originate from within the Pleistocene sequence. The depths of these horizons are greater than the 130 m implied by the depth scale on the figure, as seismic velocities in Pleistocene sediments are greater than the average Holocene velocity used to produce the depth scale (Appendix A and Fig. A1).

The 500 ms optimum offset profiles acquired northeast of Tsawwassen also show evidence of layering and unconformities within the Pleistocene sequence. Figure 27 is an east-west section that adjoins the section in Figure 17 midway between A and B. Correlation of the two sections indicates that the Pleistocene surface is the reflection at 150 ms. The Pleistocene sequence below this reflection is more than 250 m thick and consists of two units of relatively flat-lying layers separated at a depth of 250-270 m by a west-dipping unconformity. The coherent, flat-lying reflections and undisturbed layering of the upper unit (120-250 m depth) suggest that this is a dominantly glaciomarine sequence without thick till units, unlike the sequence at the north end of Figure 24 and the south end of Figure 26.

Tertiary bedrock (unit 4)

Conventional seismic reflection data collected as part of a hydrocarbon exploration program have been used to map the Tertiary bedrock surface beneath the Fraser River delta (Britton et al., 1995). The results show that the bedrock surface ranges from 390 to 1050 m in depth, and is characterized by northwest-trending ridges and troughs. The seismic data discussed in this paper were acquired with small, high-frequency sources, and do not generally have the signal strength required to reach this surface. The only exception is the 6-fold CMP P-wave survey conducted in 1990 with an 8-gauge shotgun source and 1 s record length (Table 1). These data were acquired northeast of Tsawwassen where no shallow gas attenuates the seismic signal. They show an unconformity dipping northward from approximately 400 to 600 m depth (see Fig. 2 of Hunter et al., 1998) which is interpreted to be the Tertiary surface. In this area, seismic data acquired with these recording parameters were able to image reflections up to 800 m deep.

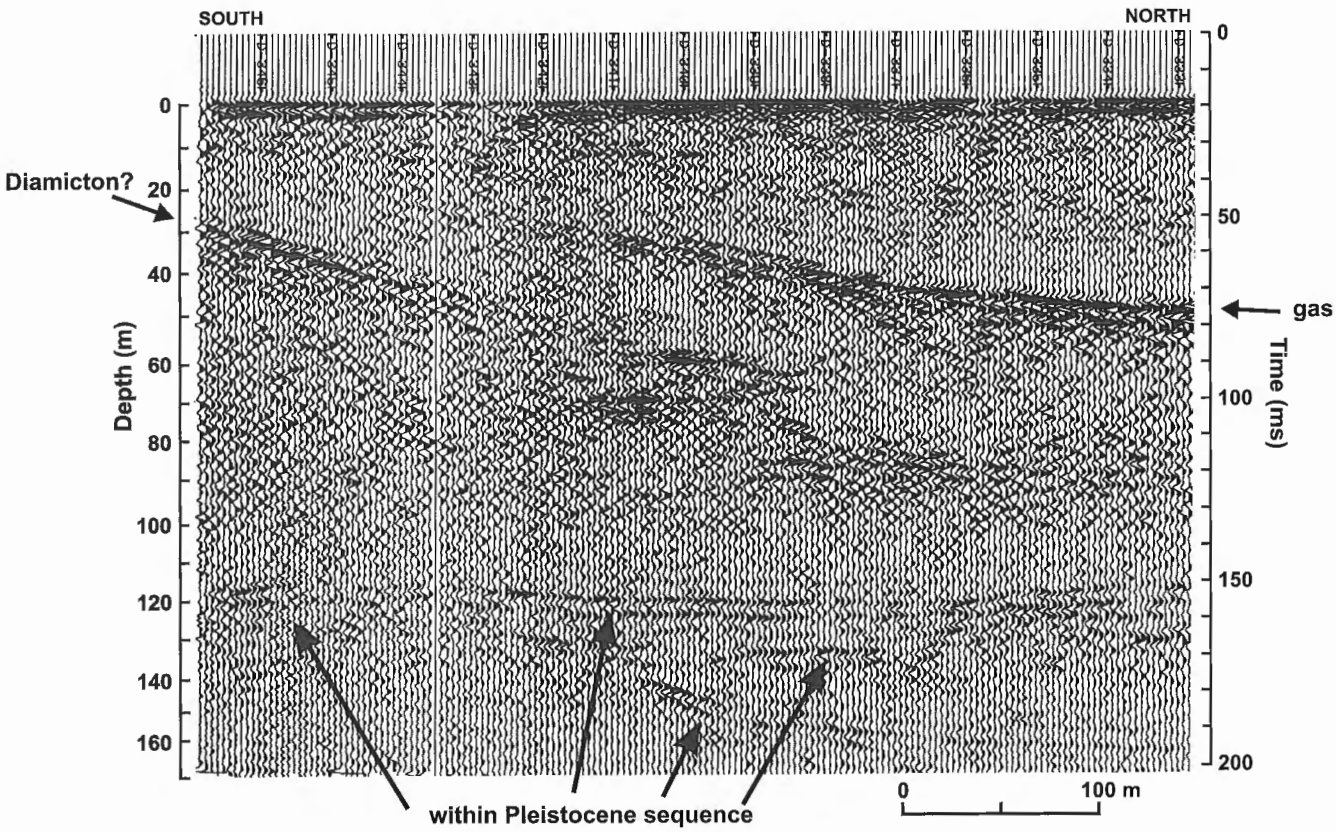

Figure 26. Northward extension of the optimum offset profile shown in Figure 24. The northward-dipping reflection at 40 m depth at the south end of the profile may be the top of the Pleistocene sequence. It can only be traced about 250 m before it disappears beneath a shallower large-amplitude reflection (gas). Weaker reflections at 150-200 ms (>130 m depth) are interpreted to be horizons within the Pleistocene sequence.

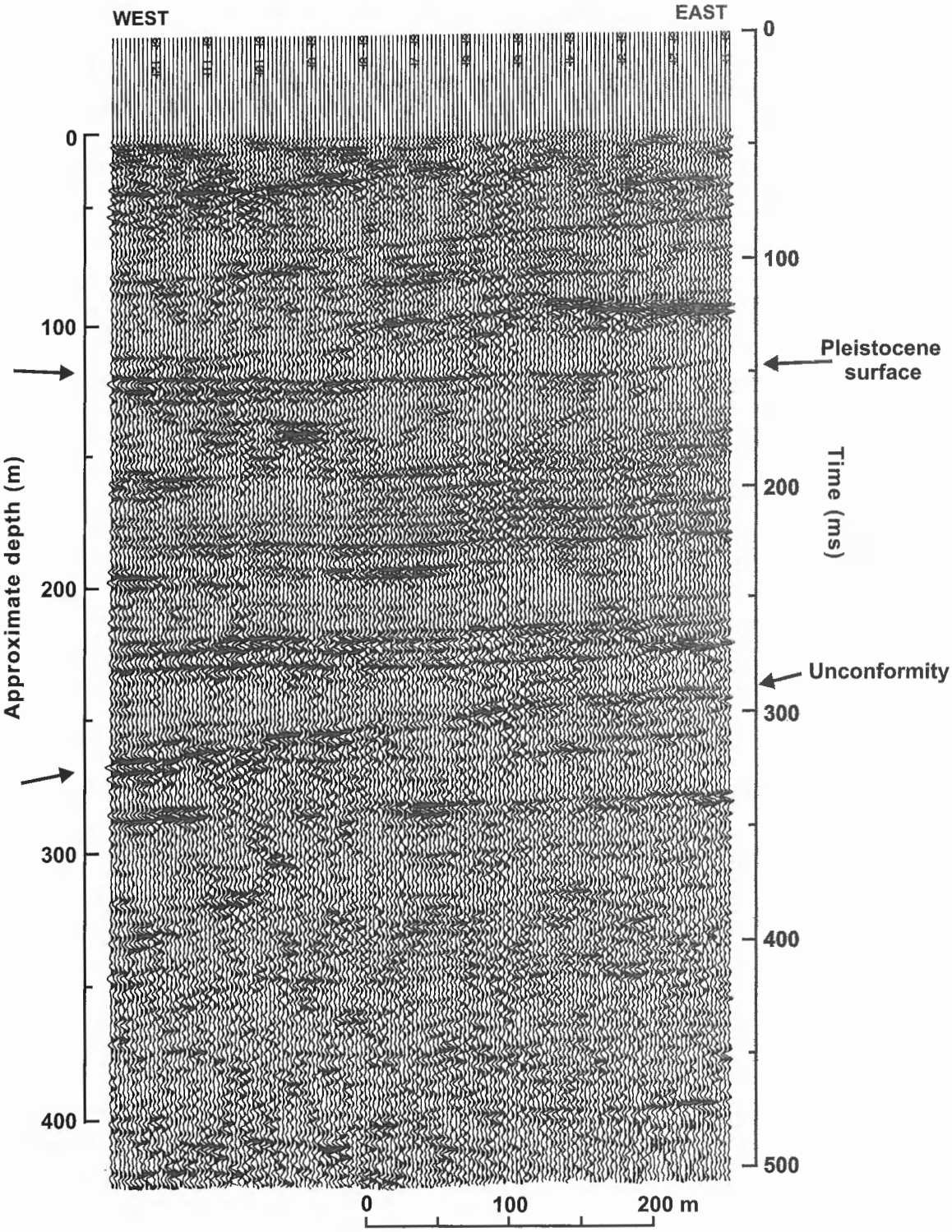

Figure 27. East-west optimum offset section recorded with a source-receiver separation of 66 m and a record length of 500 ms. The section shows thick (>250 m) Pleistocene deposits beneath 120 m of Holocene sediments. An unconformity is visible at approximately 240-270 m depth, but otherwise the Pleistocene sequence is characterized by coherent, flat-lying reflections and undisturbed layering. These deposits are interpreted to be mainly glaciomarine sediments.

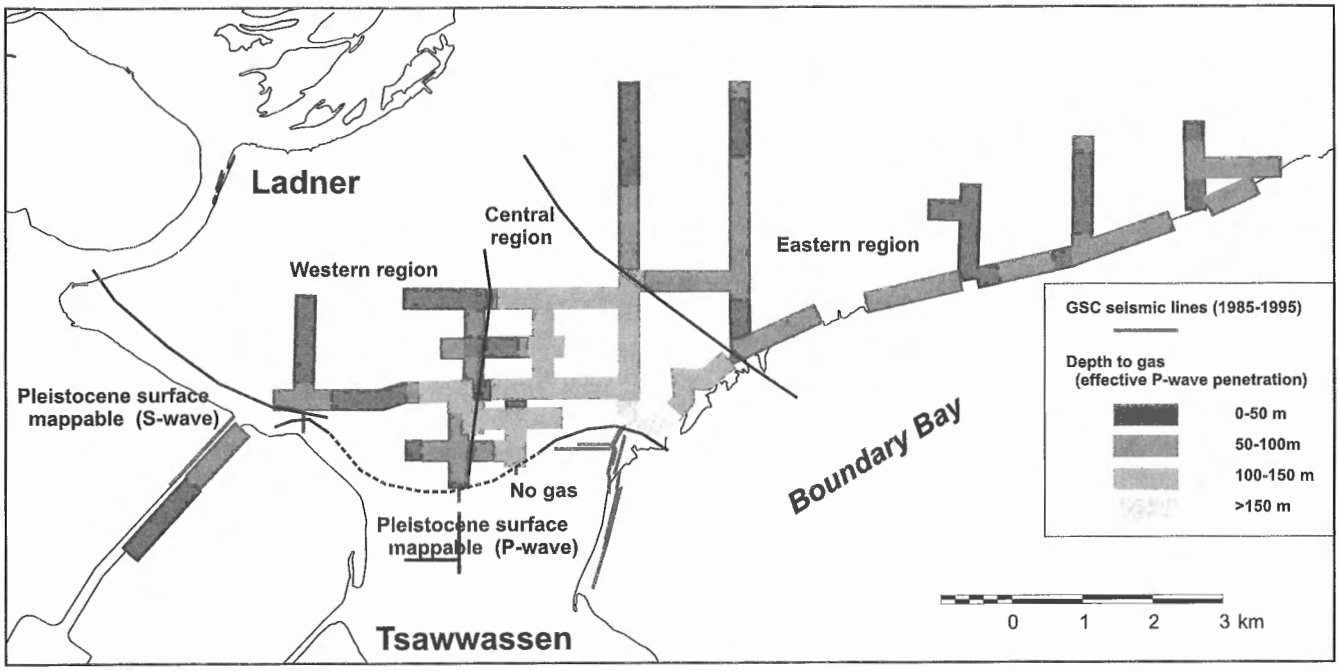

Figure 28. *Map of the southern Fraser River delta showing depths to gas (i.e. effective penetration of high-resolution P-wave energy) within the survey area. No gas has been observed directly north of the Tsawwassen upland, and the Pleistocene surface in this area can be readily mapped using P-waves.*

SUMMARY

This paper presents and summarizes representative examples of approximately 60 line-kilometres of shallow seismic reflection data that have been acquired on the Fraser River delta by the Geological Survey of Canada over the last decade. These ten years have also seen tremendous advances in engineering-seismograph and microcomputer technology, and the techniques used to acquire and process shallow seismic reflection data have improved accordingly. The data from the Fraser delta include a wide variety of optimum offset and CMP surveys using both compressional and shear waves, as attempts were made to evaluate the capabilities of these methods in this particular geological environment.

The fine-grained, water-saturated sediments of the delta surface provide a near-ideal medium for the application of high-resolution seismic reflection surveying. The geophones and shotgun source were planted in the bottom of water-filled drainage ditches. The dominant frequency of the reflection data is generally between 300 and 500 Hz, corresponding to wavelengths of 3-5 m, and a potential subsurface resolution on the metre scale. Logistical problems in locating survey lines in the urbanized areas of the northern delta (Richmond), and the poor data acquired on or near the peat bogs on the eastern delta led to a concentration of effort in the southern area. However, even there, the seismic sections are dominated by large-amplitude reflections that effectively mask all deeper structure. Drilling and downhole surveys have shown that these reflections are the result of gas trapped within the deltaic sediments. The presence of even a small amount of gas in sediments can have a profound effect on the quality of compressional-wave reflection data, causing an abrupt decrease in the seismic velocity and greatly increasing the attenuation of high-frequency signals. The result is that the depth of penetration of high-resolution compressional-wave surveys is effectively limited to the shallowest occurrence of gas. Figure 28 is a summary of the variation in depth to the top of gas observed on the seismic sections from the southern delta.

Nevertheless, the seismic sections do provide a wealth of data on the subsurface structure of the Holocene delta and underlying Pleistocene deposits in the area surveyed. Four main units are recognized in the seismic sections: unit 1 – Holocene topset sequence, unit 2 – Holocene foreset sequence, unit 3 – Pleistocene sediments, and unit 4 - Tertiary bedrock. All the sections provide some information on the Holocene units, but only in limited areas do the sections delineate the Holocene-Pleistocene boundary or image underlying units.

The shallowest unit observed on the optimum offset seismic reflection profiles is a sequence of flat-lying, low-to-moderate-amplitude reflections, interpreted to be deltaic topset deposits. This unit ranges in thickness from a few metres to more than 20 m. The source-receiver geometries used in the seismic surveys were not designed to look at these shallow depths, although a trial survey using smaller source-receiver and geophone separations demonstrated that it is possible to clearly resolve structure within this sequence and to delineate the contact between this unit and underlying foreset deposits. The topset deposits increase in thickness in an

easterly (and to a lesser extent, northerly) direction on the southern Fraser delta. The unit is about 20 m thick throughout the eastern region, whereas it is barely resolvable on seismic sections in the western region (Fig. 28) where the topset deposits are only a few metres thick (Williams and Roberts, 1989).

Beneath the topset deposits, most of the survey area is underlain by a thick unit of dipping reflections interpreted to be foreset beds. The beds dip south-southwest at average angles of 1.5-3°, although angles can reach 7-8°. Slump blocks are fairly common within this unit; observed features range in size from less than 100 to more than 300 m in length, and from 10 to more than 30 m in height. There are also a few isolated occurrences of disrupted reflections, suggesting the possibility that the foreset sequence is faulted.

Gas is trapped at various depths within the foreset unit over the entire survey area, with the exception of the area directly north of the Tsawwassen uplands (Fig. 28). It is not known whether this gas is generated locally by degeneration of organic matter, or at deeper stratigraphic levels from which it has migrated into the deltaic sediments. The gas is presumed to be trapped within the foreset sequence beneath finer grained layers; hence the large-amplitude reflections that result are still interpreted to have some stratigraphic significance.

While most of the seismic data are dominated by the large-amplitude reflections and strong signal attenuation that result from the presence of gas, profiles from different parts of the survey area differ substantially in how these characteristics are manifested. North-south profiles from the eastern region (Fig. 28) are characterized by high-amplitude, steeply dipping and laterally discontinuous reflections; east-west profiles along the Boundary Bay dyke are characterized by distinctive hyperbolic diffractions. In general, the depth of penetration of seismic energy in the eastern region decreases to the north and east. These sediments were probably deposited in a relatively deep basin in which there was frequent slumping from the rapidly advancing front of the ancestral Fraser delta. In contrast, many profiles from the western region (Fig. 28) are dominated by a single, continuous, high-amplitude reflection at shallow depth. It is clear that the amplitude of the reflection is related to the presence of gas, but its continuity and the fact that it is relatively flat lying suggest that this portion of the delta was not built out into a deep basin, but rather accumulated in relatively quiet shallow water, perhaps on an old platform of Pleistocene sediments.

The buried Holocene-Pleistocene surface is a critical element in modelling the response of the Fraser delta to earthquake shaking (Hunter et al., 1998). Unfortunately, because of limited energy penetration due to the presence of gas within the deltaic sediments, the seismic reflection data provide information on this boundary in only a few areas (Fig. 28). In the southernmost part of the survey area, the Pleistocene surface can be mapped with P-waves, and several seismic lines in that area show the surface dipping to the north to depths of 150 m or more. Farther north, the surface is obscured by high-amplitude reflections in the deltaic sequence.

An attempt has been made to better map this surface in the last few years by experimenting with both P- and S-wave CMP methods. However, P-wave CMP surveys have not been able to image the Pleistocene surface through shallow gas, at least not in areas where the surface is not marked by a major change in lithology. In contrast, shear-wave CMP surveys are better able to delineate the Pleistocene surface in areas where gas limits the penetration of compressional-wave energy, although they have not been able to resolve structure within the Holocene sequence. The signal-to-noise ratio of the shear-wave data collected to date is poor, and more work in testing shear-wave sources and surveying parameters is needed before the technique can be routinely applied to mapping the Pleistocene surface.

Very little of the shallow seismic reflection data discussed in this paper provides information on the structure of Pleistocene and Tertiary sediments underlying the Fraser delta, both because of the depths of these units and limits on penetration of seismic energy related to the presence of gas. However, some structure within the Pleistocene sequence has been observed on seismic profiles near the Tsawwassen upland. Unconformities of considerable relief occur within Pleistocene deposits in some areas. There are also thick units characterized by flat-lying reflections and undisturbed layering which are interpreted to be glaciomarine deposits. Only one seismic section imaged the Tertiary bedrock, which is at least 400 m below the surface; this surface is better mapped using conventional seismic reflection data collected for hydrocarbon exploration in the delta.

The application of seismic reflection methods on the Fraser River delta and the interpretation of the results have proved to be challenging. Some of the data from the delta are among the best high-resolution data collected anywhere by the Geological Survey of Canada, and allow a detailed examination of the subsurface structure to depths of up to several hundred metres. In other areas, penetration of seismic energy is severely limited by the presence of gas. Despite the limitations encountered in applying seismic methods on the Fraser delta, seismic reflection profiles provide a two-dimensional perspective on the subsurface that is essential in extending the detailed point source information provided by boreholes. For this reason, the data summarized here and the lessons learned in testing and applying these techniques constitute a unique and valuable contribution to the evolving understanding of the architecture and geological evolution of the Fraser River delta.

ACKNOWLEDGMENTS

Our initial testing of the shallow seismic reflection technique on the Fraser River delta in 1985 was carried out at the suggestion of J.L. Luternauer, and we appreciate his and J.J. Clague's support of this work over the ensuing decade. The data could not have been acquired without the assistance of numerous summer students who have slogged through the ditches and brambles, planting geophones and the shotgun source - notable among these have been R. Heard, B. Felix, M. Lockhard, M. Melenski, B. Ophoff, J. Udell, A. Caltagirone,

and K. Thorson. The Minipac Gas Detector used during the drilling of two boreholes by Simon Fraser University in 1991 was loaned to the Geological Survey of Canada by Continental Laboratories (1985) Ltd. of Calgary; the authors are very appreciative of this support of our research. We would also like to thank M.E. Best, J.J. Clague, and P.A Monahan, who provided thoughtful and constructive reviews which led to substantial improvements in the paper.

REFERENCES

Armstrong, J.E.
1984: Environmental and engineering application of the surficial geology of the Fraser Lowland, British Columbia; Geological Survey of Canada, Paper 83-23, 54 p.

Bates, C.R.
1996: Multi-component seismic acquisition in engineering and environmental investigations; in Proceedings, Symposium on the Application of Geophysics to Engineering and Environmental Problems, SAGEEP '95, Keystone, Colorado, p. 147-157.

Brandt, H.
1960: Factors affecting compressional wave velocity in unconsolidated marine sand sediments; Journal of the Acoustical Society of America, v. 32, p. 171-179.

Britton, J.R., Harris, J.B., Hunter, J.A., and Luternauer, J.L.
1995: The bedrock surface beneath the Fraser River delta in British Columbia based on seismic measurements; in Current Research 1995-E, Geological Survey of Canada, p. 83-89.

Christian, H.A., Mosher, D.C., Barrie, J.V., Hunter, J.A., and Luternauer, J.L.
1998: Seabed instability on the Fraser River delta; in Geology and Natural Hazards of the Fraser River Delta, British Columbia, (ed.) J.J. Clague, J.L. Luternauer, and D.C. Mosher; Geological Survey of Canada, Bulletin 525, this volume.

Clague, J., Harper, J.R., Hebda, R.J., and Howes, D.E.
1982: Late Quaternary sea levels and crustal movements, coastal British Columbia; Canadian Journal of Earth Sciences, v. 19, p. 597-618.

Clague, J.J., Luternauer, J.L., and Hebda, R.J.
1983: Sedimentary environments and postglacial history of the Fraser Delta and lower Fraser Valley, British Columbia; Canadian Journal of Earth Sciences, v. 20, p. 1314-1326.

Clague, J.J., Luternauer, J.L., Pullan, S.E., and Hunter, J.A.
1991: Postglacial deltaic sediments, southern Fraser River delta, British Columbia; Canadian Journal of Earth Sciences, v. 28, p. 1386-1393.

Clark, J.C., Johnson, W.J., and Miller, W.A.
1994: The application of high resolution shear wave seismic reflection surveying to hydrogeological and geotechnical investigations; in Proceedings, Symposium on the Application of Geophysics to Engineering and Environmental Problems, SAGEEP '94, Boston, Massachusetts, v. 1, p. 231-245.

Dallimore, S.R., Edwardson, K.A., Hunter, J.A., and Clague, J.J.
1995: Composite geotechnical logs for two deep boreholes in the Fraser River delta, British Columbia; Geological Survey of Canada, Open File 3018, 3 sheets.

Dobecki, T.L.
1993: High resolution in saturated sediments – a case for shear wave reflection; in Proceedings, Symposium on the Application of Geophysics to Engineering and Environmental Problems, SAGEEP '93, San Diego, California, v. 1, p. 319-333.

Doornenbal, J.C. and Helbig, K.
1983: High resolution seismics on a tidal flat in the Dutch Delta - acquisition, processing, and interpretation; First Break, v. 1, no. 4, p. 9-20.

Harris, J.B., Hunter, J.A., Luternauer, J.L., and Finn, W.D.L.
1995: Site response modelling of the Fraser River delta, British Columbia: preliminary results from two deep boreholes; in Current Research 1995-E; Geological Survey of Canada, p. 69-75.

Harris, J.B., Hunter, J.A., Pullan, S.E., Burns, R.A., and Good, R.L.
1996: Shallow shear wave seismic reflection profiling in the Fraser River delta, British Columbia; in Expanded Abstracts, Society of Exploration Geophysicists, 66th International Meeting, Denver, Colorado, p. 865-868.

Hasbrouck, W.P.
1987: Hammer-impact, shear-wave studies; in Shear-wave Exploration, (ed.) S.H. Danbom and S.N. Domenico; Society of Exploration Geophysicists, Geophysical Development Series, v. 1, p. 97-121.

Helbig, K.
1987: Shear waves - what they are and how they can be used; in Shear-wave Exploration, (ed.) S.H. Danbom and S.N. Domenico; Society of Exploration Geophysicists, Geophysical Development Series, v. 1, p. 19-36.

Hunter, J.A. and Burns, R.A.
1991: Determination of overburden P-wave velocities with a downhole 12-channel eel; in Current Research, Part C; Geological Survey of Canada, Paper 91-1C, p. 61-65.

Hunter, J.A., Douma, M., Burns, R.A, Good, R.L., Pullan, S.E., Harris, J.B., Luternauer, J.L, and Best, M.E.
1998: Testing and application of near-surface geophysical techniques for earthquake hazards studies, Fraser River delta, British Columbia; in Geology and Natural Hazards of the Fraser River Delta, British Columbia, (ed.) J.J. Clague, J.L. Luternauer, and D.C. Mosher; Geological Survey of Canada, Bulletin 525, this volume.

Hunter, J.A., Pullan, S.E., Burns, R.A., Gagné, R.M., and Good, R.L.
1984: Shallow seismic reflection mapping of the overburden-bedrock interface with the engineering seismograph - some simple techniques; Geophysics, v. 49, p. 1381-1385.
1989: Applications of a shallow seismic reflection method to groundwater and engineering studies; in Proceedings, Exploration '87; Third Decennial International Conference on Geophysical and Geochemical Exploration for Minerals and Groundwater, (ed.) G.D. Garland; Ontario Geological Survey, Special Volume 3, p. 704-715.

Hutchinson, I., Roberts, M.C., and Willliams, H.F.L.
1995: Stratigraphy, diatom biofacies, and palaeogeomorphology of a mid Holocene distributary channel system, Fraser River delta, British Columbia, Canada; Canadian Journal of Earth Sciences, v. 32, p. 749-757.

Johnson, W.J. and Clark, J.C.
1992: Improving subsurface resolution with the seismic reflection method: use S-waves; in Proceedings, 6th National Outdoor Action Conference, National Ground Water Association, Las Vegas, Nevada, p. 655-663.

Jol, H.M.
1988: Seismic stratigraphic analysis of the southeastern Fraser River delta, British Columbia; M.Sc. thesis, Simon Fraser University, Burnaby, British Columbia, 176 p.

Jol, H.M. and Roberts, M.C.
1988: The seismic facies of a delta onlapping an offshore island: Fraser River Delta, British Columbia; in Sequences, Stratigraphy, Sedimentology: Surface and Subsurface, (ed.) D.P. James and D.A. Leckie; Canadian Society of Petroleum Geologists, Memoir 15, p. 137-142.
1992: The seismic facies of a tidally influenced Holocene delta: Boundary Bay, Fraser River delta, B.C.; Sedimentary Geology, v. 77, p. 173-183.

Jongerius, P. and Helbig, K.
1988: Onshore high-resolution seismic profiling applied to sedimentology; Geophysics, v. 53, p. 1276-1283.

Knapp, R.W. and Steeples, D.W.
1986a: High-resolution common-depth-point seismic reflection profiling: instrumentation; Geophysics, v. 51, p. 276-282.
1986b: High-resolution common-depth-point seismic reflection profiling: field acquisition parameter design; Geophysics, v. 51, p. 283-294.

Luternauer, J.L.
1988: Geoarchitecture, evolution, and seismic risk assessment of the southern Fraser River delta, British Columbia; in Current Research, Part E; Geological Survey of Canada, Paper 88-1E, p. 105-109.
1990: 1989 field activities and accomplishments of geophysical and geotechnical land-based operations and marine/fluvial surveys, Fraser River delta, British Columbia; in Current Research, Part E; Geological Survey of Canada, Paper 90-1E, p. 235-237.
1991: 1990 field activities and accomplishments, Fraser River delta, British Columbia; in Current Research, Part A; Geological Survey of Canada, Paper 91-1A, p. 43-47.

Luternauer, J.L. and Hunter, J.A.
1996: Mapping Pleistocene deposits beneath the Fraser River delta: preliminary geological and geophysical results; in Current Research 1996-E, Geological Survey of Canada, p. 41-48.

Luternauer, J.L., Clague, J.J., and Feeney, T.D.
1991: A 367 m core from southwestern Fraser River delta, British Columbia; in Current Research, Part E; Geological Survey of Canada, Paper 91-1E, p. 127-134.

Luternauer, J.L., Clague, J.J., Hamilton, T.S., Hunter, J.A., Pullan, S.E., and Roberts, M.C.
1986: Structure and stratigraphy of the southwestern Fraser River delta: a trial shallow seismic profiling and coring survey; in Current Research, Part B; Geological Survey of Canada, Paper 86-1B, p. 707-714.

McKenna, G.T., Luternauer, J.L., and Kostaschuk, R.A.
1992: Large-scale mass wasting events on the Fraser River delta front near Sand Heads, British Columbia; Canadian Geotechnical Journal, v. 29, p. 151-156.

Miller, R.D., Anderson, N.L., Feldman, H.R., and Franseen, E.K.
1995: Vertical resolution of a seismic survey in stratigraphic sequences less than 100 m deep in southeastern Kansas; Geophysics, v. 60, p. 423-430.

Miller, R.D., Saenz, V., and Huggins, R.J.
1992: Feasibility of CDP seismic reflection to image structures in a 220-m deep, 3-m thick coal zone near Palau, Coahuila, Mexico; Geophysics, v. 57, p. 1373-1380.

Milne, W.G., Rogers, G.C., Riddihough, R.P., McMechan, G.A., and Hyndman, R.D.
1978: Seismicity of western Canada; Canadian Journal of Earth Sciences, v. 15, p. 1170-1193.

Monahan, P.A., Luternauer, J.L., and Barrie, J.V.
1993: A delta plain sheet sand in the Fraser River delta, British Columbia, Canada; Quaternary International, v. 20, p. 27-38.

Mustard, P.S. and Rouse, G.E.
1994: Stratigraphy and evolution of Tertiary Georgia Basin and subjacent Upper Cretaceous sedimentary rocks, southwestern British Columbia and northwestern Washington State; in Geology and Geological Hazards of the Vancouver Region, Southwestern British Columbia, (ed.) J.W.H. Monger; Geological Survey of Canada, Bulletin 481, p. 97-169.

Norminton, E.J.
1990: Seismic model studies of the overburden bedrock reflection: P-wave and S-wave; in Expanded Abstracts, Society of Exploration Geophysicists, 60th International Meeting, San Francisco, California, v. 1, p. 376-379.

Norminton, E.J. and Pullan, S.E.
1986: Reflection seismic software; Geological Survey of Canada, Open File 1277, two 5.25 inch diskettes to run on Apple DOS 3.3.

Pullan, S.E. and Hunter, J.A.
1987: Application of the "optimum offset" shallow reflection technique in the Fraser delta, British Columbia; in Expanded Abstracts, Society of Exploration Geophysicists, 57th International Meeting, New Orleans, Louisiana, p. 244-246.
1990: Delineation of buried bedrock valleys using the optimum offset shallow seismic reflection technique; in Geotechnical and Environmental Geophysics, v. III, Geotechnical, (ed.) S.H. Ward; Society of Exploration Geophysicists, Tulsa, Oklahoma, p. 75-87.

Pullan, S.E. and MacAulay, H.A.
1987: An in-hole shotgun source for engineering seismic surveys; Geophysics, v. 52, p. 985-996.

Pullan, S.E., Hunter, J.A., Burns, R.A., and Good, R.L.
1992: "Optimum offset" shallow seismic reflection profiles from the Okanagan Valley, British Columbia; Geological Survey of Canada, Open File 2545, 22 p.

Pullan, S.E., Hunter, J.A., Gagné, R.M., and Good, R.L.
1987: Delineation of bedrock topography at Val Gagné, Ontario, using seismic reflection techniques; in Current Research, Part A; Geological Survey of Canada, Paper 87-1A, p. 905-912.

Pullan, S.E., Hunter, J.A., and Neave, K.G.
1991a: Shallow shear wave reflection tests; in Current Research, Part D; Geological Survey of Canada, Paper 91-1D, p. 67-70.

Pullan, S.E., Jol, H.M., Gagné, R.M., and Hunter, J.A.
1989: Compilation of high resolution "optimum offset" shallow seismic reflection profiles from the southern Fraser River delta, British Columbia; Geological Survey of Canada, Open File 1992, 16 p.

Pullan, S.E., Miller, R.D., Hunter, J.A., and Steeples, D.W.
1991b: Shallow seismic reflection surveys - CDP or "optimum offset"?; in Expanded Abstracts, Society of Exploration Geophysicists, 61st International Meeting, Houston, Texas, v. 1, p. 576-579.

Roberts, M.C., Pullan, S.E., and Hunter, J.A.
1992: Applications of land-based high resolution seismic reflection analysis to Quaternary and geomorphic research; Quaternary Science Reviews, v. 11, p. 557-568.

Sharpe, D.R., Pullan, S.E., and Warman, T.A.
1992: A basin analysis of the Wabigoon area of Lake Agassiz, a Quaternary clay basin in northwestern Ontario; Géographie physique et Quaternaire, v. 46, p. 295-309.

Slaine, D.D., Pehme, P.E., Hunter, J.A., Pullan, S.E., and Greenhouse, J.P.
1990: Mapping overburden stratigraphy at a proposed hazardous waste facility using shallow seismic reflection methods; in Geotechnical and Environmental Geophysics, v. II, Environmental and Groundwater, (ed.) S.H. Ward; Society of Exploration Geophysicists, Tulsa, Oklahoma, p. 273-280.

Steeples, D.W. and Miller, R.D.
1990: Seismic reflection methods applied to engineering, environmental, and groundwater problems; in Geotechnical and Environmental Geophysics, v. I, Tutorial, (ed.) S.H. Ward; Society of Exploration Geophysicists, Tulsa, Oklahoma, p. 1-30.

Telford, W.M., Geldart, L.P., Sheriff, R.E., and Keys, D.A.
1976: Applied Geophysics; Cambridge University Press, Cambridge, England, 860 p.

Whiteley, R.J., Hunter, J.A., and Pullan, S.E.
1986: High-resolution common-offset seismic reflection profiling in the Chaophraya Basin, Bangkok, Thailand; in Expanded Abstracts, Society of Exploration Geophysicists, 56th International Meeting, Houston, Texas, v. 1, p. 104-106.

Williams, H.F.L. and Roberts, M.C.
1989: Holocene sea-level change and delta growth: Fraser River delta, British Columbia; Canadian Journal of Earth Sciences, v. 26, p.1657-1666.
1990: Two middle Holocene marker beds in vertically accreted floodplain deposits, lower Fraser River, British Columbia; Géographie physique et Quaternaire, v. 44, p. 27-32.

Zhang, S.
1990: Shallow SH-wave seismic exploration for subway construction in Shanghai; in Geotechnical and Environmental Geophysics, v. III, Geotechnical, (ed.) S.H. Ward; Society of Exploration Geophysicists, Tulsa, Oklahoma, p. 175-179.

APPENDIX A

Velocity analyses - uphole seismic surveys

Determination of average velocity as a function of depth

An accurate estimate of the compressional-wave velocity structure as a function of depth is required to convert two-way traveltime to depth on the optimum offset seismic sections. The most common method of obtaining the subsurface velocity structure involves recording 'expanded' or 'walk-away' geophone spreads composed of several sets of multichannel data. These data can be processed using velocity analysis routines to obtain estimates of the average velocities down to reflecting horizons (T^2-X^2 analyses; see, for example, Telford et al., 1976). To be used in its simplest form, this technique requires that target reflectors be flat lying. Few reflecting horizons in the project area meet this requirement.

A more accurate method of obtaining velocity information is shooting uphole surveys in a borehole. The velocity function that was used to convert the two-way traveltimes of the optimum offset seismic reflection profiles shown in this paper was calculated from the results of uphole surveys in six boreholes drilled by the Geological Survey of Canada in the project area in 1986 (Clague et al., 1991). These holes were cased with plastic liner (PVC pipe) on completion of drilling and were logged at a later date. This allowed the borehole to collapse around the plastic casing, improving the coupling between the surrounding sediments and the detector in the borehole.

In each hole, a single hydrophone was lowered in 1 m increments from the surface. At each depth, a shot was fired at the surface using the 12-gauge Buffalo gun. The data were recorded on a Nimbus 1210F seismograph using the highest time resolution (50 ms scale) with no filtering. The source was located at a set offset (6-12 m) from the hole, generally at the bottom of the nearest ditch for optimum coupling. Offsets of less than 6 m were not used to prevent generation of a significant casing wave.

The first arrival was picked for each hydrophone and logged using computer-assisted techniques. After geometrical compensation for offset, the average velocity from the surface to each depth was computed.

A compilation of average velocity vs. depth for all six 1986 boreholes is shown in Figure A1. Five of the six holes were drilled in dominantly deltaic sediments (FD86-2, 3, 4, 5, and 6). FD86-1 encountered till at shallow depth. Near-surface average velocities vary considerably from hole to hole, reflecting the effect of different thicknesses of low-velocity material above the water table. Below 30 m, most holes have similar velocity structures, with velocity gradually increasing to 1700 m/s at about 100 m depth. FD86-1 is markedly different, with higher average velocities, reaching 2000 m/s at depth. The data from FD86-1 were excluded from further analysis because the sediments encountered in that hole are not typical of the shallow sediments beneath most of the delta. The velocity data from the remaining five boreholes were averaged to obtain a mean curve from which the depth-traveltime conversion was made for the particular shot-geophone offset of each shallow reflection profile. The computed depth scale is shown on each optimum offset profile discussed in this paper; note that nonlinear effects can be observed in the shallow portions of the records as a result of the non-zero source-receiver offset. Below 116 m depth, where no uphole data are available, the depth scale was calculated assuming a velocity of 1700 m/s.

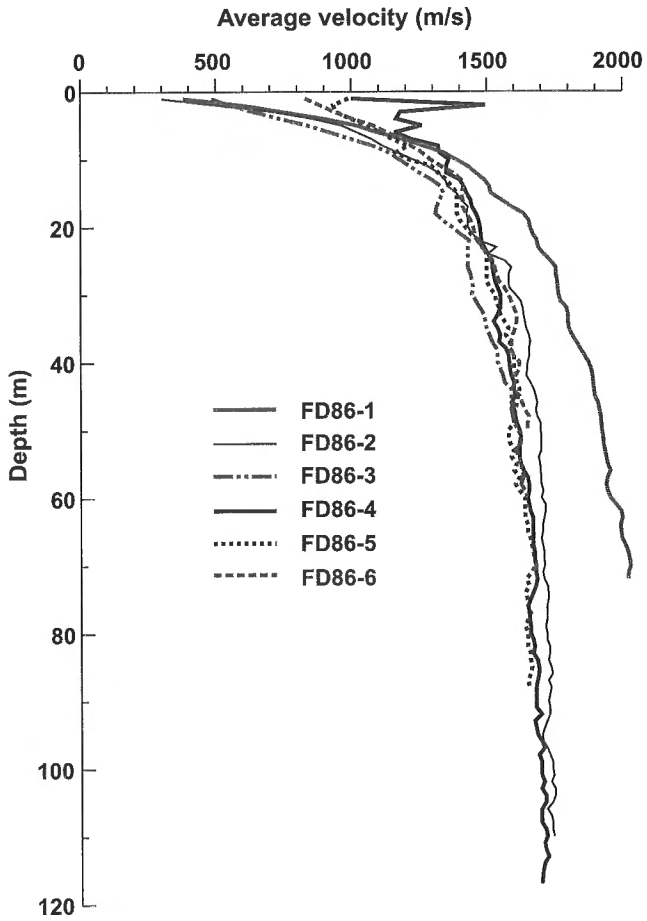

Figure A1. *Average velocity as a function of depth in six 1986 Geological Survey of Canada boreholes. The velocity profiles were calculated from data acquired with a single hydrophone in the hole and a near-surface source. The average results, which excludes data from FD86-1, were used to calculate the depth scale for the optimum offset seismic reflection profiles presented in this paper.*

Traveltime-depth conversion errors above 15 m depth could be large due to variations in near-surface velocities between boreholes. These errors decrease with depth as the average velocity is more confidently defined. At 30 m depth, the envelope of velocity variations from all data sets produces a potential depth error of 2 m; at 60 m it is 1.75 m; and at 90 m it is approximately 1.5 m. Hence for most depths, the possible error in depth is smaller than the uncertainty in picking the onset of the reflection arrival time on the seismic section.

Calculation of interval velocities as a function of depth

The above-described technique of using a single hydrophone in a hole is adequate for determining average velocities as a function of depth, but cannot be used to obtain accurate interval velocities down the hole. This is due to small uncertainties in the zero time of the records which become very significant when measuring the difference in time for energy to reach downhole positions separated by only a metre or so. In an attempt to improve the determination of downhole interval velocities, the Geological Survey of Canada designed and constructed 12- and 24-channel downhole eels with 0.5 m spacing between hydrophones (Hunter and Burns, 1991). The multichannel capacity removes the concern about the absolute accuracy of zero time and allows an interval velocity to be determined over the length of the array. However, in water-saturated sediments, the moveout of the first arrival times across 12 channels (5.5 m) is of the order of 3-5 ms, and an accurate determination of the interval velocity is limited by the error in picking these arrivals. By lowering the hydrophone array in small increments (0.5 - 1 m), it is possible to obtain a redundancy of data which may be used to reduce the significance of picking errors. Experience with this technique has shown that it can yield P-wave interval velocities accurate to within a few percent (Hunter and Burns, 1991). This technique was used to determine interval velocities in borehole SFU91-2 (Fig. 14).

Testing and application of near-surface geophysical techniques for earthquake hazards studies, Fraser River delta, British Columbia

J.A. Hunter[1], M. Douma[1], R.A. Burns[1], R.L. Good[1], S.E. Pullan[1], J.B. Harris[2], J.L. Luternauer[3], and M.E. Best[4]

Hunter, J.A., Douma, M., Burns, R.A., Good, R.L., Pullan, S.E., Harris, J.B., Luternauer, J.L., and Best, M.E., 1998: Testing and application of near-surface geophysical techniques for earthquake hazards studies, Fraser River delta, British Columbia; in Geology and Natural Hazards of the Fraser River Delta, British Columbia, (ed.) J.J. Clague, J.L. Luternauer, and D.C. Mosher; Geological Survey of Canada, Bulletin 525, p. 123–145.

Abstract: Geophysical techniques have been tested and applied on the Fraser River delta to determine the structure and geotechnical parameters of Quaternary sediments as a contribution towards earthquake hazards studies. Information has been obtained on the buried bedrock surface, Pleistocene glacial deposits, and overlying Holocene deltaic sediments using surface and borehole geophysical techniques. Considerable progress has been made in developing and testing methods for determining the shear-wave velocity structure of Fraser delta sediments. Knowledge of the shear-wave velocity structure of the delta is important for earthquake ground-motion amplification studies as well as cyclic liquefaction investigations.

Résumé : Le delta du Fraser a été le centre de l'essai et de l'application de techniques géophysiques dans le but de déterminer le style structural et les paramètres géotechniques des sédiments quaternaires de cette région, et ainsi contribuer à l'étude des risques sismiques. Des données sur la surface du substratum enfoui, les sédiments glaciaires du Pléistocène et les sédiments deltaïques sus-jacents de l'Holocène ont donc été recueillies en utilisant des techniques géophysiques en surface et dans les sondages. Des progrès considérables ont été accomplis dans l'élaboration et l'essai de méthodes pour déterminer le style structural selon les vitesses des ondes de cisaillement dans les sédiments deltaïques du fleuve Fraser. Il est important de connaître cette information que nous révèlent les ondes de cisaillement pour étudier l'amplification des ébranlements du sol causés par les séismes ainsi les phénomènes cycliques de liquéfaction.

[1] Geological Survey of Canada, 601 Booth Street, Ottawa, Ontario K1A 0E8
[2] Department of Geology, Millsaps College, 1701 N. State Street, Jackson, Mississippi 39210
[3] Geological Survey of Canada, 605 Robson Street, Vancouver, British Columbia V6B 5J3
[4] Geological Survey of Canada, Pacific Geoscience Centre, P.O. Box 6000, Sidney, British Columbia V8L 4B2

INTRODUCTION

The Fraser River delta lies in one of the highest earthquake hazard regions in Canada (Milne et al., 1978) and is currently an area of rapid urban growth. The delta plain is underlain by thick soft soils that may require increased factors of safety for earthquake loading under current National Building code guidelines (National Research Council of Canada, 1995, p. 149, Table 4.1.9.1.C). Both amplification of ground motion and liquefaction of cohesionless water-saturated soils could occur on the delta during an earthquake. Geological parameters that may have a bearing on the severity of these effects include the thickness, geotechnical properties, and subsurface structure of the unconsolidated sediments.

Recent destructive earthquakes in Mexico City (1985), San Francisco (1989), and Los Angeles (1995) have shown that the stratigraphy and structure of the unconsolidated materials in sedimentary basins can have a profound effect on the areal intensity of seismic shaking, with resulting variability in the severity of damage to buildings, transportation corridors, and other infrastructure. In such sedimentary basins, large shear-wave velocity contrasts can occur at the sediment-bedrock interface or within the unconsolidated deposits. Computer-based modelling has shown that these boundaries produce complex earthquake wave motions that can constructively interfere, or resonate, to intensify ground motion. Intensities can be further altered by focusing or defocusing of the earthquake energy at the ground surface if the critical subsurface boundaries are concave or convex (Rial et al., 1992). As well, basin edges may generate surface waves. Resonance may occur away from the basin edges, where the surface waves interact with upward-travelling energy. Several studies of the effects of basin shape and structure on ground motion amplification have recently been published (Bard and Bouchon, 1985; Rial, 1989; Seligman et al., 1989; Alvarez, 1990; Lomnitz, 1990; Schuster et al., 1990; Frankel and Vidale, 1992; Bard and Chavez-Garcia, 1993; Frankel, 1993; Graves, 1993; Chang et al., 1994). The authors of these reports have stressed the need to know the geological structure of basins and geophysical parameters such as shear-wave velocity structure and anelastic attenuation to accurately predict the complex pattern of surface ground motion that would result from a large earthquake.

Evidence for ground-motion amplification of earthquake shaking in the Fraser delta has been obtained from seismograph recordings of moderate (magnitude (M) = 5.1, 5.3) earthquakes with epicentral distances up to 140 km (Rogers et al., 1998). Observed amplification of horizontal motion is of the order of three to five at Fraser delta sites, compared to bedrock sites. This amplification appears to be related to the occurrence of thick sediments beneath the delta and possible resonance amplification associated with thin sediments at the delta edge.

Near-surface, noncohesive, water-saturated sediments on the Fraser delta may liquefy (loss of resistance of the soil to shear) during an earthquake, possibly causing damage to man-made structures (Byrne and Anderson, 1987). Guidelines on the liquefaction potential of soils for earthquakes of different magnitudes have been developed over the last 20 years; the guidelines are based on geotechnical techniques, notably the Standard Penetration Test (SPT) and the Cone Penetration Test (CPT) (Seed and Idriss, 1982; Seed and de Alba, 1986; Seed et al., 1985; Finn, 1996; Robertson and Fear, 1996). The shear-wave velocity structure of soils has also been examined as a measure of the potential for liquefaction during earthquakes (Stokoe et al., 1988b; Robertson, 1990; Stokoe, 1990; Kayen et al., 1992; Robertson et al., 1992; Andrus and Stokoe, 1996). Considerable effort has been made over the last few years to modify existing geotechnical tests (e.g. Seismic Cone Penetrometer Test, SCPT), and to develop surface and borehole geophysical methods (e.g. downhole and cross-hole shear-velocity techniques, Spectral Analysis of Surface Waves (SASW), and surface shear-wave refraction methods) to obtain better estimates of shear-wave velocities in the near-surface region (Hunter and Woeller, 1990; Robertson and Addo, 1991; Hunter et al., 1992; Hunter, 1995).

The Geological Survey of Canada has selected the Fraser delta as a test area for developing and applying high-resolution near-surface geophysical techniques. The overall aims of this research are to obtain regional subsurface geophysical data in this particular geological setting for use in geotechnical assessment of earthquake hazards, and to develop technologies that can be applied to other earthquake-prone areas of Canada.

The study area is approximately 24 km by 26 km and includes the subaerial plain of the Fraser delta and parts of adjacent Pleistocene uplands (Fig. 1). This area encompasses portions of the cities of Vancouver, Burnaby, and Richmond, and the municipality of Delta.

For the purposes of this paper, the deposits beneath the Fraser delta can be subdivided into three primary units: 1) Tertiary sedimentary rocks, primarily sandstone and shale; 2) unconsolidated sediments of Pleistocene age, mainly of glacial origin; and 3) deltaic sands and silts of Holocene age, unconformably overlying the Pleistocene materials. The specific objectives of the geophysical surveys were the following: 1) delineate the bedrock surface; 2) determine the lithology and three-dimensional structure of Holocene and Pleistocene sediments; 3) characterize the shear-wave velocity structure of near-surface sediments; and 4) delineate shear-wave seismic-impedance boundaries within the unconsolidated sediments and at the sediment-bedrock interface.

SEISMIC REFLECTION METHODS

Conventional compressional (P-) wave reflection surveys

Conventional seismic reflection surveying techniques are routinely used by the oil and gas industry to delineate structure within sedimentary rocks to depths of 5 km or more below surface. These relatively costly surveys require large, surface, seismic sources capable of producing compressional-wave impulses in the 10-100 Hz range. The signals are transmitted downwards and reflected back to surface

from compressional-wave velocity discontinuities associated with changes in lithology. The returning seismic waves are registered by arrays of geophones at the surface, and the digital records are computer processed to produce two-dimensional seismic sections that display the subsurface structure within the rock. Such data have been obtained on parts of the Fraser delta by Dynamic Oil Company of Vancouver and have been made available to the Geological Survey of Canada to help provide the regional geological framework required to assess earthquake-related hazards. Compressional-wave velocity analyses reveal large velocity contrasts at the boundary between the Quaternary deposits and bedrock; there is commonly a strong reflection from this interface in the seismic records (Britton et al., 1995).

Over 125 line-kilometres of 48-fold CDP (common depth point), 96-trace vibroseis data have been analyzed to delineate the bedrock surface beneath the Fraser delta. Depth estimates were made at approximately 200 m intervals along each line from the processed record sections. As a form of quality control, these estimates were compared with independent interpretations of the bedrock surface, obtained from detailed

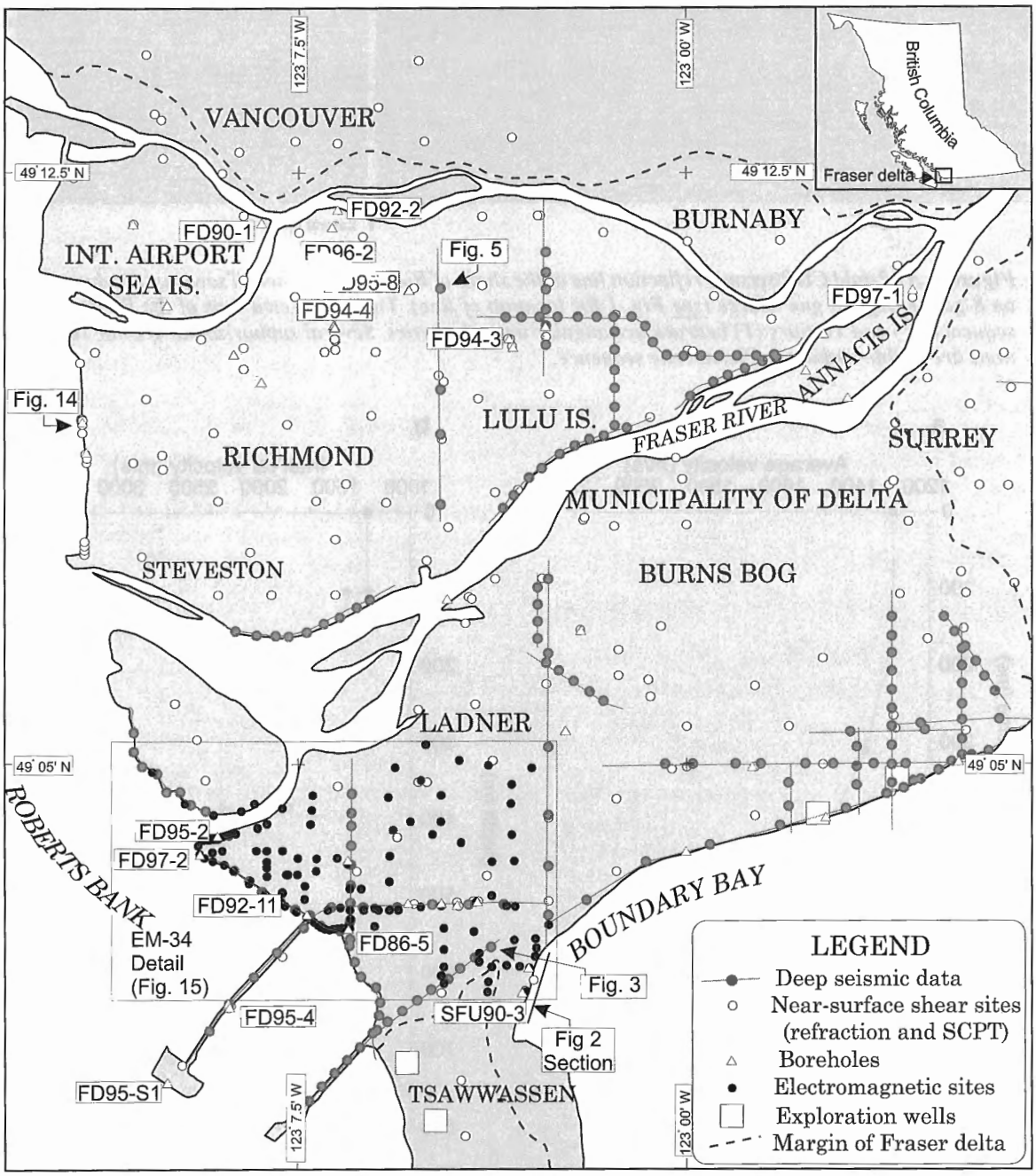

Figure 1. *Map of the Fraser delta survey area showing locations of geophysical survey sites. Sites cited in the text are labelled.*

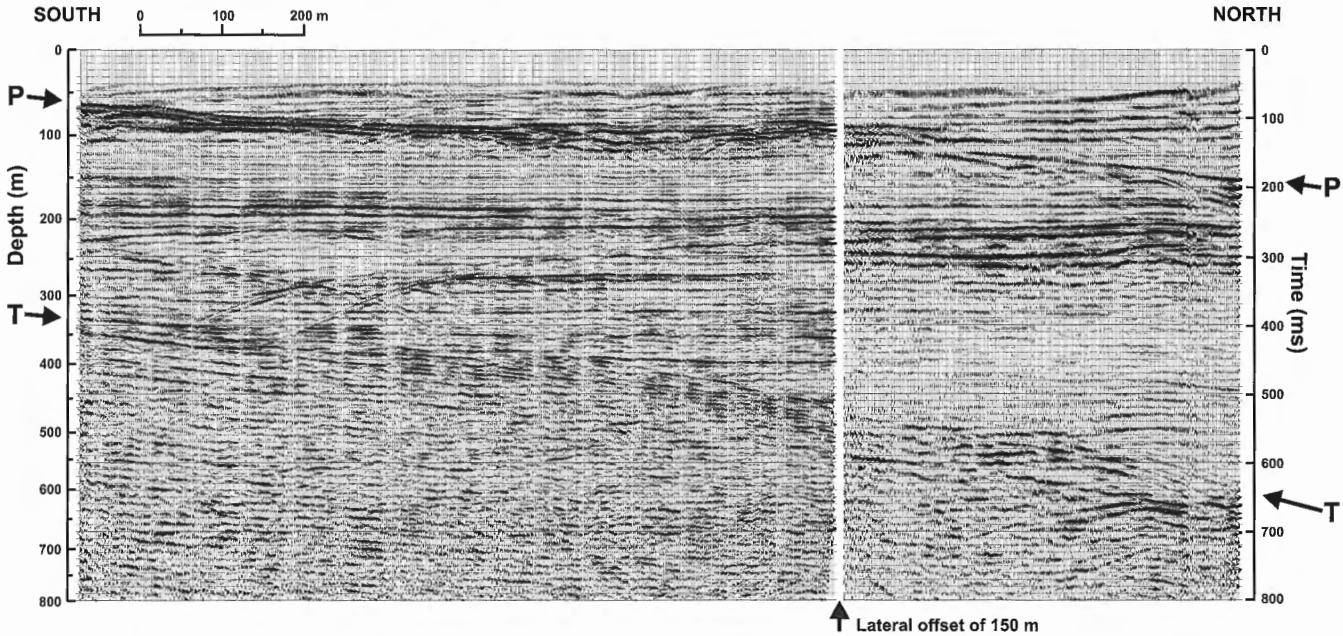

Figure 2. *A 12-fold CDP seismic reflection line at the shore of Boundary Bay near Tsawwassen, shot with an 8-gauge Buffalo gun source (see Fig. 1 for location of line). The interpreted tops of the Pleistocene sequence (P) and Tertiary (T) bedrock are angular unconformities. Several subhorizontal seismic reflections are visible within the Pleistocene sequence.*

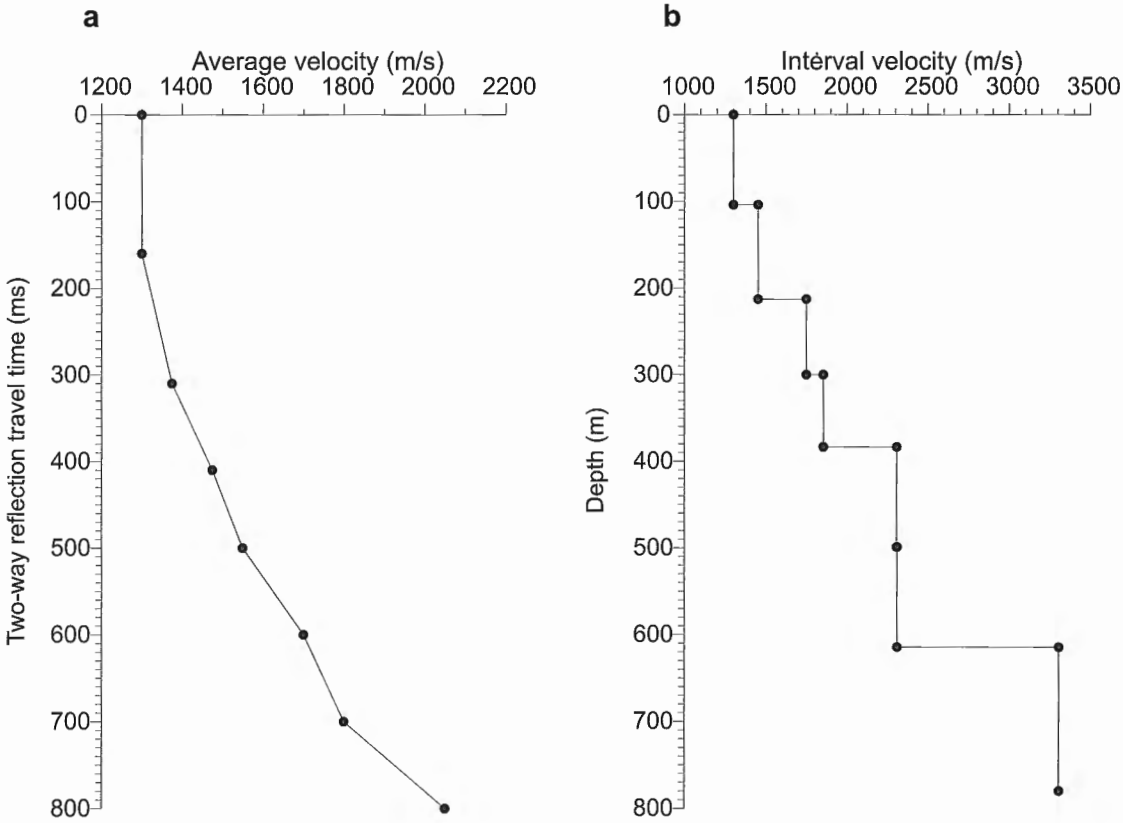

Figure 3. *Velocity analysis from deep seismic reflection data of Dynamic Oil Ltd. (see Fig.1 for location).* ***a)*** *Average compressional-wave velocity vs. two-way traveltime to reflectors.* ***b)*** *Computed interval velocities vs. depth. One hundred and eighty two locations such as this were analyzed in the survey area.*

velocity-depth analysis of the same data set at selected intervals of approximately 1 km along each line. The depth data were contoured in map form (Britton et al., 1995). A modified version of the map is included in Clague et al. (1998), and a three-dimensional perspective view can be found in Ricketts (1998).

The Geological Survey of Canada has shot one seismic section that shows the top of Tertiary bedrock (Fig. 2; details in Pullan et al., 1998). Both the Pleistocene-Tertiary and Holocene-Pleistocene boundaries are evident in this section and are marked by angular unconformities. The depth to the top of bedrock ranges from 350 m to 650 m along this short section. Elsewhere on the delta, this surface ranges from about 350 m to 1050 m deep. The average thickness of the overlying Quaternary sediments is about 500 m. Buried topographic highs and lows trend northwest and northeast, and may present significant concave and convex surfaces from which seismic energy could be focused or defocused during an earthquake.

As indicated above, the shear-wave velocity contrasts associated with geological boundaries are required for computer modelling of earthquake ground-motion amplification response. No direct shear-wave velocity measurements, however, have been made on the deeper parts of the Quaternary sequence or the upper portion of the Tertiary section. The shear-wave velocity structure can be estimated as a function of depth from compressional-wave data obtained from conventional seismic reflection surveys, using a two-step procedure. The first step is illustrated in Figure 3a, where average P-wave velocity is plotted against two-way reflection traveltime. These data, which are derived from routine computer analysis of multichannel seismic reflection data, can be used to calculate interval P-wave velocities using the Dix (1955) technique, as shown in Figure 3b. The second step involves estimating shear-wave velocities from interval P-wave velocities using an empirical relationship developed by Hunter et al. (1996b), as shown in Figure 4; the relationship was derived from measurements of compressional- and shear-wave velocities in boreholes on the Fraser delta (Dallimore et al., 1995), and from similar measurements in Tertiary sedimentary rock elsewhere. It should be noted that this relationship has been developed for local sediments and bedrock and is valid over the seismic frequency range of 20-500 Hz; it should not be applied to other sedimentary basins without additional ground-truth measurements.

An example of a shear-wave velocity-depth interpretation utilizing compressional-wave data from the Fraser delta is shown in Figure 5. A large shear-wave velocity contrast is evident at the top of Tertiary bedrock, interpreted by Britton et al. (1995) to be about 480 m deep at this site. Such contrasts are typical of the buried bedrock surface throughout the survey area. In some areas, large velocity contrasts also occur within the Quaternary succession (Hunter et al., 1996b). These velocity contrasts may be associated with the Holocene-Pleistocene boundary and reflect a difference in consolidation between deltaic and glacially overridden sediments, or they may be associated with horizons within the Pleistocene sequence.

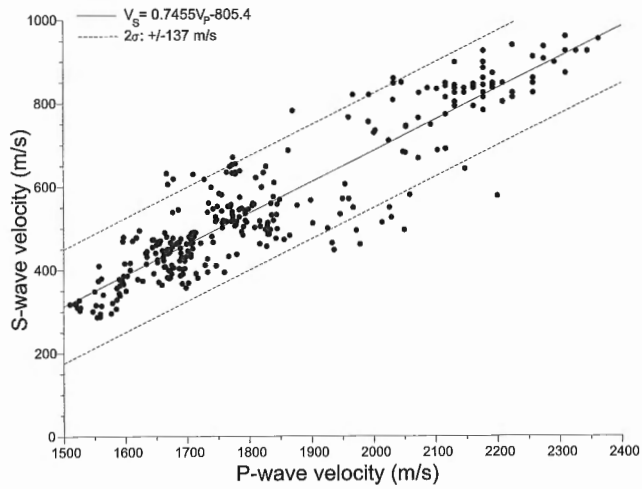

Figure 4. *Empirical relationship between shear-wave and compressional-wave seismic velocities (after Hunter et al., 1996b). The data are from Fraser delta boreholes and Tertiary bedrock of a type similar to that which underlies the survey area.*

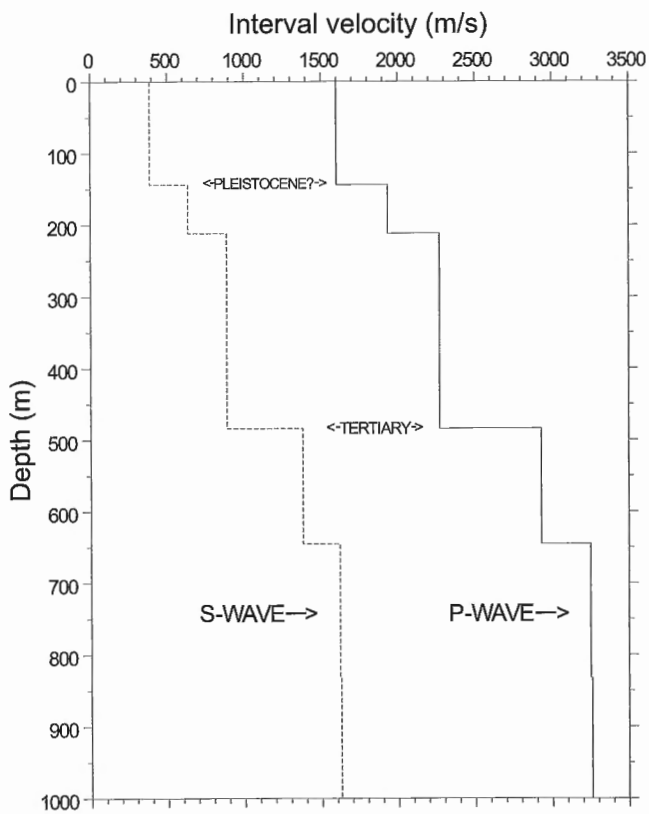

Figure 5. *P- and S-wave interval velocities from deep seismic reflection data of Dynamic Oil Ltd. (see Fig. 1 for location). P-wave velocities were computed from average velocities measured from the surface (see Fig. 3); S-wave velocities were calculated using the empirical relationship in Figure 4.*

The empirical P-S velocity relationship discussed above should be viewed only as a first step in the investigation of the shear-wave velocity structure of the Fraser delta. Direct shear-wave measurements in deep boreholes that penetrate bedrock would provide better data for computer modelling of earthquake ground motion amplification effects.

High-resolution compressional (P-) wave reflection surveys

High-resolution P-wave reflection methods (Hunter et al., 1989; Pullan et al., 1991; Roberts et al., 1992) have been tested on the southern Fraser delta for over a decade (Luternauer et al., 1986; Pullan and Hunter, 1987; Jol, 1988; Jol and Roberts, 1988; Pullan et al., 1989; Clague et al., 1991). To date, over 60 line-kilometres of data have been obtained, and reflection boundaries have been mapped to depths of 200 m or more in some areas. The optimum offset and the common-midpoint methods have been used in these surveys. Both methods require different recording equipment and seismic array geometries than the conventional reflection techniques used in oil and gas exploration. Horizontal and vertical resolution is generally higher than obtained with conventional methods, but the depth of penetration can be limited by the frequencies used, as well as other factors. Details on methods and results are summarized in Pullan et al. (1998); the reader is referred to this paper for discussions of applications and limitations of the techniques. High-resolution P-wave reflection methods developed on the Fraser delta are applicable to most other earthquake-prone areas of Canada with thick unconsolidated deposits.

High-resolution shear (S-) wave reflection surveys

Shear-wave reflection methods rely on the transmission of seismic energy via the sediment framework and can be used in areas where high-resolution P-wave reflection methods are limited by gas in the pore spaces of the sediment (Pullan et al., 1998). Experimental high-resolution shear-wave reflection surveys have recently been conducted on the Fraser delta at sites where borehole data provide some ground truth. These tests have shown that shear-wave reflections (both transverse and radial polarization modes) can be obtained where shallow gas limits the penetration of P-wave energy. Large-amplitude shear-wave reflections are associated with known shear-wave velocity contrasts measured in the boreholes. Detailed descriptions of the method and its initial applications on the Fraser delta are given by Harris et al. (1996) and Pullan et al. (1998).

Results to date suggest that the method is relatively insensitive to minor changes in shear-wave velocity within the Holocene sequence; significant reflection of energy is associated only with the large velocity contrast at the Holocene-Pleistocene boundary and with velocity contrasts in the Pleistocene sequence. Examples of this can be seen in Figure 20b of Pullan et al. (1998), which shows the interpreted Holocene-Pleistocene boundary dipping 11° north, and Figure 22 of Pullan et al. (1998), where a large-amplitude shear-wave reflector coincides with a shear-wave velocity discontinuity.

The shear-wave reflection method, although still in the early stage of testing on the delta, may offer a new approach to delineating the velocity structure associated with the Holocene-Pleistocene boundary.

BOREHOLE GEOPHYSICAL METHODS

More than 40 holes have been drilled on the Fraser delta by the Geological Survey of Canada to provide information on the Quaternary stratigraphy of the delta and on the geotechnical and geophysical properties of the sediments. Most of these holes were cased with 50-65 mm diameter PVC pipe for geophysical logging. Five different types of geophysical logs have been obtained in the boreholes: natural gamma, inductive electrical conductivity, magnetic susceptibility, multichannel P-wave (downhole), and well-lock three-component shear wave (downhole). Many of the holes have been preserved for future testing of new geophysical downhole techniques.

Natural gamma log

The natural gamma log measures gamma radiation from radioactive isotopes of potassium, uranium, and thorium which occur naturally within unconsolidated sediments. Changes in radiation in a borehole can be used to provide a qualitative estimate of lithology. Fraser delta sands have relatively low gamma count rates, commonly two times less than the count rates for silts and clays (Fig. 6, 7).

Sediments to depths of 3 to 15 m over much of the delta are dominantly silts and peats (Armstrong and Hicock, 1979; Monahan et al., 1993; Clague et al., 1998); these materials have relatively high gamma count rates. Thick distributary-channel sands beneath these fine-grained sediments (Clague et al., 1998) are characterized by relatively low gamma count rates. One or more fining-upward sequences within the sand unit can be identified on the gamma logs. Beneath the distributary-channel sands is a thick (up to 200 m) unit of silts and local sands, interpreted to be Holocene foreset and prodelta deposits (Clague et al., 1991, 1998). This sequence yields generally high gamma count rates; count rates increase as the unit fines. The base of the deltaic sequence in many boreholes is delineated by an abrupt change in the gamma count rate, which commonly coincides with a lithological discontinuity between Holocene clayey silt and Pleistocene diamicton (Dallimore et al., 1995, 1996).

The natural gamma response measured by the borehole sonde is strongly dependent on the particular tool used (i.e. the type and sensitivity of the detection electronics) and on the diameter of the borehole (for many instruments, most of the measured gamma response is from a distance of 0.5 m or less). Hence, for interpreting lithological changes within a borehole or for correlating between boreholes, the same hole diameters and casing, as well as sondes, should be maintained throughout the survey area. Most Geological Survey of Canada boreholes on the Fraser delta are of the same diameter and were completed with similar PVC casing size and wall thickness; as well, most holes were logged with the same borehole gamma sonde (Geonics EM-39G). In the few cases where

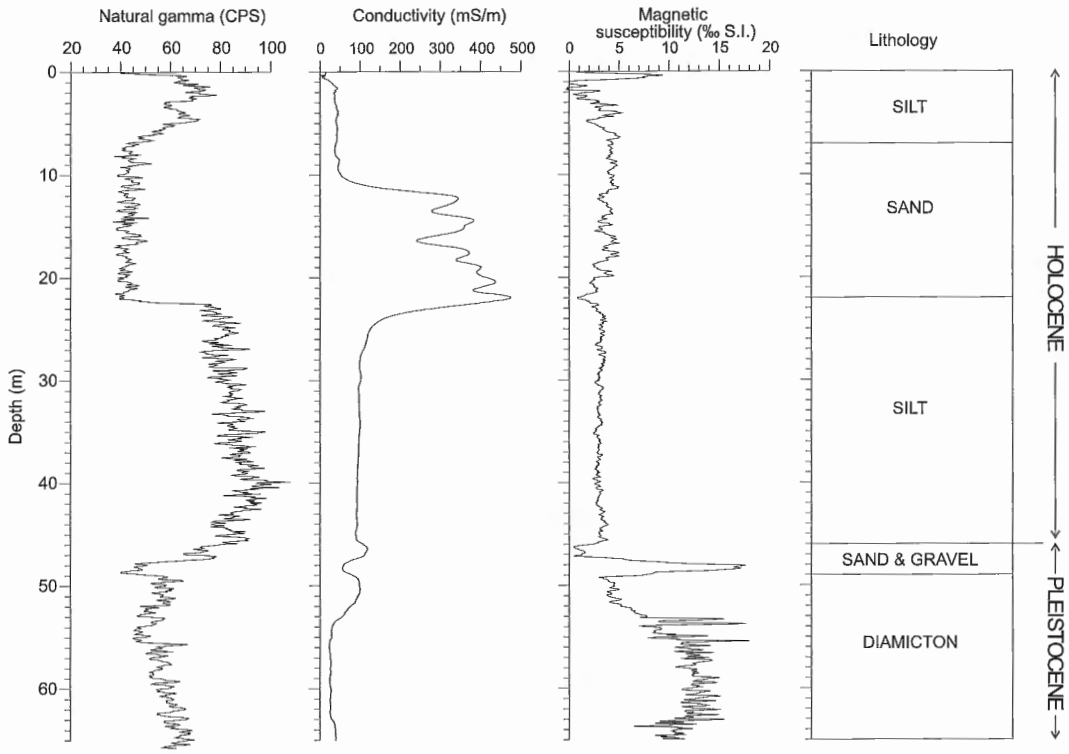

Figure 6. *Geophysical borehole logs obtained with the Geonics EM-39 system, borehole FD96-2 (see Fig.1 for location).*

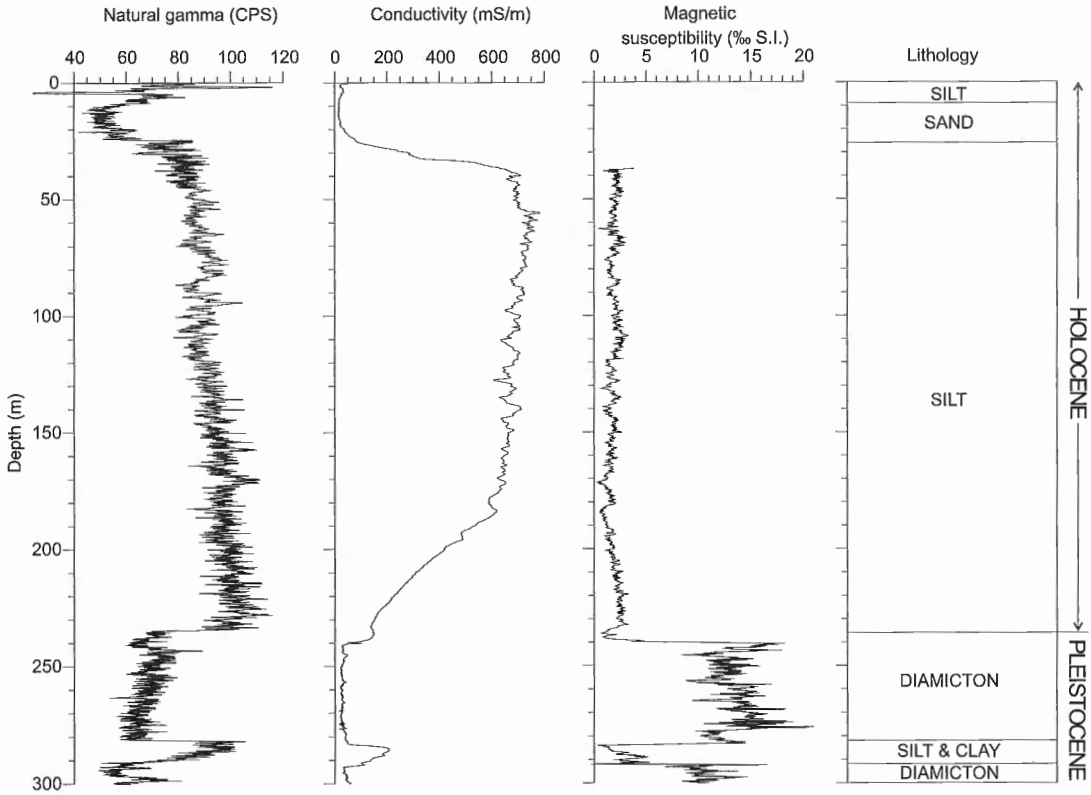

Figure 7. *Geophysical borehole logs obtained with the Geonics EM-39 system, borehole FD94-4 (see Fig.1 for location).*

different sonde types were used, careful in-hole calibration of the sondes was done over a range of sediment types to adjust overall response levels to the above-mentioned 'standard' sonde type.

The overall response of the natural gamma tool is also affected by the integration rate of the electronics (an analog system with digital output), the background noise response (ambient and instrumental), and the vertical logging speed. A high count-rate integration setting was chosen for the work on the Fraser delta, dictating a slow vertical logging speed (0.025 m/s) which has been maintained in all borehole surveys. Since radioactive decay and emission of gamma rays are random in time, measurements were made with a stationary sonde over long periods to determine statistical variation. The combined temporal and instrumental error assigned to Fraser delta gamma logs has a mid-range (70 counts per second) variation of ± 6.5 counts per second (95% confidence limits). This limits the resolution that is possible for lithological interpretations (e.g. vertical variations in count rate must exceed 2 σ to delineate a lithological change). All published Geological Survey of Canada borehole gamma logs from the Fraser delta have been presented in an unprocessed form without post-acquisition digital filtering or smoothing.

Electrical conductivity log

The electrical conductivity log can provide information on lithology because silts and sands commonly have different electrical properties. In the case of the Fraser delta, however, the conductivity log primarily reflects pore-water salinity. Figure 8 shows a correlation between pore-water salinity and the electrical conductivity of Holocene and Pleistocene sediments of a range of grain sizes, based on measurements in two deep boreholes on the Fraser delta (after Dallimore et al., 1995).

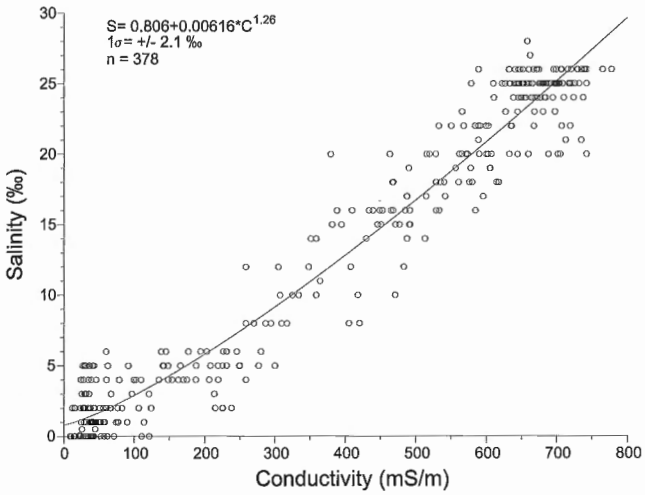

Figure 8. *Least-squares fit of salinity measured in samples and electrical conductivity measured with a Geonics EM-39 induction logging sonde, boreholes FD94-3 and FD94-4 (see Fig. 1 for location). Approximately half of the data are from Holocene deltaic sediments and half are from Pleistocene sediments.*

Other examples of electrical conductivity logs are shown in Figures 6 and 7. Variations in conductivity in these logs may be the result of groundwater flow within the sediments (Ricketts, 1998). Saline pore water is common in silts and clays throughout the Holocene section, locally to depths of 300 m (Dallimore et al., 1995, 1996). Freshwater zones, 1-40 m thick, with low electrical conductivity, occur near the surface in association with sands (Fig. 7). Hydraulic connection with the sea is possible where electrical conductivity in these near-surface sands is high (Fig. 6).

Low-conductivity waters are commonly present at the Holocene-Pleistocene boundary, with a strong gradient into more saline waters higher in the section (Fig. 7). The low salinity of pore waters in the basal Holocene silts, and the conductivity gradient, may reflect postdepositional hydrogeological processes such as salt diffusion into, or artesian pressures from, the Pleistocene succession. If the conductivity gradient is the result of salt leaching, a geotechnically sensitive condition may exist (Christian et al., 1998) wherein the postfailure residual shear strength of the basal Holocene sediments is considerably less than the original strength.

The conductivity sonde used in all Geological Survey of Canada boreholes on the Fraser delta (Geonics EM-39C) is an inductive tool which does not require direct electrical contact with the formation or fluid in the borehole and is relatively insensitive to near-sonde borehole conditions. A detailed description of the sonde and its applications is given by McNeill (1986, 1990), McNeill et al. (1988), and Taylor et al. (1989). The configuration of the sonde gives an integrated response of the conductivity to 1 m or more radially from the borehole, with vertical resolution of about 0.5 m or greater (see Taylor et al., 1989, for a detailed discussion of thin-layer response). The time constant of this tool, unlike that of the gamma sonde, is relatively small; hence a logging speed of 0.05 m/s or less was used for all surveys, yielding a vertical shift error in conductivity readings of less than 0.05 m. Sonde calibration was done routinely at all boreholes to maintain zero offset errors of less that ± 0.1 mS/m.

Magnetic susceptibility log

The magnetic susceptibility of earth materials represents the degree to which they can be magnetized in the presence of the Earth's magnetic field, and is defined as the ratio of the intensity of magnetization divided by the magnetic field strength (Telford et al., 1976). Large magnetic susceptibilities are associated with ferrimagnetic minerals, notably those composed of iron-titanium oxides; of these, magnetite has by far the highest susceptibility (Lindsley et al., 1966). The magnetic susceptibility response of fluvial, deltaic, and glacial sediments may reflect only the magnetite content of the material (McNeill et al., 1996). Commonly, however, unconsolidated sediments, such as those of the Fraser delta, contain only small quantities of magnetite; hence the overall magnetic susceptibility response is low compared to igneous rocks and many metamorphic and sedimentary rocks.

Examples of magnetic susceptibility logs are shown in Figures 6 and 7. The Holocene deltaic sediments have very low susceptibilities, but there are small differences between

fine-grained (low susceptibility) and coarse-grained (higher susceptibility) sediments. The Pleistocene sediments, in general, contain more magnetite and the Holocene-Pleistocene boundary is commonly marked by an abrupt increase in magnetic susceptibility.

The magnetic susceptibility borehole-logging sonde used in the study area (Geonics EM-39M) was developed and tested through Geological Survey of Canada–industry collaborative research. It was initially considered to be an experimental prototype, but has subsequently been developed into a commercial product. The sonde is of an electromagnetic inductive design similar to that of the electrical conductivity sonde (Geonics EM-39C); the digital recording configuration and logging-speed parameters of the two instruments are similar. A detailed discussion of the theory of operation and the resolution of the instrument is given by McNeill et al. (1996). The tool is relatively insensitive to near-sonde borehole conditions, but penetration into the formation is less than with the conductivity sonde, with an approximate response radius of 0.3 m. For Fraser delta boreholes, the tool was calibrated to give a resolution of $\pm 0.01 \times 10^{-3}$ S.I. (magnetic susceptibility is a dimensionless constant relating magnetic intensity and magnetic flux density, in Système International (S.I.) units).

Downhole compressional (P-) wave velocity log

Geological Survey of Canada, multichannel, seismic P-wave logging systems were designed and tested in house, and are variants of types in common use in the engineering geophysics industry today (Hunter and Burns, 1991). The systems in use on the Fraser delta are twelve- and twenty-four-channel, downhole hydrophone arrays consisting of groups of one or two broad-band (4-2000 Hz response) hydrophones, with a 0.5 m vertical spacing between groups. The surface energy source is a 12-gauge 'Buffalo gun' (Pullan and MacAulay, 1987). Data were recorded on a digital enhancement (stacking) seismograph. The use of many, equally spaced hydrophones in an in-hole array allows velocity interpretations that are independent of absolute zero time, previously a major source of interpretational error. As a result, relatively accurate P-wave interval velocities can now be determined and correlated with borehole lithology (Hunter and Burns, 1991).

P-wave velocities of unconsolidated water-saturated sediments are controlled by the travel path of elastic waves through both sediment grains and pore water. Water-saturated sediments with porosities of 40-50% generally yield velocities only slightly higher than that of water (1470 m/s). Small amounts of gas can decrease compressional-wave velocities to values much less than 1470 m/s (Brandt,

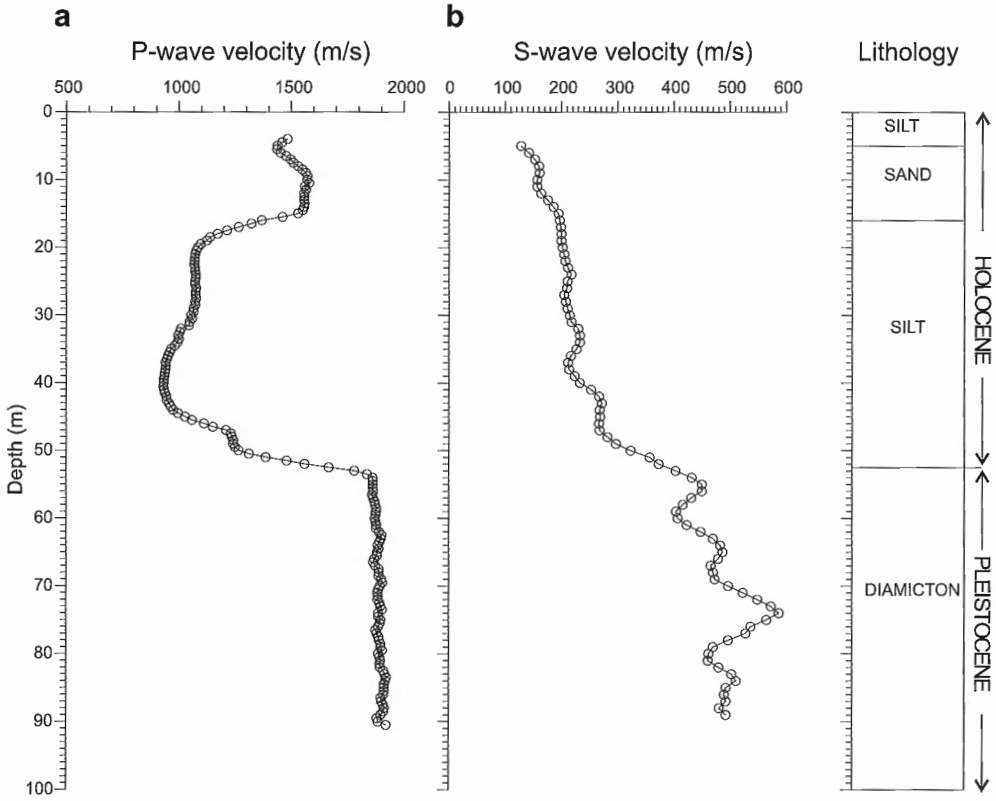

Figure 9. *Downhole seismic logs for borehole FD95-2 (see Fig. 1 for location).* ***a)*** *P-wave velocity log obtained with a 12-channel hydrophone array, 0.5 m sensor spacing, and a 5.5 m averaging window.* ***b)*** *S-wave velocity log obtained with a well-locked three-component geophone, 1 m sensor spacing, and a 10 m averaging window.*

1960). With decreasing porosity, yet full water saturation, and increasing bulk density, velocities may increase to as high as 2000-3000 m/s.

P-wave logging has been carried out in Fraser delta boreholes to obtain velocity measurements for processing high-resolution seismic reflection sections (Pullan et al., 1998), for detecting gas in sediment pore space, and for delineating major lithological boundaries (e.g. Holocene-Pleistocene boundary). An example of a P-wave velocity log is shown in Figure 9a, along with the interpreted geology. In this example, the uppermost 15 m of sediment are loose and water saturated, but are free of gas. Sediments from about 15 to 52 m depth have very low compressional-wave velocities, indicating that some gas is present in the pore space. Pleistocene sediments, present below 52 m, have velocities of about 2000 m/s, similar to values for a range of sediment types of this age beneath the Fraser delta (Dallimore et al., 1995).

Downhole shear (S-) wave velocity log

Downhole shear-wave velocity logs have been obtained on the Fraser delta using a three-component, well-locked, low-frequency (8 Hz) geophone array in a PVC-cased hole, and a surface-polarized shear-wave source. The energy source is a 5.8 kg hammer struck against a horizontal plate in firm contact with the ground. The seismic energy from the geophones was recorded with a digital seismograph. Shear-wave first-arrival times from the source to successive locations of the geophone array in the borehole (0.5-1 m vertical spacing) were determined using routine reverse-polarity trace-comparison techniques. Least-squares fits of arrival time-distance measurements for three to five contiguous sampling points (i.e. vertical intervals of 2 m or more) were used to determine interval velocities.

Shear-wave velocities increase with depth in the Holocene deltaic sequence, in accord with an established depth relationship for normally consolidated sediments (Robertson, 1990; Stokoe, 1990). There is a marked increase in shear-wave velocity at the Holocene-Pleistocene boundary (Fig. 9b). Shear-wave velocities of Pleistocene sediments vary with depth and lithology, from 400 m/s for sands and silts at shallow depth (<50 m below surface) to 800 m/s for diamicton at depths of 200 m or more. The high velocities in some of these sediments may be the result of overconsolidation caused by glacial overriding, in addition to normal time- and depth-dependent consolidation effects.

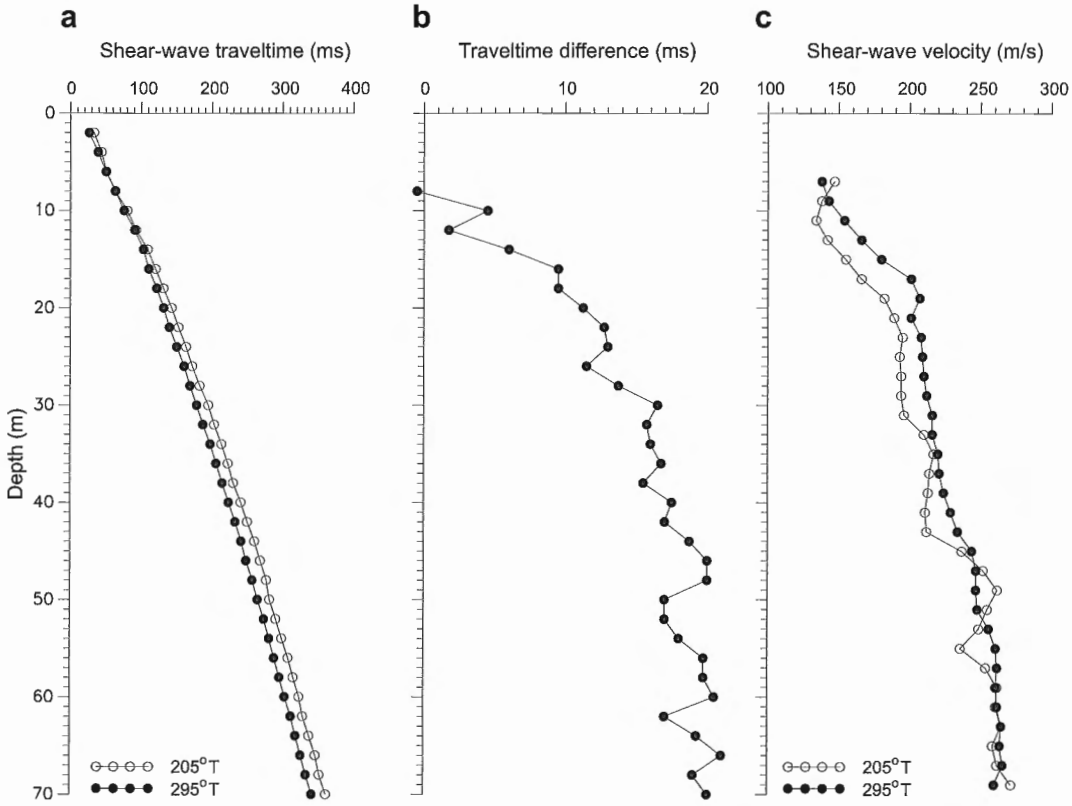

Figure 10. *Results of a shear-wave splitting experiment in borehole FD95-S1 at the Deltaport on Roberts Bank (see Fig. 1 for location). An oriented three-component well-lock geophone was moved down the hole at 2 m intervals. At each position, two orthogonal sets of polarized source data were obtained. The data were rotated during processing to obtain maximum and minimum traveltime azimuths.* ***a)*** *Traveltimes for maximum and minimum directions.* ***b)*** *Traveltime differences between fast and slow shear-wave velocity directions.* ***c)*** *Shear-wave velocities obtained using a four-point averaging window.*

An attempt has been made to obtain estimates of horizontal anisotropy of shear-wave velocity in the Fraser delta (Harris et al., 1996). Shear-wave velocity anisotropy in sediments can be caused by grain orientation during deposition or by horizontal stress anisotropy (Roesler, 1979; Lynn, 1991). Figure 10 shows results from borehole FD95-S1, located at the seaward terminus of the Deltaport causeway on the southwestern Fraser delta (Fig. 1). The plotted velocities are maximum and minimum values determined at various depths from a series of oriented surface-source polarizations and the known orientation of the three-component geophone array in the borehole. Significant horizontal anisotropy exists to a depth of 45 m in the borehole. For each data point within this anisotropic zone, the maximum and minimum polarization directions are 295° and 205° True North, respectively (± 2.5°). Three other boreholes on the Deltaport causeway, landward of FD95-S1, show no significant shear-wave horizontal anisotropy. The anisotropy observed in borehole FD95-S1 may be caused by unequal local horizontal stresses. It is interesting to note that the minimum velocity direction is parallel to the delta slope immediately seaward of the site; this direction is consistent with minimum horizontal stresses that would occur close to a submarine slope.

Seismic cone penetrometer log

A variant of the downhole shear-wave velocity method is the seismic cone penetration test (SCPT; Robertson et al., 1986). A horizontal geophone or accelerometer, installed near the tip of a standard cone penetrometer, is used as the shear-wave detector, much like a well-lock geophone. A surface shear-wave source, similar to that described above, is generally used. The advantage of this technique over the well-lock borehole geophone logging method is the superior coupling of the instrument to the formation, since the cone is pushed through the sediment. A disadvantage is that the method is limited to the maximum penetration that can be achieved with a cone penetrometer. Single cone pushes, without drill-outs, to 90 m depth are possible in Fraser delta sediments (H. Christian, pers. comm., 1997). SCPT data are available for over 70 sites on the Fraser delta studied by the Geological Survey of Canada (Fig. 1; Woeller et al., 1993a, b, 1994).

A SCPT shear-wave velocity log and, for comparison, a nearby downhole shear-wave velocity log are shown in Figure 11. The statistical error (largely the first arrival time picking error) associated with the SCPT data is slightly lower than that of the downhole data. Further comparisons of borehole and SCPT results are given by Hunter and Woeller (1990) and Hunter et al. (1991, 1993).

SURFACE GEOPHYSICAL METHODS

Surface shear-wave refraction method

A shear-wave refraction method has been tested and applied throughout the survey area (Hunter et al., 1992). Data were acquired with shear-wave sources at each end of a geophone array (a 'reversed refraction profile'). A horizontally polarized (SH) source was used since it is least affected by conversion of shear waves to compressional waves, which may result in noise at the source. In most cases the shear-wave source consisted of a weighted block struck sideways by a 7.3 kg hammer. Two directions of horizontally polarized SH energy from the source were digitally stacked using the polarity-reversing feature of the recording seismograph. At some sites, an 8-gauge Buffalo gun seismic source (Pullan and MacAulay, 1987) was used without polarized-record stacking (most impulsive surface P-wave sources are good generators of shear-wave energy).

For most of the surveys on the Fraser delta, the geophone spacing was 3 m, and array lengths were at least 210 m. In some locations, where space for longer arrays could be found and where ambient noise was relatively low, single-ended or reversed refraction arrays were lengthened to 700 m or more to achieve greater depth penetration.

Application of this refraction method requires that shear-wave velocity increases with depth, i.e. there is a positive velocity-depth gradient. Shear-wave velocity data from boreholes (see above) indicate that this condition is met on the Fraser delta. As a result of large shear-wave velocity-depth gradients peculiar to the survey area, effective penetration of

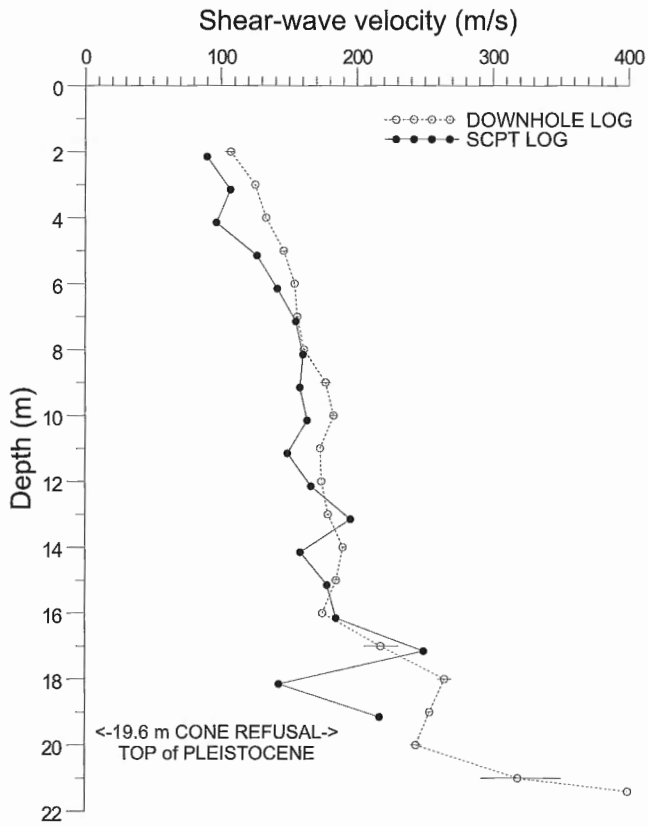

Figure 11. *Comparison of shear-wave velocities obtained with a seismic cone penetrometer and using the downhole method, borehole FD94-3 (see Fig. 1 for location). Each SCPT velocity was calculated from two traveltime measurements 1 m apart; each downhole velocity was obtained from three traveltime measurements at 1 m spacings using least-squares techniques.*

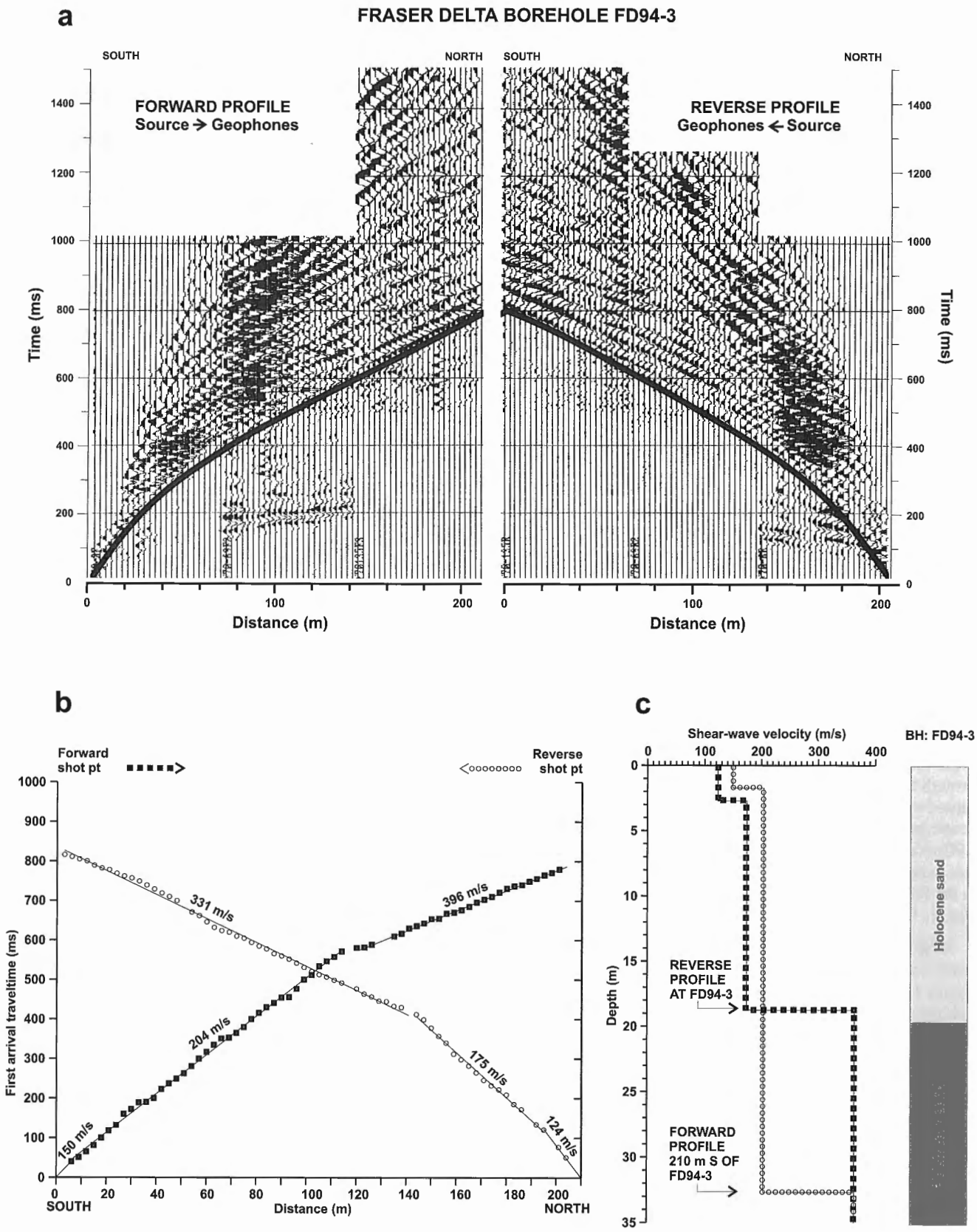

*Figure 12. Shear-wave reversed refraction profile near borehole FD94-3 (see Fig. 1 for location). **a)** Composite seismic record. **b)** First-arrival traveltime plots and apparent velocities. **c)** Velocity-depth plot.*

refraction ray paths with this method is extraordinarily good and is approximately one third the array length (this rule of thumb may not necessarily apply in other survey areas).

Velocity discontinuities were encountered at depth at several sites; correlation with borehole data (Luternauer and Hunter, 1996) indicates that the discontinuities coincide with the Holocene-Pleistocene boundary (Fig. 12). Figure 12a shows composite forward and reverse, shear-wave refraction seismic records for a site on central Lulu Island (Fig. 1). Plots of first arrival traveltime vs. offset distance for this site are shown in Figure 12b. These plots reveal a high-velocity refraction discontinuity associated with the top of the Pleistocene sequence (Fig. 12c). Analyses of first arrival traveltime plots, such as shown in Figure 12b, use both routine curve-fitting and velocity-layer interpretation methods (Hunter, 1971; Hunter et al., 1992).

Shear-wave velocity profiles have been obtained at over 100 sites on the Fraser delta. Most surveys were designed to provide detailed subsurface shear-wave velocity estimates to 30 to 50 m depth. At sites with long array lengths, velocity estimates to depths of 250 m or more have been obtained (Luternauer and Hunter, 1996).

A partial compilation of shear-wave velocities as a function of depth, based on refraction analyses and SCPT data, is shown in Figure 13. Sites where Pleistocene materials are interpreted to have high velocities are excluded from this data set. The relatively high velocity gradient immediately below the delta surface probably stems from the increase in overburden load stress with depth in normally consolidated deltaic sediments (Robertson, 1990). Although these data were obtained from widely distributed sites on the Fraser delta, the limited range of the data at most depths suggests that vertical load stress, rather than lithology, is the most important factor affecting shear-wave velocity. This well constrained, delta-wide, velocity-depth function can be used to model ground-motion amplification (Hunter, 1995). Differences in velocities in the 0-15 m depth range (Fig. 13), however, may be significant with respect to liquefaction resistance during an earthquake; this topic is discussed in a later section.

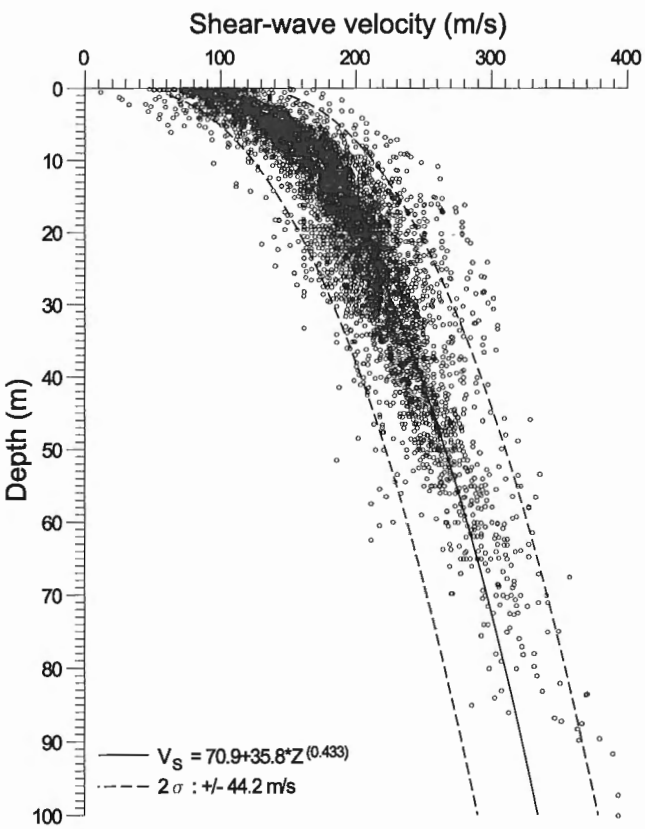

Figure 13. *Shear-wave velocity-depth data for Holocene deltaic sediments obtained from surface refraction and seismic cone penetrometer surveys (after Hunter, 1995).*

Spectral analysis of surface waves (SASW)

A ground-surface (non-invasive) technique called spectral analysis of surface waves (SASW) (Stokoe and Nazarian, 1985; Stokoe et al., 1988a; Robertson and Addo, 1991) has recently been tested in the survey area. SASW requires an impulsive, broad-band, surface seismic source, such as a hammer struck on a plate, or an in-hole shotgun source, and at least two in-line geophones capable of recording relatively low frequencies (>2 Hz). The data are analyzed for spectral components of the Rayleigh surface-wave energy, and apparent velocities are assigned to each component. Inversion of the apparent velocities yields estimates of shear-wave velocities as a function of depth. The method can detect relatively small velocity reversals at depth. Tests have shown depth penetration to be 20 m or more on the Fraser delta (Woeller et al., 1993a). Figure 14 provides a comparison of SASW and SCPT results from a site on the central Fraser delta (Fig. 1). The two data sets are similar; the differences in velocities may be related to shear-wave velocity anisotropy between vertical and horizontal travel paths.

Surface electromagnetic techniques

Surface electromagnetic methods measure variations in the magnetic field of a transmitted electromagnetic wave or pulse to determine electrical conductivity or resistivity of subsurface materials. In areas where conductivities are low, depths of penetration and vertical resolution of conductivity variations can be high; however, saline pore water within sediments of the Fraser delta presents a challenge for these methods.

The frequency domain method, which uses the Geonics EM-34 system, and the transient method, which uses the Geonics EM-47 system, have been tested on the delta. The principles and operational details of both methods are described by McNeill (1990).

The EM-34 conductivity-meter system consists of a 1 m diameter, air-cored transmitter coil and a similar-sized receiver coil operating at three frequencies and coil spacings. Measurements are usually made with the coils oriented horizontally and vertically, giving rise to six measurements of apparent conductivity. The apparent conductivity readings are analyzed using one-dimensional computer-modelling software (Stoyer and Butler, 1994) to provide conductivity

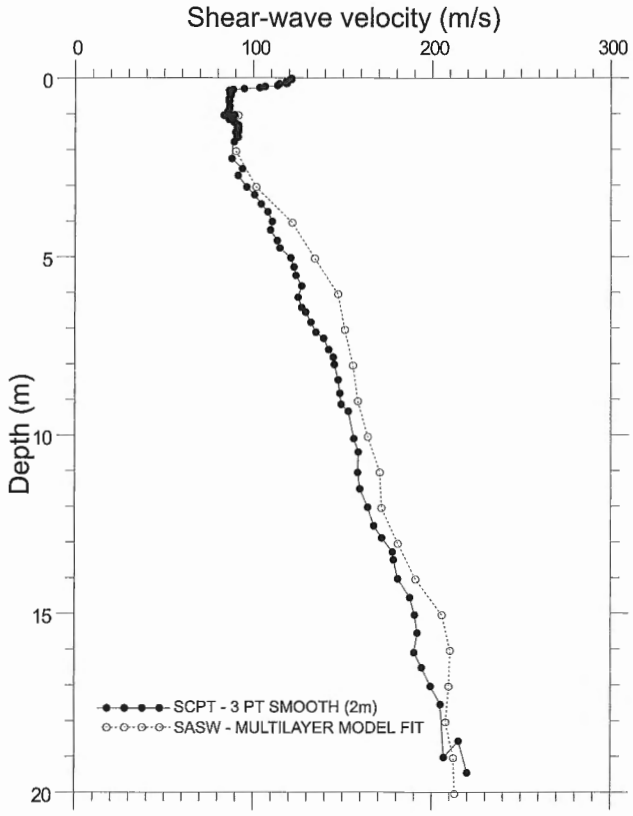

Figure 14. *Comparison of shear-wave velocity-depth data obtained with a seismic cone penetrometer and from spectral analysis of surface wave seismic data (SASW) (see Fig.1 for location).*

vs. depth plots for two or three layer models. Examples of such modelling on the Fraser delta are presented in Figure 15. In this figure, sounding models from sets of six measurements are compared to electrical conductivity measured in adjacent boreholes.

Soundings made with the EM-34 system on the Fraser delta have generally been limited to providing estimates of the conductivity and thickness of the near-surface freshwater zone, the top of the saline zone being the limit of penetration with this system (Fig. 15a). Where the saline zone is relatively thin (< 30 m), it may be possible to estimate its conductivity and thickness as well (Fig. 15b). Figure 16 shows the interpreted thickness of the near-surface freshwater zone on the southwestern Fraser river delta, based on EM-34 soundings (Hunter et al., 1996c). Limited borehole control suggests that this freshwater occurs within a sheet of Holocene distributary-channel sands (Monahan et al., 1993).

The advantage of the frequency domain method is that it can be easily used in an urban environment. Only a small area, free from fences, powerlines, and other sources of conductive anomalies and electromagnetic radiation, is required for a sounding.

The Geonics EM-47 system obtains estimates of subsurface electrical conductivity by measuring voltages resulting from the decaying magnetic field of induced eddy currents in the ground. These eddy currents are produced by a transient electromagnetic pulse transmitted through a large square loop laid out on the ground. The wire loops are typically 40 m^2, 80 m^2, or larger, and generally require a relatively large, electrically noise-free area for successful operation (e.g. fields, playgrounds, public parks). The receiver coil is relatively small (1 m in diameter) and is generally placed within the transmitter loop. Operational details relating to tests on the Fraser delta are given by Best and Todd (1996). The maximum penetration of this system in a conductive sediment environment is about 90 m.

Sounding data obtained with this transient EM system are interpreted in the form of apparent conductivity vs. depth using one-dimensional computer-modelling software (Stoyer et al., 1996). Figure 17a presents a sounding interpretation and an adjacent borehole conductivity log from a site where the top of the Pleistocene sequence is associated with a conductivity low. In contrast, Figure 17b is an example from a site where conductivities are relatively high.

EM-47 soundings are logistically more challenging in an urban environment than EM-34 surveys; however, they do provide more detailed and deeper conductivity information.

DISCUSSION

Lithology and structure of Fraser delta deposits

Surface and borehole geophysical techniques have made a fundamental contribution to defining the lithology and three-dimensional structure of Fraser delta deposits. High-resolution seismic surveys on the southern portion of the delta (Pullan et al., 1998) have provided high-quality images of structure to depths of 200 m or more and have revealed foreset beds, slumps, buried channels, and the presence of gas in the Holocene deltaic sequence.

Downhole geophysical logs have provided detailed lithological and other (e.g. pore water salinity, ferrimagnetic mineral content, presence of gas) information, which is routinely used for regional geological and geotechnical interpretations (Monahan et al., 1993; Christian et al., 1998; Clague et al., 1998). From established relations between lithology and geophysical parameters, it is now possible to conduct cost-efficient drilling programs that rely on geophysical logging with only minimal geological sampling.

Buried Pleistocene ridges or hills occur at the base of the Holocene sequence in the north-central delta (borehole FD94-3, Fig. 1) and in the southwestern area (borehole FD95-2); slopes on the flanks of these features, determined from seismic surveys, exceed 10° at some locations. One-dimensional earthquake ground-motion amplification models that assume horizontal layering may not be applicable at such sites.

The bedrock surface beneath the Fraser delta has been mapped from deep seismic reflection data (Britton et al., 1995). It occurs at depths ranging from 350 m to 1050 m and thus has considerable relief. Northwest-trending ridges and depressions (Clague et al., 1998) have been mapped in some areas, with valley width-to-depth ratios of up to 6:1 and local

slopes reaching 20°. The relief on the bedrock surface will affect the propagation of seismic energy through the overlying Quaternary deposits, causing a complex pattern of ground-motion amplification during strong earthquakes.

Notwithstanding the above contributions, little is known about the Pleistocene sequence beneath the Holocene deltaic deposits, and even less is known about the deeper bedrock materials. The recently developed high-resolution shear-wave reflection technique (Pullan et al., 1998), in concert with deep drilling, may ameliorate this problem in future.

Earthquake liquefaction resistance estimates from near-surface shear-wave velocity structure

During the last ten years, much research in North America has been directed towards the relation between shear-wave velocities of cohesionless water-saturated soils and liquefaction resistance during cyclic (earthquake) loading. A summary of recent findings and recommended methodologies is given by Andrus and Stokoe (1996). Empirically developed graphs relate surface or near-surface earthquake-shaking parameters (magnitude, severity of cyclic motion) to measured shear-wave velocities. Two relations have been suggested: cyclic stress ratio vs. normalized shear-wave velocity; and peak horizontal acceleration vs. average site shear-wave velocity (0-15 m depth).

Figure 18a shows an example of a liquefaction assessment chart for a magnitude 7.0 earthquake (after Andrus and Stokoe, 1996). On this chart, the liquefaction threshold is related to the cyclic stress ratio and normalized shear-wave velocity. The cyclic stress ratio is the ratio of earthquake-induced, average, cyclic, shear stress to the initial effective overburden stress (Andrus and Stokoe, 1996), a value dependent on the intensity of shaking at a particular site and depth. The normalized shear-wave velocity is the measured shear-wave velocity at a particular depth, modified to account for changes in effective stress with depth (see Robertson et al., 1992, for the recommended normalizing procedure). Hence, to use this chart to determine the liquefaction resistance at a site where shear-wave velocities have been measured, the earthquake magnitude and the cyclic stress-ratio variation with depth must be known. Figure 18b is a plot of normalized shear-wave velocities for Holocene sediments throughout the Fraser delta. Comparison of Figures 18a and 18b indicates

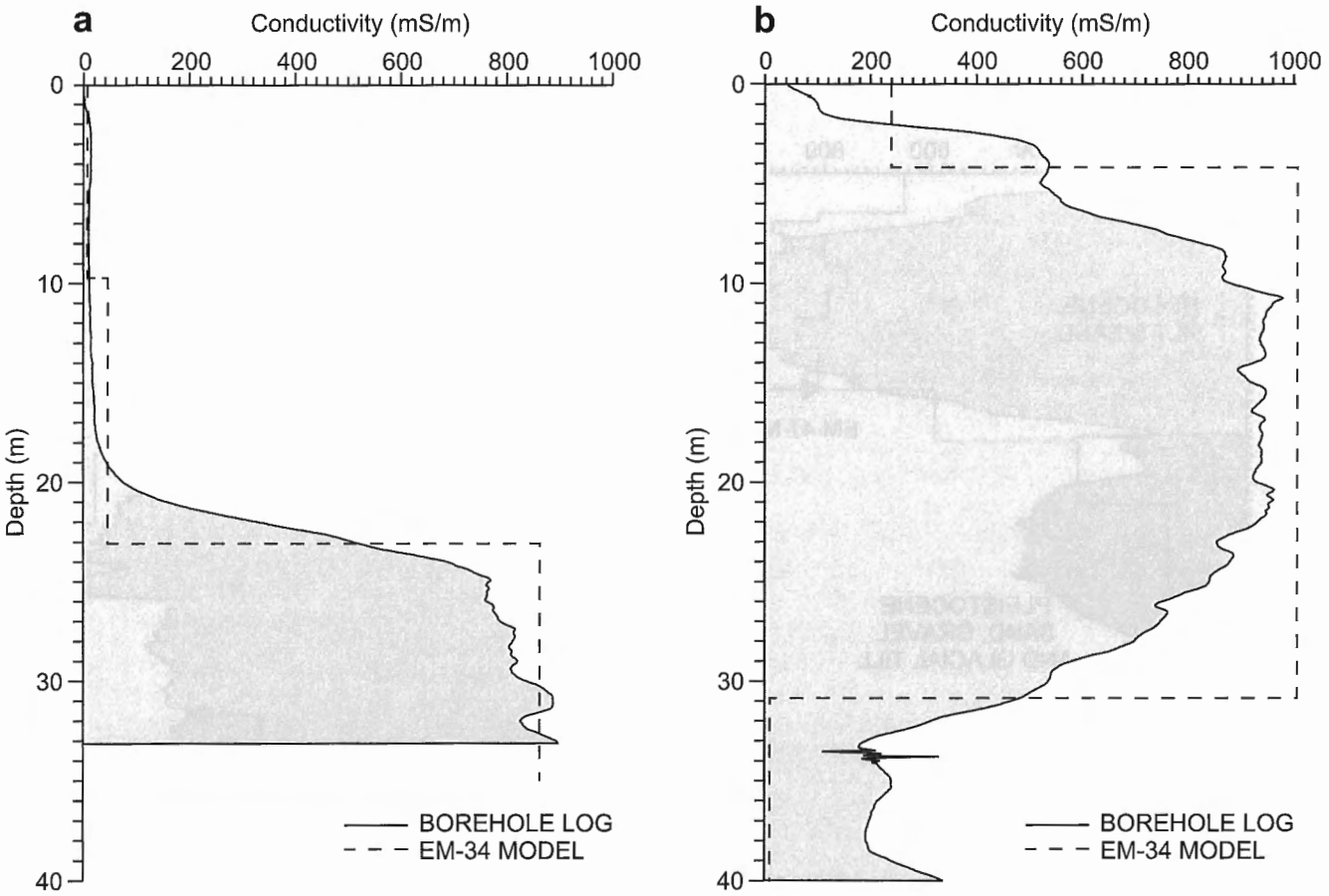

Figure 15. *Comparison of EM-34 two-layer and three-layer inversion-model results and borehole electrical conductivity measurements for two sites on the southern Fraser River delta.* ***a)*** *Borehole SFU90-3).* ***b)*** *Borehole FD86-5 (see Fig. 1 and 16 for locations).*

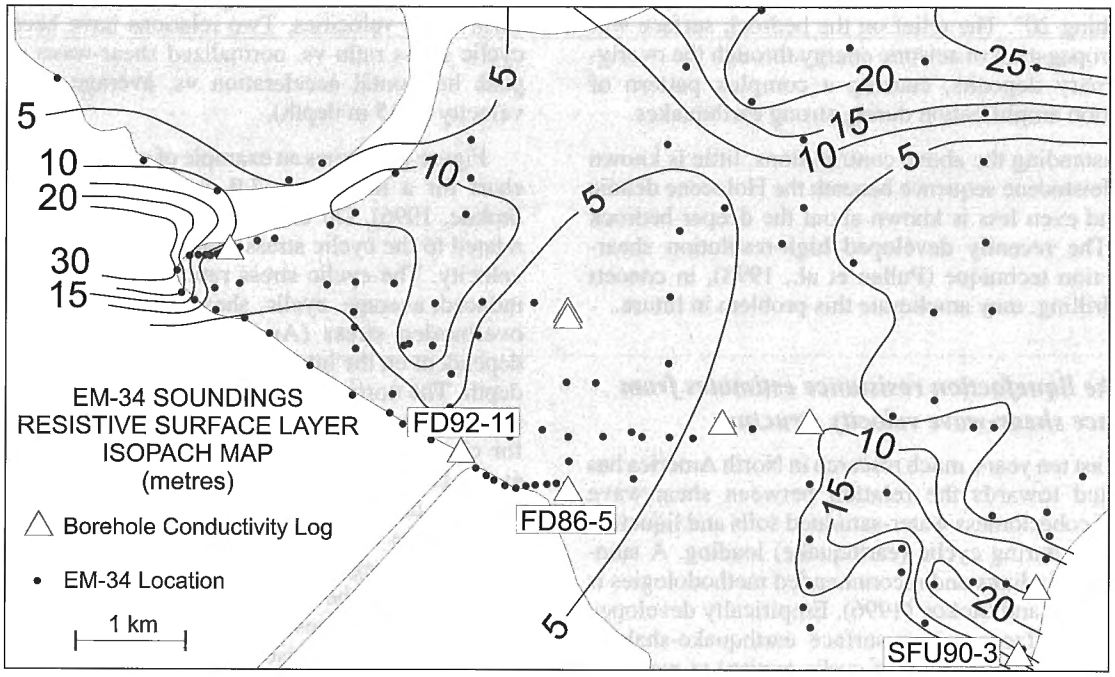

Figure 16. *Isopach map of the surface low-salinity layer on the southwestern Fraser delta based on conductivity models of EM-34 sounding data.*

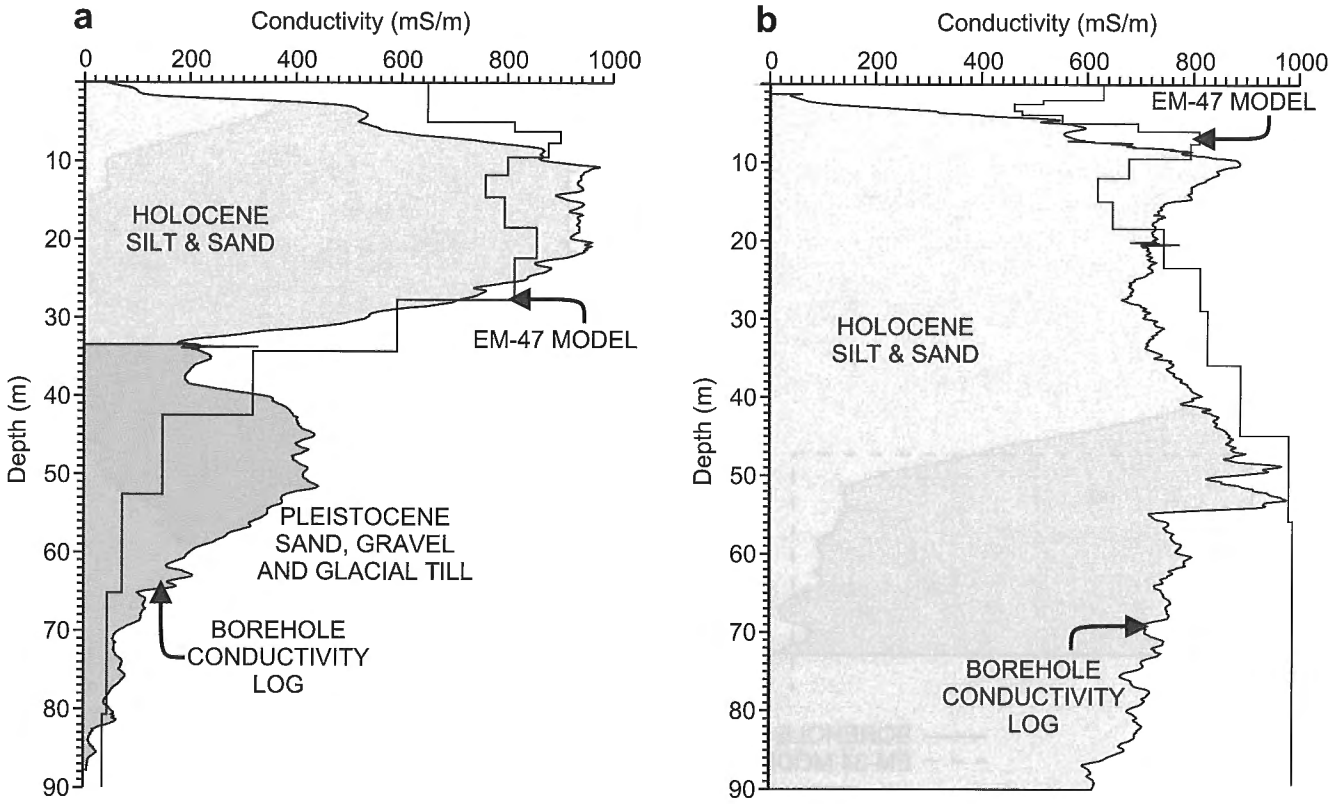

Figure 17. *Comparison of smooth model inversions of EM-47 soundings and EM-39 borehole conductivity logs at two sites on the southwestern Fraser delta (see Fig. 16 for locations).* ***a)*** *Borehole FD86-5 with a moderate thickness of conductive Holocene silts and sands overlying less conductive Pleistocene sediments.* ***b)*** *Borehole FD92-11 with thick conductive Holocene sediments.*

that water-saturated cohesionless soils at shallow depths at most sites in the survey area could liquefy during a strong earthquake if the cyclic stress ratio, to a depth of 30 m, exceeds about 0.2.

An alternative approach, also suggested by Andrus and Stokoe (1996), relates estimated, peak horizontal ground-surface acceleration for earthquake shaking and the sediment thickness-weighted average shear-wave velocity (generally in the 0-15 m depth range). The example shown in Figure 19a is for a magnitude 7.0 earthquake. For comparison, the non-normalized, thickness-weighted, average shear-wave velocity curve derived from the least-squares fit for the Fraser delta (Fig. 13), is shown in Figure 19b along with the ± two standard deviation limits. Comparison of Figures 19a and 19b suggests that there is potential for liquefaction of water-saturated cohesionless soils at shallow depths for peak horizontal accelerations greater that about 0.2 g (g = acceleration of gravity).

Earthquake amplification effects from shear-wave velocity gradients

Amplification of horizontal components of ground acceleration from vertically incident earthquake shear waves can occur where thick sediments with low shear-wave velocities overlie sediments or rock with higher shear-wave velocities. For a simple elastic model, Shearer and Orcutt (1987) have shown:

$$\text{Gradient amplification} = \rho_D V_D / \rho_S V_S$$

where ρ_D and V_D are the density and shear-wave velocity of the deep bedrock, and ρ_S and V_S are the density and shear-wave velocity of the near-surface sediments.

This formula assumes small strain, elastic wave transmission with no amplification losses due to internal reflections from velocity discontinuities, and no anelastic attenuation. Hence, it should only be considered an upper limit of possible gradient-amplification effects.

Figure 20 presents a compilation of shear-wave velocities vs. depth, taken from the regional seismic database discussed by Hunter et al. (1996b) and extended to a depth of 3500 m.

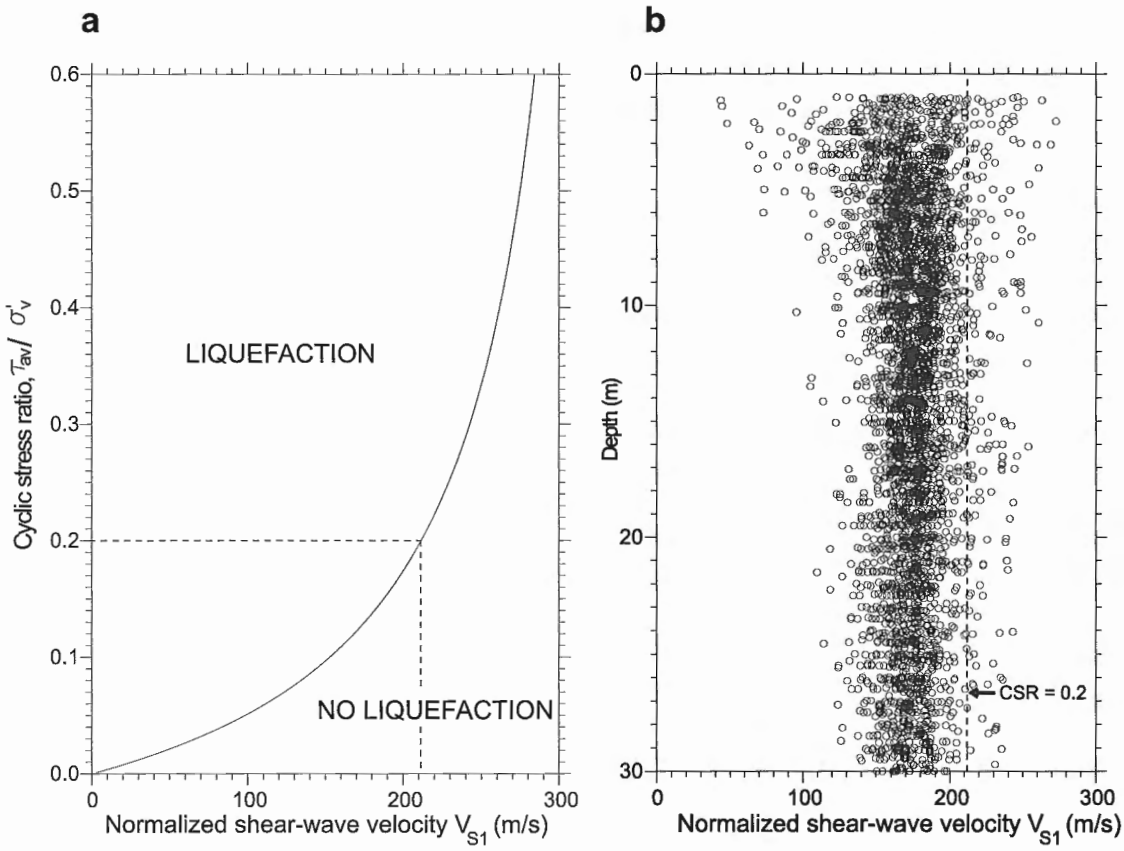

Figure 18. a) *Threshold liquefaction curve for noncohesive water-saturated sediments on a plot of cyclic stress ratio vs. normalized shear-wave velocity for an earthquake of magnitude 7.0 (after Andrus and Stokoe, 1996).* ***b)*** *Normalized shear-wave velocity data for 119 sites on the Fraser delta (after Hunter, 1995); shear-wave velocities were normalized according to the procedure given by Robertson (1990).*

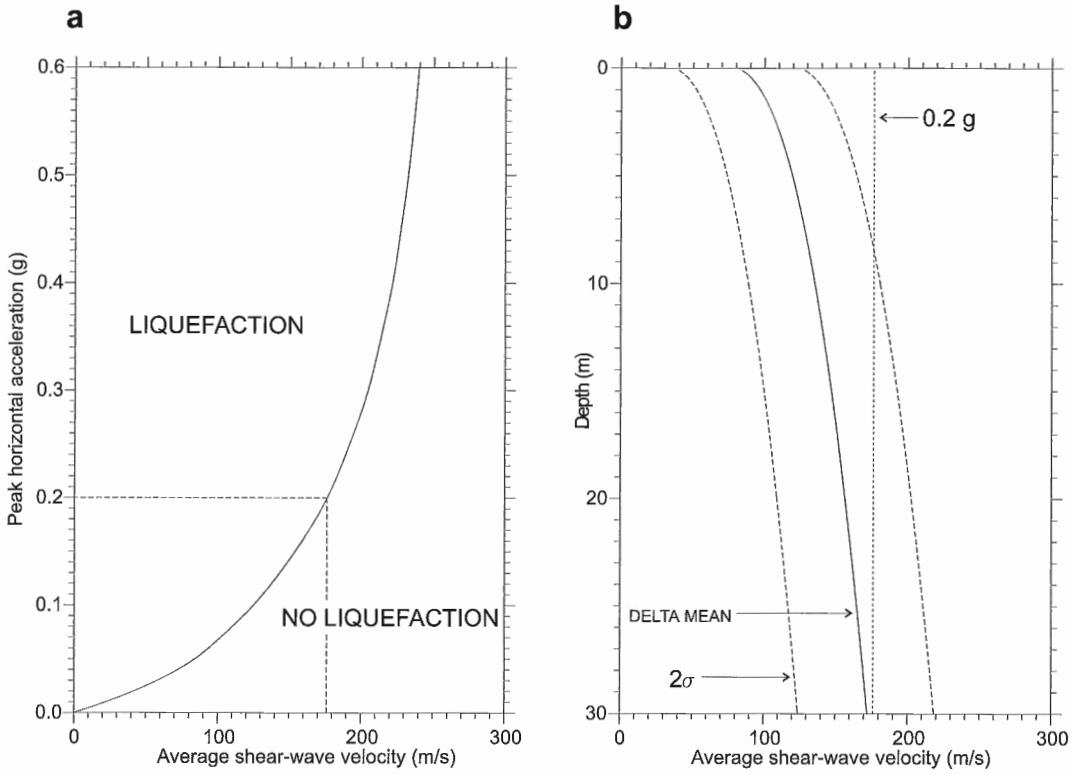

Figure 19. a) *Threshold liquefaction curve for noncohesive water-saturated sediments on a plot of peak horizontal ground acceleration vs. thickness-weighted, average, shear-wave velocity for an earthquake of magnitude 7.0 (after Andrus and Stokoe, 1996).* ***b)*** *Thickness-weighted, average, shear-wave velocity curve for Fraser delta sediments, derived from data in Figure 13; dashed lines are ± two standard deviation limits, g = gravitational acceleration at the Earth's surface.*

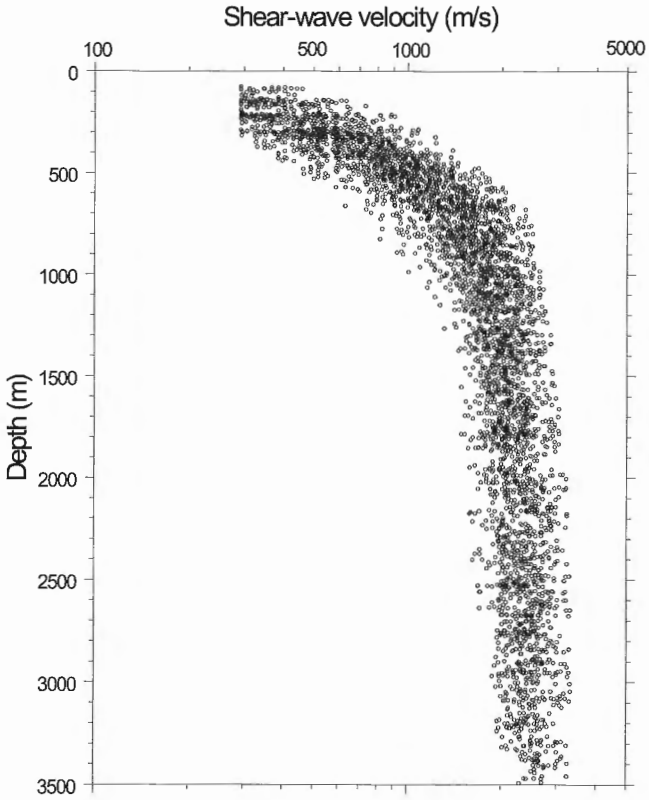

Figure 20.

Compilation of shear-wave velocities derived from seismic reflection data at 182 locations on the Fraser delta (Hunter et al., 1996b).

This figure shows an approximate ten-fold decrease in shear-wave velocities from buried bedrock to the surface on the Fraser delta; the gradient of the velocity distribution appears to be consistent from site to site. If one assumes a density contrast of 1.25 between the bedrock and near-surface Holocene sediments, the gradient amplification would be 3.5. Amplifications approaching this value were recorded by seismographs on the Fraser delta during the magnitude 5.3 Duval, Washington earthquake in 1996 (Rogers et al., 1998). For delta sites where there are significant shear-wave velocity contrasts within the Quaternary sequence (leading to transmission losses by internal reflections), or for earthquakes with larger incident strain levels, the gradient amplification effect would probably be lower than predicted with the simplifying small-strain elastic assumptions of this formulation.

Earthquake resonant amplification effects from shear-wave velocity discontinuities

Measurements made to date on the Fraser delta indicate that shear-wave velocities increase gradually with depth in the Holocene deltaic sequence, but rise abruptly (velocity contrasts of 1.5 to 3) at the Holocene-Pleistocene boundary, where there is a marked change in lithology and consolidation. As mentioned previously, there is also a significant shear-wave velocity discontinuity (contrasts of 2 to 3) at the boundary between the Quaternary succession and Tertiary bedrock.

Internal reflection of seismic waves at these seismic impedance boundaries can cause resonance or large accelerations of horizontal shear motion during shaking. For a simple one-dimensional elastic model consisting of an upper low-velocity layer overlying a higher velocity layer, the fundamental resonance frequency and higher harmonics are given by (Bard and Bouchon, 1980):

$$f_n = (2n+1)V/4H$$

where V is the thickness-weighted, average, shear-wave velocity of the upper layer (m/s), H is the thickness of the upper (surface) layer (m), and n = 0, 1, etc. for the fundamental frequency, first harmonic, etc.

For a two-layer model consisting of Quaternary and Tertiary sequences, Harris et al. (1995) showed that resonance frequencies on the Fraser delta would be in the range 0.2-0.3 Hz (3.5-5 s periods); such resonance would be of concern for the seismic response of very large structures, such as bridges, tall buildings, pipelines, and industrial facilities.

Figure 21 shows results for a two-layer model consisting of Holocene and Pleistocene sequences. The data in this figure are a summary of information obtained from Fraser delta boreholes where the Pleistocene surface was encountered and shear-wave measurements were made (see Fig. 1 for locations); these data agree well with curves derived from surface refraction and SCPT measurements. Figure 21a is a plot of depth to the velocity boundary vs. thickness-weighted, average, shear-wave velocity of the upper Holocene sediments derived from the curve shown in Figure 13. Figure 21b shows the curve of fundamental resonant frequency, f_0, as well as period, for the same depth range. This latter curve demonstrates that resonance may contribute to horizontal ground-surface accelerations in the range 0.5-10 Hz if there are large shear-wave velocity contrasts at the Holocene-Pleistocene boundary within 100 m of the ground surface. Such situations exist near the edges of the Fraser delta and at some locations in the central portion of the delta (Hunter et al., 1996a). Amplifications which are possibly associated with resonance from this surface have been observed on some seismograph records from the Duval earthquake (Rogers et al., 1998).

At the ground surface, the relative amplification of horizontal accelerations at the resonant frequencies for an elastic two-layer model, assuming no anelastic attenuation, is given by (Shearer and Orcutt, 1987):

$$\text{Resonance amplification} = \rho_L V_L / \rho_U V_U$$

where ρ_L and V_L are the density and shear-wave velocity of the lower layer, and ρ_U and V_U are the density and shear-wave velocity of the upper layer. For a two-layer Quaternary-Tertiary model, shear-wave velocities derived by Hunter et al. (1996b) suggest that the maximum amplification associated with low-frequency (long period) resonance on the Fraser delta would be 3 or less. The maximum shear-wave velocity contrast that has been measured to date at the Holocene-Pleistocene boundary is 3. Measured density contrasts at this boundary (Hunter et al., 1996a) are typically 1.16, hence the maximum resonance-amplification contribution would be about 3.5.

The gradient and resonance-amplification effects inferred from the data in Figures 20 and 21 should be considered only as conservative, rule-of-thumb guidelines since the analysis is based on one-dimensional, small-strain, elastic-wave propagation theory without consideration of anelastic attenuation or additional strain-dependent responses associated with larger earthquakes.

SUMMARY

A wide range of surface and borehole geophysical techniques have been tested and applied on the Fraser River delta to determine the structure of the Quaternary deposits and to obtain geophysical and geotechnical parameters that can be used to evaluate earthquake hazards. Large-scale multichannel reflection surveys have delineated the irregular Quaternary-Tertiary surface beneath the Fraser delta and have provided regional estimates of shear-wave velocity-depth variations. These structural and velocity data are required for two- and three-dimensional, earthquake ground-motion amplification modelling.

High-resolution reflection surveys on the southern portion of the delta have helped elucidate the internal structure of the Holocene deltaic sequence and, locally, the Pleistocene sequence. The surveys have revealed significant topographic relief on the buried Holocene-Pleistocene surface, which is also a consideration in ground-motion amplification modelling.

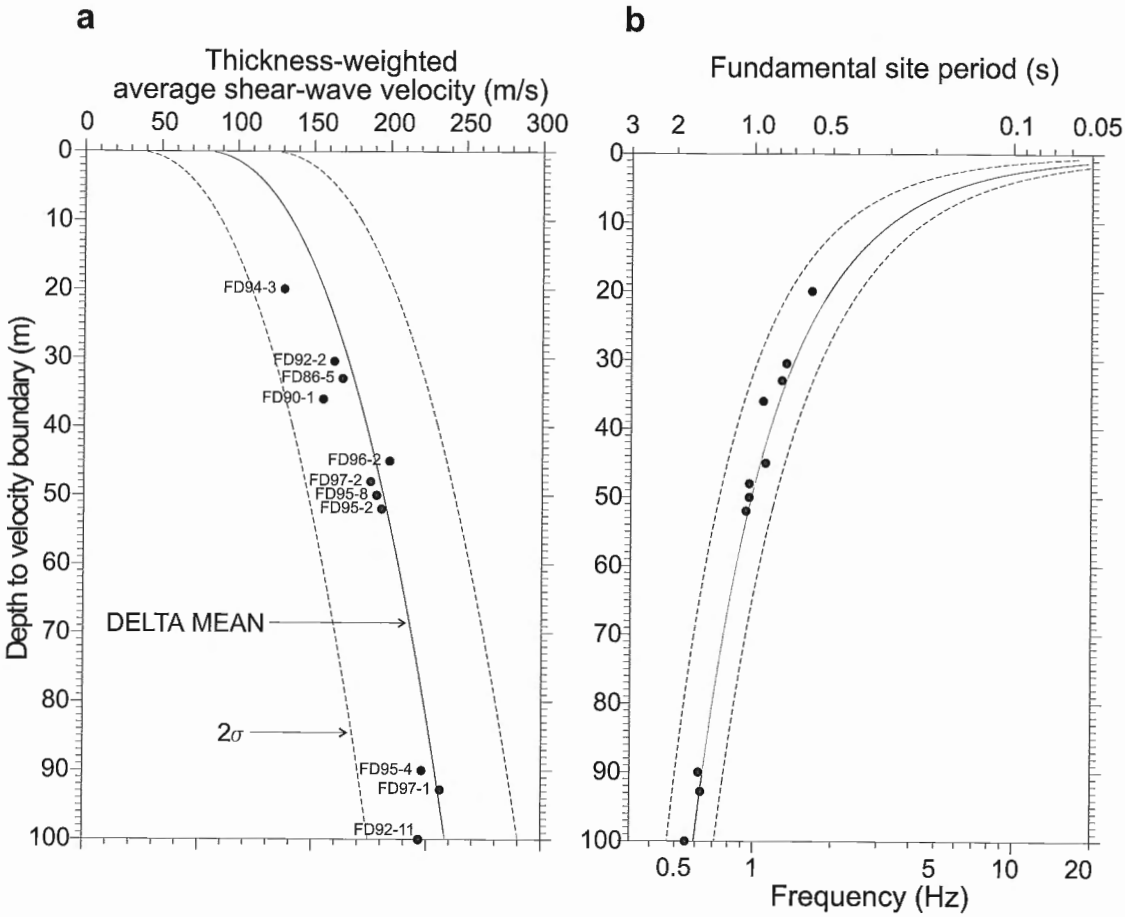

Figure 21. a) *Thickness-weighted, average, shear-wave velocity in Holocene deltaic sediments, derived from the mean curve in Figure 13; dashed lines are ± two standard deviation limits.* ***b)*** *Relationship between resonant frequencies (periods) of earthquake ground motion and depth to the Holocene-Pleistocene boundary from the velocity-depth curve in a); data are from boreholes in which Pleistocene deposits were penetrated and shear-wave velocity contrasts were measured.*

Borehole geophysical techniques have been applied in more than 40 holes drilled on the Fraser delta. Lithological information can be obtained from natural gamma and magnetic susceptibility logs, and pore-water salinity variations can be estimated from the conductivity log. The compressional-wave velocity log has been used to detect presence of gas in pore spaces and to delineate lithological boundaries. The shear-wave velocity log has provided regional velocity-depth information required for earthquake liquefaction resistance estimates and ground-motion amplification modelling. Horizontal shear-wave velocity anisotropy, found in one borehole on the Fraser delta, has been attributed to horizontal stress anisotropy in Holocene sediments. High-quality shear-wave velocity logs have also been obtained at more than 70 sites on the delta using the seismic cone penetrometer.

Surface shear-wave techniques have been used at over 100 locations on the Fraser delta to measure near-surface velocity-depth gradients. The shear-wave refraction method and the spectral analysis of surface wave method provide information to approximately 50 m below the surface; deeper penetration (to 250 m depth) has been achieved with the refraction method at favourable sites.

Electromagnetic soundings have been made on the southern Fraser delta to determine the vertical extent of saline pore water within the deltaic sequence. Much of the deltaic sediments have high pore-water salinity (high electrical conductivity). In such environments, the maximum depth of penetration of electromagnetic techniques that have been used to date is approximately 90 m. In many places, there is a strong conductivity gradient in fine-grained sediments near the base of the deltaic sequence; it is possible that saline water is being leached from this zone, giving rise to geotechnically 'sensitive clays'. Electromagnetic techniques employed to date are limited to approximately 90 m depth penetration in a saline pore-water deltaic environment.

Shear-wave velocity is perhaps the most important geophysical parameter obtained from this work for earthquake hazard applications. Delta-wide estimates of shear-wave velocity have been obtained from the ground surface to

3500 m depth using several geophysical techniques. Two buried surfaces of particular interest for earthquake modelling on the delta are the Holocene-Pleistocene and Quaternary-Tertiary surfaces. Direct measurement of the shear-wave velocity discontinuity at the Holocene-Pleistocene boundary is limited to some surface shear-wave refraction surveys and a few borehole shear-wave logs on which the boundary has been identified. Subsurface information is insufficient to map either the depth or magnitude of this velocity discontinuity over the entire delta. The Quaternary-Tertiary surface has been mapped over a large part of the delta in a reconnaissance manner; however, no direct borehole measurements have yet been made of the shear-wave velocity contrast at this boundary.

ACKNOWLEDGMENTS

We wish to thank the critical reviewers P.G. Killeen (GSC), D.C. Mosher (GSC), J.J. Clague (GSC), and W.D.L. Finn (University of British Columbia) for helpful suggestions which led to substantial improvements in this paper. SCPT and SASW tests at Geological Survey of Canada sites were done by Conetec Investigations Ltd. under the direction of Mr. David Woeller. Shear-wave seismic downhole logs in three deep (300+ m) boreholes were obtained by Frontier Geosciences Inc.; we thank Russell Hillman and Clifford Candy for processing the records and ensuring that they are of high quality. We acknowledge the support of many people who have helped with various surveys, including Upaal Attakorala (Golder Associates), Jim Britton (Dynamic Oil Ltd.), John Clows (Municipality of Delta), Dennis Dingle (Foundex Explorations Ltd.), Harry Jol (University of Wisconsin), Glen Jolly (Conetec Investigations Ltd.), Pavel Kurfurst (GSC Ottawa), Vic Levson (B.C. Geological Survey), Robert MacDonald (GSC Pacific), Pat Monahan (B.C. Geological Survey), Mike Roberts (Simon Fraser University), Ray Roussey (Sonic Drilling Ltd.), Robert Switzer (Corporation of Richmond), and Brian Todd (consultant). We especially wish to acknowledge the support of Dr. W.D.L. Finn (University of British Columbia) who, over the last decade, has provided us inspiration and guidance.

REFERENCES

Alvarez, R.
1990a: Structure of the basin of Mexico City and its relation to destruction in the earthquake of 1985; in Geotechnical and Environmental Geophysics, (ed.) S. H. Ward; Society of Exploration Geophysicists, Tulsa, Oklahoma, v. 3, p. 263-280.

Andrus, R.D. and Stokoe, K.H., II
1996: Guidelines for evaluating liquefaction resistance using in situ shear wave velocity; in Proceedings of a Symposium on Recent Developments in Seismic Liquefaction Assessment, Section 3; Conetec Ltd., Vancouver, British Columbia, p 1-23.

Armstrong, J.E. and Hicock, S.R.
1979: Surficial geology, Vancouver, British Columbia; Geological Survey of Canada, Map 1486A, scale 1:50 000.

Bard, P.Y. and Bouchon, M.
1980: The seismic response of sediment-filled valleys. Part I. The case of incident SH waves; Bulletin of the Seismological Society of America, v. 70, p. 1263-1286.
1985: The two-dimensional resonance of sediment-filled valleys; Bulletin of the Seismological Society of America, v. 75, p. 519-541.

Bard, P.Y. and Chavez-Garcia, F.J.
1993: On the decoupling of surficial sediments from surrounding geology at Mexico City; Bulletin of the Seismological Society of America, v. 83, p. 1979-1991.

Best, M.E. and Todd, B.J.
1996: Electromagnetic soundings, pseudo-resistivity logs and implications for porosity and ground water salinity; in Proceedings, Symposium of the Application of Geophysics to Engineering and Environmental Problems, Keystone, Colorado, p. 1061-1074.

Brandt, H.
1960: Factors affecting compressional wave velocity in unconsolidated marine sand sediments; Journal of the Acoustical Society of America, v. 32, p. 171-179.

Britton, J.R., Harris, J.B., Hunter, J.A., and Luternauer, J.L.
1995: The bedrock surface beneath the Fraser River delta in British Columbia based on seismic measurements; in Current Research 1995-E; Geological Survey of Canada, p. 83-89.

Byrne, P.M. and Anderson, D.L.
1987: Earthquake design in Richmond, B.C., version II; University of British Columbia, Department of Civil Engineering, Soil Mechanics Series, No. 109, 90 p.

Chang, S.W., Bray, J.D., and Seed, R.B.
1994: Geotechnical aspects of the Northridge earthquake of January 17, 1994: ground motions and damage patterns; Geotechnical News, June 1994, p. 49-52.

Christian, H.A., Mosher, D.C., Barrie, J.V., Hunter, J.A., and Luternauer, J.L.
1998: Seabed instability on the Fraser River delta; in Geology and Natural Hazards of the Fraser River Delta, British Columbia, (ed.) J.J. Clague, J.L. Luternauer, and D.C. Mosher; Geological Survey of Canada, Bulletin 525, this volume.

Clague, J.J., Luternauer, J.L., Monahan, P.A., Edwardson, K.A., Dallimore, S.R., and Hunter, J.A.
1998: Quaternary stratigraphy and evolution of the Fraser delta; in Geology and Natural Hazards of the Fraser River Delta, British Columbia, (ed.) J.J. Clague, J.L. Luternauer, and D.C. Mosher; Geological Survey of Canada, Bulletin 525, this volume.

Clague, J.J., Luternauer, J.L., Pullan, S.E., and Hunter, J.A.
1991: Postglacial deltaic sediments, southern Fraser River delta, British Columbia; Canadian Journal of Earth Sciences, v. 28, p. 1386-1393.

Dallimore, S.R., Edwardson, K.A., Hunter J.A., Clague, J.J., and Luternauer, J.L.
1995: Composite geotechnical logs for two deep boreholes in the Fraser River delta, British Columbia; Geological Survey of Canada, Open File 3018, 3 sheets.

Dallimore, S.R., Edwardson, K.A., Hunter, J.A., Meldrum, J.L., Luternauer, J.L., and Clague, J.J.
1996: Composite geotechnical logs for a deep borehole at the Richmond City Hall; Geological Survey of Canada, Open File 3356, 3 sheets.

Dix, C.H.
1955: Seismic velocities from surface measurements; Geophysics, v. 20, p. 68-86.

Finn, W.D.L.
1996: Evaluation of liquefaction potential for different earthquake magnitudes and site conditions; in Proceedings of a Symposium on Recent Developments in Seismic Liquefaction Assessment, Section 4; Conetec Ltd., Vancouver, British Columbia, p. 1-34.

Frankel, A.
1993: Three-dimensional simulations of ground motions in the San Bernadino valley, California, for hypothetical earthquakes on the San Andreas fault; Bulletin of the Seismological Society of America, v. 83, p. 1020-1041.

Frankel, A. and Vidale, J.
1992: A three-dimensional simulation of seismic waves in the Santa Clara valley, California, from a Loma Prieta aftershock; Bulletin of the Seismological Society of America, v. 82, p. 2045-2074.

Graves, R.W.
1993: Modelling three-dimensional site response effects in the Marina District basin, San Francisco, California; Bulletin of the Seismological Society of America, v. 83, p. 1042-1063.

Harris, J.B., Hunter, J.A., Burns, R.A., Good, R.L., and Luternauer, J.L.
1996: Observation of shear-wave splitting in Holocene sediments of the Fraser River delta, British Columbia; 7th International Workshop on Seismic Anisotropy, Miami, Florida, Abstracts, p. 16.

Harris, J.B., Hunter, J.A., Luternauer, J.L., and Finn, W.D.L.
1995: Site response modelling of the Fraser River delta, British Columbia: preliminary results from two deep boreholes; in Current Research 1995-E; Geological Survey of Canada, p. 69-75.

Hunter, J.A.
1971: A computer method to obtain the velocity-depth function from seismic refraction data; in Report of Activities, Part B; Geological Survey of Canada, Paper 71-1B, p. 40-48.
1995: Shear wave velocities of Holocene sediments, Fraser River delta, British Columbia; in Current Research 1995-A; Geological Survey of Canada, p. 29-32.

Hunter, J.A. and Burns, R.A.
1991: Determination of overburden P-wave velocities with a downhole 12-channel eel; in Current Research, Part D; Geological Survey of Canada, Paper 91-1D, p. 61-65.

Hunter, J.A. and Woeller, D.J.
1990: Comparison of surface, borehole, and seismic cone penetrometer methods of determining the shallow shear-wave velocity structure in the Fraser River delta, British Columbia; 60th Annual Meeting, Society of Exploration Geophysicists, San Francisco, California, Expanded Abstracts, p. 385-388.

Hunter, J.A., Dallimore, S.R., and Christian, H.A.
1996a: Borehole measurements of shear wave velocity discontinuities in Quaternary sediments, Fraser River delta, British Columbia; in Current Research 1997-A; Geological Survey of Canada, p. 159-165.

Hunter, J.A., Harris, J.B., and Britton, J.R.
1996b: Compressional and shear wave interval velocity data for Quaternary sediments in the Fraser River delta from multichannel seismic reflection surveys; Geological Survey of Canada, Open File 3325, 228 p.

Hunter, J.A., Luternauer, J.L., and Kurfurst, P.J.
1996c: Regional electromagnetic soundings with the Geonics EM-34 conductivity meter in the southern Fraser River delta, B.C.; Geological Survey of Canada, Open File 3359, 141 p.

Hunter, J.A., Luternauer, J.L., Neave, K.G., Pullan, S.E., Good, R.L., Burns, R.A., and Douma, M.
1992: Shallow shear-wave velocity-depth data in the Fraser delta, from surface refraction measurements, 1989, 1990, 1991; Geological Survey of Canada, Open File 2504, 270 p.

Hunter, J.A., Pullan, S.E., Burns, R.A., Gagne, R.M., and Good, R.L.
1989: Applications of a shallow reflection method to groundwater and engineering studies; in Proceedings Explorations '87; Third Decennial International Conference on Geophysical and Geochemical Explorations for Minerals and Groundwater, (ed.) G.D. Garland; Ontario Geological Survey, Special Volume 3, p. 704-715.

Hunter, J.A., Woeller, D.J., Addo, K.O., Luternauer, J.L., and Pullan, S.E.
1993: Application of shear wave seismic techniques to earthquake hazard mapping in the Fraser River delta, British Columbia; 63th Annual Meeting, Society of Exploration Geophysicists, Washington, D.C., Expanded Abstracts, p. 501-503.

Hunter, J.A., Woeller, D.J., and Luternauer, J.L.
1991: Comparison of surface, borehole and seismic cone penetrometer methods of determining the shallow shear wave velocity structure in the Fraser River delta, British Columbia; in Current Research, Part A; Geological Survey of Canada, Paper 91-1A, p.23-26.

Jol, H.M.
1988: Seismic stratigraphic analysis of the southeastern Fraser River delta, British Columbia; M.Sc. thesis, Simon Fraser University, Burnaby, British Columbia, 176 p.

Jol, H.M. and Roberts, M.C.
1988: The seismic facies of a delta onlapping an offshore island: Fraser River delta, British Columbia; in Sequences, Stratigraphy, Sedimentology: Surface and Subsurface, (ed.) D.P. James and D.A. Leckie; Canadian Society of Petroleum Geologists, Memoir 15, p. 137-142.

Kayen, R.E., Mitchell, J.K., Seed, R.B., Lodge, A., Nishio, S., and Coutinho, R.
1992: Evaluation of SPT-, CPT- and shear wave-based methods for liquefaction potential assessment using Loma Prieta data; in Proceedings of the Fourth Japan-U.S. Workshop on Earthquake Resistant Design of Lifeline Facilities and Countermeasures for Soil Liquefaction; National Center for Earthquake Engineering Research, Report NCEER-92-0019, v. 1, p. 177-204.

Lindsley, D.H., Andreasen, G.E., and Balsley, J.R.
1966: Magnetic properties of rocks and minerals; in Handbook of Physical Constants, (ed.) S.P. Clark; Geological Society of America, Memoir 97, p. 543-552.

Lomnitz, C.
1990: Mexico 1985: the case for gravity waves; Geophysical Journal International, v. 102, p. 569-572.

Luternauer, J.L. and Hunter, J.A.
1996: Mapping Pleistocene deposits beneath the Fraser River delta; preliminary geological and geophysical results; in Current Research 1996-E; Geological Survey of Canada, p.41-48.

Luternauer, J.L., Clague, J.J., Hamilton, T.S., Hunter, J.A., Pullan, S.E., and Roberts, M.C.
1986: Structure and stratigraphy of the southwestern Fraser River delta; a trial shallow seismic profiling and coring survey; in Current Research, Part B; Geological Survey of Canada, Paper 86-1B, p. 707-714.

Lynn, H.B.
1991: Field measurements of azimuthal anisotropy; first 60 meters, San Francisco Bay area, CA, and estimation of horizontal stresses' ratio from V_{s1}/V_{s2}; Geophysics, v. 56, p. 822-832.

McNeill, J.D.
1986: Geonics EM39 borehole conductivity meter - theory of operation; Geonics Ltd., Mississauga, Ontario, Technical Note TN-20, 14 p.
1990: Use of electromagnetic methods for groundwater studies; in Geotechnical and Environmental Geophysics, (ed.) S.H. Ward; Society of Exploration Geophysicists, Tulsa, Oklahoma, v. 1, p. 191-218.

McNeill, J.D., Bosnar, M., and Snelgrove, F.B.
1988: A borehole induction logger for monitoring groundwater contamination; Geonics Ltd; Mississauga, Ontario, Technical Note TN-25, 28 p.

McNeill, G.D., Hunter, J.A., and Bosnar, M.
1996: Application of a borehole induction magnetic susceptibility logger to shallow lithological mapping; Journal of Environmental and Engineering Geophysics, v. 0, p. 77-90.

Milne,W.G., Rogers, G.C., Riddihough, R.R., McMechan, G.A., and Hyndman, R.D.
1978: Seismicity of western Canada; Canadian Journal of Earth Sciences, v. 15, p. 1170-1193.

Monahan, P.A., Luternauer, J.L., and Barrie, J.V.
1993: A delta plain "sheet" sand in the Fraser River Delta, British Columbia, Canada; Quaternary International, v. 20, p. 27-38.

National Research Council of Canada
1995: National Building Code of Canada; National Research Council of Canada, Canadian Commission on Building and Fire Codes, Ottawa, Ontario, 571 p.

Pullan, S.E. and Hunter, J.A.
1987: Application of the "optimum offset"' shallow reflection technique in the Fraser delta, British Columbia; 56th Annual Meeting, Society of Exploration Geophysicists, New Orleans, Louisiana, Expanded Abstracts, p. 244-246.

Pullan, S.E. and MacAulay, H.A.
1987: An in-hole shotgun source for engineering seismic surveys; Geophysics, v. 52, p. 985-996.

Pullan, S.E., Hunter, J.A., Jol, H.M., Roberts, M.C., Burns, R.A., and Harris, J.B.
1998: Seismostratigraphic investigations of the southern Fraser River delta; in Geology and Natural Hazards of the Fraser River Delta, British Columbia, (ed.) J.J. Clague, J.L. Luternauer, and D.C. Mosher; Geological Survey of Canada, Bulletin 525, this volume.

Pullan, S.E., Jol, H.M., Gagne, R.M., and Hunter, J.A.
1989: Compilation of high resolution "optimum offset", shallow seismic reflection profiles from the southern Fraser River delta, British Columbia; Geological Survey of Canada, Open File 1992, 16 p.

Pullan, S.E., Miller, R.D., Hunter, J.A., and Steeples, D.W.
1991: Shallow seismic reflection surveys- CDP or "optimum offset"?; 61st Annual Meeting, Society of Exploration Geophysicists, Houston, Texas, Expanded Abstracts, v. 1, p. 576-579.

Rial, J.A.
1989: Seismic wave resonances in 3-D sedimentary basins; Geophysical Journal International, v. 99, p. 81-90.

Rial, J.A., Saltzman, N.G., and Ling, H.
1992: Earthquake-induced resonance in sedimentary basins; American Scientist, v. 80, p. 566-578

Ricketts, B.D.
1998: Groundwater flow beneath the Fraser River delta, British Columbia: a preliminary model; in Geology and Natural Hazards of the Fraser River Delta, British Columbia, (ed.) J.J. Clague, J.L. Luternauer, and D.C. Mosher; Geological Survey of Canada, Bulletin 525, this volume.

Roberts, M.C., Pullan, S.E., and Hunter, J.A.
1992: Applications of land-based high resolution seismic reflection analysis to Quaternary and geomorphic research; Quaternary Science Reviews, v. 11, p. 557-568.

Robertson, P.K.
1990: Seismic cone penetration testing for evaluating liquefaction potential; in Proceedings of a Seminar on Recent Advances in Earthquake Design Using Laboratory and In-situ Tests, Section 5; Conetec Ltd., Vancouver, British Columbia, p 1-36.

Robertson, P.K. and Addo, K.O.
1991: Recent in-situ methods to determine seismic velocity profiles; Geotechnical News, September 1991, p. 26-30.

Robertson, P.K. and Fear, C.E.
1996: Soil liquefaction and its evaluation based on SPT and CPT; in Proceedings of a Symposium on Recent Developments in Seismic Liquefaction Assessment, Section 2; Conetec Ltd., Vancouver, British Columbia, p. 1-52.

Robertson, P.K., Campanella, R.G., Gillespie, D., and Rice, A.
1986: Seismic CPT to measure in-situ shear wave velocity; American Society of Civil Engineers, Journal of the Geotechnical Division, v. 112, p. 971-802.

Robertson, P.K., Woeller, D.J., and Finn, W.D.L.
1992: Seismic cone penetrometer test for evaluating liquefaction potential under cyclic loading; Canadian Geotechnical Journal, v. 29, p. 686-695.

Roesler, S.K.
1979: Anisotropic shear modulus due to stress anisotropy; American Society of Civil Engineers, Journal of Geotechnical Engineering Division, v. 105, p. 871-880.

Rogers, G.C., Cassidy, J.F., and Weichert, D.H.
1998: Variation in earthquake ground motion on the Fraser delta from strong motion seismograph records; in Geology and Natural Hazards of the Fraser River Delta, British Columbia, (ed.) J.J. Clague, J.L. Luternauer, and D.C. Mosher; Geological Survey of Canada, Bulletin 525, this volume.

Schuster, G., Benz, H., Murphy, M., Hill, J., Sikorski, C., and Tsay, C.W.
1990: Prediction of seismic ground amplification by forward modelling techniques; in Geotechnical and Environmental Geophysics, (ed.) S.H. Ward; Society of Exploration Geophysicists, Tulsa, Oklahoma, v. 3, p. 1-21.

Seed, H.B. and de Alba, P.
1986: Use of SPT and CPT tests for evaluating the liquefaction resistance of sands; in Use of In-situ Tests in Geotechnical Engineering; American Society of Civil Engineers, Geotechnical Special Publication, No. 6, p. 281-302.

Seed, H.B. and Idriss, I.M.
1982: Ground motions and soil liquefaction during earthquakes; University of California, Earthquake Engineering Research Institute Monograph; Berkeley, California, 134 p.

Seed, H.B., Tokimatsu, K., Harder, L.F., and Chung, R.
1985: Influence of SPT procedures in soil liquefaction resistance evaluations; American Society of Civil Engineers, Journal of Geotechnical Engineering, v. 111, p. 1425-1445.

Seligman, T.H., Alvarez-Tostado, J.M., Mateos, J.L., Flores, J., and Novaro, O.
1989: Resonant response models for the Valley of Mexico - I; the elastic inclusion approach; Geophysical Journal International, v. 99, p. 789-799.

Shearer, P.M. and Orcutt, J.A.
1987: Surface and near-surface effects on seismic waves - theory and borehole seismometer results; Bulletin of the Seismological Society of America, v. 77, p. 1168-1196.

Stokoe, K.H., II
1990: In-situ seismic testing of soils for geotechnical earthquake engineering purposes; in Proceedings of a Seminar on Recent Advances in Earthquake Design Using Laboratory and In-situ Tests, Section 4; Conetec Ltd, Vancouver, British Columbia, p. 1-66.

Stokoe, K.H., II, and Nazarian, S.
1985: Use of Rayleigh waves in liquefaction studies; in Proceedings of Session on Measurement and Use of Shear Wave Velocity for Evaluating Dynamic Soil Properties, (ed.) R.D. Woods; American Society of Civil Engineers, Geotechnical Engineering Division, Denver, Colorado, p. 1-17.

Stokoe, K.H., II, Nazarian, S., Rix, G.J., Sanchez-Salinero, I., Sheu, J.C., and Mok, Y.J.
1988a: In situ seismic testing of hard-to-sample soils by surface wave method; in Proceedings, Earthquake Engineering and Soil Dynamics II; American Society of Civil Engineers, Specialty Conference, Salt Lake City, Utah, p. 264-278.

Stokoe, K.H., II, Roesset, J.M., Bierschwale, J.G., and Aouad, M.
1988b: Liquefaction potential of sands from shear wave velocity; in Proceedings, Ninth World Conference on Earthquake Engineering, Tokyo, v. III, p. 213-218.

Stoyer, C.H. and Butler, M.S.
1994: EMIX34PLUS user's manual; Interpex Ltd., Golden, Colorado, 100 p.

Stoyer, C.H., Zerilli, A., Wilson, G and Butler, M.S.
1996: TEMIXXL user's manual, Interpex Ltd., Golden, Colorado, 250 p.

Taylor, K.C., Hess, J.W., and Mazzela, A.
1989: Field evaluation of a slim-hole borehole induction tool; Ground Water Monitoring Review, Winter 1989, p. 10-14.

Telford, W.M., Geldhart, L.P., Sheriff, R.E., and Keys, D.A.
1976: Applied Geophysics; Cambridge University Press, Cambridge, England, 860 p.

Woeller, D.J., Hunter, J.A., and Luternauer, J.L.
1993a: Results of SCPT and SASW testing of the Fraser River delta sediments, British Columbia; Geological Survey of Canada, Open File 2714, 217 p.
1994: Results of seismic cone penetration testing, Fraser River delta, British Columbia, February-March 1994; Geological Survey of Canada, Open File 2956, 166 p.

Woeller, D.J., Luternauer, J.L., and Hunter, J.A.
1993b: Presentation and interpretation of seismic cone penetration test data, Fraser River delta, British Columbia; Geological Survey of Canada, Open File 2715, 80 p.

Morphology, structure, and stratigraphy of the offshore Fraser delta and adjacent Strait of Georgia

D.C. Mosher[1] and T.S. Hamilton[1]

Mosher, D.C. and Hamilton, T.S., 1998: Morphology, structure, and stratigraphy of the offshore Fraser delta and adjacent Strait of Georgia; in Geology and Natural Hazards of the Fraser River Delta, British Columbia, (ed.) J.J. Clague, J.L. Luternauer, and D.C. Mosher; Geological Survey of Canada, Bulletin 525, p. 147–160.

Abstract: The stratigraphic sequence in the southern Strait of Georgia consists of 1) folded and faulted Tertiary and older sedimentary rocks, 2) Pleistocene glacial and interglacial deposits which form distinctive ridges within the strait and below the Fraser delta, 3) glaciomarine sediments dating to the end of the last glaciation, and 4) modern Fraser delta sediments which drape underlying topography and are locally more than 300 m thick. Significant morphologic elements of the Fraser delta include an extensive delta plain, active distributary channels constrained by dikes and jetties, a 200 km^2 delta slope incised by channels, gullies, and sea valleys, an extensive prodelta, a large sedimentary failure on the southern portion of the modern delta, and an area of ridges and troughs in the centre of the Strait of Georgia that are either deformation features or sedimentary bedforms. Natural delta processes have been altered significantly by human activity.

Résumé : La séquence stratigraphique dans le sud du détroit de Georgia comprend les entités suivantes : 1) des roches sédimentaires plissées et faillées du Tertiaire et plus anciennes; 2) des dépôts glaciaires et interglaciaires du Pléistocène qui forment des crêtes distinctes dans le détroit et sous le delta du Fraser; 3) des sédiments glaciomarins datant de la fin de la dernière glaciation; 4) des sédiments récents du delta du Fraser qui recouvrent la topographie sous-jacente et qui mesurent par endroits plus de 300 mètres d'épaisseur. Parmi les éléments morphologiques d'intérêt du delta du Fraser, mentionnons une vaste plaine deltaïque, des défluents actifs limités par des digues et des jetées, un talus deltaïque couvrant une superficie de 200 kilomètres carrés (entaillé de chenaux, de ravins et de vallées sous-marines), une zone prodeltaïque étendue, une grande rupture sédimentaire sur la portion méridionale du delta récent ainsi qu'une zone de crêtes et de cuvettes dans le centre du détroit de Georgia qui sont le résultat soit de la déformation, soit de la sédimentation. Les processus deltaïques naturels ont été grandement modifiés par l'activité anthropique.

[1] Geological Survey of Canada, Pacific Geoscience Centre, P.O. Box 6000, Sidney, British Columbia V8L 4B2

INTRODUCTION

Knowledge of the unconsolidated sediments and bedrock beneath the Fraser delta and the Strait of Georgia is essential to understanding the development of the delta and its associated geohazards (Mosher et al., 1997). This paper presents results of recent geophysical and geological studies by the Geological Survey of Canada on the stratigraphy, structure, and morphology of the southern Strait of Georgia (that part south of about 48°25′N), including the marine portion of the modern Fraser delta (Fig. 1).

REGIONAL GEOLOGICAL SETTING

The regional geological setting of the Fraser River delta is presented elsewhere in this Bulletin (Clague, 1998); consequently, only a brief description is included here as context. The Strait of Georgia lies within the Georgia Basin, which is a structural and sedimentary basin situated between Vancouver Island and the British Columbia mainland. Upper Cretaceous and early Tertiary sandstones, conglomerates, and shales of the Nanaimo Group and the overlying Chuckanut and Huntington formations underlie the Georgia Basin, including

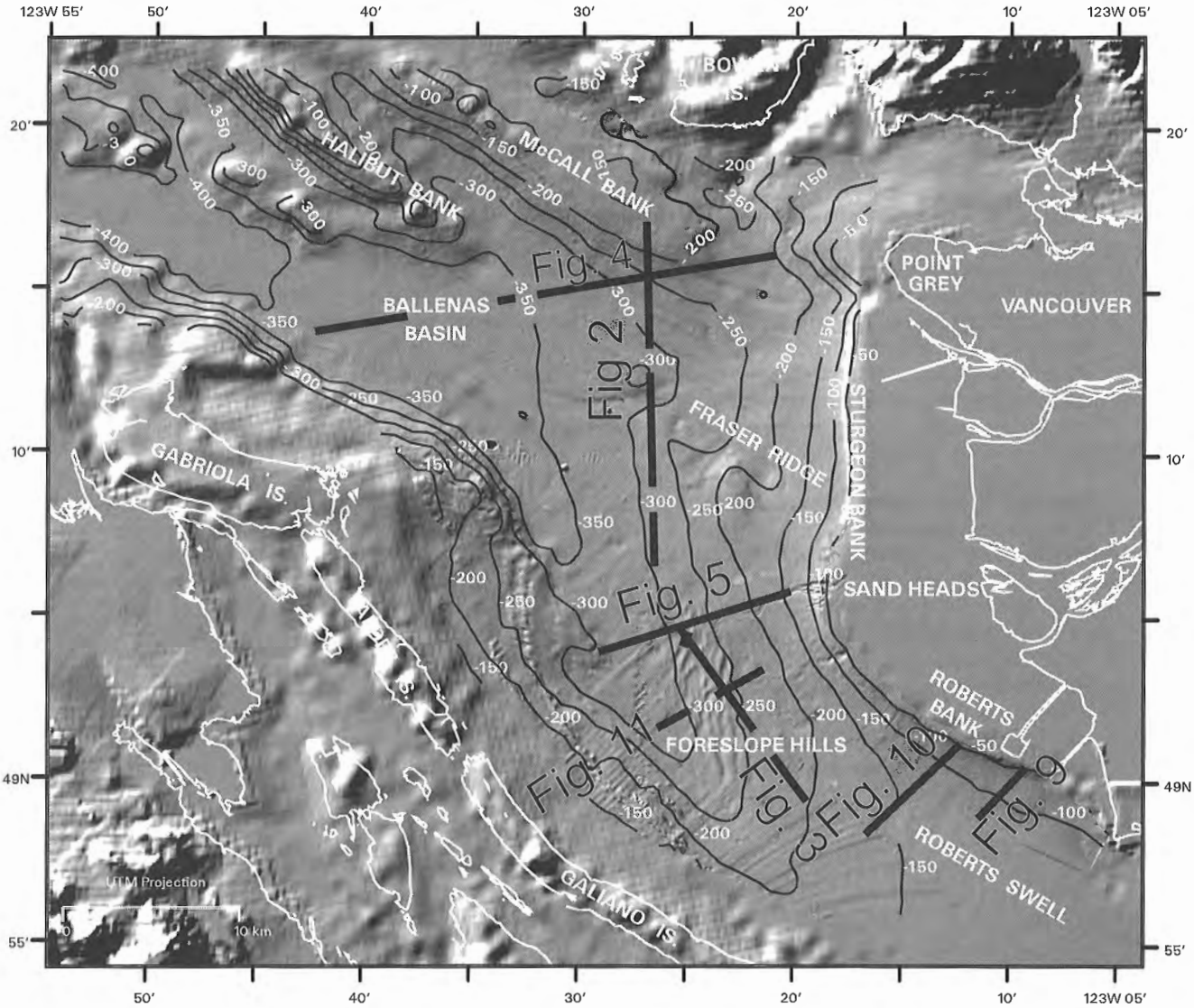

Figure 1. Obliquely illuminated, or shaded relief, image of seafloor bathymetry of the southern Strait of Georgia. Data are digitized from bathymetric field sheets and swath bathymetry surveys. Long, linear or curvilinear features on the seafloor are artifacts of the surveys, probably resulting from poor tidal corrections or positioning errors. Note the series of northwest-trending ridges in the northern part of the area, Sand Heads sea valley and the Foreslope Hills west of the Main Channel of the Fraser River, and Roberts Swell in the extreme south. Straight dark lines indicate the locations of seismic lines shown in this paper.

much of the southern Strait of Georgia (England and Hiscott, 1992; Mustard, 1994; Mustard and Rouse, 1994). These rocks were deeply eroded by glaciers during several Pleistocene glaciations and are mantled by thick Quaternary sediments throughout much of the study area. The structure and stratigraphy of the Quaternary deposits and underlying bedrock in the southern Strait of Georgia are the subjects of numerous papers that are the foundation for this summary (e.g. Tiffin, 1969; Tiffin et al., 1971; Hamilton and Luternauer, 1983; Hamilton and Wigen, 1987; Hamilton, 1991; Hart et al., 1991, 1992a, b, 1995; Mosher et al., 1995).

The Fraser River began to build its delta into the Strait of Georgia about 10 000 ^{14}C yr ago (Clague et al., 1983, 1991; Luternauer et al., 1993, 1994). Although the river has flowed continuously westward into the strait during the last 5000 years, considerable channel meandering and anastomosing is known to have occurred, even in historical times. Channel locations, however, are now fixed by dikes and jetties. Present-day deposition at the Fraser delta front is controlled by tidal, fluvial, and mass wasting processes operating in a high-energy, semi-enclosed marine basin (Luternauer, 1980; Luternauer et al., 1993).

METHODS

Stratigraphic and structural information for this paper was derived from over 5000 line-kilometres of single and multichannel (5, 10, and 40 in^3 airgun and 40 in^3 sleeve gun) and high-resolution (Huntec and Seistec) seismic reflection records (Fig. 1) (Hamilton, 1991; Hart et al., 1991, 1992a; Mosher, 1995; Mosher et al., 1995). Air and sleeve guns create a sharp noise in the water by the sudden release of compressed air. The echoes returning from this sound wave contitute a seismic reflection record. Deep seismic reflection profiles shown in this paper are 6-fold stack, 0.65 L (40 in^3) sleeve-gun multichannel records with a central frequency of about 100 Hz. The high-resolution records are Huntec DTS sparker profiles, with a centre frequency of about 1 kHz. Morphologic information (Fig. 1) has been derived from Canadian Hydrographic Service bathymetric field sheet data and from a recent swath bathymetric survey (Currie and Mosher, 1996).

STRATIGRAPHY OF THE STRAIT OF GEORGIA

Four seismostratigraphic units are recognized from seismic reflection data (Fig. 2 to 5).

Unit 1

The lowest unit is acoustic basement and is referred to as the bedrock facies by Hamilton (1991). It shows sequences of largely parallel seismic reflectors dipping up to 2° in a variety of directions (Fig. 2). The reflectors are commonly truncated at the upper surface of the unit. This surface has considerable relief, probably due to faulting and glacial erosion (Fig. 6). Bedrock crops out at the seafloor on the western side of the Strait of Georgia (Fig. 4, 5) and underlies Quaternary deposits in the center of the strait (Fig. 2 to 5). It is barely discernable through the thick sediments that underlie the delta slope (Fig. 4).

Unit 2

Unit 2 unconformably overlies bedrock. It occurs only locally, but, where present, attains thicknesses of up to 450 m. The upper surface is extremely irregular (Fig. 7), and the seismic character of the unit differs markedly both along and across strike. The unit can be divided into two acoustic facies: 1) a layered sequence with numerous, relatively horizontal reflections; and 2) a sequence with incoherent or amorphous internal reflections and a rough hummocky surface with point reflectors. Reflections in the layered facies are laterally continuous, but are locally folded, faulted, and contorted, and truncate against steep erosional walls. Figures 2, 4, and 5 show especially good examples of unit 2 and its constituent facies.

Unit 3

Units 1 and 2 are unconformably overlain by up to 130 m of sediments characterized by flat-lying, subparallel, semicoherent, high-amplitude reflections. Signal amplitudes of reflectors decrease up-section, but the reflectors become more coherent upward, probably reflecting a change in sedimentation through time. The unit infills deep troughs, is generally buried, and has limited outcrop on the seafloor (Hamilton and Luternauer, 1983). Reflections onlap the margins of troughs. Individual horizons cannot be correlated from trough to trough, but the unit generally thickens to the southeast. The few cores recovered from places where unit 3 is not covered by younger sediments consist of dense, oxidized, organic-poor, laminated and bedded silt; some of the silt contains angular or faceted pebbles. The top of the unit is marked by a regionally extensive, high-amplitude, low-frequency reflection horizon, termed reflector A (Fig. 2 to 5).

Unit 4

The uppermost unit in the succession is characterized by numerous, very low-amplitude reflections. The base of the unit is the regional 'A' reflector, and the top of the unit is the seafloor.

In the central Strait of Georgia, internal reflections of unit 4 are parallel and flat lying, and the unit is up to 200 m thick. Beneath the Fraser delta slope, these reflections dip up to 7° west and have clinoform shapes. The unit is over 250 m thick under the Sturgeon Bank slope, thins to the south over Fraser Ridge near Sand Heads, thickens again towards Canoe Passage, and, finally, thins as unit 2 comes to the surface near Point Roberts. Unit 4 is about 105 m thick at the terminus of the Roberts Bank Deltaport (Christian et al., 1995).

Sediments of unit 4 contain in situ biogenic gas (Hart and Hamilton, 1993). Shallow gas is recognized in the seismic reflection records by gas masking (absorption of acoustic energy) and gas brightening (enhancement of the impedance contrast at a boundary). In the southern half of the survey

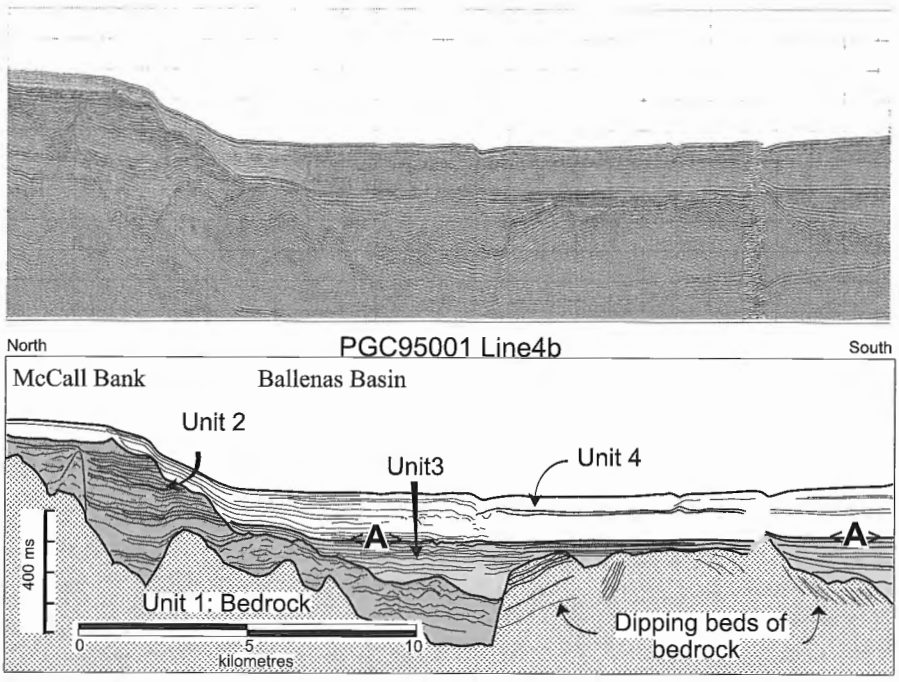

Figure 2. *Seismic reflection record across McCall Bank and Ballenas Basin to just north of the Foreslope Hills (see Fig. 1 for location). The top of the profile is the sea surface. This record provides good examples of the four seismic units. Note truncated reflectors in unit 2 (ice-eroded facies) beneath McCall Bank and dipping reflectors in the bedrock unit near the south end of the profile. The reflector labelled 'A' separates unit 3 (layered facies) from the overlying unit 4 (transparent facies).*

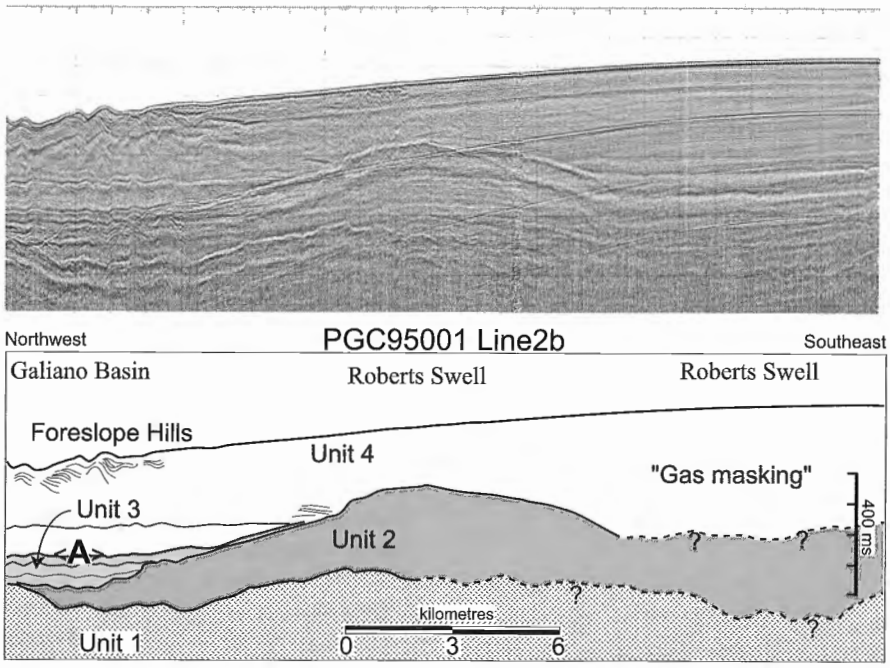

Figure 3. *Seismic reflection record across the Foreslope Hills and Roberts Swell (see Fig. 1 for location). The record shows a buried ridge of bedrock and sediment of unit 2 just south of the Foreslope Hills. Masking due to the presence of in situ biogenic gas in sediments of Roberts Swell is so intense that little detail can be discerned in the seismic section.*

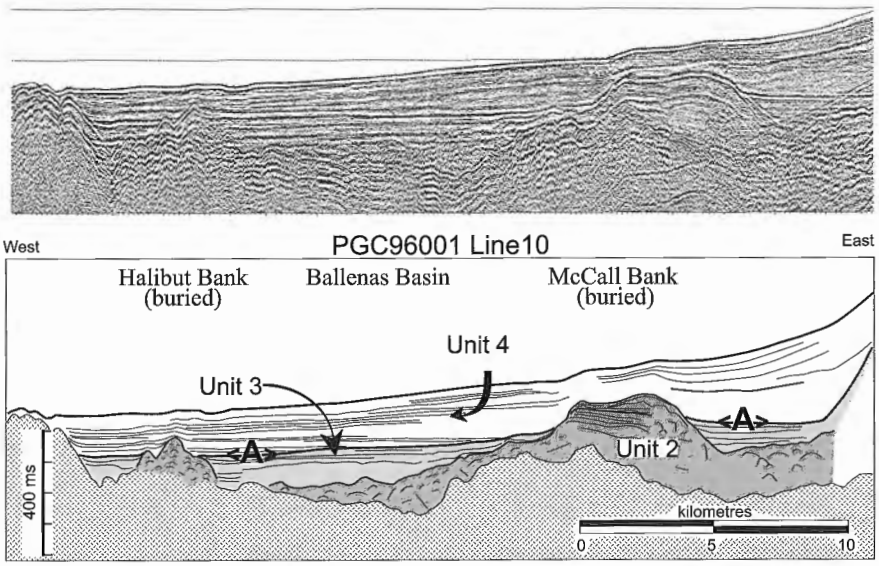

Figure 4. *Seismic reflection record across the northern part of the study area, from Gabriola Island on the west to Point Grey on the east (Fig. 1). Note that units 3 and 4 (layered and transparent facies, respectively) are finely bedded and relatively free of gas. Deeply buried ridges of unit 2 (ice-eroded facies) at the west and east ends of the profile are probably extensions of Halibut and McCall banks, respectively.*

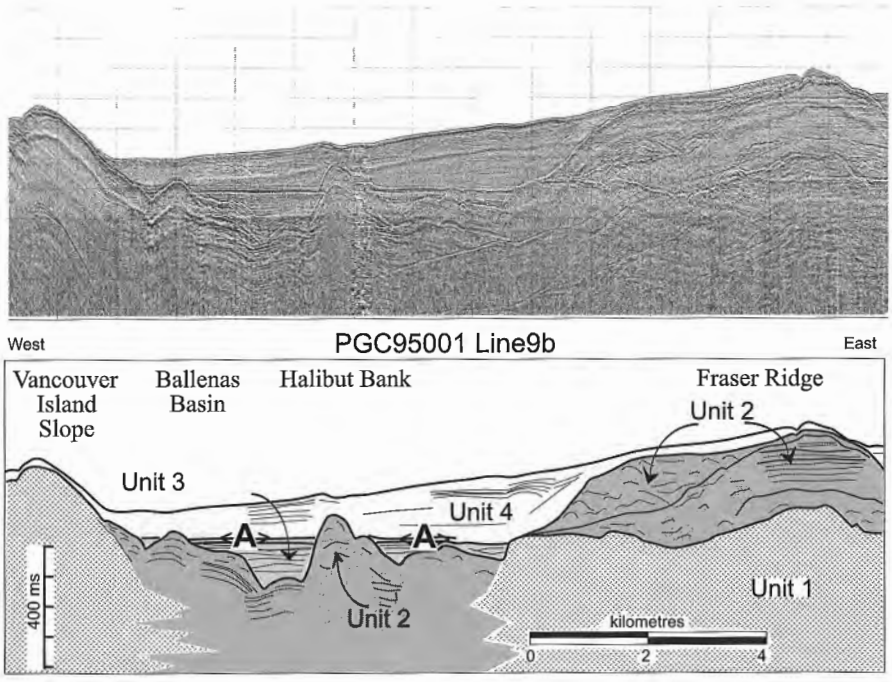

Figure 5. *Seismic reflection record across the Strait of Georgia, from Valdes Island on the west to Fraser Ridge on the east (Fig. 1). This profile shows that Fraser Ridge is composed of sediments of unit 2 (ice-eroded facies), which here comprises two subunits separated by an unconformity. The buried ridge of unit 2 just to the left of the centre of the profile may be an extension of Halibut Bank.*

area, in particular under Roberts Swell and much of the Fraser delta slope, in situ gas impedes acoustic imaging. Little detail of the subbottom stratigraphy is seen in that area as a result.

MORPHOLOGY AND SEDIMENTS

The Strait of Georgia is an elongated basin, about 250 km long and 35-45 km wide, marked by deep basins and several northwest-southeast-trending ridges and banks (Fig. 1). The Fraser River has built its delta into the southern part of the strait from the east; the delta front presently extends from Point Grey on the north to Point Roberts and Boundary Bay on the south. This progradation has reduced the width of the Strait of Georgia in this area by about one-third. Fine-grained sediments transported in the Fraser River plume cover the floor of the Strait of Georgia from the southern end of the study area to at least as far north as Texada Island. These sediments drape the underlying topography.

Hart and Barrie (1995) distinguished three principal morphological zones on the submerged portion of the Fraser delta: the subaqueous delta plain, delta slope (foreslope), and prodelta.

Subaqueous delta plain

The subaqueous part of the delta plain extends from lowest low water to the break in slope at about 10 m water depth. Surface sediments are largely sand and muddy sand; mud is restricted to protected shallow areas and is common only north of the Main Channel (Pharo and Barnes, 1976).

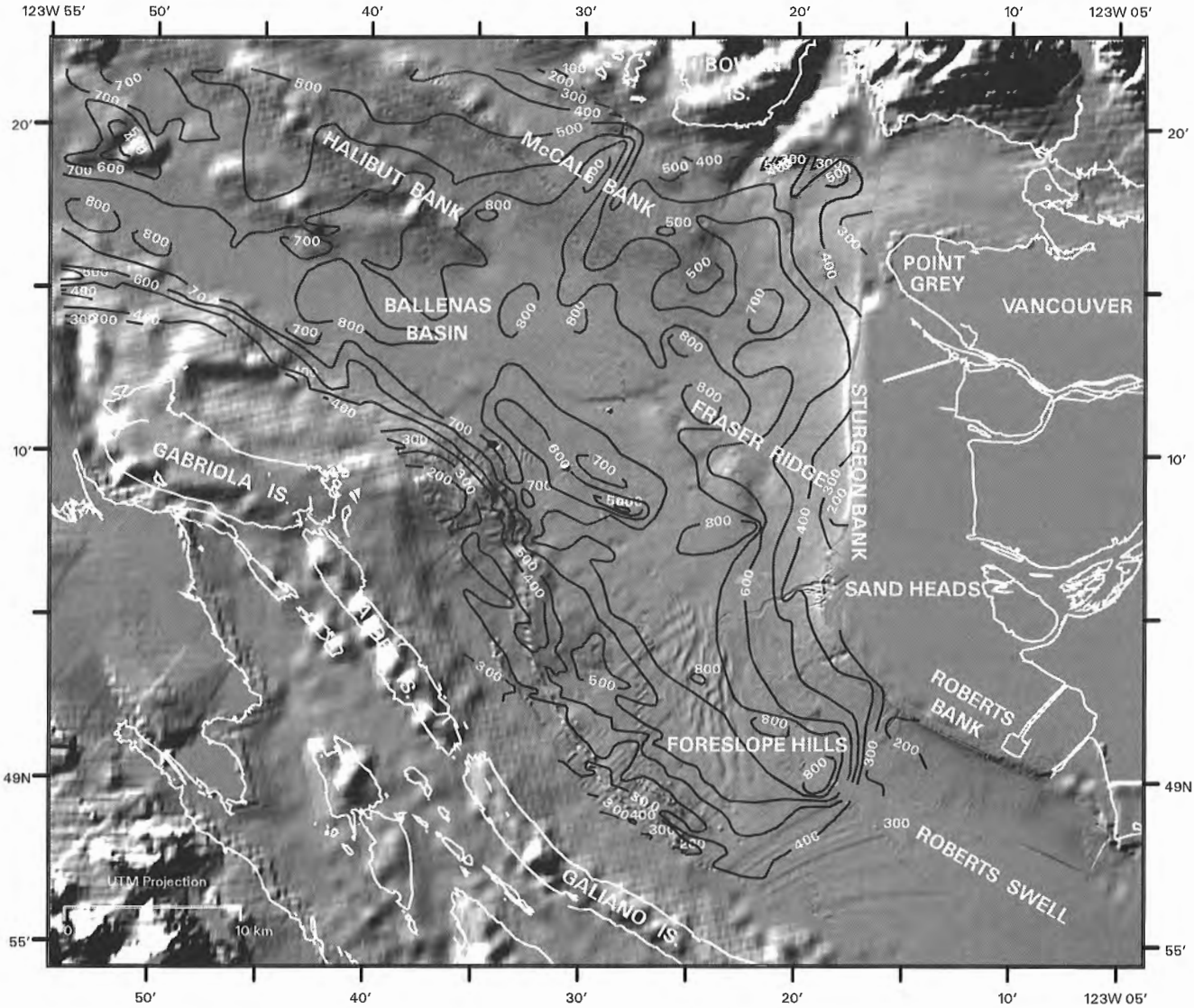

Figure 6. Contours of two-way traveltime to bedrock (from Hamilton, 1991), superimposed on shaded relief bathymetric map of the southern Strait of Georgia. Contour interval is 100 ms.

The subaqueous delta plain slopes gently westward. Its most significant features are the distributary channels that cross it, including the Main Channel, the North and Middle arms, and Canoe Passage. Each of these distributary channels has eroded the delta plain and carries sediment across the intertidal zone to the foreslope of the delta. Since the late 1800s, river flow has been constrained by dikes and jetties, and most of the discharge of the Fraser River is presently carried by the Main Channel. This channel is dredged constantly to maintain a navigable passage.

Delta slope

The active western slope of the Fraser delta ranges from 10 m to more than 250 m deep, and covers an area of 1000 km^2. The gradient of the slope ranges from 0.5° to 23°, averaging about 2°. The delta slope is steepest at its upper break. Slope sediments consist of fine-grained sand, silt, and mud; these sediments fine to the west and north away from the Main Channel (Pharo and Barnes, 1976). The slope is cut by gullies and sea valleys seaward of active distributary channels (Hart et al., 1992c, d, 1993; McKenna et al., 1992; Evoy et al., 1993; Chillarige, 1995; Chillarige et al., 1997; Christian et al., 1997a, 1998).

Sand Heads and associated sea valleys

A network of submarine channels is cut into the delta slope just seaward of Sand Heads, located at the break in slope at the mouth of the Main Channel (Fig. 8). The channels coalesce into a single steep-walled valley farther down the slope (Fig. 1, 8; see also Luternauer et al., 1998). The valley is a

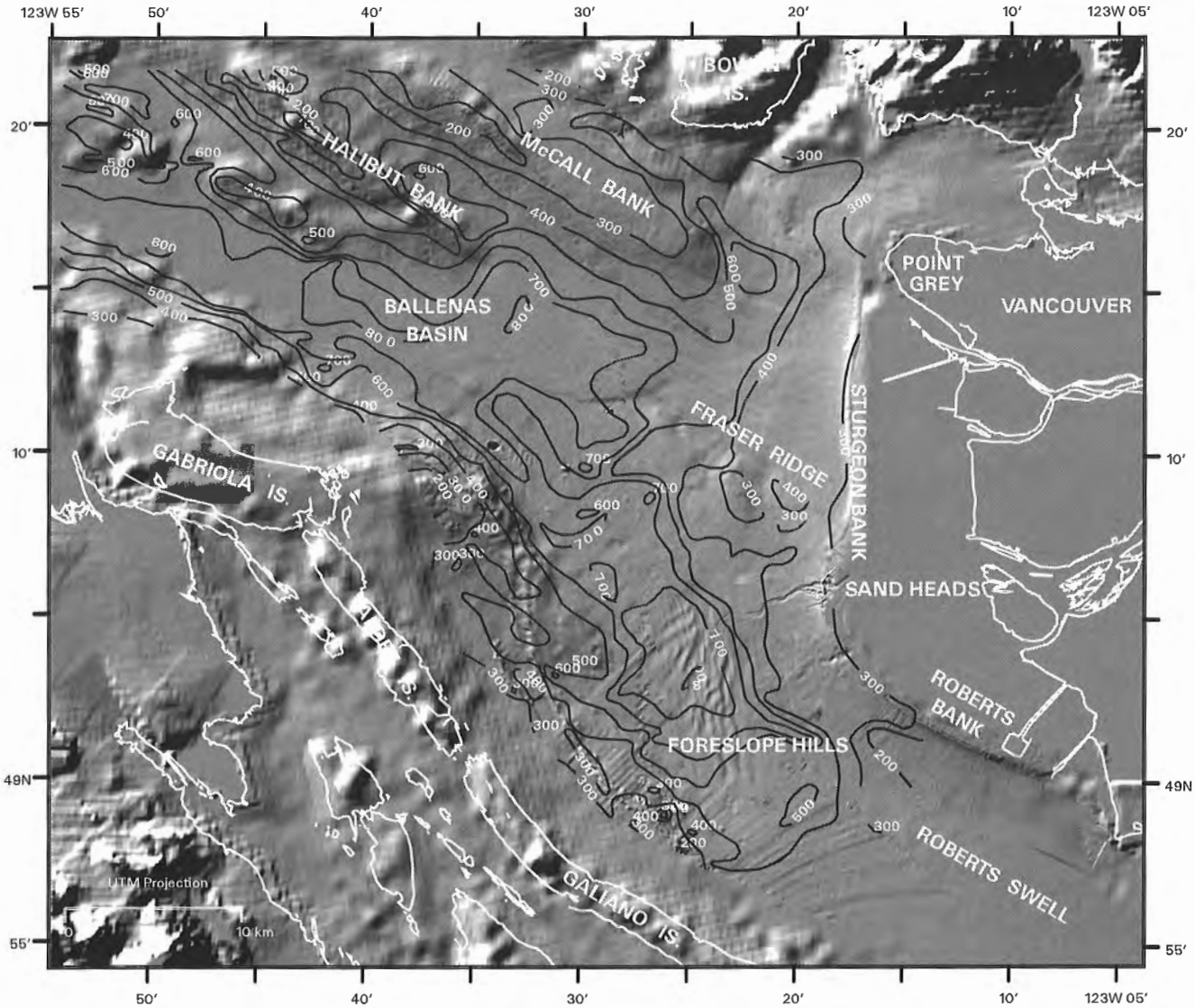

Figure 7. Contours of two-way traveltime to the top of the Pleistocene succession (from Hamilton, 1991), superimposed on shaded relief bathymetric map of the southern Strait of Georgia. Contour interval is 100 ms. Note that there is a fair correspondence between this surface and the present-day bathymetry.

curvilinear feature up to 60 m deep, 100 m wide, and 6 km long, with walls as steep as 45° (Hart et al., 1992c, d). It ends in a fan-shaped lobe of sediment that covers an area of about 30 km^2 at the base of the slope. Gullies and small valleys are also present on the delta slope off the North Arm and Canoe Passage (Fig. 8), but these are smaller than the Sand Heads system.

Southern Roberts Bank slope

The Roberts Bank Failure Complex is a 60 km^2 area of hummocky topography on the Fraser delta slope off southern Roberts Bank (Fig. 8; Terra Surveys, 1994; Currie and Mosher, 1996). This feature is characterized in seismic reflection profiles by contorted, semicoherent and incoherent internal reflections, suggestive of stacked lobes of deformed sediment (Fig. 9, 10). The wedge-shaped toe of the failure complex overlies nondeformed deltaic sediment at the base of the slope, and 1-2 m of nondeformed sediment drapes the feature. The base of the failure complex is defined by a high-amplitude, gas-brightened reflector, which is 70 m below the surface at the break in slope in the vicinity of Roberts Bank Deltaport (Fig. 9).

The seabed on the Roberts Bank slope shows sand waves and dunes that trend at right angles to bathymetric contours; evidence of active sediment transport under the action of strong flood-tidal currents (Fig. 8; Hart et al., 1992d; Kostaschuk et al., 1995; Barrie and Currie, 1997; Luternauer et al., 1998). Sediment samples collected from the sand-wave field consist of 20-68% silt and 32-80% sand (Kostaschuk et al., 1995).

Prodelta and Strait of Georgia

The distal portion of the Fraser delta (the prodelta) extends beyond the foot of the delta slope. Prodelta sediment consists largely of silty clay deposited by turbidity currents originating off distributary channnels and by settling of sediment

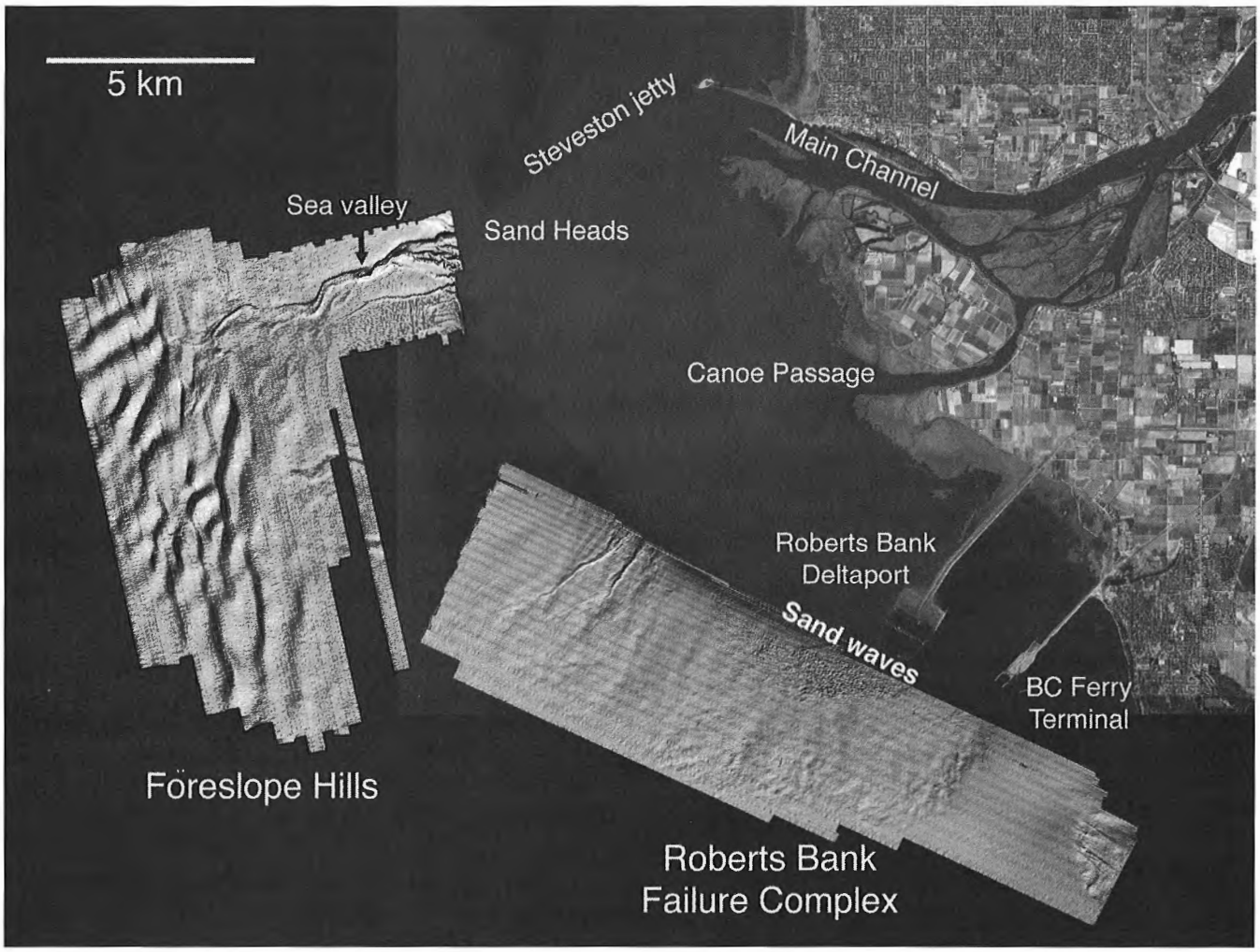

Figure 8. *Shaded-relief images of two areas off the southern Fraser delta surveyed with swath sonar (see Currie and Mosher, 1996, for details of the survey). Features of note are the Sand Heads sea valley, gullies off Canoe Passage, the Foreslope Hills, the Roberts Bank Failure Complex, and a sand-wave field just offshore of the Roberts Bank Deltaport.*

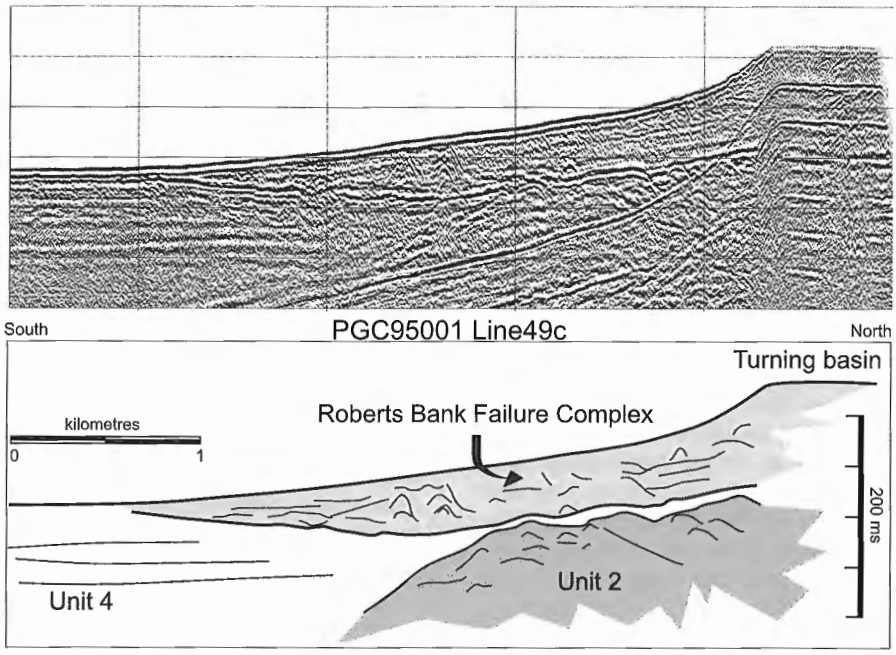

Figure 9. *Seismic reflection record across the Roberts Bank Failure Complex (Fig. 1). The failure complex is within unit 4 (transparent facies). The base of the complex is delineated by a high-amplitude, gas-brightened reflector. This reflector is about 100 ms (50-75 m) below the seafloor at the break in slope between the delta plain and the delta slope.*

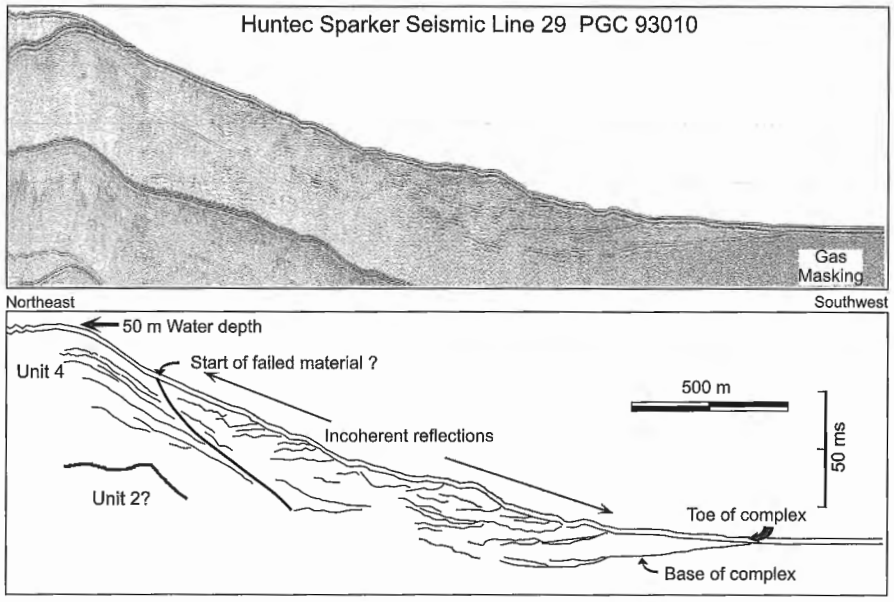

Figure 10. *Huntec DTS sparker, high-resolution, seismic reflection profile over the Roberts Bank Failure Complex just south of the profile shown in Figure 9. Note the hummocky seafloor and the incoherent to semicoherent internal reflections.*

suspended in the river plume (Pharo and Barnes, 1976). The prodelta sediment sequence thins and fines away from the delta, drapes underlying topography, and fills in low areas.

The southernmost part of the prodelta, which is referred to as Roberts Swell (Fig. 1, 3), appears to be underlain by a thick sequence of prodelta sediments that are possibly indicative of an earlier phase of delta growth (Tiffin, 1969; Hamilton, 1991). This sequence has a maximum thickness of about 500 ms (two-way traveltime), or about 330 m assuming an acoustic velocity of 1300 m/s. Roberts Swell reaches depths as shallow as 140 m in the southeast and deepens to the northwest.

North of Roberts Swell and west of Sand Heads is an area of ridges and troughs known as the Foreslope Hills (Fig. 1, 3, 8, and 11). These features cover an area of 60 km^2 at water depths between 230 and 330 m. Swath bathymetric data clearly delineate the ridges, which are up to 5 km long and 20 m high, with wavelengths of 500-600 m (Fig. 8). The orientation of the ridges changes from east-northeast in the northern part of the area to almost due north in the south (Fig. 8).

The Foreslope Hills are underlain by about 350 m of sediment. They do not mimic deeper structure, but rather appear to involve only the uppermost 100 m of the sediment sequence (Fig. 3, 11). Gas obscures the internal structure in acoustic images, but the uppermost reflections are asymmetrical and resemble cross-bedding (Fig. 3, 11).

The area north of the Foreslope Hills and west of Sturgeon Bank is crossed by three northwest-trending ridges: Fraser Ridge, Halibut Bank, and McCall Bank (Fig. 1). Fraser Ridge rises to the southeast to within 148 m of the sea surface and extends beneath the Fraser delta slope. Its north and northwest sides are steep, sloping more than 14°. Halibut Bank is as shallow as 27 m below sea level, and McCall Bank as shallow as 29 m. These ridges have steep flanks, with slopes up to 14°. Several submarine channels traverse the north flank of McCall Bank between depths of 140 and 180 m. The largest of these channels is about 4 m deep and 2.5 km long. In addition, submarine terraces occur on the flanks of these ridges and are especially conspicuous on the southern flank of McCall Bank. The terraces are typically 250-500 m wide and occur at depths of 240 to 300 m.

The deep area separating the aforementioned ridges is Ballenas Basin. It is floored by silty clay (Pharo and Barnes, 1976) and is relatively flat. A steep-sided submarine channel, up to 35 m deep, runs westward across Ballenas Basin between Halibut Bank and Fraser Ridge (Fig. 1; Hamilton and Luternauer, 1983). Extensive fields of pockmarks (gas-escape features) occur on the seafloor at water depths less than 190 m between this channel and McCall Bank (Hart and Hamilton, 1993).

DISCUSSION

Stratigraphy

The interpretation of seismic stratigraphic units is based primarily on the acoustic characteristics of the materials, analysis of short cores, and correlations with onshore geology. Unit 1 is acoustic basement in the seismic reflection records and is likely Cretaceous and Tertiary sedimentary rocks of the Nanaimo Group and the overlying Chuckanut Formation. These rocks crop out on land around the southern Strait of

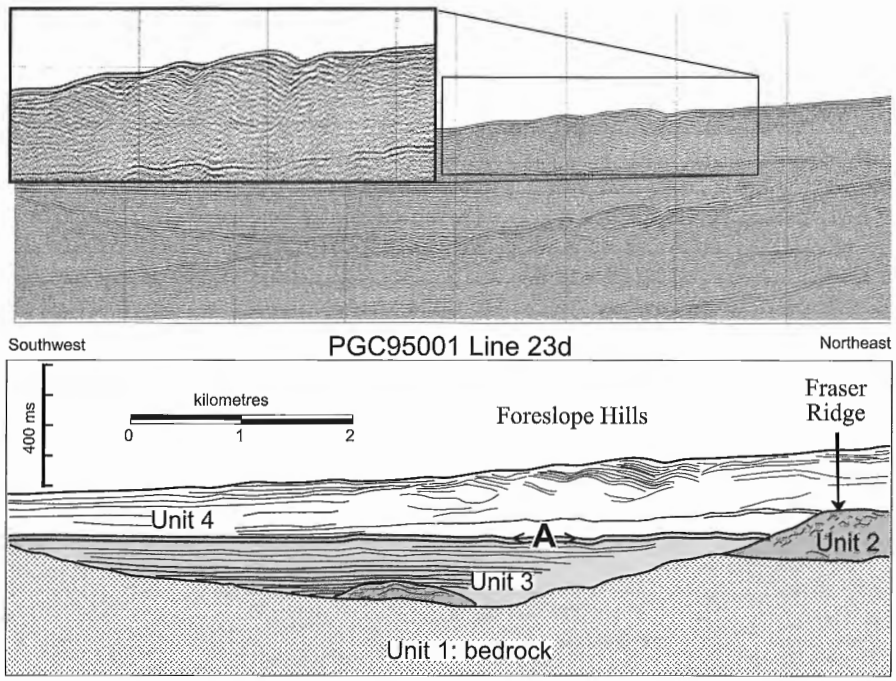

Figure 11. *Seismic reflection record over the Foreslope Hills (Fig. 1). Note the clinoform shape of the internal reflections, shown in detail in the blown-up section.*

Georgia (England and Hiscott, 1992; Mustard, 1994; Mustard and Rouse, 1994). They have been folded and thrust in a north to northwest direction. The upper surface of the unit is an unconformity formed by prolonged erosion during Late Tertiary time (England and Hiscott, 1992). The surface has been further eroded by glaciers during the Pleistocene Epoch. Glacial erosion produced northwest-trending troughs and ridges on the floor of the Strait of Georgia.

Unit 2 is interpreted to be sediments deposited mainly during the episodic advance and retreat of Pleistocene glaciers. This unit is equivalent to the seismic-reflector package called Pleistocene by Clague (1976, 1977b) and Clague et al. (1991). It includes deposits of the last glaciation (Late Wisconsinan or Fraser Glaciation), but the thickest sections are dominated by older Pleistocene deposits (see Armstrong et al., 1965; Hicock and Armstrong, 1983).

Unit 2 consists of stratified glaciomarine sediments and diamicton, represented in seismic reflection records by two distinct acoustic facies. The stratified facies comprises clay, silt, and sand deposited on the seafloor some distance from glacier margins. Contortion and faulting of the sediments are attributed to shearing at the base of a glacier, suggesting that the sediments are older than the last glaciers that occupied the area. The facies with an amorphous acoustic character and point reflectors is probably till or ice-proximal glaciomarine diamicton. The point reflectors are likely boulders. The stratified and non-stratified facies commonly occur in close association. Contacts between the two facies are commonly abrupt, but are not demarcated by a contrast in acoustic impedance. This evidence suggests that the two facies are genetically related and perhaps were deposited in close association at the margin of, and beneath, a retreating glacier. Unit 2 has been sampled in the offshore only in a deep borehole at the Roberts Bank Deltaport at a depth of 106 m below the seafloor (Christian et al., 1995). It crops out extensively, however, on nearby Point Roberts Peninsula and underlies large parts of the lowlands bordering the Strait of Georgia.

Unit 3 occurs in the troughs and basins between ridges. Hart et al. (1995) term it the lower postglacial unit. Sediments of this unit were probably deposited during retreat of glaciers at the end of the Fraser Glaciation, both from turbidity currents and by settling of hemipelagic and ice-rafted detritus from suspension (Hamilton, 1991; Hart et al., 1995).

Reflector A, which delineates the top of unit 3 on seismic reflection records (Figs. 2 to 5), probably records a significant change in oceanography and sedimentation in the Strait of Georgia during postglacial time. Clague (1977a) and Hamilton (1991) attribute it to the change from glaciomarine sedimentation to a postglacial regime dominated by Fraser delta sedimentation. This change does not explain the high impedance contrast necessary to create such a strong reflector, however.

Unit 4, the upper postglacial unit of Hart et al. (1995), overlies the layered reflector unit and largely consists of hemipelagic sediment deposited during the Holocene. The unit is the same age as foreslope deposits nearer the river mouth and associated sea valleys, which mainly consist of turbidites and debris-flow deposits. Sediments of unit 4 onlap and drape higher areas of the seafloor and fill in depressions. Internal reflections are truncated at the seafloor in some places and the unit is absent in others, suggesting that strong bottom currents have eroded it. Unit 4 is commonly obscure in subbottom acoustic records because of the presence of interstitial gas. Less than 1% gas by volume is sufficient to obstruct the acoustic signal in compressional-wave seismic reflection surveys. This gas is likely biogenic in origin, formed by decomposition of organic matter derived from the Fraser River discharge (Judd, pers. comm., 1997).

The Fraser delta

Submarine slope failures have recurred at Sand Heads during the historical period (McKenna et al., 1992). The failures are likely caused by the combined effects of high sedimentation rates, tidal drawdown, and excess pore pressures within highly gas-charged sediments (Chillarige et al., 1994, 1995, 1997a, b; Chillarige, 1995; Christian et al., 1997a, b, 1998; Luternauer et al., 1998). Such failures are believed to be the dominant mechanism for generating and maintaining the sea valley system off Sand Heads. Hart et al. (1992a) identified debris-flow deposits within the Sand Heads sea valley and concluded that valley-confined debris flows are responsible for transporting coarse-grained sediment past the delta slope. The large lobe of sediment at the base of the sea valley is probably a debris-flow fan (Hart et al., 1992c, d).

As a consequence of channel entrainment and channel dredging (Kostaschuk et al., 1998; Luternauer et al., 1998), sediment supply to the delta front has been greatly reduced in this century. Much of the sediment that now reaches Sturgeon Bank and the adjacent slope is fine grained and settles out of a buoyant plume. Without dikes and jetties, distributary channels would be able to shift across the delta plain, sediment would be more evenly distributed to the delta front, and ephemeral surface features would be rapidly buried. The foreslope would likely receive relatively more sediment than the deeper slope apron because sea valleys, which can be viewed as slope bypass conduits, would probably not develop to the same extent as they have at Sand Heads in this century. Distributary channels probably would shift too often to allow the development of a large sea valley. A consequence of channel shifting is that the grain size of sediment deposited at any one site would vary greatly through time, giving rise to bedded deposits. Shallow boreholes and cores on the delta slope or within paleo-foreslope deposits (Monahan et al., 1993; Christian et al., 1994, 1995, 1997b) commonly are finely stratified and consist of alternating layers of sand, silt, and mud.

The Roberts Bank Failure Complex may be a delta-slope deposit related to the discharge of one or more former, rapidly shifting, distributary channels. The rough topography appears to include subtle channels and levees that trend downslope. Incoherent and semicoherent internal reflections are suggestive of small stacked lobate failures. The toe of the complex overlies undisturbed deltaic deposits (Fig. 9), suggesting that sediment ran out onto the seafloor. We suggest that large amounts of sediment were delivered to the slope by a distributary channel located south of the present Main Channel, and that this sediment was carried into deeper water

along small underdeveloped sea valleys. Debris lobes accumulated at the seaward ends of the valleys. No large sea valleys formed in this area because distributary channels did not remain in the same place for lengthy periods.

Several hypotheses have been advanced to explain the Foreslope Hills. Mathews and Shepard (1962), Terzaghi (1962), and Hamilton and Wigen (1987) postulated that they are the displaced mass resulting from a large failure of the slope of the Fraser delta. Hamilton and Wigen (1987) further suggested that a significant tsunami might have followed the failure. Shepard (1967) speculated the Foreslope Hills may be mud diapirs, similar in origin to those on the Mississippi delta (Prior and Coleman, 1984). Tiffin et al. (1971) and Luternauer and Finn (1983) concluded that the Foreslope Hills consist of folded sediments deformed by instability farther upslope. Hart (1993) suggested that the asymmetry in the internal structure of the hills, evident on seismic reflection profiles, is the result of shear caused by in situ rotational displacement in a downslope direction. Christian et al. (1997a, 1998) suggest a link between delta progradation (driving stress) and creep-deformation (yielding in weak seafloor strata), supporting the compressional folding hypothesis.

Recent swath bathymetry and subbottom reflection data show that the Foreslope Hills are asymmetrical both in surface form and internal structure. The hills are steeper on the upslope side, and clinoform or asymptotic internal reflections reveal internal asymmetry in the upslope direction (Fig. 3, 11). The asymmetry is similar to what might be expected of migrating sediment waves. Asymmetric submarine mud waves of similar size to the Foreslope Hills, and showing evidence of upslope migration, have been observed elsewhere on deep-water submarine fans, for example the Barra Fan (Howe, 1996), Hueneme Fan (Piper et al., 1995), and Var Fan (Savoye et al., 1993). It is possible, therefore, that the Foreslope Hills are large sediment waves, generated by turbidity currents from the Sand Heads sea valley, possibly in combination with strong tidal currents. In the case of the Barra Fan, Howe (1996) postulated that the sediment waves may have been initiated by bottom currents, but are maintained by turbidity currents. Troughs at the eastern edge of the Foreslope Hills, nearest the Sand Heads sea valley, contain what appear to be ponded turbidites. Howe (1996) observed similar infilling of troughs between ridges on the Barra Fan. To date, the evidence is inconclusive as to the origin of these features.

SUMMARY

The Strait of Georgia is the submerged part of the Georgia Basin. The sedimentary fill in the southern Strait of Georgia is subdivided into four seismostratigraphic units, based on seismic reflection records. These units record the geologic development of the strait and the Fraser delta.

The lowest and oldest unit (unit 1) consists of folded and faulted Late Cretaceous and Tertiary sedimentary rocks. This unit is unconformably overlain by a Pleistocene succession comprising till and glaciomarine and marine sediments (unit 2). The Pleistocene deposits underlie northwest-trending ridges that have been sculpted by glaciers flowing down the Strait of Georgia. Unit 3 consists of glaciomarine sediments deposited as late Pleistocene glaciers retreated from the Strait of Georgia. These sediments mainly occur in depressions and troughs, and are probably turbidites deposited some distance from glacier margins. The uppermost unit in the succession (unit 4) consists of sediments deposited during Holocene progradation of the Fraser delta. This unit underlies the Fraser delta and floors much of the southern Strait of Georgia, thinning from east to west and south to north. It is more than 200 m thick under the tidal flats of the Fraser delta and up to 100 m thick in the deep basins of the southern Strait of Georgia. Near the Fraser delta, unit 4 sediments are deposited by turbidity currents, debris flows, and hemipelagic processes. Farther from the delta, the sediments are deposited mainly by fallout of fine-grained silt and clay suspended from the Fraser River plume and by unconfined, low-density turbidity currents.

The Fraser River has discharged into the Strait of Georgia for the last 10,000 years and has produced a large delta consisting of an extensive plain, including a broad intertidal zone, and an equally extensive delta slope. Active distributary channels which cross the delta plain are now fixed in their locations by dikes and jetties. Channel training and dredging have affected natural river sedimentation and sediment delivery to the delta front. Reduced supply of sand to the delta front and erosion of a deep sea valley off Sand Heads are the likely results of this human activity. Debris-flow deposits, turbidites, and hemipelagic sediments are the dominant seafloor sediments near the base of the sea valley. Hemipelagic sediments become more common with increasing distance from the river mouth.

Before the Fraser River was diked and dredged, frequent channel shifts caused sediment to be delivered to a larger part of the delta slope than today, with less bypassing of the delta front. Evidence for channel shifting includes the presence of a sheet of distributary-channel sands beneath most of the delta plain and the presence of alternating layers of sand, silt, and mud in cores from the delta slope. The Roberts Bank Failure Complex may be a relict delta-slope deposit that accumulated at the mouth of one or more, former, rapidly shifting distributary channels.

The Foreslope Hills are a large area of ridges and troughs on the seafloor west of the Sand Heads sea valley. The origin of this feature is uncertain, but the most plausible explanations are these: 1) in situ rotational failure caused by high sediment pore pressures; 2) compressional soft-sediment deformation resulting from lateral stresses from the prograding delta; and 3) sediment waves generated by strong bottom currents in combination with hyperpycnal flow from the Fraser River.

ACKNOWLEDGMENTS

We wish to express our appreciation to the many people who helped collect data that made this paper possible, especially the technical staff at the Pacific Geoscience Centre. Richard Franklin painstakingly digitized the bathymetric

field sheets for the Strait of Georgia, and Robert Kung produced the shaded relief images. We thank David Piper for valuable discussion concerning the genesis of the Foreslope Hills. David Prior, Ralph Currie, and John Clague provided valuable scientific and editorial comment.

REFERENCES

Armstrong, J.E., Crandell, D.R., Easterbrook, D.J., and Noble, J.B.
1965: Late Pleistocene stratigraphy and chronology in southwestern British Columbia and northwestern Washington; Geological Society of America Bulletin, v. 76, p. 321-330.

Barrie, J.V. and Currie, B.G.
1997 Anthropogenic alteration of the natural evolution of the Fraser River delta, Canada: in Pacific Coasts and Ports; in Proceedings, 13th Australian Coastal and Ocean Engineering Conference and 6th Australasian Port and Harbour Conference, Christchurch, New Zealand, v. 1, p. 99-106

Chillarige, A.V.
1995: Liquefaction and seabed instability in the Fraser River delta; Ph.D. thesis, University of Alberta, Edmonton, Alberta, 356 p.

Chillarige, A.R.V., Morgenstern, N.R., Robertson, P.K., and Christian, H.A.
1995: Characterization of Fraser River delta sand; in Proceedings, 48th Canadian Geotechnical Conference, Vancouver, British Columbia, v. 2, p. 711-720.
1997a: Evaluation of in-situ state of Fraser River sand; Canadian Geotechnical Journal, v. 34, p. 510-519.

Chillarige, A.R.V., Robertson, P.K., Morgenstern, N.R., and Christian, H.A.
1997b: Seabed instability due to flow liquefaction in the Fraser River delta; Canadian Geotechnical Journal, v. 34, p. 520-533.

Chillarige, A.R.V., Robertson, P.K., Morgenstern, N.R., Christian, H.A., and Woeller, D.J.
1994: Evaluation of wave effects on seabed instability in the Fraser River delta; in Proceedings, 47th Canadian Geotechnical Conference, Halifax, Nova Scotia, p. 186a-186j.

Christian, H.A., Barrie, J.V., Hunter, J.A., Luternauer, and Monahan, P.A.
1995: Deep hole geotechnical investigation, Westshore Terminal, Roberts Bank Superport, March 6-31, 1995; report by Geological Survey of Canada to British Columbia Hydro and Power Authority, Burnaby, British Columbia, 20 p.

Christian, H.A., Monahan, P.A., and Barrie, J.V.
1994: Deep-hole geotechnical investigation adjacent to the BC Hydro Canoe Pass submarine cable terminal, Fraser River Delta, British Columbia; Geological Survey of Canada, Open File 2861, 26 p.

Christian, H.A., Mosher, D.C., Barrie, J.V., Hunter, J.A., and Luternauer, J.L.
1998: Seabed instability on the Fraser River delta; in Geology and Natural Hazards of the Fraser River Delta, British Columbia, (ed.) J.J. Clague, J.L. Luternauer, and D.C. Mosher; Geological Survey of Canada, Bulletin 525, this volume.

Christian, H.A., Mosher, D.C., Mulder, T., Barrie, J.V., and Courtney, R.C.
1997a: Geomorphology and potential slope instability on the Fraser River delta foreslope, Vancouver, British Columbia; Canadian Geotechnical Journal, v. 34, p. 432-446.

Christian, H.A., Woeller, D.J., Robertson, P.K., and Courtney, R.C.
1997b: Site investigations to evaluate flow liquefaction slides at Sand Heads, Fraser River delta; Canadian Geotechnical Journal, v. 34, p. 384, 397.

Clague, J.J.
1976: Quadra Sand and its relation to the late Wisconsin glaciation of southwest British Columbia; Canadian Journal of Earth Sciences, v. 13, p. 803-815.
1977a: Holocene sediments in the northern Strait of Georgia, British Columbia; in Report of Activities, Part A; Geological Survey of Canada, Paper 77-1A, p. 51-58.
1977b: Quadra Sand: A study of the late Pleistocene geology and geomorphic history of coastal southwest British Columbia; Geological Survey of Canada, Paper 77-17, 26 p.

Clague, J.J. (cont.)
1998: Geological setting of the Fraser River delta; in Geology and Natural Hazards of the Fraser River Delta, British Columbia, (ed.) J.J. Clague, J.L. Luternauer, and D.C. Mosher; Geological Survey of Canada, Bulletin 525, this volume.

Clague, J.J., Luternauer, J.L., and Hebda, R.J.
1983: Sedimentary environments and postglacial history of the Fraser delta and lower Fraser valley, British Columbia; Canadian Journal of Earth Sciences, v. 20, p. 1314-1426.

Clague, J.J., Luternauer, J.L., Pullan, S.E., and Hunter, J.A.
1991: Postglacial deltaic sediments, southern Fraser River delta, British Columbia; Canadian Journal of Earth Sciences, v. 28, p. 1386-1393.

Currie, R.C. and Mosher, D.C.
1996: Swath bathymetric surveys in the Strait of Georgia, British Columbia; in Current Research 1996-E, Geological Survey of Canada, p. 33-40.

England, T.D.J. and Hiscott, R.N.
1992: Lithostratigraphy and deep-water setting of the upper Nanaimo Group (Upper Cretaceous), outer Gulf Islands of southwestern British Columbia; Canadian Journal of Earth Sciences, v. 29, p. 574-595.

Evoy, R.W., Moslow, T.F., Patterson, R.T., and Luternauer, J.L.
1993: Patterns and variability in sediment accumulation rates, Fraser River delta foreslope, British Columbia, Canada; Geo-Marine Letters, v. 13, p. 212-218.

Hamilton, T.S.
1991: Seismic stratigraphy of unconsolidated sediments in the central Strait of Georgia: Hornby Island to Roberts Bank; Geological Survey of Canada, Open File 2350, 9 sheets.

Hamilton, T.S. and Luternauer, J.L.
1983: Evidence of seafloor instability in the south-central Strait of Georgia: a preliminary compilation; in Current Research, Part A; Geological Survey of Canada, Paper 83-1A, p. 417-421.

Hamilton, T.S. and Wigen, S.O.
1987: The Foreslope Hills of the Fraser Delta: implications for tsunamis in Georgia Strait; International Journal of the Tsunamis Society, v. 5, p. 15-33.

Hart, B.S.
1993: Large-scale in situ rotational failure on a low-angle delta slope: the Foreslope Hills, Fraser Delta, British Columbia, Canada; Geo-Marine Letters, v. 13, p. 219-226.

Hart, B.S. and Barrie, J.V.
1995: Environmental geology of the Fraser Delta, Vancouver; Geoscience Canada, v. 22, p. 172-183.

Hart, B.S. and Hamilton, T.S.
1993: High-resolution acoustic mapping of shallow gas in unconsolidated sediments beneath the Strait of Georgia, British Columbia; Geo-Marine Letters, v. 13, p. 49-55.

Hart, B.S., Barrie, J.V., Christian, H.A., Hamilton, T.S., Davis, A.M., and Law, L.K.
1993: Marine geological, geophysical and geotechnical investigations of the submarine portions of the Fraser Delta: implications for submarine failures; in Proceedings, Canadian Coastal Conference, Vancouver, British Columbia.

Hart, B.S., Barrie, J.V., Currie, R.G., Luternauer, J.L., Prior, D.B., and Macdonald, R.D.
1991: High resolution seismic and side-scan sonar mapping of the Fraser Delta front and adjacent Strait of Georgia, British Columbia; in Current Research, Part E; Geological Survey of Canada, Paper 91-1E, p. 19-23.

Hart, B.S., Hamilton, T.S., Barrie, J.V., Currie, R.G., and Prior, D.B.
1992a: Marine geophysical and geological surveys of the Fraser Delta slope and adjacent Strait of Georgia: 1991 geophysical survey tracklines and 1983-1992 core locations; Geological Survey of Canada, Open File 2543, 5 sheets.

Hart, B.S., Hamilton, T.S., Barrie, J.V., and Prior, D.B.
1995: Seismic stratigraphy and sedimentary framework of a deep-water Holocene delta: the Fraser delta, Canada; in Geology of Deltas, (ed.) M.N. Oti and G. Postma; A.A. Balkema, Rotterdam, Netherlands, p. 167-178.

Hart, B.S., Horel, G., Olynyk, H.W., and Frydecky, I.
1992b: An airgun seismic survey of the Fraser Delta slope; in Current Research, Part E; Geological Survey of Canada, Paper 92-1E, p. 33-39.

Hart, B.S., Prior, D.B., Barrie, J.V., Currie, R.G., and Luternauer, J.L.
1992c: A river mouth submarine channel and failure complex, Fraser Delta, Canada; Sedimentary Geology, v. 81, p. 73-87.

Hart, B.S., Prior, D.B., Hamilton, T.S., Barrie, J.V., and Currie, R.G.
1992d: Patterns and styles of sedimentation, erosion and failure, Fraser Delta slope, British Columbia; in Geotechnique and Natural Hazards; BiTech Publishers, Vancouver, British Columbia, p. 365-372.

Hicock, S.R. and Armstrong, J.E.
1983: Four Pleistocene formation in southwest British Columbia: their implications for patterns of sedimentation of possible Sangamonian to early Wisconsinan age; Canadian Journal of Earth Sciences, v. 20, p. 1232-1247.

Howe, J.A.
1996: Turbidite and contourite sediment waves in the northern Rockall Trough, North Atlantic Ocean; Sedimentology, v. 43, p. 219-234.

Kostaschuk, R.A., Luternauer, J.L., Barrie, J.V., Werth von Deichmann, L., and LeBlond, P.H.
1995: Subtidal dune morphology and sediment transport: Fraser River delta, British Columbia; Canadian Journal of Earth Sciences, v. 32, p. 852-859.

Kostaschuk, R.A., Luternauer, J.L., and Church, M.A.
1998: Sedimentary processes in the estuary; in Geology and Natural Hazards of the Fraser River Delta, British Columbia, (ed.) J.J. Clague, J.L. Luternauer, and D.C. Mosher; Geological Survey of Canada, Bulletin 525, this volume.

Luternauer, J.L.
1980: Genesis of morphological features on the western delta front of the Fraser River, British Columbia - status report of knowledge; in The Coastline of Canada, (ed.) S.B. McCann; Geological Survey of Canada, Paper 80-10, p. 381-396.

Luternauer, J.L. and Finn, W.D.L.
1983: Stability of the Fraser River delta front; Canadian Geotechnical Journal v. 20, p. 603-616.

Luternauer, J.L., Barrie, J.V., Christian, H.A., Clague, J.J., Evoy, R.W., Hart, B.S., Hunter, J.A., Killeen, P.G., Kostaschuk, R.A., Mathewes, R.W., Monahan, P.A., Moslow, T.F., Mwenifumbo, C.J., Olynyk, H.W., Pattersno, R.T., Pullan, S.E., Roberts, M.C., Robertson, P.K., Tarbotton, M.R., and Woeller, D.J.
1994: Fraser River delta: geology, geohazards and human impact; in Geology and Geological Hazards of the Vancouver Region, Southwestern British Columbia, (ed.) J.W.H. Monger; Geological Survey of Canada, Bulletin 481, p. 197-220.

Luternauer, J.L., Clague, J.J., Hunter, J.A.M., Pullan, S.E., Roberts, M.C., Woeller, D.J., Kostaschuk, R.A., Moslow, T.F., Monahan, P.A., and Hart, B.S.
1993: The Fraser River delta, British Columbia: architecture, geological dynamics and human impact; in Deltas of the World, (ed.) R. Kay; American Society of Civil Engineers, New York, New York, p. 99-114.

Luternauer, J.L., Mosher, D.C., Clague, J.J., and Atkins, R.J.
1998: Sedimentary environments of the Fraser delta; in Geology and Natural Hazards of the Fraser River Delta, British Columbia, (ed.) J.J. Clague, J.L. Luternauer, and D.C. Mosher; Geological Survey of Canada, Bulletin 525, this volume.

Mathews, W.H. and Shepard, F.P.
1962: Sedimentation of the Fraser River delta, British Columbia; American Association of Petroleum Geology Bulletin, v. 46, p. 1416-1438.

McKenna, G.T., Luternauer, J.L., and Kostaschuk, R.A.
1992: Large-scale mass-wasting events on the Fraser River delta front near Sand Heads, British Columbia; Canadian Geotechnical Journal, v. 29, p. 151-156.

Monahan, P.A., Luternauer, J.L., and Barrie, J.V.
1993: A delta plain sheet sand in the Fraser River delta, British Columbia, Canada; Quaternary International, v. 20, p. 27-38.

Mosher, D.C.
1995: Southern Roberts Bank nearshore survey: PGC95003; Geological Survey of Canada, Open File 3308, 21 p.

Mosher, D.C., Christian, H.A., Hunter, J.A., and Luternauer, J.L.
1997: Onshore/offshore geohazards in the Vancouver region of western Canada: field modelling and mapping techniques and results; in Proceedings, International Symposium on Engineering Geology and the Environment, Athens, Greece; A.A. Balkema, Rotterdam, The Netherlands, p. 875-883.

Mosher, D.C., Nichols, B.C., and Scientific Party of PGC95001
1995: Multichannel and high resolution seismic reflection survey of the marine portion of the Fraser River Delta, Vancouver, British Columbia: Tully PGC95001; in Current Research 1995-E, Geological Survey of Canada, p. 37-45.

Mustard, P.S.
1994: The Upper Cretaceous Nanaimo Group, Georgia Basin; in Geology and Geological Hazards of the Vancouver Region, Southwestern British Columbia, (ed.) J.W.H. Monger; Geological Survey of Canada, Bulletin 481, p. 3-25.

Mustard, P.S. and Rouse, G.E.
1994: Stratigraphy and evolution of Tertiary Georgia Basin and subjacent Upper Cretaceous sedimentary rocks, southwestern British Columbia and northwestern Washington State; in Geology and Geological Hazards of the Vancouver Region, Southwestern British Columbia, (ed.) J.W.H. Monger; Geological Survey of Canada, Bulletin 481, p. 27-95.

Pharo, C.H. and Barnes, W.C.
1976: Distribution of surficial sediments of the central and southern Strait of Georgia; Canadian Journal of Earth Sciences, v. 13, p. 684-696.

Piper, D.J.W., Normark, W.R., and Hiscott, R.N.
1995: Holocene sand body geometry, Hueneme Fan, California Borderland; in Atlas of Deep Water Environments: Architectural Style in Turbidite Systems, (ed.) K.T. Pickering, R.N. Hiscott, N.H. Kenyon, F. Ricci Lucchi, and R.D.A. Smith; Chapman and Hall, London, England, p. 203-207.

Prior, D.B. and Coleman, J.M.
1984: Submarine slope instability; in Slope Instability, (ed.) D. Brunsden and D.B. Prior; Wiley, New York, New York, p. 419-455.

Savoye, B., Piper, D.J.W., and Droz, L.
1993: Plio-Pleistocene evolution of the Var deep-sea fan off the French Riviera; Marine and Petroleum Geology, v. 10, p. 550-571.

Shepard, F.P.
1967: Delta-front diapirs off Magdalena River, Columbia, compared with hills off other large deltas; Gulf Coast Association of Geological Societies, Transactions, v. 17, p. 316-325.

Terra Surveys Ltd.
1994: The Roberts Bank failure deposit, Fraser River Delta, British Columbia; report to Geological Survey of Canada, Pacific Geoscience Centre, Sidney, British Columbia, 29 p.

Terzaghi, K.
1962: Discussion, Sedimentation of Fraser River delta, British Columbia; Bulletin of American Association of Petroleum Geologists, v. 46, p. 1438-1443.

Tiffin, D.L.
1969: Continuous seismic reflection profiling in the Strait of Georgia, British Columbia; Ph.D. thesis, University of British Columbia, Vancouver, British Columbia, 177 p.

Tiffin, D.L., Murray, J.W., Mayers, I.R., and Garrison, R.E.
1971: Structure and origin of Foreslope Hills, Fraser Delta, British Columbia; Bulletin of Canadian Petroleum Geology, v. 19, p. 589-600.

Plant macrofossil, pollen, diatom, and foraminiferal biofacies of the Fraser delta

I. Hutchinson[1], R.T. Patterson[2], and R.W. Mathewes[3]

Hutchinson, I., Patterson, R.T., and Mathewes, R.W., 1998: Plant macrofossil, pollen, diatom, and foraminiferal biofacies of the Fraser delta; in Geology and Natural Hazards of the Fraser River Delta, British Columbia, (ed.) J.J. Clague, J.L. Luternauer, and D.C. Mosher; Geological Survey of Canada, Bulletin 525, p. 161–175.

Abstract: The Fraser River delta plain supports a diverse array of marine and terrestrial ecological communities. A mosaic of marshes, sand flats, and mud flats in the intertidal zone and wet meadows, shrub lands, bogs, and riparian woodlands above the limit of tides can be linked by a successional model that relates ecological communities to elevation and substrate characteristics. Paleoecological investigations of plant macrofossils, pollen, diatom, and foraminifers have proven useful in 1) reconstructing late-glacial and early Holocene conditions in the Strait of Georgia, 2) reconstructing small-scale changes in relative sea level, 3) assessing flood frequency, and 4) explaining autogenic changes related to fire occurrence in raised bogs on the delta plain.

Résumé : La plaine deltaïque du fleuve Fraser est l'habitat de communautés écologiques et terrestres d'une grande diversité. Un modèle successif qui met en corrélation les communautés écologiques avec l'altitude et les caractéristiques du substrat permet de relier la mosaïque des marécages, des estrans sableux et des estrans boueux de la zone intertidale aux prairies humides, aux broussailles, aux tourbières et aux boisés riverains qu'on observe au-dessus de la limite des marées. Les études paléoécologiques des macrofossiles de plantes, de pollens, de diatomées et de foraminifères se sont avérées utiles pour 1) reconstituer les conditions de la fin de la dernière glaciation et de l'Holocène précoce dans le détroit de Georgia, 2) reconstituer les changements à petite échelle du niveau marin relatif, 3) évaluer la fréquence des crues et 4) expliquer les changements autogènes liés aux feux de tourbières soulevées sur le territoire de la plaine deltaïque.

[1] Department of Geography and Institute for Quaternary Research, Simon Fraser University, Burnaby, British Columbia V5A 1S6
[2] Ottawa-Carleton Geoscience Centre and Department of Earth Sciences, Carleton University, Ottawa, Ontario K1S 5B6
[3] Department of Biological Sciences and Institute for Quaternary Research, Simon Fraser University, Burnaby, British Columbia V5A 1S6

INTRODUCTION

The Fraser River delta has been built out into the deep waters of the semienclosed marine basin of the Strait of Georgia during the Holocene Epoch (Luternauer et al., 1993). The delta now extends more than 20 km west from its apex near New Westminster and covers an area of about 1000 km^2 (Mathews and Shephard, 1962). The structure of the delta has been determined from onshore and offshore drilling and seismic surveys (Luternauer et al., 1993; Monahan et al., 1993). These geological and geophysical investigations have benefited from complementary and ancillary research on the paleoecology of the delta. In this paper we review these paleoecological investigations and assess their contribution to our understanding of the development of the Fraser delta.

Paleoenvironmental conditions are inferred from assemblages of fossil organisms using modern community-environment relationships. Although deltaic communities exhibit substantial local variation, their distribution is largely controlled by the elevation of the surface and the properties of the substrate. Progressive aggradation of the delta surface induces shifts in the distribution of ecological communities and predictable changes in the structure of the community at a site. A model of successional change based on elevation-aggradation-community structure relationships can be used to analyze variations in paleoecological communities through time. Departures from the successional sequence predicted by the model may indicate unstable conditions associated with shifts in distributary-channel position or changes in sea level.

In this paper we present a simple successional model that can be used as a diagnostic tool in paleoecological research on the Fraser delta, and discuss the most important paleoecological studies that have been conducted there to date. We focus on vascular plants (macrofossils and pollen), diatoms, and foraminifers, which are the main fossil groups used in past paleoecological studies.

Although our focus is on the Fraser delta itself, it should be noted that paleoecological research in neighbouring areas can also contribute to a better understanding of the evolution of the Fraser delta. For example, variations in delivery of water and sediment to the delta front are linked to changes in the climate and vegetation of the Fraser River basin, which can be documented by paleoecological analysis. In addition,

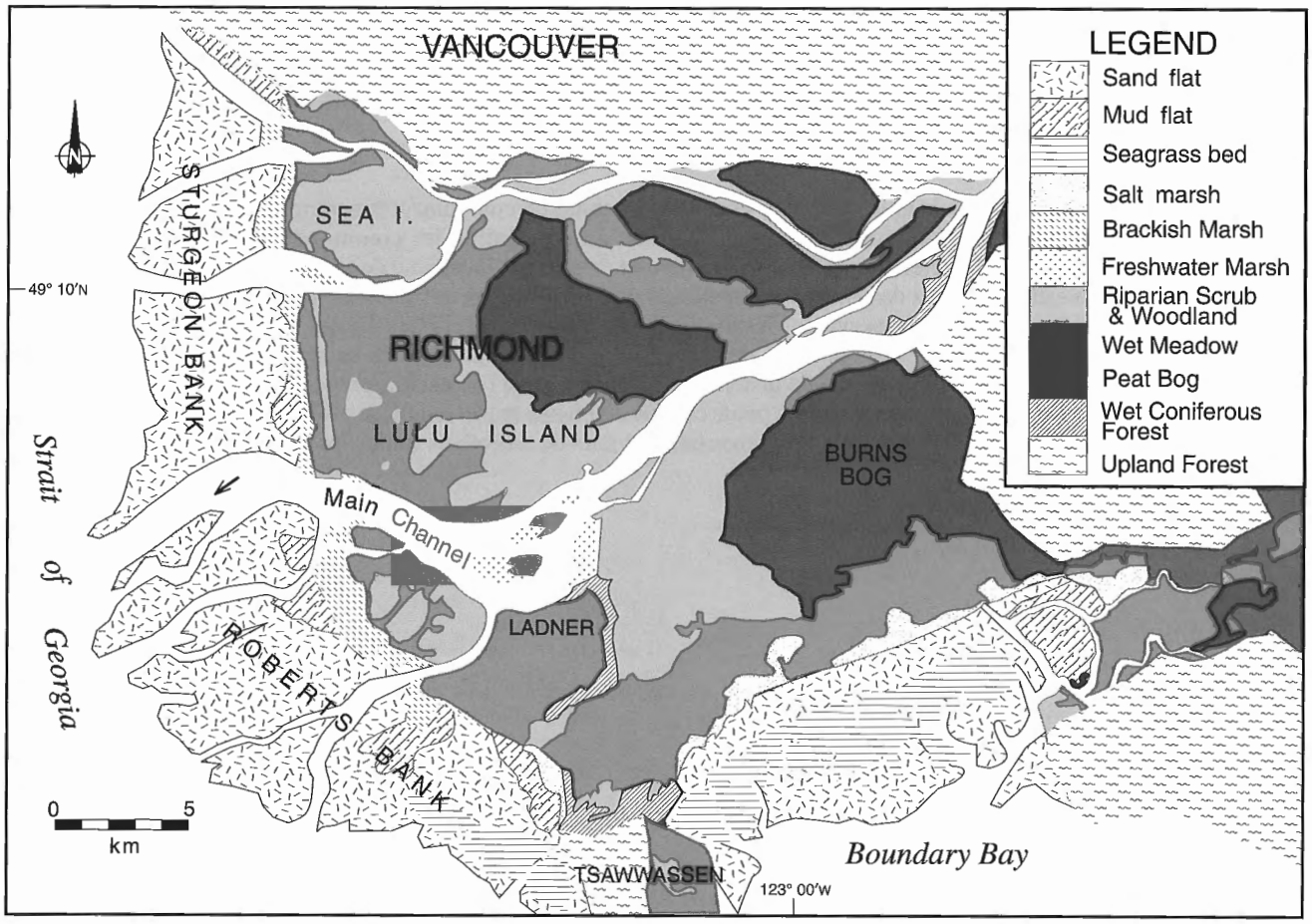

Figure 1. Plant communities and associated habitats of the Fraser River delta in the early historical period; adapted from North and Teversham (1979).

changes in sea or land level, which strongly affect the rate of growth of the delta, can be documented through paleoecological study of the coastal margins of the Strait of Georgia.

MODERN BIOTIC COMMUNITIES OF THE FRASER DELTA

The primary division of habitats in deltaic environments is between marine and terrestrial realms. The marine realm comprises the area below low tide, i.e. the subtidal zone. In morphological terms this is equivalent to the prodelta, the delta slope, and the lower delta plain. The ecological communities of the subtidal zone are often poorly known because of sampling difficulties.

The intertidal zone is the transitional area between the marine and terrestrial realms. The width of the intertidal zone in a deltaic environment is largely determined by the local tidal range. In the case of the Fraser River delta, the maximum tidal range is about 4 m (Milliman, 1980), and the intertidal zone is relatively broad (up to 7 km). Some 80% of this area consists of unvegetated sand and mud flats (Fig. 1). Parts of the upper subtidal zone and lower intertidal zone are occupied by beds of eelgrass (*Zostera* spp.), and the upper, vegetated part of the intertidal zone supports salt and brackish marsh communities. Intertidal marshes and tidal flats on the Fraser delta have undergone some disturbance in the last century as a result of river training, channel diversion, and construction.

The natural landscape above the high-water mark has been extensively altered in this century, but the distribution of natural biotic communities has been reconstructed from the field notes of the original land surveyors (North and Teversham, 1979). The vegetation map derived from these notes (Fig. 1) reveals a complex mosaic of aquatic, semiaquatic, and terrestrial plant communities: sloughs, freshwater marshes, wet meadows and shrub lands, bogs, and riparian forests. From a paleoecological perspective this map is very useful; it not only provides a typology of modern ecological communities, but also shows their relative extent and distribution.

Prior to settlement, wet meadows covered about 40% of the upper delta plain, bogs about 30%, shrub lands and riparian woodlands about 20%, and flowing-water ecosystems (distributary channels, sloughs) about 10%. Bogs dominated interdistributary areas on the eastern part of the delta, whereas wet meadows and riparian shrub communities were common to the west. Freshwater marsh occurred as ribbons along the margins of active channels and sloughs and as pioneer communities on mid-channel bars. Coniferous forest was common on the channel banks, particularly near the apex of the delta.

Small differences in the elevation of the Fraser River delta plain, and related differences in tidal submergence, water-table depth, substrate salinity, and sediment mobility have given rise to a variety of deltaic habitats which support diverse ecological communities. These communities lie along a bifurcating successional sequence with more-or-less isolated endpoints (Fig. 2). The first steps in the successional series are undifferentiated prodelta and slope environments. These environments are succeeded by intertidal habitats. On the upper delta plain, we recognize a successional sequence associated with aggradation in poorly drained interdistributary areas, culminating in the development of oligotrophic raised bogs (Fig 50 in Hebda, 1977). An independent successional sequence is linked to aggradation on relatively well drained channel banks; this sequence passes from freshwater marsh, through riparian woodland, to wet coniferous forest (Fig. 2).

Organic materials produced in these communities may be preserved at the site of origin (autochthonous material) or they may be entrained by wind or water and deposited elsewhere (allochthonous material). Paleoecologists focus on those organic components that are abundant and readily identifiable, have high preservation potential, and display community structures that are strongly influenced by local environmental conditions. The taxa included in this paper (plant macrofossils, pollen, diatoms, and foraminifers) are widely used in Quaternary studies in coastal areas for these reasons (e.g. Scott and Medioli, 1986; Warner, 1990; Jonasson and Patterson, 1992). Generalized distributions of these taxa along a deltaic marine-terrestrial gradient are shown in Figure 3.

Paleoenvironmental reconstruction on the Fraser River delta has been made more difficult as a result of settlement. The paleoecologist can no longer examine pristine communities in order to determine environmental influences. Habitat alienation, the introduction of alien species, and urban and industrial pollution have drastically altered biotic assemblages on the Fraser delta in the last century. Because the relative abundance of species in present-day communities may not be the same as in their presettlement counterparts, the characterization of modern analogues requires careful sampling of native biofacies. The dominant species, and general ecological characteristics, of these native biofacies are described below.

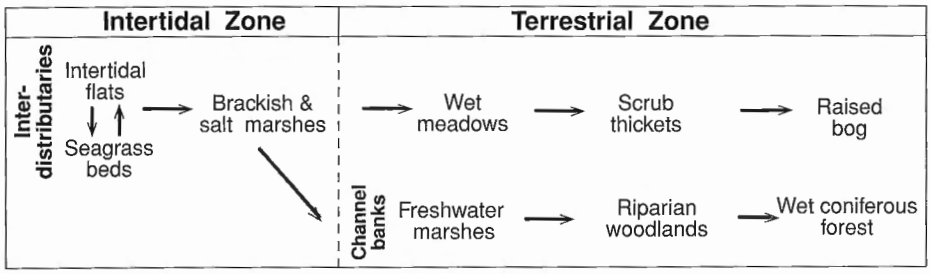

Figure 2.

Generalized successional pathways for plant communities on the Fraser River delta.

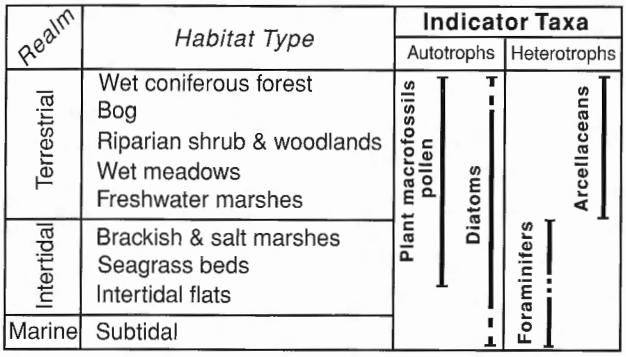

Figure 3. *Generalized distributions of taxa discussed in this paper. Solid lines indicate habitats where the taxa are abundant; broken lines indicate sparse populations. Autotrophs are capable of photosynthesis; heterotrophs feed on other organisms.*

Subtidal zone

The subtidal zone includes the slope of the Fraser delta and the floor of the southern Strait of Georgia to the west. The environment of this area is strongly influenced by the Fraser River, which supplies 80% of the total runoff to the Strait of Georgia, and by tides, currents, and winds which mix the water column (LeBlond, 1983). Substrates in the subtidal zone consist of mud derived from suspended material in the Fraser River plume and coarser grained material transported by sediment gravity flows down channels or valleys cut into the Fraser delta slope (Luternauer et al., 1983).

Prodelta and delta-slope biofacies

Photosynthetic marine micororganisms such as dinoflagellates and diatoms live as plankton in the surface waters of the Strait of Georgia. They cannot live in the low-light conditions of the prodelta environment, so the dinoflagellates and diatoms that are commonly found in prodelta sediments are all allochthonous, as are terrestrially derived pollen and spores (Dobell, 1976; Mathewes, unpublished data). Whereas the organic cell walls of pollen, spores, and dinoflagellates resist dissolution as they settle through the prodelta water column, diatom valves are constructed from silica and tend to dissolve in these silica-deficient waters (Sancetta, 1989). As a consequence, the diatom assemblage in prodelta sediments consists of only the most robust of the marine planktonic species, plus those brackish and freshwater species that survive transport in the Fraser River plume (Shim, 1977; Harrison et al., 1983).

The foraminiferal fauna in prodelta sediments, however, is largely autochthonous. This fauna is strongly influenced by the relatively low salinity conditions of the southern Strait of Georgia and by the texture of the substrate. The prodelta and lower delta slope encompass part of the '*Elphidium-Elphidiella*' biofacies which occurs at water depths of about 50 to 200 m (Cockbain, 1963). *Cribroelphidium excavatum*, the dominant species in this assemblage (Cockbain, 1963), and the other important species of this biofacies, *Buccella frigida*, *Elphidiella nitida*, and *Nonionella stella*, are common in relatively shallow marine waters along the entire west coast of North America (Culver and Buzas, 1985). Elements of this fauna are present, however, at greater depths elsewhere in the Strait of Georgia.

Fine-grained sediments in deep water have a more diverse and abundant foraminiferal fauna than sands of the upper delta slope (Williams, 1989). Rapid sedimentation and frequent slumping of the sands near the upper slope break inhibit establishment of foraminifer and diatom populations. Some delta-slope sediments, however, contain an abundance of allochthonous species reworked from tidal-flat, marsh, or channel-margin habitats and carried down the slope by sediment gravity flows (Evoy et al., 1993).

Intertidal zone

The distribution of intertidal biota on the Fraser delta, as on other temperate deltas, is linked to the elevation of the tidal platform, which determines the extent to which marine organisms are subject to dessication, and terrestrial organisms to inundation. Other factors that influence the character of the biota are the salinity of inundating and interstitial waters and the texture, organic content, and redox status of the substrate.

At present, all Fraser River distributaries discharge onto the western delta front. As a consequence, the water covering Sturgeon and Roberts banks (Fig. 1) at high tide is relatively fresh, particularly during summer when the Fraser River is in flood. Surface salinities are commonly ≤5‰ when marsh plants are actively growing, and these marshes are dominated by sedges and grasses that are tolerant of weakly saline conditions (Fig. 4). Very small amounts of fresh water are discharged into Boundary Bay (Fig. 1) at the southern front of the delta. Waters on the tidal flats and marshes in this area are consequently much more saline (~25‰) during the growing season. High rates of evaporation in mid-summer can render infrequently inundated areas at higher elevations in the Boundary Bay marshes hypersaline (>35‰). Because of their relatively high salinity, these marshes resemble true salt marshes in their species composition (Fig. 4).

The distribution of biota on the tidal flats themselves seems to be more controlled by substrate mobility than by salinity. We, therefore, discuss the tidal-flat environment in terms of the biofacies associated with sand- and mud-dominated substrates.

Sand-flat biofacies

The sediment load of the Fraser River is extremely rich in sand-sized material (Milliman, 1980), consequently most of the Fraser delta intertidal platform is mantled by sand. With the exception of eelgrass beds, these areas are unvegetated, and the sandy substrate is mobile. The lower and middle tidal flats are floored by horizontally bedded, fine- to medium-grained sand, which is commonly bioturbated, and contains whole or fragmented shells. These clean sands grade into silty sands of the mid to upper tidal flats.

The seagrass ecosystem of the Fraser River delta consists of native eelgrass (*Zostera marina*), the exotic *Zostera japonica*, and minor ditch grass (*Ruppia maritima*). The most important of these species from a paleoecological point of view is *Z. marina* which grows abundantly on sand flats at subtidal to lower intertidal elevations (Fig. 4). It is common on southern Roberts Bank and in Boundary Bay where water turbidity is relatively low. Although the shoots and pollen of *Z. marina* may be redeposited by tides and waves, the rhizomes of this species have a high potential for in situ preservation, and are a potentially useful paleoelevation indicator.

The sand-flat diatom community consists of benthic species which grow attached to sand grains or eelgrass stems, and marine planktonic species. Sand-flat deposits on Sturgeon Bank contain a benthic diatom assemblage with brackish or brackish-marine affinities; *Amphora staurophora* is the most common species (Fig. 4). The diatom communities in Boundary Bay are more marine in character and strongly resemble sand-flat communities in the Pacific Northwest (Rao and Lewin, 1976; Hemphill-Haley, 1995) and elsewhere (e.g. Vos and de Wolf, 1993). *Achnanthes delicatula* is the most common benthic diatom in sands of the lower and middle intertidal zone in Boundary Bay (Fig. 4). Marine planktonic diatoms, which are abundant in the lower and middle intertidal zone in Boundary Bay, are less common in the muddy sands of the upper intertidal zone (Hutchinson et al., 1995). Allochthonous fresh and fresh-brackish species derived from distributary-channel margins and brackish marshes may be a significant component of these sand-flat assemblages.

Foraminiferal colonization of lower intertidal sand flats is inhibited by the unstable substrate. Except for allochthonous offshore and marsh foraminifers, and arcellaceans carried down from the high marsh, these sand flats are barren (Fig. 4). Sand flats at higher elevations, however, have a limited foraminiferal fauna dominated by *Milliamina fusca* (Williams, 1989; Patterson, 1990).

Mud-flat biofacies

Mud has accumulated on the western foreshore of the Fraser delta in sheltered locations. Diatom assemblages on the mud flats include many species that are found in sand-flat environments (Hutchinson, unpublished data), but tend to be dominated by species which prefer fine-textured substrates, such as *Navicula digitoradiata* (Laws, 1988).

Foraminiferal assemblages on the mud flats consist of virtually monospecific populations of *Trochammina pacifica* (Patterson, 1990). This biofacies is restricted to elevations between -1.1 and -0.5 m in areas stabilized by eelgrass. The dominance of *T. pacifica* is probably related to the organic-rich substrate in the upper marsh at the western front of the

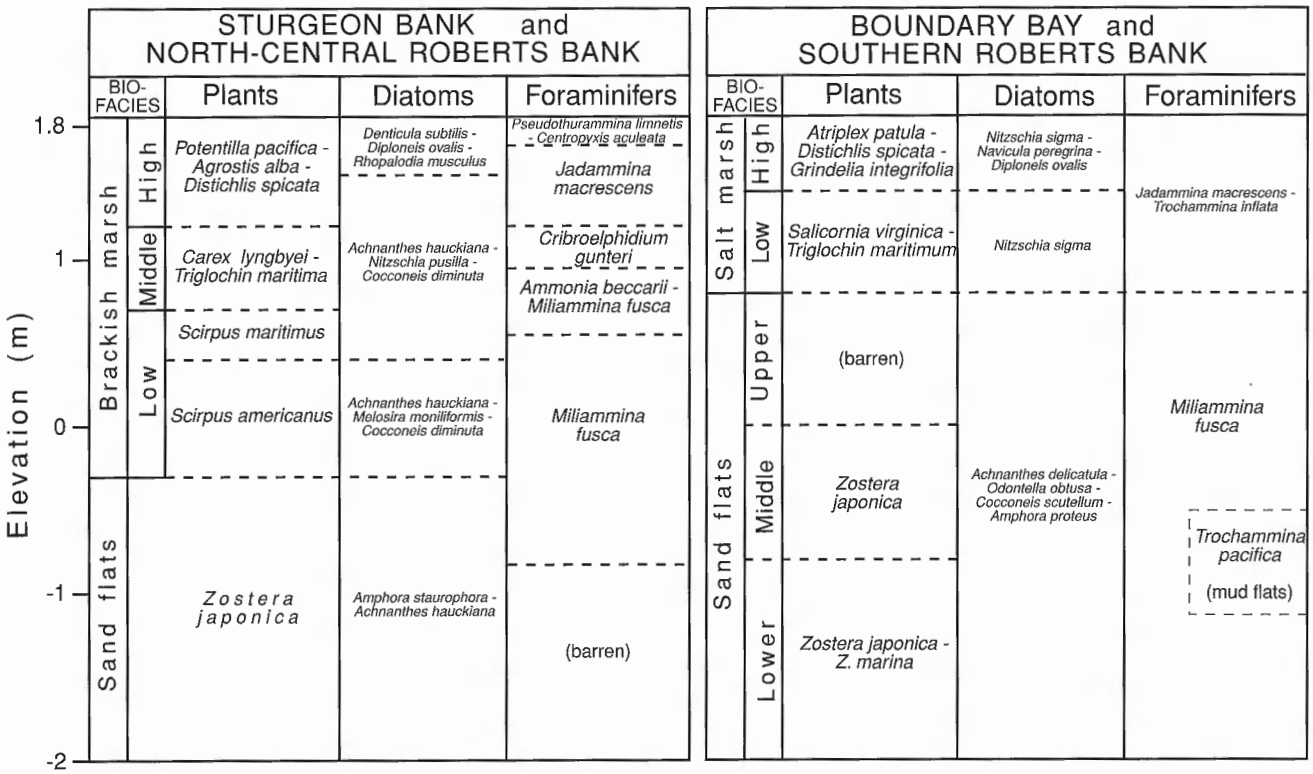

Figure 4. *Elevational ranges of key taxa in brackish (Sturgeon Bank and north-central Roberts Bank) and saline (Boundary Bay and southern Roberts Bank) areas of the intertidal zone on the Fraser delta. Sources: Shepperd (1981), Hutchinson (1982), Williams (1989), Patterson (1990), Baldwin and Lovvorn (1994), I. Hutchinson (unpublished data).*

delta. This species is abundant in similar habitats elsewhere along the west coast of North America (Watkins, 1961; Bandy et al., 1965).

Brackish-marsh biofacies

Because of the low ambient salinity, the brackish-marsh biofacies extends below mean sea level on the intertidal platform (Fig. 4). Several biotic zones with restricted elevation ranges are recognized on the basis of the relative abundance of various species of plants, diatoms, and foraminifers. In terms of plant distribution, there is a strong gradient in biodiversity with elevation. Low-marsh plant communities consist almost entirely of bulrushes (*Scirpus* spp.); high-marsh communities have a more complex and diverse structure (Hutchinson, 1982). Marsh-plant macrofossils, particularly rhizomes and leaf bases, have proven to be useful paleoelevation indicators on the Fraser delta (e.g. Styan and Bustin, 1983) and elsewhere in the Pacific Northwest (e.g. Atwater et al., 1995).

Diatom assemblages in brackish marshes of the Fraser delta have not been extensively investigated, but appear to consist of a diverse mix of benthic species, most with brackish affinities. Low- and middle-marsh assemblages are difficult to distinguish (Hutchinson, unpublished data), but high-marsh assemblages are relatively distinct (Fig. 4), consisting primarily of fresh-brackish species that can withstand dessication (aerophile species), such as *Navicula pusilla* and *Diploneis ovalis*. Similar diatom assemblages have been described at other estuaries in the Pacific Northwest (e.g. Hemphill-Haley, 1993, 1995; Nelson and Kashima, 1993).

Foraminiferal assemblages in brackish-marsh sediments on Sturgeon Bank were investigated by Williams (1989) and Patterson (1990). The lowest zone consists of a *Miliammina fusca* biofacies which extends from areas on the upper tidal flats stabilized by *Zostera japonica* into the low marsh. Similar foraminiferal assemblages have been described at equivalent elevations in other Northern Hemisphere temperate marshes (Lutze, 1968; Ellison and Nichols, 1976; Scott and Medioli, 1980; Scott et al., 1981; De Rijk, 1995).

Miliammina fusca is the dominant foraminifer on the upper sand flats and in the lower part of the low-marsh zone on both north-central Roberts Bank and Sturgeon Bank (Fig. 4). It is also common in the upper part of the low-marsh zone, where *Ammonia beccarii* is the dominant species. This faunal assemblage extends into the upper middle marsh, where *Cribroelphidium gunteri* replaces *A. beccarii* (Patterson, 1990). As elsewhere, the low and middle marshes support substantial numbers of calcareous foraminifers (Phleger, 1965, 1966, 1970; Scott, 1976), but the tests of these species dissolve soon after death in the weakly acidic marsh sediments (Scott and Medioli, 1980).

The foraminiferal fauna of the high-marsh zone on Sturgeon and Roberts banks is dominated by *Jadammina macrescens*. The biofacies is similar to the high-marsh assemblage in brackish marshes in Nova Scotia (Scott and Medioli, 1980). *Pseudothurammina limnetis* and the arcellacean *Centropyxis aculeata* are common near the limit of tides. *Centropyxis aculeata* is an opportunisitic species that can withstand salinities up to 5‰ and much more hostile conditions than most other arcellaceans. The narrow vertical range of this biofacies makes it extremely useful for paleo-sea-level studies (Patterson et al., 1985; Guilbault et al., 1995).

Salt-marsh biofacies

True salt marshes occupy the upper intertidal zone in Boundary Bay and at the western delta front near Tsawwassen (Fig. 1). The floristic character of the Boundary Bay salt marsh and its successional development have been described by Shepperd (1981). Accretion of mud and organic detritus on the tidal flats leads to the replacement of pioneering stands of arrowgrass (*Triglochin maritimum*) and pickleweed (*Salicornia virginica*) by high-marsh species such as saltgrass (*Distichlis spicata*) and gumweed (*Grindelia integrifolia*). Orache (*Atriplex patula*), an annual halophyte, is common at disturbed sites near the high-tide limit. Pollen in this environment is derived largely from local stands of chenopods (e.g. *Salicornia*), amaranths (e.g. *Atriplex*), and grasses (Hebda, 1977; Shepperd, 1981).

Diatom assemblages in the salt marshes are diverse; allochthonous marine species transported from subtidal and lower intertidal areas by winter storms (e.g. *Odontella* spp., *Cocconeis* spp., and *Amphora* spp.) commonly outnumber autochthonous species, particularly in areas where eelgrass detritus is deposited. The most common autochthonous species in the Boundary Bay salt marsh is *Nitzschia sigma* (Fig. 4). *Nitzschia terrestris* and *Denticula subtilis* are common in the marsh-upland transition zone.

Foraminiferal assemblages in the Boundary Bay salt marsh are similar to those of the high-marsh zone of the brackish marsh at Sturgeon Bank; the assemblages are dominated by *Jadammina macrescens* and include significant numbers of *Trochammina inflata*. Similar assemblages are widespread in other salt-marsh environments (e.g. Phleger, 1970; Scott, 1976).

Terrestrial zone

Distributary-channel biofacies

Diatom assemblages in the modern Fraser River distributaries contain a mixture of planktonic and benthic freshwater species, with *Aulacoseira granulata* and *Achnanthes minutissima* respectively dominating these two groups (Beak Consultants, 1981; Hutchinson, unpublished data). The planktonic species may be autochtonous, but phytoplankon productivity in the distributaries is very low because of weak light penetration through the turbid water column (Harrison et al., 1983). In-channel diatom populations are therefore likely derived from the flushing of seasonal ponds and sloughs, and from the erosion of distributary-channel banks by floods.

Freshwater-marsh biofacies

Prior to settlement, freshwater marshes occupied the margins of all major distributary channels and the extensive network of sloughs that criss-crossed the Fraser delta (Ham, 1987).

The freshwater marshes that still remain are regularly submerged at high tide and are flooded for longer periods during the summer freshet. The vegetation at lower elevations in these marshes consists of bulrushes (*Scirpus* spp.) and sedges (*Carex* spp., *Eleocharis* spp.). Cattail (*Typha latifolia*), buckbean (*Menyanthes trifoliata*), and skunk cabbage (*Lysichiton americanum*) are common at higher elevations and also in freshwater marshes beyond the influences of tides (Bradfield and Porter, 1982). The pollen spectrum in these marshes is dominated by regional arboreal species; sedge, grass, and skunk cabbage are important secondary elements (Williams and Hebda, 1991).

The common diatoms in freshwater marshes are the same as those found in high brackish marshes; *Denticula subtilis*, *Diploneis ovalis*, *Pinnularia lagerstedtii*, and *Navicula cryptocephala* are the most abundant taxa (Hutchinson, unpublished data). Arcellacean faunas replace foraminifers in freshwater marshes. Not enough research has been carried out to define diatom and arcellacean assemblages in the various subenvironments of this habitat.

Riparian-woodland biofacies

Channel banks above the freshwater marsh are occupied by riparian woodlands dominated by red alder (*Alnus rubra*), black cottonwood (*Populus trichocarpa*), Sitka spruce (*Picea sitchensis*), and willow (*Salix* spp.), with a well developed shrub understorey consisting of salmonberry (*Rubus spectabilis*) and red-osier dogwood (*Cornus stolonifera*) (Williams and Hebda, 1991). Inorganic sediment and allochthonous organic detritus are deposited in these woodlands during floods. Arboreal species dominate the pollen spectrum (Williams and Hebda, 1991), suggesting a mainly local source, but diatom assemblages are equivalent to those from freshwater marshes, and may be dominantly allochthonous (Hutchinson, unpublished data).

Wet-meadow and shrub-land biofacies

Large areas of the western and southern Fraser delta plain were seasonally flooded grasslands before agricultural clearing and drainage destroyed this habitat (North and Teversham, 1984). The diatom biofacies of this environment is dominated by freshwater aerophilic species such as *Navicula mutica* (Hutchinson et al., 1995). Freshwater planktonic species which colonize seasonal ponds on the upper delta plain (e.g. *Aulacoseira* spp.) may be a minor component of this assemblage.

Raised-bog biofacies

Peat bogs are the end member of the interdistributary successional pathway on the Fraser delta (Fig. 2). They develop in distal areas of the upper delta plain, beyond the limit of tides, where low rates of clastic sedimentation allow *Sphagnum* moss to become established as ground cover. The mat of *Sphagnum* restricts water flow and acidifies the substrate. Freshwater marsh species are quickly replaced by Ericaceae (e.g. Labrador tea, *Ledum groenlandica*), which are tolerant of wet acidic soils and low nutrient supply (Hebda, 1977). Variable growth of *Sphagnum* around the base of shrubs produces a hummocky bog surface; higher areas may then be colonized by lodgepole pine (*Pinus contorta*) and birch (*Betula* spp.). These communities undergo complex successional changes linked to fire, the hummock-hollow cycle, and increased elevation of the bog surface (Hebda, 1977; Styan and Bustin, 1983). Slow decomposition of organic matter in this wet and acidic environment promotes peat accretion and the development of a raised bog; some of the bogs on the Fraser delta have achieved elevations of more than 5 m.

The pollen spectrum in Fraser delta bogs is dominated by pine, Ericaceae, and alder (Hebda, 1977). Birch pollen and bracken (*Pteridium*) spores are locally abundant in better-drained areas at bog margins. Few diatoms can survive in this highly acidic environment; consequently, diatom assemblages are generally sparse and have low biodiversity. The main species are acidophilic and include *Pinnularia divergentissima* and *Eunotia* spp. (Hutchinson, unpublished data).

LATE QUATERNARY BIOFACIES

Late Pleistocene and Holocene macrofossil, pollen, diatom, and foraminiferal assemblages of the Fraser delta have been described from samples collected from cores and exposures. In this section, we review several studies in which the description of these assemblages has resulted in an improved understanding of depositional environments and environmental interactions. Pleistocene and early Holocene

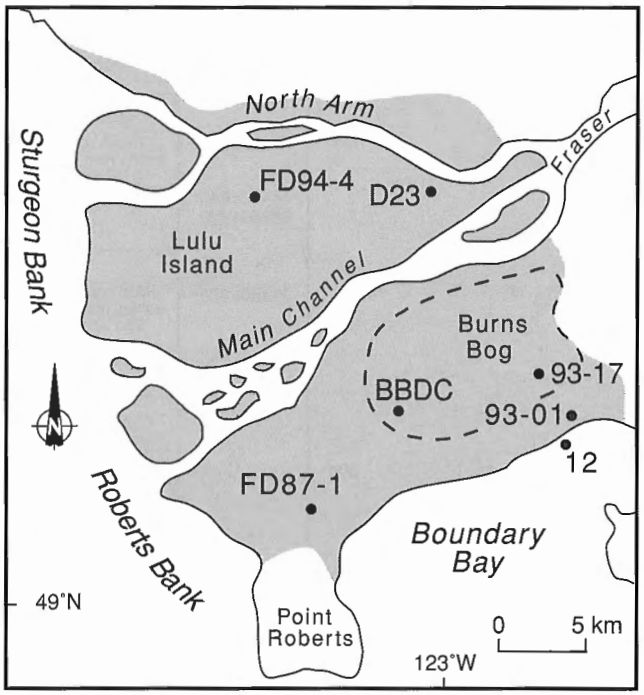

Figure 5. *Location of cores discussed in the paper; shaded area is the Fraser delta.*

depositional environments have been assessed from an analysis of pollen and foraminifers in two long cores, FD87-1 (367 m) and FD94-4 (304 m) (Fig. 5; Patterson and Cameron, 1991; Patterson and Luternauer, 1993; Mathewes, unpublished data). Middle and late Holocene environments, particularly on the southern delta, have been reconstructed from pollen and diatom assemblages in many short cores (Shepperd, 1981; Styan and Bustin, 1983; Clague et al., 1991; Williams and Hebda, 1991; Hutchinson et al., 1995).

Pleistocene biofacies

Two major predeltaic foraminiferal biofacies have been identified in cores FD87-1 and FD94-4: a cassidulinid-dominated assemblage found in the basal parts of both cores; and a *Cribroelphidium barletti* biofacies found only in FD87-1 (Fig. 6).

The cassidulinid-dominated biofacies, found in diamicton and clayey sediments between 347.5 and 367 m in core FD87-1 and between 284 and 287 m in core FD94-4, is dominated by *Cassidulina reniforme*. This species lives in

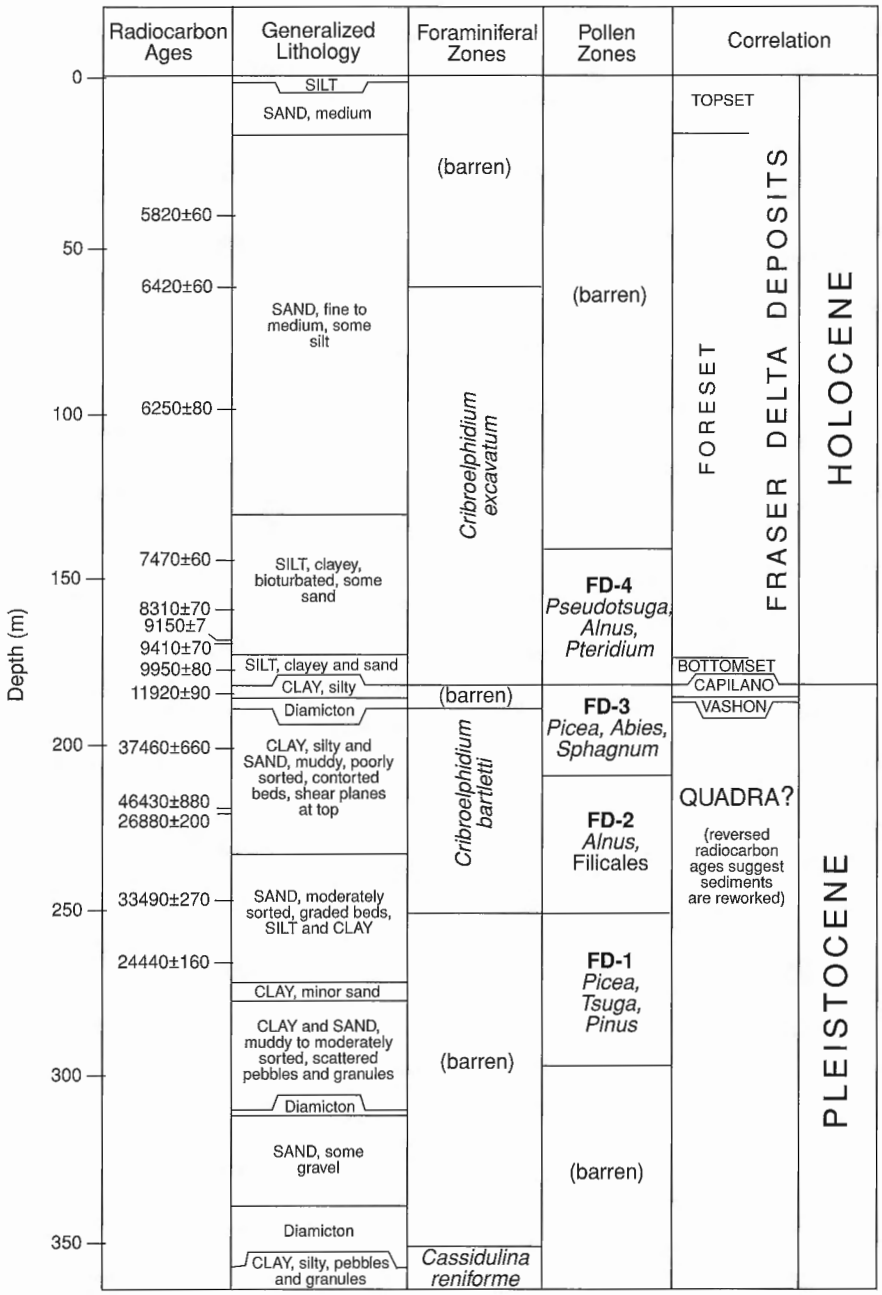

Figure 6. *Stratigraphy and biofacies, core FD87-1.*

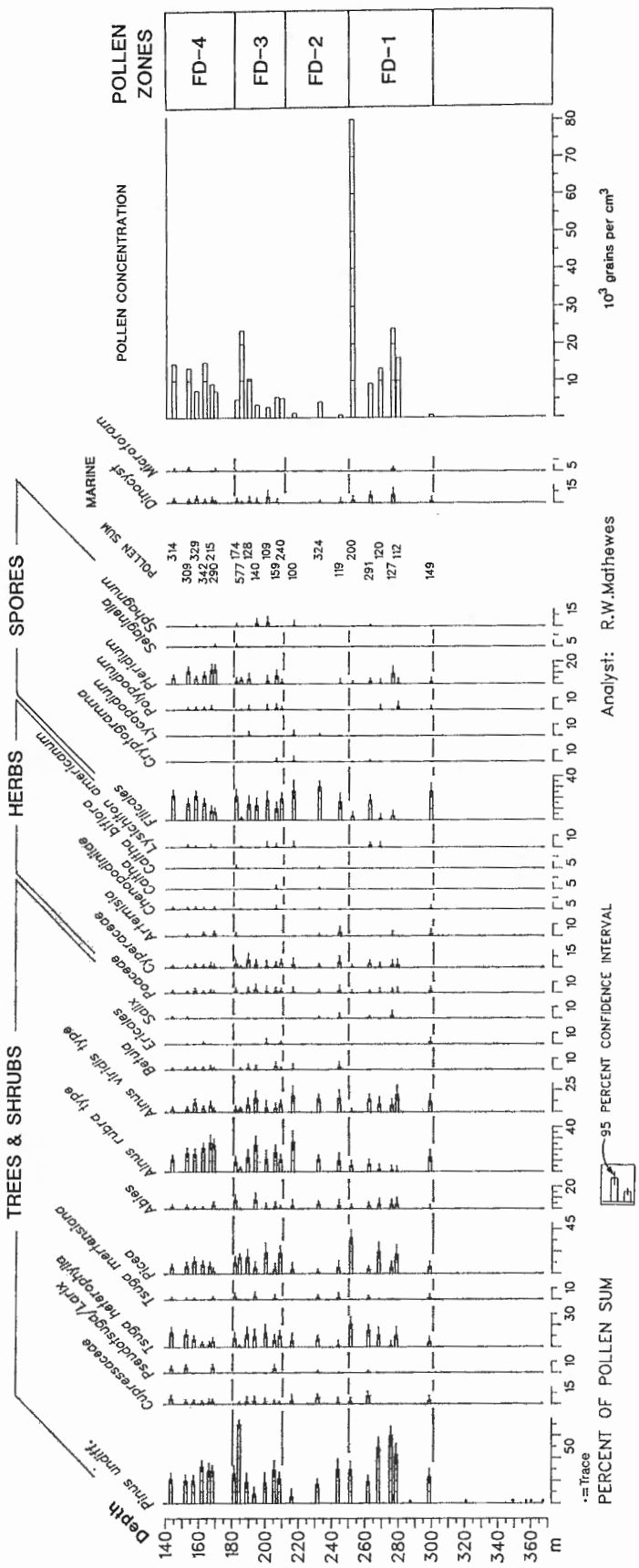

Figure 7. Pollen diagram for core FD87-1.

ice-proximal glaciomarine environments (e.g. Bahnson et al., 1974; Elverhøi et al., 1980; Osterman, 1984) and has been reported from similar late-glacial environments in eastern Canada (Sejrup and Guilbault, 1980; Scott et al., 1989) and British Columbia (Patterson, 1993; Patterson et al., 1995). The present-day and paleodistributions of the major taxa of this biofacies indicate deposition in cold saline (≥27‰) water approximately 100-200 m deep (Guilbault, 1980, 1989). The sediments containing this biofacies may correlate with the Semiahmoo Drift of Early Wisconsin age (Armstrong, 1975), but they could also be older.

The *Cribroelphidium bartletti* biofacies occurs between 192.9 and 256 m in core FD87-1 in silt and clay which are continuous with underlying barren sediments. *Cribroelphidium bartletti* has been recorded in shallow marine sediments (<150 m water depth) at high latitudes (Loeblich and Tappan, 1953; Todd and Low, 1967; Smith, 1970; Bergen and O'Neil, 1979).

Of the 35 sediment samples selected for analysis of pollen and spores from core FD87-1, only those samples between 140 and 300 m depth contained enough palynomorphs for quantitative analysis. Four pollen assemblage zones (FD-1 to FD-4) were identified in this interval based on abundances of characteristic taxa (Fig. 7). Although some of the pollen and spores were likely reworked from older deposits, the four pollen zones appear to correlate with the geological units in the core.

FD-1 (*Pinus-Picea-Tsuga* zone, 250-300 m) represents the first sediments that contain enough palynomorphs for quantitative analysis. The abundance of tree pollen suggests at least a partially forested landscape during this interval. Pollen zones FD-2 (*Alnus-Filicales* zone, 210-250 m) and the lower part of FD-3 (*Picea-Abies-Sphagnum* zone, 180-210 m) span the interval of the *C. bartletti* biofacies. Reversals in radiocarbon dates render the age of these deposits problematical (Fig. 6) and suggest that much of this material may be reworked.

The upper part of the FD-3 pollen zone (Fig. 7) is reliably dated to the period from 12 000 to 10 000 ^{14}C yr B.P. (Fig. 6). Although some of the material in these late Pleistocene deposits is reworked, the relatively high abundances of pine, alder and spruce pollen (Fig. 7) match pollen spectra from other late-glacial deposits in the region (Heusser, 1973).

Holocene biofacies

Prodelta and delta-foreslope biofacies

Prodelta and lower delta-slope muds contain a low-diversity foraminiferal fauna dominated by *Cribroelphidium excavatum*, *Buccella frigida*, and *Elphidiella hannai* (Fig. 6; Patterson and Cameron, 1991; Patterson and Luternauer, 1993). This biofacies is found at depths of 67 to 180 m in core FD87-1 and 65 to 120 m in core FD94-4, similar to the depth at which it occurs in the present-day marine environment. *Cribroelphidium excavata*, which dominates this assemblage, is widely distributed at shallow depths in temperate and polar seas at the present (Phleger, 1952; Loeblich and Tappan, 1953; Miller et al., 1982). It is also common in late Pleistocene glaciomarine deposits, constituting 50-80% of the foraminiferal fauna (Feyling-Hanssen, 1976; Knudsen, 1976; Osterman, 1984; Rodriguez and Richard, 1986; Hald and Vorren, 1987; Patterson, 1993; Patterson et al., 1995). Its presence in temperate environments indicates a salinity below that of standard sea water (35‰).

There are several forms of *C. excavatum*, but only the '*clavatum*' variant has been found in Fraser delta deposits dating from the early and middle Holocene. This form is indicative of either cold, normal-salinity marine waters (sometimes described as a 'warm ice-margin fauna'; Scott et al., 1989), or waters with slightly reduced salinities (Miller et al., 1982). The greater abundance of *C. excavatum* in early postglacial deposits, and the dominance of the '*clavatum*' form, suggest that water temperature (and/or salinity) in the Strait of Georgia was somewhat lower during the early Holocene than at present.

The conclusion that the regional climate was cooler in the early Holocene is, however, at odds with the paleoclimatic reconstruction based on the pollen record. Pollen zone FD-4, which correlates with the lower part of the *C. excavatum* zone, is characterized by large amounts of Douglas-fir (*Pseudotsuga menziesii*) and red alder pollen, and bracken spores (Fig. 7). This assemblage is typical of early Holocene pollen assemblages at other sites in southwestern British Columbia (Heusser, 1983; Mathewes, 1985) and western Washington (Heusser, 1977), which have been interpreted as indicating a warmer and drier climate than at present (Mathewes 1985; Cwynar, 1987). This being the case, one might expect higher surface temperatures in the Strait of Georgia at that time.

Foraminifers become increasingly less common higher in the delta-slope sequence and are absent in upper-slope, channel, and tidal-flat sands (Patterson and Cameron, 1991; Patterson and Luternauer, 1993). As mentioned previously, the high mobility of these sandy sediments curtails foraminiferal colonization. Foraminifers generally disappear at about 20 to 30 m depth in cores, but the range is from as little as 10 m in core FD91-1 to over 70 m in cores FD87-1 (Fig. 6) and FD88A-1 (Patterson and Cameron, 1991; Patterson and Luternauer, 1993).

Tidal-flat and intertidal-marsh biofacies

A buried peat bed, which crops out on the foreshore of Boundary Bay (Fig. 8a; Kellerhals and Murray, 1969; Shepperd, 1981; Styan and Bustin, 1983), was laid down in a

*Figure 8. Stratigraphy and plant macrofossil and microfossil assemblages of selected short cores from the Fraser River delta (core sites shown in Fig. 5): **a)** major diatom groups in core 93-01, from Hutchinson et al. (1995); **b)** selected pollen types, core 12; adapted from Shepperd (1981); **c)** biozones and plant macrofossils, core BBDC, adapted from Hebda (1977); **d)** major diatom groups, core 93-17, from Hutchinson et al. (1995). Figures 8a and 8d are reproduced with permission of the National Research Council of Canada.*

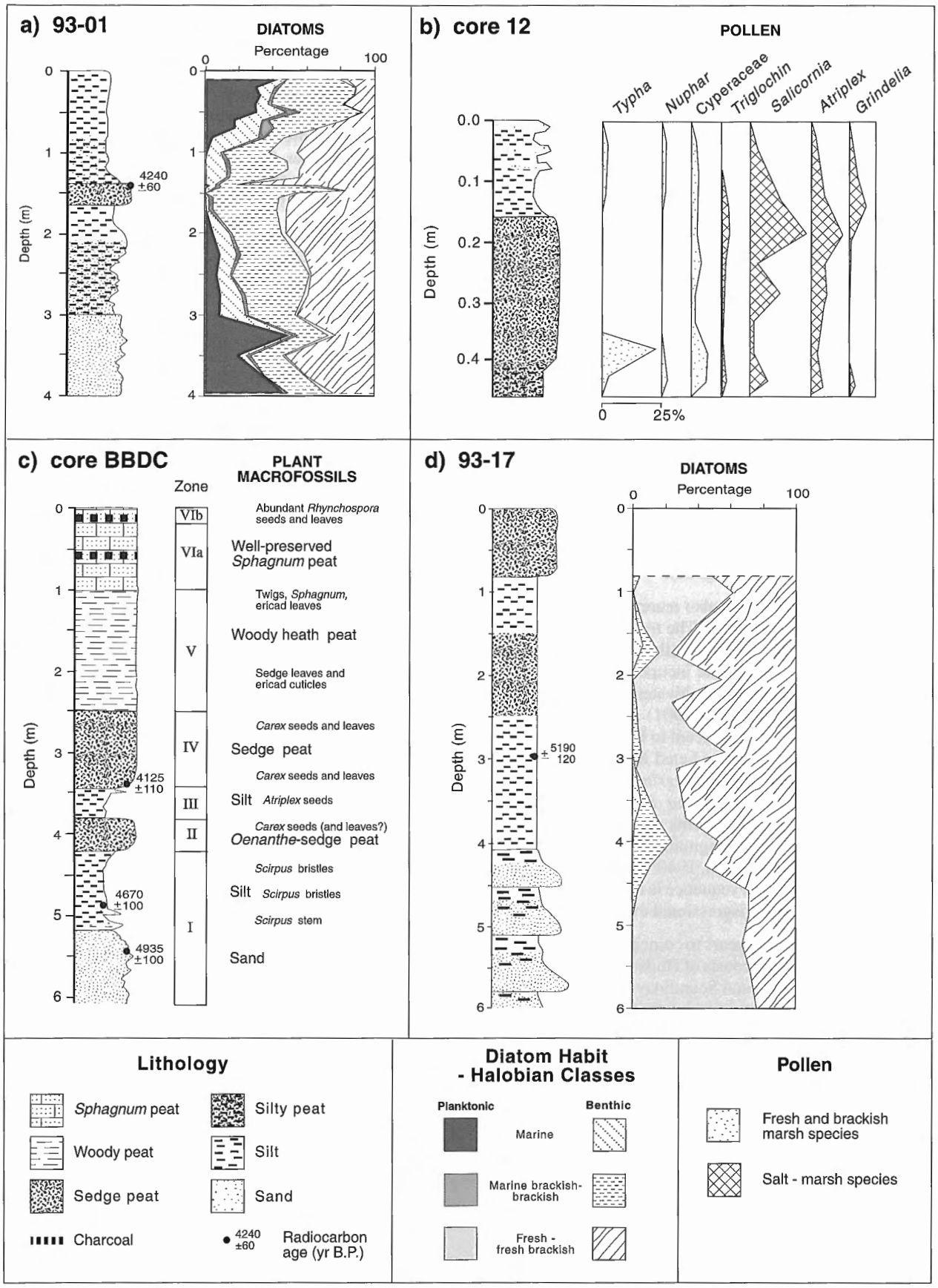
a) 93-01
DIATOMS
Percentage
0
100
Depth (m)
4240 ±60
b) core 12
POLLEN
Typha
Nuphar
Cyperaceae
Triglochin
Salicornia
Atriplex
Grindelia
Depth (m)
0
25%
c) core BBDC
PLANT MACROFOSSILS
Zone
VIb
VIa
V
IV
III
II
I
Abundant Rhynchospora seeds and leaves
Well-preserved Sphagnum peat
Twigs, Sphagnum, ericad leaves
Woody heath peat
Sedge leaves and ericad cuticles
Carex seeds and leaves
Sedge peat
Carex seeds and leaves
Silt Atriplex seeds
Carex seeds (and leaves?)
Oenanthe-sedge peat
Scirpus bristles
Silt Scirpus bristles
Scirpus stem
Sand
Depth (m)
4125 ±110
4670 ±100
4935 ±100
d) 93-17
DIATOMS
Percentage
0
100
Depth (m)
5190 ± 120
Lithology
Sphagnum peat
Woody peat
Sedge peat
Charcoal
Silty peat
Silt
Sand
4240 ±60
Radiocarbon age (yr B.P.)
Diatom Habit - Halobian Classes
Planktonic
Benthic
Marine
Marine brackish-brackish
Fresh - fresh brackish
Pollen
Fresh and brackish marsh species
Salt - marsh species

brackish-freshwater marsh environment after the abandonment of distributary channels on the southern flank of the delta about 5000 years ago (Hutchinson et al., 1995). Underlying and overlying clastic sediments are tidal-flat deposits.

A typical tidal-flat aggradational sequence in the Boundary Bay foreshore area is found in the lower part of core 93-01 (Fig. 5, 8a). A basal sand unit contains high percentages of marine planktonic and brackish-marine benthic diatoms (Fig. 8a; Hutchinson et al., 1995). The marine planktonic component steadily decreases through the overlying, interbedded sandy muds which were deposited in the middle and upper intertidal zone, and benthic brackish species such as *Nitzschia levidensis* become dominant. Pollen of freshwater aquatic plants (e.g. *Typha* and *Nuphar*) (Fig. 8b; Shepperd, 1981), fern spores (Shepperd, 1981), and fresh-brackish diatoms (Fig. 8a) are abundant in the lower part of the peat, indicating succession to a freshwater-marsh environment.

Abundant sedge macrofossils in the middle of the peat (Styan and Bustin, 1983) herald the return of brackish marsh conditions, and mark the onset of a short-lived oscillation in sea level at around 4200 ^{14}C years BP. The transgressional phase of this oscillation is recorded by an increase in the pollen of salt-marsh plants in the upper part of the peat (Fig. 8b), the subsequent transition to muddy sands, and the gradual increase in marine and marine-brackish diatoms in these sands and the overlying silts (Fig. 8a).

This sea-level oscillation is also recorded in core BBDC from western Burns Bog (Fig. 5). The transition from freshwater peats (Fig. 8c: zone II) to peaty silts containing *Atriplex* seeds (zone III) marks the marine incursion (Hebda, 1977). The silts in turn are overlain by freshwater peats, signalling a marine regression. Clague et al. (1991) recorded a similar sequence in a core from a site adjacent to BBDC. The silt unit in this core, which was also bracketed by peats, contained intertidal diatoms (e.g. *Navicula peregrina*) and foraminifers (*Miliammina fusca*, *Trochammina inflata*). Silts with brackish-marine pollen and diatoms overlying freshwater sedge peats and underlying sphagnum peats are also known from central Lulu Island (Hansen, 1940; Hutchinson, unpublished data). The Lulu Island sequence is undated, but the silt unit may mark the same transgressional event.

This marine incursion appears to coincide with a sea-level oscillation identified on the coasts of Hudson Bay (Fairbridge and Hillaire-Marcel, 1977) and Scandinavia (Mörner, 1980). The effects of this transgression may have been magnified on the southern front of the Fraser delta by the contemporaneous closure of the distributary-channel network in this area (Hutchinson et al., 1995).

Distributary-channel biofacies

Core 93-17 from eastern Burns Bog (Fig. 5) records a distributary paleochannel in the final stages of abandonment (Fig. 8d). Cyclic, fining-upward, sand-silt sequences in the lower part of the core were deposited by floods from a nearby channel. These sediments contain a meagre diatom assemblage composed largely of abraded valves of *Aulacoseira granulata*, a robust planktonic diatom which can withstand fluvial transport (Hutchinson et al., 1995). Closure of the channel is indicated by increased deposition of fines and organics in the upper part of the core (Fig. 8d). These sediments have high concentrations of diatoms, mainly benthic freshwater species associated with shallow, standing water or wet substrates. Whereas diatom biofacies in abandoned channel deposits at upstream sites such as 93-17 are characterized by freshwater species, biofacies from sites closer to the channel mouth have high frequencies of brackish and marine diatoms (Hutchinson et al., 1995).

Freshwater-marsh, wet-meadow, and riparian-woodland biofacies

Fluvial overbank deposits of the upper delta plain and their associated pollen biofacies have been described by Williams and Hebda (1991) from a 15 m vibracore (D23; Fig. 5) from central Lulu Island. A thin, basal, tidal-flat sand is overlain by silts containing skunk cabbage, sedge, and grass pollen, and horsetail spores. The inferred vegetation is similar to the present-day vegetation in freshwater marshes on the upper delta plain. Abundant pollen of herbaceous species and low-shrub pollen indicate that the site was frequently flooded by the Fraser River at this time. A zone with significant shrub pollen (sweet gale (*Myrica gale*), Ericaceae, and Rosaceae) overlies the freshwater marsh deposit. Williams and Hebda (1991) inferred that this change from marsh to swamp occurred because the site had aggraded to a higher elevation and was less subject to flooding. The successional sequence outlined in Figure 2 suggests that the swamp would in time be replaced by a raised bog, but increases in red alder and skunk cabbage pollen higher in the sequence indicate that the area became a riparian woodland. The site was again being flooded frequently, either in response to a rise in base level or a shift in the position or discharge of a nearby distributary channel.

Raised-bog biofacies

The upper half of core BBDC (Fig. 8c) records a typical raised bog succession on the Fraser delta (Hebda, 1977). The salt-marsh or upper tidal-flat deposits of zone III are overlain by peat deposited in a freshwater sedge marsh or fen (zone IV). The fen deposits, in turn, are overlain by heath shrubland peat (zone V). The heath habitat was gradually colonized by *Sphagnum* mosses and Ericaceae species characteristic of a bog environment. The uppermost unit (zone VI) consists almost entirely of *Sphagnum* peat. This sequence follows the successional path in interdistributary areas shown in Figure 2.

Changes in plant macrofossils and pollen in zone VI illustrate the role of fire in mediating the development of the *Sphagnum* hummock-hollow cycle (Hebda, 1977, fig. 7). Large fires in the bog are recorded by charcoal layers in the peat (Fig. 8c). These fires destroy higher, drier moss hummocks and the heath plants that grow on them. Reduced growth of peat in these patches converts them to wet acid hollows, which are colonized by sedges (e.g. *Rhynchospora*). Peat deposition is rapid in these wet microenvironments which subsequently regenerate into *Sphagnum* hummocks.

DISCUSSION AND CONCLUSIONS

A reconstruction of the natural landscape of the Fraser delta in the early historical period reveals a mosaic of wet meadows and shrub lands, bogs, and riparian woodlands above the limit of tides, and marshes, sand flats, and mud flats in the intertidal zone. These environments can be linked by a successional model that relates ecological communities to elevation and the character of the substrate.

Intertidal and subtidal habitats on the Fraser delta have changed in the last century, due to human activity, but the ecological structure of these communities, prior to settlement, has been determined with some confidence from their modern counterparts. In contrast, most of the natural vegetation of the upper delta plain has been lost, making the task of the paleobotanist or palynologist difficult. Present-day plant communities on the delta plain may not provide good analogues for their prehistoric counterparts, and surface pollen collections may bear little resemblance to pollen spectra from earlier times. Despite these problems, there is sufficient baseline information on the distribution and character of modern biofacies to at least identify paleobiofacie

Plant macrofossils play an important role in these investigations, not only as raw materials for AMS radiocarbon dating, but also as indicators of the ambient physical environment and plant-community composition. Together with pollen, spores, diatoms, and foraminifers, plant macrofossils (including detrital wood and buried stumps) provide information on past environmental conditions such as climate, water depth, temperature, and salinity, and the relative elevation of the site.

The examples discussed in this paper demonstrate that some progress has been made in reconstructing paleoenvironmental change on the Fraser delta. We have shown the value of paleoecological investigations in 1) reconstructing late-glacial and early Holocene conditions in the Strait of Georgia (core FD87-1); 2) reconstructing small-scale marine transgressions and regressions (cores BBDC, 12, and 93-01); 3) assessing flood frequency in interdistributary areas (core D23); and 4) developing models to explain autogenic changes associated with fire occurrence in raised bogs (core BBDC).

These paleoecological investigations are primarily reconnaissance studies focusing on changes in particular macro- or microfossil assemblages in local areas on the Fraser delta. A synthesis of the development of the Fraser delta's ecological mosaic can only be achieved if future workers link species and community responses to deltaic processes via integrated geological-paleoecological analyses. This approach is exemplified by the analysis of paleoseismic activity in southwestern British Columbia by Mathewes and Clague (1994), and on the Fraser delta by Clague et al. (1998).

ACKNOWLEDGMENTS

We thank John Clague and Richard Hebda for their painstaking reviews of earlier drafts of this paper. Ray Squirrell and Paul de Grace helped draft the illustrations. The work on which this paper is based was funded in part by grants from the Natural Science and Engineering Research Council (Patterson, Mathewes) and the Department of Energy, Mines and Resources, now the Department of Natural Resources (Patterson).

REFERENCES

Armstrong, J.E.
1975: Quaternary geology, stratigraphic studies, and revaluation of terrain inventory maps, Fraser Lowland, British Columbia; in Report of Activities, Part A; Geological Survey of Canada, Paper 75-1A, p. 377-380.

Atwater, B.F., Nelson, A.R., Clague, J.J., Carver, G.A., Yamaguchi, D.K., Bobrowsky, P.T., Bourgeois, J., Darienzo, M.E., Grant, W.C., Hemphill-Hailey, E., Kelsey, H.M., Jacoby, G.C., Nishenko, S.P., Palmer, S.P., Peterson, C.D., and Reinhart, M.A.
1995: Summary of coastal geological evidence for past great earthquakes at the Cascadia subduction zone; Earthquake Spectra, v. 11, p. 1-18.

Bahnson, H., Peterson, K.S., Konradi, P.B., and Knudsen, K.L.
1974: Stratigraphy of Quaternary deposits in the Skaerumhede II boring: lithology, molluscs and foraminifera; Danmarks Geologiske Undersøgelse, Ärbog 1973, p. 27-62.

Baldwin, J.R. and Lovvorn, J.R.
1994: Habitats and tidal accessibility of the marine foods of dabbling ducks and brant in Boundary Bay, British Columbia; Marine Biology, v. 120, p. 627-638.

Bandy, O.L., Ingle, J.C., Jr., and Resig, J.M.
1965: Foraminiferal trends, Hyperion outfall, California; Limnology and Oceanography, v. 10, p. 314-332.

Beak Consultants
1981: Environmental impact statement of proposed improvements to the Fraser River shipping channel; report to Public Works Canada, Pacific Region, Vancouver, British Columbia.

Bergen, F.W. and O'Neil, P.
1979: Distribution of Holocene foraminifera in the Gulf of Alaska; Journal of Paleontology, v. 53, p. 1267-1292.

Bradfield, G.E. and Porter, G.L.
1982: Vegetation structure and diversity of a Fraser estuary tidal marsh; Canadian Journal of Botany, v. 60, p. 445-451.

Clague, J.J., Lichti-Federovich, S., Guilbault J.-P., and Mathewes, R.W.
1991: Holocene sea level change, south-coastal British Columbia; in Current Research, Part A; Geological Survey of Canada, Paper 91-1A, p. 15-21.

Clague, J.J., Naesgaard, E., and Mathewes, R.W.
1998: Geological Evidence for Prehistoric Earthquakes; in Geology and Natural Hazards of the Fraser River Delta, British Columbia, (ed.) J.J. Clague, J.L. Luternauer, and D.C. Mosher; Geological Survey of Canada, Bulletin 525, this volume.

Cockbain, A.E.
1963: Distribution of foraminifera in Juan de Fuca and Georgia straits, British Columbia, Canada; Cushman Foundation for Foraminiferal Research, Contributions, v. 14, p. 37-57.

Culver, S.J. and Buzas, M.A.
1985: Distribution of Recent benthic foraminifera off the North American Pacific coast from Oregon to Alaska; Smithsonian Contributions to the Marine Sciences, No. 26, 234 p.

Cwynar, L.C.
1987: Fire and the forest history of the North Cascade Range; Ecology, v. 68, p. 791-802.

De Rijk, S.
1995: Salinity control of the distribution of salt marsh foraminifera (Great Marshes, Massachusetts); Journal of Foraminiferal Research, v. 25, p. 156-165.

Dobell, P.E.R.
1976: A study of dinoflagellate cysts from recent marine sediments of British Columbia; Ph.D. thesis, University of British Columbia, Vancouver, British Columbia, 176 p.

Ellison, R.L. and Nichols, M.M.
1976: Modern and Holocene foraminifera in the Chesapeake Bay region; in First International Symposium on Benthonic Foraminifera of the Continental Margins, Part A, Ecology and Biology, (ed.) C. Schafer and B.R. Pelletier; Maritime Sediments, Special Publication 1, p. 131-151.

Elverhøi, A., Liestøl, O., and Nagy, Y.
1980: Glacial erosion, sedimentation and microfauna in the inner part of Kongsfjorden, Spitsbergen; Norsk Polarinstitutt Skrifter, v. 172Z, p. 33-61.

Evoy, R.W., Moslow, T.F., Patterson, R.T., and Luternauer, J.L.
1993: Patterns and variability in sediment accumulation rates, Fraser River delta foreslope, British Columbia, Canada; Geo-Marine Letters, v. 13, p. 212-218.

Fairbridge, R.W. and Hillaire-Marcel, C.
1977: A 8,000-yr palaeoclimatic record of the 'Double-Hale' 45-yr solar cycle; Nature, v. 268, p. 413-416.

Feyling-Hanssen, R.W.
1976: A mid-Wisconsinian interstadial on Broughton Island, Arctic Canada, and its foraminifera; Arctic and Alpine Research, v. 8, p. 161-182.

Guilbault, J.-P.
1980: A stratigraphic approach to the study of the Late-Glacial Champlain Sea deposits with the use of foraminifera; Licentiat thesis, Aarhus University, Aarhus, Denmark, 294 p.
1989: Foraminiferal distribution in the central and western parts of the Late Pleistocene Champlain Sea basin, Eastern Canada; Géographie physique et Quaternaire, v. 43, p. 3-26.

Guilbault, J-P., Clague, J.J., and Lapointe, M.
1995: Amount of subsidence during a late Holocene earthquake - evidence from fossil tidal marsh foraminifera at Vancouver Island, west coast of Canada; Palaeogeography, Palaeoclimatology, Palaeoecology, v. 118, p. 49-71.

Hald, M. and Vorren, T.O.
1987: Foraminifera stratigraphy and environment of the late Weichselian deposits on the continental shelf off Troms, northern Norway; Marine Micropalaeontology, v. 12, p. 129-160.

Ham, L.
1987: An archaeological resource overview of Richmond B.C.; British Columbia Archaeology Branch, Victoria, British Columbia, Permits 1986-19 and 1987-1, 105 p.

Hansen, H.P.
1940: Paleoecology of two peat bogs in southwestern British Columbia; American Journal of Botany, v. 27, p. 144-149.

Harrison, P.J., Fulton, J.D., Taylor, F.J.R., and Parsons, T.R.
1983: Review of the biological oceanography of the Strait of Georgia: pelagic environment; Canadian Journal of Fisheries and Aquatic Sciences, v. 40, p. 1064-1094.

Hebda, R.J.
1977: The paleoecology of a raised bog and associated deltaic sediments of the Fraser River delta; Ph.D. thesis, University of British Columbia, Vancouver, British Columbia, 183 p.

Hemphill-Haley, E.
1993: Taxonomy of recent and fossil (Holocene) diatoms (Bacillariophyta) from northern Willapa Bay, Washington; United States Geological Survey, Open-File Report 93-289, 151 p.
1995: Diatom evidence for earthquake-induced subsidence and tsunami 300 yr ago in southern coastal Washington; Geological Society of America Bulletin, v. 107, p. 367-378.

Heusser, C.J.
1973: Environmental sequence following the Fraser advance of the Juan de Fuca lobe, Washington; Quaternary Research, v. 3, p. 284-306.
1977: Quaternary palynology of the Pacific slope of Washington; Quaternary Research, v. 8, p. 282-306.

Heusser, L.E.
1983: Palynology and paleoecology of postglacial sediments in an anoxic basin, Saanich Inlet, British Columbia; Canadian Journal of Earth Sciences, v. 20, p. 873-885.

Hutchinson, I.
1982: Vegetation - environment relations in a brackish marsh, Lulu Island, Richmond, B.C.; Canadian Journal of Botany, v. 60, p. 452-462.

Hutchinson, I., Roberts, M.C. and Williams, H.F.L.
1995: Stratigraphy, diatom biofacies and palaeogeomorphology of a mid-Holocene distributary channel system, Fraser River delta, British Columbia, Canada; Canadian Journal of Earth Sciences, v. 32, p. 749-757.

Jonasson, K. and Patterson, R.T.
1992: Preservation potential of marsh benthic foraminifera from the Fraser River delta, British Columbia; Micropaleontology, v. 38, p. 289-301.

Kellerhals, P. and Murray, J.W.
1969: Tidal flats at Boundary Bay, Fraser River delta, British Columbia; Bulletin of Canadian Petroleum Geology, v. 17, p. 67-91.

Knudsen, K.L.
1976: Foraminifera faunas in Weichselian stadial and interstadial deposits of the Skaerumhede boring, Jutland Denmark; in First International Symposium on Benthonic Foraminifera of Continental Margins, Part B, Paleoecology and Biostratigraphy, (ed.) C. Schafer and B.R. Pelletier; Maritime Sediments, Special Publication 1, p. 131-151.

Laws, R.A.
1988: Diatoms (Bacillariophyceae) from surface sediments in the San Francisco Bay estuary; Proceedings, California Academy of Sciences, v. 45, p. 133-254.

LeBlond, P.H.
1983: The Strait of Georgia: functional anatomy of a coastal sea; Canadian Journal of Fisheries and Aquatic Sciences, v. 40, p. 1026-1032.

Loeblich, A. R., Jr. and Tappan, H.
1953: Studies of Arctic foraminifera; Smithsonian Miscellaneous Collections, v. 121, 150 p.

Luternauer, J.L., Clague, J.J., Hunter, J.A.M., Pullan, S.E., Roberts, M.C., Woeller, D.J., Kostaschuk, R.A., Moslow, T.F., Monahan, P.A., and Hart, B.S.
1993: The Fraser River delta, British Columbia: architecture, geological dynamics and human impact; in Deltas of the World, (ed.) R.Kay; American Society of Civil Engineers, New York, New York, p. 99-113.

Luternauer, J.L, Clague, J.J., and Pharo, C.H.
1983: Substrates of the Strait of Georgia, British Columbia; Canadian Journal of Fisheries and Aquatic Sciences, v. 40, p. 1026-1032.

Lutze, C.F.
1968: Jahresgang der foraminiferen-fauna in der Bottsand-Lagune; Meyniana, v. 18, p. 13-30.

Mathewes, R.W.
1985: Paleobotanical evidence for climatic change in southern British Columbia during late-glacial and Holocene time; in Critical Periods in the Quaternary Climatic History of Northern North America, (ed.) C.R. Harington; National Museums of Canada, National Museum of Natural Sciences, Syllogeus Series, no. 5, p. 397-422.

Mathewes, R.W. and Clague, J.J.
1994: Detection of large prehistoric earthquakes in the Pacific Northwest using microfossil analysis; Science, v. 264, p. 688-691.

Mathews, W.H. and Shepard, F.P.
1962: Sedimentation of Fraser River delta, British Columbia; American Association of Petroleum Geologists Bulletin, v. 46, p. 1416-1443.

Miller, A.A.L., Scott, D.B., and Medioli, F.S.
1982: *Elphidium excavatum* (Terquem); ecophenotypic versus subspecific variation; Journal of Foraminiferal Research, v. 12, p. 116-144.

Milliman, J.D.
1980: Sedimentation in the Fraser River and its estuary, southwestern Brittish Columbia (Canada); Estuarine and Coastal Shelf Science, v. 10, p. 609-613.

Monahan, P.A., Luternauer, J.L., and Barrie, J.V.
1993: A delta plain sheet sand in the Fraser River delta, British Columbia, Canada; Quaternary International, v. 20, p. 27-38.

Mörner, N-A.
1980: The northwest European "sea-level laboratory" and regional Holocene eustasy; Palaeogeography, Palaeoclimatology, Palaeoecology, v. 29, p. 281-300.

Nelson, A.R. and Kashima, K.
1993: Diatom zonation in southern Oregon tidal marshes relative to vascular plants, foraminifera, and sea level; Journal of Coastal Research, v. 9, p. 673-697.

North, M.E.A. and Teversham, J.M.
1979: Vegetation of the southwestern Fraser lowland, 1858-1880; Canada Department of Environment, Lands Directorate, Vancouver, British Columbia, Fraser River Delta and Estuary Map Series, 1:50 000.
1984: The vegetation of the floodplain of the lower Fraser, Serpentine and Nicomekl rivers; Syesis, v. 17, p. 47-66.

Osterman, L.
1984: Benthic foraminifera zonation of a glacial/interglacial transition from Frobisher Bay, Baffin Island, North West Territories, Canada; in Benthos '83, Second International Symposium on Benthic Foraminifera, (ed.) H.J. Orleti; Elf Aquitane, Esso REP, TOTAL, CFP, Bordeaux, France, p. 471-476.

Patterson, R.T.
1990: Intertidal benthic foraminiferal biofacies on the Fraser River delta, British Columbia: modern distribution and paleoecological importance; Micropaleontology, v. 36, p. 183-199.
1993: Late Quaternary benthic foraminiferal biofacies and paleoceanography of Queen Charlotte Sound and southern Hecate Strait, British Columbia; Journal of Foraminiferal Research, v. 23, p. 1-18.

Patterson, R.T. and Cameron, B.E.
1991: Paleoenvironmental significance of the foraminiferal biofacies succession in the late Quaternary Sediments of the Fraser River delta, British Columbia; Journal of Foraminiferal Research, v. 21, p. 228-243.

Patterson, R.T. and Luternauer, J.L.
1993: Holocene foraminiferal faunas from cores collected on the Fraser River delta, British Columbia: a paleoecological interpretation; in Current Research, Part A; Geological Survey of Canada, Paper 93-1A, p. 245-254.

Patterson, R.T., Guilbault, J.-P., Thomson, R.E., and Luternauer, J.L.
1995: Foraminiferal evidence of Younger Dryas isochronous cooling on the British Columbia shelf, west coast of Canada; Géographie physique et Quaternaire, v. 49, p. 409-428.

Patterson, R. T., MacKinnon, K. D., Scott, D. B., and Medioli, F. S.
1985: Arcellaceans ("thecamoebians") in small lakes of New Brunswick and Nova Scotia: modern distribution and Holocene stratigraphic changes; Journal of Foraminiferal Research, v. 15, p. 114-137.

Phleger, F.B., Jr.
1952: Foraminifera distribution in some sediment samples from the Canadian and Greenland arctic; Cushman Foundation for Foraminiferal Research, Contributions, v. 3, p. 80-89.
1965: Patterns of marsh foraminifera, Galveston Bay, Texas; Limnology and Oceanography, v. 10 (Supplement), p. R169-R184.
1966: Patterns of living marsh foraminifera in south Texas coastal lagoons; Boletin de la Sociedad Geológica Mexicana, v. 28, p. 1-44.
1970: Foraminiferal populations and marine marsh processes; Limnology and Oceanography, v. 15, p. 522-534.

Rao, V.N.R. and Lewin, J.
1976: Benthic marine diatom flora of False Bay, San Juan Island, Washington; Syesis, v. 9, p. 173-213.

Rodriguez, C.G. and Richard, S.H.
1986: An ecostratigraphic study of late Pleistocene sediments of the western Champlain Sea Basin, Ontario and Quebec; Geological Survey of Canada, Paper 85-22, 33 p.

Sancetta, C.
1989: Processes controlling the accumulation of diatoms in sediments: a model derived from British Columbian fjords; Paleoceanography, v. 4, p. 235-251.

Scott, D.B.
1976: Quantitative studies of marsh foraminiferal patterns in southern California and their application to Holocene stratigraphic problems; in First International Symposium on Benthonic Foraminifera on Continental Margins, Part A, Ecology and Biology, (ed.) C.T. Schafer and B.R. Pelletier; Maritime Sediments, Special Publication, v. 1, p. 153-170.

Scott, D.B. and Medioli, F.S.
1980: Quantitative studies of marsh foraminiferal distributions in Nova Scotia. Implications for sea level studies; Cushman Foundation for Foraminiferal Research, Special Publication No. 17, 58 p.
1986: Foraminifera as sea-level indicators; in Sea-Level Research: A Manual for the Collection and Evaluation of Data, (ed.) O. van de Plassche; Geo Books, Norwich, United Kingdom, p. 435-456.

Scott, D.B., Baki, V., and Younger, C.D.
1989: Late Pleistocene-Holocene paleoceanographic changes on the eastern Canadian margin: stable isotopic evidence; Palaeogeography, Palaeoclimatology, Palaeoecology, v. 74, p. 279-295.

Scott, D.B., Williamson, M.A., and Duffett, T.E.
1981: Marsh foraminifera of Prince Edward Island: their recent distribution and application to former sea level studies; Maritime Sediments and Atlantic Geology, v. 17, p. 98-129.

Sejrup, H.-P. and Guilbault, J.-P.
1980: *Cassidulina reniforme* and *C. obtusa* (Foraminifera), taxonomy, distribution, and ecology; Sarsia, v. 65, p. 79-85.

Shepperd, J.E.
1981: Development of a salt marsh on the Fraser Delta at Boundary Bay, British Columbia, Canada; M.Sc. thesis, University of British Columbia, Vancouver, British Columbia, 99 p.

Shim, J.H.
1977: Distibutional ecology of planktonic diatoms in the Strait of Georgia, B.C.; Journal of the Oceanographic Society of Korea, v. 12, p. 13-32.

Smith, R.K.
1970: Late glacial foraminifera from southeast Alaska and British Columbia and a world-wide high northern latitude shallow-water faunal province; Archives des Sciences, v. 23, p. 675-702.

Styan, W.B. and Bustin, R.M.
1983: Sedimentology of Fraser River delta peat deposits: a modern analogue for some deltaic coals; International Journal of Coal Geology, v. 3, p. 101-143.

Todd, R. and Low, D.
1967: Recent foraminifera from the Gulf of Alaska and southeastern Alaska; United States Geological Survey, Professional Paper 573-A, 58 p.

Vos, P.C. and De Wolf, H.
1993: Reconstruction of sedimentary environments in Holocene coastal deposits of the southwest Netherlands; the Poortvliet boring, a case study of palaeoenvironmental research; Hydrobiologia, v. 269/270, p. 297-306.

Warner, B.G. (ed.)
1990: Methods in Quaternary ecology; Geoscience Canada, Reprint Series, No. 5, 170 p.

Watkins, J.G.
1961: Foraminiferal ecology around the Orange County, California, ocean sewer outfall; Micropaleontology, v. 7, p. 199-206.

Williams, H.F.L.
1989: Foraminiferal zonations on the Fraser River delta and their application to paleoenvironmental interpretations; Palaeogeography, Palaeoclimatology, Palaeoecology, v. 73, p. 39-50.

Williams, H.F.L. and Hebda, R.J.
1991: Palynology of Holocene top-set aggradational sediments of the Fraser River delta, British Columbia; Palaeogeography, Palaeoclimatology, Palaeoecology, v. 86, p. 297-311.

Geological evidence for prehistoric earthquakes

J.J. Clague[1], E. Naesgaard[2], and R.W. Mathewes[3]

Clague, J.J., Naesgaard, E., and Mathewes, R.W., 1998: Geological evidence for prehistoric earthquakes; in Geology and Natural Hazards of the Fraser River Delta, British Columbia, (ed.) J.J. Clague, J.L. Luternauer, and D.C. Mosher; Geological Survey of Canada, Bulletin 525, p. 177–194.

Abstract: Geological and paleoecological evidence for two large, late Holocene earthquakes was found on the Fraser River delta and nearby Serpentine River floodplain. Both earthquakes triggered sudden land-level changes, and one caused extensive liquefaction. The younger quake occurred about 1700 years ago and is marked by submergence throughout the south-coastal region. Sand dykes, sand blows, and deformed strata at many sites on and near the Fraser delta may be products of the same earthquake; if so, earthquakes large and close enough to the delta to produce extensive liquefaction may be rare events. The land-level change and liquefaction may record a great (magnitude (M) = 8+) plate-boundary earthquake on the Cascadia subduction zone, for which there is considerable evidence on the Pacific coasts of southern Washington and northern Oregon. However, they are more likely the result of a large crustal earthquake of about the same age within the North America plate. An older earthquake, which occurred about 3600 years ago, is marked by slight emergence of the Fraser delta and submergence on southern Vancouver Island. This pattern of deformation is consistent with a plate-boundary earthquake.

Résumé : Des données géologiques et paléoécologiques ont permis de prouver que, au cours de l'Holocène tardif, deux gros séismes ont frappé la région du delta du Fraser et de la plaine d'inondation de la rivière Serpentine. Les deux séismes ont déclenché des ruptures subites du sol et l'un des deux a causé de nombreux phénomènes de liquéfaction des sédiments. Le plus récent des deux séismes a eu lieu il y a quelque 1 700 ans et a causé la submergence de toute la côte méridionale. Ici et là sur le delta du Fraser et à proximité, des dykes de sable, des éruptions de sable et des couches déformées pourraient avoir été formés à la suite du même séisme. Si tel est le cas, la fréquence des séismes suffisamment violents et assez près du delta pour produire de nombreux phénomènes de liquéfaction serait rare. Les ruptures du sol et les phénomènes de liquéfaction pourraient être attribuables à un séisme de forte magnitude ($M \geq 8$) déclenché à la limite de deux plaques dans la zone de subduction de Cascadia, lequel séisme a laissé de nombreux indices sur la côte pacifique du sud de l'État de Washington et du nord de l'Oregon. Cependant, il est plus probable que les ruptures du sol et les phénomènes de liquéfaction soient le résultat d'un gros séisme crustal qui se serait produit dans la plaque nord-américaine à peu près à la même époque. Un séisme plus ancien, survenu il y a 3 600 ans, s'est traduit par une légère émergence du delta du Fraser et une submergence dans la partie sud de l'île de Vancouver. Ces observations abondent dans le sens d'un séisme déclenché à la limite de deux plaques.

[1] Geological Survey of Canada, 605 Robson Street, Vancouver, British Columbia V6B 5J3
[2] MacLeod Geotechnical Ltd., Suite 201-20 Brooksbank Avenue, North Vancouver, British Columbia V7J 2B8
[3] Department of Biological Sciences and Institute for Quaternary Research, Simon Fraser University, Burnaby, British Columbia V5A 1S6

INTRODUCTION

The Vancouver metropolitan area, with a population of nearly two million people, lies in a region with the potential for large earthquakes (Milne et al., 1978; Rogers, 1988, 1994). Historically, no earthquakes have caused damage to structures in Vancouver; however, geological evidence indicates that this area has been shaken by very large earthquakes during the late Holocene, prior to European settlement. There are three possible sources for damaging earthquakes in the region: 1) the boundary between the Juan de Fuca and North America plates; 2) faults within the North America plate; and 3) faults within the Juan de Fuca plate (Fig. 1; Rogers, 1994, 1998).

Great subduction, or plate-boundary, earthquakes (M = 8+) occur at intervals ranging from a few centuries, or less, to more than a thousand years at the Cascadia subduction zone in the northwestern United States and southwestern Canada (Atwater et al., 1995; Darienzo and Peterson, 1995; Atwater and Hemphill-Haley, 1996). There is abundant coastal geological

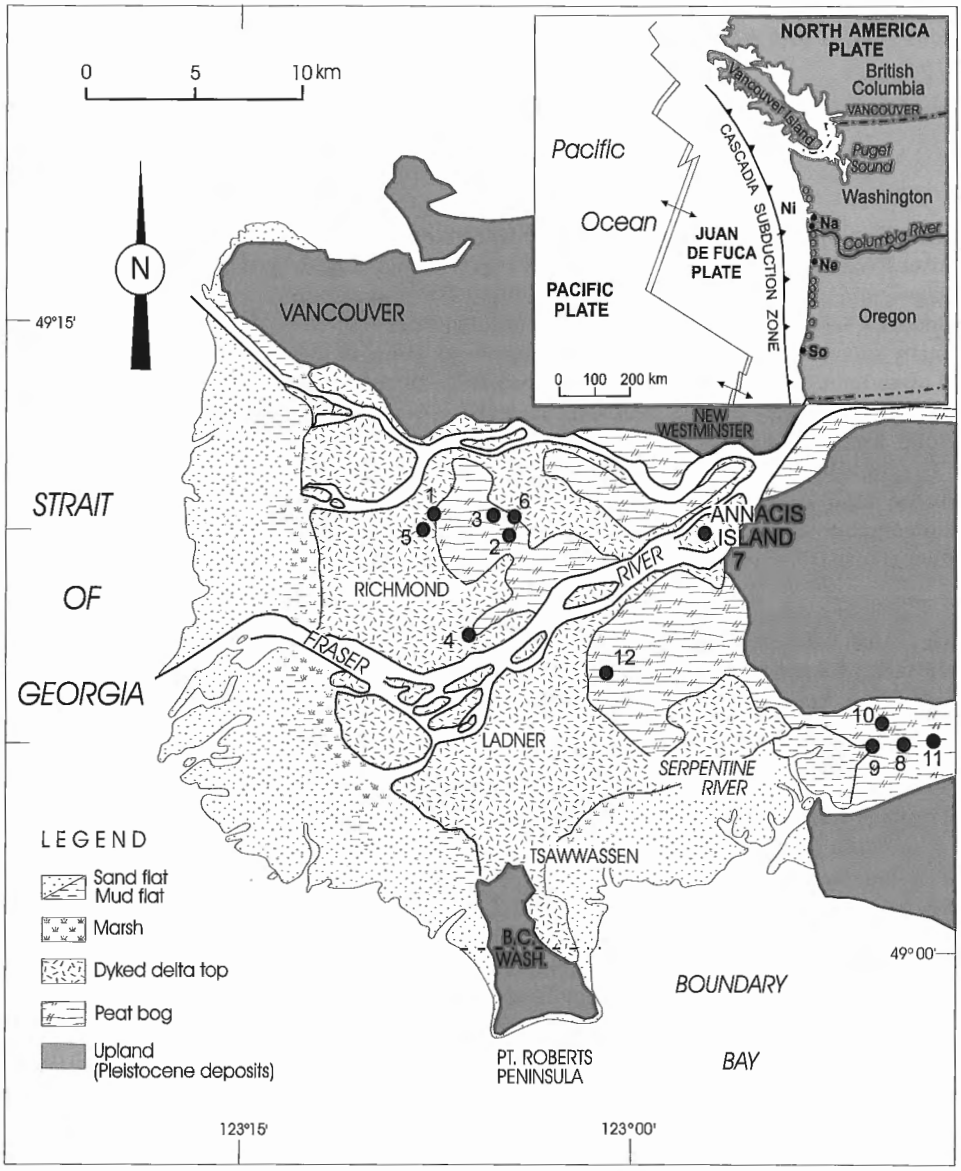

Figure 1. Map of the Fraser River delta and surrounding area, showing sites where evidence of late Holocene liquefaction or land-level change has been found; see Table 1 for site details. Inset map shows the general plate-tectonic setting of the region and estuaries in Washington and Oregon where there is evidence of sudden coastal subsidence about 1700 years ago. Solid dots locate four sites with the precise ages on this event (Ni – Niawiakum River, Na – Naselle River, Willapa Bay; Ne – Netarts Bay; So – South Slough, Coos Bay); open dots locate other sites with less precise ages.

evidence for several plate-boundary earthquakes in the past 3500 years, the most recent about AD 1700 (Nelson et al., 1995; Satake et al., 1996). The earthquakes have left signs of sudden land-level change, tsunamis, and shaking along the outer coasts of British Columbia, Washington, Oregon, and northern California (Atwater, 1992, 1994; Clarke and Carver, 1992; Nelson, 1992a, b; Clague and Bobrowsky, 1994a, b; Darienzo et al., 1994; Obermeier, 1994a; Atwater et al., 1995; Darienzo and Peterson, 1995; Guilbault et al., 1995, 1996; Hemphill-Haley, 1995; Jacoby et al., 1995; Atwater and Hemphill-Haley, 1996; Nelson et al., 1996a, b).

Large earthquakes within the North America plate (crustal earthquakes) have left similar geological signs (Bucknam et al., 1992; Clarke and Carver, 1992). These earthquakes and much deeper (subcrustal) quakes in the Juan de Fuca plate are smaller, but more frequent, than great plate-boundary events. Crustal and subcrustal earthquakes represent a considerable hazard because they are relatively frequent (on average, there is one magnitude 6+ event every 10 to 15 years in southern British Columbia or Washington; Shedlock and Weaver, 1991; Rogers, 1994), and because their epicentres can be close to cities, including Vancouver. At other subduction zones, such earthquakes have occurred both independently of, and concurrently with, plate-boundary earthquakes.

In this paper, we review published geological and paleobotanical evidence from the Fraser River delta for large prehistoric earthquakes. Evidence has been found on the Fraser delta for coseismic liquefaction and sudden land-level changes. At least one of the inferred earthquakes occurred at about the same time as a great Cascadia plate-boundary earthquake recorded in sediments at several localities on the outer coasts of Washington and Oregon. We argue, although not conclusively, that ground shaking strong enough to produce widespread liquefaction on the Fraser delta occurs very infrequently.

SETTING

The Fraser River delta plain extends 15 to 23 km west and south into the Strait of Georgia from a narrow gap in Pleistocene uplands at New Westminster (Fig. 1). The inhabited portion of the delta is protected by levees and lies 0-2 m above mean sea level, with the water table within 2 m of the surface. Very gently sloping tidal flats and the fringing subtidal part of the delta plain extend up to 9 km from the dyked edge of the delta.

The Fraser delta has formed since the disappearance of the last Cordilleran Ice Sheet 13 000-11 000 ^{14}C years BP (Clague et al., 1983). The postglacial deltaic sequence has a maximum known thickness of over 300 m and unconformably overlies Pleistocene stratified sediments, tills, and glaciomarine diamictons (Clague et al., 1991, 1998; Luternauer et al., 1993, 1994). The surface sediments of the delta plain are floodplain and intertidal silts and silty sands, commonly 3 to 15 m thick, and peat up to 8 m thick. These sediments overlie a unit of well sorted, fine- to medium-grained sand that is 10 to 20 m thick, commonly has a sharply defined base with several metres of local relief, fines upward, and is interpreted to be a complex of distributary-channel sand (Monahan et al., 1993; Clague et al., 1998). This unit is nearly continuous under the dyked delta plain and the inshore part of the western tidal flats and was deposited in channels that migrated across and eroded the former tidal flats and floodplain of the delta. It is the source of most of the sand dykes and sand blows documented below. The distributary-channel sand unit overlies a thick sequence of silty and sandy foresets and silty and clayey bottomsets analogous to sediments presently being deposited on the Fraser delta slope (Clague et al., 1983, 1991; Luternauer et al., 1993, 1994, 1998).

LIQUEFACTION FEATURES

Sand dykes are sedimentary injections that cut across bedding; in contrast, sand sills are injected parallel to the bedding. Sand blows (also called sand boils and sand volcanoes) are bodies of sand that have been vented onto the ground surface. They commonly are mound-shaped, but become flatter soon after they form, due to erosion.

At many sites on and adjacent to the Fraser delta, large numbers of sand dykes and sills intrude near-surface clayey silt and peat (Fig. 1, Table 1). At some of the sites, sand and

Table 1. Sites on the Fraser delta and Serpentine River floodplain where liquefaction features or evidence for land-level change have been found.

Site, Fig. 1	Location Lat. N	Long. W	Site details
1	49°10.5'	123 °07.5'	Building excavation, Kwantlen College, Richmond
2	49°09.9 '	123°05.1'	Drainage ditch, Hwy. 99 south of Westminster Hwy., Richmond
3	49°10.7'	123°05.8'	Drainage ditch, Hwy. 99 north of Hwy. 91 exit, Richmond
4	49°07.9'	123°05.9'	Construction site, southeast of intersection of Steveston Hwy. and Shell Rd., Richmond
5	49°09.9'	123°08.0'	Drill core from building site near Anderson Rd., Richmond
6	49°10.8'	123°04.9'	Construction site, northwest of intersection of Hwy. 91 and Jacombs Rd., Richmond
7	49°09.8'	122°57.1'	Excavation, sewage treatment facility, Annacis Island, Delta
8	49°05.3'	122°49.3'	River bank, Serpentine River west of Highway 99A, Surrey
9	49°05.3'	122°50.4'	River bank, Serpentine River at Highway 99 bridge, Surrey
10	49°05.9'	122°49.9'	Dug pit, 14091 Colebrook Rd., Surrey
11	49°05.5'	122°48.1'	Trench, west of intersection of 48th Ave. and 152nd St., Surrey
12	49°06.6'	123°01.1'	Piston core, Burns Bog, Delta

silt blows are associated with the dykes. These liquefaction features have been found in building excavations, in drill core, and in river banks (Clague et al., 1992).

Description of features

Dykes and sills

Near-surface dykes and sills have been documented at nine sites on the Fraser delta and the nearby Serpentine River floodplain (Clague et al. 1992, 1997; Naesgaard et al., 1992). They consist mainly of sand, although dykes of silt were found at one site on the Serpentine River floodplain (Mathewes and Clague, 1994). Contacts between the dykes and sills, and the sediments that they cut, are sharp everywhere. The dykes cut steeply (commonly 45-90°) through cohesive clayey silt (Fig. 2). At sites where the surface materials are peat, the dykes flatten out at the top of the clayey silt and in the lower part of the peat (Fig. 3, 4) and, in some cases, extend laterally several metres as thin sills. If not seen to be extensions of the clearly intrusive, steeply dipping dykes, these layers might mistakenly be attributed to river flooding or tsunamis. The dykes do not penetrate vertically more than 30 cm into the peat. The reason for this is that the upper part of the peat is fibrous and has low specific gravity and high tensile strength, making it easier for sand and water to intrude horizontally than to fracture vertically.

The dykes range in thickness from less than 1 mm to approximately 30 cm. They commonly thin upward, but there is considerable variation in thickness of dykes and sills over short distances. It is not uncommon, for example, for a dyke or sill to pinch out over distances of 10 to 20 cm, only to reappear farther up, or along, the section. Within peat, sand intrusions occur as discontinuous layers ranging from 1 mm to a few centimetres in thickness. In places, secondary stringers and fingers of sand and silt extend away from the main structures, giving rise to a zone of thin, lacy, interdigitating sand stringers within the peat.

Some of the larger dykes at sites 2 and 3 (Fig. 1) occur in pairs, with a fan-like geometry in profile (Fig. 3, 4). These dykes are close to one another at the base of the exposure and may merge at depth, but they diverge sharply and become flatter upward. The structure at site 4 bifurcates in a similar manner but, interestingly, the beds between the bifurcating arms of this structure are about 40 cm higher than the same beds on opposite sides (Fig. 5). This indicates that either the

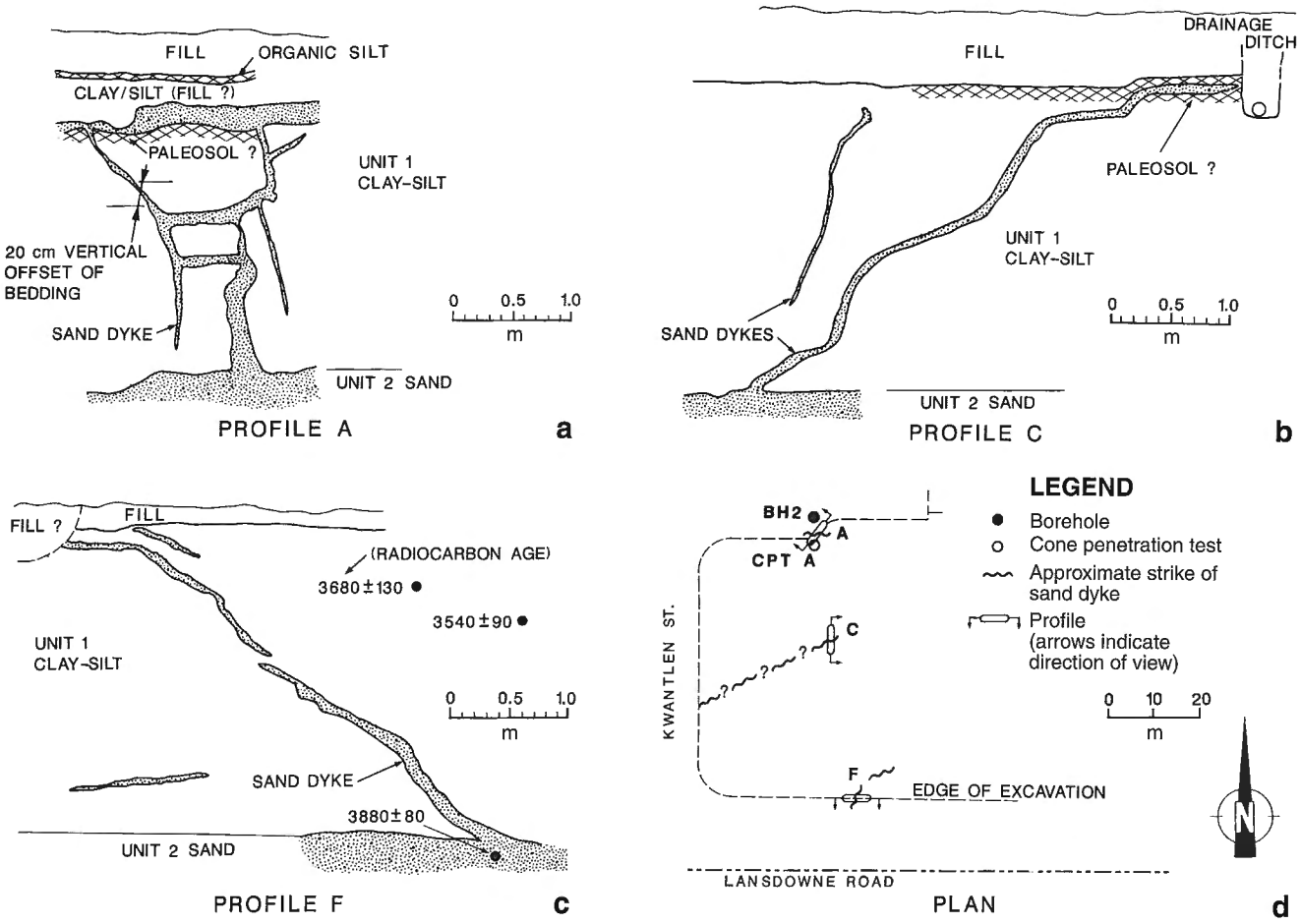

*Figure 2. Profiles of three representative sand dykes (A, C, and F) at site 1 on the Fraser delta (modified from Clague et al., 1992, Fig. 4). A plan of the dykes is shown in (**d**).*

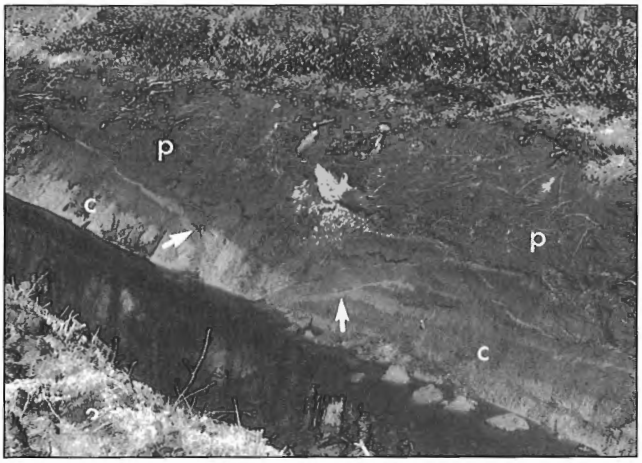

Figure 3. Two large bifurcating sand dykes (arrowed) exposed in a drainage ditch at site 2 on the Fraser delta (Clague et al., 1992, Fig. 6). The dykes cut steeply through clayey silt (c) and flatten out in the overlying peat (p). See Figure 4 for a sketch of the dykes. The ditch is about 2 m deep.

sediments between the arms of the dyke were heaved upward at the time of injection, or the flanks subsided. In contrast, sediments above some of the dykes at sites 2, 3, and 4 dip gently downward toward the axis of the structures. This suggests subsidence due to expulsion of water and sediment from below.

Some of the dykes and sills have no internal structure, whereas others are stratified (Fig. 6). Where present, stratification is parallel to the margins of the dykes and sills and is defined by subtle differences in grain size within the sand. Graded beds were observed in one sill (Fig. 6), but these are uncommon. Thin layers of massive and laminated silt and sandy silt are also present; some of these layers separate sand layers within the dykes, but most occur at the margins. Where the dykes and sills thin and feather out, especially in peat, they may commonly consist of silt and mud, rather than sand. The fractures in which this fine-grained sediment was deposited may have been too small to allow the passage of the higher-viscosity, fluidized sand.

Occasional rip-up clasts of mud, silt, and peat are present in some of the sand dykes. Most of the clasts are clayey silt, which is the common sediment hosting the dykes.

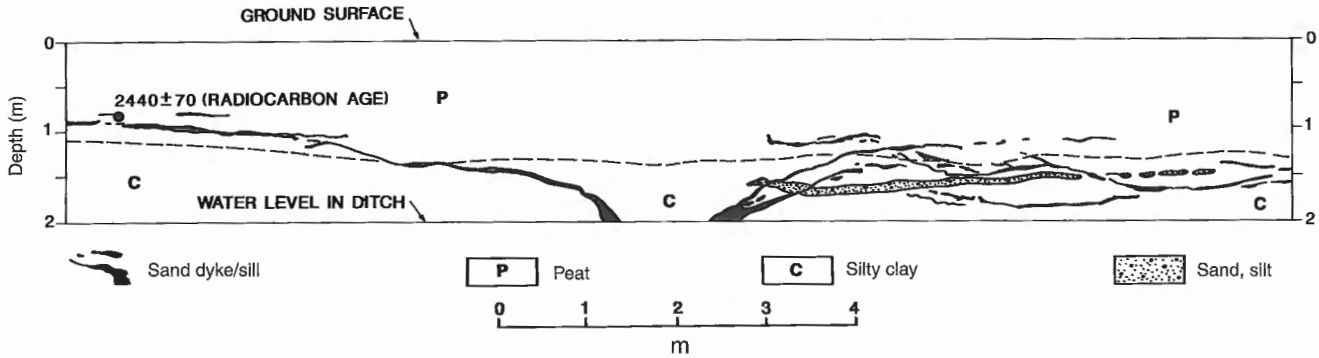

Figure 4. Profile of sand dykes and sills shown in Figure 3 (modified from Clague et al., 1992, Fig. 7).

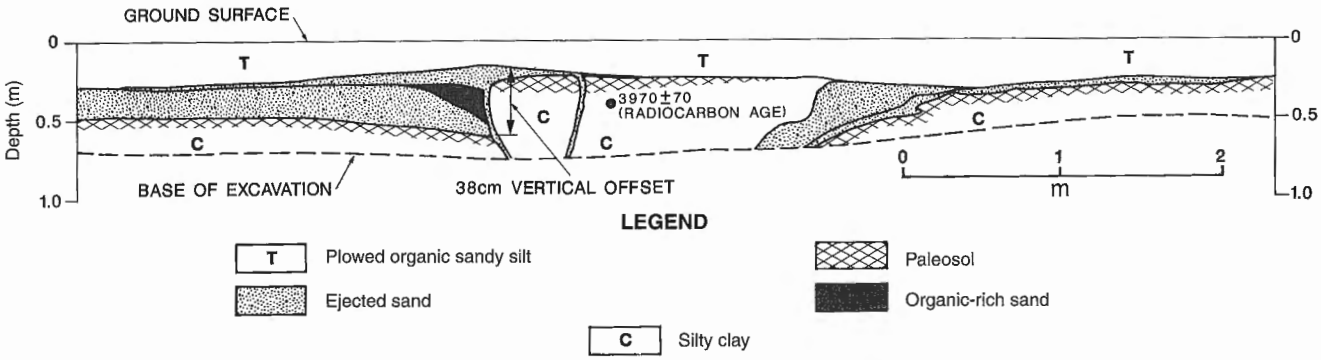

Figure 5. Profile of sand dykes and vented sand exposed in the shallow wall of a building excavation at site 4 on the Fraser delta (modified from Clague et al., 1992, Fig. 9). The vented sand directly overlies a paleosol. It displays stratification indicative of emplacement during either multiple events or multiple pulses within a single event. Note the vertical displacement of the paleosol and the subjacent clayey silt along the two main feeder dykes.

Blows

There is evidence for venting of sand onto a floodplain at sites 1, 4, and 7, and for expulsion of silt onto a marsh at site 8 (Fig. 1).

Two sand dykes at site 1 extend to the top of what is likely a paleosol (a buried organic soil) developed in the surface clayey silt unit. Each dyke is continuous with a horizontal layer of sand that directly overlies the paleosol (Fig. 2a, b).

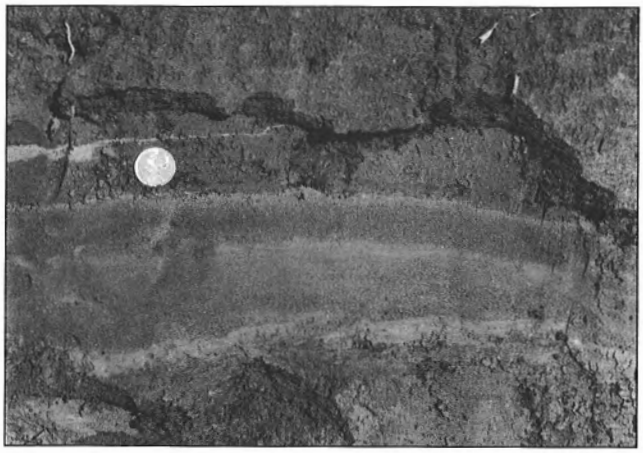

Figure 6. *Stratification within a sill at site 4 on the Fraser delta (Clague et al., 1992, Fig. 14). Two graded sand beds are bounded by thin layers of silt which delineate the margins of the sill. The coin is 24 mm in diameter.*

The sand layer shown in Figure 2a has an exposed length of about 5 m and thins laterally in both directions away from what is presumed to be the feeder dyke.

The low walls of the excavation at site 4 reveal the relationship between steeply dipping sand dykes and a conspicuous brown paleosol that underlies the tilled zone (Fig. 5). The paleosol is about 10 cm thick, has a prismatic structure in its upper part, and becomes lighter coloured with depth. Sand dykes cut sharply through the paleosol and are connected to flat-lying masses of sand that directly overlie the paleosol and thin in both directions away from the dykes. These masses of sand are up to 25 cm thick near the source dykes and extend laterally up to several metres. Most are massive, but some, including those shown in Figure 5, are stratified. Where present, stratification is parallel to the margins of the sand bodies and is defined by thin layers of silt, mud, and organic detritus, as well as by variations in grain size within the sand.

The features shown in Figure 5 provide evidence that injection and extrusion of sand were accompanied by vertical displacements of the intruded sediments. The paleosol and underlying mud are offset about 40 cm vertically along the two main feeder dykes. A wedge of sand is banked up against the displaced hanging wall of one of the feeder dykes. This sand, in turn, appears to have been cut by the dyke and covered by more sand.

Two large sand blows were observed in the wall of a dewatered pit dug in 1994 and 1995 during the expansion and upgrading of a sewerage treatment facility on Annacis Island (site 7, Fig. 1). The sand blows, which are up to 1 m thick and 25 m wide (Fig. 7), are tapering wedges of well sorted, massive to

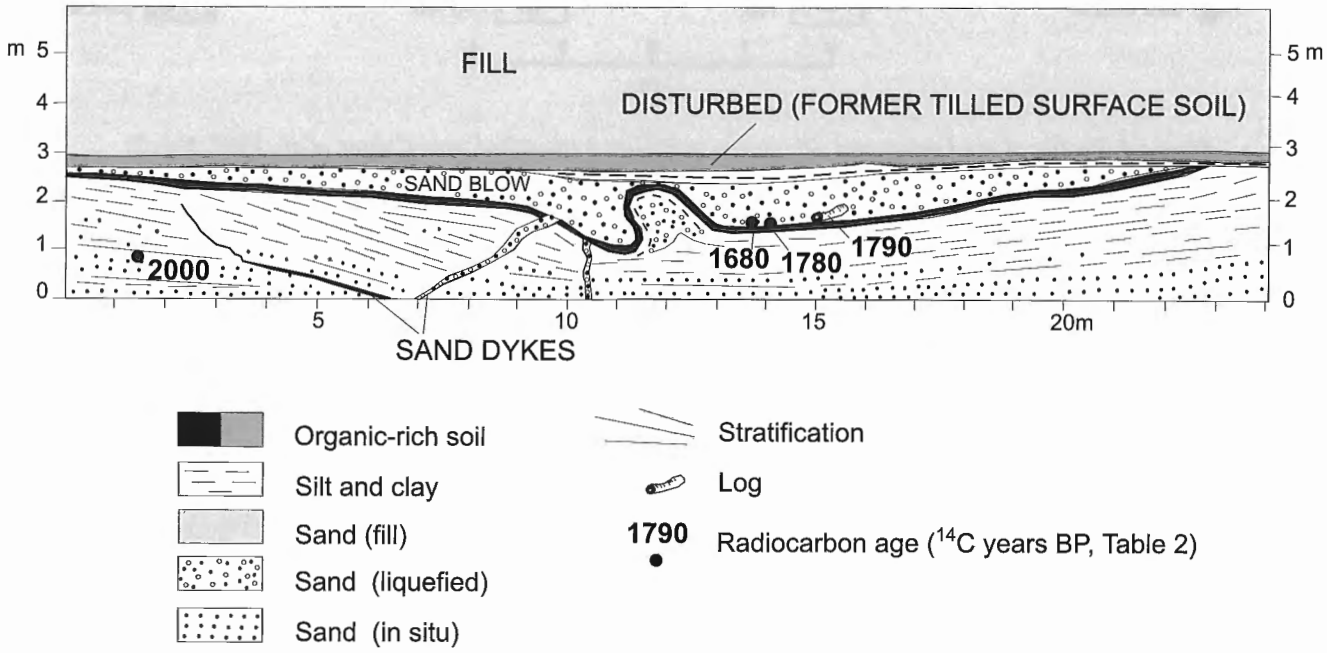

Figure 7. *Sketch of a large sand blow and feeder dykes exposed in the wall of an excavation at site 7 on Annacis Island (modified from Clague et al., 1997). Note the tight fold developed in the thin organic-rich soil underlying the sand blow, and the gentle dip of injected sediments towards the centre of the structure.*

weakly stratified sand. They are overlain successively by a discontinuous thin unit of clayey silt, by organic-rich soil which marks the tilled surface of Annacis Island prior to industrial development, and by sand fill (Fig. 7). The blows sharply overlie a thin layer of brown peaty mud and silty peat with abundant detrital wood, conifer foliage, and in situ roots of woody plants (a paleosol). A large log (4+ m long, 15 cm wide) with preserved bark was found on the surface of this paleosol directly beneath the sand. The paleosol overlies interbedded, olive grey silt and fine-grained sand deposited in a fluvial environment. The upper part of the latter unit is mainly thin-bedded silt; sand beds increase in number and thickness towards the bottom of the exposure, and the lowest exposed sediments are silty sand and sand. Clean sand more than 12 m thick, below the base of the pit, is interpreted to be part of a distributary-channel complex.

Sediments beneath the sand blows are deformed and injected by sand dykes. The paleosol is buckled and overturned near the centre of one of the blows; a bulbous mass of what is interpreted to be liquefied sand forms the core of this structure (Fig. 7). Layering in the interbedded silt-sand unit is also warped beneath the sand blow.

A mound of vented silty mud is exposed in the bank of Serpentine River (site 8), just south of the Fraser delta (Fig. 1, 8, 9). This mound mantles peat and is covered by intertidal mud. The mound is continuous downward with dykes of silty mud containing upward-displaced peat clasts. The sharp contact between the intertidal mud and peat, and plant microfossil changes across this contact, are evidence for sudden submergence at this site (see 'Land-level Changes', below). The stratigraphic relations further show that liquefaction and submergence occurred at the same time, suggesting that both phenomena are the result of a large earthquake (Mathewes and Clague, 1994).

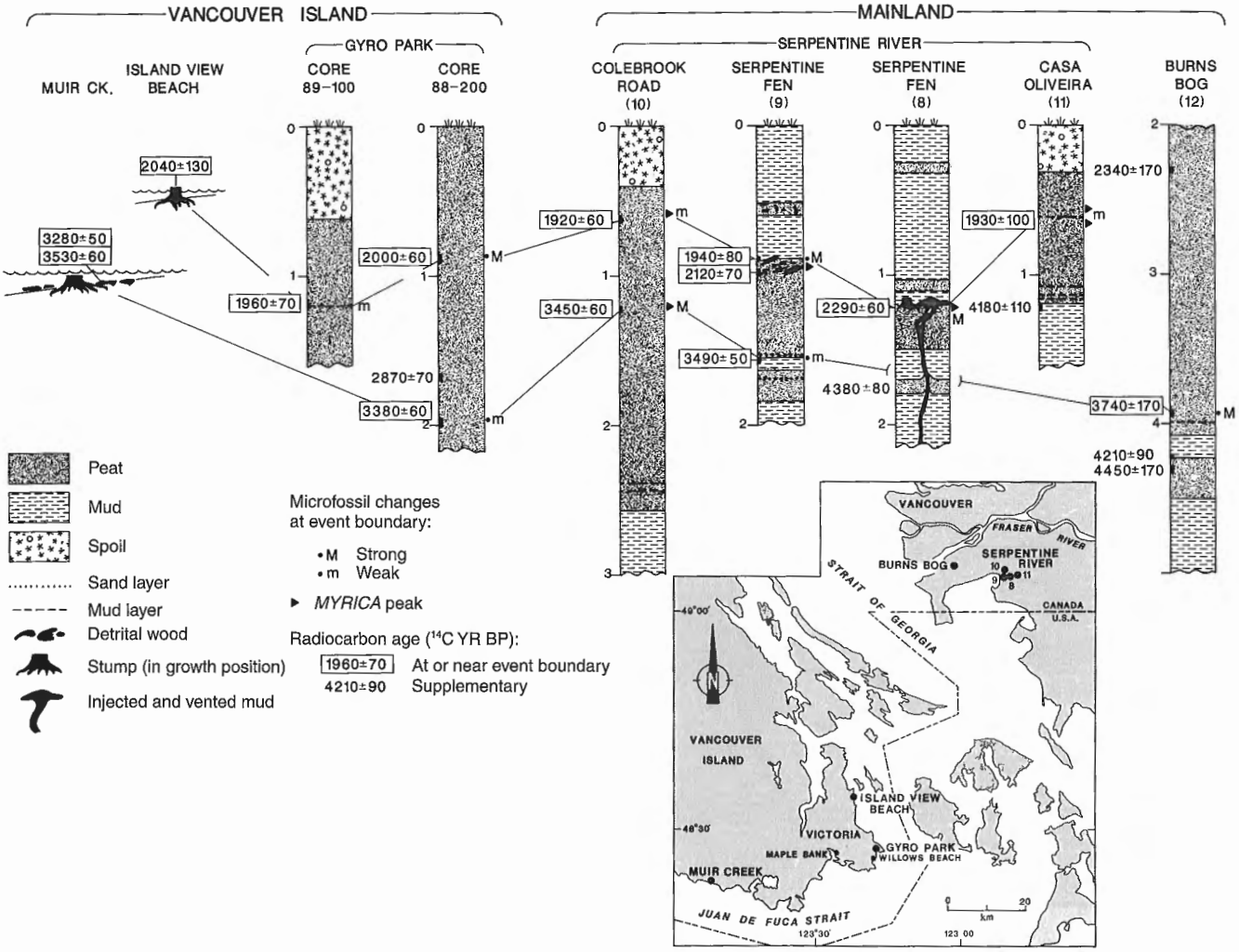

Figure 8. Stratigraphic sections and correlations of two inferred earthquakes about 3600 and 1700 years ago (modified from Fig. 1 and 2 of Mathewes and Clague, 1994). The left side of each section is labelled with the depth (in centimetres) and the radiocarbon age (in ^{14}C years before present). Symbols on the right side indicate microfossil changes at the event boundaries. Correlations are based on radiocarbon ages in boxes (at or near event boundaries, see Table 2 for details; other ages are supplemental) and microfossil changes.

Age of liquefaction features

Radiocarbon dating shows that all observed liquefaction features are younger than ca. 3500 ^{14}C years old (Table 2). Dating at two sites (7 and 8) is sufficiently precise to show that the features there are about the same age, i.e. 1700-2000 ^{14}C years old. The possibility that the sand dykes and blows at the other sites are also of this age is not precluded by the available data.

The age of liquefaction is particularly well constrained at site 7, on Annacis Island, where three radiocarbon ages have been obtained on samples resting on the paleosol directly beneath vented sand (Fig. 7, Table 2). The outermost nine annual rings of a bark-covered log that was lying on the ground surface when it was buried by sand gave an age of 1790 ± 60 ^{14}C years BP. Because fallen trees in the Vancouver area rapidly lose their bark due to exposure and bacterial decay, the dated log probably had not been dead for more than a decade or two before it was buried. Thus, the liquefaction event probably is not much younger than this age. This outer-ring age is in agreement with two other radiocarbon ages from the top of the paleosol directly below vented sand, one of 1780 ± 70 ^{14}C years BP on a branch or root and another of 1680 ± 60 ^{14}C years BP on western red cedar (*Thuja plicata*) foliage. The three ages meet the criteria for contemporaneity of Ward and Wilson (1978); their weighted mean is 1763 ± 42 ^{14}C years BP, which corresponds to a calendric age range of 1542-1815 cal years BP (2σ limits).

There is no conclusive evidence from the sites examined to date for more than one liquefaction event on the Fraser delta (Clague et al., 1992). There are cross-cutting dykes and layers within intruded and vented sand bodies at some sites; this could be the result of either multiple injections during one earthquake or two or more separate events. If there had been two or more events more than several decades apart, sand blows should occur at different stratigraphic levels, at least at some sites, and no such evidence has yet been found. However, it should be noted that, with the exception of peats, sediments hosting sand dykes and blows at individual sites were deposited over short periods of time, probably tens to hundreds of years; thus opportunities for stratigraphic separation of sand blows may be limited.

Origin of features

Clague et al. (1992) reviewed possible causes of liquefaction on the Fraser delta and concluded that the sand dykes and blows that occur there are probably seismically generated. Notably, the Fraser delta features meet several criteria required to demonstrate a seismic origin (Obermeier et al., 1990, p. 5): 1) They show "evidence for an upward-directed, strong hydraulic force that was suddenly applied and of short duration". 2) They resemble liquefaction features generated by historical earthquakes in similar settings (Obermeier, 1988, 1994b; Obermeier et al., 1990; Tuttle et al., 1990; Sims and Garvin, 1995). 3) They are not located in areas where other phenomena, notably artesian discharge, might produce similar features. 4) They probably formed in one or more discrete, short episodes that individually affected a large area; these episodes were separated by lengthy periods during which no such features formed.

Liquefaction assessment

Here we consider the possible range of earthquake magnitudes and source distances that could generate the sand dykes and sand blows at Annacis Island, where we have abundant geotechnical information and good chronological control. We also compare the frequency of liquefaction events inferred

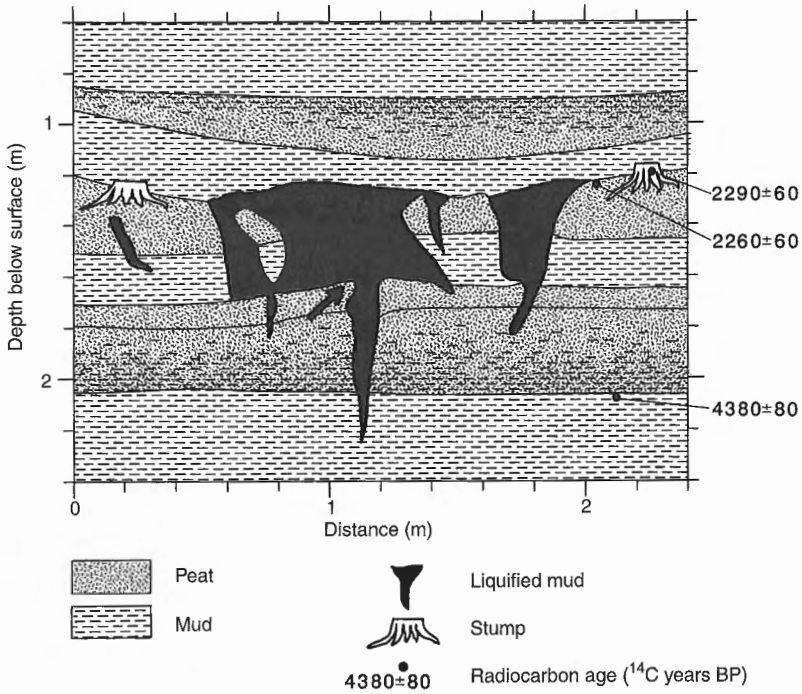

Figure 9.

Sketch of an exposure at site 8 along the Serpentine River showing evidence for contemporaneous liquefaction and submergence attributed to a large earthquake about 1700 years ago. Liquefied clayey silt occupies complex dykes and upward-widening vents. The liquefied sediment separates freshwater peat with in situ stumps from overlying intertidal mud.

from field observations and dating with the frequency calculated using current seismic models and liquefaction assessment procedures.

Magnitude/source distance relationship

Ambraseys (1988) developed an empirical relationship between earthquake magnitude and the maximum distance, from the epicentre, of liquefaction (Fig. 10 inset). We used this relationship to define areas within which earthquakes of different magnitudes might cause liquefaction at Annacis Island (shown as concentric circles centred on Annacis Island in Fig. 10). This plot suggests that:

- a great plate-boundary earthquake **may be** responsible for the sand dykes and sand blows on the Fraser delta (see 'Source of Earthquakes', below).
- the earthquake that caused the liquefaction on the Fraser delta had a minimum magnitude of 6, assuming that all sand dykes and blows on the delta (Fig. 1) are the same age; and
- there is only one historical earthquake in the Pacific Northwest (a magnitude 7.4 event in northern Washington in 1872; Malone and Bor, 1979) that possibly could liquefy Fraser delta sediments. However, the exact magnitude and location of this event are uncertain.

Table 2. Radiocarbon ages bearing on the age of liquefaction features and sudden land-level change on the Fraser delta and Serpentine River floodplain.

Radiocarbon age (yr BP)[a]	$\delta^{13}C$ (‰)	Laboratory no.[b]	Dated material	Depth (m)[c]	Comment (inference)
Site 1					
3540 ± 90	-26.6	GSC-5153	Wood fragments	1.4	Maximum age for liquefaction
3650 ± 140		GSC-5124	*Picea* branch	0.5	Maximum age for liquefaction
3680 ± 130	-28.1	GSC-5144	Wood fragments	1.1	Maximum age for liquefaction
3880 ± 80	-24.8	GSC-5111	*Picea* wood fragment	3	Maximum age for liquefaction
Site 2					
2440 ± 70		TO-2636	*Scirpus* seeds	1.5	Maximum age for liquefaction
Site 4					
3970 ± 70		TO-2637	Charcoal	0.5	Maximum age for liquefaction
Site 7					
1680 ± 60		TO-4709	*Thuja plicata* leaves	ca. 3	Maximum age for liquefaction[d]
1780 ± 80	-24.3	GSC-5865	*Pinus* branch or root	ca. 3	Maximum age for liquefaction[d]
1790 ± 60	-21.5	GSC-5857	*Thuja plicata* log[e]	ca. 3	Maximum age for liquefaction[d]
2000 ± 60	-24.2	GSC-5983	*Picea*sp. branch	ca. 4	Maximum age for liquefaction
Site 8					
2260 ± 60		TO-4311	Branch	1.2	Maximum age for liquefaction and shift from shrub land to tidal marsh (subsidence)
2290 ± 60		TO-4057	In situ conifer root	1.2	Maximum age for liquefaction and shift from shrub land to tidal marsh (subsidence)
Site 9					
1940 ± 80	-24.8	GSC-5254	*Picea* wood fragment	0.9	Maximum age for shift from shrub land to tidal marsh (subsidence)
2120 ± 70	-24.7	GSC-5179	*Picea* log	0.9	Maximum age for shift from shrub land to tidal marsh (subsidence)
3490 ± 50		TO-2133	*Scirpus* seeds	1.5	Change from lagoonal sediments to freshwater peat (uplift)
Site 10					
1920 ± 60		TO-2631	Wood fragment	0.6	Maximum age for sudden microfossil changes
3450 ± 60		TO-2118	*Scirpus* seeds	1.2	Many microfossil changes (marine incursion, uplift)
Site 11					
1930 ± 100		S-3185	Peat	0.6	Approximate age of 2-cm muddy peat bed, decline in *Myrica*, presence of brackish microfossils (marine incursion, subsidence)
Site 12					
3740 ± 170		S-3190	Peat	3.9	Sharp decline in brackish pollen and diatoms, increase in freshwater microfossils (uplift)

[a] Age in radiocarbon years BP (before AD 1950).
[b] Laboratories: GSC, Geological Survey of Canada; S, Saskatchewan Research Council; TO, IsoTrace Laboratory (University of Toronto).
[c] Depth below present land surface.
[d] Liquefaction features are probably only slightly younger than radiocarbon age.
[e] Outermost nine rings of a log with preserved bark resting on top of paleosol beneath vented sand.

Table 3. Calculated probabilities of liquefaction.

Seismic model[a]	Magnitude scaling method[b]	Ground response amplification[c]	Annual probability of liquefaction[d]	Liquefaction return period[d] (a)
NBCC	Seed	Yes	0.547×10^{-2}	183
B.C. Hydro	Seed	Yes	0.523×10^{-2}	191
NBCC	NCEER	Yes	0.411×10^{-2}	243
B.C. Hydro	NCEER	Yes	0.314×10^{-2}	318
NBCC	Seed	No	0.290×10^{-2}	345
B.C. Hydro	Seed	No	0.243×10^{-2}	412
NBCC	NCEER	No	0.226×10^{-2}	442
B.C. Hydro	NCEER	No	0.148×10^{-2}	676

[a] NBCC = National Building Code of Canada seismic model, with Hasegawa et al. (1981) attenuation (Basham et al. 1982); BC Hydro = B.C. Hydro and Power Authority seismic model, with Crouse (1991) and Idriss (1993) attenuations (Little 1993). The two seismic models are based on historical seismicity and regional tectonic features; neither incorporates great plate-boundary earthquakes on the Cascadia subduction zone.

[b] Seed = Seed et al. (1983); NCEER = National Center for Earthquake Engineering Research committee draft recommendations (Finn 1996).

[c] Yes = incorporates ground-response amplification factor of Borcherdt (1994), calculated assuming a shear-wave velocity of 182 m/sec for the upper 30 m and a reference shear-wave velocity of 555 m/sec; this gives values that vary with ground acceleration, but are commonly about 1.4. No = no ground-response amplification.

[d] Liquefaction probabilities and return periods were calculated with a modified version of the program EQRISK, using the method of Seed and de Alba (1986) and the SCPT penetration resistance at 9.4 m depth (Fig. 11); the calculations include a 1σ offset on the attenuation relationship.

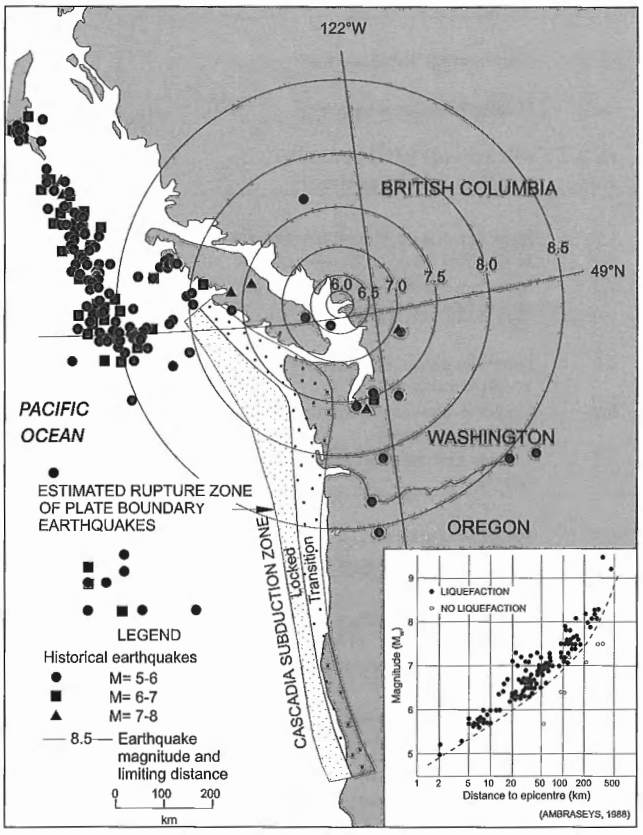

Figure 10.

Map of the Pacific Northwest showing, as concentric circles, maximum distances that earthquakes of different magnitudes can be from Annacis Island while still causing liquefaction there (based on the relationship of Ambraseys, 1988; inset) (modified from Clague et al., 1997, Fig. 5). Moderate and large historical earthquakes and the inferred source zone of great plate-boundary earthquakes on the Cascadia subduction zone (adapted from Hyndman and Wang, 1993, Fig. 1) are also shown.

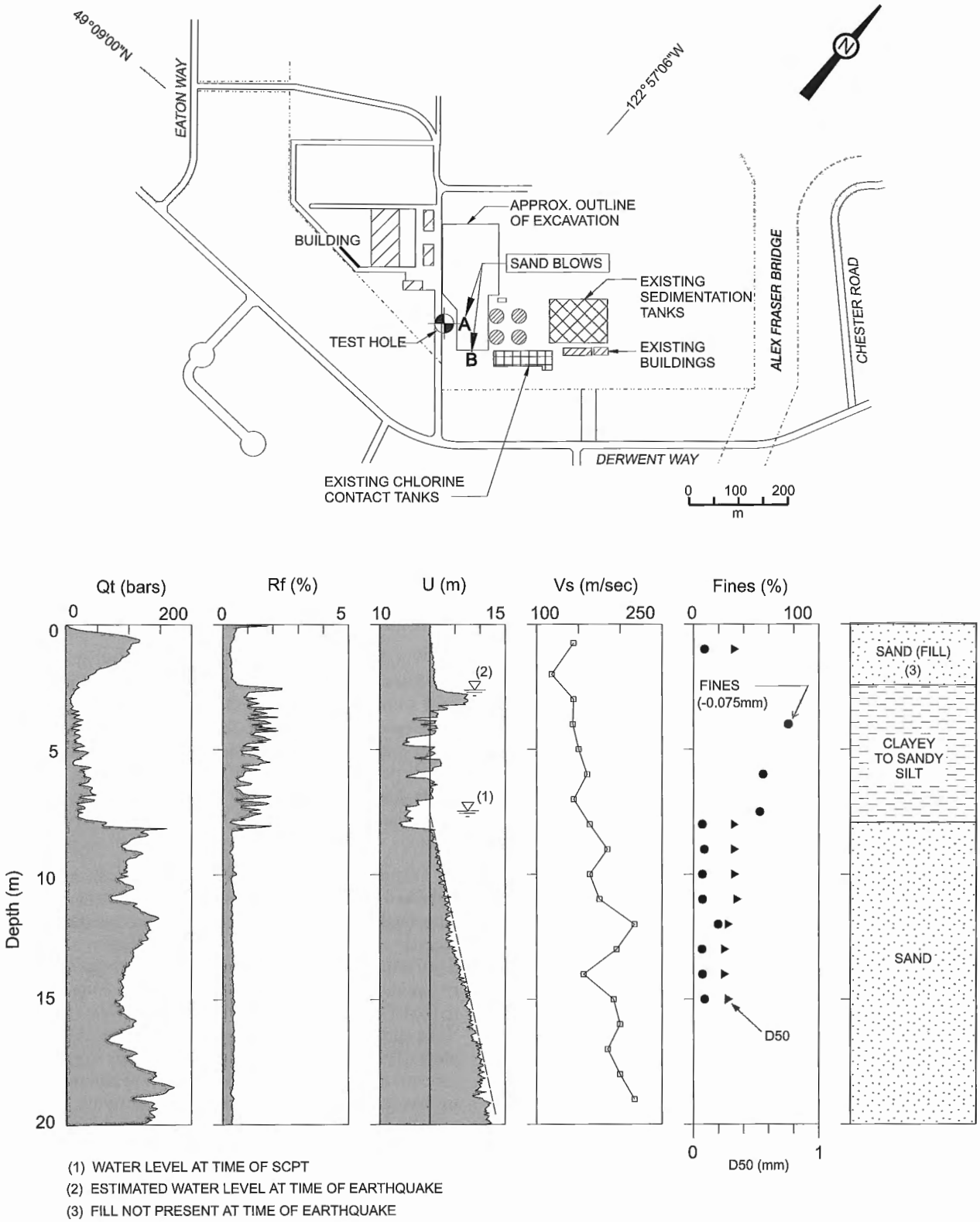

Figure 11. *Top: map of the Annacis Island sewage treatment facility (site 7, Fig. 1) and surrounding area, showing the locations of studied liquefaction features and auger and cone penetrometer test holes. Bottom: seismic cone penetrometer (SCPT) logs, grain-size data for samples recovered from an auger hole, and interpreted lithologies.* Q_t *– cone tip bearing pressure;* R_f *– cone friction ratio; U – pore pressure behind the cone tip;* V_s *– shear-wave velocity; fines – percent <75 μm;* D_{50} *– median diameter are also shown. (Modified from Clague et al., 1997, Fig. 2.)*

Probability of liquefaction

The probability of liquefaction at Annacis Island was calculated from seismic cone penetration test (SCPT) data (Fig. 11), using two seismic source models — the National Building Code of Canada (NBCC) model (Basham et al., 1982) and the British Columbia Hydro and Power Authority model (B.C. Hydro and Klohn Leonoff, 1992; Little, 1993). Both models are probabilistic in nature and are based on historical seismicity and on seismic source zones defined from regional tectonic features. Neither model includes great plate-boundary earthquakes, because such earthquakes have not occurred during historical time; including such earthquakes would increase the calculated probability of liquefaction.

Liquefaction was assessed according to the method of Seed and de Alba (1986), using both the original magnitude scaling factors of Seed et al. (1983) and the more recent factors recommended by a committee of the National Center for Earthquake Engineering Research (NCEER) (Finn, 1996). The stress reduction factor (r_d) of Byrne and Anderson (1987) for a typical Fraser delta sediment profile was employed. Ground-response amplification was included in the analysis using the procedure of Borcherdt (1994). SCPT data were corrected so that they would be representative of the ground-surface and water-table conditions about 1700 years ago (i.e., effects of the surface fill and pumping of water at the site were removed). Probabilities of liquefaction, shown in Table 3, were calculated with the computer program EQRISK (McGuire, 1976), modified to incorporate Seed and de Alba's liquefaction assessment procedure. Epistemic uncertainties in the seismic and liquefaction models were not considered in the analysis.

The results of the above analysis indicate that, if there has been only one major liquefaction event on the Fraser delta in the last 1700 years, the liquefaction assessment procedure currently used in the region (Fraser Delta Task Force, 1991) overestimates liquefaction risk (Table 3, row 1). This procedure uses the NBCC seismic model, median + 1σ attenuation values, Seed and Idriss's magnitude scaling factors, and ground-motion amplification of approximately 1.4. Use of the more recent B.C. Hydro seismic model with NCEER magnitude scaling factors gives larger return periods, but the values are only about half those inferred from field evidence (Table 3).

LAND-LEVEL CHANGES

Sudden changes in land level in the Vancouver area around 3600 and 1900 years ago have been interpreted as evidence of coseismic uplift and subsidence (Mathewes and Clague, 1994). The younger of the two earthquakes ('younger event') probably produced the liquefaction features described above; if so, it is about 1700, rather than 1900, years old. (Note: Mathewes and Clague (1994) concluded that this earthquake occurred about 1900 years ago, but the pertinent radiocarbon ages are maxima and the true age of the earthquake could be somewhat younger.)

No liquefaction features dating to the older earthquake have yet been found, but there is good stratigraphic and paleoecological evidence for this event at some sites (see 'Older earthquake', below).

Younger earthquake

At one of the Serpentine River sites (8) and possibly at Annacis Island (site 7), liquefaction was accompanied by rapid submergence, thought to be caused by subsidence during an earthquake.

Mounds of clayey silt were erupted onto a low-lying peaty surface at site 8 on the Serpentine River floodplain (Fig. 8, 9). This surface is abruptly overlain by tidal mud. The contact between the peat and the overlying mud coincides with a sharp decline in pollen of sweet gale (*Myrica gale*) and corresponding increases in pollen of Chenopodiaceae, Malvaceae, and other brackish indicators (Mathewes and Clague, 1994). These vegetation changes are consistent with minor submergence of the site. The stratigraphic relations show that submergence occurred at the same time as liquefaction, which suggests that both phenomena are the result of an earthquake. The time of this event is constrained by radiocarbon ages on an in situ stump and detrital wood near, but below, the top of the peat at sites 8 and 9. The ages, 1940 ± 80, 2120 ± 70, and 2290 ± 60 ^{14}C years BP (Table 2), are maxima for the time of submergence and therefore the earthquake.

Woody peat is abruptly overlain by mud at several other localities along the Serpentine River. At each site, there is a shift to more brackish conditions, indicative of minor submergence. At site 11, the farthest inland of the Serpentine River sites, this event is marked by a 2 cm thick layer of muddy peat dated at 1930 ± 100 ^{14}C years BP (Fig. 8). There is a sharp drop in *Myrica* pollen in the muddy peat layer, which suggests that the local shrub land was briefly replaced by herbaceous vegetation, probably as a result of submergence.

Disturbance, possibly related to coseismic subsidence, is indicated by pollen recovered from sediments at site 7 on Annacis Island (Fig. 12). The paleosol below the vented sand records a stable terrestrial surface; its pollen assemblage is dominated by spores of polypody ferns (*Polypodium*) and by tree pollen, mainly lodgepole pine (*Pinus contorta*), western red cedar (*Thuja plicata*), western hemlock (*Tsuga heterophylla*), Sitka spruce (*Picea sitchensis*, Fig. 13a), fir (*Abies*), and red alder (*Alnus rubra*). This pollen assemblage suggests a humid forested environment. Polypody ferns are common epiphytes in wet coastal forests, commonly growing, along with mosses, in bark fissures and on branches of old spruce and alder trees. The vented sand, which buries the paleosol, is barren of microfossils. The overlying clayey silt contains very high concentrations (>100,000 grains m/L) of red alder pollen, as well as abundant pollen of skunk cabbage (*Lysichitum americanum*) and cattail (*Typha latifolia*) (Fig. 13b); this, coupled with low concentrations of conifer pollen, indicates a local swampy environment. These data indicate that the site was wetter during deposition of the clayey silt than it was immediately before the earthquake. A possible explanation for this change is that subsidence during the earthquake converted a floodplain forest into a swamp. Subsidence was not

enough, however, to bring the site within the range of tidal influence (the paleosol is presently about 1 or 2 m above the upper limit of tides).

There is evidence for sudden submergence on southern Vancouver Island shortly after 2000 ^{14}C years ago (Mathewes and Clague, 1994), possibly coincident with submergence and liquefaction on the Fraser delta and along the Serpentine River (Fig. 8). In situ fossil stumps 1.0 to 1.5 m below the upper limit of tides at Island View Beach, north of Victoria, record a rapid transgression during the late Holocene. One of the stumps yielded a radiocarbon age of 2040 ± 130 ^{14}C years BP (Table 1). In a nearby marsh, mud containing intertidal diatoms sharply overlies freshwater peat at the same stratigraphic level as the stumps (Clague, 1989). The presence of mud laminae and increases in the concentration of brackish pollen and diatoms in cores and trenches dug at Gyro Park (Fig. 8), a former marsh in Victoria, is consistent with submergence around 2000 ^{14}C years ago.

In summary, sites up to 80 km apart in south-coastal British Columbia may have subsided during a large earthquake about 1700 years ago. The inferred pattern of deformation of

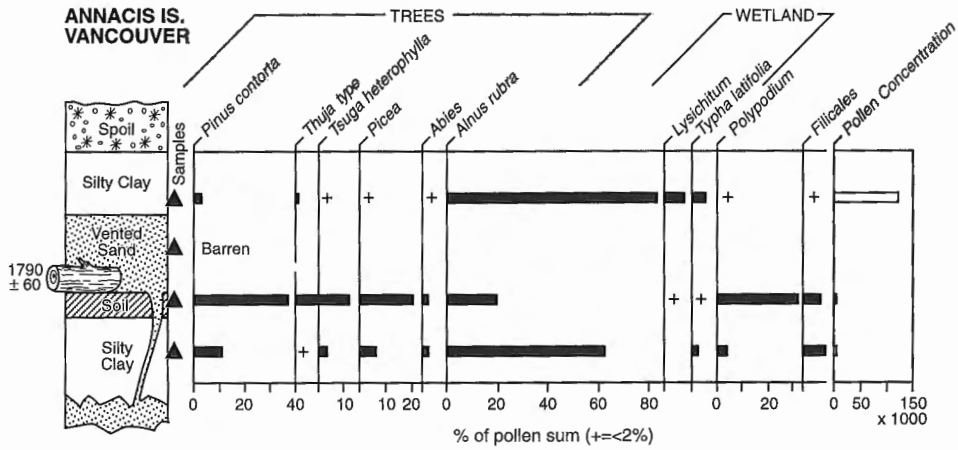

Figure 12. Microfossil diagram showing relative frequencies of selected pollen and spores in sediments at site 7 on Annacis Island. The pollen assemblage of the paleosol is markedly different from that of the clayey silt above the vented sand (see text for details).

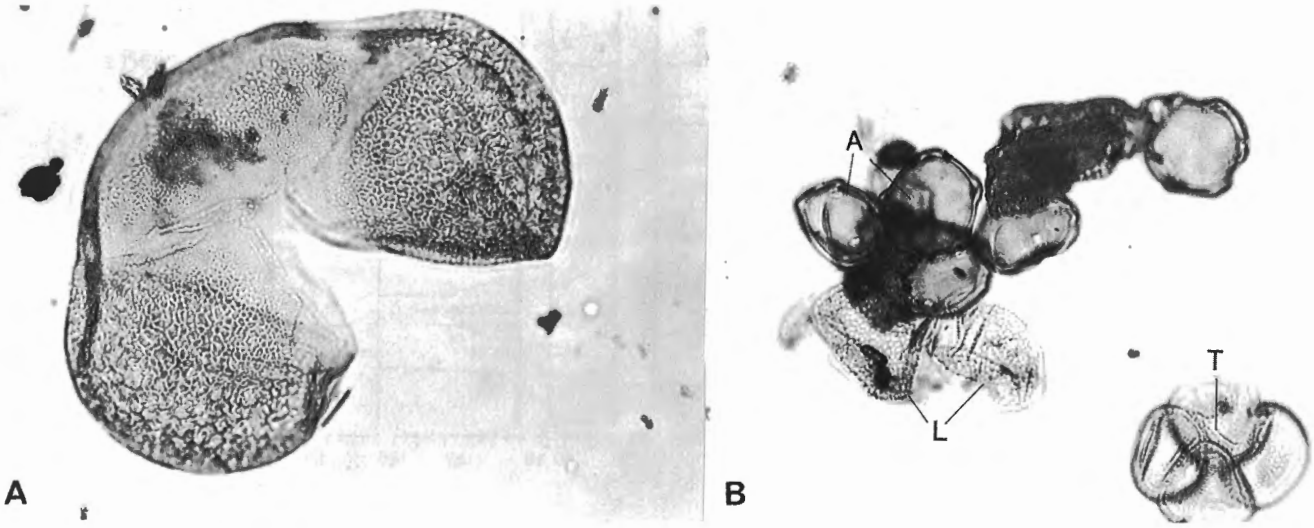

***Figure 13.** Representative pollen from sediments at site 7 on Annacis Island. **a)** A spruce pollen grain from the paleosol underlying one of the sand blows. Spruce pollen constitutes 20% of the total pollen in the soil, indicating that spruce trees were growing at or near the site. **b)** Wetland pollen assemblage from clayey silt above the vented sand. Red alder (A), skunk cabbage (L), and cattail (T) pollen indicate a local swampy environment. Magnification = 500x.*

this earthquake is different from that of the older earthquake, which is discussed below, consequently their sources may be different (see 'Source of Earthquakes', below).

Older earthquake

An earthquake around 3600 years ago is recorded at site 10 in the Serpentine River area by the sudden replacement, at 3450 ± 60 ^{14}C years BP, of a herb wetland by a shrub-land community with abundant Myrica (Fig. 14). This suggests that the site became slightly higher and drier, which is consistent with uplift.

The disappearance of foraminifers after the event (Fig. 14) supports this inference. Before 3400 ^{14}C years BP, foraminifers were deposited episodically in the freshwater marsh at site 10. A final incursion of brackish water is recorded by tests of the intertidal foraminifer *Trochammina inflata*, marine diatoms, a small increase in seaside arrow grass (*Triglochin*-type) pollen, and Malvaceae pollen identical to the upper-tidal marsh species *Sidalcea hendersonii*. The incursion of brackish water coincides with the inferred uplift and may have been produced by a seismically generated wave that washed inland and left traces of intertidal biota. Emergence at site 10 was followed by a period of gradual subsidence, indicated by a decrease in *Myrica* pollen and increases in pollen of wetland taxa such as *Typha latifolia* and spores of the aquatic alga *Spirogyra* and *Sigmopollis* (Fig. 14).

Similar changes, consistent with a regression and uplift, are evident at nearby sites. For example, at site 12 on the Fraser delta, a fossil assemblage with classical salinity indicators (*Ruppia maritima*, Chenopodiaceae, foraminifers) was suddenly replaced by a freshwater community around 3740 ± 170 ^{14}C years BP (Fig. 8). At site 9 along the Serpentine River, a brackish, aquatic (lagoonal?) sediment containing seeds of *Rumex maritima*, *Ruppia maritima*, and spines of stickleback fish (*Gasterosteus*) is abruptly overlain by freshwater-marsh peat; the change occurred about 3490 ± 50 ^{14}C years BP.

A large earthquake dating to about 3600 years ago is also recorded on the coast of southern Vancouver Island, but there the evidence indicates submergence rather than emergence (Mathewes and Clague, 1994). Rooted stumps, logs, branches, cones, and a peaty forest soil are exposed at low tide at the mouth of Muir Creek (Fig. 8), west of Victoria. Nearby, the fossil forest is abruptly overlain by silt and sand containing brackish-water diatoms. Wood from the peat bed has been dated at 3280 ± 50 and 3530 ± 60 ^{14}C years BP, suggesting that the forest was submerged and killed at about that time. The same transgression is also recorded at Gyro Park. There, a shift to wetter and more brackish conditions about 3380 ± 170 ^{14}C years BP is suggested by large increases in cattail pollen and *Sigmopollis* spores and the presence of brackish-water diatoms.

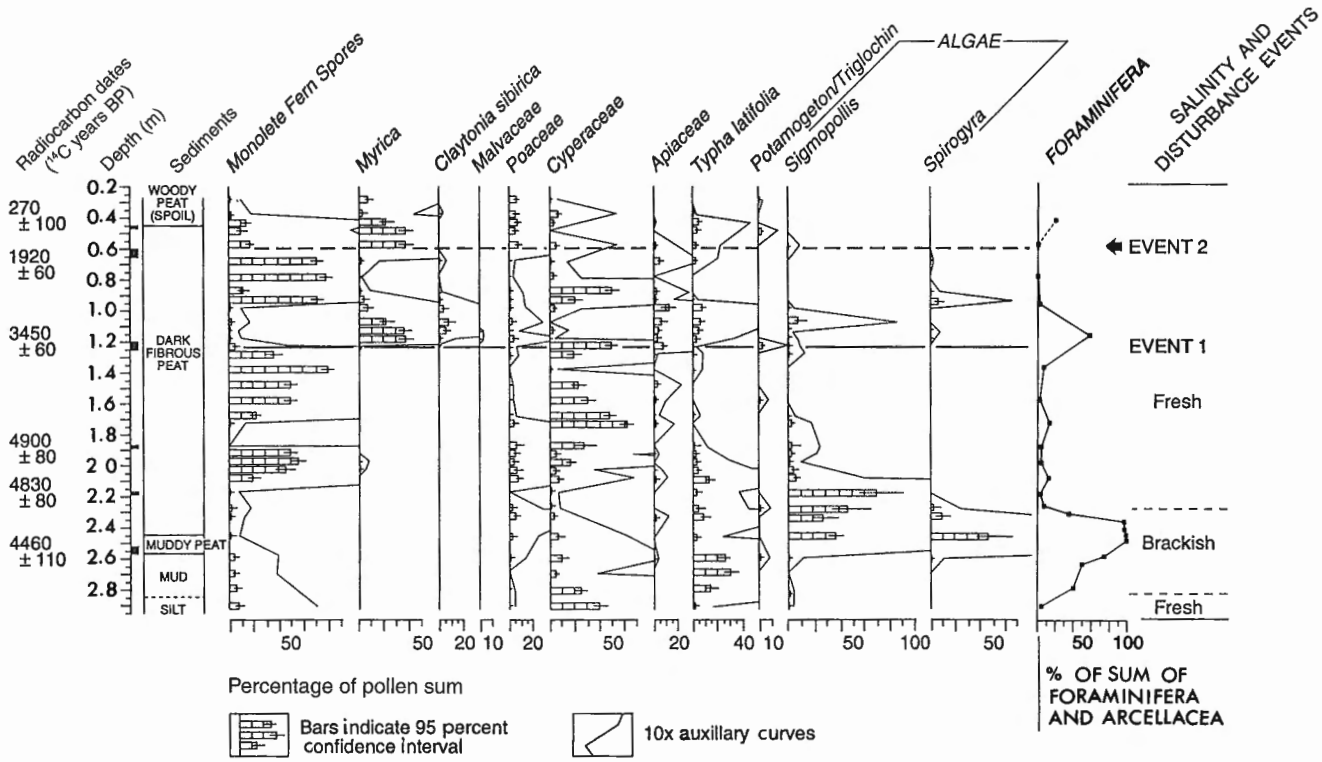

Figure 14. *Microfossil diagram showing relative frequencies of selected pollen, spores, and foraminifers in sediments at site 10 in the Serpentine River area (modified from Mathewes and Clague, 1994, Fig. 3). Two periods of rapid vegetation change, delimited by samples spaced 5 cm apart, are labelled events 1 and 2.*

SOURCE OF EARTHQUAKES

Younger earthquake

Liquefaction on the scale of that at Annacis Island appears to be a rare occurrence — no evidence has yet been found on the Fraser delta for more than one major liquefaction event in the last few thousand years; and none of the ten moderate to large (M = 6-7.5) earthquakes that have occurred in southwestern British Columbia and western Washington in the last 150 years (Shedlock and Weaver, 1991; Rogers, 1994) has caused Fraser delta sediments to liquefy. This raises two related questions that have important implications for earthquake hazard assessment — is the liquefaction recorded at Annacis Island and elsewhere on the Fraser delta the result of an earthquake of the same size as the largest historical events, but with an epicentre unusually close to Vancouver? Or do the features record a much larger (M = 8-9), distant earthquake at the plate boundary?

The evidence from the Fraser delta does not allow us to definitively answer these questions, but the earthquake that generated the sand dykes and blows at Annacis Island about 1700 years ago may be associated with a plate-boundary earthquake of about the same age that caused tidal wetlands along the Pacific coast of Washington and Oregon to subside (Atwater, 1992; Darienzo et al., 1994; Atwater and Hemphill-Haley, 1996; Nelson et al., 1996a).

It is possible that these two earthquakes are, in fact, one event. Because great earthquakes at some subduction zones have occurred only hours or days apart, radiocarbon dating cannot demonstrate that buried soils of the same radiocarbon age subsided at exactly the same time (Atwater, 1992; Darienzo et al., 1994; Nelson et al., 1996a). However, researchers have recently suggested that the evidence of sudden subsidence and tsunamis within a few hundred years of 1700 cal years BP at many estuaries in Washington and Oregon records the same earthquake (Darienzo and Peterson, 1995; Nelson et al., 1996b).

Radiocarbon ages that suggest a great earthquake about this time have been obtained on a variety of materials from possibly correlative soils at many estuaries in Washington, Oregon, and northern California (Fig. 1; Atwater, 1992; Clarke and Carver, 1992; Nelson, 1992a, b; Briggs, 1994; Darienzo and Peterson, 1995; Atwater and Hemphill-Haley, 1996). The earthquake (or earthquakes) about 1700 years ago has been most precisely dated at three estuaries, as much as 350 km apart, in Washington and Oregon (Fig. 1, 15). The weighted mean of three accelerator mass spectrometer (AMS) radiocarbon ages on herbaceous plants rooted in the top of a buried marsh soil at Naselle River, Washington, is 1742 ± 27 ^{14}C years BP. Two AMS ages on rooted plants and three AMS ages on conifer buds and leaves from a correlative soil at Netarts Bay, Oregon, have a mean age of 1747 ± 23 ^{14}C years BP. The mean of three AMS ages on similar materials from the top of a buried soil described by Ota et al. (1995) at South Slough, Coos Bay, Oregon, is 1736 ± 48 ^{14}C years BP. If two additional gas proportional radiocarbon ages from a nearby correlative soil studied by Nelson et al. (1996a) are included, the mean for South Slough becomes 1755 ± 35 ^{14}C years BP. These means compare well with the

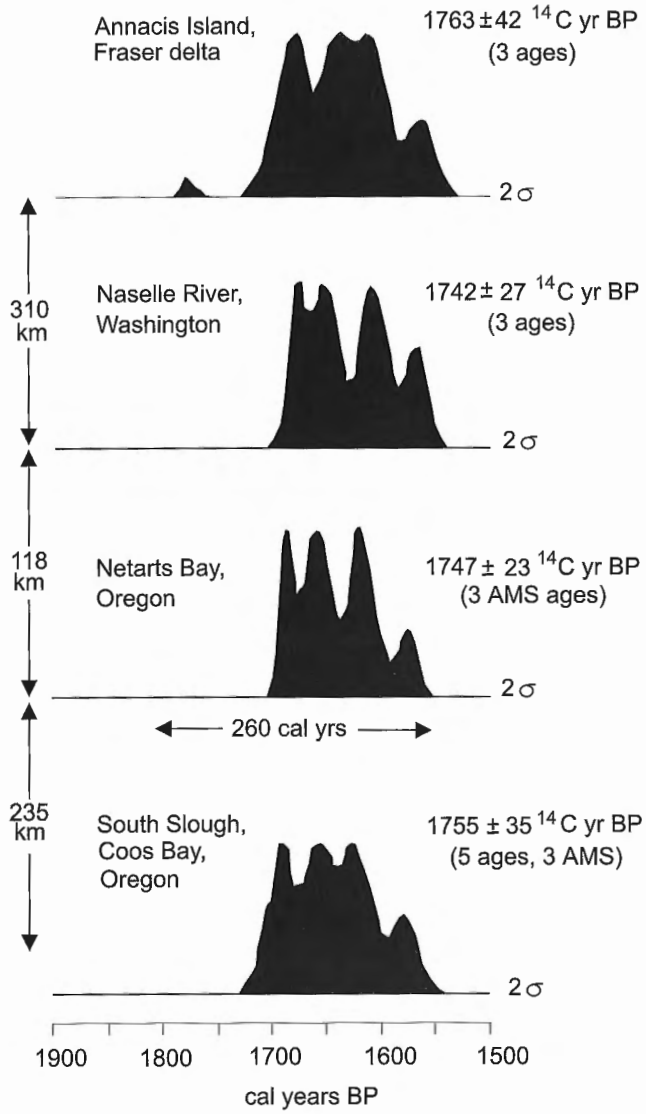

Figure 15. *Calibrated age-probability distributions for the mean of three ^{14}C ages from Annacis Island (Table 2) and for mean ages from coseismically subsided soils at three sites in Washington and Oregon (Clague et al., 1997, Fig. 4). The probability distributions include 2σ age intervals calculated using the decadal calibration data set of Stuiver and Becker (1993) (method of Stuiver and Reimer, 1993). An error multiplier of 1.0 was applied to AMS ages (Nelson et al., 1995) and 1.5-2.0 to gas proportional ages (note error multipliers expand laboratory-quoted errors to cover uncertainties in reproducibility and systematic bias; for a discussion, see Stuiver and Pearson, 1993). The numbers next to distributions are the mean and standard deviation of averaged ages and, in parentheses, the number of ages. Vertical arrows show distances between sites; South Slough is 650 km south of Annacis Island. Mean ages from all sites are statistically indistinguishable (test of Ward and Wilson, 1978).*

mean of the three ages from the top of the buried soil at Annacis Island (1763 ± 42 ^{14}C years BP; Table 2, Fig. 15). The ages used to calculate the means at each site, as well as the mean ages themselves, are statistically indistinguishable at the 2σ level. Calibration of the means from each site yields intervals that span more than 200 years (Fig. 15), an interval far too long to preclude the occurrence of a series of M = 8 plate-boundary earthquakes along the subduction zone, rather than a single M = 9 earthquake. Furthermore, many of the radiocarbon ages are on detrital material that grew before the time of burial, thus the earthquake (or earthquakes) may have occurred as much as several decades after this interval of time.

An alternative hypothesis, which is also consistent with the radiocarbon data, is that the earthquake responsible for the liquefaction at Annacis Island was a crustal event related to a larger plate-boundary earthquake, with minutes, days, or years separating the two events. We have no way of testing this hypothesis, but the very low shear strength of the subduction thrust fault separating the Juan de Fuca and North America plates favours a situation in which a plate-boundary earthquake could trigger a large earthquake in the crust east of the plate boundary (Wang et al., 1995). Contemporaneous slip on faults in the North America plate and on the plate boundary has been advanced as a possible explanation for inferred coseismic deformation in the southern Puget Lowland of Washington (Bucknam et al., 1992) and in northern California (Clarke and Carver, 1992). Sudden uplift along one or more crustal faults in the Puget Lowland about 1000 years ago (Bucknam et al., 1992; Bucknam and Biasi, 1994) may have occurred at the same time as localized subsidence and venting of sand on the Pacific coast; the subsidence and venting may be due to plate-boundary rupture (Atwater, 1992).

The deformation pattern inferred for the younger earthquake is more compatible with a large crustal earthquake than a plate-boundary event. Southern Vancouver Island and the adjacent mainland coast dropped slightly during this earthquake, but at least the eastern part of this area is outside the zone of expected coseismic subsidence for a Cascadia plate-boundary earthquake (see "Older earthquake", below).

The liquefaction analysis presented above precludes neither a plate-boundary nor crustal source for the earthquake that caused the liquefaction at Annacis Island and other sites on the Fraser delta. Ambraseys' data indicate that a M = 8 plate-boundary earthquake centred on the northern Cascadia subduction zone could liquefy sediments at Annacis Island; a M = 9 earthquake, involving rupture of much of the plate boundary, could have a similar effect (Fig. 10). The data also indicate that the minimum magnitude of the earthquake(s) that produced the liquefaction features on the Fraser delta is about 6.

Older earthquake

The pattern of submergence on southern Vancouver Island and minor emergence near Vancouver about 3600 years ago fits the expectation of coseismic deformation caused by a great plate-boundary earthquake along the Cascadia subduction zone (Plafker, 1969; Plafker and Savage, 1970; Dragert and Rogers, 1988). Rupture of the Juan de Fuca – North America plate boundary beneath the eastern North Pacific Ocean would trigger coincident uplift of the continental shelf off the west coast of Vancouver Island, subsidence of much of Vancouver Island, and, possibly, minor uplift of the British Columbia mainland coast to the east. This deformation is the surface manifestation of the release of elastic strain stored at the locked plate boundary (Savage, 1983; Hyndman and Wang, 1993). There is geological evidence from the coasts of southern Washington and northern Oregon for a plate-boundary earthquake of about the same age as the older earthquake in British Columbia (Darienzo and Peterson, 1990).

SUMMARY

The Fraser River delta is located in an area with the potential for large earthquakes, and it contains extensive shallow subsurface sands that are susceptible to coseismic liquefaction. There is geological and paleoecological evidence on the Fraser delta and the nearby Serpentine River floodplain for two large earthquakes during the late Holocene. Sudden land-level changes caused by these earthquakes are recorded as abrupt lithologic and microfossil changes in low-lying wetland stratigraphic sequences. In addition, one of the earthquakes extensively liquefied sediments on, and in the vicinity of, the Fraser delta.

The younger of the two documented earthquakes occurred about 1700 years ago. Study sites along the shores of the southern Strait of Georgia were suddenly submerged at this time, due to coseismic subsidence. Probably at the same time, shallow subsurface sands on the Fraser delta and along the Serpentine River liquefied, generating dykes and blows of sand and silt. The vigorous upward movement of liquefied sediment also deformed the strata through which it flowed.

These events may record a great (M = 8+) plate-boundary earthquake that ruptured part or all of the Cascadia subduction zone. A plate-boundary earthquake of approximately the same age has been documented on the Pacific coasts of southern Washington and northern Oregon, using geological evidence. More likely, the ca. 1700-year-old earthquake recorded on the Fraser delta was a large quake within the crust of the North America plate, either related to or independent of plate-boundary rupture. Whatever the source, data from the Fraser delta suggest that earthquakes capable of producing extensive liquefaction in this area are rare events.

An older earthquake, dating to about 3600 years ago, is marked by minor emergence of the Fraser delta and submergence on southern Vancouver Island. The inferred pattern of crustal deformation is consistent with a great plate-boundary earthquake.

REFERENCES

Ambraseys, N.N.
1988: Engineering seismology; Earthquake Engineering and Structural Dynamics, v. 17, p. 1-105.

Atwater, B.F.
1992: Geologic evidence for earthquakes during the past 2000 years along the Copalis River, southern coastal Washington; Journal of Geophysical Research, v. 97, p. 1901-1919.
1994: Geology of liquefaction features about 300 years old along the lower Columbia River at Marsh, Brush, Price, Hunting, and Wallace Islands, Oregon and Washington; United States Geological Survey, Open-File Report 94-209, 64 p.

Atwater, B.F. and Hemphill-Haley, E.
1996: Preliminary estimates of recurrence intervals for great earthquakes of the past 3500 years at northeastern Willapa Bay, Washington; United States Geological Survey, Open-File Report 96-001, 88 p.

Atwater, B.F., Nelson, A.R., Clague, J.J., Carver, G.A., Yamaguchi, D.K., Bobrowsky, P.T., Bourgeois, J., Darienzo, M.E., Grant, W.C., Hemphill-Haley, E., Kelsey, H.M., Jacoby, G.C., Nishenko, S.P., Palmer, S.P., Peterson, C.D., and Reinhart, M.A.
1995: Summary of coastal geologic evidence for past great earthquakes at the Cascadia subduction zone; Earthquake Spectra, v. 11, p. 1-18.

Basham, P.W., Weichert, D.H., Anglin, F.M., and Berry, M.J.
1982: New probabilistic strong seismic ground motion maps of Canada: a compilation of earthquake source zones, methods and results; Canada Earth Physics Branch, Open File 82-33, 202 p.

B.C. Hydro and Klohn Leonoff
1992: Liquefaction hazard assessment for the Lower Mainland region; British Columbia Hydro and Power Authority and Klohn Leonoff Ltd., Report No. H2474a, 44 p.

Borcherdt, R.D.
1994: New developments in estimating site effects on ground motion; Applied Technology Council, Seminar on New Developments in Earthquake Ground Motion Estimation and Implications for Engineering Design Practice, ATC-35, p. 10-1 – 10-44.

Briggs, G.G.
1994: Coastal crossing of the elastic strain zero isobase, Cascadia margin, south central Oregon coast; M.Sc. thesis, Portland State University, Portland, Oregon, 251 p.

Bucknam, R.C. and Biasi, G.P.
1994: An improved estimate of the time of a prehistoric earthquake in the southwest Puget Sound region, Washington; Geological Society of America, Abstracts with Programs, v. 26, no. 7, p. A-522.

Bucknam, R.C., Hemphill-Haley, E., and Leopold, E.B.
1992: Abrupt uplift within the past 1700 years at southern Puget Sound, Washington; Science, v. 258, p. 1611-1614.

Byrne, P.H. and Anderson, D.L.
1987: Earthquake design in Richmond, B.C., Version II; University of British Columbia, Department of Civil Engineering, Soil Mechanics Series, No. 109, 90 p.

Clague, J.J.
1989: Late Quaternary sea level change and crustal deformation, southwestern British Columbia; in Current Research, Part E; Geological Survey of Canada, Paper 89-1E, p. 233-236.

Clague, J.J. and Bobrowsky, P.T.
1994a: Evidence for a large earthquake and tsunami 100-400 years ago on western Vancouver Island, British Columbia; Quaternary Research, v. 41, p. 176-184.
1994b: Tsunami deposits beneath tidal marshes on Vancouver Island, British Columbia; Geological Society of America Bulletin, v. 106, p. 1293-1303.

Clague, J.J., Luternauer, J.L., and Hebda, R.J.
1983: Sedimentary environments and postglacial history of the Fraser Delta and lower Fraser Valley, British Columbia; Canadian Journal of Earth Sciences, v. 20, p. 1314-1326.

Clague, J.J., Luternauer, J.L., Monahan, P.A., Edwardson, K.A., Dallimore, S.R., and Hunter, J.A.
1998: Quaternary stratigraphy and evolution of the Fraser delta; in Geology and Natural Hazards of the Fraser River Delta, British Columbia, (ed.) J.J. Clague, J.L. Luternauer, and D.C. Mosher; Geological Survey of Canada, Bulletin 525, this volume.

Clague, J.J., Luternauer, J.L., Pullan, S.E., and Hunter, J.A.
1991: Postglacial deltaic sediments, southern Fraser River delta, British Columbia; Canadian Journal of Earth Sciences, v. 28, p. 1386-1393.

Clague, J.J., Naesgaard, E., and Nelson, A.R.
1997: Age and significance of earthquake-induced liquefaction features near Vancouver, British Columbia, Canada; Canadian Geotechnical Journal, v. 34, p. 53-62.

Clague, J.J., Naesgaard, E., and Sy, A.
1992: Liquefaction features on the Fraser delta: evidence for prehistoric earthquakes?; Canadian Journal of Earth Sciences, v. 29, p. 1734-1745.

Clarke, S.H., Jr. and Carver, G.A.
1992: Late Holocene tectonics and paleoseismicity, southern Cascadia subduction zone; Science, v. 255, p. 188-192.

Crouse, C.B.
1991: Ground-motion attenuation equations for earthquakes on the Cascadia subduction zone; Earthquake Spectra, v. 4, p. 201-236.

Darienzo, M.E. and Peterson, C.D.
1990: Episodic tectonic subsidence of late Holocene tidal marshes, northern Oregon coast, central Cascadia margin; Tectonics, v. 9, p. 1-22.
1995: Magnitude and frequency of subduction-zone earthquakes along the northern Oregon coast in the past 3,000 years; Oregon Geology, v. 57, p. 3-12.

Darienzo, M.E., Peterson, C.D., and Clough, C.
1994: Stratigraphic evidence for great subduction-zone earthquakes at four estuaries in northern Oregon: Journal of Coastal Research, v. 10, p. 850-876.

Dragert, H. and Rogers, G.C.
1988: Could a megathrust earthquake strike southwestern British Columbia?; Geos, v. 17, no. 3, p. 5-8.

Finn, W.D.L.
1996: Evaluation of liquefaction potential for different earthquake magnitudes and site conditions; in Recent Developments in Seismic Liquefaction Assessment; ConeTec Investigations Ltd., Vancouver, British Columbia, 34 p.

Fraser Delta Task Force
1991: Earthquake design in the Fraser delta – Task Force report; City of Richmond, British Columbia, 42 p.

Guilbault, J.-P., Clague, J.J., and Lapointe, M.
1995: Amount of subsidence during a late Holocene earthquake – evidence from fossil tidal marsh foraminifera at Vancouver Island, west coast of Canada; Palaeogeography, Palaeoclimatology, Palaeoecology, v. 118, p. 49-71.
1996: Foraminiferal evidence for the amount of coseismic subsidence during a late Holocene earthquake on Vancouver Island, west coast of Canada; Quaternary Science Reviews, v. 15, p. 913-937.

Hasegawa, H.S., Basham, P.W., and Berrry, M.J.
1981: Attenuation relations for strong seismic ground motion in Canada; Seismological Society of America Bulletin, v. 71, p. 1943-1962.

Hemphill-Haley, E.
1995: Diatom evidence for earthquake-induced subsidence and tsunami 300 yr ago in southern coastal Washington; Geological Society of America Bulletin, v. 107, p. 367-378.

Hyndman, R.D. and Wang, K.
1993: Thermal constraints on the zone of major thrust earthquake failure: the Cascadia subduction zone; Journal of Geophysical Research, v. 98, p. 2039-2060.

Idriss, I.M.
1993: Procedures for selecting earthquake ground motions at rock sites; National Institute of Standards and Technology, Report NIST GCR 93-625, 7 p.

Jacoby, G.C., Carver, G., and Wagner, W.
1995: Trees and herbs killed by an earthquake 300 yr ago at Humboldt Bay, California: Geology, v. 23, p. 77-80.

Little, T.E.
1993: Report to the Ministry of Transportation and Highways on seismic ground motion parameters for Oak Street and Port Mann bridges; British Columbia Hydro and Power Authority, Report No. H2723, 42 p.

Luternauer, J.L., Barrie, J.V., Christian, H.A., Clague, J.J., Evoy, R.W., Hart, B.S., Hunter, J.A., Killeen, P.G., Kostaschuk, R.A., Mathewes, R.W., Monahan, P.A., Moslow, T.F., Mwenifumbo, C.J., Olynyk, H.W., Patterson, R.T., Pullan, S.E., Roberts, M.C., Robertson, P.K., Tarbotton, M.R., and Woeller, D.J.
1994: Fraser River delta: geology, geohazards and human impact; in Geology and Geological Hazards of the Vancouver Region, Southwestern British Columbia, (ed.) J.W.H. Monger; Geological Survey of Canada, Bulletin 481, p. 197-220.

Luternauer, J.L., Clague, J.J., Hunter, J.A.M., Pullan, S.E., Roberts, M.C., Woeller, D.J., Kostaschuk, R.A., Moslow, T.F., Monahan, P.A., and Hart, B.S.
1993: The Fraser River delta, architecture, geological dynamics and human impact; in Deltas of the World, (ed.) R. Kay; American Society of Civil Engineers, New York, p. 99-113.

Luternauer, J.L., Mosher, D.C., Clague, J.J., and Atkins, R.J.
1998: Sedimentary environments of the Fraser delta; in Geology and Natural Hazards of the Fraser River Delta, British Columbia, (ed.) J.J. Clague, J.L. Luternauer, and D.C. Mosher; Geological Survey of Canada, Bulletin 525, this volume.

Malone, S.D. and Bor, S.
1979: Attenuation patterns in the Pacific Northwest based on intensity data and the location of the 1872 North Cascades earthquake; Seismological Society of America Bulletin, v. 69, p. 531-576.

Mathewes, R.W. and Clague, J.J.
1994: Detection of prehistoric large earthquakes in the Pacific Northwest by microfossil analysis; Science, v. 264, p. 688-691.

McGuire, R.K.
1976: Fortran computer program for seismic risk analysis; United States Geological Survey, Open-File Report 76-67, 68 p.

Milne, W.G., Rogers, G.C., Riddihough, R.P., McMechan, G.A., and Hyndman, R.D.
1978: Seismicity of western Canada; Canadian Journal of Earth Sciences, v. 15, p. 1170-1193.

Monahan, P.A., Luternauer, J.L., and Barrie, J.V.
1993: A delta plain sheet sand in the Fraser River delta, British Columbia, Canada; Quaternary International, v. 20, p. 27-38.

Naesgaard, E, Sy, A., and Clague, J.J.
1992: Liquefaction sand dykes at Kwantlen College, Richmond, B.C.; in Geotechnique and Natural Hazards; BiTech Publishers, Vancouver, p. 159-166.

Nelson, A.R.
1992a: Discordant ^{14}C ages from buried tidal-marsh soils in the Cascadia subduction zone, southern Oregon coast; Quaternary Research, v. 38, p. 75-90.
1992b: Holocene tidal-marsh stratigraphy in south-central Oregon – evidence for localized sudden submergence in the Cascadia subduction zone; in Quaternary Coasts of the United States: Marine and Lacustrine Systems, (ed.) C.P. Fletcher and J.F. Wehmiller; Society for Sedimentary Geology, Special Publication 48, p. 287-301.

Nelson, A.R., Atwater, B.F., Bobrowsky, P.T., Bradley, L.-A., Clague, J.J., Carver, G.A., Darienzo, M.E, Grant, W.C., Krueger, H.W., Sparks, R., Stafford, T.W., Jr., and Stuiver, M.
1995: Radiocarbon evidence for extensive plate-boundary rupture about 300 years ago at the Cascadia subduction zone; Nature, v. 378, p. 371-374.

Nelson, A.R., Jennings, A.E., and Kashimi, K.
1996a: An earthquake history derived from stratigraphic and microfossil evidence of relative sea-level change at Coos Bay, southern coastal Oregon; Geological Society of America Bulletin, v. 108, p. 141-154.

Nelson, A.R., Shennan, I., and Long, A.J.
1996b: Identifying coseismic subsidence in tidal-wetland stratigraphic sequences at the Cascadia subduction zone of western North America; Journal of Geophysical Research, v. 101, p. 6115-6135.

Obermeier, S.F.
1988: Liquefaction potential in the central Mississippi Valley; United States Geological Survey, Bulletin 1832, 21 p.
1994a: Preliminary limits for the strength of shaking in the Columbia River valley and the southern half of coastal Washington, with emphasis for a Cascadia subduction zone earthquake about 300 years ago; United States Geological Survey, Open-File Report 94-589, 40 p.
1994b: Using liquefaction-induced features for paleoseismic analysis; Chapter A in Using Ground-Failure Features for Paleoseismic Analysis, (ed.) S.F. Obermeier and R.W. Jibson; United States Geological Survey, Open-File Report 94-663, 58 p.

Obermeier, S.F., Jacobson, R.B., Smoot, J.P., Weems, R.E., Gohn, G.S., Monroe, J.E., and Powars, D.S.
1990: Earthquake-induced liquefaction features in the coastal setting of South Carolina and the fluvial setting of the New Madrid fault zone; United States Geological Survey, Professional Paper 1504, 44 p.

Ota, Y., Nelson, A.R., Umitsu, M., Kaoru, K., and Matsushima, Y.
1995: Interpreting an earthquake history from the stratigraphy of late Holocene intertidal deposits in South Slough, Coos Bay, Oregon, USA; Journal of the Geographical Society of Japan, v. 104, p. 94-106 [in Japanese].

Plafker, G.
1969: Tectonics of the March 27, 1964 Alaska earthquake. United States Geological Survey, Professional Paper 543-I, 74 p.

Plafker, G. and Savage, J.C.
1970: Mechanism of the Chilean earthquakes of May 21 and 22, 1960; Geological Society of America Bulletin, v. 81, p. 1001-1030.

Rogers, G.C.
1988: An assessment of the megathrust potential of the Cascadia subduction zone; Canadian Journal of Earth Sciences, v. 25, p. 844-852.
1994: Earthquakes in the Vancouver area; in Geology and Geological Hazards of the Vancouver Region, Southwestern British Columbia, (ed.) J.W.H. Monger; Geological Survey of Canada, Bulletin 481, p. 221-229.

Rogers, G.C. (cont.)
1998: Earthquakes and earthquake hazard in the Vancouver area; in Geology and Natural Hazards of the Fraser River Delta, British Columbia, (ed.) J.J. Clague, J.L. Luternauer, and D.C. Mosher; Geological Survey of Canada, Bulletin 525, this volume.

Satake, K., Shimazaki, K., Tsuji, Y., and Ueda, K.
1996: Time and size of a giant earthquake in Cascadia inferred from Japanese tsunami records of January 1700; Nature, v. 379, p. 246-249.

Savage, J.C.
1983: A dislocation model of strain accumulation and release at a subduction zone; Journal of Geophysical Research, v. 88, p. 4984-4996.

Seed, H.B. and de Alba, P.
1986: Use of SPT and CPT tests for evaluating the liquefaction resistance of sands; in Proceedings, In Situ '86, (ed.) S.P. Clemence; American Society of Civil Engineers, Geotechnical Special Publication No. 6, p. 281-302.

Seed, H.B., Idriss, I.M., and Arango, I.
1983: Evaluation of liquefaction potential using field performance data; American Society of Civil Engineers, Journal of Geotechnical Engineering Division, v. 109, p. 458-481.

Shedlock, K.M. and Weaver, C.S.
1991: Program for earthquake hazard assessment in the Pacific Northwest; United States Geological Survey, Circular 1067, 29 p.

Sims, J.D. and Garvin, C.D.
1995: Recurrent liquefaction induced by the 1989 Loma Prieta earthquake and 1990 and 1991 aftershocks: implications for paleoseismicity; Seismological Society of America Bulletin, v. 85, p. 51-65.

Stuiver, M. and Becker, B.
1993: High-precision decadal calibration of the radiocarbon time scale, AD 1950-6000 BC; Radiocarbon, v. 35, p. 35-65.

Stuiver, M. and Pearson, G.W.
1993: High-precision bidecadal calibration of the radiocarbon timescale, AD 1950-500 BC and 2500-6000 BC; Radiocarbon, v. 35, p. 1-23.

Stuiver, M. and Reimer, P.J.
1993: Extended ^{14}C data base and revised CALIB 3.0 ^{14}C age calibration program; Radiocarbon, v. 35, p. 215-230.

Tuttle, M., Law, K.T., Seeber, L., and Jacob, K.
1990: Liquefaction and ground failure induced by the 1988 Saguenay, Quebec, earthquake; Canadian Geotechnical Journal, v. 27, p. 580-589

Wang, K., Mulder, T., Rogers, G.C., and Hyndman, R.D.
1995: Case for very low coupling stress on the Cascadia subduction fault; Journal of Geophysical Research, v. 100, p. 12,907-12,918.

Ward, G.K. and Wilson, S.R.
1978: Procedures for comparing and combining radiocarbon age determinations: a critique; Archaeometry, v. 20, p. 19-34.

Variation in earthquake ground motion on the Fraser delta from strong-motion seismograph records

G.C. Rogers[1], J.F. Cassidy[1], and D.H. Weichert[1]

Rogers, G.C., Cassidy, J.F., and Weichert, D.H., 1998: Variation in earthquake ground motion on the Fraser Delta from strong-motion seismograph records; in Geology and Natural Hazards of the Fraser River Delta, British Columbia, (ed.) J.J. Clague, J.L. Luternauer, and D.C. Mosher; Geological Survey of Canada, Bulletin 525, p. 195–210.

Abstract: Strong ground-motion recordings of the magnitude (M_W) = 5.3 1976 Pender Island, British Columbia and M_W = 5.1 1996 Duvall, Washington earthquakes provide the best constraints, to date, on seismic site response on the Fraser delta. At low frequencies, seismic amplification occurs on the thick soils of the Fraser delta relative to rock and firm-soil sites. The amplification is more pronounced in the horizontal component of ground motion than in the vertical. At high frequencies, modest attenuation is observed on the thick soils. The crossover from amplification to attenuation occurs in the 5-8 Hz bandwidth. The largest ground accelerations recorded were not on the thickest sediments, but nearer the edge of the delta where the deltaic sediments and underlying Pleistocene sediments are thinner. This represents a hazard that should be taken into account when siting buildings near the delta edge.

Résumé : Les enregistrements des ébranlements du sol provoqués par les forts séismes de l'île Pender (Colombie-Britannique) en 1976 (M_W = 5,3) et de Duvall (État de Washington) en 1996 (M_W = 5,1) sont ceux qui permettent le mieux, à ce jour, d'établir comment se comporteraient les matériaux du delta du Fraser s'ils étaient soumis aux ondes d'un séisme. Aux basses fréquences, une amplification des ondes sismiques a été enregistrée aux sites du delta du Fraser où les sédiments sont épais, et non à ceux où le substratum ou le sol ferme est à faible profondeur. L'amplification de la composante horizontale de l'ébranlement du sol est plus marquée que celle de sa composante verticale. Aux hautes fréquences, on note une atténuation faible des ondes aux sites où les sédiments sont épais. Le passage de l'amplification à l'atténuation se situe dans la largeur de bande de 5 à 8 Hz. Ce n'est pas dans les sédiments les plus épais que l'on a constaté les plus fortes accélérations mais plus près de la bordure du delta, où les sédiments deltaïques et les sédiments pléistocènes sous-jacents sont plus minces. Il faudrait donc tenir compte de cette information lorsqu'on prévoit construire des bâtiments près de la bordure du delta.

[1] Geological Survey of Canada, Pacific Geoscience Centre, P.O Box 6000, Sidney, British Columbia V8L 4B2

INTRODUCTION

It has long been recognized that the amplitude of seismic waves can be altered by local geological structure (e.g. Milne, 1898). This is especially true for thick sedimentary basins. Amplification has been documented in thick sedimentary basins for a number of recent damaging earthquakes: the 1985 Mexico earthquake (Celebi et al., 1987); the 1989 Loma Prieta earthquake (Hough et al., 1990); the 1994 Northridge earthquake (Pitarka and Irikura, 1996); and the 1995 Kobe earthquake (Kawase, 1996). For a recent summary of some previous studies and references, see Field (1996).

The Fraser delta, just south of Vancouver (Fig. 1), is made up of soft sediments, mainly silts and sands, up to 300 m thick that have been deposited since the last glaciation (Clague et al., 1998). These soft sediments rest on top of firmer glacial sediments (mainly tills and sands) up to 500 m thick that extend beyond the present delta and mantle most of the surrounding uplands. The delta has a substantial and growing residential population as well as a number of vital economic facilities including manufacturing and port facilities, a liquified natural-gas plant, and the Vancouver International Airport. The delta also has a ferry terminal and hydroelectric transmission facilities which are critical links to Vancouver Island. It is thus important to understand the potential for amplification of seismic shaking on soils in this region, one of Canada's most seismically active areas. Note that we use the term 'soil' in this paper in the engineering sense, i.e. 'not rock'.

A network of self-triggering strong-motion seismographs around the Fraser delta was first laid out in the late 1960s and early 1970s, specifically to study soil response to seismic waves (Milne and Rogers, 1971; Rogers, 1976). It comprises north-south and east-west lines of instruments that cross the modern delta and extend onto the adjacent uplands, with reference instruments placed on bedrock. In recent years, the network has been upgraded with digital instruments and B.C. Hydro has deployed instruments at electrical transmission facilities.

Two earthquakes have provided strong-motion data sets for the Fraser delta region, one on May 16, 1976 ($M_W = 5.3$) and a second on May 3, 1996 ($M_W = 5.1$). The 1976 earthquake was located beneath Pender Island about 30 km south of the delta (Fig. 1) at a depth of 62 km (Rogers and Baldwin, 1989). This earthquake occurred within the subducting Juan de Fuca plate. The 1996 earthquake was a shallow event (4 km depth) within the crust of the North America plate near Duvall, Washington (Fig. 2) about 170 km southeast of the Fraser delta (Thomas et al., 1996).

In addition to strong-motion records of the Pender and Duvall earthquakes on or near the Fraser delta, we also utilize digital broadband and short-period records of the Canadian National Seismograph Network (CNSN) and its predecessor, the digital short-period Western Canadian Telemetered Network (WCTN), to examine the frequency-dependent site response on the Fraser delta, relative to firm-soil and bedrock sites.

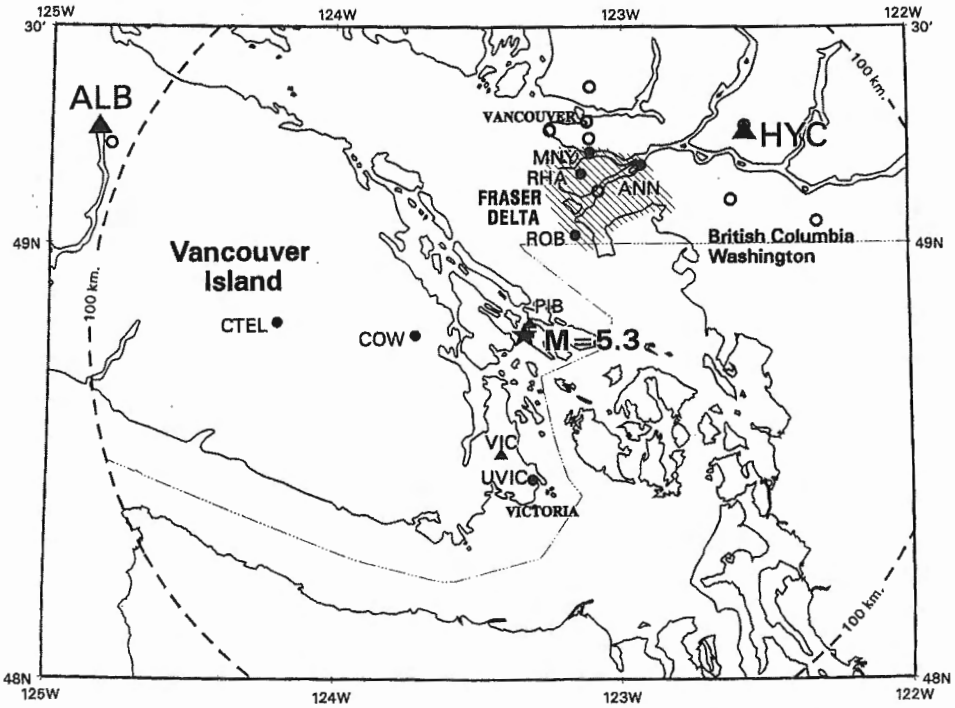

Figure 1. Map showing the epicentre of the 1976 Pender Island $M_W = 5.3$ earthquake relative to the Fraser delta (hatched area), locations of strong-motion instruments (circles; filled circles are triggered sites), and short-period vertical component instruments (triangles). The dashed line denotes an epicentral distance of 100 km.

Before interpreting these data in terms of the local soil structure, we first describe the data set for each of the earthquakes and consider earthquake source and travel-path effects. These two earthquakes are very different; the Pender Island earthquake was a deep event with shorter, but more vertical travel paths, whereas the 1996 Duvall earthquake was a shallow crustal earthquake with longer travel paths. Hence, potential source and path effects must be considered before attempting to constrain the local site response on the Fraser delta.

THE FRASER DELTA

The Fraser delta (Fig. 3) has been developing since the retreat of glaciers, approximately 11,000 years ago (Clague et al., 1998). Bedrock is about 200-1000 m below the delta, with an average depth of about 500 m (Britton et al., 1995). The sediments beneath the delta are Holocene deltaic deposits and Pleistocene glacial and interglacial deposits. The Holocene sediments are up to about 300 m thick (Luternauer and Hunter, 1996) and are mainly silts and sands. The Pleistocene sediments are mostly ice-compacted tills and glaciomarine silts and sands that overlie Tertiary bedrock. Shear-wave velocity in the Holocene sequence increases with depth (Hunter, 1995) with typical average values in the range of 200 to 300 m/s, but about 100 m/s near the surface in many places. The Pleistocene sediments typically have an average shear-wave velocity near 500 m/s but with considerable variability. The shear-wave velocity of the underlying Tertiary bedrock is 1500 m/s or greater. The Holocene sediments thin rapidly to the north at the edge of the basin (Fig. 3a). They are about 300 m thick in the basin centre near strong-motion instrument sites ARN and RHA, and only a few metres thick on the north side of the Fraser River at site MNY. In contrast, the Pleistocene sediments thin to the north more gradually and extend beyond the Fraser delta and mantle most of the greater Vancouver area (see cross-section in Fig. 4). Depth to the Tertiary bedrock (Fig. 3b) is about 800 m in the centre of the delta (sites ARN, RHA) and about 200-400 m near the North Arm of the Fraser River (sites KID, MNY, ANN), where the Holocene sediments pinch out. There are some localized highs on the buried bedrock and Pleistocene surfaces, such as one near station EBT.

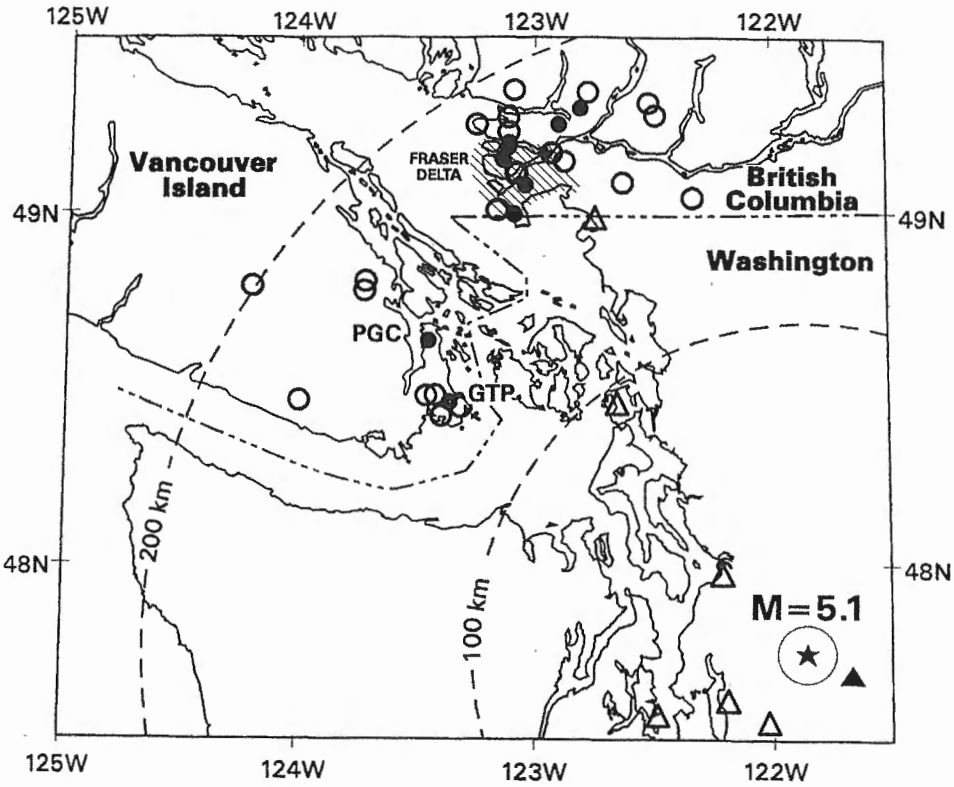

Figure 2. Map showing the epicentre of the 1996 M_W = 5.1 Duvall earthquake, the Fraser delta (hatched area), and locations of the strong-motion instruments in southern British Columbia and northern Washington. Circles are instruments operated by the Geological Survey of Canada and British Columbia Hydro and Power Authority, triangles are strong-motion instruments operated by the United States Geological Survey. In both cases filled symbols denote instruments that triggered during the earthquake.

THE STRONG-MOTION DATA SETS

The instruments that recorded the 1976 Pender Island earthquake (Fig. 1) are different from those that recorded the 1996 Duvall earthquake (Fig. 2). The instruments deployed in 1976 were analogue, recording on paper or 70 mm film. All of the instruments in the Fraser delta region used a 1 s pendulum for a trigger that required a horizontal displacement of 0.5 mm to commence operation. By contrast, all the instruments that triggered in 1996 were digital recording and had an adjustable three-component trigger, sensitive to 1-12 Hz energy (thresholds set between 0.4-1.0%g (g = acceleration of gravity)). The more sophisticated triggers on the modern instruments provide a higher record return, and the digital nature of the data gives a higher resolution, particularly for low-amplitude records such as we analyze in this paper. Details of the instrument types and trigger thresholds are given in Tables 1 and 2.

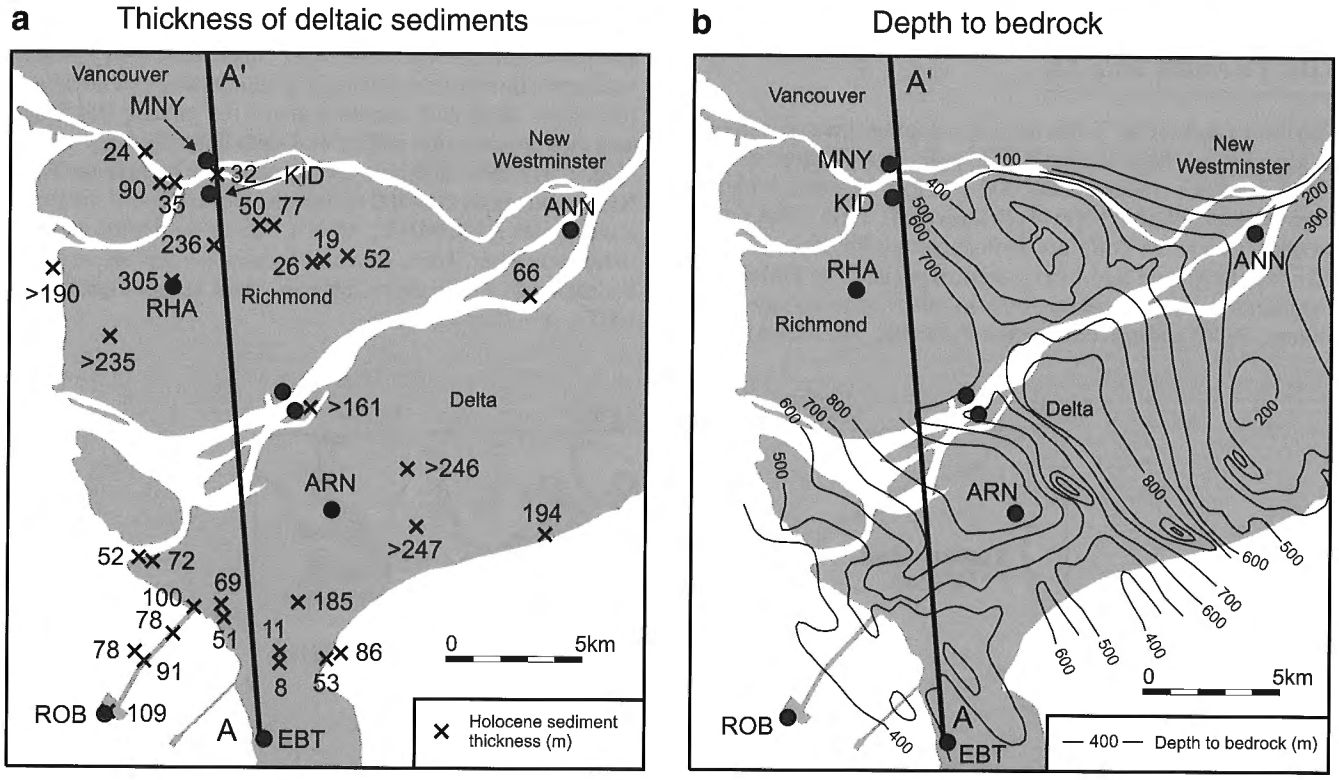

Figure 3. a) Thickness of Holocene sediments (in m) on the Fraser delta from borehole and surface geophysical studies (adapted from Luternauer and Hunter, 1996). Locations of strong-motion instruments relevant to this study are shown as filled circles. A simplified cross-section along line A-A' is shown in Figure 4. b) Depth to the Tertiary bedrock in the Fraser delta area from borehole and surface geophysical studies (adapted from Britton et al., 1995). The area north of the Fraser River is not well mapped.

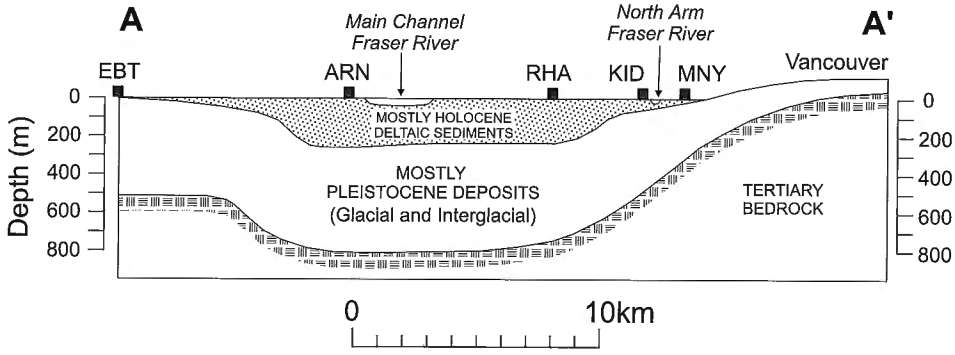

Figure 4. Simplified cross-section of the Fraser delta along line A-A' in Figure 3 showing Holocene and Pleistocene sediments and Tertiary bedrock.

Table 1. 1976 strong-motion seismograph station information.

Station	Instrument	Lat. °N Long. °W	Distance[1] (km)	Azimuth[2] (°)	Soil[3]	Peak acceleration (cm/s^2) SH	SZ	Z
Firm-soil triggers								
CTEL	SMA-1	48.843 124.074	62	270	20 m or more of dense gravelly till	34.7	34.9	31.7
COW	SMA-1	48.786 123.723	27	268	25 m or more of sand and gravel	46.1	56.2	39.2
UVIC	SMA-1	48.463 123.307	38	176	gravelly sand	35.0	31.1	20.7
Fraser delta triggers								
ANN	RFT250	49.181 122.929	52	36	~100 m (H) ~150 m (P)	52.8	41.9	11.5
ROB	RFT250	49.018 123.170	28	30	~100 m (H) ~400 m (P)	24.3	18.9	9.5
MNY	RFT250	49.210 123.110	49	21	~3 m (H) ~200 m (P)	32.3	25.6	15.4
RHA	AR-240	49.163 123.136	43	21	~300 m (H) ~500 m (P)	36.6	28. 0	5.8
Fraser delta non-triggers								
***	RFT250	49.124 123.077	41	28	~150 m (H) ~450 m (P)	–	–	–

Note: only stations that triggered are assigned station names (see Fig. 1 and 10a for locations).
[1] Epicentral distance.
[2] Direction from epicentre to station.
[3] H, Holocene sediments; P, Pleistocene sediments.

Table 2. 1996 strong-motion seismograph station information.

Station	Instrument trigger	Lat. °N Long. °W	Distance[1] (km)	Azimuth[2] (°)	Soil[3]	Peak acceleration (cm/s^2) SH	SV	V
Firm-soil/bedrock								
BND	SSA-2 0.004g	49.263 122.899	184.2	335.5	very dense sandy till	4.9	4.3	2.6
GTP	SSA-2 0.006g	48.474 123.359	137.4	305.9	~20 m silty clay over till	4.3[4]	8.5[4]	4.4[4]
MDN	SSA-2 0.004g	49.309 122.806	177.4	346.4	>7 m very dense silty/ sandy soil	10.9[4]	9.0[4]	3.2[4]
PGC	SSA-1 0.001g	48.651 123.449	154.6	310.4	granitic bedrock	4.6	3.3	1.8
Fraser delta triggers								
ARN	SSA-2 0.004g	49.091 123.042	172.3	329.7	~350 m (H) ~500 m (P)	9.4	6.8	1.5
EBT	SSA-2 0.004g	49.008 123.090	166.3	327. 0	~500 m (P)	6. 0	3.2	1.5
KID	SSA-2 0.004g	49.199 123.114	185.3	330.2	~45 m (H) >150 m (P)	12.8	13.6	2.9
MNY	SSA-2 0.01g	49.210 123.11	186.1	330.5	~3 m (H) ~200 m (P)	15. 0	6.9	3.7
RHA	SSA-2 0.01	49.163 123.136	182.7	329.2	~300 m (H) ~500 m (P)	9. 0	10.7	2.3
Fraser delta non-triggers								
ANN	SSA-2 0.01g	49.181 122.929	177. 0	333.7	~100 m (H) ~150 m (P)	<10.0	<10.0	<10.0
ROB	SSA-2 0.01g	49.018 123.170	170.6	325.6	~100 m (H) ~400 m (P)	<10.0	<10.0	<10.0
***	SSA-2 0.01g	49.124 123.077	176.7	329.6	~150 m (H) ~450 m (P)	<10.0	<10.0	<10.0
***	SA-2 0.01g	49.126 123.082	177. 0	329.6	~150 m (H) ~450 m (P)	<10.0	<10.0	<10.0

Note: only stations that triggered are assigned station names (see Fig. 2 and 10b for locations).
[1] Epicentral distance.
[2] Direction from epicentre to station.
[3] H, Holocene sediments; P, Pleistocene sediments.
[4] Seismograms are dominated by a strong resonance likely caused by structures at the recording site.

All of these records can best be described as 'weak' strong motion and are barely in the range of ground motion that strong-motion seismographs are designed to record. Because the amplitude of the records is not much above the resolution of the instruments, and because some of the records are of short duration, we have not attempted to analyze at frequencies below 0.5 Hz (2 s period) even though we would expect significant amplification at lower frequencies on the deeper parts of the delta.

The 1976 (M = 5.3) Pender Island earthquake data

This earthquake triggered seven strong-motion instruments in southwest British Columbia (Fig. 1), four on the Fraser delta, and three on southern Vancouver Island. It was also recorded on four nearby digital short-period vertical-component WCTN seismographs. The Fraser delta strong-motion sites that triggered were ANN, MNY, RHA, and ROB. The latter two stations are very thick soil sites, with 300 m (RHA) and 100 m (ROB) of Holocene sediments and bedrock depths of 800 m (RHA) and 400 m (ROB). Station MNY is located at the north edge of the Fraser Delta (Fig. 3a) where the Holocene sediments are about 3 m thick and depth to bedrock is estimated at about 200 m. Site ANN has a bedrock depth of about 250 m, and the Holocene sediments are about 100 m thick. Unfortunately, none of the nearby instruments sited on bedrock triggered. However, the instrument at station CTEL on Vancouver Island (Fig. 1), which did trigger, is about the same distance from the epicentre as the Fraser delta, but is on firm soil (very dense sandy-gravelly till). The depth to bedrock near CTEL ranges from 20 m to 55 m. We compare the character of horizontal motion at the Fraser delta sites with the CTEL record.

Figure 5 shows strong-motion acceleration records of the Pender Island earthquake at Fraser delta sites ANN, MNY, and CTEL. This figure illustrates 3 points: 1) although the horizontal components of ground motion at sites ANN and MNY were similar in amplitude to that at the firm-soil site CTEL, there was a significant difference in the frequency content, with the thicker delta-soil sites being dominated by longer-period energy; 2) the duration of strong shaking was much longer at ANN than at CTEL; and 3) the vertical component of ground shaking was less at the Fraser delta sites than at CTEL.

Prior to interpreting these records in terms of site response, we need to consider potential source radiation, rupture directivity, and travel-path effects. In Figure 6 we consider potential source effects and show the P-wave and S-wave radiation patterns with the station locations plotted on the focal sphere. The S-wave pattern is resolved into transverse (SH) and radial (SV) components. Most of the strong-motion and WCTN sites are well away from the P-wave nodal plane. Unfortunately, most of the Fraser delta sites are close

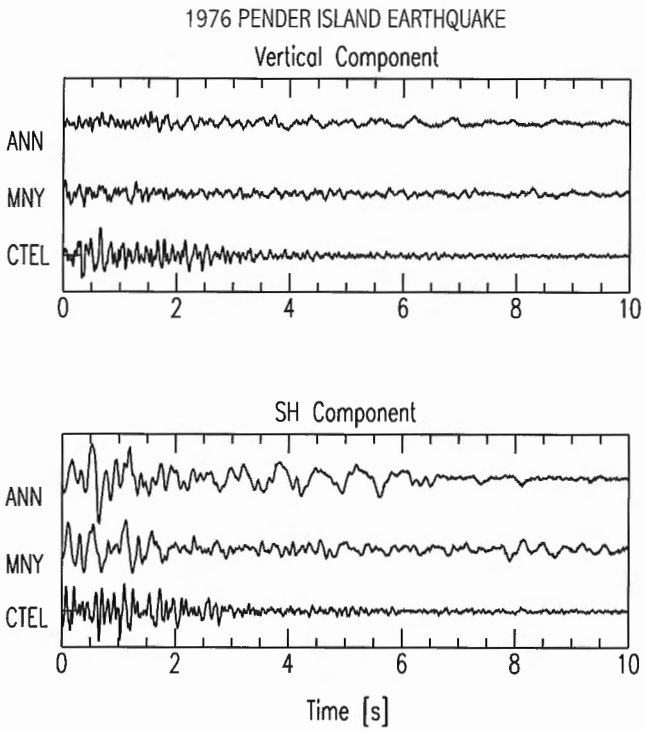

Figure 5. *Unfiltered vertical (top) and horizontal (bottom) acceleration records of the 1976 Pender Island earthquake at stations ANN and MNY on the Fraser delta, and CTEL, a firm-soil site on Vancouver Island. All traces are plotted at the same scale. For the SH component, both ANN and MNY are dominated by longer period waves, and exhibit a longer duration of strong shaking than CTEL. The long-period 'ringing' at ANN suggests a resonance effect. The vertical component of motion at the Fraser delta sites is of lower amplitude than that at the firm-soil site.*

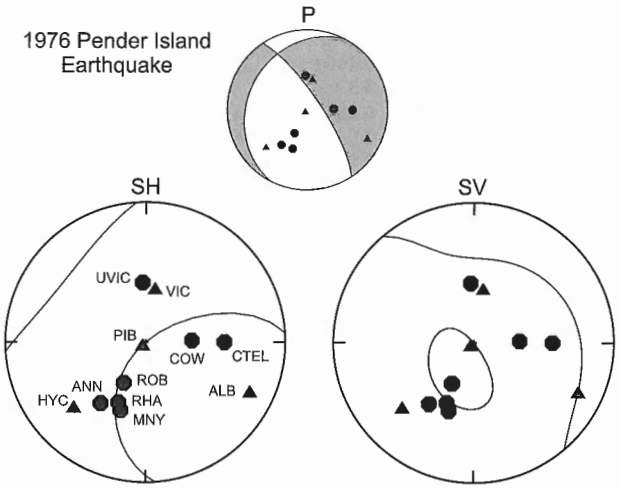

Figure 6. *P-wave, SH-wave, and SV-wave radiation patterns for the focal mechanism (lower hemisphere projection; strike 326°, dip 76°, slip -113°) of the 1976 Pender Island earthquake (Rogers, 1983); locations of the strong-motion sites (filled circles) and short-period WCTN sites (triangles) are superimposed. The strong-motion sites on the Fraser delta (ANN, ROB, RHA, and MNY) are near-nodal for both SH and SV waves. Horizontal amplitudes at these sites may be lower than those at stations farther from the nodal planes (e.g. CTEL).*

to SH and SV nodal planes, which are radiation minima. This raises a caution that the amplitude of both SH and SV energy radiated towards adjacent stations may be different and thus not directly comparable.

Fraser delta sites ANN, ROB, and MNY (azimuth = 20-36°) are at a very different azimuth from the epicentre than CTEL (azimuth = 270°). Fortunately, there are WCTN short-period vertical-component digital recordings of this earthquake from two bedrock sites (Fig. 1) at similar azimuths to the strong-motion recordings. HYC is just northeast of the Fraser delta at an azimuth of 47° from the epicentre (similar to the Fraser delta strong-motion sites, but more distant — 77 km). ALB on Vancouver Island at an azimuth of 296° from the epicentre is similar to CTEL, but more distant (121 km). Comparison of the velocity spectra at these two WCTN sites (Fig. 7) shows no difference in either the frequency of the energy peak or overall appearance, indicating that source directivity and propagation effects are not significantly different at these two azimuths and thus are probably not a concern in analyzing the strong-motion records.

The 1996 (M = 5.1) Duvall earthquake data

The Fraser delta strong-motion sites that triggered during the Duvall earthquake (Fig. 2) were RHA and ARN, both thick soil sites (about 300 m of Holocene sediments, and bedrock at about 800 m depth); KID and MNY near the delta edge (about 30 m and 3 m of Holocene sediments, respectively, and bedrock is at least 200 m deep); and EBT located on a Pleistocene high (bedrock depth of about 500 m). It is noteworthy that the strong-motion instrument at Annacis Island (ANN), which recorded the highest acceleration and longest duration shaking during the Pender Island earthquake, did not trigger during the 1996 earthquake. Firm-soil strong-motion instruments in the lower mainland that triggered in 1996 were BND and MDN; both instruments are situated on several metres of dense till overlying bedrock. The only strong-motion recording on rock was from PGC on southern Vancouver Island (Fig. 2), which is situated on granitic bedrock (quartz diorite).

In Figure 8 we compare vertical and horizontal records for stations PGC (bedrock), RHA (thickest Holocene sediment), and MNY (near the edge of the delta). The highest accelerations, at 2-3 Hz in the unfiltered waveforms, were recorded at MNY; the lowest were at the bedrock site (PGC). In contrast to records of the Pender Island earthquake (Fig. 5), the frequency content of these records is similar. Also, amplification at the thick-soil sites relative to bedrock occurs for both horizontal and vertical components of motion, but is greatest for the horizontal components. In contrast, the Pender Island records showed amplification only for the horizontal component of motion.

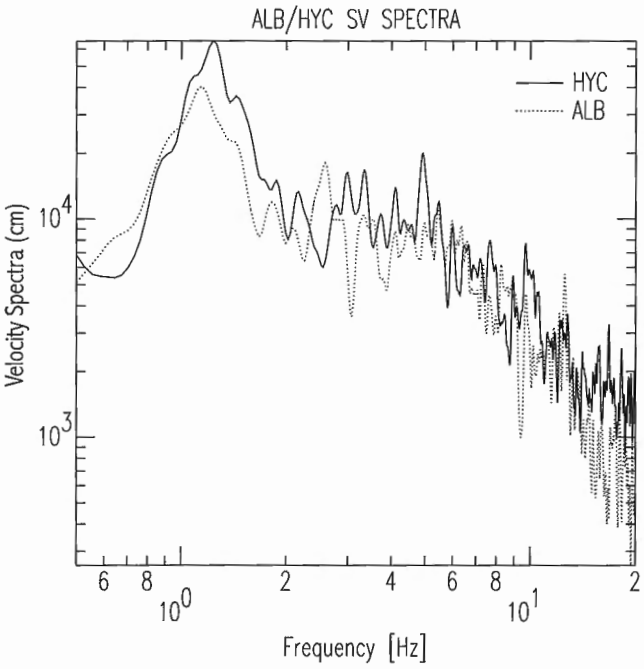

Figure 7. Comparison of the SV spectra of the 1976 Pender Island earthquake at short-period vertical seismographs at bedrock sites HYC on the Lower Mainland and ALB on Vancouver Island. Despite their different azimuths from the epicentre, the spectra are very similar, indicating that rupture directivity and path effects are not important when comparing Fraser delta strong-motion recordings with those on Vancouver Island.

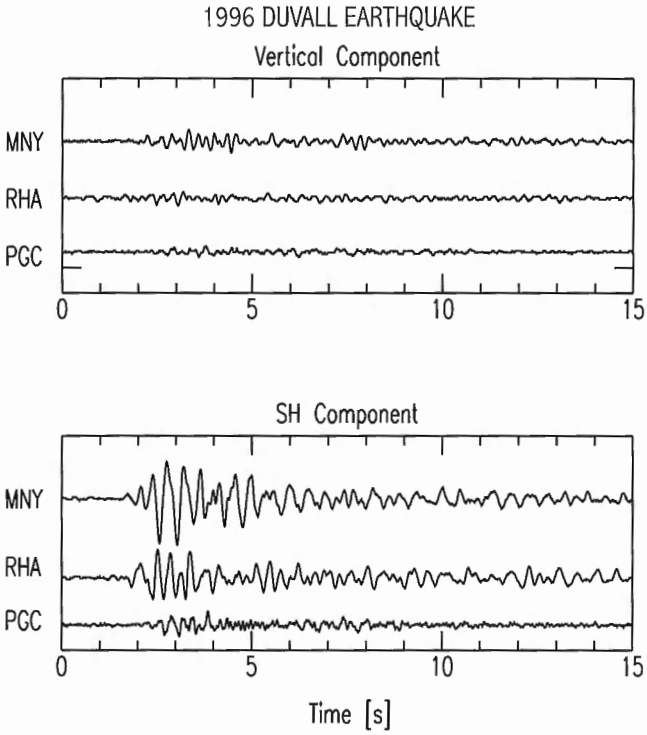

Figure 8. Unfiltered vertical (top) and horizontal (bottom) acceleration records of the 1996 Duvall earthquake at stations MNY and RHA on the Fraser delta, and PGC, a rock site on Vancouver Island. All traces are plotted at the same scale. Both RHA and MNY show amplification, relative to rock, particularly in the horizontal component of motion.

Source and travel-path effects are not a problem for this data set because all of the Fraser delta strong-motion sites, and the PGC bedrock site are away from SH and SV radiation minima (nodal lines on the radiation patterns in Fig. 9). The range in distance from the epicentre of the earthquake to the sites considered in this study is small enough (140-180 km) that differences due to path effects will be minimal, thus we feel confident that we can use the PGC recordings as meaningful bedrock reference spectra for the Fraser delta.

In addition to the strong-motion data, we have utilized short-period vertical-component recordings made on the WCTN, and three-component broadband recordings made on CNSN stations in southern British Columbia. For these data sets, the instrument response was removed, and the velocity records differentiated to form acceleration records for direct comparison with the strong-motion recordings. At PGC, where broadband, short-period, and strong-motion records were all obtained, the processed broadband and short-period acceleration records are in excellent agreement with the strong-motion recordings.

DATA ANALYSIS

To analyze the 1976 Pender Island earthquake, we redigitized the original film records. We contracted a commercial service in California that uses a computer-based laser-beam trace-following system, specifically designed for digitizing 70 mm film from strong-motion instruments. RHA was a paper record and so the original hand-digitized data used in the Weichert and Milne (1980) report were used. Linear trends and DC offsets were removed from the seismograms and they were rotated, based on the earthquake-to-station azimuth, to form the radial (SV) and transverse (SH) components. We analyzed SH waves in this study, and used the vertical component of the SV waves to compare peak values of horizontal and vertical motion.

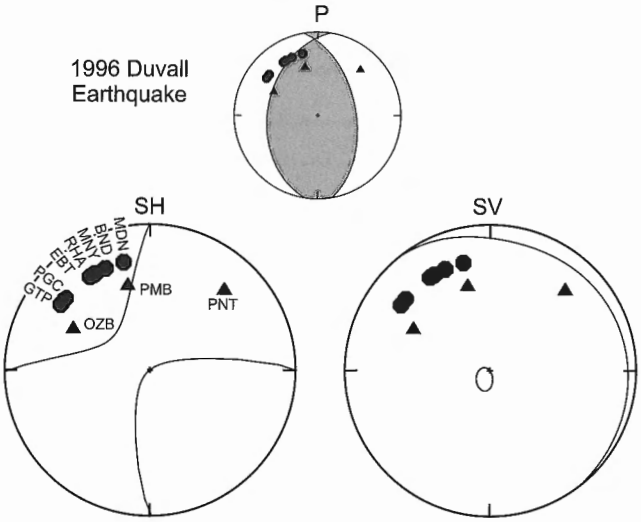

Figure 9. *P-wave, SH-wave, and SV-wave radiation patterns for the focal mechanism (lower hemisphere projection; strike 350°, dip 52°, slip 78°) for the 1996 Duvall earthquake; locations of the strong-motion sites (filled circles) and broadband sites (filled triangles) are superimposed. P-wave amplitude variations may be significant since the sites on the Fraser delta are close to nodal, but we do not analyze P waves in this paper. All stations considered in this study are far enough away from S-wave nodal planes that amplitude variations should be negligible.*

Peak ground acceleration

Peak ground accelerations measured at strong-motion instrument sites on and around the Fraser delta during the 1976 and 1996 earthquakes are listed in Tables 1 and 2 and shown in Figures 10a and 10b, respectively. In addition, in Figure 10b, the instruments that did not trigger during the 1996 earthquake provide upper limits for peak ground acceleration at their locations because they have acceleration triggers. Note that these peak accelerations were at 2-3 Hz for the Duvall earthquake and 1.5-3 Hz for the Pender Island earthquake. Accelerations for the Pender Island earthquake were higher than those of the Duvall earthquake due to the slightly larger size (M_W = 5.3 vs. M_W = 5.1) and the closer proximity (30-50 km vs. 140-180 km) of the Pender Island event. In both cases, most of the instruments that triggered were on very thick deltaic deposits. However, in both cases, not all of the instruments on the delta triggered; in particular, instruments on deep soil near the Main Channel of the Fraser River did not trigger. Instruments on rock in the Vancouver area did not trigger during either of these earthquakes.

To demonstrate that the peak acceleration values at the Fraser delta sites are anomalously high relative to rock or firm-soil sites, we plotted, for the Duvall earthquake, (Fig. 11) peak horizontal acceleration versus epicentral distance for the strong-motion data set (rock, thin firm soil, and thick soil) and for the broadband data set (rock sites). In all cases, the peak acceleration occurred within the first 5 s of the S-wave train. It is clear that the thick-soil sites on the Fraser delta have significantly higher (2-5 times) peak horizontal accelerations than bedrock or thin firm-soil sites.

The solid line in Figure 11 represents the strong ground-motion attenuation relation proposed for the year 2000 National Building Code of Canada (Adams et al., 1996). It is based on the Boore et al. (1993, 1994) relations, extended beyond 100 km by inclusion of an anelastic attenuation term (Atkinson, 1995). The Boore et al. studies utilized earthquakes in California, and the curve shown is appropriate for rock sites (as defined by Boore et al. (1993, 1994): Class A, S-wave velocity > 750 m/s). While it is not the focus of this paper, the Duvall earthquake provides one of the first opportunities to compare this proposed ground-motion relation with data in southern British Columbia from a crustal earthquake with a magnitude greater than 5. The horizontal accelerations in Figure 11 drop off more rapidly with distance than the proposed relationship. However, we note that these observations reflect only a single M = 5.1 earthquake with travel paths greater than 100 km and in a small azimuthal range from the epicentre.

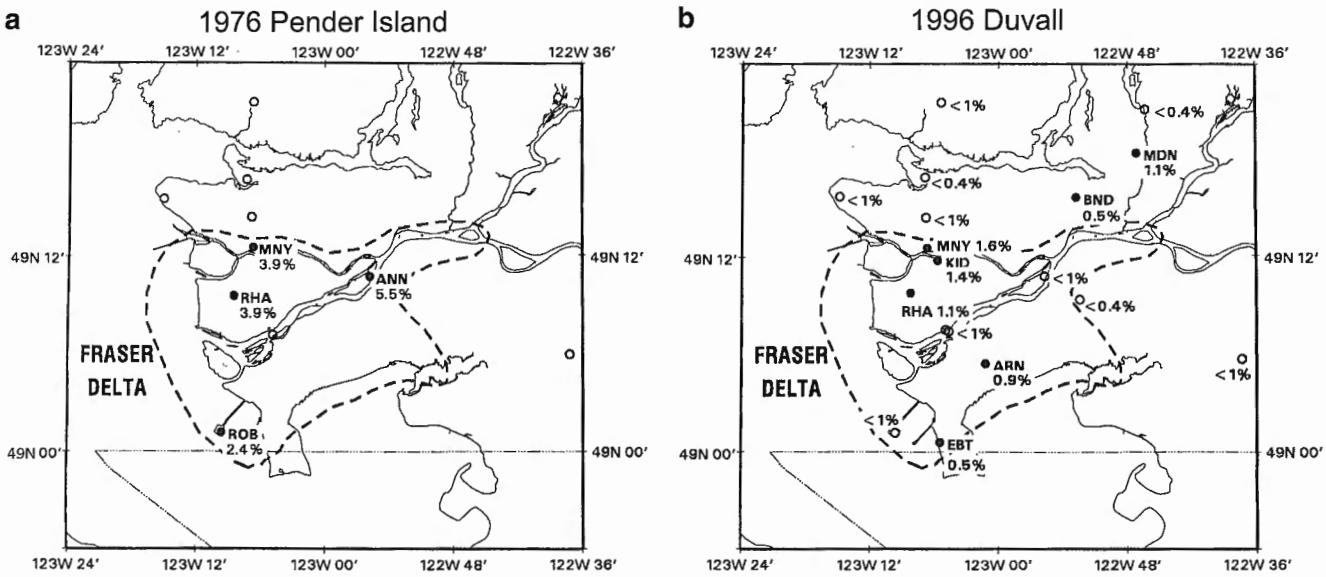

*Figure 10. Peak horizontal accelerations (in %g (g = acceleration of gravity)) recorded for the (**a**) 1976 Pender Island and (**b**) 1996 Duvall earthquakes. Readings were made from unfiltered waveforms. Instruments that did not trigger (open circles) provide an upper bound on peak acceleration at those locations. The dashed line outlines the Fraser delta.*

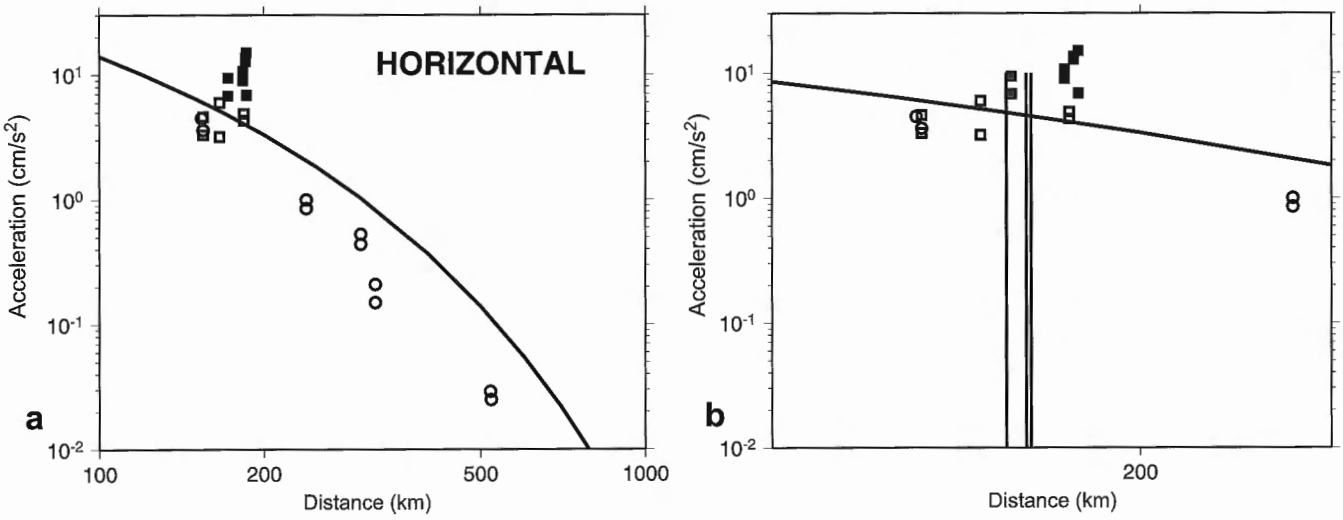

*Figure 11. **a**) Measured peak horizontal (SH) acceleration versus hypocentral distance for the 1996 Duvall earthquake (adapted from Cassidy et al., 1997). Data are from strong-motion records (squares), and broadband records (circles). Filled squares denote stations on the Fraser delta. The curve is the strong ground-motion attenuation relation proposed for the year 2000 National Building Code of Canada for rock sites (see text). Note that sites on the Fraser delta have significantly higher peak accelerations than sites on rock or on firm soil. **b**) Peak horizontal accelerations in the Fraser delta area (the region between the dotted lines in (a); curve as described above. The thick black line is as described above. The vertical lines are constraints provided by strong-motion instruments that did not trigger during the Duvall earthquake (i.e. peak acceleration is less than the top of the bar). Thick vertical lines represent Fraser delta thick-soil sites (Fig. 10b); thin lines are rock or firm-soil sites.*

Frequency dependence

The frequency dependence of the amplification becomes apparent when the spectra of the two earthquakes are compared at different strong-motion sites. For spectral analysis, the amplitudes are corrected for geometric spreading at the correct hypocentral distance to make direct comparisons of spectral amplitude possible. All spectra were smoothed using an eleven-point running-mean average (0.5 Hz full-width).

1976 Pender Island earthquake

The strong-motion seismograms for the Pender Island earthquake range from 7-30 s in length. Except for RHA, the 7 s record, we used a 10 s data window at each site for consistency. Due to the relatively short window length, we only considered frequencies greater than 0.5 Hz (2 s period) in this analysis, even though we would expect resonance at lower frequencies on the deepest soils of the delta (e.g. Harris et al., 1995). Frequencies higher than 20 Hz (0.05 s period) were not considered either, as noise dominates the spectra at these frequencies.

We compared the SH spectra of a firm-soil site on Vancouver island (CTEL) to spectra at sites near the northern edge of the delta (MNY and ANN) in Figure 12 and near the centre (RHA) and southern edge (ROB) of the delta in Figure 13. ANN and ROB both have about 100 m of Holocene sediments beneath them, underlain by differing amounts of Pleistocene sediments (about 150 m at ANN and about 400 m at ROB). The spectra in Figure 12 were computed using the waveforms shown in Figure 5. Note the frequency dependence of the response. At low frequencies (<5 Hz), the SH spectra at the thick-soil Fraser delta sites have significantly higher amplitudes relative to CTEL, whereas at higher frequencies, the amplitudes are attenuated relative to CTEL. The peak in the ANN spectra near 1 Hz likely reflects a resonance caused by the velocity structure of the local soil profile. Energy near this frequency is apparent in the raw waveforms (Fig. 5). A similar peak at 1.5 Hz is visible in the ROB spectrum. While CTEL is not a bedrock site (20-65 m of dense gravelly, sandy till), we would expect any soil-induced resonance effects to be confined to the high-frequency end of the spectra (in the 3-10 Hz bandwidth, depending on the exact velocity and depth to bedrock – see quarter wavelength discussion in the section titled "Seismic Hazard Implications", below). One or more of the peaks at the high-frequency end of the CTEL spectrum may be a result of soil resonance. With the exception of such resonance, we hypothesize that the spectral shape at CTEL should approximate that on bedrock.

At the low-frequency end of the spectral window that we have chosen, all of the Fraser delta spectra show amplification of about 5-10 times relative to CTEL. Very small amplitudes define these low frequencies; they approach the width of the photographic trace on the original seismograms at 0.5 Hz. We are concerned that the size of this amplification relative to CTEL may be an artifact of data processing related to the difficulty of accurately recovering low amplitudes. Three observations suggest this: 1) the spectra from the Duvall earthquake (following section) show an amplification

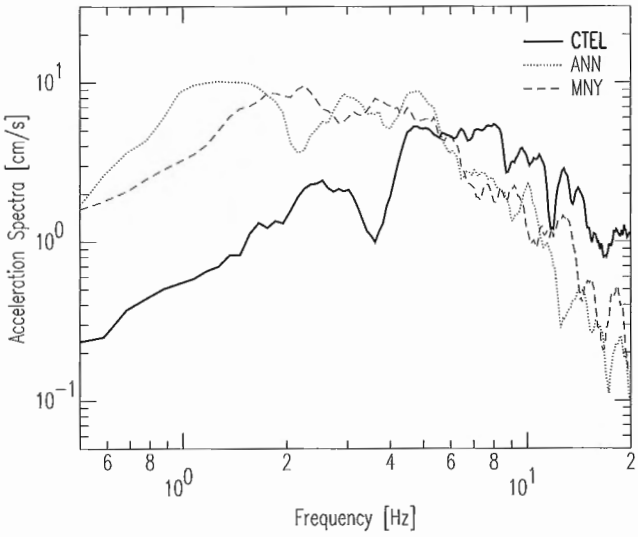

Figure 12. Smoothed horizontal (SH) spectra of strong motion for the 1976 Pender Island earthquake. CTEL is a firm-soil site on Vancouver Island; ANN and MNY are Fraser delta sites, with bedrock at least 200 m deep and Holocene sediments about 100 m (ANN) and a few metres (MNY) thick. Frequency-dependent amplification is evident in the spectra. For frequencies less than about 5 Hz, spectral amplitudes of horizontal motion on the Fraser delta are greater than on firm soil (CTEL). At frequencies above 5 Hz, ground motions on the Fraser delta are attenuated relative to CTEL.

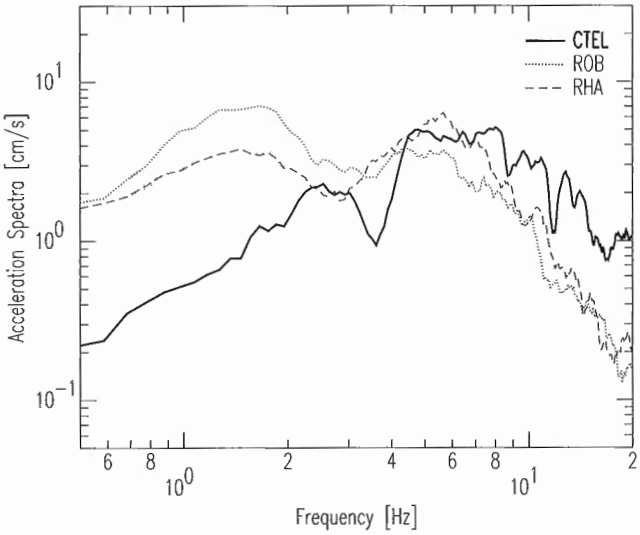

Figure 13. Smoothed horizontal (SH) spectra of strong motion for the 1976 Pender Island earthquake. Here, Fraser delta sites with thick Holocene sediments (ROB, 100 m; RHA, 300 m) are compared to firm-soil site CTEL. Note the similar pattern to that of Fraser delta sites ANN and MNY (Fig. 12); at low frequencies spectral amplitudes of horizontal motions on the Fraser delta are greater than amplitudes on firm soil, whereas at frequencies above about 5 Hz, ground motions on the Fraser delta are attenuated relative to CTEL.

factor of about 3-4 at these frequencies; 2) spectra computed from another digitization of the same seismograms (Weichert and Milne, 1980) show an amplification of about 2-3 at these frequencies; and 3) the spectral values at low frequencies are not robust and change by factors of 2-4 when slight changes are made to record length. The spectral amplitudes at the low-frequency end may be fictitious, but the resonance peaks near 1-2 Hz at ANN and ROB are robust in our experiments with the data and also appear in an analysis of the hand digitized records (Weichert and Milne, 1980).

1996 Duvall earthquake

Figures 14 and 15 show the spectra for the Duvall earthquake. These spectra were calculated using 15 s data windows. The spectra in Figure 14 were calculated using the seismograms in Figure 8. The spectra at all sites are similar in that the bulk of the energy falls in the 1-5 Hz bandwidth, likely due to a source and path effect. We compared the only rock strong-motion recording of this earthquake (PGC - quartz diorite) to thick-soil strong-motion recordings at RHA, MNY, ARN, and KID. RHA and ARN are near the centre of the delta; MNY and KID are near the northern edge. Figures 14 and 15 clearly illustrate the frequency-dependent amplification effects of thick-soil sites versus rock. There is a general amplification, up to a factor of about 4 (RHA), at lower frequencies and a modest attenuation at higher frequencies, with the crossover between amplification and attenuation in the 5-8 Hz bandwidth. Similar observations have been made in other areas (e.g. Margheriti et al., 1994), with crossover frequencies between 4-8 Hz, depending on the soil and basin characteristics.

Sites near the edge of the delta exhibit spectral peaks, up to an amplification factor of 7 over the PGC rock site: near 2 Hz at MNY (Fig. 14) and near 1.5 Hz at KID (Fig. 15). The KID spectra also show three pronounced peaks at higher frequencies which are not evident at the other deep-soil sites (Fig. 15). The peaks near 4 Hz and 6 Hz correlate with near surface velocity steps documented in well logs from the site. A peak near 3 Hz is present at most of the B.C. Hydro electrical switch-yard sites. At GTP and MDN energy near that frequency dominates the seismograms (Weichert et al., 1996). We suspect that the peak near 3 Hz at KID is also due to resonant oscillation of structures common to the electrical switch-yards.

In analyzing these records from the 1996 earthquake we found none of the difficulties of unstable spectra at lower frequencies that we noted above in analysis of the 1976 records. The modern digital instruments provide high-quality data even near their limit of resolution.

Sites recording both earthquakes

Two sites on the Fraser delta (RHA and MNY) triggered during both earthquakes. In Figure 16 we compare the spectra for the two earthquakes. They are very similar, even though the earthquakes have very different focal mechanisms and travel paths. This suggests that many of the spectral features may be due to the seismic response of the site. The most notable differences in the spectra are the low in spectral amplitude

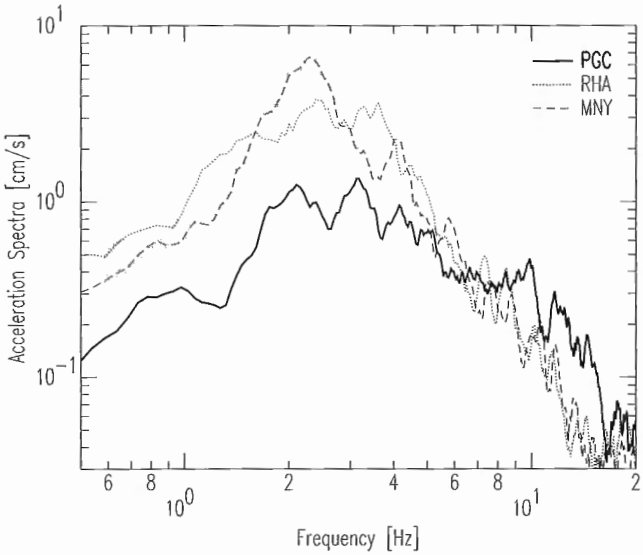

Figure 14. Smoothed horizontal (SH) spectra of strong motion for the 1996 Duvall earthquake. PGC is a rock site on Vancouver Island; RHA and MNY are Fraser delta sites with 300 m and a few metres of Holocene sediments, respectively. A pattern similar to that of the Pender Island earthquake is observed, with frequency-dependent amplification. At frequencies less than about 5 Hz, spectral amplitudes of horizontal motions are amplified on the Fraser delta, relative to the rock site at PGC. At frequencies above about 8 Hz, ground motions on the Fraser delta are attenuated relative to PGC.

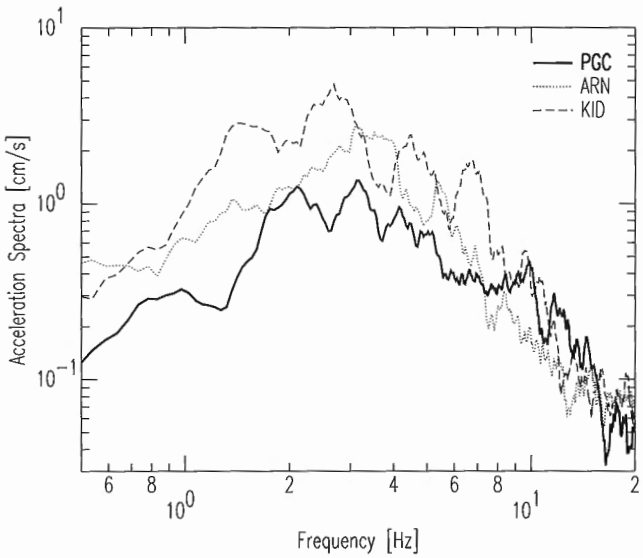

Figure 15. Smoothed horizontal (SH) spectra of strong motion for the 1996 Duvall earthquake. PGC is a bedrock site on Vancouver Island; ARN and KID are Fraser delta sites with 250 m and 30 m of Holocene sediments, respectively. The pattern is similar to that for Fraser delta sites MNY and RHA (Fig. 14); however ARN shows less amplification than RHA, even though both are thick soil sites.

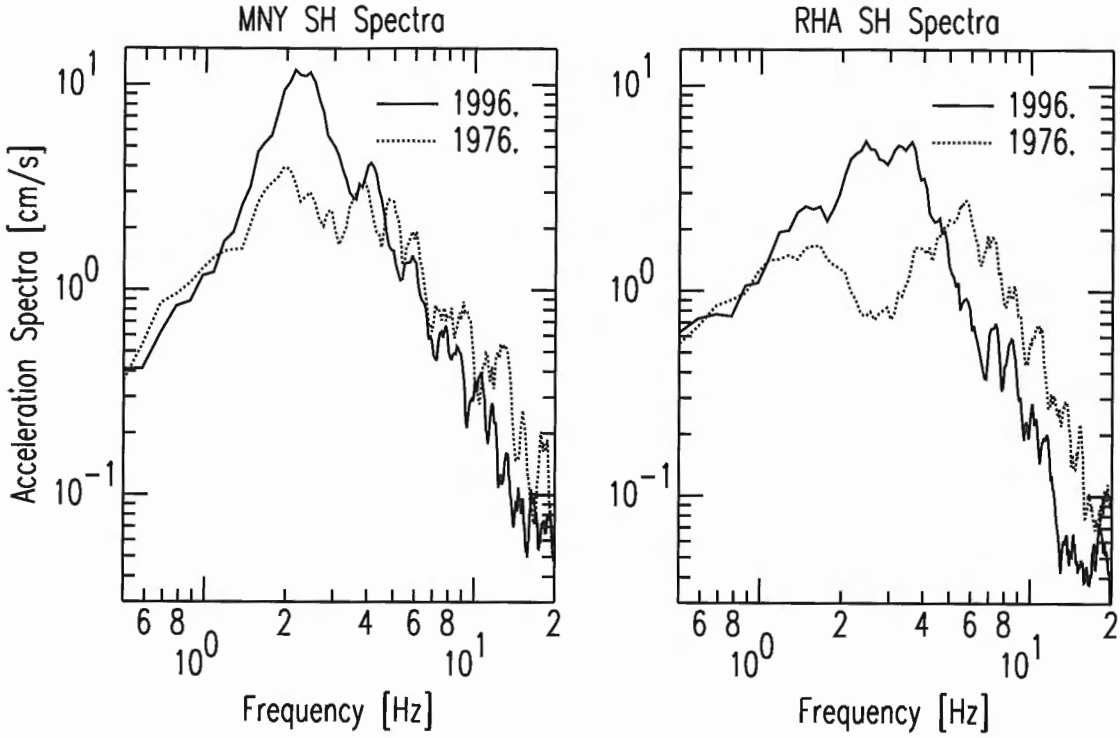

Figure 16. *Comparison of smoothed horizontal (SH) spectra of strong motion for the 1976 and 1996 earthquakes at Fraser delta sites MNY (left) and RHA (right). The spectra have been corrected for geometrical spreading (the 1996 travel paths are about 180 km, whereas the 1976 paths are about 80 km) and for differences in earthquake magnitude (M_W = 5.3 for the 1976 earthquake; M_W = 5.1 for the 1996 event). The spectra have not been corrected for anelastic attenuation (Q) - the longer travel path, and greater attenuation of higher-frequency energy, for the 1996 event explain the lower amount of high-frequency energy in the 1996 spectra. The low in energy at 2-4 Hz in the 1976 spectra is likely a source radiation-pattern effect, as these stations are near an SH minimum (Fig. 6).*

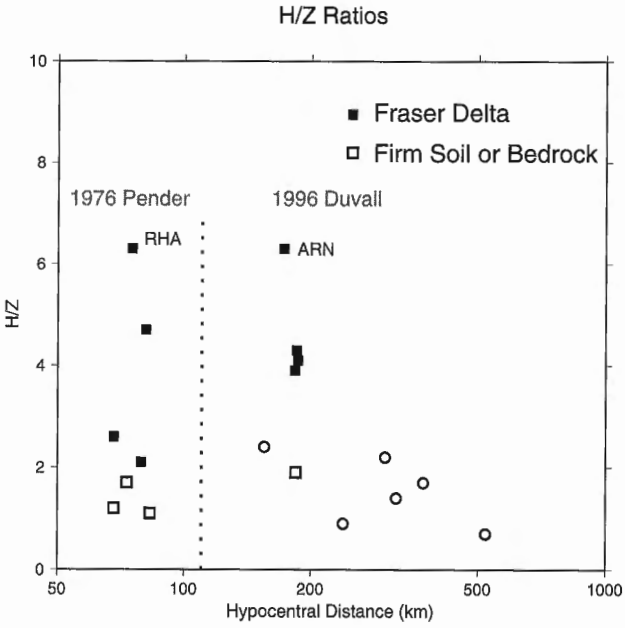

Figure 17.

Peak horizontal to peak vertical acceleration ratios (H/Z) plotted as a function of hypocentral distance for strong-motion sites (squares) and three-component broadband sites (circles) for the two earthquakes. The dotted vertical line separates the two data sets. Fraser delta sites have an average H/Z ratio of 4.3 ± 1.4, compared to 1.5 ± 0.5 for rock and firm-soil sites. The high H/Z ratio (6.2) for ARN in the 1996 data set is due to a low vertical-component amplitude at that site; the SH amplitude at ARN is similar to that at the other three Fraser delta sites that have H/Z ratios near 4. The two low Fraser delta values (2.1 and 2.6) for the Pender Island earthquake are attributed to source radiation effects; these sites are near both SH and SV nodal planes (Fig. 6). The consistent H/Z values for the firm-soil and rock sites over a hypocentral distance range of 75-500 km suggests that the H/Z ratio is independent of distance.

in the 2 to 4 Hz range in the 1976 spectra and the higher amplitudes at frequencies above about 5 Hz in the 1976 spectra. The low in the 2-4 Hz range is likely due to the Fraser delta sites being close to the node in SH radiation from the 1976 earthquake (Fig. 6), which means that less energy in the dominant spectral band of the source is radiated in their direction. The difference in the high-frequency spectra levels between the two earthquakes is likely related to the differences in epicentral distance. These spectra have not been corrected for anelastic attenuation ('Q'), which is frequency dependent, because we do not have values for frequency-dependent 'Q' in this region. However, we would expect more high-frequency energy to be attenuated over the longer travel paths from the 1996 earthquake, and this is likely the difference observed in the high-frequency levels between the two earthquakes.

The similarities between the spectra of these very different earthquakes at the same sites are a strong argument for using spectra of 'weak' ground motion to determine seismic site response. This has been done successfully elsewhere (e.g. Hartzell et al., 1996). The advantage of using 'weak' strong motion is that it is not necessary to rely on triggered strong-motion seismographs. Data for site response can be gathered at a higher rate using continuously recording seismographs, and with modern, high-dynamic range instruments, the data can be in the mid range of the instrument sensitivity rather than near the limit of resolution.

Peak horizontal/peak vertical acceleration ratios

These recordings also provide the first estimates of horizontal-to-vertical ratios for peak acceleration for rock and Fraser delta sites. Here we add observations from the 1976 Pender Island earthquake to those presented by Cassidy et al. (1997) for the 1996 Duvall earthquake. The ratios were obtained using peak accelerations measured from the unfiltered SH-waveform (H) and the vertical component of the SV-waveform (Z) (Tables 1 and 2) . H/Z ratios, plotted as a function of hypocentral distance in Figure 17, are 4.3 ± 1.4 for the Fraser delta sites (KID, MNY, RHA, ARN, ROB, and EBT) compared to 1.5 ± 0.5 for the firm-soil and rock sites. The large scatter in the 1976 H/Z ratios for the Fraser delta sites is attributed to earthquake source effects, as all of these sites are near both SH and SV nodal lines (Fig. 6). The large H/Z ratio (6.3) for the 1996 earthquake at ARN is due to a smaller vertical-component amplitude at this site. We note that the SH amplitude here is comparable to that at other Fraser delta sites (e.g. RHA – see Table 1).

The 1976 and 1996 data collectively cover a distance range of 70-520 km. The uniformity of the ratios over this distance range, with the exception of the 1976 Fraser delta values described above, suggests that H/Z is independent of hypocentral distance. The rock H/Z ratio of 1.5 is slightly higher than that observed for eastern Canadian rock sites (about 1.3 at 3 Hz). The H/Z ratio for Fraser delta soil sites is similar to that obtained in other areas of thick soil, for example, ratios of 3-5 on soil sites in southern Ontario (Atkinson, 1996) and in the Coachella Valley, California (Field, 1996).

SEISMIC HAZARD IMPLICATIONS

On the deep soils of the Fraser delta, the strong-motion seismographs record spectral amplification of up to 4 at lower frequencies compared to the PGC rock site and up to 2 compared to nearby firm-soil site BND. Modest attenuation is observed at higher frequencies with a crossover from amplification to attenuation in the 5-8 Hz bandwidth (Fig. 18). During earthquakes, structures are damaged mainly by earthquake energy near the natural resonant period of the structure. This resonant period is approximately 0.1N, where N is the number of storeys in the structure. Thus, the observed amplification at lower frequencies (longer periods) will affect mainly taller buildings (up

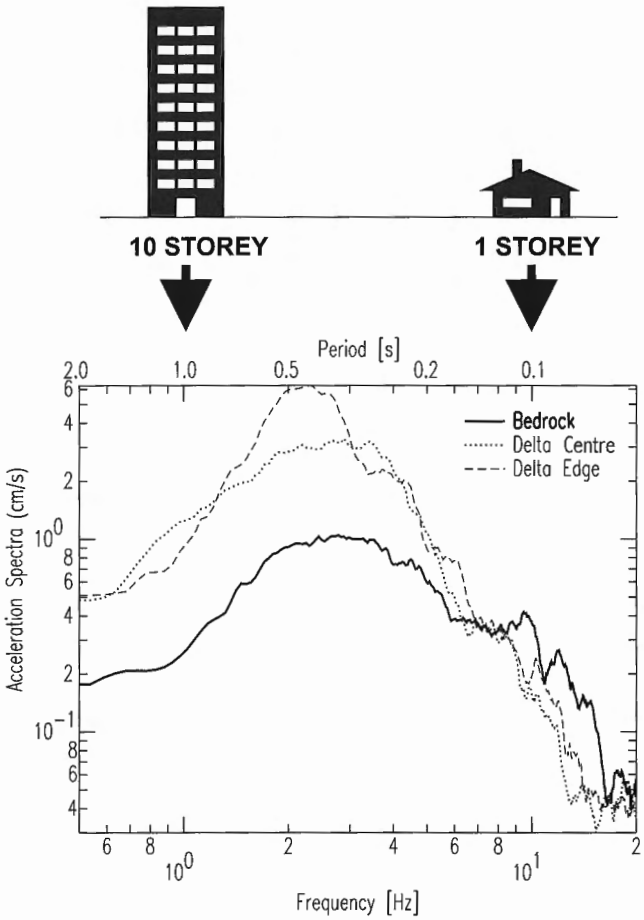

Figure 18. *Log-log plot of smoothed horizontal (SH) spectra of strong-motion recordings of the 1996 Duvall earthquake at a rock site (PGC), a site near the delta centre (RHA), and a site near the edge of the delta (MNY). These spectra are filtered with a 21-point (1 Hz full-width) running-mean average. The amplification at longer periods will affect mainly taller buildings. In contrast, one- or two-storey buildings (the most common structures on the delta) will experience comparable, or less severe shaking near their resonant periods than similar structures built on rock or firm soil. The pronounced peak near 0.5 seconds (2 Hz) at the delta-edge site is likely due to seismic resonance in the soil column.*

to 20 stories at the low end of the spectra we present). In contrast, 1-2 storey structures (typical residential structures, and the most common type of structure on the delta) will experience less severe shaking near their resonant period than similar structures on rock or firm soil (Fig. 18). The National Building Code of Canada (NBCC) requires a factor of 2 in base shear over rock or firm-soil sites for engineered structures on deep (>15 m) very soft soil (table 4.1.9.1.C. in National Research Council of Canada, 1995). Thus, the observed amplification in the centre of the delta in the spectral range presented here is largely taken care of in the current NBCC.

The situation is different, however, near the edge of the delta. Here, both the Holocene and Pleistocene deposits thin to the point where soil resonances of seismic waves in the soil column are in the range of the fundamental resonant periods of common buildings. We see resonances at about 1-2 Hz (0.5-1 s period) near the North Arm of the Fraser River at sites MNY, KID, and ANN, which produce a higher amplification over a narrow frequency range (Fig. 18). ROB, near the southern edge of the delta, also seems to show such a resonance. The spectral amplification at MNY is about a factor of 7 greater than the PGC rock site and about factor of 5 greater than the nearby firm-soil site BND (Fig. 19). This soil resonance is a hazard that should be considered when siting buildings near the edge of the delta, since ground motions can exceed the nominal NBCC requirements for structures build on deep soft soil.

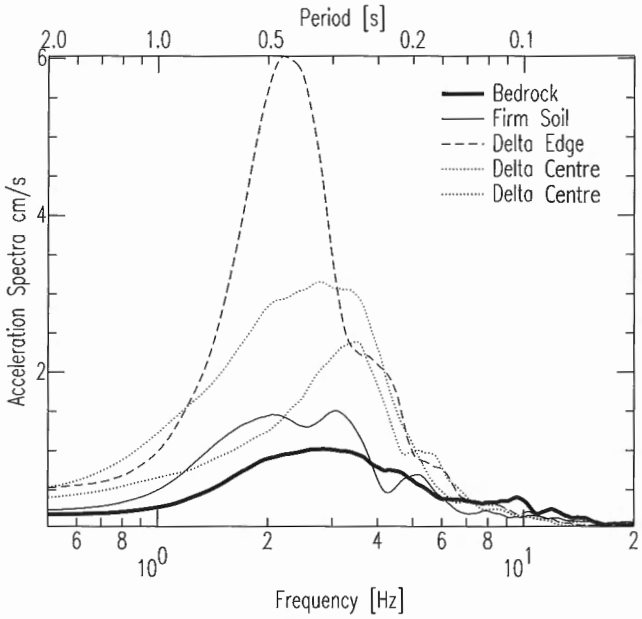

Figure 19. *Log-linear plot of the same three spectra as in Figure 18, with another site near the centre of the delta (ARN) and a thin firm-soil site (BND) added. The log-linear plot facilitates the comparison of peak values and emphasizes the amplification near the delta edge relative to rock and firm-soil sites and the difference in character of two sites in the centre of the delta.*

We truncated our spectra at 0.5 Hz (2 s period) because of the low amplitudes defining the lower frequencies on the strong-motion seismograph recordings. However, we would expect amplification at longer periods in the centre of the delta. The natural frequency (inverse of the fundamental resonant period) of a soil site is generally equal to the average S-wave velocity divided by four times the soil thickness (the so-called "quarter wavelength" rule). This kind of simple analysis predicts amplifications at periods longer than 2 s in the centre of the delta, which could present a hazard to larger structures such as extremely tall buildings or large bridges. More sophisticated one-dimensional analyses using the computer program SHAKE (Schnabel et al., 1972) also predict significant amplification at periods greater than the range shown in the spectra that we present here (Sy et al., 1991; Harris et al., 1995).

Quarter wavelength analysis also predicts the observed resonances noted above near the edge of the delta. We do not require focusing or other three-dimensional effects that have been used elsewhere to explain amplification on deep sedimentary basins (e.g. Rial et al., 1991, 1992; Field, 1996) to explain the character of the spectra recorded on the Fraser delta. We also see no evidence of a large 'basin-edge effect' on the seismograms (e.g. Field, 1996). This edge effect is the result of constructive interference between shear waves and surface waves that produces large amplitudes later in the wave train. It has been observed to produce high amplitudes near the edges of some sedimentary basins and may have influenced the damage pattern in the 1995 Kobe earthquake (Kawase, 1996). However, we emphasize that basin-edge and three-dimensional effects are very path-specific phenomena, depending on both the direction of incoming seismic energy and the nature of the structure at the edge of the basin.

CONCLUSIONS

Strong-motion seismograph records of the 1976 Pender Island and 1996 Duvall earthquakes provide the best constraints to date on amplification of seismic waves on the Fraser delta. The data show that peak ground motions are amplified on the thick soils of the Fraser delta, but this amplification is frequency dependent. For the crustal Duvall earthquake, at relatively low frequencies on the thick soils in the centre of the delta, the spectral amplitudes of SH motion are up to twice a nearby firm-soil site and up to four times greater than a granitic rock site on Vancouver Island. At higher frequencies, ground motions on thick soils are slightly attenuated relative to rock. The crossover between amplification and attenuation occurs in the 5-8 Hz bandwidth. This means that typical 1-2 storey residential structures on the delta will experience slightly less shaking near their resonant period than similar structures located on rock.

Analysis of the 1976 Pender Island strong-motion seismograph records shows the same pattern relative to a firm-soil site, with amplification at low frequencies, attenuation at high frequencies, and evidence for resonance near the delta edge. Unfortunately, the level of amplification at the low end of the 1976 spectra cannot be confidently calculated because

the level of ground motion defining these low frequencies is near the optical resolution of the instruments deployed at that time. The amplification observed at all sites for both earthquakes is most pronounced in the horizontal components of ground motion. The horizontal to vertical ratio calculated for thick-soil sites is 4.3, whereas it is 1.5 for rock and firm-soil sites.

The largest peak horizontal ground accelerations measured for both earthquakes, at frequencies of 2-3 Hz, were not on the thickest sediments, but nearer the edge of the delta. The spectral amplification is up to a factor of seven greater than the PGC rock site and up to a factor of 5 greater than the nearby firm-soil site BND. Near the edge of the delta, both the Holocene and Pleistocene deposits thin to the point that resonances of seismic waves in the soil column are in the range of the fundamental resonant periods of common buildings. This represents a hazard that should be considered when siting buildings near the edge of the delta, as ground motions may exceed nominal National Building Code of Canada design requirements.

ACKNOWLEDGMENTS

We gratefully acknowledge reviews by Scott Dunbar, Peter Basham, and John Clague. Much of the data was provided by British Columbia Hydro and Power Authority, and Tim Little and Bo Chandra have been most helpful in providing information on B.C. Hydro sites.

REFERENCES

Adams, J., Weichert, D.H., Halchuck, S., and Basham, P.
1996: Trial seismic hazard maps of Canada - 1995: final values for selected cities; Geological Survey of Canada, Open File Report 3283, 97 p.

Atkinson, G.M.
1995: Attenuation and source parameters of earthquakes in the Cascadia region; Bulletin of the Seismological Society of America, v. 85, p. 1327-1342.
1996: The high-frequency shape of the source spectrum for earthquakes in eastern and western Canada; Bulletin of the Seismological Society of America, v. 86, p. 106-112.

Boore Boore, D.M., Joyner, W.B., and Fumal, T.E.
1993: Estimation of response spectra and peak accelerations from western North American earthquakes: an interim report; United States Geological Survey, Open-File Report 93-509, 72 p.
1994: Estimation of response spectra and peak accelerations from western North American earthquakes: an interim report, Part 2; United States Geological Survey, Open-File Report 94-127, 40 p.

Britton, J.R., Harris, J.B., Hunter, J.A., and Luternauer, J.L.
1995: The bedrock surface beneath the Fraser River delta in British Columbia based on seismic measurements; in Current Research 1995-E, Geological Survey of Canada, p. 83-89.

Cassidy, J.F., Rogers, G.C., and Weichert, D.H.
1997: Strong ground motion recordings on the Fraser Delta, British Columbia, of the M = 5.3 Duvall, Washington earthquake; Bulletin of the Seismological Society of America, v. 87, p. 1354-1361.

Celebi, M., Dietel, C., Prince, J., Onate, M., and Chavez, G.
1987: Site amplification in Mexico City (determined from 19 September 1985 strong-motion records and from recordings of weak motions); in Ground Motion and Engineering Seismology, (ed.) A.S. Cakmak; Elsevier, Amsterdam, Netherlands p. 141-152.

Clague, J.J., Luternauer, J.L., Monahan, P.A., Edwardson, K.A., Dallimore, S.R., and Hunter, J.A.
1998: Quaternary stratigraphy and evolution of the Fraser delta; in Geology and Natural Hazards of the Fraser River Delta, British Columbia, (ed.) J.J. Clague, J.L. Luternauer, and D.C. Mosher; Geological Survey of Canada, Bulletin 525, this volume.

Field, E.H.
1996: Spectral amplification in a sediment-filled valley exhibiting clear basin-edge-induced waves; Bulletin of the Seismological Society of America, v. 86, p. 991-1005.

Harris, J.B., Hunter, J.A., Luternauer, J.L., and Finn, W.D.L.
1995: Site response modelling of the Fraser River delta, British Columbia: preliminary results from two deep boreholes; in Current Research 1995-E, Geological Survey of Canada, p. 69-75.

Hartzell, S., Leeds, A., Frankel, A., and Michael, J.
1996: Site response for urban Los Angeles using aftershocks of the Northridge earthquake; Bulletin of the Seismological Society of America, v. 86, p. S168-S192.

Hough, S.E., Borcherdt, R.D., Friberg, P.A., Busby, R., Field, E., and Jacob, K.H.
1990: The role of sediment-induced amplification in the collapse of the Nimitz Freeway during the October 17, 1989 Loma Prieta earthquake; Nature, v. 344, p. 853-855.

Hunter, J.A
1995: Shear wave velocities of Holocene sediments, Fraser River delta, British Columbia; in Current Research 1995-A, Geological Survey of Canada, p. 29-32.

Kawase, H.
1996: The cause of the damage belt in Kobe: "the basin-edge effect," constructive interference of the direct S-wave with the basin-induced diffracted/Raleigh waves; Seismological Research Letters, v. 67, p. 25-34.

Luternauer, J.L. and Hunter, J.A.
1996: Mapping Pleistocene deposits beneath the Fraser River delta: preliminary geological and geophysical results; in Current Research 1996-E, Geological Survey of Canada, p. 41-48.

Margheriti, L., Wennerberg, L., and Boatwright, J.
1994: A comparison of coda and S-wave spectral ratios as estimates of site response in the southern San Francisco Bay area; Bulletin of the Seismological Society of America, v. 84, p. 1815-1830.

Milne, J.
1898: Seismology (1st edition); Kegan Paul, Trench Truber and Co. Ltd., London, United Kingdom, 320 p.

Milne, W.G. and Rogers, G.C.
1971: Earthquake engineering research at Victoria Geophysical Observatory; in Proceedings, 1st Canadian Conference on Earthquake Engineering, University of British Columbia, Vancouver, British Columbia, p. 27-37.

National Research Council of Canada
1995: National building code of Canada, 1995; Commission on Building and Fire Codes, National Research Council of Canada, 571 p.

Pitarka, A. and Irikura, K.
1996: Basin structure effects on long-period strong motions in the San Fernando Valley and the Los Angeles Basin from the 1994 Northridge earthquake and an aftershock; Bulletin of the Seismological Society of America, v. 86, p. S126-S137.

Rial, J.A., Saltzman, N.G., and Ling, H.
1991: Computation of eigenmodes of resonant sedimentary basins of arbitrary shape by semiclassical and variational methods; Wave Motion, v. 14, p. 377-398.
1992: Earthquake-induced resonance in sedimentary basins; American Scientist, v. 80, p. 566-578.

Rogers, G.C.
1976: A survey of the Canadian strong motion seismograph network; Canadian Geotechnical Journal, v. 13, p. 79-85.
1983: Seismotectonics of British Columbia; Ph.D. thesis, University of British Columbia, Vancouver, British Columbia, 247 p.

Rogers, G.C. and Baldwin, R.E.
1989: The 1976 Pender Island earthquake; Seismological Research Letters, v. 60, p. 7.

Schnabel, P.B., Lysmer, J., and Seed, H.B.
1972: SHAKE: a computer program for earthquake response analysis of horizontally layered sites; University of California, Berkeley, Earthquake Engineering Research Center, Report EERC-72/12, 3 diskettes.

Sy, A., Henderson, P.W., Lo, R.C., Siu, D.Y., Finn, W.D.L., and Heidebrecht, A.C.
1991: Ground motion response for the Fraser delta, British Columbia; Proceedings, 4th International Conference on Seismic Zonation, Stanford, California, v. 2, p. 343-350.

Thomas, G.C., Crosson, R.S., Cohec, B., and Qaman, T.
1996: The May 2, 1996 Duvall, Washington earthquake and aftershock sequence; Eos (Transactions, American Geophysical Union), v.77, p. 523 (abstract).

Weichert, D.H. and Milne, W.G.
1980: Canadian strong motion records; Canada Department of Energy Mines and Resources, Earth Physics Branch, Open-File Report 80-1, 22 p.

Weichert, D.H., Cassidy, J.F., Rogers, G.C., Little, T., and Chandra, B.
1996: Canadian strong ground motions from the May 1996, Duvall, Washington, earthquake; Geological Survey of Canada, Open File Report 3390, 75 p.

Site amplification modelling of the Fraser delta, British Columbia

J.B. Harris[1], J.A. Hunter[2], J.L. Luternauer[3], and W.D.L. Finn[4]

Harris, J.B., Hunter, J.A., Luternauer, J.L., and Finn, W.D.L., 1998: Site amplification modelling in the Fraser Delta, British Columbia; in Geology and Natural Hazards of the Fraser River Delta, British Columbia, (ed.) J.J. Clague, J.L. Luternauer, and D.C. Mosher; Geological Survey of Canada, Bulletin 525, p. 211–216.

Abstract: Newly acquired and interpreted geological and geophysical data from two borehole sites on the Fraser River delta, and a newly prepared map of the depth to bedrock underlying the delta, indicate that the architecture of the delta is significantly different from that used for current site response models. SHAKE analysis for the two borehole sites shows that there is likely to be considerable long-period response (3.5 to 5.0 s) because the deltaic and/or Pleistocene sequences at these locations are interpreted to be thicker and, at depth, less dense than previously assumed. The presence of significant long-period ground motions has important implications for the stability of large structures on the delta. Seismic response of the delta will also likely be affected by the highly irregular bedrock surface beneath the delta which may focus or disperse earthquake energy.

Résumé : Selon de nouvelles données géologiques et géophysiques acquises à partir de deux sondages dans les matériaux du delta et selon une carte récente de la profondeur à laquelle se trouve le substratum sous le delta, il semble que l'architecture du delta soit très différente de celle qui est utilisée pour construire les modèles actuels du comportement des matériauxs à divers sites. Une analyse des diagraphies faites dans les deux sondages (à l'aide de SHAKE) montre que les ondes devraient avoir une période considérablement longue, allant de 3,5 à 5,0 s; en effet, l'interprétation fait ressortir que tant les séquences deltaïques que pléistocènes à ces endroits sont plus épaisses et, en profondeur, moins denses qu'on ne le prévoyait. Le fait que les ondes aient une période significativement longue a des incidences importantes sur la stabilité des gros ouvrages construits sur le delta. En outre, il se peut que le comportement des matériaux soit modifié par la surface très irrégulière du substratum sous le delta, laquelle pourrait concentrer ou disperser l'énergie d'un séisme.

[1] Department of Geology, Millsaps College, 1701 N. State Street, Jackson, Mississippi 39210
[2] Geological Survey of Canada, 601 Booth Street, Ottawa, Ontario K1A 0E8
[3] Geological Survey of Canada, 605 Robson Street, Vancouver British Columbia V6B 5J3
[4] Department of Civil Engineering, University of British Columbia, Vancouver, British Columbia V6T 1W5

INTRODUCTION

Areas underlain by thick deposits of unconsolidated sediments, such as the Fraser River delta in southwestern British Columbia, are known to experience greater levels of earthquake damage due to amplification of seismic waves than areas underlain by rock. The delta's architecture, its location within the most seismically active region in Canada, and the rapid growth of communities situated on it have raised concerns about the area's seismic vulnerability.

As part of a continuing effort to identify and help assess earthquake hazards of the Fraser delta, the Geological Survey of Canada (GSC) has initiated a project to model the response of the thick sediment deposits to earthquake ground motions. Two newly available data sets were used as a framework for the modelling (Fig. 1): 1) geological and geophysical data from two 300 m deep boreholes (FD94-3 and FD94-4) were used to evaluate the geotechnical properties of the Quaternary sediments (Dallimore et al., 1995); and 2) industry seismic reflection profiles were used to evaluate the depth to bedrock (Tertiary) beneath the delta (Britton et al., 1995). This paper discusses preliminary one-dimensional site response modelling based on geological models constructed using these new data, and compares the results with the response of previously existing geotechnical models of the delta. The results demonstrate the importance of accurate geological characterization in site response modelling.

GEOLOGICAL SETTING

The Fraser River delta, western Canada's largest, is composed of a thick sequence of unconsolidated sands and silts underlain by nonlithified glacial and interglacial sediments (Luternauer et al., 1994). The Quaternary deposits lie unconformably on a Tertiary bedrock surface with high relief: depth to bedrock ranges from hundreds of metres to more than 1000 m (Britton et al., 1995).

In borehole FD94-3, the Holocene deltaic sequence is 19 m thick and is underlain by Pleistocene sands and clays. In contrast, the Holocene-Pleistocene boundary in borehole FD94-4 occurs at a depth of 236 m and is marked by a firm glacial till (no till was found in borehole FD94-3). Tertiary bedrock was not encountered in either borehole, a surprising result given previous estimates of depth to bedrock (Byrne and Anderson, 1987; Finn and Nichols, 1988; Sy et al., 1991).

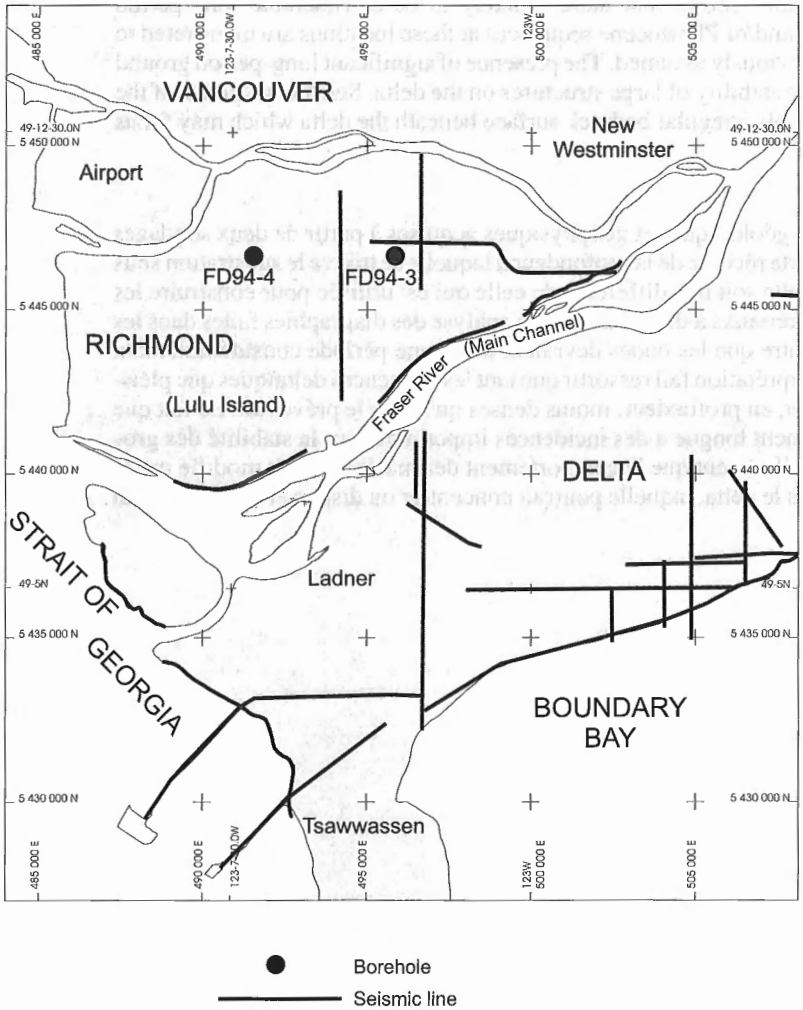

Figure 1.

Locations of boreholes (FD94-3 and FD94-4) and industry seismic reflection profiles within the Fraser delta area.

SITE RESPONSE MODELLING

Computer modelling programs have been developed to analyze the site response of the sediment column to bedrock ground motions. The most widely used program is SHAKE (Schnabel et al., 1972), a one-dimensional site response modelling routine designed to propagate vertically incident shear waves from bedrock through a column of horizontally layered soil horizons. The key parameter in determining the dynamic response of a site to seismic loading is the low-strain shear modulus (G_{max}) of the individual layers making up the soil column. G_{max} can be calculated as the product of the square of the soil layer's shear-wave (S-wave) velocity and its mass density. Other necessary parameters include layer thicknesses and estimates of the strain-dependent response of the shear modulus and damping.

Shear-wave velocities

Detailed downhole S-wave surveys were completed in boreholes FD94-3 and FD94-4 (Dallimore et al., 1995) with good-quality, S-wave velocity measurements to a depth of 300 m at each site (Fig. 2). Because Tertiary strata were not encountered in either borehole, depths to bedrock were estimated from industry seismic reflection data (Britton et al., 1995). This newly available data set indicates that Quaternary sediments are significantly thicker than has been previously considered in site response modelling of the Fraser delta area (Fig. 3). S-wave velocities of the deeper post-Tertiary sequence were estimated using the combined S-wave and compressional-wave (P-wave) velocity data recorded in boreholes FD94-3 and FD94-4 (Dallimore et al., 1995) and P-wave interval velocities available from the industry seismic reflection data (Hunter et al., 1996).

Site models

Shear-wave velocity data (Dallimore et al., 1995; Hunter et al., 1996) and density measurements (Dallimore et al., 1995) were used to calculate the variation in G_{max} versus depth for boreholes FD94-3 and FD94-4 (Fig. 4). Based on the depth-to-bedrock map (Fig. 3), the Quaternary section is estimated to be 495 m thick at FD94-3 and 700 m thick at FD94-4. Figure 4 also shows G_{max} versus depth for five 'typical' models of the delta that have been published in the geotechnical literature (Byrne and Anderson, 1987; Finn and Nichols, 1988; Sy et al., 1991) and have been widely used in site response modelling of the delta. These models are based primarily on shallow-borehole information, in general with poorly supported estimates of geological conditions and geotechnical parameters below 100 m depth. However, when examined collectively, the models shown in Figure 4 offer an indication of the range in site conditions that might be present in the delta area.

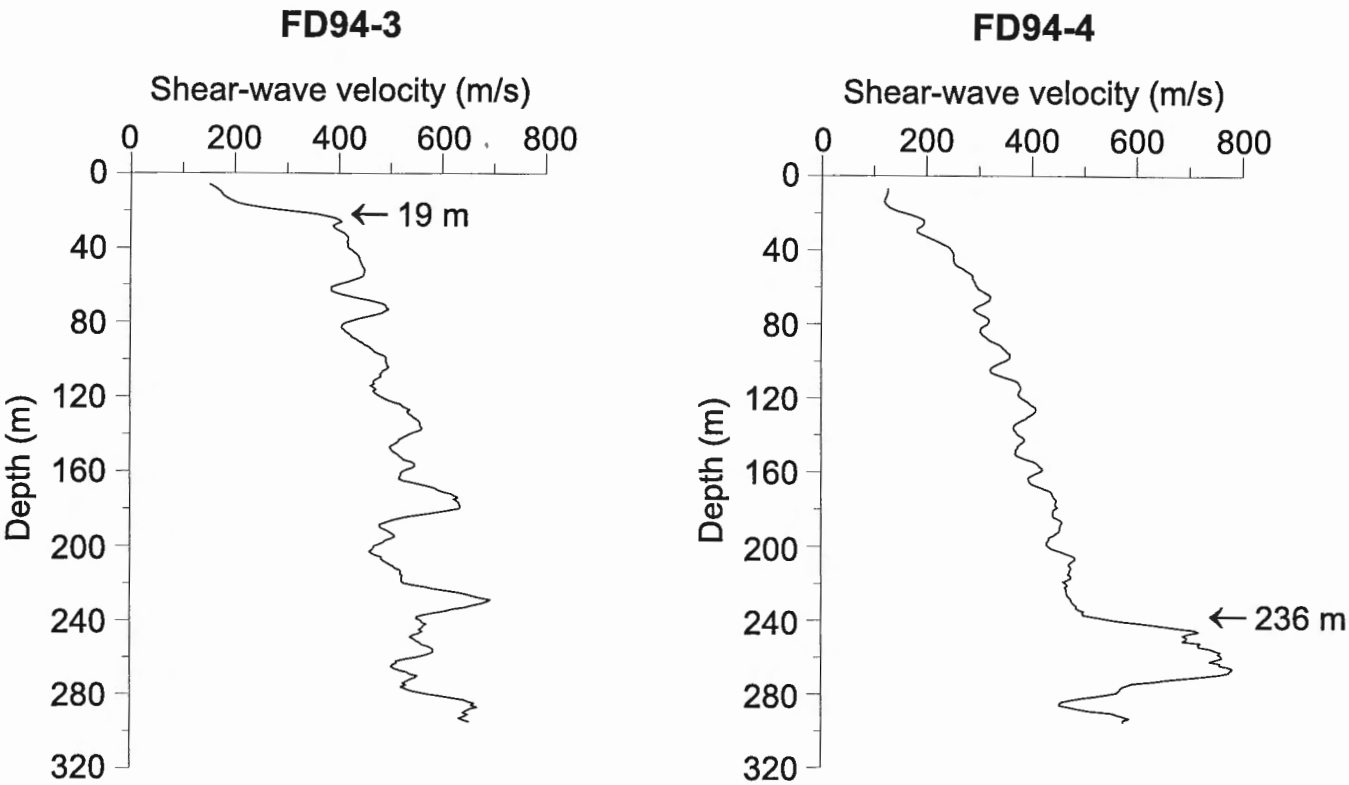

Figure 2. *Shear-wave velocities recorded in boreholes FD94-3 and FD94-4. Note the difference in depth to Pleistocene deposits (marked by arrows).*

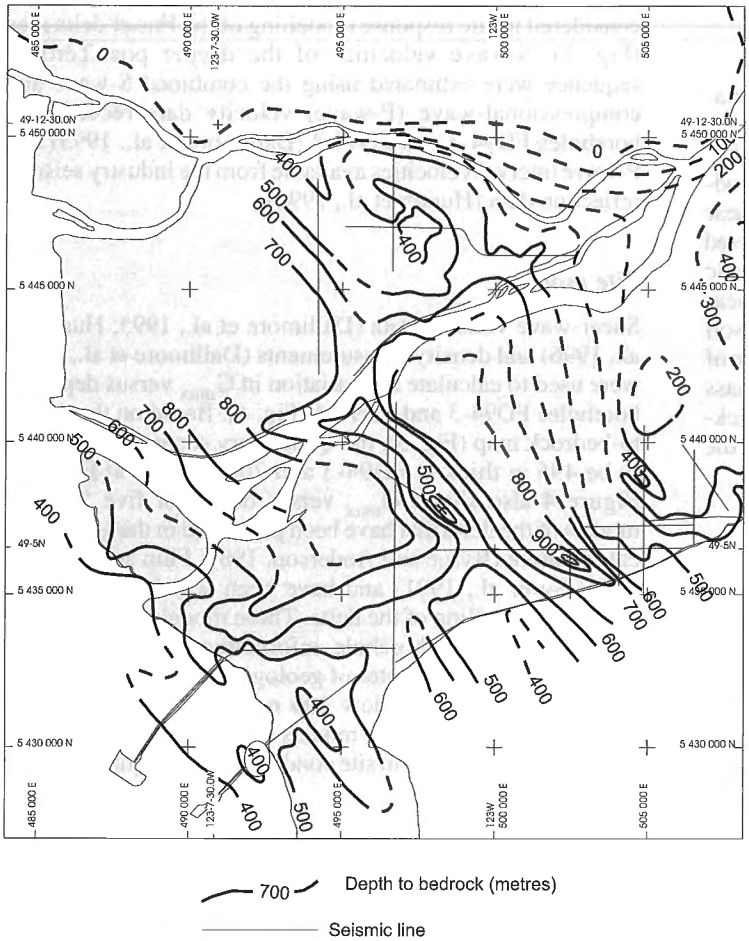

Figure 3.

Interpreted depth to Tertiary bedrock beneath the Fraser delta based on industry seismic reflection data (Britton et al., 1995).

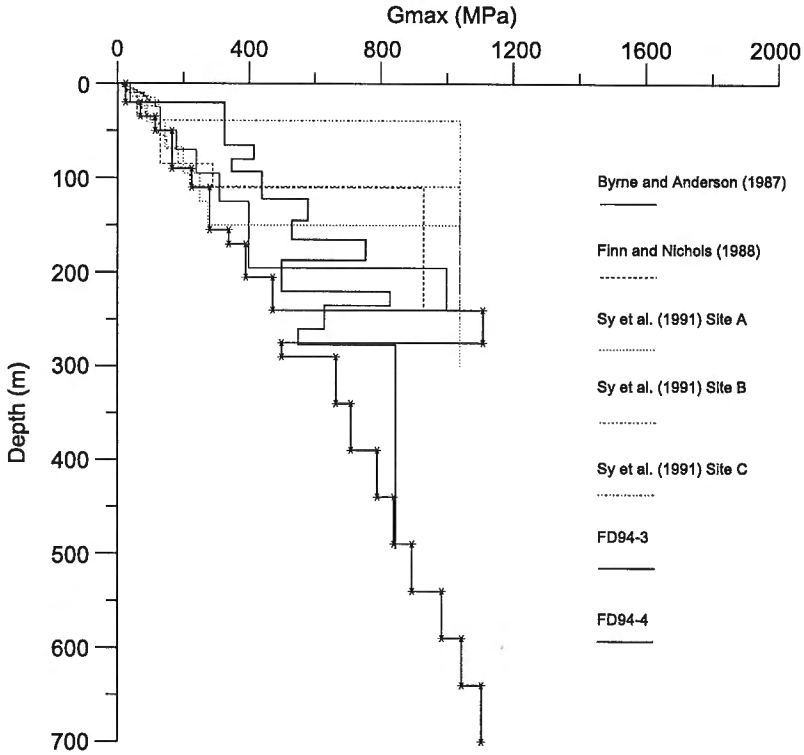

Figure 4.

G_{max} versus depth for the two deep boreholes (FD94-3 and FD94-4) and five existing geotechnical models of the Fraser delta.

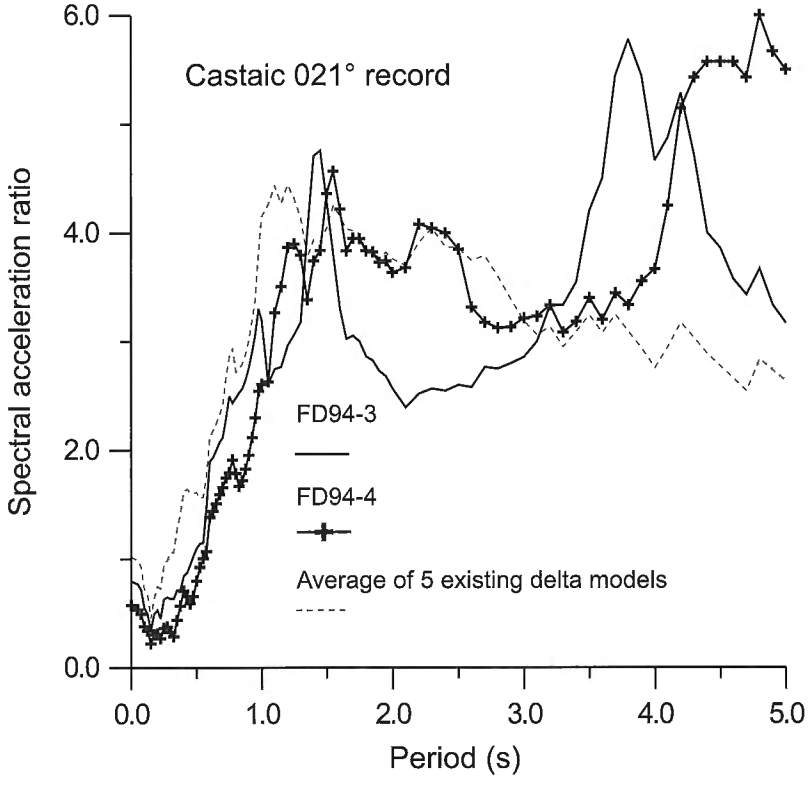

Figure 5.

Spectral ratios for the models shown in Figure 4 using record Castaic 021°.

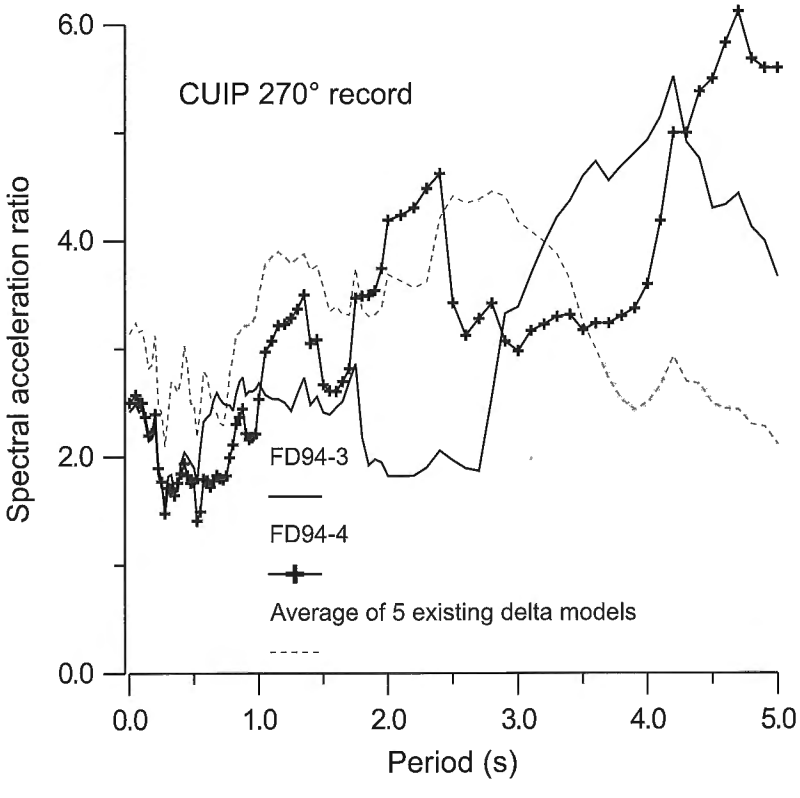

Figure 6.

Spectral ratios for the models shown in Figure 4 using record CUIP 270°.

PRELIMINARY OBSERVATIONS

Two earthquake-acceleration time histories were propagated through the seven site models (FD94-3, FD94-4, and the five existing delta models) using WESHAKE (Sykora et al., 1991), an updated version of SHAKE designed to run on personal computers. The acceleration records used were Castaic 021° (1971 San Fernando earthquake) and CUIP 270° (1985 Michoacán earthquake). The Castaic record (epicentral distance ≈ 30 km) was scaled to a peak acceleration of 0.21 g (g = acceleration of gravity), and the CUIP record (epicentral distance ≈ 375 km) was scaled to a peak acceleration of 0.035 g. The earthquake records and scaled acceleration values are consistent with those used in previous ground-motion amplification studies of the Fraser delta (Byrne and Anderson, 1987; Finn and Nichols, 1988; Sy et al., 1991) and simulate seismic events (local (Castaic) and subduction zone (CUIP)) of primary concern to the Fraser delta area (Rogers, 1994). The modulus reduction and damping curves used in the site amplification analysis are from Sy et al. (1991).

In order to evaluate amplification as a function of period, spectral ratios (5% damped acceleration-response spectra at the surface divided by 5% damped acceleration-response spectra at bedrock) were calculated for each of the seven site models using both acceleration records. Figures 5 and 6 show spectral-acceleration ratios of FD94-3, FD94-4, and the average of the five existing delta models for the Castaic 021° and CUIP 270° records, respectively. Spectral-ratio peaks (site periods) for the average of the five existing delta models occur at periods shorter than 3.0 s (peak ratio of approximately 4), while site periods for FD94-3 and FD94-4 show significantly higher long-period response (peak ratios approaching 6 for periods longer than 3.5 s). Predominant site periods of 3.5 to 4.0 s are seen at FD94-3, whereas FD94-4 has a predominant site period of 4.5 s.

CONCLUSIONS

No bedrock was encountered in two recent 300 m deep boreholes on the Fraser delta (Dallimore et al., 1995). A new map of depth to Tertiary bedrock beneath the delta (Fig. 3; Britton et al., 1995) shows the bedrock surface to be, on average, about two times deeper than has been previously assumed for geotechnical modelling. Preliminary ground-motion amplification analysis using geotechnical site models based on this new geological and geophysical information suggests that significantly longer-period (3.5 to 5.0 s) site response is likely for the Fraser delta. Not only does this long-period amplification potential have significant implications on the response of large structures (i.e. bridges, tall buildings, industrial facilities, pipelines) to earthquake ground motions, but it also calls into question the applicability of one-dimensional site response analysis (e.g. SHAKE modelling) for the Fraser delta. Sykora et al. (1991, p. 18) state "... for periods greater than 4 sec, motions are likely to be significantly affected by two-dimensional effects and surface wave energy and are not well represented with SHAKE." The depth-to-bedrock map (Fig. 3) shows numerous structures that are likely to produce two- and three-dimensional effects such as trapping and focusing of seismic energy.

There are still many unresolved questions regarding the geology and seismic vulnerability of the Fraser delta; however, these new data (Britton et al., 1995; Dallimore et al., 1995) should allow our picture of the delta and its potential seismic hazards to become clearer by establishing a geological framework for future earthquake-hazard modelling.

REFERENCES

Britton, J.R., Harris, J.B., Hunter, J.A., and Luternauer, J.L.
1995: The bedrock surface beneath the Fraser River delta in British Columbia based on seismic measurements; in Current Research 1995-E, Geological Survey of Canada, p. 83-89.

Byrne, P.M. and Anderson, D.L.
1987: Earthquake design in Richmond, B.C., Version II; University of British Columbia, Department of Civil Engineering, Soil Mechanics Series, No. 109, 90 p.

Dallimore, S.R., Edwardson, K.A., Hunter, J.A., Clague, J.J., and Luternauer, J.L.
1995: Composite geotechnical logs for two deep boreholes in the Fraser River delta, British Columbia; Geological Survey of Canada, Open File 3018, 1 sheet.

Finn, W.D.L. and Nichols, A.M.
1988: Seismic response of long-period sites: lessons from the September 19, 1985, Mexican earthquake; Canadian Geotechnical Journal, v. 25, p. 128-137.

Hunter, J.A., Harris, J.B., and Britton, J.R.
1996: Compressional and shear wave interval velocity data for Quaternary sediments in the Fraser River delta from multichannel seismic reflection surveys; Geological Survey of Canada, Open File 3325, 228 p.

Luternauer, J.L., Barrie, J.V., Christian, H.A., Clague, J.J., Evoy, R.W., Hart, B.S., Hunter, J.A., Killeen, P.G., Kostaschuk, R.A., Mathewes, R.W., Monahan, P.A., Moslow, T.F., Mwenifumbo, C.J., Olynyk, H.W., Patterson, R.T., Pullan, S.E., Roberts, M.C., Robertson, P.K., Tarbotton, M.R., and Woeller, D.J.
1994: Fraser River delta: geology, geohazards, and human impact; in Geology and Geological Hazards of the Vancouver Region, Southwestern British Columbia, (ed.) J.W.H. Monger; Geological Survey of Canada, Bulletin 481, p. 197-220.

Rogers, G.C.
1994: Earthquakes in the Vancouver area; in Geology and Geological Hazards of the Vancouver Region, Southwestern British Columbia, (ed.) J.W.H. Monger; Geological Survey of Canada, Bulletin 481, p. 221-229.

Schnabel, P.B., Lysmer, J., and Seed, H.B.
1972: SHAKE: A computer program for earthquake response analysis of horizontally layered sites; University of California, Berkeley, Earthquake Engineering Research Center, Report EERC-72/12, 3 diskettes.

Sy, A., Henderson, P.W., Lo, R.C., Siu, D.Y., Finn, W.D.L., and Heidebrecht, A.C.
1991: Ground motion response for the Fraser delta, British Columbia; in Proceedings, 4th International Conference on Seismic Zonation, Stanford, California, v. 2, p. 343-350.

Sykora, D.W., Wahl, R.E., and Wallace, D.C.
1991: WESHAKE for personal computers; U. S. Army Corps of Engineers, Geotechnical Earthquake Engineering Software, Instructional Report GL-91-1, 215 p. and 1 diskette.

Seabed slope instability on the Fraser River delta

H.A. Christian[1], D.C. Mosher[2], J.V. Barrie[2], J.A. Hunter[3], and J.L. Luternauer[4]

Christian, H.A., Mosher, D.C., Barrie, J.V., Hunter, J.A., and Luternauer, J.L., 1998: Seabed slope instability on the Fraser River delta; in Geology and Natural Hazards of the Fraser River Delta, British Columbia, (ed.) J.J. Clague, J.L. Luternauer, and D.C. Mosher; Geological Survey of Canada, Bulletin 525, p. 217–230.

Abstract: The Fraser River delta lies in one of the most earthquake-prone regions in Canada and is composed, in part, of loose sands that have a high seismic liquefaction potential. Engineering investigations at the western margin of the Fraser delta have demonstrated that seismic liquefaction is possible on the existing delta slope. There are several areas of past and present slope instability at the delta front. Present examples include chronic retrogressive slumping and debris flows at the mouth of the Main Channel and slow downslope creep movements in adjacent areas, where sediments are accumulating on the delta slope. Prehistoric mass movements may have been triggered by liquefaction during past earthquakes or may be related to recurrent slumping at the mouths of former distributary channels. In addition, failure may be linked to leaching of metastable marine sediments at the base of the Holocene deltaic sequence. Spontaneous failures occurring at present at the river mouth are due to the combined effects of rapid sedimentation and slope over-steepening, shallow gas held within the sediment mass, and tidal loading.

Résumé : Le delta du fleuve Fraser se trouve dans l'une des régions où la sismicité est la plus élevée du Canada et se compose, en partie, de sable non consolidé qui pourrait se liquéfier s'il était soumis à de fortes secousses sismiques. Les études techniques menées sur la bordure ouest du delta du Fraser ont mis en évidence la possibilité que des phénomènes de liquéfaction d'origine sismique se produisent au niveau du talus du delta. Le front deltaïque est ponctué de plusieurs zones d'instabilité du talus, tant anciennes qu'actuelles. Parmi les exemples actuels, on compte un glissement rétrogressif récurrent et des coulées de débris à l'embouchure du chenal principal ainsi que des reptations lentes vers le bas du talus dans les zones adjacentes, là où les sédiments s'accumulent sur le talus du delta. Quant aux mouvements de masse préhistoriques, ils ont pu être des phénomènes de liquéfaction de sédiments déclenchés par des séismes ou être l'un des glissements récurrents à l'embouchure d'anciens défluents. Les ruptures pourraient aussi être attribuables au lessivage de sédiments marins métastables à la base de la séquence deltaïque holocène. Aujourd'hui, les ruptures spontanées qui se produisent à l'embouchure du fleuve sont causées par les effets combinés d'une sédimentation rapide et d'un surraidissement des talus, par le piégeage de gaz dans les sédiments peu profonds et par l'action des marées.

[1] Geological Survey of Canada, P.O. Box 1006, Dartmouth, Nova Scotia B2Y 4A2
[2] Geological Survey of Canada, Pacific Geoscience Centre, P.O. Box 6000, Sidney, British Columbia V8L 4B2
[3] Geological Survey of Canada, 601 Booth Street, Ottawa, Ontario K1A 0E8
[4] Geological Survey of Canada, 605 Robson Street, Vancouver, British Columbia V6B 5J3

INTRODUCTION

Analysis of the stability of marine sediments requires knowledge of geology, geomorphology, and the geotechnical characteristics of the sediments and their response to external loading (e.g. earthquakes, rapid sedimentation). Research has been conducted by the Geological Survey of Canada (GSC) offshore of the Fraser River delta to identify seafloor instability processes and to determine the distribution, magnitude, and frequency of slope failures, mainly using geophysical techniques (Christian et al., 1994a). Research into the mechanisms of failure has employed in situ methods to evaluate the seismic liquefaction potential of seafloor sediments at key sites (Christian et al., 1994b). Modern geological processes have been studied to identify and explain past, large-scale slope failures.

This paper is a summary of recent GSC research on modern and relict slope instability processes on the Fraser delta, with a view toward quantitatively assessing and understanding trigger mechanisms. The research reported herein complements geological mapping activities carried out by the GSC by providing a regional framework of seafloor geohazards which could potentially affect engineered installations.

Geological and geophysical mapping of the western margin of the Fraser River delta has identified several areas of large-scale instability related to delta progradation over weak silts and clays flooring the Strait of Georgia. Large prehistoric failure complexes are present at the base of the delta slope off Sand Heads and Roberts Bank (Fig. 1), and other smaller failures have occurred historically wherever the Main Channel of the Fraser River has discharged large quantities of sediment onto the delta slope.

The processes responsible for this instability are not well understood. Geotechnical investigation of sediments at the delta front indicate a high potential for widespread flow-liquefaction during a future large earthquake. However, sediments at the mouth of the Main Channel periodically spontaneously liquefy and evolve into mobile flow slides in the

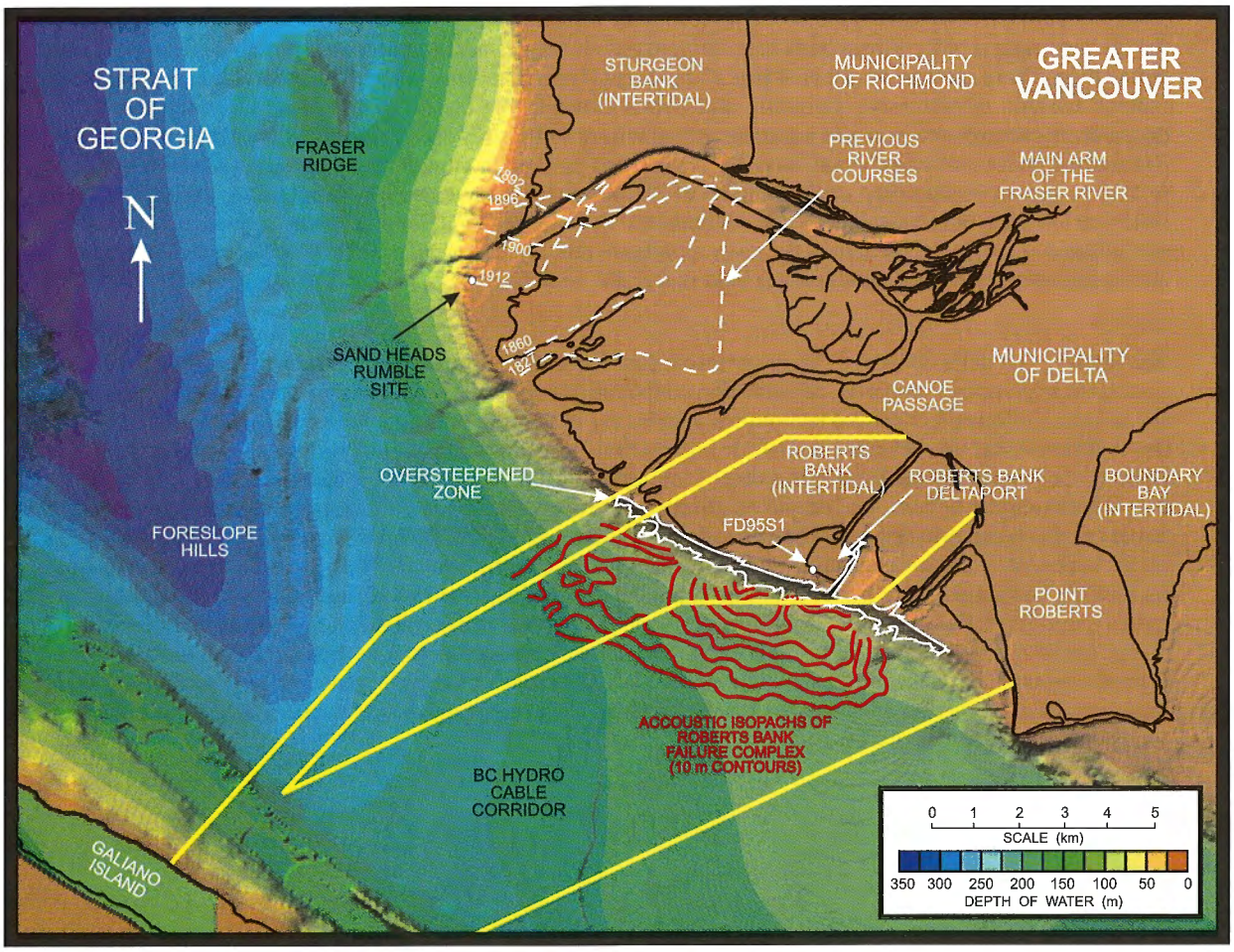

Figure 1. Location map of southern Strait of Georgia showing the southwestern Fraser River delta, intertidal flats, locations of past river channels, the B.C. Hydro cable corridor, and the Roberts Bank Deltaport (location of Westshore Terminals Coalport). Isopach map shows acoustic thickness of Roberts Bank Failure Complex (after Hart and Olynyk (1994)).

absence of earthquake shaking, and much of the prehistoric instability at the delta front is associated with areas off the mouths of former distributary channels.

BACKGROUND

The Fraser delta, situated in one of the most seismically active regions in Canada, is a large body of mainly sandy and silty sediments deposited during progradation of the Fraser River into the Strait of Georgia over the past 10 000 years. The marine portion of the Fraser delta hosts one of the busiest public ferry terminals in the world, the largest bulk shipping facility in western Canada, a major hydroelectric and communication cable corridor that provides electrical power to southern Vancouver Island, and a large seasonal fishery (Fig. 1).

The delta front has been extensively investigated using a variety of onshore and marine geophysical and geotechnical methods. Subsurface investigations carried out by the GSC include wash and rotary borehole sampling, electric resistivity and seismic cone penetration testing (CPT), and downhole, crosshole, and surface shear-wave measurements (Hunter et al., 1991; Christian et al., 1994b, 1995; Dallimore et al., 1995; Christian and Woeller, 1996). In addition, an effort is now being made to assess the role of groundwater through downhole pore-pressure monitoring and pore water/gas sampling.

These activities have provided evidence for both active and relict slope instability, including steep erosional escarpments near points of river discharge, deep upper-slope sea valleys, shallow-seated rotational movements at mid-slope, debris lobes and fans at the base of the delta slope, local disruption of acoustic reflections, and creep folding, primarily in soft gas-charged sediments. Evidence for instability at the present time is most apparent off the Main Channel at Sand Heads (Fig. 2). Within, and at the base of, the active sea valleys are lobes of sediment deposited by debris flows and turbidity currents that originated on the steep valley walls off the Main Channel mouth. Relict incised sea valleys apparent in high-resolution bathymetric records elsewhere on the delta slope are associated with older distributary channels (Fig. 1).

Strong geological evidence exists for very large earthquakes on the west coast of Canada about 300 and 1700 years ago (Clague and Bobrowsky, 1994; Mathewes and Clague, 1994; Satake et al., 1996); many other smaller earthquakes

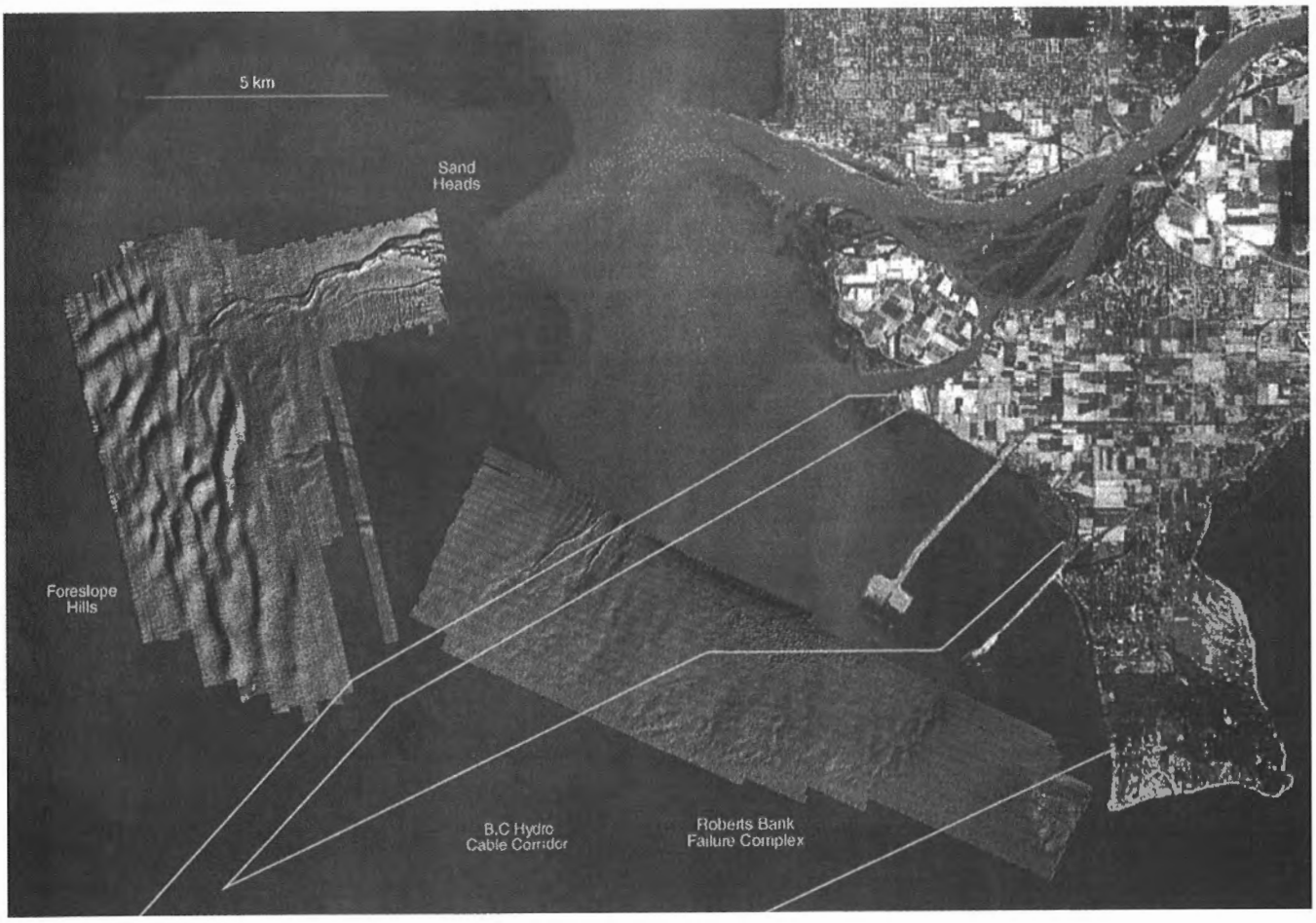

Figure 2. *Shaded-relief multibeam image of the seafloor in areas of known slope instability at the Fraser delta front (after Currie and Mosher, 1996).*

have probably also affected the Fraser delta in recent times. Strong shaking may trigger flow liquefaction on steep slopes at the front of the delta.

The seismic liquefaction resistance of recently deposited sediments at the western margin of the Fraser delta has been only partially evaluated. Geotechnical site investigations have shown that the delta slope and crest may be susceptible to seismic liquefaction during extreme events (moment magnitude 7.5 with a peak horizontal surface acceleration of at least 0.2 g (g = acceleration of gravity)), involving post-failure deformations ranging from lateral spreading to flow sliding (Christian et al., 1994b). A possible consequence would be damage to major port facilities located at the crest of the slope or to submarine electrical transmission cables on the Roberts Bank slope.

SETTING

The subaerial part of the Fraser River delta is a dyked floodplain that extends up to 23 km westward from a gap in the Pleistocene uplands at New Westminster and is underlain by silt and peat. Sandy tidal flats up to 9 km wide border the dyked floodplain on the west and are bounded by a slope that descends into the Strait of Georgia at angles ranging from an average of 15° near the crest to less than 1° at its base. The base of the slope lies in 100 to 300 m of water, deepening to the north. Steeper slopes, typically 20 to 45°, occur within sea valleys off Sand Heads and Canoe Passage. The delta slope is underlain dominantly by clayey silt north of the Main Channel, and sandy silt and sand to the south (Clague et al., 1983, 1991). The Steveston Jetty constrains the Main Channel where it crosses the tidal flats, preventing further migration and concentrating sediment discharge at the delta front in the vicinity of Sand Heads.

Peats and intertidal floodplain silts are more than 15 m thick at the apex of the delta and thin westward to less than 1 m at the western margin of the delta plain. These sediments are underlain by a sheet of distributary-channel sands up to 30 m thick (Monahan et al., 1993a, b). The channel sands tend to be looser than littoral sands deposited at the shoreline because they have not been densified by wave action (Pryor, 1973; de Mulder and Westerhoff, 1985), and they have a high susceptibility to seismic liquefaction (Watts et al., 1992). However, younger sands at the seaward margin of the tidal flats are even looser and possess a greater liquefaction potential (Christian and Woeller, 1996).

The distributary-channel sand sheet unconformably overlies a thick sequence of delta-slope deposits (foresets) consisting of interbedded sands and silty sands (Fig. 3). The slope deposits, in turn, overlie prodelta silts and clayey silts. Individual layers can be traced only short distances based on CPT logs (P.A. Monahan, pers. comm., 1994). Slope deposits beneath southernmost Roberts Bank consist primarily of sands and silty sands, but elsewhere they are mainly silts with localized sand-dominated units up to 30 m thick. Geophysical records and CPT correlations suggest that foreset beds dip seaward at angles up to 7° (Monahan et al., 1993a, b).

Deltaic deposits overlie Pleistocene till and stratified sediments (Luternauer et al., 1993). The surface separating the deltaic and Pleistocene sequences has up to 300 m of relief (Hamilton, 1991; Harris et al., 1995).

Seismic-reflection records over much of the subaerial delta plain and in many offshore areas are obscured by shallow gas, which absorbs acoustic energy. The gas is primarily biogenically derived methane, produced by decomposition of large quantities of organic material that is carried to the sea by the Fraser River. In situ pore-fluid sampling indicates that a large portion of the void space of sediments at the seaward margin of the delta is occupied by free gas. Farther offshore, free gas is less concentrated (less than 1% by volume) because of high back pressures, but is more ubiquitous.

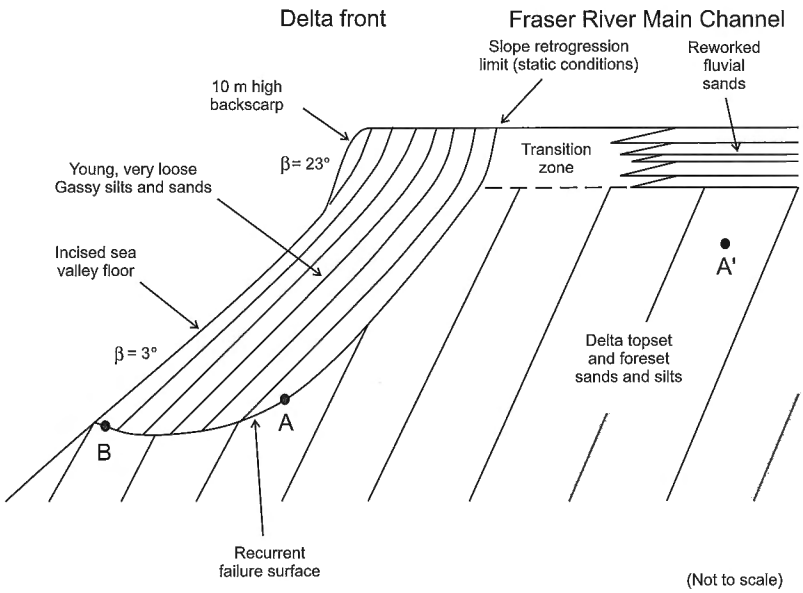

Figure 3.

Interpretive cross-section of the Fraser delta in the vicinity of the modern river mouth at Sand Heads. The section is normal to the slope along a major sea valley.

SEA VALLEYS

A network of submarine channels is incised into the delta slope at Sand Heads (Fig. 1, 2, 3). These channels coalesce into a single large sea valley farther down the slope. The sea valley is up to 60 m deep, 100 m wide, and 6 km long. It was created, and continues to be maintained, by mass wasting at Sand Heads (Hart et al., 1992a). Channelized debris flows transport sediment to the base of the slope where it is deposited, along with turbidites, on debris aprons and fans. These flows bypass the upper slope, limiting sedimentation there to primarily relatively fine-grained suspension deposits until a new sea valley develops.

Failures caused by spontaneous liquefaction have been documented at the head of the Sand Heads sea valley since the construction of the Steveston Jetty (McKenna and Luternauer, 1987). Much research has been done in an attempt to explain these events. Hungr (1993) reviewed historical data and concluded that the trigger mechanism, although unknown, did not involve seismicity, as no earthquakes coincided with documented mass movements. Terzaghi (1956) observed that many unexplained subaqueous flow slides in sands around the world occurred during or shortly after extremely low tides.

The most recent observed liquefaction slide in the Fraser delta occurred in July 1985 and involved the rapid mass wasting of at least 10^6 m^3 of sediment and retrogression of the head of the principal sea valley to within 100 m of the Sand Heads lighthouse (McKenna and Luternauer, 1987; Atkins and Luternauer, 1991). The depression left by this failure has since been entirely filled in with sediment (Fig. 4). Backscarps developed during this and other liquefaction

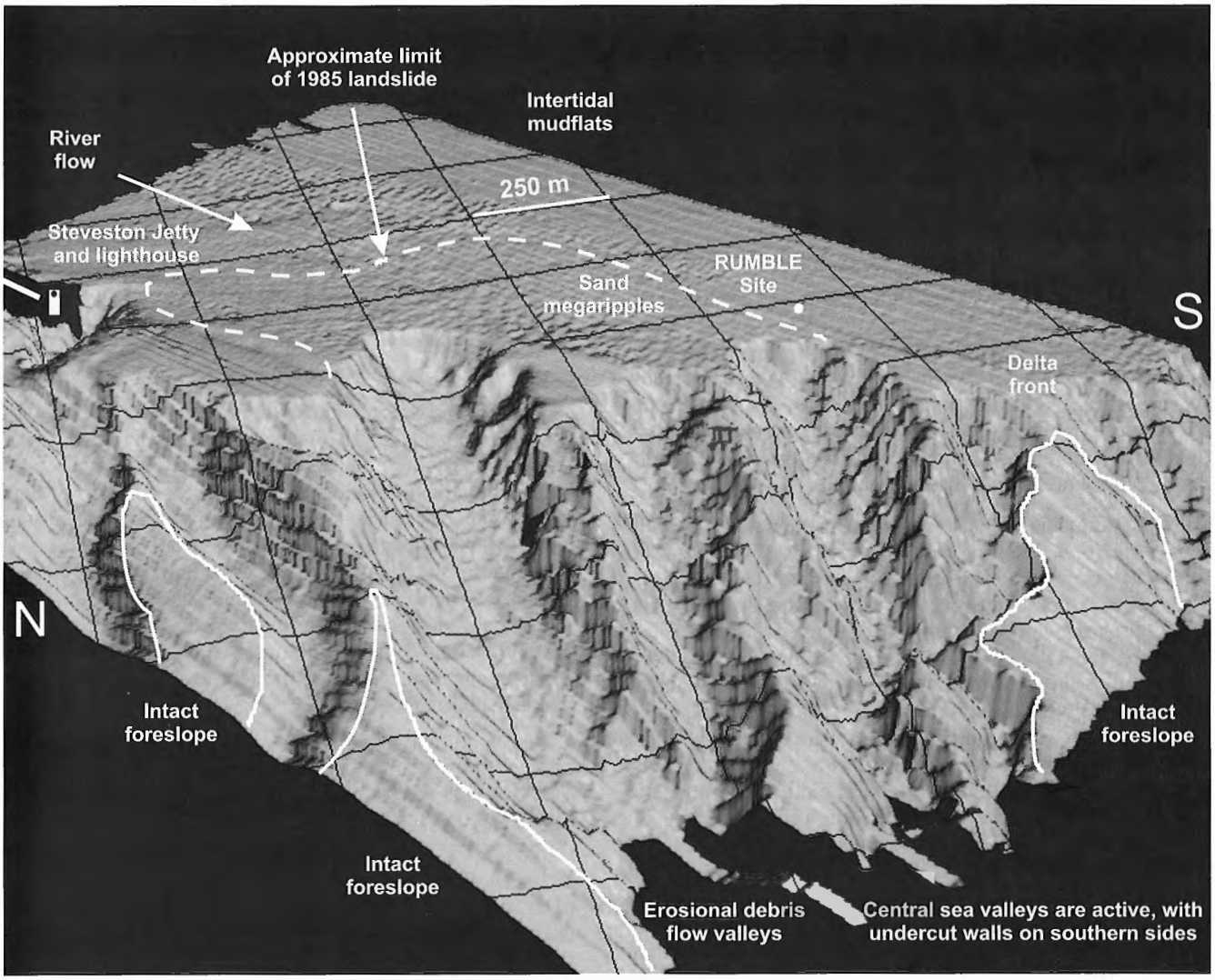

Figure 4. Shaded-relief bathymetry of the Sand Heads area, showing submarine canyons at the mouth of the Fraser River, the approximate extent of the 1985 underwater landslide, the location of the Sand Heads lighthouse, and the RUMBLE study site. Intact portions of the delta slope are marked. Sea valleys north of the Steveston Jetty are inactive and are slowly being filled with sediment.

failures typically have angles no greater than 23°, which is about half of the angle of internal friction of clean Fraser River sand in undrained shear (Chillarige et al., 1995). Hence they are difficult to explain as naturally occurring failures.

Static triggering of distributary-mouth flow slides

Instability at the river mouth appears to be partly related to high sedimentation during the spring freshet from May through July. Radiocarbon dating of material from cores collected at Sand Heads indicates that sedimentation rates there locally exceed 0.18 m/a (J.V. Barrie, pers. comm., 1995). Dredging and construction of the Steveston Jetty have altered sedimentation patterns and may have locally increased delta-front instability, since large volumes of sand formerly stored upstream in distributary bars are now transported directly to the top of the delta slope.

Wave and tidally induced pore pressures were monitored adjacent to the Sand Heads lighthouse in an attempt to determine the trigger mechanism for liquefaction and subsequent flow sliding and to check the initial assumption of fully saturated conditions. Wave loading on the scale of that present in the Strait of Georgia is not sufficient to trigger failure on these slopes (Chillarige et al., 1994), but tidal drawdown can, under some circumstances, initiate static liquefaction. In areas of high sedimentation, the density of sandy sediments is low, allowing collapse during shear failure.

Typically, the post-failure shear strength is a fraction of the peak strength, allowing the sediment mass to deform in an uncontrolled manner, evolving into a highly mobile flow slide. Such flows accelerate as they enter the sea valley system and can travel great distances, only coming to rest on flatter slopes where driving stresses are fully resisted by the large-strain (remoulded) shear strength. Non-thixotropic slide masses thereafter remain in a marginally stable state and can be reactivated by additional shear stress.

High sedimentation on a submarine slope can lead to high static shear stresses, but observations show that failure usually occurs at much lower angles than expected. One possible explanation is that some process causes an increase in internal pore pressure, thereby reducing the effective stress and, consequently, the available shear strength during shear. However, a fully saturated, freely draining sand deposit cannot sustain static pore pressures in excess of the hydrostatic pressure. Previously, submarine sediments were thought to fail in a fully saturated condition (i.e. free gas was not present). This now appears to be an incorrect assumption, based on field sampling and testing which show that high concentrations of methane gas are present in sediments filling the 1985 landslide depression at Sand Heads (Christian et al., 1994b; Christian and Woeller, 1996). Geophysical data suggest that such gas is widespread; acoustic P-wave velocities measured by downhole and seismic CPT methods are much lower than those in gas-free sediments.

Long-term in situ monitoring at the head of a sea valley at Sand Heads (RUMBLE (Remote underwater monitoring before liquefaction events) study area; Fig. 4) has shown that pore pressure at a depth of 5 m is attenuated by about 75% relative to the tides and follows the tidal curve by up to 60 minutes (Fig. 5, 6). Excess pore pressures, calculated by subtracting the measured pore pressure from the hydrostatic value, range up to 16.5 kPa, approaching the 20 kPa required to trigger static liquefaction within the slope.

Finite element analysis of the shear-stress state preceding the 1985 failure indicates that liquefaction failure began at a depth of 36 m beneath the slope at the head of the sea valley (Chillarige et al., 1995). This is illustrated schematically on the Mohr-Coulomb diagram in Figure 7, where the static stress state is depicted for the pre-slide 1985 Sand Heads geometry (point A), along with the collapse surface for clean sand which defines the stress state during the onset of strain-softening behaviour.

A falling spring tide produces a critical stability condition in an unsaturated sediment mass by lowering the effective stress state toward point B in Figure 7, inducing strain softening of the sediment. In a fully saturated sediment possessing no gas, the effective stress would remain unchanged and the effective stress state would not deviate from point A. Conversely, a rising tide increases the effective stress, since the pore pressure is slower to respond and the sediment mass strain-hardens. If, during an extremely low tide, a loose cohesionless slope approaches failure due to a gas-delayed pore-pressure response, deformations may become large, leading to a flow slide. The static driving stresses induced by gravity remain unchanged, thus the slope loses integrity as it strain-softens. Fully saturated underwater slopes can remain statically stable indefinitely as long as no failure trigger mechanism exists. The assumption of a fully equalized pore pressure response to tidal drawdown may be invalid, however, if free gas is present within the sediment mass.

Based on extrapolation of field data, we conclude that extreme spring tides of 5 m in the Strait of Georgia are capable of reducing the static effective stress by the 20 kPa needed to initiate liquefaction failure in gassy sands and silts at Sand Heads. Laboratory triaxial testing of Fraser River sand samples, reconstituted to densities measured in geotechnical investigations at Sand Heads, shows a high susceptibility to collapse, since the post-failure steady-state shear strength is considerably lower than the in situ static shear stress at the head of the delta slope (Chillarige et al., in press a, b). Future spontaneous flow slides are thought to be inevitable in the Sand Heads area.

SHALLOW ROTATIONAL FAILURES ON THE DELTA SLOPE

Sidescan sonar surveys over the upper delta slope southwest of Sand Heads have revealed a series of sub-parallel sinusoidal ridges trending roughly parallel to bathymetric contours (Fig. 2; Hart et al., 1992a). The ridges measure 60 to 100 m from crest to crest, are several metres in height, and are composed of silty sands and clayey silts. Hart et al. (1992a) interpreted these features as shallow rotational failures produced by rapid sedimentation, with each ridge representing a back-tilted block. They further suggested that the zone of failure

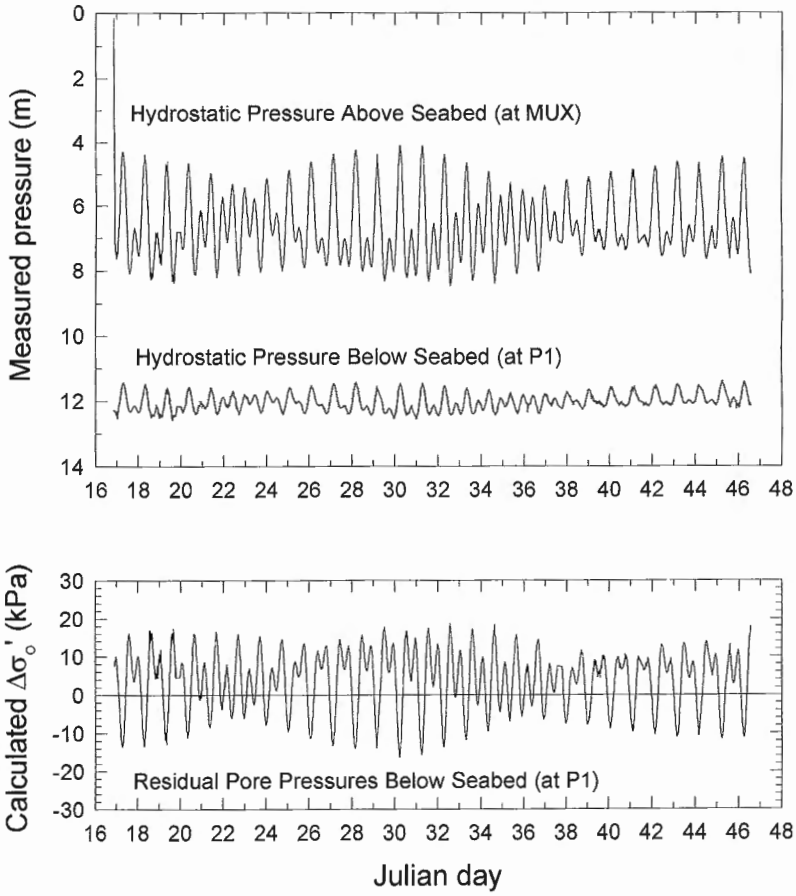

Figure 5.

Data record from a liquefaction detection experiment (RUMBLE) conducted in 1995 at Sand Heads, showing tidal elevations measured by a pressure gauge on the seabed (MUX-data multiplexor) and the sediment pore-pressure response measured at the tip of a sub-seabed probe (piezometer P1). Variations in effective stress ($\Delta\sigma_0'$) were calculated directly from changes in sediment pore pressure (Δu) (Christian and Woeller, 1996).

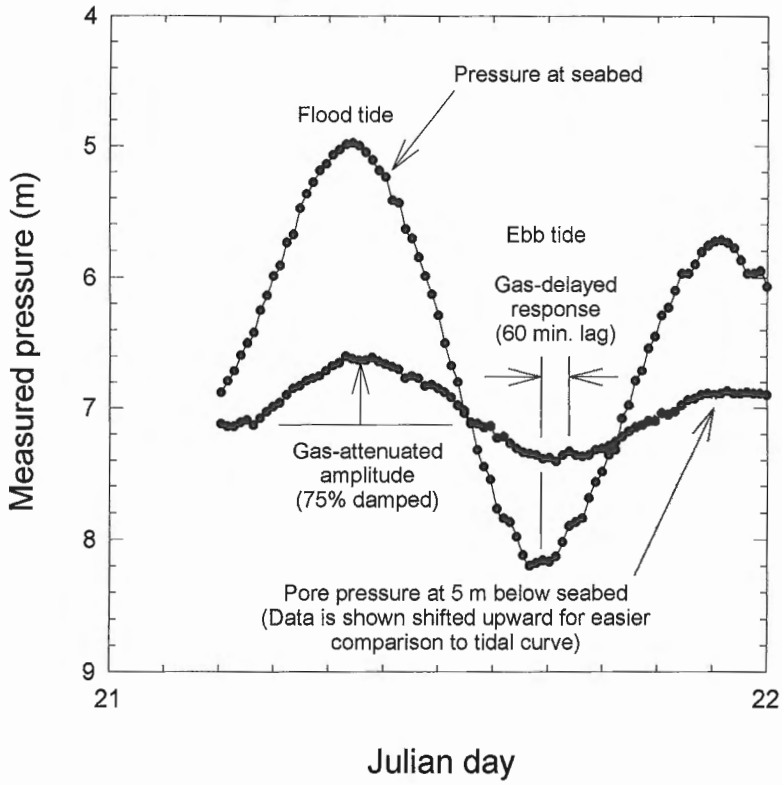

Figure 6.

Enlargement of RUMBLE field-data record of January 21, 1995. The tidal range was about 3.2 m, yet the corresponding pore pressure was only about 0.7 m due to gas damping. The observed 60-minute lag results in a reduction in effective stress and available shear strength.

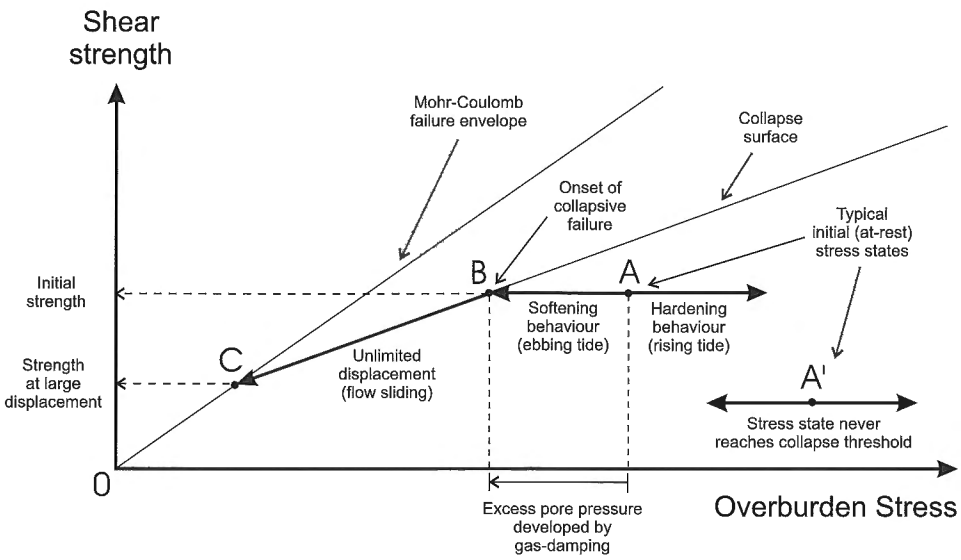

Figure 7. *Idealized Mohr-Coulomb shear response for typical monotonic loading conditions in loose sands subjected to tidal variations and a gas-damped pore-pressure response. For level seafloor (A′) well away from a slope, initial shear stresses are low and tidal loading cannot induce failure. For an element near a slope (A), static shear stresses may exceed the large-strain strength (C), leading to development of a flow slide, if liquefaction is triggered. Pore pressure buildup during tidal drawdown can induce softening and, ultimately, static liquefaction failure (at B).*

extends to the floor of the Strait of Georgia and ends in the Foreslope Hills. Recent multibeam bathymetric imagery shows that the ridges are restricted to the steepest part of the slope. The strength of sediment resting on this part of the delta slope is very low, and the load imposed by sedimentation upslope leads to continuous slow downslope movement (Terzaghi, 1962). Extensive gas masking in high-resolution reflection profiles prevents definition of the internal structure of the ridges, but Hart et al. (1992a) observed that the zone of instability is limited to the area of most active sedimentation and concluded that a widespread failure surface lies about 3 m below the seafloor.

FORESLOPE HILLS

The Foreslope Hills are a series of elongated sub-parallel ridges developed in soft gas-charged silts and clays at the base of delta slope, in water depths of 230 to 330 m (Fig. 1, 2). The ridges cover an area of about 60 km^2, are up to 5 km long and 20 m high, and have wavelengths of 500-600 m. They are oriented in a west-northwest direction in the north, trend almost due north in the south, and abut an outcropping Pleistocene high known as Fraser Ridge (Fig. 1).

The location and orientation of the Foreslope Hills suggest a genetic relationship with the Fraser delta, and many hypotheses have been advanced to explain their origin. Mathews and Shepard (1962) and Terzaghi (1962) postulated that they might be a translational landslide mass produced by a large failure higher on the slope. Shepard (1967) speculated that they may be mud diapirs. Tiffin et al. (1971) and Luternauer and Finn (1983) concluded that the Foreslope Hills are compressional folds developed in weak sediments at the toe of a failure farther upslope. Hart (1993) reviewed available geophysical data and argued that the ridges are associated with landward-dipping shear planes produced by extensional rotation. He noted that the ridges are markedly asymmetric, with steeper slopes on their upslope sides; yet turbidites infilling the troughs showed no signs of tilting. Currie and Mosher (1996) interpreted the Foreslope Hills as a complex suite of sediment bedforms created by currents (see also Mosher and Hamilton,1998).

Figure 8 shows vectors of driving stress superimposed on shaded-relief bathymetry obtained from multibeam mapping (Christian et al., 1995). The orthogonal intersection of principal shear-stress vectors with ridge crests suggests that gravitational loads imposed by progradation of the delta, coupled with downslope creep of lower slope sediments, could have produced the Foreslope Hills, as suggested by Luternauer and Finn (1983). If this is the case, the failure was non-catastrophic and could not have generated a tsunami, as proposed by Hamilton and Wigen (1987).

The existence of such a large failure in an area where the seafloor slopes less than 1° suggests that the delta foreset rests on similar weak materials and may possess, at best, only marginal long-term static stability. Dynamic earthquake loading

may, in addition, cause cyclically induced deformations and progressive failure within the bottomset sequence at depth, as well as cyclic liquefaction of near-surface sediments on the delta slope (N.R. Morgenstern, pers. comm., 1994). Insufficient data exist at present to adequately address these issues.

ROBERTS BANK FAILURE COMPLEX

Offshore geophysical records have revealed a large (40 km^2) area of chaotic and disrupted strata on the Fraser delta slope between Canoe Passage and Point Roberts (Fig. 1, 2), interpreted as resulting from upslope failure (Hart et al., 1992b). This feature, referred to as the Roberts Bank Failure Complex, extends to the base of the slope (Christian et al., 1994b). Its upslope limit is poorly defined, due to steeper slopes that affect the quality of the acoustic data. Large sand waves developed on the seafloor also scatter acoustic energy. The failure complex, however, may extend beneath the tidal flats, since the deepest reflectors do not appear to emerge at the seafloor on the slope.

There are several possible explanations for the Roberts Bank Failure Complex. One possibility is that it formed by seismic liquefaction of a large area of the delta slope during a prehistoric earthquake. Another hypothesis, advanced by D.B. Prior (pers. comm., 1994), is that it is a stacked sequence of sediment lobes emplaced by repeated upslope failure in the vicinity of former distributary channels, as is occurring today off Sand Heads. A third explanation invokes progressive straining within the delta bottomset sequence, leading to a redistribution of shear stresses and propagation of failure into surficial sediments resting on the slope, as described by Hansbo et al. (1985). This hypothesis has not been fully evaluated due to the difficulty of obtaining high-quality geotechnical data from the depths and zones of interest. In this context, however, onshore site investigations have shown

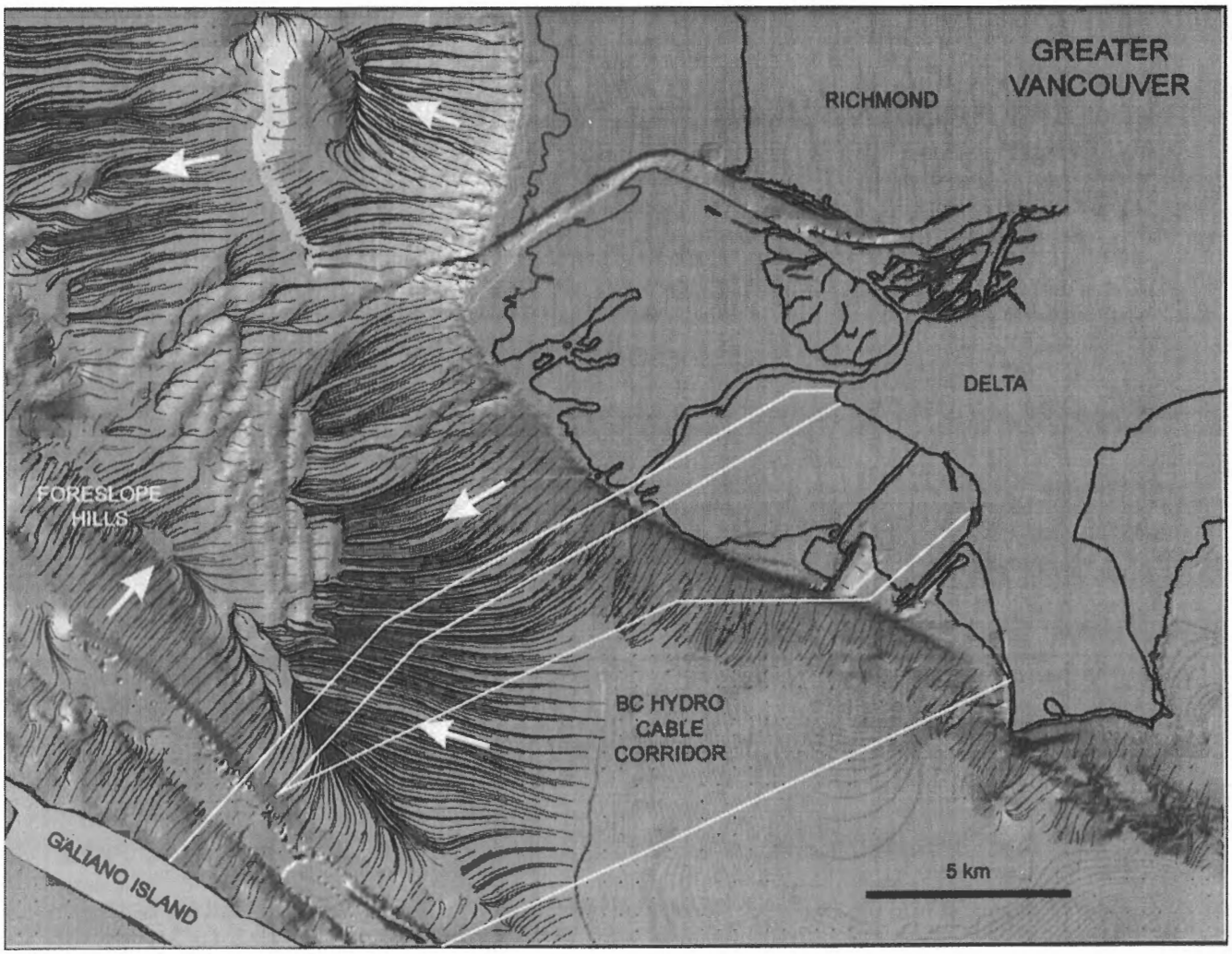

Figure 8. *Shaded-relief image of the seafloor at the western front of the Fraser delta, overlain by vectors of driving (shear) stress. Ridge crests of the Foreslope Hills are nearly perpendicular to the principle stress vectors, suggesting that there is a link between unbalanced driving stresses produced by deltaic progradation over weak marine sediments and compressional deformation of the prodelta sequence.*

that deep groundwater leaching may have a significant impact on the static and dynamic stability of the delta front. Leaching of marine sediments by fresh groundwater leads to a marked reduction in the post-failure or ultimate shear strength (Skempton and Northey, 1952). This process is described in more detail in the next section.

The Roberts Bank Failure Complex has not been precisely dated, although radiocarbon ages of wood taken from cores of the uppermost strata show it to be younger than about 1000 years. The failure complex predates abandonment of Canoe Passage because its northern surface is incised by channels that were active when the Fraser River flowed through this passage. Clague et al. (1983) reviewed historical charts and maps of the delta front dating from 1827 and determined that the main distributary channel of the Fraser River has migrated northward from southern Roberts Bank since that time (Fig. 1).

The origin of the Roberts Bank Failure Complex is not as critical an issue as the future behaviour of the steeper upslope region during a large earthquake. The upper part of the Roberts Bank slope may still experience cyclic softening during earthquake loading, even though the Fraser River no longer supplies sediment to this area. Engineering investigations have demonstrated a high collapse potential to depths of 10 to 15 m below the seafloor over most of the upper slope (Christian et al., 1994b). Widespread lateral spreading and localized flow slides are anticipated, since static driving stresses near the crest of the slope appear to exceed the estimated post-shaking shear strength (i.e. the static factor of safety against sliding is less than 1; Fig. 9).

EFFECTS OF GROUNDWATER ON DELTA STABILITY

The shear behaviour of fine-grained sediments can be characterized by their sensitivity, which is the ratio of the intact to remoulded undrained strength. Skempton and Northey (1952) examined a variety of marine clays that had been leached by fresh groundwater and concluded that a linear empirical relationship exists between sensitivity and pore-water salinity (Fig. 10). Failure in highly sensitive clays often occurs rapidly, with little or no warning, and the brittle clays

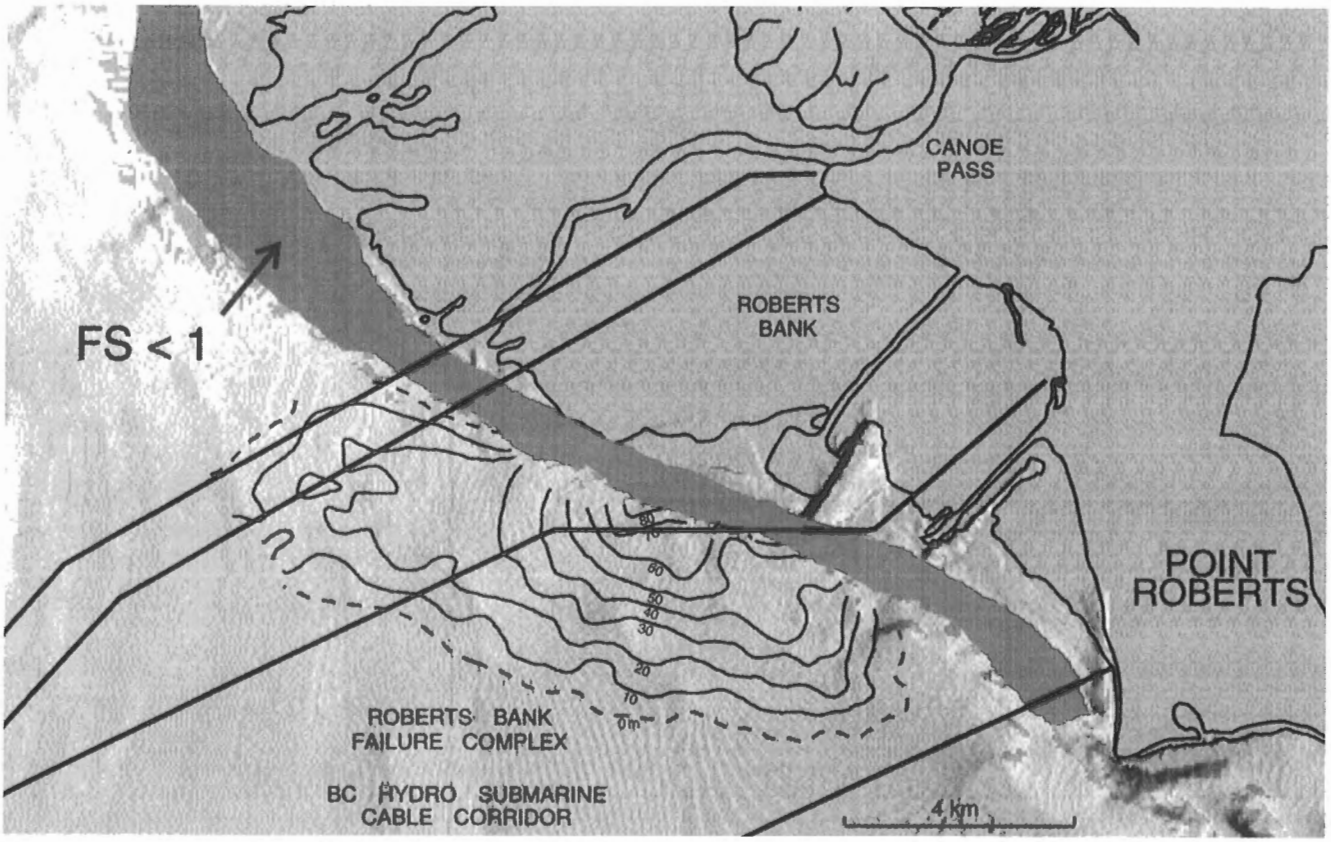

Figure 9. *Area of the Roberts Bank slope where the post-failure static factor of safety against sliding is less than 1, assuming widespread cyclic liquefaction. The calculated depth of the failure surface is 4 to 5 m over the upper Roberts Bank slope if it is assumed that the large-strain undrained shear strength is 0.06 times the effective vertical stress. This assumption is supported by observations of very low cone penetration resistance and shear-wave velocity in soundings at the break in slope. Deformations involve lateral spreading and may involve flow sliding within the B.C. Hydro submarine cable corridor. Isopach map shows acoustic thickness of Roberts Bank Failure Complex (after Hart and Olynyk (1994)).*

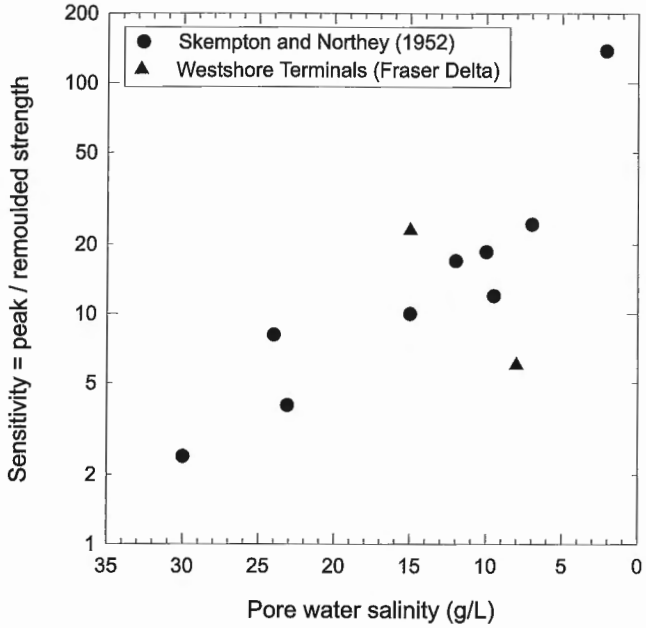

Figure 10. *Relation between pore water salinity and soil sensitivity for various leached marine clays (data from Skempton and Northey, 1952) and moderately sensitive clayey silts from the base of the Fraser delta sequence (borehole FD95S1, 106-109 m).*

transform into a viscous fluid. The zone of failure generally expands into intact portions of the destabilizing soil mass, and affected areas can be extensive.

Moderately sensitive, marine silty clays and clayey silts lie at the base of the Fraser delta sediment sequence (Fig. 11; Christian et al., 1995). These sediments overlie Pleistocene strata and were deposited in earliest Holocene time before being buried by the prograding delta.

The stability of this unit is a concern. Geophysical logging of deep boreholes on the delta plain has demonstrated that there is freshwater within the sediments and that, locally, there are artesian conditions within the underlying Pleistocene deposits (Christian et al., 1995; Dallimore et al., 1995; Ricketts, 1998). Geotechnical investigations during construction of the Annacis Island Bridge showed that excess pore pressures exist at the base of the Holocene sequence at the head of the Fraser delta (Bazett and McCammon, 1986). Low-plasticity clayey silts below a depth of 106 m in a deep borehole drilled at the Roberts Bank Deltaport have low to moderate sensitivities (5 to 20), corresponding to marine muds possessing a pore-water salinity of 5 to 15 g/L (Fig. 12). Chloride ions may have been leached from clay minerals in these sediments by upwelling groundwater, leading to an induced moderate sensitivity and a high strain-softening potential.

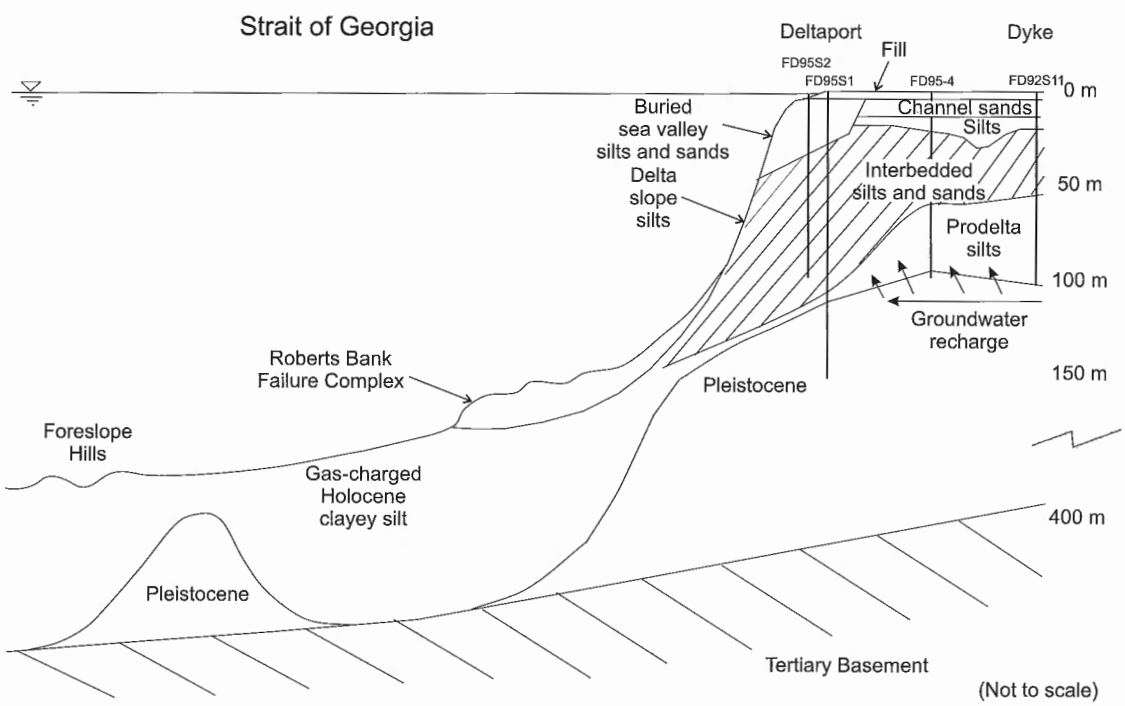

Figure 11. *Diagrammatic geological section through Roberts Bank in the vicinity of the Deltaport. Key stratigraphic elements are shown in relation to the failure complex at the base of the delta slope. Boundaries are schematic and are based on scant deep-borehole and CPT sounding information, supported by high-resolution reflection profiles.*

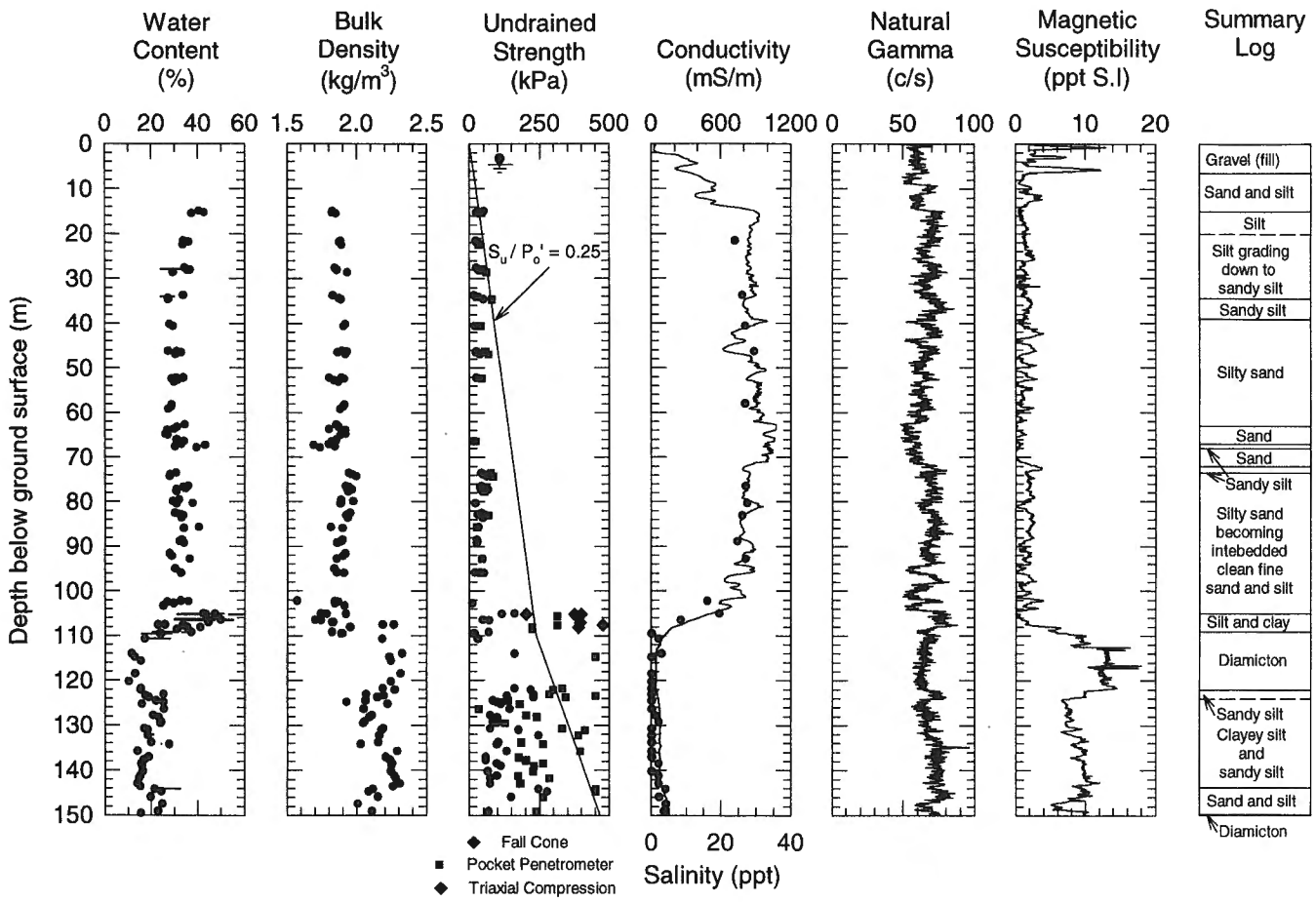

Figure 12. Geotechnical and geophysical logs for borehole FD95S1 at the Deltaport on Roberts Bank. Holocene sands and silts overlie a thin clay unit beginning at a depth of 106 m. Pleistocene strata occur below 109 m. The low salinities within the fine-grained unit at the base of the Holocene sequence may be the result of upward migration of fresh groundwater from Pleistocene deposits.

An important consequence of the identification of sensitive sediments beneath the Fraser delta slope is that dynamic earthquake loading may result in strain softening at depth, which could, in turn, trigger a more widespread progressive failure, potentially destabilizing overlying sediments. This mechanism should be considered in future stability analyses as a distinct process from gravity-induced creep deformation of the lower delta slope.

CONCLUSION

Areas of slope instability at the front of the Fraser delta have been identified through a major collaborative effort involving government, universities, and industry, using a variety of state-of-the-art geophysical and geotechnical methods. This work has shown that retrogressive flow slides occur at the crest of the delta independently of earthquakes and may involve progressive failure in underlying metastable marine sediments. The findings of this research assist in evaluating the potential impact of mass movements on key installations, including seafloor electrical-transmission cables and port facilities, as well as providing data for modelling the initiation of slide-generated tsunamis.

Slope instability near the river mouth is linked to reductions in shear strength during extremely low tides, gas-compressibility effects resulting from decomposition of organic material, and high static shear stresses within the delta slope. The high collapse potential of river-mouth sands is due to rapid sedimentation and a lack of time for consolidation. Because the sediments are loose in their intact state, post-failure deformations tend to be uncontrolled once liquefaction is triggered. Areas most prone to large-scale failure during a major earthquake are steeper slopes near the crest of the delta, especially near the river mouth.

The existence of fine-grained, moderately sensitive sediments at the base of the Fraser delta sequence has been verified through deep geological and geotechnical investigations. These sediments may play an important role in static and cyclic slope stability, because of their large-strain shear-strength capacity and the existence of underlying artesian pressures. The Foreslope Hills occur downslope from these

sensitive sediments and are a product of large-scale slope instability. GSC research has identified compressional creep-folding of weak sediments in advance of the prograding delta as the most likely explanation for the Foreslope Hills, although other mechanisms cannot be entirely discounted.

The existence of a large failure complex at the base of Roberts Bank slope underscores the need for further research into the effects of dynamic loading on the stability of metastable sediments underlying the delta slope. The origin of the Roberts Bank Failure Complex is uncertain; several processes may have been active simultaneously and it is not clear which might have dominated. The geomorphology of the failure complex, however, is suggestive of a prolonged period of flow sliding off the mouth of a former large river distributary.

Future static movements on the Fraser delta slope could be overshadowed by the effects of a major local earthquake, with catastrophic consequences for sensitive facilities at the delta front. Improved understanding of both the physical processes that operate at the delta front and the stability of the deltaic sediments will permit the importance of naturally occurring progradation and recession of the delta to be evaluated against the more extreme threat posed by strong shaking and seismic liquefaction.

ACKNOWLEDGMENTS

We thank P.A. Monahan for CPT-based interpretations, M. Johns for micropaleontological analyses, I. Frydecky for navigational support, R. Macdonald, R. Good, and R. Burns for downhole geophysical testing, and J. Harries for interpretations of shear-wave anisotropy. An early version of this paper was reviewed by S.R. Dallimore and N.R. Morgenstern. The authors are grateful to J.J. Clague for helpful constructive criticism. Financial support was provided by the Panel for Energy Research and Development (PERD) and the British Columbia Hydro and Power Authority.

REFERENCES

Atkins, R.J. and Luternauer, J.L.
1991: Re-evaluation of slope failure volume estimates involving 3D computer graphics for the Fraser River delta front, British Columbia; in Current Research, Part E, Geological Survey of Canada, Paper 91-1E, p. 59-65.

Bazett, D.J. and McCammon, N.R.
1986: Foundations of the Annacis cable-stayed bridge; Canadian Geotechnical Journal, v. 23, p. 458-471.

Chillarige, A.R.V., Morgenstern, N.R., Robertson, P.K., and Christian, H.
1995: Characterization of Fraser River delta sand; in Proceedings, 48th Canadian Geotechnical Conference, Vancouver, British Columbia, v. 2, p. 711-720.
in press a: Seabed instability due to flow liquefaction in the Fraser River delta; Canadian Geotechnical Journal.

Chillarige, A.R.V., Robertson, P.K., Morgenstern, N.R., and Christian, H.A.
in press b: Evaluation of in-situ state of Fraser River delta sand; Canadian Geotechnical Journal.

Chillarige, A.R.V., Robertson, P.K., Morgenstern, N.R., Christian, H.A., and Woeller, D.J.
1994: Evaluation of wave effects on seabed instability in the Fraser River delta; in Proceedings, 47th Canadian Geotechnical Conference, Halifax, Nova Scotia, p. 186a-186j.

Christian, H.A. and Woeller, D.J.
1996: Investigation of spontaneous liquefaction flow slides at the margin of the Fraser River delta, Vancouver, British Columbia; in Proceedings, 2nd International Congress on Environmental Geotechnics, Osaka, Japan, v. 1, p. 337-342.

Christian, H.A., Barrie, J.V., MacDonald, R., Monahan, P.A., Hunter, J.A., and Luternauer, J.L.
1995: Slope instability on Roberts Bank, Fraser River delta, Vancouver, British Columbia; in Proceedings, 48th Canadian Geotechnical Conference, Vancouver, British Columbia, v. 2, p. 937-946.

Christian, H.A., Mulder, T., Courtney, R.C., Mosher, D.C., Barrie, J.V., Currie, R.G., Olynyk, H.W., and Monahan, P.A.
1994a: Slope instability on the Fraser River delta foreslope, Vancouver, British Columbia; in Proceedings, 47th Canadian Geotechnical Conference, Halifax, Nova Scotia, p. 155-165.

Christian, H.A., Woeller, D.W., Weemes, I., and Robertson, P.K.
1994b: Use of SASW and SCPT to evaluate liquefaction potential of the Fraser delta foreslope, Vancouver, British Columbia; in Proceedings, 47th Canadian Geotechnical Conference, Halifax, Nova Scotia, p. 166-175.

Clague, J.J. and Bobrowsky, P.T.
1994: Evidence for a large earthquake and tsunami 100-400 years ago on western Vancouver Island, British Columbia; Quaternary Research, v. 41, p. 176-184.

Clague, J.J., Luternauer, J.L., and Hebda, R.J.
1983: Sedimentary environments and postglacial history of the Fraser Delta and lower Fraser Valley, British Columbia; Canadian Journal of Earth Sciences, v. 20, p. 1314-1326.

Clague, J.J., Luternauer, J.L., Pullan, S.E., and Hunter, J.A.
1991: Postglacial deltaic sediments, southern Fraser River delta, British Columbia; Canadian Journal of Earth Sciences, v. 28, p. 1386-1393.

Currie, R.G. and Mosher, D.C.
1996: Swath bathymetric surveys in the Strait of Georgia, British Columbia, Canada; in Current Research 1996-E, Geological Survey of Canada, p. 33-40.

Dallimore, S.R., Edwardson, K.A., Hunter, J.A., Clague, J.J., and Luternauer, J.L.
1995: Composite geotechnical logs for two deep boreholes in the Fraser River delta, British Columbia; Geological Survey of Canada, Open File 3018, 2 sheets.

de Mulder, E.F.J. and Westerhoff, W.E.
1985: Geology; in The Netherlands Commemorative Volume (Proceedings, 11th International Conference on Soil Mechanics and Foundation Engineering, San Francisco, California), (ed.) E.H. de Leeuw; The Netherlands Member Society, Beverwijk, Netherlands, p. 19-28.

Hamilton, T.S.
1991: Seismic stratigraphy of unconsolidated sediments in the central Strait of Georgia: Hornby Island to Roberts Bank; Geological Survey of Canada, Open File 2350, 9 sheets.

Hamilton, T.S. and Wigen, S.O.
1987: The Foreslope Hills of the Fraser Delta: implications for tsunamis in Georgia Strait; International Journal of the Tsunami Society, v. 5, p. 15-33.

Hansbo, P., Larsson, R., Runesson, K., and Wiberg, N-E.
1985: On the behaviour of natural slopes with emphasis on progressive failure; in Proceedings, 11th International Conference on Soil Mechanics and Foundation Engineering, Rio De Janeiro, Brazil, v. 2, p. 757-760.

Harris, J.B., Hunter, J.A., Luternauer, J.L., and Finn, W.D.L.
1995: Site amplification modelling of the Fraser Delta, British Columbia; in Proceedings, 48th Canadian Geotechnical Conference, Vancouver, British Columbia, v. 2, p. 947-962.

Hart, B.S.
1993: Large-scale in situ rotational failure on a low-angle delta slope: the Foreslope Hills, Fraser Delta, British Columbia, Canada; Geo-Marine Letters, v. 13, p. 219-226.

Hart, B.S. and Olynyk, H.W.
1994: The Roberts Bank failure deposit, Fraser River delta, British Columbia; Terra Surveys Ltd., report to the Geological Survey of Canada, Contract XSA93-00030-(603) 1A, 29 p.

Hart, B.S., Prior, D.B., Barrie, J.V., Currie, R.G., and Luternauer, J.L.
1992a: A river mouth submarine channel and failure complex, Fraser Delta, Canada; Sedimentary Geology, v. 81, p. 73-87.

Hart, B.S., Prior, D.B., Hamilton, T.S., Barrie, J.V., and Currie, R.G.
1992b: Patterns and styles of sedimentation, erosion and failure, Fraser Delta slope, British Columbia; in Geotechnique and Natural Hazards; BiTech Publishers, Vancouver, British Columbia, p. 365-372.

Hungr, O.
1993: Sand Heads Lightstation risk assessment; Thurber Engineering Ltd., report to Canadian Coast Guard, Vancouver, British Columbia, 32 p.

Hunter, J.A., Woeller, D.J., and Luternauer, J.L.
1991: Comparison of surface, borehole and seismic cone penetrometer methods of determining the shallow shear wave velocity structure in the Fraser River delta, British Columbia; in Current Research, Part A, Geological Survey of Canada, Paper 91-1A, p. 23-26.

Luternauer, J.L. and Finn, W.D.L.
1983: Stability of the Fraser River delta front; Canadian Geotechnical Journal, v. 20, p. 603-616.

Luternauer, J.L., Clague, J.J., Hunter, J.A.M., Pullan, S.E., Roberts, M.C., Woeller, D.J., Kostaschuk, R.A., Moslow, T.F., Monahan, P.A., and Hart, B.S.
1993: The Fraser River delta, architecture, geological dynamics and human impact; in Deltas of the World, (ed.) R. Kay; American Society of Civil Engineers, New York, New York, p. 99-113.

Mathewes, R.W. and Clague, J.J.
1994: Detection of large prehistoric earthquakes in the Pacific Northwest by microfossil analysis; Science, v. 264, p. 688-691.

Mathews, W.H. and Shepard, F.P.
1962: Sedimentation of Fraser River delta, British Columbia; American Association of Petroleum Geology Bulletin, v. 46, p. 1416-1438.

McKenna, G.T. and Luternauer, J.L.
1987: First documented large failure at the Fraser River delta front, British Columbia; in Current Research, Part A, Geological Survey of Canada, Paper 87-1A, p. 919-924.

Monahan, P.A., Luternauer, J.L., and Barrie, J.V.
1993a: A delta plain "sheet" sand in the Fraser River Delta, British Columbia, Canada; Quaternary International, v. 20, p. 27-38.

Monahan, P.A., Luternauer, J.L., and Barrie, J.V. (cont.)
1993b: Subsurface mapping of the Fraser River delta: implications for delta front instability; in Proceedings, 4th Canadian Conference on Marine Geotechnical Engineering, St. John's, Newfoundland, v. 2, p. 451-463.

Mosher, D.C. and Hamilton, T.S.
1998: Morphology, structure, and stratigraphy of the Offshore Fraser delta and adjacent Strait of Georgia; in Geology and Natural Hazards of the Fraser River Delta, British Columbia, (ed.) J.J. Clague, J.L. Luternauer, and D.C. Mosher; Geological Survey of Canada, Bulletin 525, this volume.

Pryor, W.A.
1973: Permeability-porosity patterns and variations in some Holocene sand bodies; American Association of Petroleum Geology Bulletin, v. 57, p. 162-189.

Ricketts, B.D.
1998: Groundwater flow beneath the Fraser River delta, British Columbia; a preliminary model; in Geology and Natural Hazards of the Fraser River Delta, British Columbia, (ed.) J.J. Clague, J.L. Luternauer, and D.C. Mosher; Geological Survey of Canada, Bulletin 525, this volume.

Satake, K., Shimazaki, K., Tsuji, Y., and Ueda, K.
1996: Time and size of a giant earthquake in Cascadia inferred from Japanese tsunami records of January 1700; Nature, v. 379, p. 246-249.

Shepard, F.P.
1967: Delta-front diapirs off Magdalena River, Columbia, compared with hills off other large deltas; Transactions, Gulf Coast Association of Geological Societies, v. 17, p. 316-325.

Skempton, A.W. and Northey, R.D.
1952: The sensitivity of clays; Geotechnique, v. 3, p. 30-53.

Terzaghi, K.
1956: Varieties of submarine slope failure; Proceedings of the 8th Texas Conference on Soil Mechanics and Foundation Engineering, University of Texas, Austin, Bureau of Engineering Research, Special Publication No. 29, 41 p.
1962: Discussion [of Sedimentation of Fraser River delta, British Columbia, by W.H. Mathews and F.P. Shepard]; American Association of Petroleum Geologists Bulletin, v. 46, p. 1438-1443.

Tiffin, D.L., Murray, J.W., Mayers, I.R., and Garrison, R.E.
1971: Structure and origin of Foreslope Hills, Fraser delta, British Columbia; Canadian Petroleum Geology Bulletin, v. 19, p. 589-600.

Watts, B.D., Seyers, W.C., and Stewart, R.A.
1992: Liquefaction susceptibility of Greater Vancouver area soils; in Geotechnique and Natural Hazards; BiTech Publishers, Vancouver, British Columbia, p. 145-157.

Seismic liquefaction potential of the southwestern margin of the Fraser River delta

H.A. Christian[1]

Christian, H.A., 1998: Seismic liquefaction potential of the southwestern margin of the Fraser River delta; in Geology and Natural Hazards of the Fraser River Delta, British Columbia, (ed.) J.J. Clague, J.L. Luternauer, and D.C. Mosher; Geological Survey of Canada, Bulletin 525, p. 231–240.

Abstract: Geotechnical investigations at the southwestern margin of the Fraser delta indicate that seismic liquefaction failure is possible and might result in lateral spreading, slope flattening, and flow sliding. Comparisons were made between cone-derived parameters and cyclic stress ratios predicted from empirical relationships between earthquake magnitude, peak horizontal acceleration, and overburden stress. Loose sandy silt and sand at the crest of the delta slope appear susceptible to cyclic liquefaction to a depth of about 25 m below the seafloor. Post-liquefaction deformations could potentially include lateral spreading of the area behind the crest of the slope, as well as localized flow sliding at and immediately below the crest of Roberts Bank slope.

Résumé : Les recherches géotechniques menées sur la bordure sud-ouest du delta du Fraser indiquent qu'il est possible qu'une rupture par liquéfaction d'origine sismique se produise et qu'elle provoque un déplacement latéral de matériaux, un aplatissement du talus et des glissements-coulées. Des comparaisons ont été faites entre, d'une part, les paramètres mesurés à l'aide d'un pénétromètre à pointe conique et, d'autre part, les rapports de contraintes cycliques prévus à partir de relations empiriques entre la magnitude des séismes, l'accélération horizontale maximale et le poids des couches sus-jacentes. Le silt sableux et le sable non consolidés accumulés au niveau de la crête du talus semblent être propices à une liquéfaction cyclique jusqu'à une profondeur d'environ 25 mètres sous le plancher océanique. Une liquéfaction pourraient, entre autres, provoquer un déplacement latéral des matériaux derrière la crête du talus et déclencher des glissements-coulées juste au-dessus ou au niveau de la crête du talus du banc Roberts.

[1] Geological Survey of Canada, P.O. Box 1006, Dartmouth, Nova Scotia B2Y 4A2

INTRODUCTION

The Fraser River delta is located in an area of moderate to high seismicity and supports a number of facilities that are critical to the economy of British Columbia, including port facilities and submarine transmission cables that supply electrical power to southern Vancouver Island (Fig. 1). Facilities at the western margin of the delta plain could be damaged during a moderate to large earthquake by submarine landslides or by a loss of foundation stability resulting from earthquake-induced liquefaction and limited lateral spreading (Christian et al., 1998). Static gravitational forces on the delta slope impose an additional load which could increase post-liquefaction displacements, resulting in uncontrolled flow slides in soils that have a high potential for strain softening when subjected to cyclic loading. ('Soil' is used in this paper in an engineering sense; i.e. all types of unconsolidated sediments overlying bedrock.)

Cyclic liquefaction arising from strong earthquake shaking has been recognized for nearly twenty years as a major hazard on the onshore part of the Fraser delta (Byrne, 1978; Luternauer and Finn, 1983; Byrne and Anderson, 1987; Watts et al., 1992). The problem was first addressed by Byrne and Anderson (1987) who, on behalf of the Municipality of Richmond, made recommendations to the geotechnical and structural engineering community on seismic criteria used in the design of foundations on the delta. Watts et al. (1992) summarized the likely impacts of earthquake shaking on the various types of soils constituting the Fraser delta, and identified distributary-channel sands as being particularly susceptible to cyclic liquefaction. Until very recently, however, little information existed on the geology and geotechnical characteristics of sediments on the delta slope; and the possibility that these deposits could also liquefy during a strong earthquake had not been fully evaluated.

The Geological Survey of Canada recently conducted field investigations to evaluate the susceptibility of the deltaic deposits to seismic liquefaction. Key nearshore and offshore

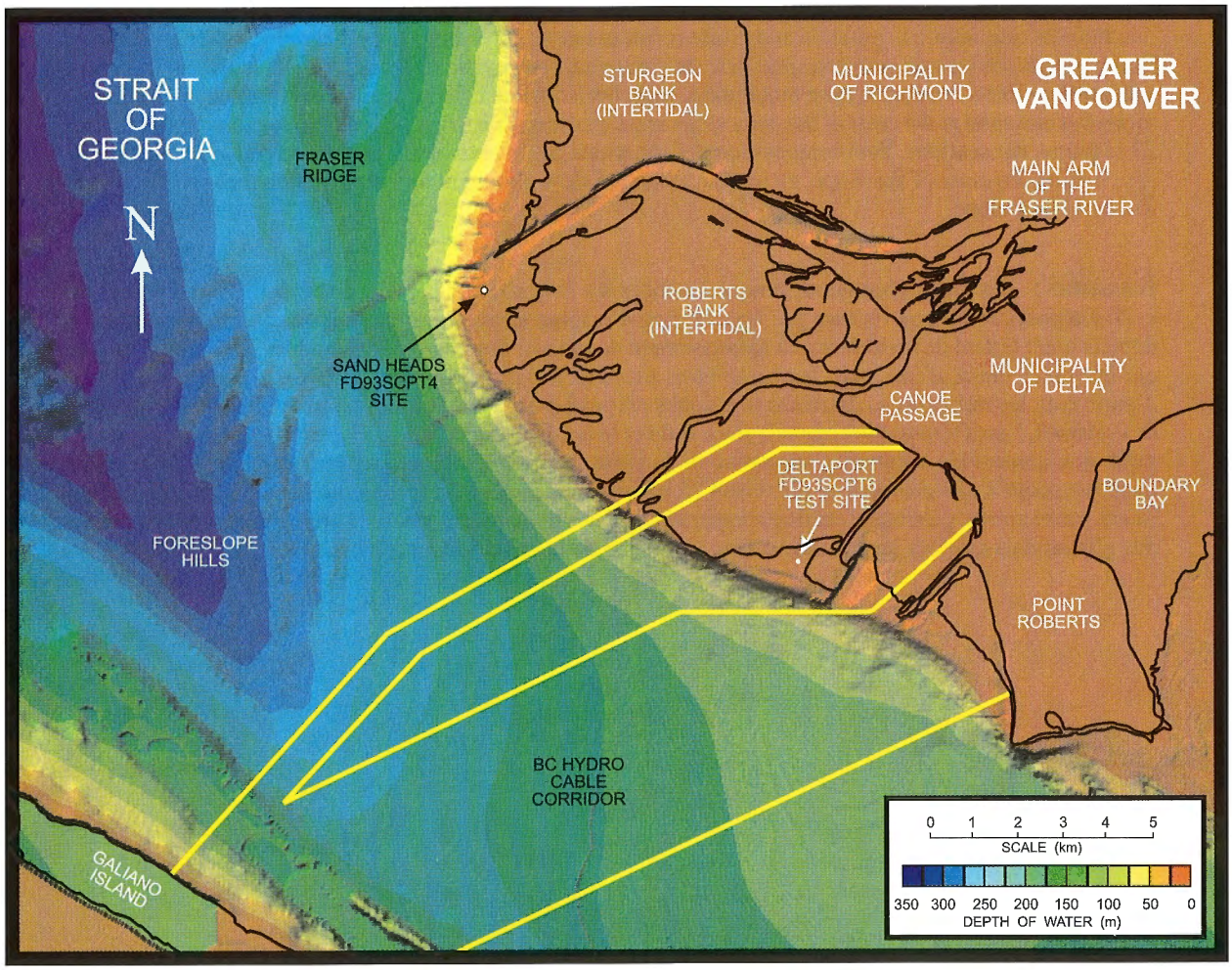

Figure 1. *Shaded-relief bathymetric map of the southern Strait of Georgia, showing the southwestern margin and slope of the Fraser River delta and locations of geotechnical investigation sites at Sand Heads and Roberts Bank Deltaport.*

sites at the southwestern delta front (Fig. 1) were investigated between 1993 and 1995, after geophysical surveys showed these areas to be potentially unstable (Hart et al., 1992; Christian et al., 1994a, 1995). The work involved wash and rotary borehole sampling; electric resistivity and seismic cone penetration testing; downhole, crosshole, and surface shear-wave measurements; and piezometric monitoring of the groundwater regime. This paper presents the results of this research, focusing on the engineering response of the upper deltaic deposits to strong seismic shaking.

SETTING

The Fraser River delta extends southwest and west from a gap in the Pleistocene uplands at New Westminster, to the shores of the Strait of Georgia and Boundary Bay. The delta has been built entirely during the last 10 000 years, following the last glaciation (Clague et al., 1983). At the extreme southwestern margin of the delta, which is the area of concern in this paper, are the B.C. Ferry Terminal, Roberts Bank Deltaport, and one of the two submarine hydroelectric transmission and telecommunication cable corridors connecting the British Columbia mainland with Vancouver Island (Fig. 1). The delta slope, which lies immediately seaward of the Ferry Terminal and the Deltaport, is steepest (averaging 8 to 15°) near its crest, in 20 to 80 m of water, and is nearly flat at its base, at depths ranging from 100 m in the south to 350 m in the north.

The uppermost soils beneath the Fraser delta plain are silt, sand, and peat deposited in tidal flat, floodplain, and bog environments. These soils range in thickness from about 15 m near the apex of the delta to 5 m at the western margin of the dyked floodplain. The tidal-flat and floodplain deposits are underlain by a laterally extensive sheet of distributary-channel sand up to 30 m thick, which has an erosional base and locally comprises two or more fining-upward sequences (Monahan et al., 1993). The sand was deposited in abandoned channels as the Fraser River migrated across the delta plain, extensively reworking older deltaic deposits. The sand sheet is discontinuous and locally absent at the western margin of the delta, and extensive areas of soft, intertidal, sandy and clayey silt are preserved outside present distributary channels, seaward of the dykes on Roberts and Sturgeon banks. Historic training of these channels has halted the natural shifting of the river and substantially altered sedimentation at the delta front. Sedimentation is now restricted largely to the vicinity of the mouths of active distributary channels, which are areas of chronic instability.

METHODS

Laboratory cyclic shear test results are strongly influenced by the initial state of the soil (characterized by the void ratio, effective confining stress, and soil structure), the intensity and duration of cyclic loading (the cyclic shear-stress ratio and the number of cycles of strong motion), and material characteristics such as grain size and fines content (Been et al., 1986; Robertson and Wride, 1997).

It is generally difficult to obtain representative samples of sandy soils in an undisturbed state, therefore various methods of in situ testing have been developed to better characterize such soils and determine their susceptibility to cyclic liquefaction (Robertson and Campanella, 1985). The most widely used of these in situ methods are the standard penetration test (SPT), cone penetration test (CPT), and acoustic-profiling techniques such as the seismic cone penetration test (SCPT), spectral analysis of surface waves (SASW), and crosshole, uphole, and downhole shear-wave tests. All these methods have been applied on the Fraser delta by the Geological Survey of Canada as part of a collaborative seismic liquefaction assessment involving university and industry partners.

Evaluation of cyclic liquefaction potential from cone penetration resistance

The cone penetration test was chosen as the preferred method for evaluating resistance to cyclic liquefaction in loose sandy soils at the western margin of the Fraser delta. CPT data were supplemented with data acquired through in situ shear-wave velocity testing, which are reported elsewhere (Christian et al., 1994b).

Figure 2 is a drawing of a typical cone penetrometer, showing various sensors (Fig. 2). The cone is pushed vertically into the ground at a constant rate using a drill rig, which is mounted on a floating barge for offshore investigations (Christian and Woeller, 1996). The cone penetrometer has load cells which measure penetration resistance ahead of, and around, the tip, as well as skin friction on a shaft-mounted sleeve. A transducer measures soil pore pressure through a glycerin-filled hydraulic filter mounted immediately behind the tip. The cone also has tilt sensors to monitor vertical deviation during penetration. Seismic cone penetrometers are fitted with horizontally or vertically mounted geophones, which are used to measure the velocity of shear waves generated at the ground surface (Robertson et al., 1986).

Charts have been developed relating penetration resistance (q_t), sleeve friction (f_s or F_s), and pore pressure (U) response to many useful geotechnical parameters (Robertson, 1995). Cone resistance and shear-wave velocity-based techniques are now widely accepted parameters for evaluating cyclic liquefaction potential in sandy soils. Cone penetration resistance is measured by the load cell behind the cone tip, and is related to soil shear strength, density, and grain size. Robertson (1995) normalized cone resistance (q_{tIN}) to account for overburden stress effects, allowing an evaluation of liquefaction susceptibility that is independent of burial depth and, hence, confining stress. Sleeve friction is measured by the load cell mounted on the cone sleeve and is an excellent indicator of material type and stiffness; this parameter is low in sand and high in plastic clay. Pore pressure is measured through a filter stone located immediately behind the cone tip and senses changes in soil type, fines content, stress history, plasticity, and equilibrium groundwater pressure. Friction ratio (R_f) is obtained by dividing sleeve friction by cone resistance and is expressed in percent. Friction ratio can also be normalized for overburden stress and expressed in dimensionless form (Robertson, 1995). Differential

pore-pressure ratio (DPPR) is computed from measured and hydrostatic pore pressures, and is used to classify soils. Classification charts based on these parameters are useful in subdividing a soil profile into stratigraphic units with different engineering properties (Campanella and Robertson, 1982; Robertson, 1995).

Cone penetration resistance is related to the cyclic resistance ratio (CRR), which at the point of cyclic liquefaction is equivalent to the cyclic stress ratio (CSR) imposed by earthquake shaking. Byrne and Anderson (1987) recommended that an earthquake of moment magnitude (M) = 7.5, with 15 cycles of strong motion and a peak horizontal (firm-ground) acceleration of 0.21 g (g = acceleration of gravity), be used in calculating CSR for engineering design in Richmond. This idealized ('design') earthquake is estimated to have a return period of 475 years, or an annual probability of 0.0021, based on empirical data relating earthquake magnitude to frequency of occurrence (Rogers, 1988). Seed and Idriss (1971) provided an empirical expression for estimating cyclic stress ratios developed during strong earthquake shaking:

$$CSR=\frac{\tau_{eq}}{\sigma_o'}=0.65\frac{\sigma_o}{\sigma_o'}a_{max}r_d$$

where τ_{eq} is the cyclic shear stress induced by earthquake shaking, σ_o and σ_o' are the total and effective overburden stresses, respectively, a_{max} is the peak ground acceleration, and r_d is a site-dependent reduction factor that accounts for increasing soil stiffness with depth.

A cyclic liquefaction correlation developed by Robertson and Wride (1997) is shown in Figure 3. The data in this figure were collected from level-ground sites that experienced cyclic liquefaction during an M = 7.5 earthquake (manifested as surface cracking, sand boils, or toppled structures). The empirical correlation shown in Figure 3 is based on data from sampled intervals of clean sand having no fines. Seed et al. (1985) modified the position of the CSR curve to account for lower penetration resistances encountered in silty sands, for fine contents ranging from 5 to 35%. Interpretation of cyclic liquefaction potential in silty sands requires that this correction be made to arrive at an equivalent clean sand resistance ratio, otherwise estimates of CRR will be overly conservative.

For soils with more than about 35% fines, cone penetration resistance is a poor measure of density. Development of undrained conditions around the cone tip greatly reduces the penetration resistance, and applied corrections are larger than the measurements themselves. As a consequence, other methods

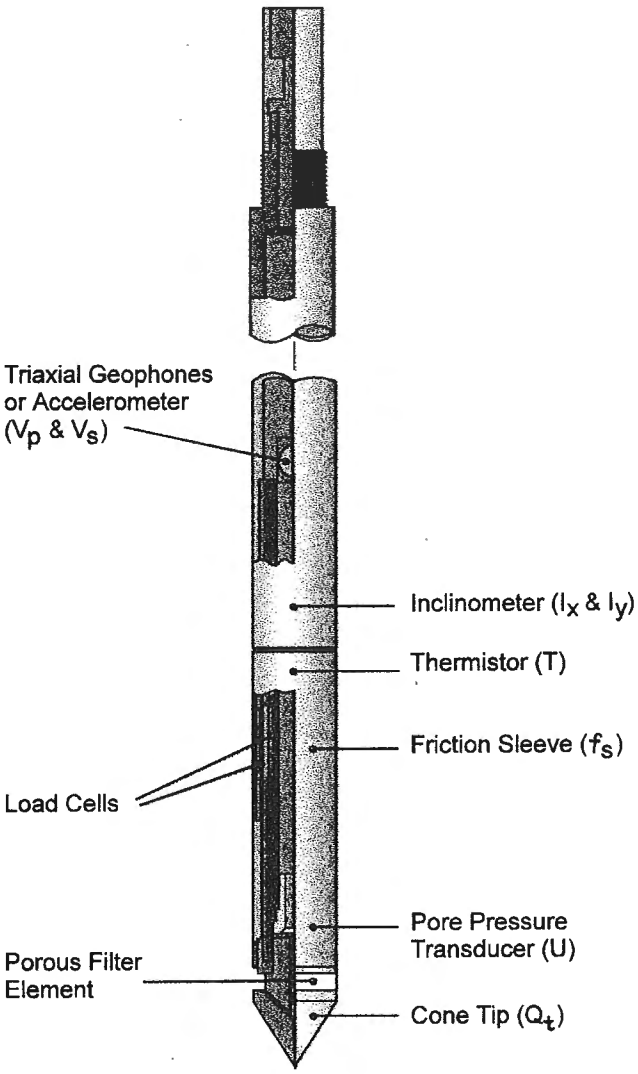

Figure 2. Schematic drawing of a cone penetrometer, showing its sensors (figure courtesy of ConeTec Investigations Ltd.).

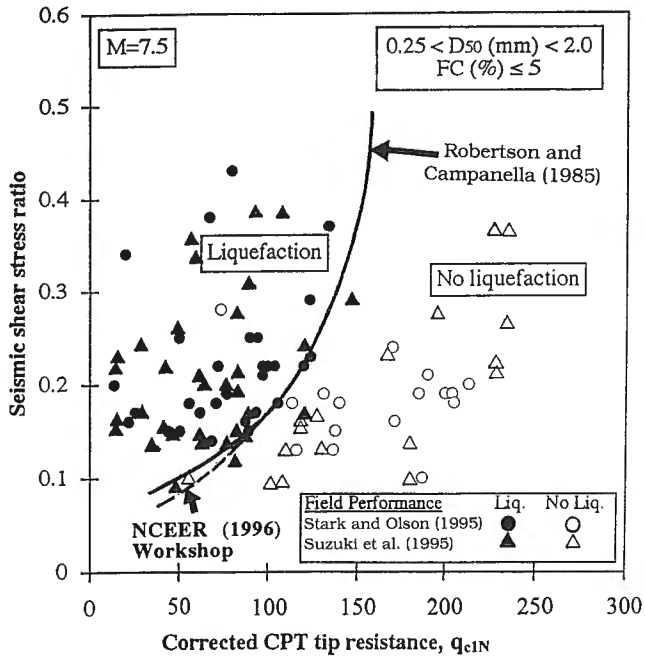

Figure 3. Relationship between cyclic stress ratio and normalized cone penetration resistance, q_{t1N}, for clean sands under level-ground conditions (modified from Robertson and Wride, 1997).

of evaluating cyclic liquefaction potential are used (Marcuson et al., 1990). Recently, correlations have been made between fines content and CPT-based soil classifications, allowing more accurate adjustment of normalized cone penetration resistance to an equivalent clean-sand value, for comparison to the expected CSR for a particular design earthquake (Robertson and Wride, 1997).

A stepwise interpretive process is followed when using CPT data to evaluate cyclic liquefaction potential (Robertson and Wride, 1997). Fines content is estimated from normalized cone resistance and normalized friction ratio, and is then used to correct the normalized cone resistance within silty intervals. The result is a normalized, equivalent, clean-sand cone resistance $(q_{tIN})_{cs}$. From $(q_{tIN})_{cs}$, maximum cyclic resistance ratio can be estimated for an earthquake of any magnitude. Values of CRR are obtained from the curve separating liquefied from non-liquefied soils, as suggested by the U.S. National Committee on Earthquake Engineering (Fig. 3), and these values are then compared to cyclic stress ratios induced by strong ground shaking (note that the seafloor is the datum for calculating CSR). Recent research has shown that $(q_{tIN})_{cs}$ can be an excellent indicator of flow-liquefaction potential in loose clean sands; specifically, strain softening has been observed in triaxial extension tests, coincident with equivalent normalized cone resistance values less than 50 (P.K. Robertson, pers. comm., 1997). (Flow liquefaction is a term used to describe collapse of a soil during shear failure, resulting in unlimited deformations. Such failures occur in very loose sediments where the post-failure shear strength is lower than static shear stresses imposed by gravity. Generally, collapsive failures on slopes steeper than about 6° change rapidly into flow slides which accelerate downslope and travel considerable distances.)

SEISMIC LIQUEFACTION POTENTIAL ON THE UPPER DELTA SLOPE

CPT data from the southwestern Fraser delta were first used to classify the soils, as suggested by Robertson (1995), and then used to estimate the fines content according to the recommendations of Robertson and Wride (1997). Results are for a CPT test (FD93SCPT4) carried out in 1993 at Sand Heads at the mouth of Main Channel of the Fraser River (Fig. 1) are shown in Figures 4 and 5. The soils at this site are some of the youngest deposits at the delta front and possess the lowest resistance to cyclic liquefaction. Results for a site near the Deltaport on southern Roberts Bank (FD93SCPT6), where the soils are estimated to be about 1000 years older, are presented in Figures 6 and 7. Detailed descriptions of the two

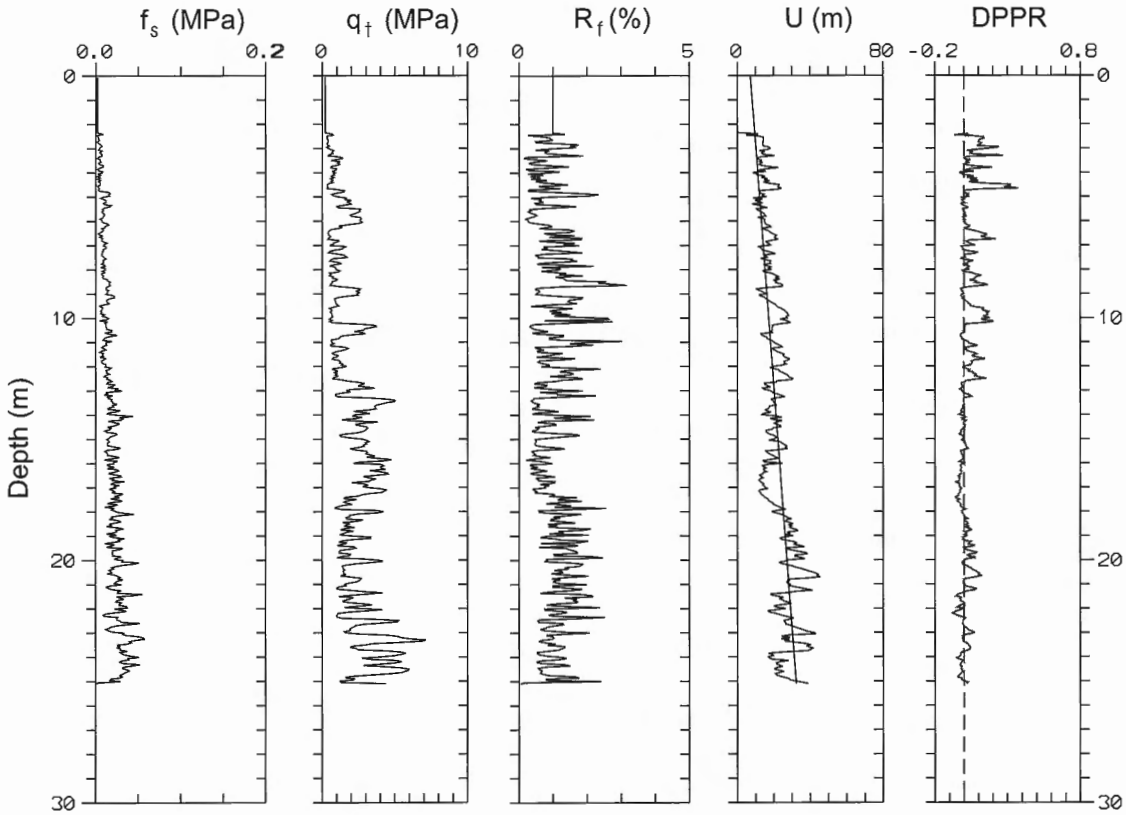

Figure 4. CPT data for the Sand Heads site (FD93SCPT4); f_s – sleeve friction, q_t – cone resistance, R_f – friction ratio, U – measured pore-water pressure, DPPR – differential pore-pressure ratio (DPPR). The soil sequence consists of interbedded, very loose to loose sand (fines content less than 5%) and non-plastic sandy silt. The low penetration resistances indicate that the soils are highly collapsible and could flow if liquefaction is triggered.

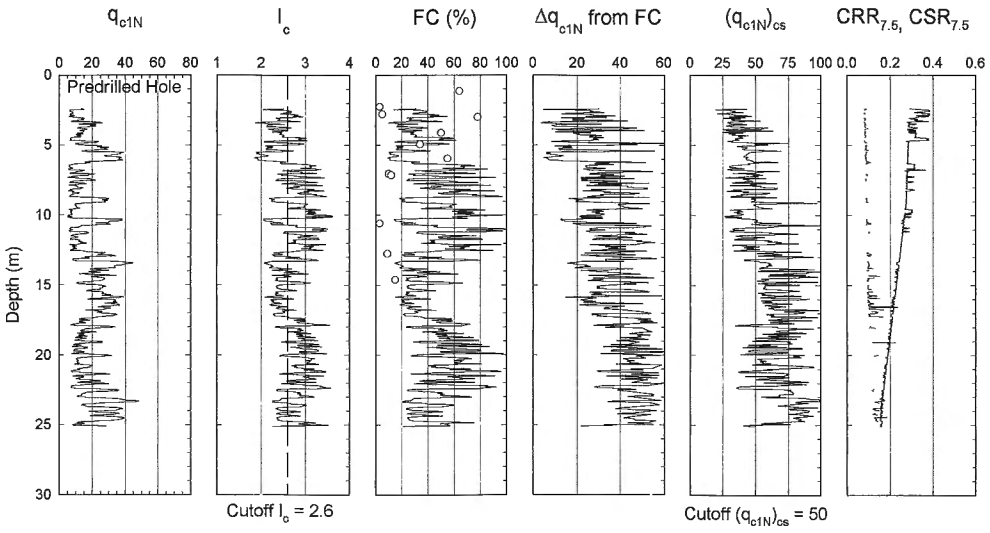

Figure 5. *Evaluation of cyclic liquefaction potential at the Sand Heads study site. Cone resistance was corrected for differences in fines content estimated from the soil-behaviour index (I_c); I_c was derived from CPT data. Fines contents obtained from grain size analysis of borehole samples (FC) are also plotted (open circles), for comparison with the I_c-based estimates. Intervals with fines contents greater than 35% cannot be analyzed using these methods and must be evaluated with specialized laboratory tests (dashed line indicates the analytical cutoff of $I_c > 2.6$). Cyclic resistance ratios ($CRR_{7.5}$) were not calculated for these finest portions of the soil sequence. The cyclic stress ratio for a M = 7.5 earthquake ($CSR_{7.5}$, shown as a solid line) is larger than the cyclic resistance ratio ($CRR_{7.5}$), suggesting that cyclic liquefaction can occur to a depth of at least 25 m below the seafloor.*

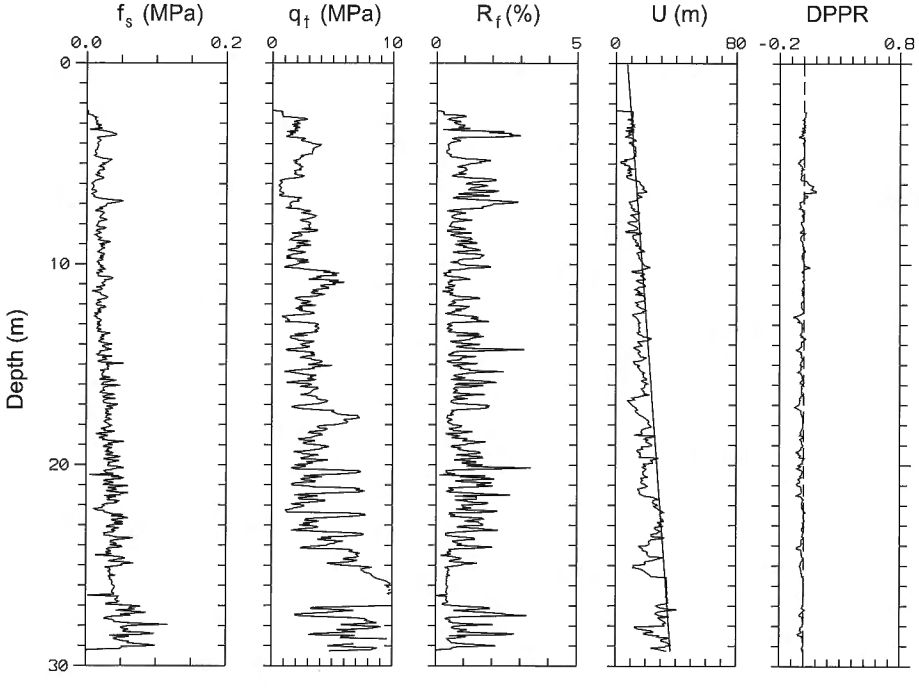

Figure 6. *CPT data for the Roberts Bank Deltaport site (FD93SCPT6); f_s – sleeve friction, q_t – cone resistance, R_f – friction ratio, U – measured pore-water pressure, DPPR – differential pore-pressure ratio (DPPR). The soil sequence consists of interbedded, loose silty sand and sandy silt, with some thin silt layers; a clean sand bed occurs at 5-7 m depth.*

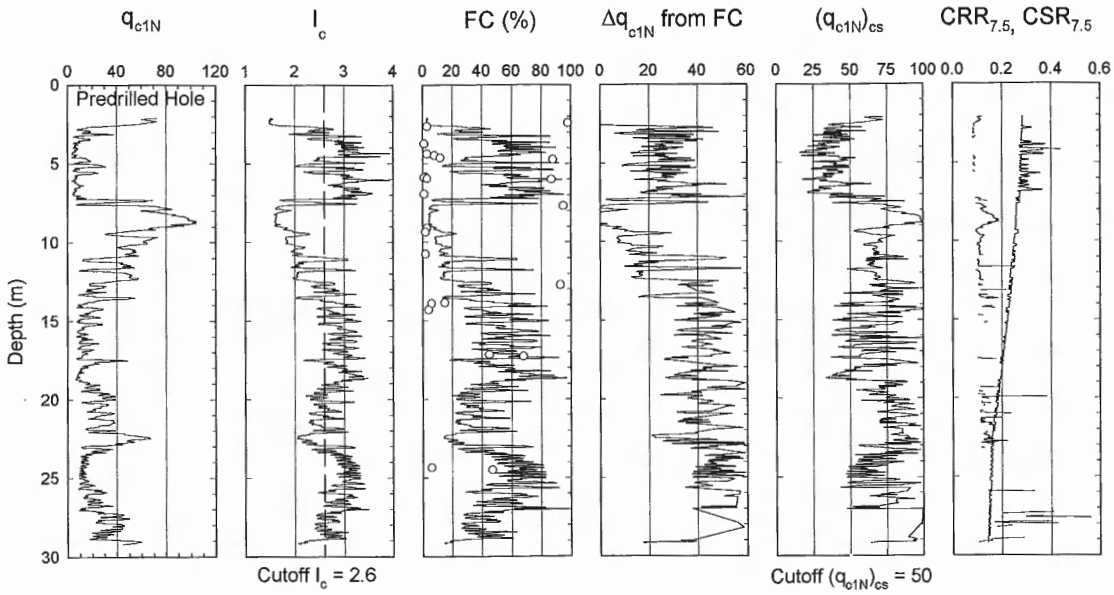

Figure 7. *Evaluation of cyclic liquefaction potential at the Roberts Bank Deltaport study site (see Fig. 5 caption and text for ame[illegible]al details). Cyclic liquefaction is indicated to a depth of about 23 m below the seafloor during the design earthquake.*

study sites can be found in a companion paper (Christian et al., 1998) and in Christian et al. (1997a). Predicted fines contents are shown in Figures 5 and 7 for comparison with grain-size data from samples obtained from mud-rotary boreholes close to the CPT sites. Parts of the soil sequence at both sites are sandy silt and silt; prediction of the cyclic liquefaction potential is limited to sandier portions of the sequence.

The sequence at Sand Heads comprises interlayered, thin-bedded silt and sand, and thick layers of clean, massive sand containing silt rip-up clasts. The massive sand layers are interpreted to be sediment gravity-flow deposits (P.A. Monahan, pers. comm., 1993) derived from adjacent slopes (Christian et al., 1998). The percentage of fines in sand beds, based on grain-size analysis, is generally less than 20% (Fig. 5).

The resistance to cyclic liquefaction at Sand Heads was found to be very low to a depth of at least 25 m; it is lower than the cyclic stress ratios induced by a M = 7.5 earthquake with a peak horizontal firm-ground acceleration of 0.22 g. A clean sand zone at 5 to 7 m depth gave $(q_{tlN})_{cs}$ values of less than 50, which is the threshold for flow liquefaction. Soils to a depth of about 13 m at this site are considered to be highly susceptible to flow liquefaction (Christian et al., 1997b).

CPT testing at the more southerly site adjacent to the Roberts Bank Deltaport showed a somewhat greater resistance to cyclic liquefaction and lesser threat of flow liquefaction. Fine contents of sandy layers range from 1 to 8%; in contrast, some silt beds contain more than 85% fines (Fig. 7). The soils at this site are susceptible to cyclic liquefaction to a depth of about 25 m below the seafloor but since $(q_{tlN})_{cs}$ values are greater than 50 through much of the sequence, flow liquefaction is not considered likely, except possibly within thin sandy beds at depths between 14 and 19 m. While the data suggest that flow liquefaction is unlikely, conditions may be worse in shallower water at the crest of the slope wherever there are fine sands. Preliminary investigations indicate, however, that the upper 10 to 30 m of the sequence in this area is loose silt and sandy silt, and that clean sand is largely absent near the seafloor. Flow-liquefaction is less likely to occur in such fine-grained sediments because of interparticle cohesive forces. Soft, cohesive soils yield plastically and do not suffer complete collapse unless they are brittle or otherwise metastable (sensitive).

POST-LIQUEFACTION LATERAL DISPLACEMENTS

The potential for flow liquefaction (essentially unlimited displacement) or cyclic liquefaction (limited displacement) can be evaluated from in situ test data, by comparing the present state of the soils to the threshold state for flow-liquefaction (Robertson and Wride, 1997). In addition, compilations of in situ test data from sites that have and have not liquefied during past earthquakes are useful for determining if a particular site can withstand strong shaking.

It is important to note that a soil may experience cyclic liquefaction during strong seismic shaking, but may not be loose enough to collapse and form a flowslide. Also, the static shear stress imposed by gravitational loading must be greater than the post-liquefied steady-state shear strength for a flowslide to develop. Flow liquefaction is not a concern on level ground, since shear stresses are always lower than the ultimate or steady state strength. Loose, cohesionless soils on

slopes steeper than about 6° can be expected to flow when liquefied. Limited lateral displacements may occur in denser deposits on both sloping or level ground.

While flow liquefaction appears to be possible over much of the upper delta slope, CPT data are scarce in water depths greater than 10 m, making this conclusion somewhat subjective. Sufficient data exist just landward of the crest of the slope, however, to undertake a preliminary analysis of potential lateral displacements arising from cyclic liquefaction. This is useful in evaluating possible minimum anticipated displacements and illustrates the importance of proximity to the delta slope.

Lateral spreading behind the slope crest on Roberts Bank

Loss of foundation-bearing capacity, differential settlement, and horizontal displacement due to lateral spreading are common consequences of cyclic liquefaction beneath flat or gently sloping sites that are underlain by saturated cohesionless soils. Lateral spreading occurs in response to both dynamic, earthquake-generated inertial forces and static gravitational forces acting on soil layers above and below liquefiable zones (Bartlett and Youd, 1992). Lateral spreads move in a downslope direction or towards a free face.

The empirical method of Bartlett and Youd (1992) can be used to estimate lateral-spreading displacements on level or gently sloping ground where the soils have sufficient resistance to prevent flow liquefaction. Bartlett and Youd (1992) compiled geotechnical data from sites at which lateral spreading has occurred during earthquakes and subjected them to a stepwise multiple-linear regression analysis to identify variables that correlate most strongly with horizontal ground displacement. These variables include earthquake magnitude (M), horizontal distance to energy source (R), height and geometry of the free face (W), ground slope (S), total thickness of loose, granular, liquefiable soils (T_{15}) (maximum of 15 m), average fines content within liquefiable layers (F_{15}), and average median grain size ($D50_{15}$). For sites with a free face, Bartlett and Youd (1992) give the following relation for horizontal ground displacement, D_H:

$$logD_H=A+BM+Clog(R)+DR+Elog(W)+Flog(T_{15})+Glog(100-F_{15})+HD50_{15}$$

where A = -16.3658, B = 1.1782, C = -0.9275, D = -0.0133, E = 0.6572, F = 0.3483, G = 4.5270, and H = -0.9224. The equation for gently sloping sites, where there is no free face, is:

$$logD_H=I+BM+Clog(R)+DR+Jlog(S)+Flog(T_{15})+Glog(100-F_{15})+HD50_{15}$$

where I = -15.7870, J = 0.4293, and the other constants are as above. Bartlett and Youd (1992) recommended that, where both sloping ground and a free face exist, they should be analyzed separately and the larger displacement used for hazard assessment.

These empirical equations were used to estimate the magnitude of displacements that might arise from cyclic liquefaction on southern Roberts Bank. Bathymetry in the vicinity of the Deltaport was taken from sounding charts (Swan Wooster Engineering, 1982). The effect of the free face presented by the Fraser delta slope was estimated by assuming an

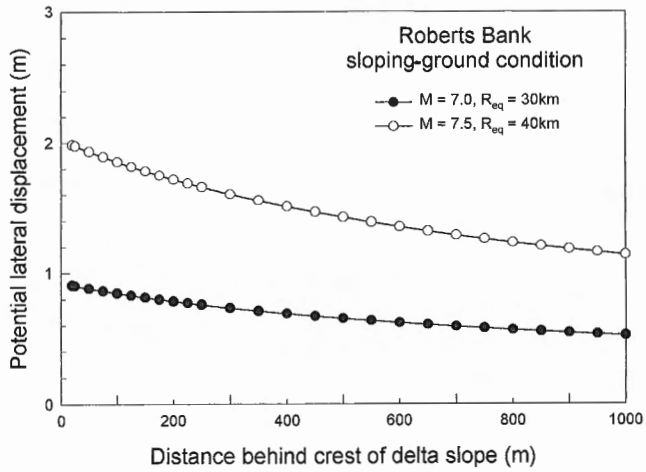

Figure 8. *Lateral spread displacements at the Roberts Bank Deltaport site, calculated for two hypothetical earthquakes – sloping-ground situation. Displacements predicted for the M = 7.5 earthquake range from 2 m at the crest of the slope to less than l m at a location l000 m landward; these displacements are about twice those of the M = 7.0 event. Because the average angle of the upper delta slope in this area exceeds 6%, the analysis is conservative and flow failure is possible.* R_e *is the equivalent epicentral radius, an empirical parameter which accounts for attenuation of seismic energy with distance (Bartlett and Youd, 1992).*

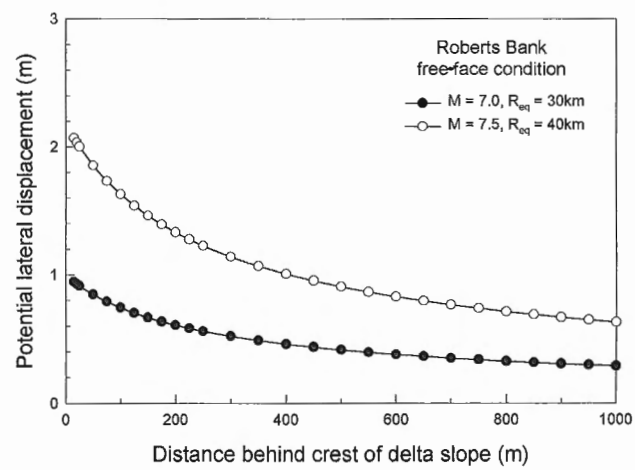

Figure 9. *Lateral spread displacements at the Roberts Bank Deltaport site, calculated for two hypothetical earthquakes – free-face situation. Displacements predicted for M = 7.5 and M = 7.0 earthquakes range from 2 m and 1 m, respectively, near the slope break to about 0.7 and 0.3 m at a setback of 1000 m.*

unsupported height of 25 m, which corresponds to the estimated thickness of liquefiable material, as determined from CPT data. The average angle of the delta slope west of the Roberts Bank Deltaport is 8°, but the seafloor between the crest of the slope and the facility is inclined only 2.5° (Swan Wooster Engineering, 1982). Earthquakes of magnitude 7.0 and 7.5, with epicentral distances of 30 and 40 km, respectively, were used in the analysis.

Plots of lateral displacements directly behind the slope crest are shown in Figures 8 and 9. Horizontal displacements are greatest near the top of the slope and decrease landward. It should be noted, however, that these estimates are only approximate and may differ substantially from actual values. Additionally, this technique evaluates only lateral-spreading-type deformation, but some flow liquefaction is also likely to occur in soils at the delta crest. The displacements in Figures 8 and 9 should, therefore, be taken as minimum estimates.

CONCLUSIONS

Recent geotechnical investigations have identified loose sandy soils near the crest of the southwestern Fraser delta slope. The seismic liquefaction response of these deposits to the design earthquake (moment magnitude 7.5) was evaluated using cone penetration data. The soils at Sand Heads have a high cyclic liquefaction potential to a depth of about 25 m below the seafloor. Low cone penetration resistances suggest that strain softening could occur during liquefaction, resulting in localized flow slides. In general, flow slides are most likely at the mouths of active and recently active distributary channels. The potential for cyclic liquefaction is somewhat lower elsewhere on the delta front, possibly because the soils in these areas have a longer history of densification.

Lateral-spreading displacements at the crest of the delta slope on southern Roberts Bank might exceed 2 m during a M = 7.5 earthquake, but would be lower near the Deltaport because of foundation improvements that were made during construction. Estimates of potential displacements in deeper water on the delta slope are highly problematic, due to a paucity of in situ geotechnical data. Further research is required to evaluate the seismic liquefaction potential and large-strain response of delta front silt deposits, given the risk of damage to key infrastructure.

ACKNOWLEDGMENTS

Funding for this research was provided by PERD (Panel for Energy Research and Development) and B.C. Hydro and Power Authority. The author is grateful to P.A. Monahan, N.R. Morgenstern, J. Howie, and D.G. Gillespie for valuable input, advice, and assistance throughout the project, and to J.J. Clague, D.C. Mosher, and P.K. Robertson for reviewing drafts of the paper.

REFERENCES

Bartlett, S.F. and Youd, T.L.
1992: Empirical prediction of liquefaction-induced lateral spread; Journal of Geotechnical Engineering, American Society of Civil Engineers, v. 121, p. 249-261.

Been, K., Crooks, J.H.A., Becker, D.E., and Jefferies, M.G.
1986: The cone penetrometer test in sands: part I, state parameter interpretation; Geotechnique, v. 36, p. 239-249.

Byrne, P.M.
1978: An evaluation of the liquefaction potential of the Fraser Delta; Canadian Geotechnical Journal, v. 15, p. 32-46.

Byrne, P. M. and Anderson, D.L.
1987: Earthquake design in Richmond, B.C., version 2; University of British Columbia, Department of Civil Engineering, Soil Mechanics Series, No. 109, 87 p.

Campanella, R.G. and Robertson, P.K.
1982: State of the art in in-situ testing of soils: developments since 1978; University of British Columbia, Department of Civil Engineering, Soil Mechanics Series, No. 56, 23 p.

Christian, H.A. and Woeller, D.J.
1996: Investigation of spontaneous liquefaction flow slides at the margin of the Fraser River delta, Vancouver, British Columbia; Proceedings, 2nd International Congress on Environmental Geotechnics, Osaka, Japan, v. 1, p. 337-342.

Christian, H.A., Mosher, D.C., Barrie, J.V., Hunter, J.A., and Luternauer, J.L.
1998: Seabed slope instability on the Fraser River delta; in Geology and Natural Hazards of the Fraser River Delta, British Columbia, (ed.) J.J. Clague, J.L. Luternauer, and D.C. Mosher; Geological Survey of Canada, Bulletin 525, this volume.

Christian, H.A., Mosher, D.C., Mulder, T., Barrie, J.V., and Courtney, R.C.
1997a: Slope instability on the Fraser River delta foreslope, Vancouver, British Columbia; Canadian Geotechnical Journal, v. 34, p. 432-446.

Christian, H.A., Mulder, T., and Courtney, R.C.
1995: Seabed slope instability of the Fraser River delta, Vancouver, British Columbia, Canada; Geological Survey of Canada, Open File 2412, 1 sheet.

Christian, H.A., Mulder, T., Courtney, R.C., Mosher, D.C., Barrie, J.V., Currie, R.G., Olynyk, H.W., and Monahan, P.A.
1994a: Slope instability on the Fraser River delta foreslope, Vancouver, British Columbia; in Proceedings, 47th Canadian Geotechnical Conference, Halifax, Nova Scotia, p. 155-165.

Christian, H.A., Woeller, D.J., Robertson, P.K., and Courtney, R.C.
1997b: Site investigations to evaluate flow liquefaction slides at Sand Heads, Fraser River delta; Canadian Geotechnical Journal, v. 34, p. 384-397.

Christian, H.A., Woeller, D.J., Weemes, I., and Robertson, P.K.
1994b: Use of SASW and SCPT to evaluate liquefaction potential of the Fraser delta foreslope, Vancouver, British Columbia; in Proceedings, 47th Canadian Geotechnical Conference, Halifax, Nova Scotia, p. 166-175.

Clague, J.J., Luternauer, J.L., and Hebda, R.J.
1983: Sedimentary environments and postglacial history of the Fraser Delta and lower Fraser Valley, British Columbia; Canadian Journal of Earth Sciences, v. 20, p. 1314-1326.

Hart, B.S., Prior, D.B., Barrie, J.V., Currie, R.G., and Luternauer, J.L.
1992: A river mouth submarine channel and failure complex, Fraser Delta, Canada; Sedimentary Geology, v. 81, p. 73-87.

Luternauer, J. and Finn, W.D.L.
1983: Stability of the Fraser River delta front; Canadian Geotechnical Journal, v. 20, p. 603-616.

Marcuson, III, W.F., Hynes, M.E., and Franklin, A.G.
1990: Evaluation and use of residual strength in seismic safety analysis of embankments; Earthquake Spectra, v. 6, p. 529-572.

Monahan, P.A., Luternauer, J.L., and Barrie, J.V.
1993: A delta plain sheet sand in the Fraser River delta, British Columbia, Canada; Quaternary International, v. 20, p. 27-38.

Robertson, P.K.
1995: Soil classification using the CPT; Canadian Geotechnical Journal, v. 27, p. 151-158.

Robertson, P.K. and Campanella, R.G.
1985: Liquefaction potential of sands using the cone penetration test; Journal of the Geotechnical Engineering Division, American Society of Civil Engineers, v. 22, p. 298-307.

Robertson, P.K. and Wride, C.E.
1997: Cyclic liquefaction and its evaluation based on SPT and CPT; in Proceedings, National Committee on Earthquake Engineering Research (NCEER) Workshop, Salt Lake City, Utah, 52 p.

Robertson, P.K., Campanella, R.G., Gillespie, D., and Rice, A.
1986: Seismic CPT to measure in-situ shear wave velocity; Journal of Geotechnical Engineering, American Society of Civil Engineers, v. 112, p. 791-803.

Rogers, G.C.
1988: An assessment of the megathrust earthquake potential of the Cascadia subduction zone; Canadian Journal of Earth Sciences, v. 25, p. 844-852.

Seed, H.B. and Idriss, I.M.
1971: Simplified procedure for evaluating soil liquefaction potential; Journal of the Geotechnical Engineering Division, American Society of Civil Engineers, v. 97, p. 458-482.

Seed, H.B., Tokimatsu, K., Harder, L.F., and Chung, R.
1985: Influence of SPT procedures in soil liquefaction resistance evaluations; Journal of Geotechnical Engineering, American Society of Civil Engineers, v. 111, p. 1425-1445.

Stark, T.D. and Olson, S.M.
1995: Liquefaction resistance using CPT and field case histories; Journal of Geotechnical Engineering, American Society of Civil Engineers, v. 121, p. 856-869.

Suzuki, Y., Tokimatsu, K., Koyamada, K., Taya, Y., and Kubota, Y.
1995: Field correlation of soil liquefaction based on CPT data; Proceedings, International Symposium on Cone Penetration Testing (CPT'95), Linkoping, Sweden, v. 2, p. 583-588.

Swan Wooster Engineering
1982: Westshore Terminals Ltd. intermediate phase expansion, marine civil works sounding plan; Swan Wooster Engineering Co., Vancouver, British Columbia, 1 sheet.

Watts, B.D., Seyers, W.C. and Stewart, R.A.
1992: Liquefaction susceptibility of Greater Vancouver area soils; in Geotechnique and Natural Hazards; BiTech Publishers Ltd., Vancouver, British Columbia, p. 145-157.

Groundwater flow beneath the Fraser River delta, British Columbia; a preliminary model

B.D. Ricketts[1]

Ricketts, B.D., 1998: Groundwater flow beneath the Fraser River delta, British Columbia; a preliminary model; in Geology and Natural Hazards of the Fraser River Delta, British Columbia, (ed.) J.J. Clague, J.L. Luternauer, and D.C. Mosher; Geological Survey of Canada, Bulletin 525, p. 241–255.

Abstract: A three-dimensional numerical simulation of groundwater flow in the Fraser delta provides the basis for assessing some of the factors contributing to regional flow. For the purposes of modelling, the architecture of the delta and adjacent upland areas has been subdivided into three primary stratigraphic units: the postglacial delta; Pleistocene glacial and interglacial deposits; and Tertiary bedrock. Each unit contains a complex array of aquifers and aquitards. The model boundaries approximate natural hydraulic boundaries. Shallow groundwater beneath the Fraser delta is recharged by a combination of precipitation and topography-driven flow from the uplands. Simulated hydraulic gradients at the water table are shallow (0.1-0.25 m/km). The model indicates the possibility of groundwater flow to the delta front. This is supported by electrical conductivity data which show mixing of seawater and freshwater as far west as the low-tide limit. Submarine seepage resulting from groundwater flow could raise pore-water pressures, thereby decreasing sediment shear strength and increasing the susceptibility of the delta front to failure.

Résumé : Une simulation numérique tridimensionnelle de l'écoulement des eaux souterraines dans le delta du Fraser constitue le fondement de l'évaluation de certains facteurs jouant un rôle dans l'écoulement régional. Aux fins de la modélisation, l'architecture du delta et des hautes terres adjacentes a été subdivisée en trois unités stratigraphiques primaires : le delta postglaciaire; les dépôts glaciaires et interglaciaires du Pléistocène; le substratum du Tertiaire. Chaque unité contient un réseau complexe d'aquifères et d'aquitards. Les limites du modèle correspondent approximativement à diverses limites naturelles (marées, aires d'alimentation et partage des eaux). Les eaux souterraines qui circulent à faible profondeur sous le delta du Fraser sont réalimentées par les précipitations et l'eau provenant des hautes terres. Les gradients hydrauliques simulés au niveau phréatique sont faibles (0,1-0,25 m/km). Le modèle indique la possibilité d'un écoulement d'eau souterraine jusqu'au front deltaïque. Il s'appuie sur les données de conductivité électrique qui mettent en évidence un mélange d'eau de mer et d'eau douce aussi loin à l'ouest que la limite de la marée basse. L'infiltration des eaux souterraines dans le milieu sous-marin pourrait augmenter la pression de l'eau interstitielle, ce qui aurait pour effet de diminuer la résistance au cisaillement des sédiments et d'accroître la vulnérabilité du front deltaïque aux ruptures.

[1] Department Of Earth Sciences, University of Waikato, Private Bag 3105, Hamilton, New Zealand

INTRODUCTION

The Fraser River delta is the modern, actively growing extension of the Fraser Lowland, a region of glacial and interglacial sedimentation at the margin of the Strait of Georgia (Fig. 1). It is the river's final testament to a 1200 km journey through almost one third of British Columbia.

There is little groundwater use on the Fraser delta, because of seawater intrusion into shallow aquifers and because most of the area is linked to the Regional District (surface) water supply. Consequently, little is known about the water table, groundwater recharge, and groundwater flow beneath the delta plain. Nevertheless, hydrogeological conditions in the delta are an important consideration for many human activities, including foundation construction in areas of excess pore pressure, assessment of seismic risk (viz. liquefaction of shallow saturated sediment), and flood management (e.g. rising water tables). Slope failure on the submarine portion of the delta poses a threat to major facilities at the delta front and to electrical transmission cables that cross the Strait of Georgia. Several failures have occurred in the last two decades (Luternauer and Finn, 1983; McKenna et al., 1992) and have been attributed largely to sediment loading at distributary-channel mouths. Other causes, such as earthquakes, interstitial gas, and loading by storm waves and tidal currents have also been suggested for such failures (Hart et al., 1992; Luternauer et al., 1994; Harris et al., 1995). However, the role that groundwater flow and seepage plays in delta-front failure has not been considered. If submarine groundwater seepage does take place, it could potentially raise sediment pore pressure, thus decreasing shear strength and increasing the possibility of failure.

This paper develops a preliminary hydrogeological model for the Fraser River delta in order to simulate groundwater flow at different stratigraphic levels beneath the delta plain. Model results are used to depict the water table under the shallow part of the delta, as well as potentiometric surfaces and flow vectors at deeper stratigraphic levels. Based on the model results, a preliminary assessment is made of the efficacy of submarine groundwater seepage as a cause of delta-slope failure.

CONCEPTUAL GROUNDWATER FLOW IN THE FRASER DELTA

Groundwater flows from areas of high fluid potential to areas of low fluid potential (Fig. 2). The driving force for regional flow is topography (Toth, 1963; Bredehoeft et al., 1982). Regions of high elevation tend to be areas of groundwater recharge and regions of low elevation, areas of discharge.

Groundwater flow is commonly depicted as nested, recharge-discharge flow systems representing circulation at local, intermediate, and regional depths. Local flow systems are generally shallow and are determined by local topography. Local flow on the Fraser delta is likely recharged only by precipitation on the delta plain itself; this flow probably discharges directly into Fraser River, smaller streams and drains,

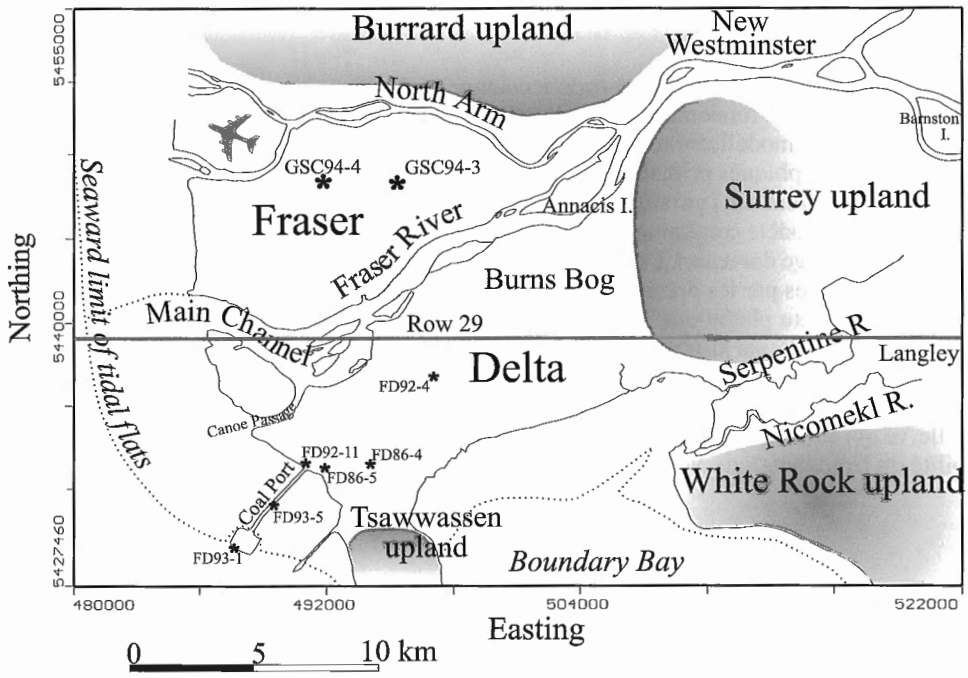

Figure 1. Map of the Fraser River delta and adjacent uplands, showing locations of Geological Survey of Canada boreholes. Map coordinates are UTMs and correspond to the coordinates of model grids in Figures 6-10. The line labelled 'Row 29', locates the section of Figures 6 and 9.

and possibly the sea. Other examples of local flow systems in the Fraser Lowland are the unconfined Abbotsford and Brookswood aquifers, both of which are recharged by direct precipitation. Groundwater travel times in these local systems probably range from months to years (Liebscher et al., 1992). Water-table elevations in the local flow systems respond rapidly to seasonal variations in precipitation, commonly changing as much as 4 m between wet and dry seasons (Halstead, 1986).

Intermediate systems are represented by deeper flow within the Holocene delta and older Pleistocene deposits. Examples include flow recharged on the Burrard, Surrey, and White Rock uplands and discharged into the Fraser delta and Nicomekl-Serpentine drainage basin. Travel times in intermediate flow systems of the Fraser Lowland and delta are largely unknown, but probably range from hundreds to thousands of years based on comparisons with similar systems elsewhere (Freeze and Cherry, 1979).

If submarine groundwater seepage does take place at the delta front, it is mostly likely driven by local and intermediate flow systems. Whether the fluid potential in the local delta system alone is sufficient to drive this process is unknown, particularly if it is competing with an intruding saline wedge.

Regional flow encompasses groundwater recharge in the Coast Mountains, mostly through fractures in metasedimentary and intrusive rocks, and flow of connate water deep within Tertiary and older bedrock (Fig. 2; Ricketts and Liebscher, 1994). The residence time of connate water at these depths (hundreds of metres) is unknown but may be on the order of hundreds of thousands of years. Freshwater has been observed at depths up to 930 m in exploratory oil wells (J. Britton, pers. comm., 1996), but it is not know if it plays a role in shallow groundwater discharge to either subaerial or submarine environments.

ARCHITECTURE OF THE FRASER DELTA

The Fraser delta is underlain by three principal sedimentary packages separated by major unconformities: the postglacial (Holocene) delta; Pleistocene glacial and interglacial deposits; and Tertiary bedrock (Fig. 3). The summary of stratigraphy that follows outlines those characteristics that are relevant to the three-dimensional groundwater model. More detailed discussions of stratigraphy and sedimentology are found in Armstrong (1981, 1984) and Clague et al. (1991, 1998).

The Holocene delta

For about the last 10 000 years, the Fraser River has emptied into the Strait of Georgia, building a complex wedge of sediment that, in places, is more than 300 m thick and pinches out where it onlaps a late-glacial unconformity exposed in the adjacent Surrey, Burrard, and Tsawwassen uplands (Fig. 1, 4). The unconformity occurs at the base of the Late Pleistocene Vashon Drift (Clague et al., 1991). Surficial geology mapping of the delta plain (Armstrong and Hicock, 1979, 1980) has delineated areas of bog (e.g. Burns Bog, Fig. 1), sandy

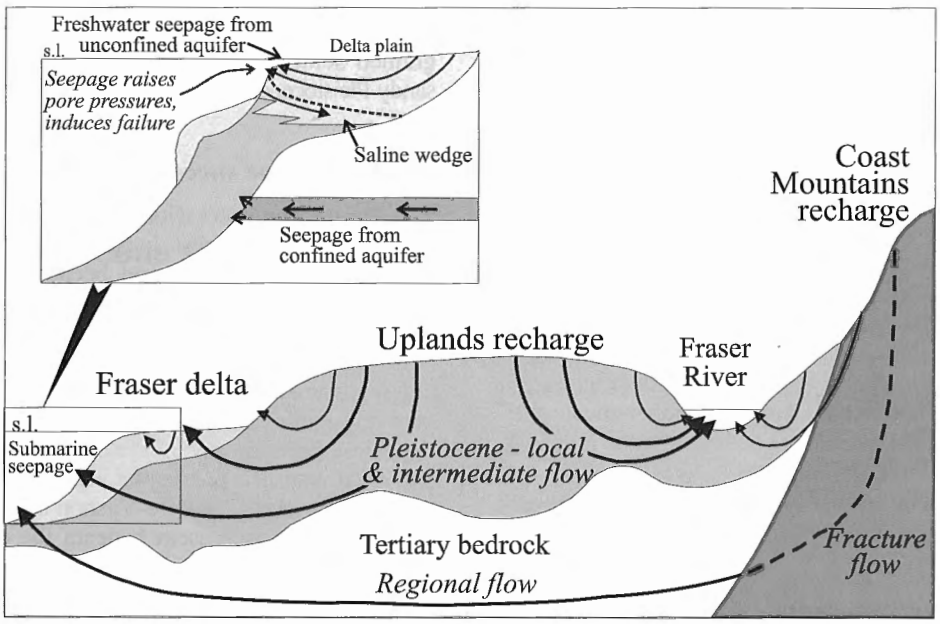

Figure 2. *Conceptual groundwater flow along a east-west profile across the Fraser delta, Fraser Lowland, and Coast Mountains, illustrating local, intermediate, and regional groundwater flow systems. The inset depicts fresh groundwater seepage from confined and unconfined aquifers at the delta front, failure of the delta front, and intrusion of a saline wedge.*

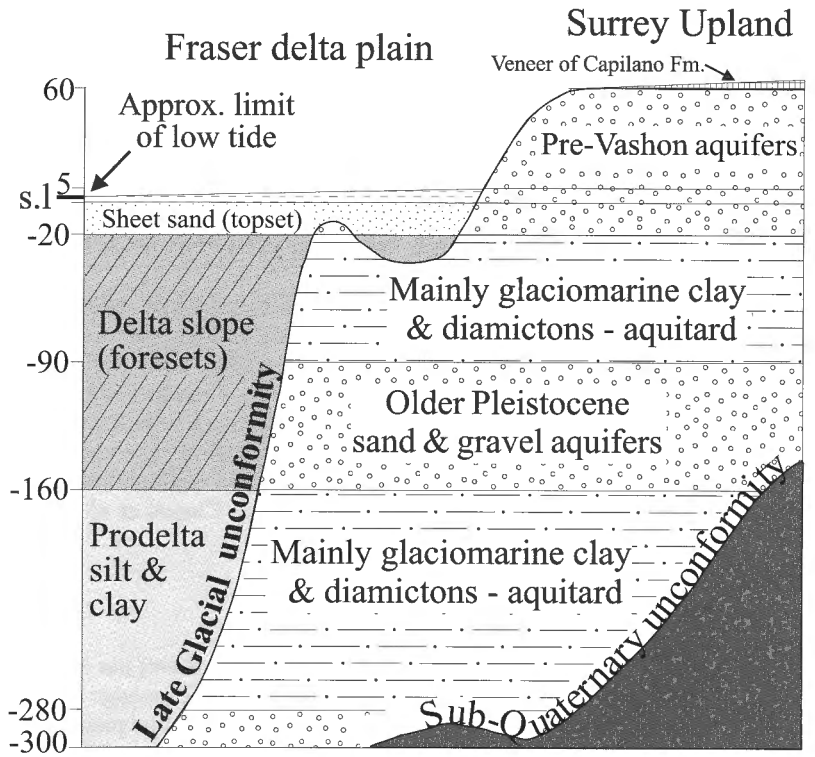

Figure 3.

Schematic profile of the Fraser River delta and western Fraser Lowland, showing the primary hydrostratigraphic units. Unconformities separate three profoundly different sedimentary packages — the postglacial delta, Pleistocene glacial and interglacial deposits, and Tertiary bedrock (see Fig. 4).

distributary channels, muddy floodplain deposits, and tidal flats up to 9 km wide (collectively the 'modern delta' layer in Fig. 3; for more detail on these environments and sediments, see Luternauer et al., 1998). A more-or-less continuous sheet of sand, generally 8 to 20 m thick, underlies this surface veneer (Monahan et al., 1993; labelled 'sheet sand' in Fig. 3). The sheet sand consists of one or more fining-upward, sand-silt packages that represent a complex amalgamation of laterally migrating distributary channels (Clague et al., 1991; Monahan et al., 1993), and in a general way can be viewed as the delta topset unit. This unit is also characterized by subhorizontal reflections in high-resolution seismic-reflection profiles (Pullan et al., 1989, 1998). In this paper it is called the 'sheet-sand aquifer'.

Thick delta-slope deposits underlie the sheet sand. High-resolution seismic-reflection profiles south of the main river channel show that these deposits are up to 170 m thick (Jol and Roberts, 1988; Pullan et al., 1989; Clague et al., 1991). The slope deposits dip approximately 5-7° southwest beneath the southern part of the delta. Deep boreholes indicate they consist of fine-grained sand and silt beds (Clague et al., 1991; Luternauer et al., 1991; Dallimore et al., 1995). Mud- and silt-dominated prodelta beds gradationally underlie the slope package.

The late-glacial unconformity

Glacial erosion of Late Pleistocene strata has produced an unconformity with up to 300 m of relief beneath the Fraser delta, and more than 400 m of relief from the top of the Surrey upland (Fig. 4). Borehole intersections of the unconformity define two major depressions north and south of the Main Channel. Pleistocene lithologies beneath the Holocene delta include silt, sand, gravel, and diamicton.

Relief on the unconformity plays an important role in directing groundwater flow, in addition to exerting significant control over the stratigraphic architecture of the Fraser delta. For example, downward flow of water through fine-grained delta deposits is focused towards more permeable, sandy Pleistocene layers that intersect the late-glacial surface.

The Pleistocene succession

The Pleistocene succession beneath the Fraser delta varies considerably in thickness, in part because it infills deeply dissected Tertiary bedrock and because glaciers eroded the Pleistocene deposits immediately before the Holocene delta began to accumulate. Late Pleistocene deposits are locally exposed on the adjacent uplands and include thick, sandy drift and nonglacial sediments (Clague, 1977; Armstrong, 1981), here referred to as the 'pre-Vashon aquifer'. The pre-Vashon deposits are commonly overlain by a veneer of glaciomarine silt, sand, and gravel (Armstrong and Hicock, 1979, 1980; Armstrong, 1981). The pre-Vashon aquifer extends into the subsurface and is present beneath the delta (e.g. borehole GSC94-3; Dallimore et al., 1995).

Older Pleistocene deposits underlie the pre-Vashon aquifer under the Fraser delta and elsewhere in the Fraser Lowland. The stratigraphic scheme illustrated in Figure 3 is a simplification for the purpose of modelling, based on lithological and hydraulic criteria. Thick units designated 'aquifers' consist primarily of interbedded coarse- and fine-grained deposits. Units designated 'aquitards' are made up predominantly of

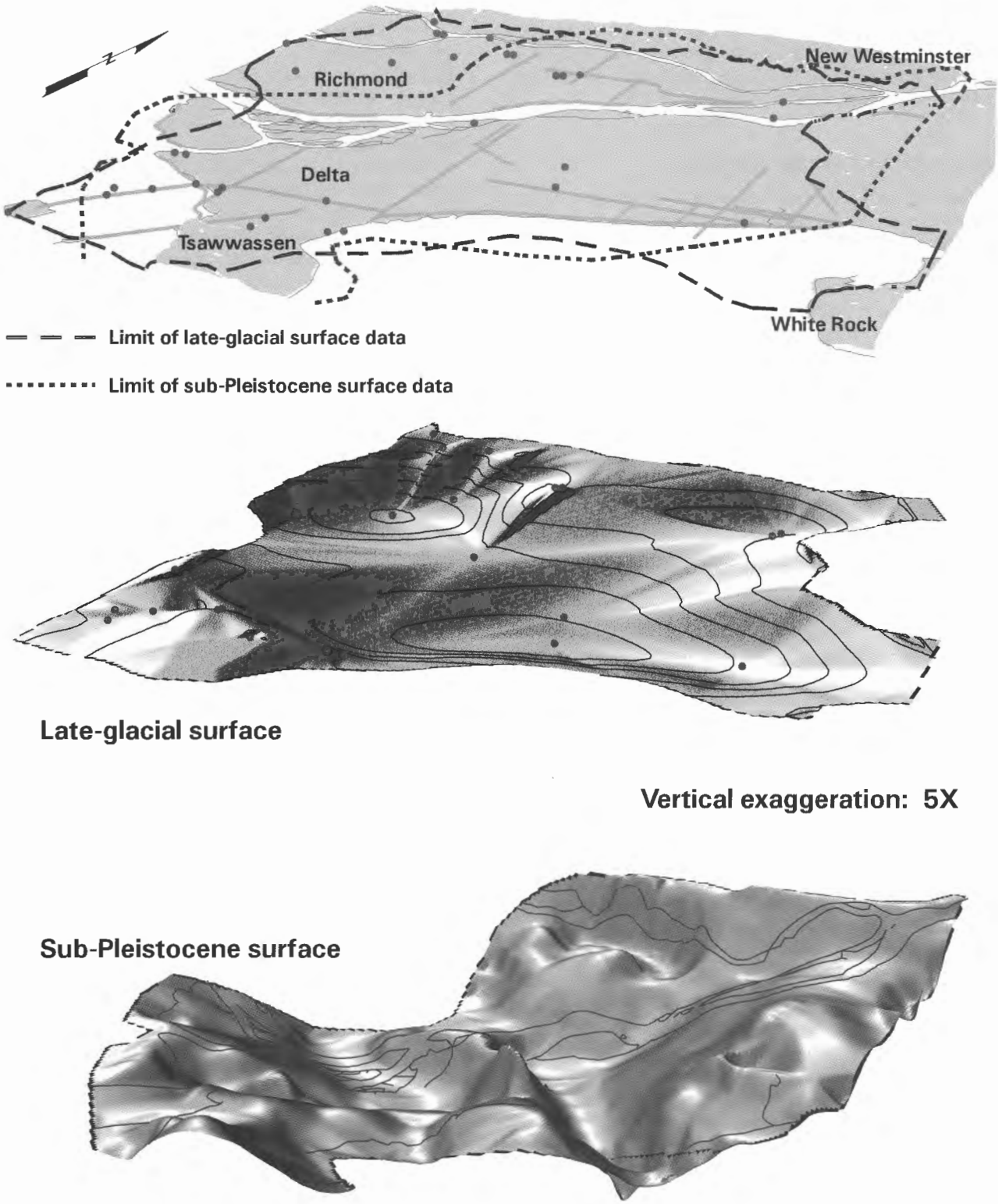

Figure 4. Graphical reconstructions, viewed from the southeast, of the Fraser delta plain (top), and the late-glacial and sub-Pleistocene (Tertiary) surfaces. The form of the late-glacial surface is based on a relatively small number of boreholes (dots) and is therefore an approximation. The zero contour coincides with the edge of Pleistocene uplands bordering the Fraser delta. In comparison, the Tertiary bedrock surface is based on industry seismic-reflection profiles and a few oil-well intersections and is better defined (Britton et al., 1995). The shoreline and the Fraser River channel have been added to the Tertiary surface for reference. Vertical exaggeration is 5.

low-permeability deposits, typically clay, silt, and diamicton. Aquifer and aquitard thicknesses and depths are averages determined from stratigraphic sections of Armstrong (1984) and from boreholes in the Geological Survey of Canada water-well database (Ricketts and Dunn, 1995).

The sub-Pleistocene unconformity

The Tertiary surface has marked relief — it lies up to 800 m below the Fraser delta, but is exposed well above sea level just to the north on the Burrard upland (Fig. 4). Data used to define the surface come from oil company seismic-reflection profiles (Britton et al., 1995). East of the delta, the surface has been delineated mostly from borehole data (Hamilton and Ricketts, 1994). Prominent, north- to northwest-trending trenches or valleys are cut in the Tertiary bedrock beneath the Pleistocene fill. The paleovalley trends are parallel to modern drainage patterns (e.g. Pitt and Stave lakes), and may be controlled, in part, by late Neogene or early Pleistocene faulting. Early to mid-Pleistocene strata progressively onlap the unconformity.

Tertiary bedrock

Oil exploration wells drilled near the Fraser delta indicate that up to 1200 m of Miocene-Pliocene sandstone and mudstone overlie a thick, shallow-dipping panel of Paleocene-Eocene conglomerate, sandstone, and minor mudstone and coal. Tertiary deposition in the area was dominated by fluvial processes (Mustard and Rouse, 1994).

GENERAL ATTRIBUTES OF FRASER DELTA AQUIFERS AND GROUNDWATER

Despite the plethora of geological and geophysical studies on the Fraser River delta, there is very little data that is directly related to groundwater, such as porosity and hydraulic conductivity (K). In this study, the lithological characteristics of aquifers and aquitards are derived from descriptions of boreholes and outcrops, and comparisons with similar units elsewhere in the Fraser Lowland.

The most important Holocene aquifer is the sheet sand, part of the delta topset unit. It is overlain by floodplain silt, silty sand, and peat (Monahan et al., 1993); depending on the distribution of these facies, the aquifer is either unconfined or semiconfined. Consequently, it is reliant on local recharge (from precipitation) and is the most susceptible to contamination. Fining-upward, sand-to-silt cycles in the sheet-sand aquifer impart a vertical anisotropy, i.e. a decreasing-upwards component of hydraulic conductivity within each cycle. Samples collected from the sheet sand on the southern part of the delta have yielded values of K averaging about 3×10^{-2} to 5×10^{-2} cm/s (Wood, 1996; L. Smith, personal communication, 1996). The larger value is used for an average horizontal conductivity in the simulations (Table 1). Isotropic conditions are assumed, although it is recognized that the vertical component of hydraulic conductivity could vary by one or two orders of magnitude from the horizontal conductivity.

Grain-size data are available for Holocene and Pleistocene sands intersected in boreholes GSC94-3 and GSC94-4 (Dallimore et al., 1995). Estimates of hydraulic conductivity were made for selected samples of fine- to medium-grained sand, using the empirical relationship $K = A\,(d_{10})^2$, where A is a constant, and the particle diameter (d_{10}) is read at the point where 10% (by weight) of the sample is finer and 90% is coarser than d_{10} (Fig. 5). Values of 4.0×10^{-2} to 4.4×10^{-2} cm/s obtained by this method, fall within the range of values estimated by Wood (1996).

Delta slope deposits consist of fine-grained sand, silt, and mud. Silty clay at the top of the slope succession has a measured K of 1.2×10^{-8} cm/s (L. Smith, pers. comm., 1996). However, the presence of sandy layers in the slope sequence suggests that the average value of K is larger. Prodelta silt and mud probably have K values similar to those of the muddy component of the slope deposits.

Table 1. Hydrostratigraphic units and corresponding hydraulic conductivities used in the Fraser delta groundwater model.

Hydrostratigraphic unit	K (cm/s)
Sheet-sand aquifer	5×10^{-2}
Delta-slope silt and sand	1×10^{-4}
Prodelta mud and silt	5×10^{-6}
Pre-Vashon aquifers	3.5×10^{-2}
Clay-till aquitard	1×10^{-7}
Tertiary bedrock	8×10^{-7}

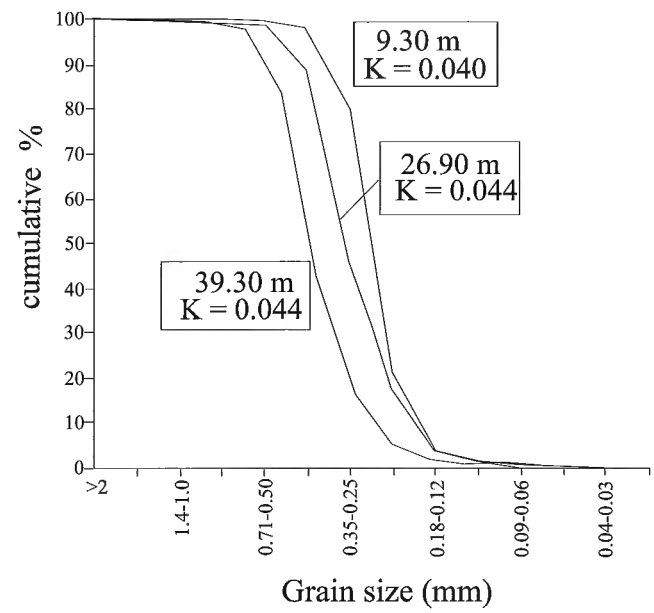

Figure 5. Graphs of cumulative grain size and calculated values of K for samples from borehole GSC94-3. The sample at 9.3 m depth is from the sheet-sand aquifer; the other two samples are from pre-Vashon aquifers.

Pleistocene aquifers beneath the Fraser delta are confined by thick clay, silt, and diamicton aquitards. Sand and gravel beds are present in the aquitards, but indications elsewhere in Fraser Lowland are that these beds, although locally important for water supply, are laterally discontinuous; they are not considered in the present models. About two-thirds of the pre-Vashon aquifer is exposed in the uplands bordering the Fraser delta; the remaining aquifers only occur below sea level. Most groundwater in the confined aquifers is probably derived by vertical leakage from confining aquitards. A hydraulic conductivity of 4.4 x 10^{-2} cm/s, estimated from grain-size data from borehole GSC94-3, is a reasonable average for the coarse- and medium-grained sand components of the pre-Vashon aquifer (Fig. 5). However, finer-grained sand and silt layers also occur in these aquifers, and hence the average value used for modelling all the Pleistocene aquifers is 3.5 x 10^{-2} cm/s (Table 1).

Porosity in Tertiary sandstone and conglomerate in the Fraser Lowland is probably a combination of intergranular and fracture porosity (Ricketts and Liebscher, 1994), but very little quantitative textural data are available for these rocks. Gordy (1988) cites an average porosity of 15% for Paleocene-Eocene sandstone in the region. A drill-stem test at 930 m depth, in Tertiary strata south of Langley, recorded a permeability of about 8 millidarcys (i.e. K = 8 x 10^{-6} cm/s; J. Britton, pers. comm., 1996).

Seawater has intruded parts of the Holocene Fraser delta. This is indicated by salinity profiles and electromagnetic data collected near the delta front and along the lower reaches of the Fraser River (Hunter et al., 1994; Christian et al., 1995).

SIMULATION OF GROUNDWATER FLOW

Geological models, like those of other disciplines, are tools for predicting what will happen to a particular physical or chemical system when stresses are applied to it. Numerical groundwater models can predict fluid flow under different geological conditions, the effects of water withdrawal or injection, the direction and time of travel of contaminant plumes, and the effects of streams, drains, recharge, and evapotranspiration.

Model structure

A program for three-dimensional groundwater modelling (MODFLOW), originally developed for the United States Geological Survey by M. McDonald and A. Harbaugh, is used to simulate flow in the Fraser delta. The model extends from 60 m above, to 300 m below, sea level and includes all of the delta to about the low-tide limit, the Surrey, Burrard, Tsawwassen, and White Rock uplands, and part of the Nicomekl-Serpentine valley (Fig. 1). The model consists of a

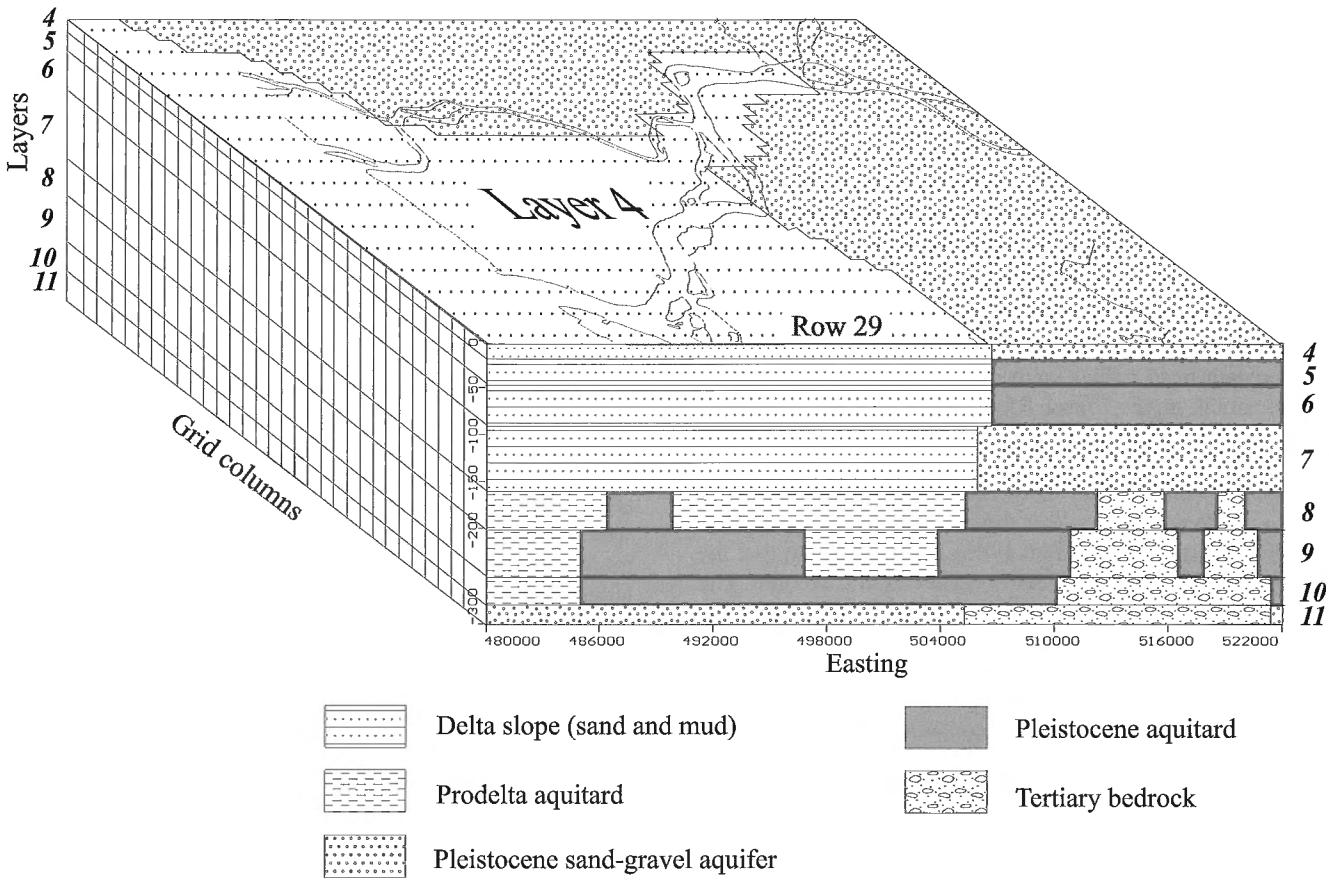

Figure 6. *An example of layer geometry and lithology for the groundwater flow model (row 29; see Fig. 1 for location). Vertical exaggeration is 50.*

three-dimensional layered grid in which cells are assigned aquifer-aquitard properties (conductivity and storage values) and boundary-head conditions. For example, a constant head boundary regulates flow in and out of cells to maintain a specified, constant hydraulic head throughout the simulation. At the other extreme, a no-flow boundary prohibits flow in or out of a cell. The model is used to simulate a potentiometric surface for the semiconfined sheet-sand aquifer (this surface approximates the water table) and potentiometric surfaces for deeper, confined aquifers.

The model grid is 50 rows by 60 columns for each of 11 hydrostratigraphic layers (Fig. 6). Cells are about 0.5 km wide and long. The model boundaries were chosen to coincide approximately with hydraulic boundaries:

- The western and southern boundaries are the low-tide limits of the delta plain, except in the Tsawwassen-Coal Port area where the boundary is seaward of the tidal limit. The southern boundary also corresponds approximately to the southern edges of the Tsawwassen and White Rock uplands, both of which are recharge areas for the delta.
- The eastern model boundary coincides approximately with the eastern edges of the Surrey and White Rock uplands. These upland recharge areas are separated by the Nicomekl-Serpentine valley.
- The northern model boundary is the approximate east-west drainage divide on Burrard upland.

The onlap relationships between Fraser delta and Pleistocene hydrostratigraphic units, and between Pleistocene units and Tertiary bedrock, can be incorporated into the model by varying the hydraulic properties of specific layers (Fig. 7). Maps of the late-glacial and sub-Pleistocene unconformities were used to determine the disposition of various units. Some units are known to have complex stratification and textures with marked lateral and vertical variations, and are therefore anisotropic. However, very little is known of the hydraulic properties of these units; thus as an additional simplification, I assume that the hydrostratigraphic units are isotropic.

Constant head values were applied to the main distributary channels of the Fraser River — Main Channel, North Arm, and Canoe Passage. This choice is justified as long as there is good hydraulic connection between the river and the sheet-sand aquifer. Observation of tidal signals in wells adjacent to the river suggests that the connection is indeed good (e.g. Bazett and McCammon, 1986). Note however, that the model itself does not take tidal fluctuations into account. The river level in Parsons Channel (Barnston Island), at the upstream end of the model area, was taken to be 3.0 m above mean low tide, and water levels in Fraser River are assumed to decrease regularly to zero to the low-tide limit (data from Ages and Woollard, 1994). A constant head of zero was applied to coastal water bodies, and constant heads up to 1 m were added to the lowest reaches of the Nicomekl River.

Several iterations of the model were run, with adjustments to variables such as hydraulic conductivity and recharge. For example, it was necessary to reduce recharge over the delta to 130 mm/a, to avoid unrealistically high water-table values. Recharge of groundwater by precipitation was applied to cells in the top layer of the model, or where no flow boundaries are present, to the uppermost active cells. Total recharge was taken to be the sum of direct inflow to the water table, minus surface runoff and evapotranspiration. East of New Westminster, recharge was set at 250 mm/a.

The Fraser delta plain is crisscrossed by many drainage ditches. Seven drains, which simulate the removal of water from an aquifer, were added to the model. There are very few, if any, water-production wells on the delta, and therefore water withdrawal was assumed to be zero.

Model calibration

Limited groundwater data are available to calibrate the models, therefore the model was adjusted to simulate a water table that approximates the delta plain topography (Fig. 8). Cone penetrometer tests on the western half of the delta plain support this approach, in that measured instantaneous pore pressures indicate normal hydrostatic conditions, at least to depths of 20 to 30 m (Monahan et al., 1993; Woeller et al., 1993a, b). Local overpressured intervals are thin (<5m) and generally correspond to fine-grained sediments.

Groundwater recharge to the sheet-sand aquifer (layers 3 and 4; Fig. 6, 7) derives from direct precipitation on the delta plain and adjacent uplands. Modelled head values for the pre-Vashon aquifer in layers 3 and 4 correlate reasonably well with observed static levels in wells in the White Rock area (Fig. 8; Halstead, 1986; B.C. Ministry of Environment water-well data). Artesian flow conditions in the Nicomekl-Serpentine valley, derived from upland recharge, are also simulated, although the modelled head values are higher than observed values. Artesian flow conditions, encountered in geotechnical boreholes near the Alex Fraser bridge (Annacis Island) and derived from recharge on the Surrey upland (Bazett and McCammon, 1986), correspond well with simulated heads in that area.

Model results

The simulations indicate that local flow systems are present beneath the Fraser delta and bordering uplands (Fig. 9). Groundwater in the sheet-sand aquifer flows towards the Fraser River and shorelines from two hydraulic divides (Fig. 8). As expected, the hydraulic potential decreases seaward, with gradients steepest in upland areas and decreasing more gradually across the delta plain. Simulated gradients along the divides in the south delta and north delta areas are 0.25 m/km and 0.1 m/km respectively. Artesian pressures on the eastern part of the delta plain, which in this model are 2-3 m above the surface, are generated from local flow systems originating on the Surrey and Burrard uplands.

Simulated hydraulic gradients in the deeper, confined Pleistocene sand aquifers (e.g. layer 11, Fig. 10) are lower than in layer 3. Most of the local flow systems appear to have been dampened at these depths (280-300 m below sea level), consistent with the findings of regional flow studies elsewhere (Bredehoeft et al., 1982). An exception in this case is located beneath the Fraser River near New Westminster

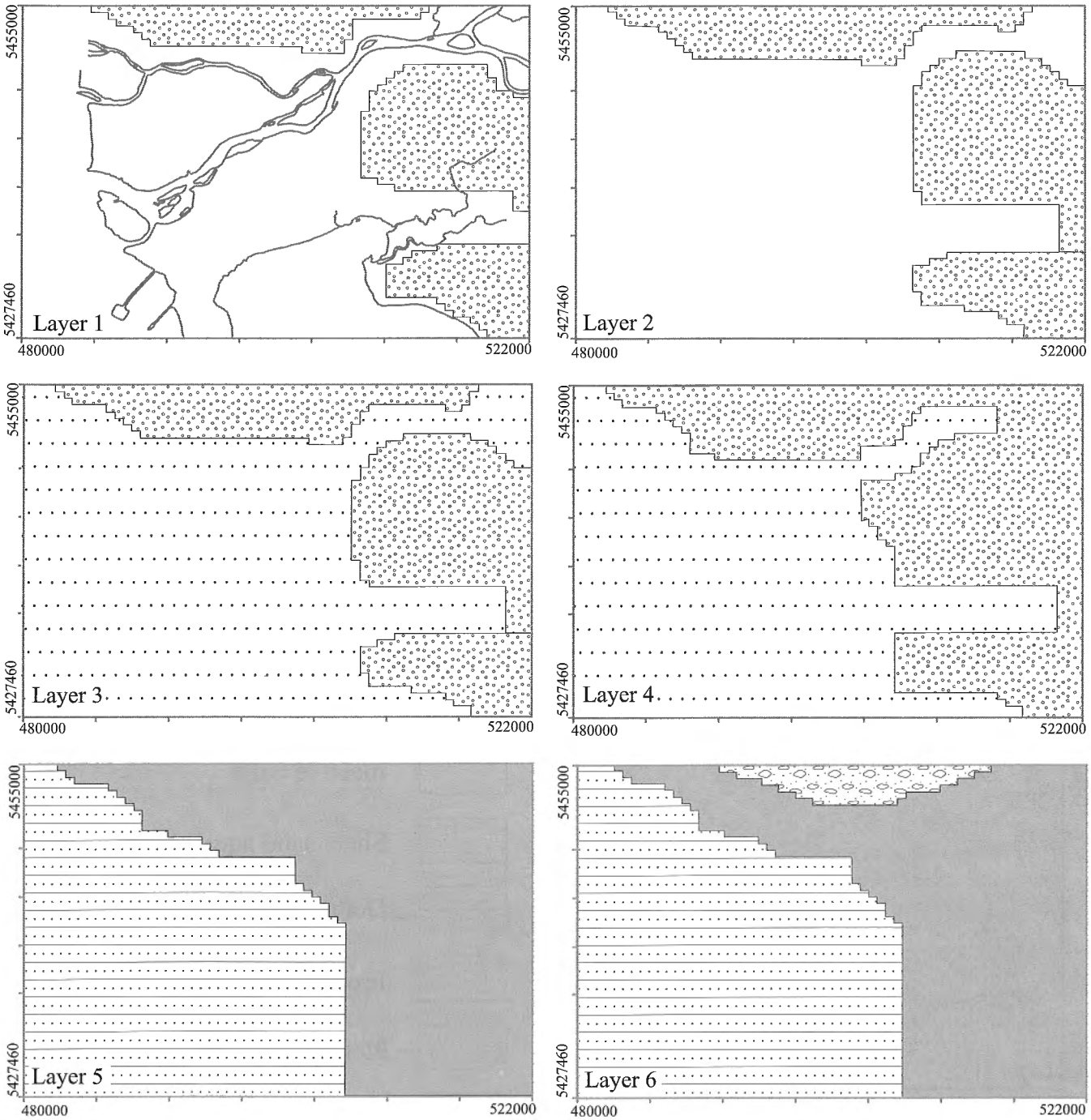

Figure 7. *Hydraulic conductivity distribution in the 11 model layers. Distributions of Pleistocene and Tertiary strata were determined using overlay maps of the unconformity surfaces (Fig. 4). The Pleistocene pre-Vashon aquifers in layers 1 and 2 are at higher elevations than the delta plain, and all cells outside this domain in these layers are designated inactive. An example of the vertical distribution of layers is shown in Figure 6.*

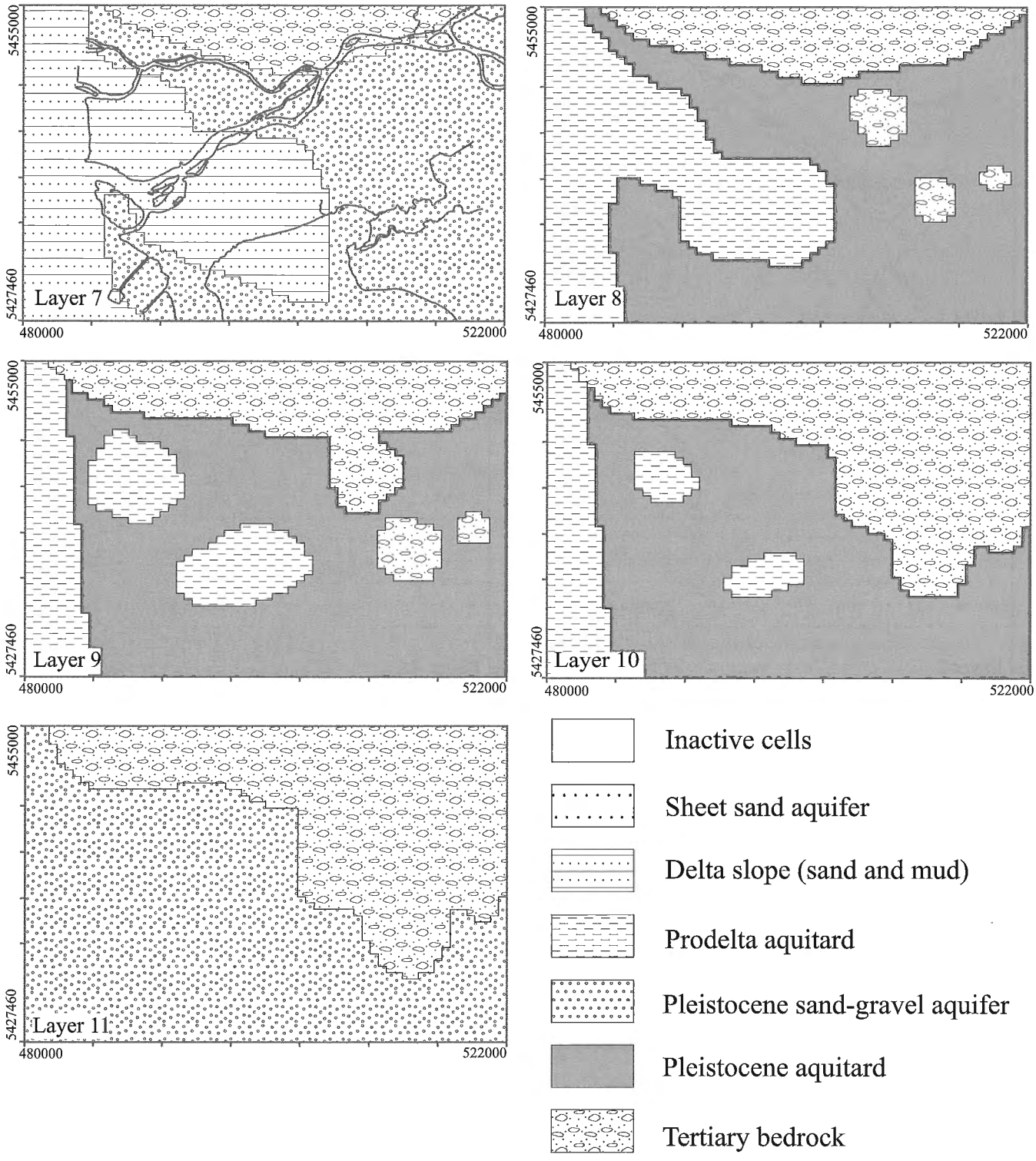

Figure 7. *(cont.)*

(Fig. 10). The steepest gradients in layer 11 are associated with Tertiary bedrock which crops out on the Burrard upland near the northern boundary of the model. From a regional perspective, this is consistent with a south-dipping Tertiary sedimentary succession (Mustard and Rouse, 1994) of low hydraulic conductivity.

Recharge to deeper, confined aquifers probably occurs by vertical leakage through Pleistocene clay, silt, and diamicton. However, recharge from Tertiary sandstone and conglomerate units may also be significant because: 1) the hydraulic conductivity of coarse-grained Tertiary lithologies is two or three orders of magnitude greater than that of fine-grained Pleistocene deposits; and 2) fluid pressures in freshwater at 930 m depth in Tertiary sandstone, are about 1000 KPa greater than normal hydrostatic pressures, indicating an upward component of flow (assuming a hydrostatic gradient of 9.5-10 KPa/m).

In general, groundwater flow has a strong upward component in aquifers and aquitards beneath the outer part of the delta plain and tidal flats. This is consistent with observations of artesian pressures in fine-grained delta slope and prodelta deposits (e.g. Christian et al., 1995). It is also consistent with

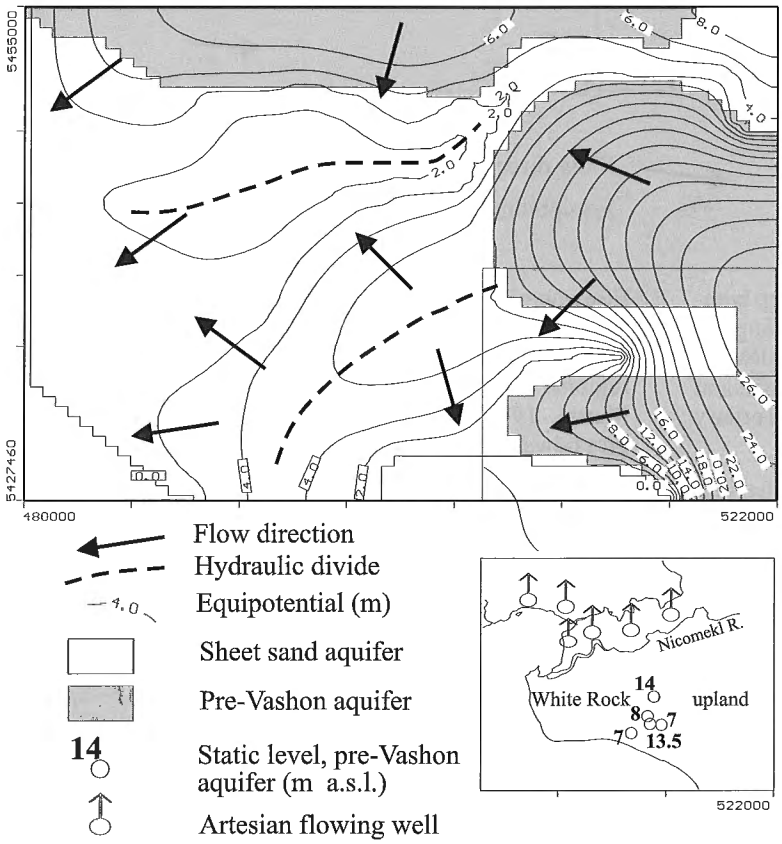

Figure 8.

Predicted potentiometric surface for the upper part of the sheet-sand aquifer (layer 3); this surface approximates the water table. The shaded area corresponds to the pre-Vashon aquifer in layer 3. Static levels measured in the pre-Vashon aquifer on the White Rock upland, and artesian flowing wells in the Nicomekl-Serpentine valley, which are used to calibrate the model, are shown on the inset.

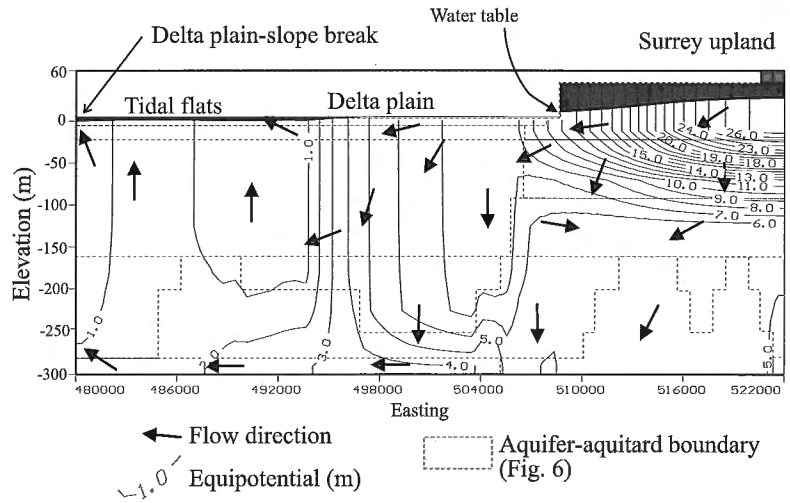

Figure 9.

An example of a model profile (row 29; see Fig. 1) showing the water table, simulated local and intermediate flow systems, the outline of hydrostratigraphic units (see Fig. 6), and groundwater flow directions. Note upward flow beneath the tidal flats. The hydraulic gradient is much steeper beneath the Surrey upland than beneath the delta. According to this model, the upland areas are driving the intermediate-scale flow. Vertical exaggeration is 50.

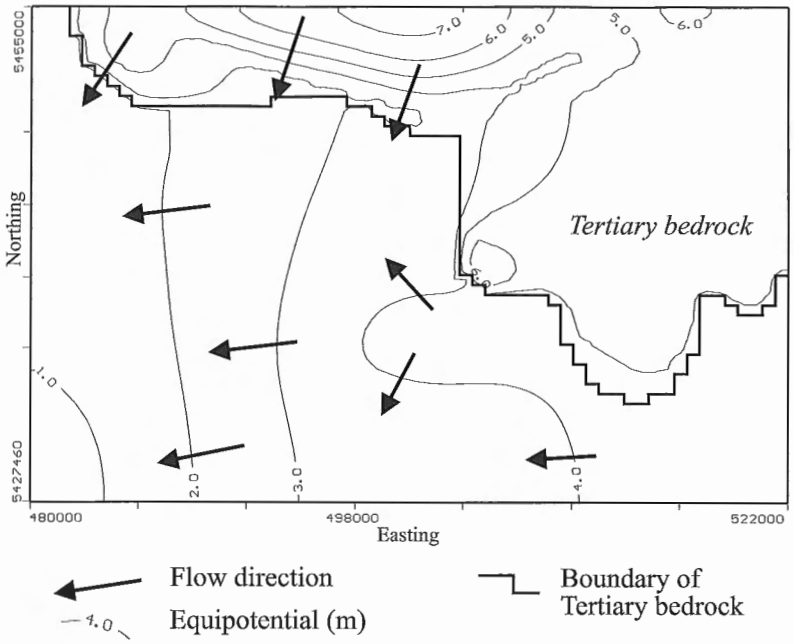

Figure 10.

Predicted potentiometric surface for the deepest Pleistocene aquifer and Tertiary bedrock (layer 11; see Fig. 7). Flow is predominantly west and southwest. The aquifer is recharged by flow from Tertiary bedrock and by leakage from overlying Pleistocene aquitards (Fig. 9). The steepest hydraulic gradients originate in Tertiary bedrock beneath the Burrard upland.

low salinities encountered in sand and silt units in deep boreholes. The low salinities require continual flushing by landward-derived freshwater, to either counteract saltwater intrusion or dilute saline connate water; i.e. a sufficient hydraulic head exists in the deep units, including Tertiary bedrock.

An important consequence of the model results is that seaward flow of freshwater beneath the tidal flats and submarine seepage at the delta front is likely. Groundwater flow under Boundary Bay is also possible. Groundwater expelled at the seepage face must originate higher on the delta plain or on the adjacent uplands. Maximum flow velocities for the sheet-sand aquifer in layers 3 and 4 are 1.4 m/day and 1.1 m/day, respectively. Average flow velocities will be lower because of aquifer anisotropy and heterogeneity, and the effects of tidal flux; therefore, groundwater residence times calculated from these values are minima. This means that groundwater that is recharged to local flow systems 10 km from the delta front will take a minimum of about 20 years to reach a possible seepage face. Residence times for groundwater in the deeper aquifers are about two orders of magnitude longer. However, even these rates are much higher than flow rates in prodelta and delta-slope aquitards, which range from 0.0001-0.001 m/day.

DISCUSSION

Given the results of the groundwater flow simulations, the significance of submarine groundwater seepage is examined as a possible cause of slope failure on the Fraser delta front. Submarine groundwater seepage is common in coastal plains, deltas, and some carbonate platforms. For example, freshwater artesian-flow conditions were encountered during drilling through carbonate platform rocks up to 120 km from the Florida coast and 130 m below the sea floor (Manheim, 1967). Elsewhere on the Atlantic coast, groundwater flow occurs in an eastward-thickening, Cretaceous to Holocene sedimentary wedge, and submarine seepage is associated with local and regional flow systems (Harsh and Laczniak, 1990; Leahy and Martin, 1993; Richardson, 1994). The extent of sub-sea groundwater flow depends on aquifer extent, hydraulic continuity, and, in particular, elevation and topographic relief of the recharge area (Toth, 1963; Bredehoeft et al., 1982). If the topographic drive is insufficient, the seaward flow of groundwater will be counteracted by landward migration of a saline wedge.

Slope failure is a natural phenomenon on most deltas. Delta-slope failures can be viewed as one of the many processes that transport sediment basinward. The causes of slope failure are many and varied and include those intrinsic to the delta depositional system. Christian et al. (1995) suggested that failures of the Fraser delta slope may result from a reduction in the mechanical strength of marine clay caused by freshwater leaching deep in the delta. As evidence, they cited positive pore pressures and salinity gradients in deep boreholes (Dallimore et al., 1995).

Clay leaching, although a feasible process, would be interminably slow given the exceedingly low hydraulic conductivity of clay-rich sediments ($<10^{-6}$ cm/s). In comparison, groundwater flow in interbedded sand and gravel is several orders of magnitude greater than in clay. Therefore, if groundwater beneath the delta has sufficient hydraulic potential and the permeable layers intersect the delta front or slope, the resulting seepage could profoundly increase pore pressures in the surficial delta deposits and induce failure.

Hydraulic gradients with significant vertical components have been documented in some deep (100-300 m) boreholes drilled on the delta (Dallimore et al., 1995). Artesian flow conditions, encountered in boreholes drilled during construction of Alex Fraser bridge, show that head values increase to

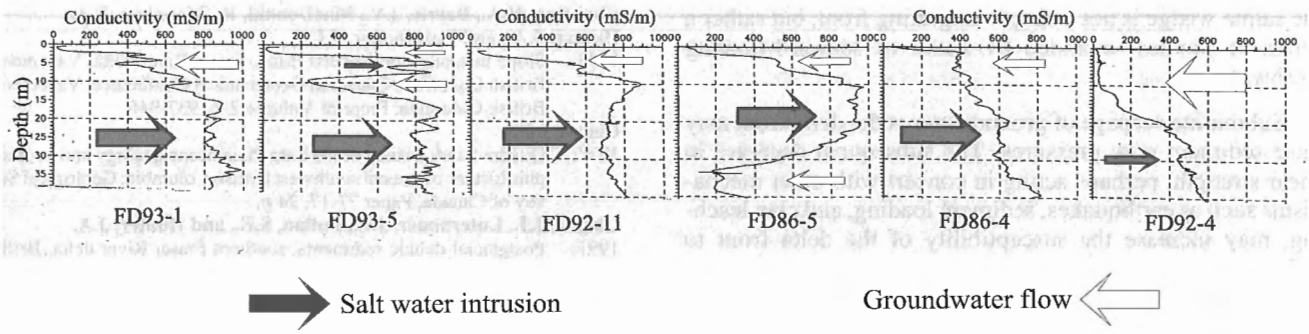

Figure 11. *Conductivity profiles for boreholes in the Coal Port-south delta area (see Fig. 1 for locations). The profiles extend through the sheet-sand aquifer and the upper part of the delta slope succession. Arrows indicate the inferred direction and relative magnitude of seawater intrusion and groundwater flow. Borehole data from Hunter et al. (1994).*

8 m above sea level at depths of 85 m (Bazett and McCammon, 1986). The driving force for these higher pore pressures is the elevated topography in uplands bordering the Fraser delta. Elevated heads (artesian flow) are probably maintained in the sheet-sand aquifer by the thin, but leaky, fine-grained sand-silt-mud layer that covers most of the delta plain. There is good reason, therefore, to suspect that groundwater could find its way to the delta front, although actual pore-pressures at the seepage face are unknown.

Flow in the shallow sheet-sand aquifer may take place above a local saline wedge. Measurements of pore-water conductivity in several boreholes on the delta (Hunter et al., 1994) document a salinity profile expected from intrusion of a saline wedge into the sheet-sand aquifer, namely a downwards increase in conductivity (Fig. 11). Zones of low conductivity probably result from mixing and more efficient flushing by seaward-flowing groundwater. Although there is considerable variation in conductivity profiles among boreholes, the general trend is one of landward-decreasing salinities. However, mixing of fresh groundwater (<200 mS/m; Hunter et al., 1994) with seawater is apparent even in the westernmost borehole, located at the seaward margin of the tidal flats (Coal Port, Fig. 1). The conductivity profiles (Fig. 11) and contoured conductivity values in the south delta area (Hunter et al., 1996) further demonstrate that the geometry of the intruding saline wedge is complex and perhaps should be viewed as a series of landward migrating plumes, separated by areas of focused, fresh or brackish, seaward-flowing groundwater, rather than as a simple migrating saline front. For example, groundwater flow focused beneath the Main Channel could contribute to delta-front failure near Sand Heads.

There is no direct evidence of fresh- or brackish-water seepage at the front of the Fraser delta. However, the conclusions drawn from the modelling presented in this paper can be tested by careful measurement of pore pressures in boreholes at the delta front, direct measurement of submarine seepage, and more detailed conductivity profiling. Such studies might reveal the geometry of seaward-migrating freshwater plumes.

CONCLUSIONS

Three-dimensional numerical simulations of groundwater flow in the Fraser delta have been conducted to generate a water-table map and assess some of the factors contributing to regional flow. The stratigraphy of the delta and adjacent upland areas has been subdivided into three essential units: the postglacial (Holocene) delta; Pleistocene glacial and interglacial deposits; and Tertiary bedrock. Each unit contains aquifers and aquitards, the geometry of which have been simplified for the purposes of modelling. For example the sandy, delta topset layer (the sheet-sand aquifer) is modelled as a contiguous, semiconfined to unconfined aquifer. Model boundaries approximate natural hydraulic boundaries and include low-tide limits at the coast and drainage divides on the uplands.

Shallow groundwater beneath the Fraser delta is recharged by a combination of direct precipitation and topography-driven flow from adjacent uplands. Recharge to the deeper Pleistocene aquifers is mostly from topography-driven flow and vertical leakage through aquitards. Simulated hydraulic gradients in the sheet-sand aquifer have low values parallel to hydraulic divides (0.1-0.25 m/km). Artesian pressures observed in the eastern part of the delta plain are simulated reasonably well; modelled heads are 2-3 m above the delta plain surface. The artesian flow is probably the result of flow systems originating in the Surrey and Burrard uplands.

Computed maximum flow velocities for the sheet-sand aquifer range from 1.1 to 1.4 m/day; average velocities are lower because of aquifer anisotropy and heterogeneity. This means that groundwater will take a minimum of about 20 years to travel a distance of 10 km beneath the delta plain.

The model results indicate the likelihood of seaward flow of freshwater beneath the tidal flats. Therefore, submarine seepage at the delta front is also possible. Electrical conductivity profiles from boreholes on the delta show that mixing of seawater (the saline wedge) and seaward-flowing groundwater takes place as far west as the low-tide limit. However,

the saline wedge is not a simple migrating front, but rather a series of plumes separated by zones of seaward-flowing freshwater.

Submarine seepage of groundwater at the delta front may raise sediment pore pressures. The subsequent decrease in shear strength, perhaps acting in concert with other mechanisms such as earthquakes, sediment loading, and clay leaching, may increase the susceptibility of the delta front to failure.

ACKNOWLEDGMENTS

This paper has benefited greatly from generous contributions from several individuals. Al Ages (Department of Fisheries and Oceans, Canada) provided data on the Fraser River; Leslie Smith (University of British Columbia) provided unpublished hydraulic conductivity data from samples collected at the B.C. Hydro Kidd 2 substation; and Jim Britton (Dynamic Oil Ltd.) made available oil-well logs and drill-stem test data. Mel Best, Jim Hunter, and John Luternauer (Geological Survey of Canada), and Hugh Liebscher (Environment Canada) kept me reasonably honest when interpreting stratigraphic, hydrostratigraphic, and geophysical data. Andrew Makepeace created the GIS base maps. Tony Sperling (Sperling Hansen Associates) and Bob Turner (Geological Survey of Canada) are thanked for their critical reviews, and John Clague is gratefully acknowledged for his editorial skills.

REFERENCES

Ages, A.B. and Woollard, A.L.
1994: The salinity intrusion in the Fraser River: observations of salinities, temperatures and currents by time-series and hovercraft coverage, 1985, 1986, 1987; Canada Department of Fisheries and Oceans, Canadian Data Report of Hydrography and Ocean Sciences, no. 126, 166 p.

Armstrong, J.E.
1981: Post-Vashon Wisconsin glaciation, Fraser Lowland, British Columbia; Geological Survey of Canada, Bulletin 322, 34 p.
1984: Environmental and engineering applications of the surficial geology of the Fraser Lowland, British Columbia; Geological Survey of Canada, Paper 83-23, 54 p.

Armstrong, J.E. and Hicock, S.R.
1979: Surficial geology, Vancouver, British Columbia; Geological Survey of Canada, Map 1486A, scale 1:50 000.
1980: Surficial geology, New Westminster, British Columbia; Geological Survey of Canada, Map 1484A, scale 1:50 000.

Bazett, D.J. and McCammon, N.R.
1986: Foundations of the Annacis cable-stayed bridge; Canadian Geotechnical Journal, v. 23, p. 458-471.

Bredehoeft, J.D., Back, W., and Hanshaw, B.B.
1982: Regional ground-water flow concepts in the United States: historical perspective; in Recent Trends in Hydrogeology, (ed.) T.N. Narasimhan; Geological Society of America, Special Paper 189, p. 297-316.

Britton, J.R., Harris, J.B., Hunter, J.A., and Luternauer, J.L.
1995: The bedrock surface beneath the Fraser River delta from seismic measurements; in Current Research, 1995-E; Geological Survey of Canada, p. 83-89.

Christian, H.A., Barrie, J.V., MacDonald, R., Monahan, P.A., Hunter, J.A., and Luternauer, J.L.
1995: Slope instability on Roberts Bank, Fraser River delta, Vancouver, British Columbia; Canadian Geotechnical Conference, Vancouver, British Columbia, Preprint Volume 2, p. 937-946.

Clague J.J.
1977: Quadra Sand: a study of the Late Pleistocene geology and geomorphic history of coastal southwest British Columbia; Geological Survey of Canada, Paper 77-17, 24 p.

Clague, J.J., Luternauer, J.L., Pullan, S.E., and Hunter, J.A.
1991: Postglacial deltaic sediments, southern Fraser River delta, British Columbia; Canadian Journal of Earth Sciences, v. 28, p. 1386-1393.

Clague, J.J., Luternauer, J.L., Monahan, P.A., Edwardson, K.A., Dallimore, S.R., and Hunter, J.A.
1998: Quaternary stratigraphy and evolution of the Fraser delta; in Geology and Natural Hazards of the Fraser River Delta, British Columbia, (ed.) J.J. Clague, J.L. Luternauer, and D.C. Mosher; Geological Survey of Canada, Bulletin 525, this volume.

Dallimore, S.R., Edwardson, K.A., Hunter, J.A., Clague, J.J., and Luternauer, J.L.
1995: Composite geotechnical logs for two deep boreholes in the Fraser River delta, British Columbia; Geological Survey of Canada, Open File 3018, 1 sheet.

Freeze, R.A. and Cherry, J.A.
1979: Groundwater; Prentice-Hall, Engelwood Cliffs, New Jersey, 604 p.

Gordy, P.L.
1988: Evaluation of the hydrocarbon potential of the Georgia depression; British Columbia Ministry of Energy, Mines and Petroleum Resources, Geological Report 88-03.

Halstead, E.C.
1986: Ground water supply - Fraser Lowland, British Columbia; Environment Canada, Inland Waters Directorate, National Hydrology Research Institute Paper No. 26, Scientific Series No. 145, 80 p.

Hamilton, T.S. and Ricketts, B.D.
1994: Contour map of the sub-Quaternary bedrock surface, Strait of Georgia and Fraser Lowland; in Geology and Geological Hazards of the Vancouver Region, Southwestern British Columbia, (ed.) J.W.H. Monger; Geological Survey of Canada, Bulletin 481, p. 193-196.

Harris, J.B., Hunter, J.A., Luternauer, J.L., and Finn, W.D.L.
1995: Site amplification modelling of the Fraser Delta, British Columbia; Canadian Geotechnical Conference, Vancouver, British Columbia, Preprint Volume 2, p. 947-954.

Harsh, J.F. and Laczniak, R.J.
1990: Conceptualization and analysis of ground-water flow system in the coastal plain of Virginia and adjacent parts of Maryland and North Carolina; United States Geological Survey, Professional Paper 1404-7, 100 p.

Hart, B.S., Prior, D.B., Barrie, J.V., Currie, R.G., and Luternauer, J.L.
1992: A river mouth submarine channel and failure complex, Fraser Delta, Canada; Sedimentary Geology, v. 81, p. 73-87.

Hunter, J.A., Luternauer, J.L., and Kurfurst, P.J.
1996: Regional electromagnetic soundings with the Geonics EM-34 conductivity meter in the southern Fraser River delta, B.C.; Geological Survey of Canada, Open File 3359, 141 p.

Hunter, J.A., Luternauer, J.L., Roberts, M.C., Monahan, P.A., and Douma, M.
1994: Borehole geophysical logs, Fraser River delta (92G), British Columbia; Geological Survey of Canada, Open File 2841, 30 p.

Jol, H.M. and Roberts, M.C.
1988: The seismic facies of a delta onlapping an offshore island: Fraser River delta, British Columbia; in Sequences, Stratigraphy, Sedimentology: Surface and Subsurface, (ed.) D.P. James and D.A. Leckie; Canadian Society of Petroleum Geologists, Memoir 15, p. 137-142.

Leahy, P.P. and Martin, M.
1993: Geohydrology and simulation of ground-water flow in the northern Atlantic coastal plain aquifer system; United States Geological Survey, Professional Paper 1404-K, 81 p.

Liebscher, H., Hii, B., and McNaughton, D.
1992: Nitrates and pesticides in the Abbotsford aquifer; Environment Canada, Inland Waters Directorate, Vancouver, British Columbia, 83 p.

Luternauer, J.L. and Finn, W.D.L.
1983: Stability of the Fraser River delta front; Canadian Geotechnical Journal, v. 20, p. 603-616.

Luternauer, J.L., Clague, J.J., and Feeney, T.D.
1991: A 367 m core from southwestern Fraser River delta, British Columbia; in Current Research, Part E; Geological Survey of Canada, Paper 91-1E, p. 127-134.

Luternauer, J.L., Barrie, J.V., Christian, H.A., Clague, J.J., Evoy, R.W., Hart, B.S., Hunter, J.A., Killeen, P.G., Kostaschuk, R.A., Mathewes, R.W., Monahan, P.A., Moslow, T.F., Mwenifumbo, C.J., Olynyk, H.W., Patterson, R.T., Pullan, S.E., Roberts, M.C., Robertson, P.K., Tarbotton, M.R., and Woeller, D.J.
1994: Fraser River delta: geology, geohazards and human impact; in Geology and Geological Hazards of the Vancouver Region, Southwestern British Columbia, (ed.) J.W.H. Monger; Geological Survey of Canada, Bulletin 481, p. 197-220.

Luternauer, J.L., Mosher, D.C., Clague, J.J., and Atkins, R.J.
1998: Sedimentary environments of the Fraser delta; in Geology and Natural Hazards of the Fraser River Delta, British Columbia, (ed.) J.J. Clague, J.L. Luternauer, and D.C. Mosher; Geological Survey of Canada, Bulletin 525, this volume.

Manheim, F.T.
1967: Evidence for submarine discharge of water on the Atlantic continental slope of thesouthern United States, and suggestions for further research; New York Academy of Sciences, Transactions, Series 2, v. 29, p. 839-853.

McKenna, G.T., Luternauer, J.L., and Kostaschuk, R.A.
1992: Large-scale mass-wasting events on the Fraser River delta front near Sand Heads, British Columbia; Canadian Geotechnical Journal, v. 29, p. 151-156.

Monahan, P.A., Luternauer, J.L., and Barrie, J.V.
1993: A delta plain sheet sand in the Fraser River delta, British Columbia, Canada; Quaternary International, v. 20, p. 27-38.

Mustard, P.S. and Rouse, G.E.
1994: Stratigraphy and evolution of Tertiary Georgia Basin and subjacent Upper Cretaceous sedimentary rocks; southwestern British Columbia and northwestern Washington State; in Geology and Geological Hazards of the Vancouver Region, Southwestern British Columbia, (ed.) J.W.H. Monger; Geological Survey of Canada, Bulletin 481, p. 97-169.

Pullan, S.E., Hunter, J.A., Jol, H.M., Roberts, M.C., Burns, R.A., and Harris, J.B.
1998: Seismostratigraphic investigations of the southern Fraser River delta; in Geology and Natural Hazards of the Fraser River Delta, British Columbia, (ed.) J.J. Clague, J.L. Luternauer, and D.C. Mosher; Geological Survey of Canada, Bulletin 525, this volume.

Pullan, S.E., Jol, H.M., Gagne, R.M., and Hunter, J.A.
1989: Compilation of high resolution 'optimum offset' shallow seismic reflection profiles from the southern Fraser River delta, British Columbia; Geological Survey of Canada, Open File 1992, 8 p.

Richardson, D.L.
1994: Hydrology and analysis of the ground-water-flow system of the Eastern Shore, Virginia; United States Geological Survey, Water-Supply Paper 2401, 108 p.

Ricketts, B.D. and Dunn, D.
1995: The groundwater database, Fraser Valley, British Columbia; in Current Research, 1995-A; Geological Survey of Canada, p. 7-10.

Ricketts, B.D. and Liebscher, H.
1994: The geological framework of groundwater in the Greater Vancouver area; in Geology and Geological Hazards of the Vancouver Region, Southwestern British Columbia, (ed.) J.W.H. Monger; Geological Survey of Canada, Bulletin 481, p. 287-298.

Toth, J.
1963: A theoretical analysis of groundwater flow in small drainage basins; Journal of Geophysical Research, v. 68, p. 4795-4812.

Woeller, D.J., Hunter, J.A., and Luternauer, J.L.
1993a: Results of SCPT and SASW testing of the Fraser River delta sediments, British Columbia (92G/2,3); Geological Survey of Canada, Open File 2714, 224 p.

Woeller, D.J., Luternauer, J.L., and Hunter, J.A.
1993b: Presentation and interpretation of seismic cone penetration test data, Fraser River delta, British Columbia; Geological Survey of Canada, Open File 2715, 60 p.

Wood, E.A.
1996: Comparison of hydraulic conductivity test methods for the Kidd2 site in Richmond, B.C.; B.A.Sc. thesis, University of British Columbia, Vancouver, British Columbia.

Geochemistry of seafloor sediments from the Strait of Georgia, British Columbia

C.E. Dunn[1]

Dunn, C.E., 1998: Geochemistry of seafloor sediments from the Strait of Georgia, British Columbia; in Geology and Natural Hazards of the Fraser River Delta, British Columbia, (ed.) J.J. Clague, J.L. Luternauer, and D.C. Mosher; Geological Survey of Canada, Bulletin 525, p. 257–270.

Abstract: Sediment samples from 127 seafloor sites in the Strait of Georgia were analyzed to determine the spatial distribution of a wide range of chemical elements. Concentrations are mostly close to normal background levels for marine mud; however, locally several groups of elements are relatively enriched. West of Burrard Inlet enrichments of Al, Fe, K, and Mg coincide with slightly elevated levels of Hg, Pb, Sb, Cu, F, Nb, and Rb, reflecting clay minerals, derived mostly from the Fraser River, but also from Howe Sound and Burrard Inlet. Other multi-element associations include a resistate fraction (REEs, Ti, Th, U, Be, Au); elements deposited under reducing conditions in relatively deep water (Na, Br, S, B, Mn, Co); a carbonate fraction (Ca, Sr, CO_2) with Zr and Hf; and an organic fraction (C, P, As, Zn). Factor analysis provides insight to element associations and indicates a possible anthropogenic component for Ag, Ba, Cu, F, Hg, Ni, Pb, Sb, and Zn.

Résumé : Des échantillons de sédiments prélevés à 127 sites sur le plancher sous-marin du détroit de Georgia ont été analysés pour déterminer la répartition spatiale d'un grand nombre d'éléments chimiques. Les concentrations correspondent pour la plupart aux teneurs de fond habituels pour les boues marines; cependant, plusieurs groupes d'éléments sont, par endroits, présent en quantités relativement plus grandes. À l'ouest de l'inlet Burrard, de fortes concentrations de Al, Fe, K et Mg coïncident avec des concentrations légèrement élevées de Hg, Pb, Sb, Cu, F, Nb et Rb; cette observation reflète la présence de minéraux argileux, provenant principalement du fleuve Fraser mais également du détroit de Howe et de l'inlet Burrard. D'autres associations de plusieurs éléments incluent une fraction de résistats (ÉTR, Ti, Th, U, Be et Au); des éléments déposés dans des conditions de réduction dans des eaux relativement profondes (Na, Br, S, B, Mn et Co); une fraction de carbonates (Ca, Sr et CO_2) avec Zr et Hf qui ont une répartition semblable; et une fraction organique (C, P, As et Zn). Une analyse factorielle permet de mieux comprendre les associations d'éléments et indique que Ag, Ba, Cu, F, Hg, Ni, Pb, Sb et Zn sont peut-être d'origine anthropique.

[1] Geological Survey of Canada, 601 Booth Street, Ottawa, Ontario K1A 0E8

INTRODUCTION

During the past 30 years, several researchers have examined aspects of the chemistry of sediments in the Fraser River delta (Waldichuk et al., 1968; Grieve and Fletcher, 1976) and the Strait of Georgia (Waldichuk, 1983; Macdonald et al., 1991). Delaney and Turner (1994) reviewed trace-element databases in the Vancouver map area and listed several studies that involved the monitoring of a few sites in the Strait of Georgia for a limited range of elements. From a review of these studies it was apparent that no systematic multi-element geochemical sampling program had been undertaken in the Strait of Georgia.

This report is a summary of a program to provide fundamental baseline data on the content of chemical elements in seafloor sediments from the southern Strait of Georgia (Fig. 1). The sample material that was available for study was collected primarily for sedimentological purposes and, therefore, was not ideal for geochemical analysis. Normally, sediment cores are required to differentiate natural from anthropogenic inputs of chemical elements, and such material was not available for this work. It is emphasized that the objective of the present study is to provide a general indication of element levels in seafloor sediments from the Strait of Georgia using available grab sediment samples. The objective was not to conduct an exhaustive environmental study aimed at differentiating natural from anthropogenic inputs.

A Geological Survey of Canada Open File (Dunn et al., 1996) supplements this report, and contains full program details, listings of all data, statistical summaries, element-distribution maps, and a bathymetric map.

METHODS

Sample collection and preparation

One hundred and twenty-seven grab samples of muddy and sandy sediment were collected during a scientific cruise of CSS *Tully* in November 1992. Samples were collected from water depths of 50 to 350 m, except at ten sites on tidal flats off Lulu Island and along the Fraser River.

A Shipek grab sampler was used to scoop up approximately 200-500 g of the top 10 cm of sediment below the seafloor. Evoy et al. (1993) estimated that the average sediment accumulation rate at a site they described as 'offshore background', west of Sturgeon Bank (Lulu Island, Fig. 1) at a water depth of 200 m, is 0.76 cm/a. They further estimated that sediments from several sites up to 20 km farther south accumulated at rates ranging from 0.49 to more than 2.92 cm/a. Assuming that similar sedimentation rates prevail throughout the survey area, the top 10 cm of material collected for this study accumulated within the past 20 years. This estimate, however, is only approximate because sedimentation rates in the southern Strait of Georgia are strongly influenced by seafloor topography and currents.

All sediment samples were freeze-dried, and a 5-10 g portion of each sample was subjected to geochemical analysis. Ninety-seven of the samples were fine mud, 20 were sandy mud, and the 10 samples from shallow water were sand. Samples were gently disaggregated with an agate mortar and pestle, and any shell fragments or pebbles were removed with plastic tweezers. Clay-rich samples were ground to a fine

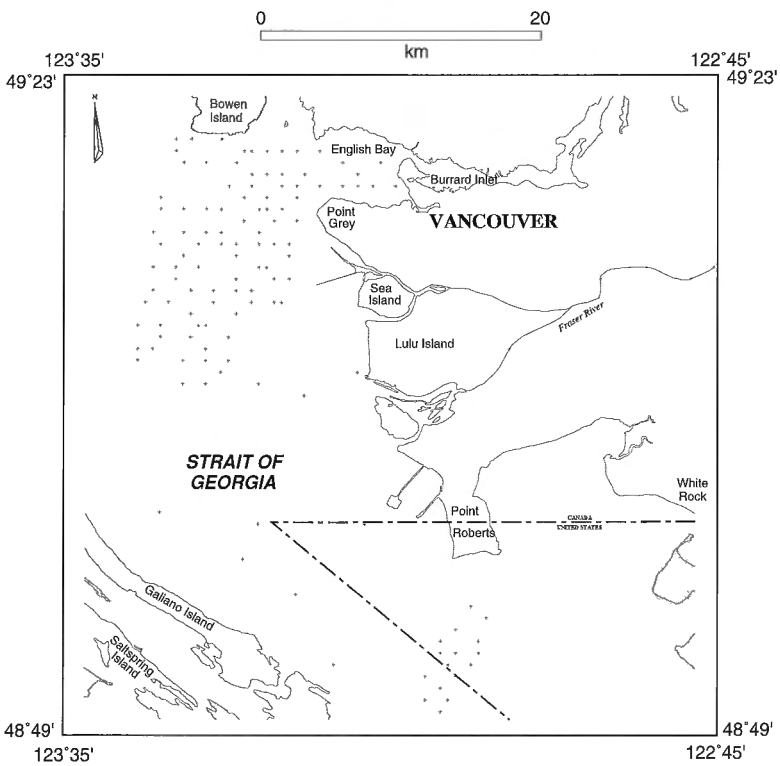

Figure 1.

Map of survey area showing sample locations.

powder in the agate mortar, and the sandy samples were ground in a ceramic ball mill. The maximum grain size after grinding was 50 µm, but most grains were smaller.

Analysis

The analytical program used the following techniques:

X-ray fluorescence (XRF) analysis for the major oxides of Al, Ca, Fe, K, Mg, Mn, P, Si, Ti, Na, and for trace elements Ba, Nb, Rb, Sr, and Zr

Approximately 1.5 g of sediment powder was ignited in a muffle furnace, and the loss-on-ignition at 900°C was recorded. During this procedure, traces of volatile elements (e.g. F, Cl, Br, Hg), water (moisture [H_2O^-] and structurally bound [H_2O^+]), and CO_2 were lost. A 1 g aliquot of each sample was then fused with $LiBO_2$. Element concentrations were determined using the methods of Rousseau (1984a, b). The XRF method is nondestructive and provides the total concentration of each element, regardless of chemical bonding.

Instrumental neutron activation analysis (INAA) for Ag, As, Au, Ba, Br, Ca, Ce, Co, Cr, Cs, Eu, Fe, Hf, Hg, Ir, La, Lu, Na, Nd, Ni, Rb, Sb, Sc, Se, Sm, Sn, Ta, Tb, Th, U, W, Yb, Zn

Approximately 0.5 g of dry powder (not ignited) was weighed accurately in a polyethylene vial and sent to Activation Laboratories Ltd. (Ancaster, Ontario) for analysis by instrumental neutron activation. INAA, like XRF, is nondestructive and provides the total content of each element in the samples.

Inductively-coupled plasma emission spectrometry (ICP-ES) following an aqua regia digestion

A 0.5 g portion of each dry powder (not ignited) was digested with 3 ml of a 3:1:2 mixture of HCl-HNO_3-H_2O (aqua regia) at 95°C for one hour, then diluted to 10 ml with distilled water. For some elements, this leach is partial because the aqua regia digestion fails to release into solution all elements that are structurally bound within crystal lattices. The partial release of elements provides an indication of their relative stability in the sediments. Table 1 lists the elements determined by ICP-ES for which adequate precision and accuracy were obtained, and their determination limits. An estimate is given of the percentage of each element released into solution during the aqua regia digestion.

Other methods for determining F, Cl, S, C, and Hg

The elements Fl, Cl, and S were determined on 100 mg portions of dry powders (not ignited) by the method of Hall et al. (1986). Pyrohydrolysis was used to separate the elements from their matrix, and concentrations were determined by ion chromatography (Dionex). Determination limits are 50 ppm for F and S, and 100 ppm for Cl.

Carbon dioxide was determined by acid evolution. The content of organic C was estimated from the difference between total C, determined by combustion, and carbonate C, determined by acid evolution.

Mercury was determined on dry sediment samples by cold-vapour atomic absorption spectrometry, involving reduction of mercury ions to metallic mercury and flushing with H_2 into the atomic absorption spectrometer.

Analytical precision and accuracy

Data quality was monitored throughout all analytical programs by inserting, within each batch of 20 samples, two subsamples of a single sample selected at random (i.e. a duplicate sample for determining analytical precision and sample homogeneity), and one sample of the National Research Council (NRC) standard marine mud #BCSS-1 (for determining the accuracy of the analytical procedures). Details on data quality are given in Dunn et al. (1996).

Data presentation

For simplicity and because of space limitations, the maps included in this paper show data for the total sample population. Element distributions for each of the three groups of sediments (mud, sandy mud, sand) are given in Dunn et al. (1996, Appendix B). The dots on the distribution maps (Fig. 2-7) are proportional in size to concentrations of the elements. This method of data presentation is useful for displaying spatial trends of enrichment and depletion; however, the absolute values themselves should be considered before assessing whether unusually high concentrations are present. Table 2 provides data to assist in such evaluations. For example, the data for lead (Fig. 3) show that the spread between the median and maximum concentrations is small, i.e. 12-28 ppm Pb.

Table 1. Elements analyzed by ICP-ES.

Element		Unit of measure	Determination limit	Approximate % leached by acid digestion[1]
Silver	Ag	ppm	0.1	100 (?)
Aluminum	Al	%	0.01	25 - 30
Boron	B	ppm	2	<25
Barium	Ba	ppm	1	10-20
Beryllium	Be	ppm	0.2	most?
Calcium	Ca	%	0.01	50
Cadmium	Cd	ppm	0.2	100 (?)
Cobalt	Co	ppm	1	90-100
Chromium	Cr	ppm	1	40
Copper	Cu	ppm	1	100
Iron	Fe	%	0.01	80-90
Mercury[2]	Hg	ppb	10	100 (?)
Potassium	K	%	0.01	20-25
Lanthanum	La	ppm	1	80
Lithium	Li	ppm	2	100 (?)
Magnesium	Mg	%	0.01	70-80
Manganese	Mn	ppm	1	100
Molybdenum	Mo	ppm	2	100 (?)
Sodium	Na	%	0.01	45-60
Nickel	Ni	ppm	1	90-100
Phosphorus	P	%	0.001	60-70
Lead	Pb	ppm	2	80-100
Strontium	Sr	ppm	1	20-25
Titanium	Ti	%	0.02	30
Vanadium	V	ppm	1	30
Zinc	Zn	ppm	1	70-90

Note: All values are above the determination limit except some analyses for Ag, B, Be, Cd, and Mo.
[1] Determined by comparison with standard marine mud sample BCSS-1 and/or concentrations obtained by XRF or INAA
[2] Determined by cold-vapour atomic absorption spectrometry.

Table 2. Comparison of median concentrations of elements in mud from the Strait of Georgia, NRC Standard Reference marine muds, and marine muds and shales from around the world.

Oxide/ element	Median in Strait of Georgia (this study)	NRC marine sediments	World average[1]	Type of sediment or sedimentary rock[1]
Determination by XRF (major oxides)				
Al_2O_3 (%)	14	12.23[2]	15.47	Shale
CaO (%)	2.44	2.92[2]	3 - 5	Marine mud and shale
Fe_2O_3 (%)	6.4	6.96[2]	9.3	Deep-sea mud
K_2O (%)	2.06	1.50[2]	2.81	Marine mud
MgO (%)	2.96	2.41[2]	2.5	Shale
MnO (%)	0.07	0.07[2]	4.9	North Pacific deep-sea mud
Na_2O (%)	3.5	4.40[2]	4	Marine mud
P_2O_5 (%)	0.23	0.23[2]	0.15	Shelf clay (0.28% in deep-sea mud)
SiO_2 (%)	58	55.7[2]	54	Clay derived from rocks of intermediate composition
TiO_2 (%)	0.75	0.70[2]	0.71	Deep-sea sediment
Determination by XRF (trace elements)				
Ba (ppm)	550	–	546	Shale
Nb (ppm)	10	–	10	Shale
Rb (ppm)	74	–	128	Shale
Sr (ppm)	260	277[2]	130-280	Marine sediment
Zr (ppm)	130	–	180	North Pacific deep-sea mud
Determination by INAA				
As (ppm)	8.3	11.1[3]	9 - 11	Marine mud
Au (ppb)	4	–	1.6 - 4.2	Nearshore clay-rich silt - Canadian Arctic
Br (ppm)	85	–	111	Barents-sea mud (top 1 cm)
Ce (ppm)	42	–	73	North American shale
Co (ppm)	15	17.5[2]	12	Atlantic deep-sea mud
Cr (ppm)	84	113[2]	84-110	North Pacific deep-sea mud
Cs (ppm)	2.5	4[3]	6	Modern sediment
Eu (ppm)	1.01	–	1.2	North American shale
Hf (ppm)	3.3	–	4.6	Deep-sea mud
La (ppm)	20.3	–	37	North American shale
Lu (ppm)	0.26	–	0.4	North American shale
Nd (ppm)	18	–	33	North American shale
Sb (ppm)	0.7	0.59[3]	1 - 2	Marine mud
Sc (ppm)	14	–	19	North Pacific deep-sea mud
Sm (ppm)	3.8	–	5.7	North American shale
Th (ppm)	5.7	–	4.8	Marine mud
U (ppm)	1.7	–	2.3	Marine mud
Yb (ppm)	1.81	–	3.1	North American shale
Zn (ppm)	120	119[3]	85	North Pacific deep-sea mud
Determination by ICP-ES				
Ag (ppm)	0.4	0.18[4]	0.1 - 0.3	Clay-rich sediment
B (ppm)	25[5]	–	230 - 2500	Saline clay
Be (ppm)	0.2	1.3[3]	2.5	Deep-sea mud
Cd (ppm)	0.2	0.25[3]	0.24	Marine mud
Cu (ppm)	42	39[4]	300	North Pacific deep-sea mud
Li (ppm)	27	74[4]	49 - 70	Pacific Ocean deep-sea mud
Mo (ppm)	1	1.9[3]	4 - 18	Pacific Ocean deep-sea mud
Ni (ppm)	39	44[2]	39	Nearshore marine mud (world-wide)
Pb (ppm)	12	22[4]	51	North Pacific mud
V (ppm)	50	127[2]	120	Deep-sea sediment
Determination by miscellaneous chemical methods				
C_{org} (%)	1.4	2.1[4]	–	
Hg (ppb)	95	92[4]	400	Shale
F (ppm)	579	–	200 - 400	Marine mud
S (ppm)	1724	1800[4]	1100	Marine mud (wide range in concentrations)

1 From Wedepohl (1969).
2 NRC marine sediment reference material PACS-1 - mud from Esquimalt Harbour.
3 NRC marine sediment reference material BCSS-1 - mud from Baie des Chaleurs (Gulf of St. Lawrence).
4 NRC marine sediment reference material MESS-2 - mud from the Beaufort-sea.
5 Partial extraction.

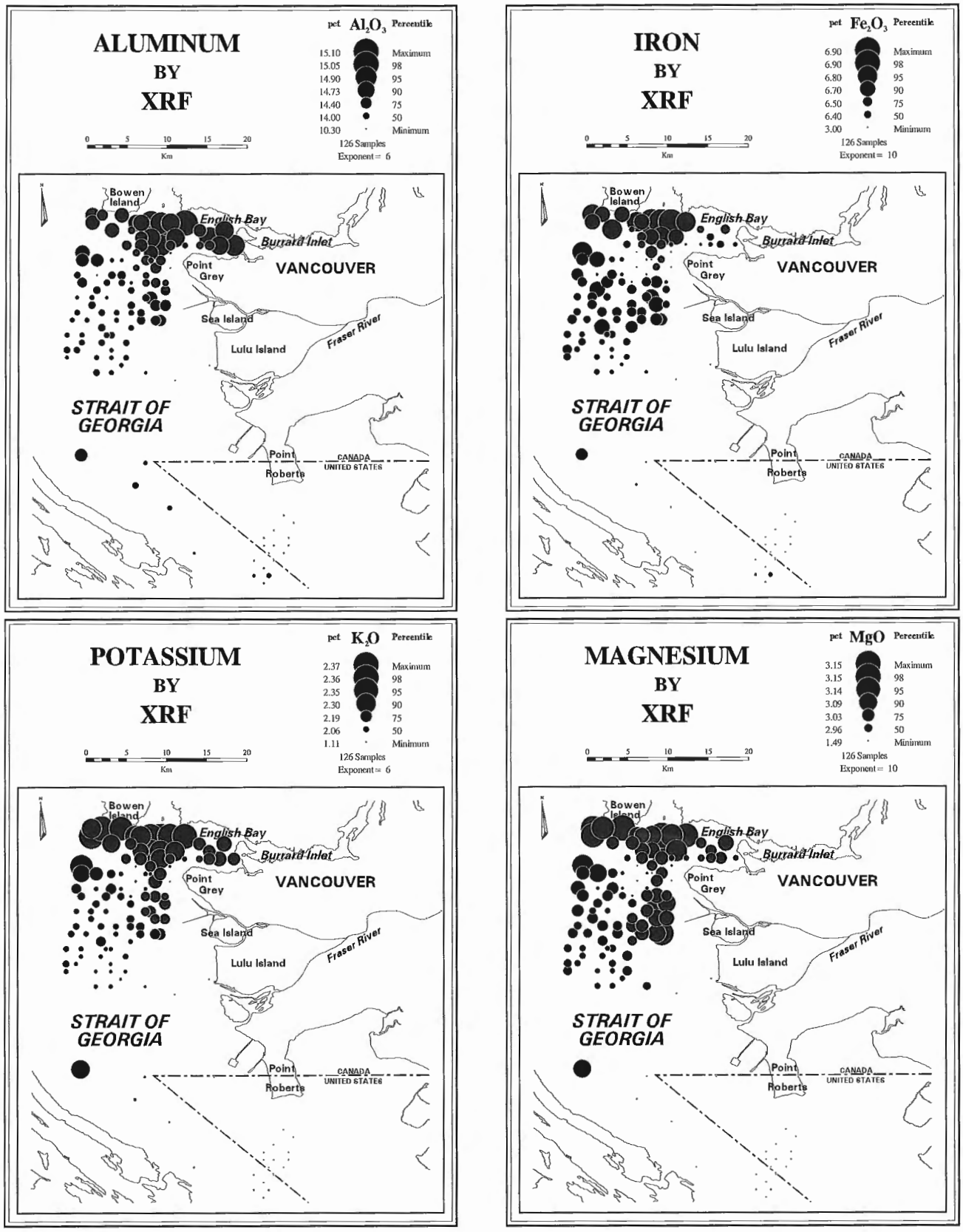

Figure 2. *Distribution patterns of Al_2O_3, Fe_2O_3, K_2O, and MgO in Strait of Georgia sediments. Elemental enrichments are related to aluminosilicate minerals and ferromagnesian clay minerals.*

There is a distinct relative enrichment of lead in the northern part of the survey area, but lead levels in Strait of Georgia sediments are mostly lower than average concentrations in marine muds from elsewhere (Table 2).

RESULTS

With some exceptions, element concentrations in muddy sediments are higher than those in sands. The exceptions are higher silica concentrations in sands because of their high quartz content, locally higher concentrations of Mn (mostly as oxides coating sand particles), and Ca, Sr, and Ba (associated with carbonates in the southern part of the survey area, south of Roberts Bank).

Median concentrations of elements in Strait of Georgia sediments are very similar to concentrations in the National Research Council (NRC) standard marine muds (PACS-1, BCSS-1, and MESS-2) from sites around Canada (Table 2). The standard from Esquimalt Harbour (PACS-1), however, is contaminated, and unusually enriched in a number of trace elements. Therefore, for most trace elements, concentrations in the other standards are used for comparison with the Strait of Georgia values. In order to further evaluate the chemical composition of mud from the Strait of Georgia, data compiled in the Handbook of Geochemistry (Wedepohl, 1969) have been reviewed and are summarized in Table 2. For many elements no data are available for nearshore muds; in these instances values for deep-sea muds are given. Typically, deep-sea muds are considerably more enriched in Fe and Mn than muds from shallower waters. In general, trace-element concentrations in Strait of Georgia sediments are similar to, or less than, concentrations in marine muds from around the world. Comparison with analyses of ancient shales derived mostly from shallow seas shows that muddy sediments from the Strait of Georgia are depleted in most elements.

Elements that display similar distribution patterns in the Strait of Georgia have been grouped together in Figures 2 to 7. Each figure shows four elements with similar distribution patterns related to a particular chemical or physical factor. These 'factors' are discussed separately in the following sections.

Major elements – clay factor

Figure 2 shows that, for the data set as a whole, concentrations of Al, K, Fe, and Mg are relatively high at water depths of 25 to 250 m in the northern part of the survey area (English Bay and approaches to Howe Sound). Compared to marine muds elsewhere (Table 2), concentrations are moderate to low, with no site unusually enriched in any of these elements.

The tidal regime off the Fraser delta is rectilinear, with the northwesterly flowing flood tide stronger than the southeasterly ebb. As a result, fine-grained sediment is transported in suspension north from the mouth of the Fraser River. Fine-grained, potassium-rich aluminosilicates (e.g. clay minerals such as illite) and ferromagnesian-rich minerals (e.g. chlorite and smectite) are deposited from suspension in English Bay and southern Howe Sound, giving rise to the relatively high concentrations of Al, K, Fe, and Mg in those areas. No data are available on the clay mineralogy of seafloor sediments from the Strait of Georgia, but X-ray diffraction analysis of samples of Holocene mud obtained from boreholes on the Fraser delta shows that the dominant clay mineral is chlorite, with secondary illite and minor smectite (S. Dallimore, personal communication, 1996).

A factor that probably contributes significantly to the relative concentration of these major elements in the northern part of the survey area is the southward flux of water and sediment from Howe Sound, north of Bowen Island. Surface waters in Howe Sound have low salinity due to the high influx of freshwater from the surrounding mountains and the hinterland (Percival et al., 1992). Mixing of these low-salinity waters with waters of the Strait of Georgia could promote flocculation and precipitation of clay minerals. Waters moving westward into English Bay from Burrard Inlet, east of Vancouver, may also carry clay minerals into the northern part of the survey area.

Trace elements – clay factor

Several trace elements show patterns of relative concentration that are similar to those of the major elements depicted in Figure 2. Figure 3 shows distributions of four such metals - Hg, Pb, Sb, and Cu. Absolute concentrations of these metals are not high. Mercury values range from below the determination level of 10 ppb to a maximum of 175 ppb, all below the average for shales (400 ppb Hg, Table 2). At the northern end of the survey area, however, mercury levels are mostly in excess of 100 ppb, greater than values to the south. Lead concentrations are low in all samples, ranging from 15 to 28 ppm in the north to mostly less than 15 ppm in the south. The antimony data, obtained by INAA, are extremely precise and accurate, therefore the minor differences in concentrations (Fig. 3) are real and not attributable to analytical error. The maximum concentration of 1.2 ppm Sb is similar to the average for marine muds (Table 2). Copper concentrations are highest in the northeast, reaching a maximum of 120 ppm. Fluorine, niobium, and rubidium also exhibit similar distribution patterns to the elements shown on Figures 2 and 3 (Dunn et al., 1996).

Many elements, notably the rare earths, Cs, Co, Sc, Li, and Zn, are also enriched in the north relative to some other areas. However, they also show enrichment at other locations, most commonly in deeper waters to the west.

The similarity of the spatial patterns of these trace elements and the phyllosilicate-related major elements (Fig. 2) is the result of at least two factors. First, some trace elements travel within the crystal structures of clay-mineral particles from their source to their site of deposition. Second, trace elements may be adsorbed on clay minerals. Phyllosilicates have a large surface area relative to their volume and therefore have many attachment sites for cations, anions, and polar molecules. Adsorption may take place during transport in marine waters, or in areas where physicochemical conditions change. Examples of the latter are the transition zone between freshwater and saline waters off the mouth of the Fraser

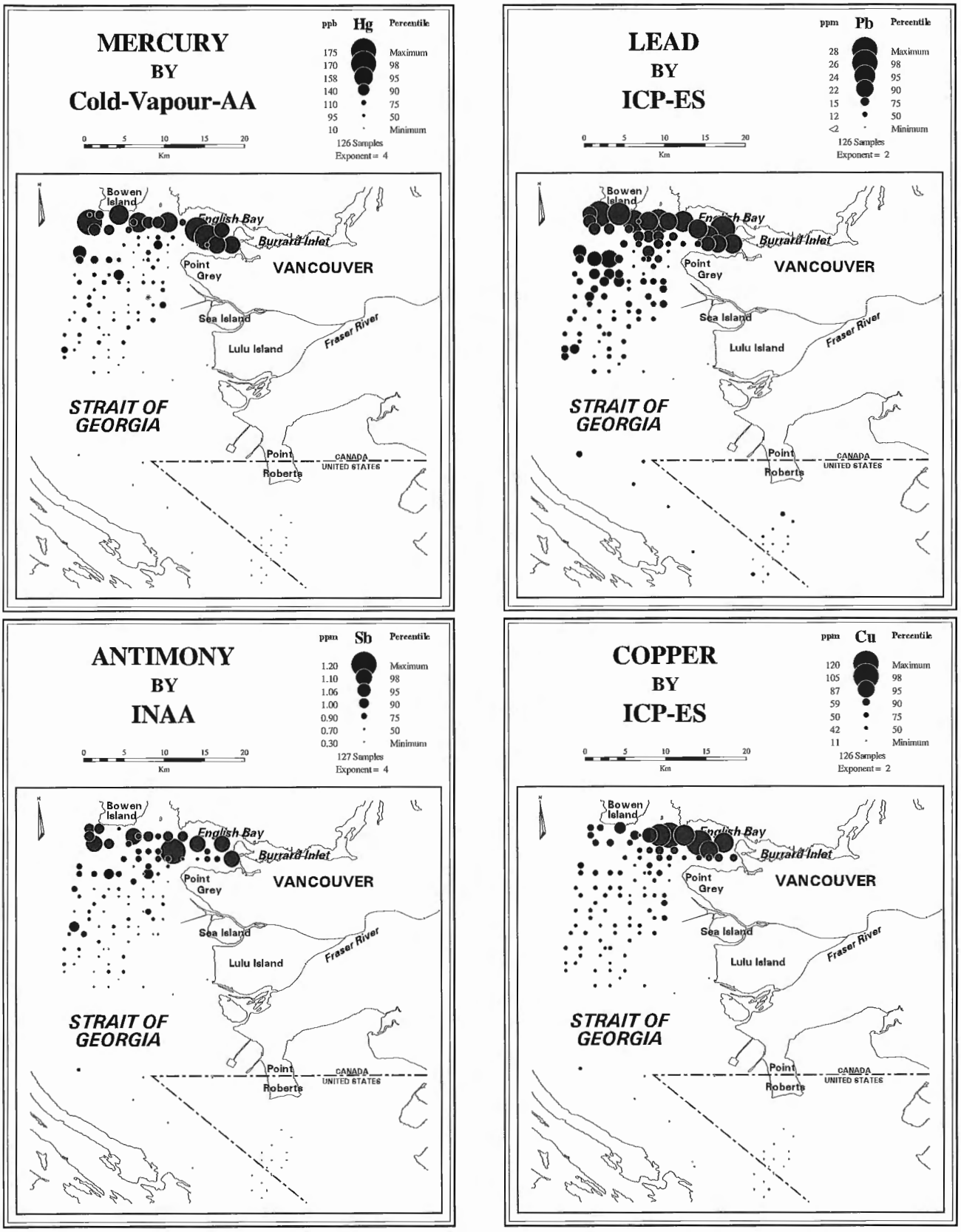

Figure 3. Distribution patterns of Hg, Pb, Sb, and Cu in Strait of Georgia sediments. Elemental enrichments are associated mainly with fine-grained aluminosilicate minerals.

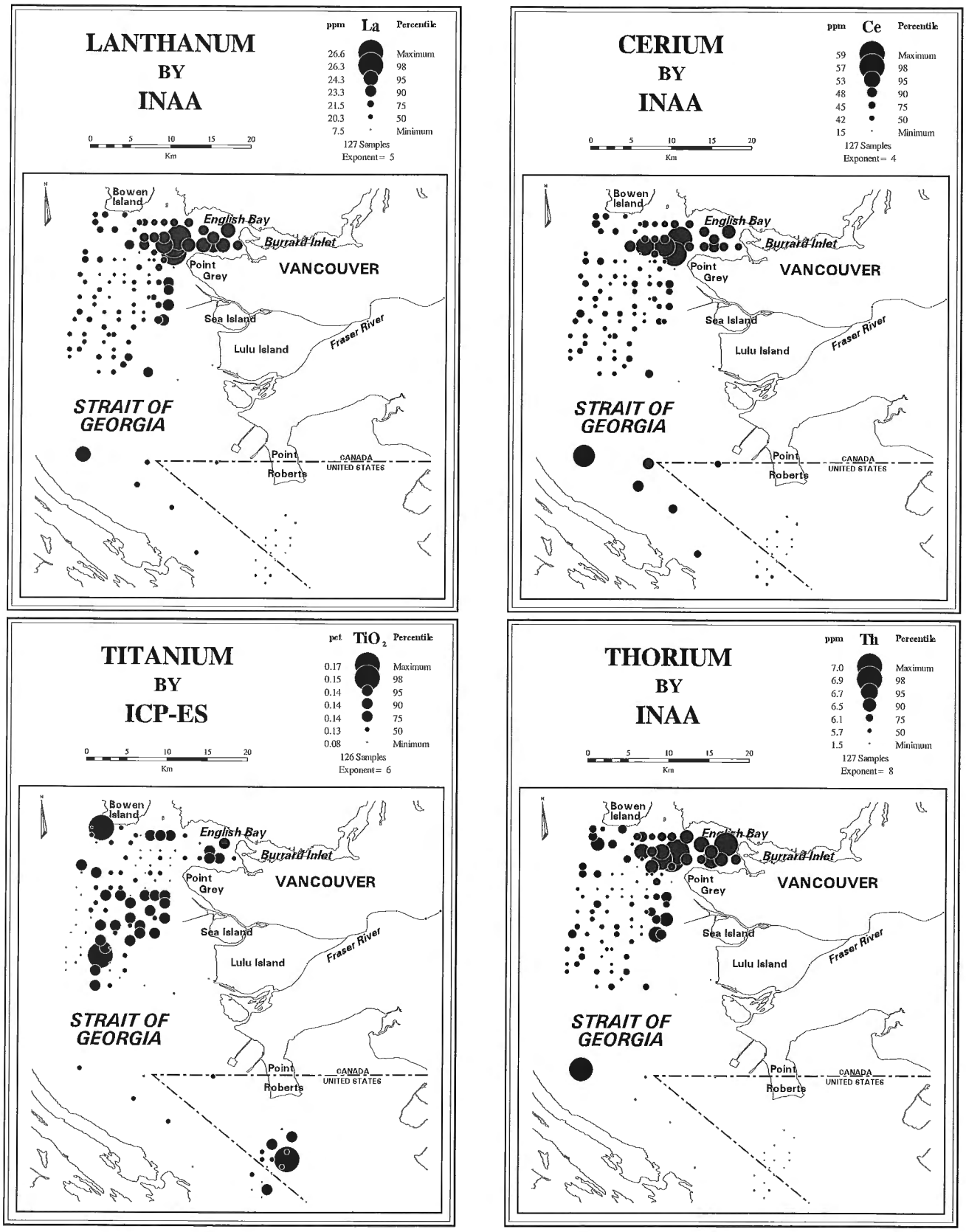

Figure 4. Distribution patterns of La, Ce, TiO_2, and Th in Strait of Georgia sediments. Elemental enrichments are related, in part, to resistate minerals.

River, the area where relatively fresh surface waters enter the Strait of Georgia from Howe Sound, and the area where waters of Burrard Inlet and English Bay mix.

Some trace-element enrichment in the northern part of the survey area could be the result of anthropogenic inputs. There is undoubtedly a flux of elements to the Strait of Georgia from human activities in the Vancouver area, but the grab samples used in this study are not ideally suited for quantifying this contribution; as mentioned previously, carefully collected and dated cores are required for this purpose. It is worth noting, however, that no sample yielded metal concentrations that are abnormally high. If anthropogenic inputs are responsible for the slightly elevated levels of Cu, Hg, and Pb shown in Figure 3, the question then arises as to why there are concomitant higher levels of elements such as Nb, Sc, Th, and the rare earth elements (Fig. 4) for which an anthropogenic source is not evident. Equally, a natural source (clay minerals) and local physicochemical conditions (mixing of low-salinity waters derived from Howe Sound and Burrard Inlet with marine waters of the Strait of Georgia) could explain the distribution patterns that are observed. It is probable that there is some influx of metals from human activity in the Vancouver area, but it is unlikely that this is the sole source of metal enrichment. This issue cannot be resolved by analysis of the samples used for this study.

Trace elements – resistate fraction

The levels of several elements are relatively elevated in sediments on the Fraser delta slope west of Lulu and Sea Islands, and off Point Grey, in waters that are 50 to 200 m deep. This suite includes elements that are characteristically elevated in resistate fractions of sediments (e.g. monazite, ilmenite, rutile), notably Th, Ti and the rare earth elements (REEs). Figure 4 shows distributions of two of the REEs (La and Ce), Ti and Th. The other REEs that were determined (Nd, Sm, Eu, Yb, and Lu) have similar distribution patterns.

There is moderate sediment enrichment in U, Be, and Au at these sites. At several locations, Au concentrations are unusually high (up to 35 ppb), an order of magnitude above background levels for marine sediments.

The distribution patterns of elements shown in Figure 4 are somewhat similar to those in Figures 2 and 3. The main difference is a lack of resistate-element concentrations on the north side of English Bay, westward to Bowen Island. The relatively high concentrations of resistate elements off Point Grey could be related to erosion of Pleistocene granitic sands which crop out in the sea cliffs there (J.J. Clague, pers. comm., 1996). The fine-grained fractions of these sediments were winnowed by waves and currents and transported to the west and north, giving rise to silt with relative enrichment of resistate minerals.

Deep-water elements

Figure 5 shows distribution patterns of several elements with relatively elevated values in sediments in the western part of the survey area where water depths exceed 300 m. These elements include Na, Br, S, aqua-regia-extractable B (less than 25% of the total; see Table 1), Mn, Co, and to a lesser extent Fe, Sc, Cs, V, and Zn. There is also S enrichment at the south end of the survey area. The deep waters in the western part of the study area are relatively undisturbed, and it is here that elements not scavenged by suspended particulates ultimately accumulate, mostly adsorbed on clay minerals in the quiet reducing conditions that prevail there.

Carbonate fraction

Sediments on Roberts Bank, south of Point Roberts, are enriched in Ca and Sr (Fig. 6). The carbon dioxide content of the sediments shows a similar distribution pattern, demonstrating that these elements are associated with carbonates. The carbonate content of the sediments is highest (locally over 5% $CaCO_3$) in this area.

The elements Zr and Hf show similar patterns of enrichment (Fig. 6). These elements have a close geochemical affinity, but are not usually elevated in carbonate-rich sediments. It is likely that the Zr and Hf occur in zircon, and that the slightly elevated concentrations are the result of a minor sediment enrichment in this heavy mineral, perhaps because of low accumulation of clay or winnowing of silty sediments (J.L. Luternauer, pers. comm., 1995). Zircon is present in Pleistocene sediments at Point Roberts, and at Point Grey (J.J. Clague, pers. comm., 1996) where Zr and Hf enrichment also occurs.

Organic fraction

Figure 7 shows four elements with distribution patterns dissimilar to those described above. All four of these elements have concentrations that are normal for marine muds (Table 2). Organic carbon is likely the controlling factor for what appears to be a partial association among these elements. The highest contents of organic carbon occur in sediments from some of the deepest waters of the study area, west of Sea Island. Some of the highest concentrations of P and As also are found in this area, although there is a second area of P and As enrichment in the northern part of the survey area. Zinc enrichment is greatest in the north where it is associated with the major elements and trace metals shown in Figures 2 and 3, but there is also moderate Zn enrichment west of Sea Island. The inference is that the distribution of Zn, and to a lesser extent P and As, is controlled by several factors, one of which is the organic fraction. No doubt other elements are associated with the organic fraction, but their associations with other sediment fractions obscure this relationship.

Factor analysis

A factor analysis was performed in order to gain greater insight into element relationships. Distributions of data are approximately normal, and there are few extreme values (Dunn et al., 1996). Consequently the data were not log transformed, nor were outliers removed, prior to generating correlation coefficients in preparation for factor analysis. Table 3

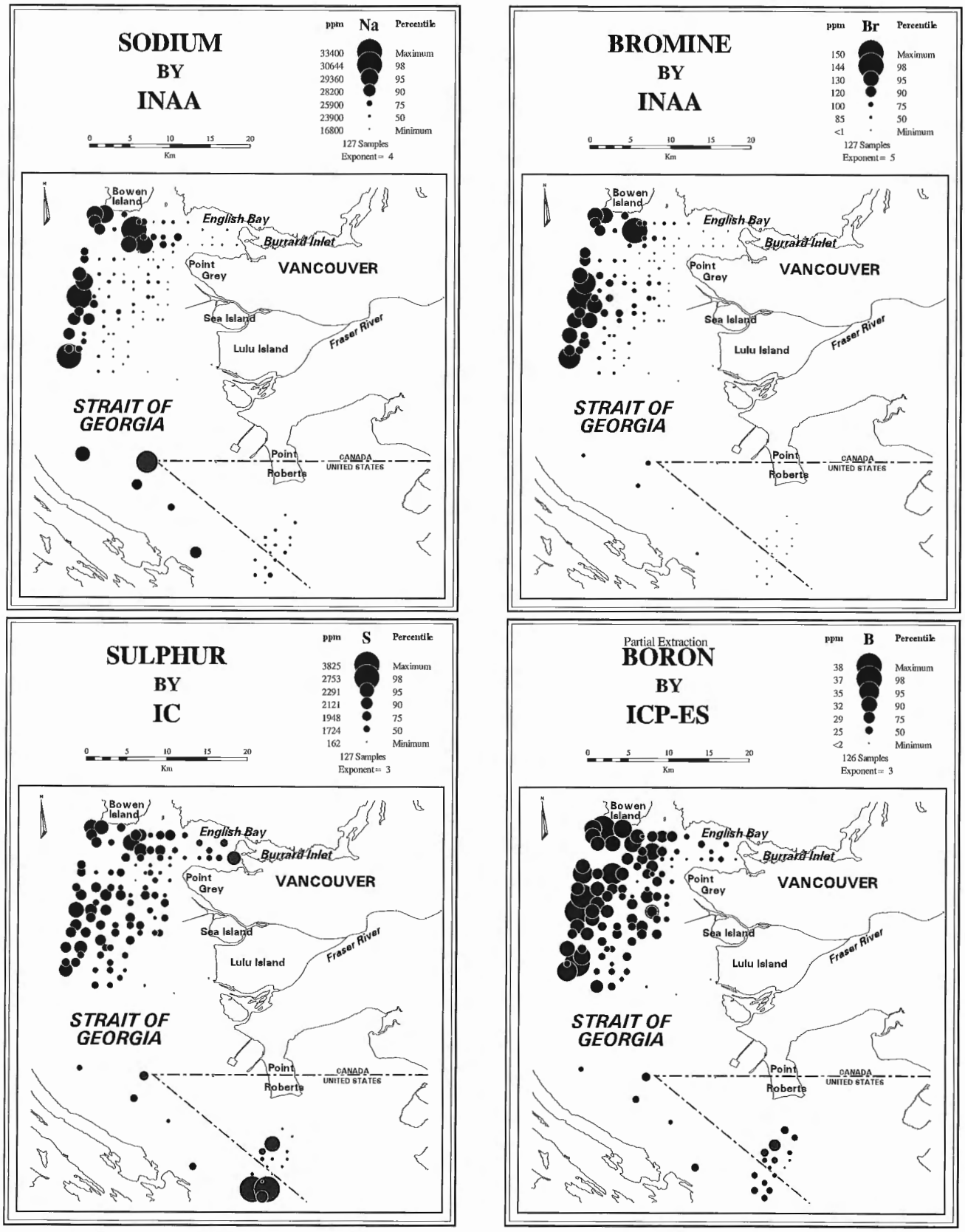

Figure 5. Distribution patterns of Na, Br, S, and B in Strait of Georgia sediments. Elemental enrichments are associated with fine-grained sediments in deep water.

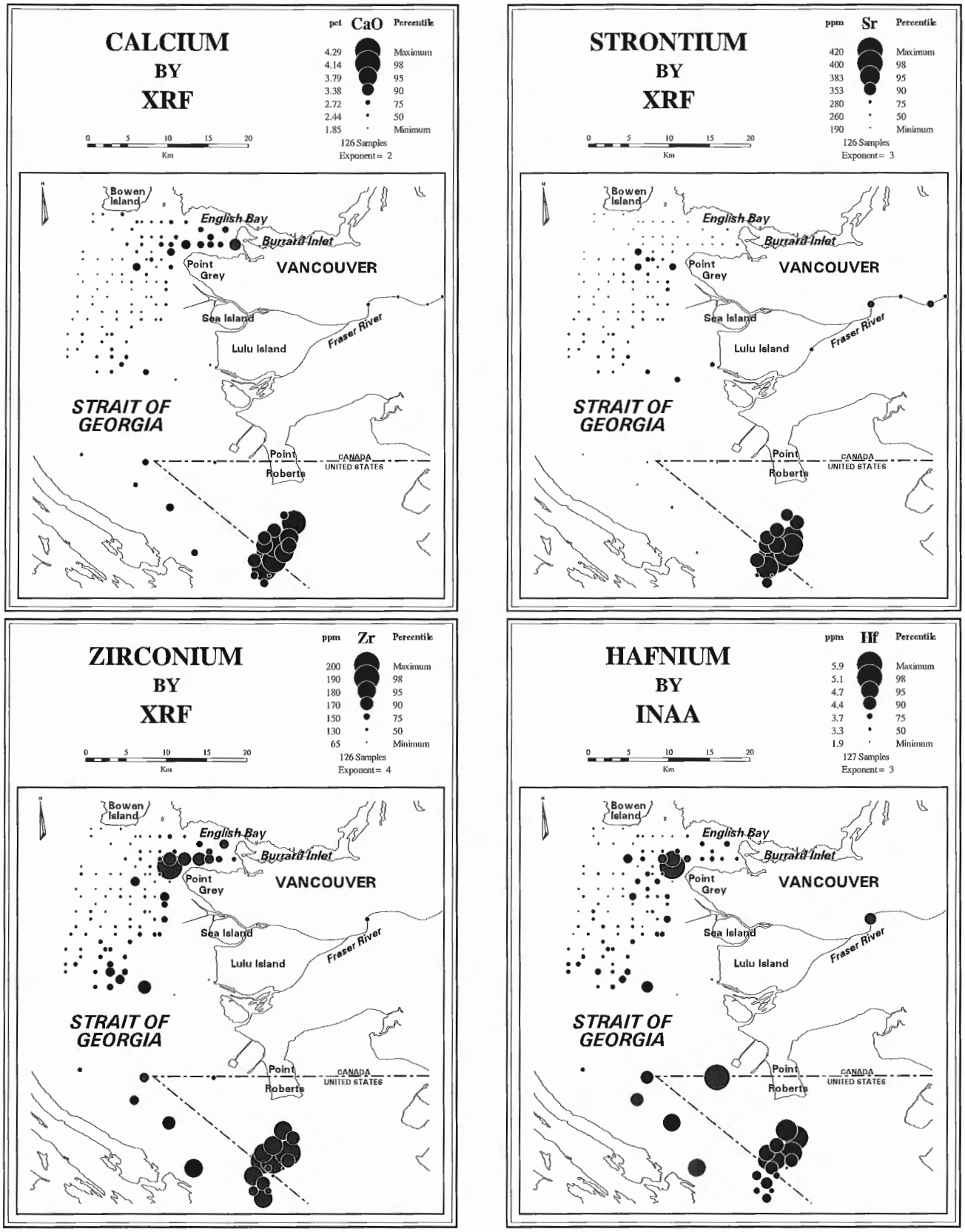

Figure 6. Distribution patterns of CaO, Sr, Zr, and Hf in Strait of Georgia sediments. Elemental enrichments indicate an association of carbonates (Ca, Sr) and zircon (Zr, Hf).

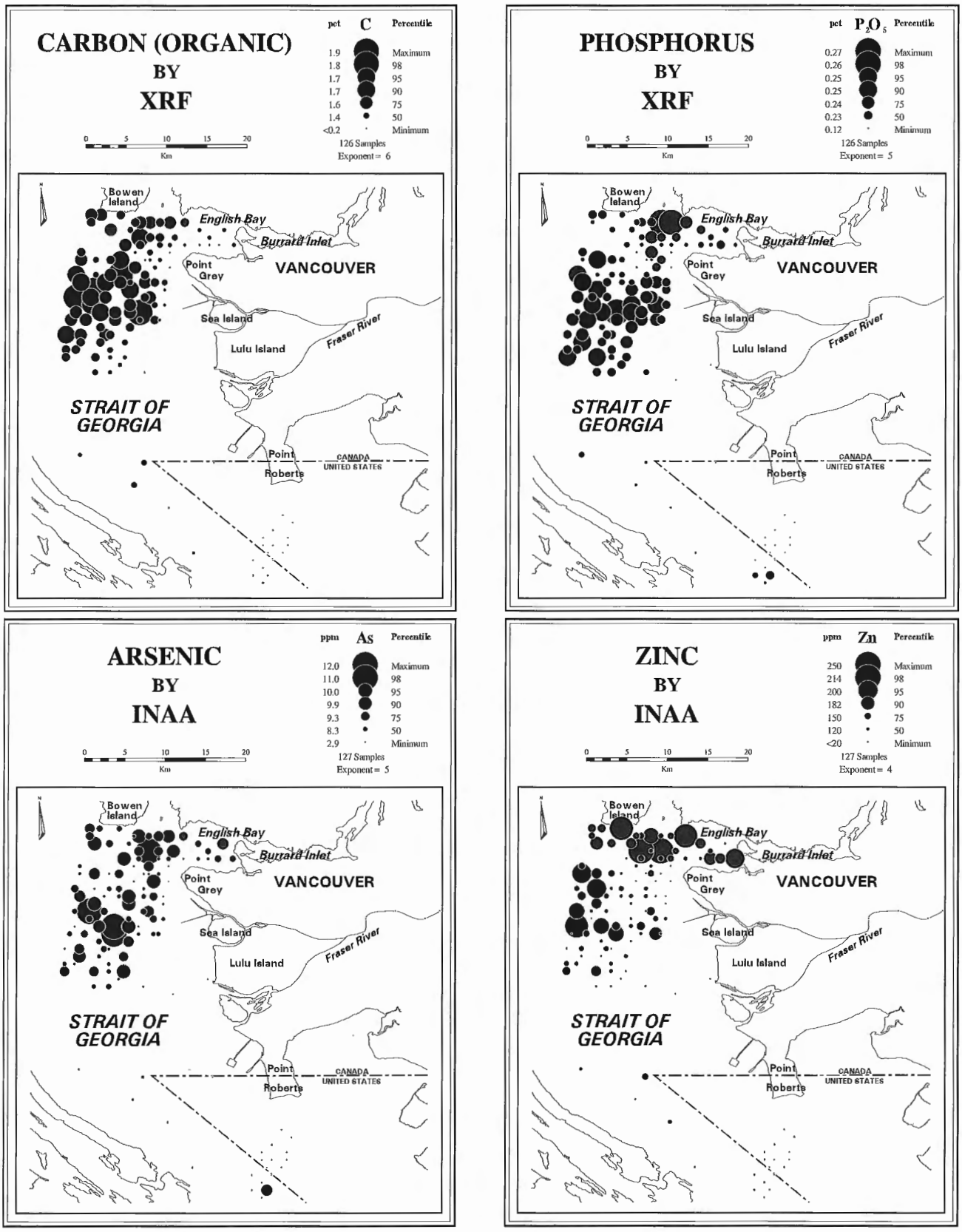

Figure 7. Distribution patterns of organic C, P_2O_5, As, and Zn in Strait of Georgia sediments. Elemental enrichments are related, in part, to organic-rich fine-grained sediments.

Table 3. Factor analysis of 68 chemical parameters (loadings >0.5, except for factors 4, 5, and 6).

	Factor 1	Factor 2	Factor 3	Factor 4	Factor 5	Factor 6
Eigenvalue	33.3	6.3	5.4	3.7	2.0	1.6
% of variation	49.0	9.3	8.0	5.4	3.0	2.4
Cumulative %	49.0	58.3	66.3	71.7	74.7	77.1
Factor Loading						
>0.9	C_{org},Br,Fe,K,Br,Na (Si)	–	–	–	–	–
0.7 – 0.9	Al,Mg,Li,Zn,P,S,Hg,B, V,Sc,Rb,Cs, Co	Cr,Ce,Yb,La,Sm	CO_2,Ca,Zr	Ag,Ba	Ti	–
0.5 – 0.7	F,Sm,Pb,La,Ni,Ce, Cu,Sb,U,Eu,Yb (Sr)	Eu,Nd,Nb,Hf,Th, U,Ti	Hf,Sr	Cu	Fe	Au,Cd
0.3 – 0.5	–	–	–	Pb,Ni,Sb,Hg Zn,F	V,Sr	Mo

Note: Elements in parentheses are negative loadings, indicating an inverse relationship.

summarizes the results obtained after applying a varimax rotation of orthogonal axes (Kaiser, 1958). Elements are grouped in order of decreasing factor loading.

Interpretation of factor analysis results relies on an understanding of the subject matter and recognition of associations which can be meaningfully explained. There is no definitive statistical test to determine the validity of the associations, but two quantitative measures can be used for guidance — eigenvalues and factor loadings.

Commonly, factors with eigenvalues greater than 1.0, which account for several percent of the data variability, are meaningful. The first six factors in this study have eigenvalues greater than 1.0, and each accounts for more than two percent of the data variation. Interpretation of factor-analysis associations with lower eigenvalues and low loadings should be approached with caution, and becomes increasingly subjective as the values decrease. For the first two or three factors, loadings less than 0.5 are usually not significant. With increasing factor number, elements with high factor loadings are fewer, and values of 0.3-0.5 may be significant.

For this study, a conservative cut-off value of 1.5 has been adopted for eigenvalues. In addition, a cut-off has been applied to loadings of 0.5 for factors with eigenvalues greater than 5, and 0.3 for factors with eigenvalues less than 5, but greater than 1.5. Factor loadings between 0.3 and 0.5 are discussed only for factors 4, 5, and 6. Appropriate caveats are given in the following discussion.

The first factor (Table 3) has many elements with strong loadings and accounts for 49% of the data variability. The associations are attributed to the clay-mineral fraction of the sediment. However, elements that have a close affinity with the organic fraction also contribute to factor 1 loadings. The high loading for organic carbon suggests that, through much of the survey area, organic material and elements associated with it, have a strong chemical affinity for the clay-mineral fraction. Elements of the deep-water fraction (Br, Na, B, S) also have high loadings on this factor.

The second factor, which accounts for 9.3% of the data variability and has an eigenvalue of 6.3, represents the resistate fraction (REEs, Th, U, Cr, Hf, Ti). The third factor accounts for 8% of data variability and represents the carbonate fraction (CO_2, Ca, Sr), with the Zr/Hf association discussed above. The fourth factor accounts for 5.4% of the data variability and has an eigenvalue of 3.7. It is of interest in that it keys in on a suite of heavy metals, dominated by Ag, Ba, and Cu, with minor positive loadings (0.3-0.5) for Pb, Hg, Sb, Zn, Ni, and F. Some of these metals may have been introduced from anthropogenic sources; although loadings are low and therefore of arguable validity, they may be a subtle indicator of contamination from industrial activity in the Vancouver area.

The final two factors in Table 3 account for 3% (factor 5) and 2.4% (factor 6) of the data variability. Their moderately large eigenvalues (2.0 and 1.6, respectively) indicate real, although subtle, element associations. Fe/Ti (loading greater than 0.5) and V (loading of 0.48) in factor 5 may be derived from a small ilmenite component of the sediments. Factor 6 is dominated by Au and Cd (loadings greater than 0.5) and Mo (loading of 0.43); it may correspond to a small precious-metal component.

Eight additional factors have eigenvalues larger than 1.0, but collectively account for only about 11% of the data variability. There is no clear explanation for their loadings, and they probably represent mostly analytical and sampling noise.

SUMMARY

This data set is a 1992 snapshot of the chemistry of seafloor sediments in the southern Strait of Georgia. As such, it can be used to monitor future changes in sediment chemistry in the Strait. Levels of elements are mostly close to those recorded in similar marine environments elsewhere in the world. Visual examination of element-distribution plots indicates several suites of elements that are associated. The geographic distribution of these element suites can be attributed to naturally occurring factors — clay minerals, resistate minerals, carbonates, organic material, or quiet reducing conditions in deep water. Some elements are partitioned among two or more of these factors. There are no unusual metal enrichments indicative of significant metal contamination of the sediments, but

factor analysis reveals a suite of heavy metals, dominated by Ag and Ba, with a weak association of Cu, F, Hg, Ni, Pb, Sb, and Zn, that may in part be attributable to anthropogenic sources. Recent studies at the University of British Columbia have found an enrichment of a few hundred parts per billion Ag in nearshore sediments off Sea Island, associated with former discharges from a sewage treatment plant (T. Pedersen, pers. comm., 1996). Studies of cores are in progress to determine late Holocene variations in sediment chemistry that might indicate recent metal enrichment, and to more clearly define anthropogenic sources of metals in the Strait of Georgia.

ACKNOWLEDGMENTS

I thank Vaughn Barrie and John Luternauer of the Geological Survey of Canada (GSC) for supplying the samples used in this study and for many useful discussions concerning the Fraser delta and Strait of Georgia. I thank also the following GSC personnel: Trudie Forbes for providing information related to the samples and their collection; Brian Sawyer for information on the bathymetry of the survey area; Alice MacLaurin for preparing the samples for analysis; Peter Belanger and his staff for undertaking the XRF analyses; Stephen Adcock for developing the computer programs for most of the data processing; Dan Boyle, Graeme Bonham-Carter, John Clague, and Leah Bendell-Young (Simon Fraser University) for constructive criticism of this manuscript; and especially Robin Balma and Wendy Spirito for producing the maps and data listings included in our Open File (Dunn et al., 1996). I also benefitted from discussions with Bob Turner, Tark Hamilton, Patrick MacLaren, and participants of several Fraser delta workshop meetings. The United States Government is gratefully acknowledged for permission granted for the CSS *Tully* to enter U.S. territorial waters to collect a few sediment samples south of Roberts Bank. This project was funded by the Geological Survey of Canada under a newly developed environmental geochemistry program.

REFERENCES

Delaney, T.A. and Turner, R.J.W.
1994: A preliminary directory of trace element databases available in the Vancouver map area; in Geology and Geological Hazards of the Vancouver Region, Southern British Columbia, (ed.) J.W.H. Monger; Geological Survey of Canada, Bulletin 481, p. 299-316.

Dunn, C.E., Balma, R.G., and Spirito, W.A.
1996: Geochemistry of marine sediments from the Strait of Georgia, British Columbia; Geological Survey of Canada, Open File 3052, 189 p.

Evoy, R.W., Moslow, T.F., Patterson, R.T., and Luternauer, J.L.
1993: Patterns and variability in sediment accumulation rates, Fraser River delta foreslope, British Columbia, Canada; Geo-Marine Letters, v. 13, p. 212-218.

Grieve, D.A. and Fletcher, W.K.
1976: Heavy metals in deltaic sediments of the Fraser River, British Columbia; Canadian Journal of Earth Sciences, v. 13, p. 1683-1693.

Hall, G.E.M., MacLaurin, A.I., and Vaive, J.E.
1986: The analysis of geological materials for fluorine, chlorine and sulphur by pyrohydrolysis and ion chromatography; Journal of Geochemical Exploration, v. 26, p. 177-186.

Kaiser, H.F.
1958: The varimax criterion for analytical rotation in factor analysis; Psychology, v. 23, p. 187-200.

Macdonald, R.W., Macdonald, D.M., O'Brien, M.C., and Gobeil, C.
1991: Accumulation of heavy metals (Pb, Zn, Cu, Cd), carbon and nitrogen in sediments from the Strait of Georgia, B.C., Canada; Marine Chemistry, v. 34, p. 109-135.

Percival, J.B., Mudroch, A., Hall, G.E.M., and Dunn, C.E.
1992: Geochemical studies in the Howe Sound drainage basin, British Columbia; in Current Research, Part A; Geological Survey of Canada, Paper 92-1A, p. 1-11.

Rousseau, R.M.
1984a: Fundamental algorithm between concentration and intensity in XRF analysis: 1 – theory; X-Ray Spectrometry, v. 13, no. 3, p. 115-120.
1984b: Fundamental algorithm between concentration and intensity in XRF analysis: 2 – practical; X-Ray Spectrometry, v. 13, no. 3, p. 121-125.

Waldichuck, M.
1983: Pollution in the Strait of Georgia: a review; Canadian Journal of Fisheries and Aquatic Sciences, v. 40, p. 1142-1167.

Waldichuk, M., Markert, J.R., and Meikle, J.H.
1968: Fraser River Estuary, Burrard Inlet, Howe Sound and Malaspina Strait physical and chemical oceanographic data, 1957-1966; Fisheries Research Board of Canada, Manuscript Report, Series 939; 2 volumes, 244 p. and 277 p.

Wedepohl, K.H.
1969: Handbook of geochemistry (vol. II, sections 1 - 5); Springer-Verlag, New York [with additions in 1970, 1972, 1974, 1978].